NASA/CR-2002-211774

Design and Test of an Improved Crashworthiness Small Composite Airframe

James E. Terry
Terry Engineering, Andover, Kansas

Steven J. Hooper and Mark Nicholson
National Institute for Aviation Research
Wichita State University, Wichita, Kansas

August 2002

The NASA STI Program Office . . . in Profile

Since its founding, NASA has been dedicated to the advancement of aeronautics and space science. The NASA Scientific and Technical Information (STI) Program Office plays a key part in helping NASA maintain this important role.

The NASA STI Program Office is operated by Langley Research Center, the lead center for NASA's scientific and technical information. The NASA STI Program Office provides access to the NASA STI Database, the largest collection of aeronautical and space science STI in the world. The Program Office is also NASA's institutional mechanism for disseminating the results of its research and development activities. These results are published by NASA in the NASA STI Report Series, which includes the following report types:

- TECHNICAL PUBLICATION. Reports of completed research or a major significant phase of research that present the results of NASA programs and include extensive data or theoretical analysis. Includes compilations of significant scientific and technical data and information deemed to be of continuing reference value. NASA counterpart of peer-reviewed formal professional papers, but having less stringent limitations on manuscript length and extent of graphic presentations.

- TECHNICAL MEMORANDUM. Scientific and technical findings that are preliminary or of specialized interest, e.g., quick release reports, working papers, and bibliographies that contain minimal annotation. Does not contain extensive analysis.

- CONTRACTOR REPORT. Scientific and technical findings by NASA-sponsored contractors and grantees.

- CONFERENCE PUBLICATION. Collected papers from scientific and technical conferences, symposia, seminars, or other meetings sponsored or co-sponsored by NASA.

- SPECIAL PUBLICATION. Scientific, technical, or historical information from NASA programs, projects, and missions, often concerned with subjects having substantial public interest.

TECHNICAL TRANSLATION. English-language translations of foreign scientific and technical material pertinent to NASA's mission.

Specialized services that complement the STI Program Office's diverse offerings include creating custom thesauri, building customized databases, organizing and publishing research results . . . even providing videos.

For more information about the NASA STI Program Office, see the following:

- Access the NASA STI Program Home Page at ***http://www.sti.nasa.gov***

- Email your question via the Internet to help@sti.nasa.gov

- Fax your question to the NASA STI Help Desk at (301) 621-0134

- Telephone the NASA STI Help Desk at (301) 621-0390

- Write to:
  NASA STI Help Desk
  NASA Center for AeroSpace Information
  7121 Standard Drive
  Hanover, MD 21076-1320

NASA/CR-2002-211774

Design and Test of an Improved Crashworthiness Small Composite Airframe

James E. Terry
Terry Engineering, Andover, Kansas

Steven J. Hooper and Mark Nicholson
National Institute for Aviation Research
Wichita State University, Wichita, Kansas

National Aeronautics and
Space Administration

Langley Research Center
Hampton, Virginia 23681-2199

Prepared for Langley Research Center
under Contract NAS1-20427

August 2002

The use of trademarks or names of manufacturers in this report is for accurate reporting and does not constitute an official endorsement, either expressed or implied, of such products or manufacturers by the National Aeronautics and Space Administration.

Available from:

NASA Center for AeroSpace Information (CASI)
7121 Standard Drive
Hanover, MD 21076-1320
(301) 621-0390

National Technical Information Service (NTIS)
5285 Port Royal Road
Springfield, VA 22161-2171
(703) 605-6000

Project Overview

The purpose of this small business innovative research (SBIR) program was to evaluate the feasibility of developing small composite airplanes with improved crashworthiness. Phase II research was conducted in five tasks.

Task 1) Refine the seat development started in Phase I by analysis and further testing.

Task 2) Develop a dynamic analysis method for the engine mount. Verify the method with quasi-static ½ scale model tests, both onto a hard surface and into soft soil.

Task 3) Develop a dynamic analysis method for the impact event which includes the engine mount, airframe structure, and under floor energy absorbers

Task 4) Design and fabricate two airplanes and test at the NASA Impact Dynamics Research Facility, one onto a hard surface and the second onto soft soil. These tests attempted to match the test conditions of prior NASA tests as closely as practical to allow direct comparison with prior data.

Task 5) Refine the design of the airplanes based on the results of the first two tests, fabricate two additional airplanes, and repeat the first two tests at the NASA Impact Dynamics Research Facility.

A finite element analysis program which analyzed dynamic non-linear large deflection problems was used to predict engine mount and airframe responses to impact. The engine mount analysis was conducted on three dimensional models while the airplane models were two dimensional. Half scale quasi-static tests were made of the engine mount on a hard surface and of the engine mount and cowling combination onto soft soil. These tests showed that the engine mount was substantially stronger than predicted using design values of yield strength. They also showed that soil response was different than expected and several additional tests were used to characterize the soil response.

The first full scale test onto a hard surface showed that the dynamic strength of the engine mount was much higher than the quasi-static tests had indicated leading to high acceleration loads. A new engine mount and cowling design based on the half scale soft soil test performed well in the second full scale test onto soft soil. However, the dummies hit the instrument panel due to seat and shoulder harness inertia reel failures. Harness loads were well above allowable limits while airframe accelerations were within the survivable range.

The first two full scale airplanes had been over strength and weight and the third and fourth airplanes were designed and fabricated to be much closer to minimum weight. Both airplanes (3 and 4) had the same basic structure in an attempt to demonstrate that the same design could protect the occupants in both hard surface and soft soil impacts. Hard surface impacts have higher normal than longitudinal loading while soft soil impacts are just the reverse.

One of the primary goals of the program was to absorb the impact energy outside the cabin structure to minimize the injury potential due to cabin deformations. This tends to move the energy absorbing material away from the center of gravity which increases the angular acceleration of the airplane upon impact. The strength of the secondary impact due to aircraft rotation is thereby increased so that all seats see a double impact. Strength of the secondary impact increases going aft in the airplane making the second impact stronger than the first at the rear seat location. A stroking seat installed in the rear location worked well in the second hard surface test as did a developmental seat installed in the pilot position. Airplane dynamics were

much improved with the improved engine mount and structure leading to a survivable test with no known injury producing problems.

Restraint systems were improved for the second soft soil test by installing an air bag in the pilot position and load limiting shoulder harnesses for both front seat positions. Cowling and engine mount performance were similar to those of the first soft soil test leading to airframe accelerations well within the survivable range and the restraint systems kept the occupant loads well in the survivable range.

These tests indicate that improved survivability is possible, compared to prior NASA tests of conventional airplanes, for symmetrical impacts at approximately stall speed for this class of airplanes for a relatively severe impact angle onto both hard and soft soil surfaces. The benefits of stroking seat designs and restraint systems including air bags and load limiting shoulder harnesses were shown. The airframe weight penalty is approximately 50 pounds with air bags adding another 12 pounds and load limiting shoulder harnesses an additional 1 pound.

Foreword

This report documents the results of Phase II of NASA SBIR Contract NAS1-20427, Design and Test of an Improved Crashworthiness Small Composite Airframe. Program manager and principal investigator was James E. Terry, president and owner of Terry Engineering who provided the dynamics analysis, structural concept and loads, structural design of the third and fourth airplanes, as well as overall program management.

Wichita State University's National Institute of Aviation Research, under the direction of Dr. Steve Hooper, provided facilities and conducted the half scale tests, conducted seat tests in their impact dynamics facility, and provided analytical support. Mark Nicholson, a graduate student, fabricated the half scale test rig and conducted the half scale tests with the principal investigator's assistance. Michael Dennis, Oregon Aero, provided the design and fabrication of the seat cushions. Rigid foam materials for the seat tests were provided by General Plastics. The air bag was provided by Simula Technologies, Inc. and energy absorbing seats were obtained from Impact Dynamics, Inc. and JAARS. Cirrus Design fabricated the test airframes and Task Research fabricated the half scale test items and the engine mounts. Lisa Jones (NASA technical monitor) conducted the tests at the NASA Impact Dynamics Research Facility.

Table of Contents

1. Introduction 1
2. Lessons From Prior Test and Design Philosophy 3
3. Seat Evaluation 4
4. Test Facilities 4
  4.1 Half Scale Test Setup 4
    4.1.1 Test Rig 4
    4.1.2 Instrumentation 5
    4.1.3 Difference between Static and Dynamic Loading 5
  4.2 Full Scale Test Facilities 5
    4.2.1 NASA Impact Dynamics Research Facility 5
    4.2.2 Instrumentation 6
    4.2.3 Anthropomorphic Dummies 6
5. Hard Surface Impact 7
  5.1 Analysis of Engine Mount 7
  5.2 Half Scale Hard Surface Tests 8
    5.2.1 Mount 1 8
    5.2.2 Mount 2 8
    5.2.3 Mount 3 8
    5.2.4 Mount 4 8
    5.2.5 Mount 5 8
    5.2.6 Comparison of ½ Scale tests to Analysis 8
    5.2.7 Mount 6 9
  5.3 Airplane Dynamic Analysis 10
  5.4 Design Concept, Tests 1& 2 11
  5.5 Full Scale Test 1, Hard Surface 12
    5.5.1 Test Conditions 12
    5.5.2 Test Data 13
    5.5.3 Comparison of Analysis to Test Results 14
    5.5.4 Key Observations 14
  5.6 Airplane Dynamic Analysis Revisions 14
  5.7 Design Concepts, Tests 3 & 4 17
  5.8 Full Scale Test 4, Hard Surface 19
    5.8.1 Seats 19
    5.8.2 Test Conditions 20
    5.8.3 Test Data 20
    5.8.4 Comparison of Analysis to Test Results 21
    5.8.5 Key Observations 21
  5.9 Impact Attitude Variations 22
6. Soft Soil Impact 22
  6.1 Half Scale Soft Soil Tests 22
    6.1.1 Soil Characterization 22
    6.1.2 California Bearing Ratio 22
    6.1.3 Airfield Index 22
    6.1.4 Soil Box for ½ Scale Tests 22
    6.1.5 Soil Preparation 23
    6.1.6 Mount 6 Test 1 24
    6.1.7 Wood Cowl Tests 24
    6.1.8 Soil Friction Tests 24
    6.1.9 Wood Block Tests 25
    6.1.10 Mount 6 Test 2 26
    6.1.11 Mount 6 Hard Surface Test 26

6.1.12 Mount 8 - ½ Scale Soft Soil Test 3 27
6.1.13 Mount 9 - ½ Scale Soft Soil Test 4 27
6.1.14 Shot-put, Dynamic versus Static 27
6.2 Full Scale Test 2, Soft Soil 28
6.2.1 Test Conditions 28
6.2.2 Test Data 28
6.2.3 Key Observations 29
6.3 Full Scale Test 3, Soft Soil 29
6.3.1 Restraint Systems 29
6.3.2 Test Conditions 31
6.3.3 Test Data 31
6.3.4 Key Observations 32
7. Weight Penalty 32
8. Summary of Results 34
9. Recommendations 34
10. References 36

1. Introduction

The crashworthiness of general aviation aircraft represents an important design consideration. In the years 1972 through 1981, more than 12,500 people were killed and more than 6,600 seriously injured in general aviation accidents [1-2][1]. More recently, there were an average of 756 fatalities per year in general aviation accidents for the years 1991 through 1995 [3]. The NTSB studied a number of accidents in detail and concluded that fatalities could be reduced 20% if all occupants wore shoulder harnesses and 88% of seriously injured occupants would have less serious injuries if shoulder harnesses were worn. Energy absorbing seats could reduce injury severity of 34% of the seriously injured occupants and reduce fatalities about 2%. A number of failures contributing to injury severity included such factors as:

Seat feet or frame failure
Seat track failure
Seat pan failure
Seat belt or belt attachment failure

Structural design of the aircraft was not addressed.

In 1982, 77% of fixed wing general aviation fatalities were in single reciprocating engine aircraft, 19% in twin reciprocating engine aircraft, and 4% for all turbine powered aircraft [4]. This indicates that the largest life saving potential is with single engine airplanes with improved survivability features but it is just this type of airplane in which it is most difficult to provide the necessary energy absorbing structure.

In general, the emphasis of current airplane designs was placed on good handling characteristics, performance, and costs. Minimal emphasis was placed on crashworthiness and little or no crashworthiness data were available for this class of airplanes. The design of any airplane requires many compromises and some of these affect crashworthiness. The quarter chord of the MAC (mean aerodynamic chord) is generally located near or under the front seats for static stability requirements leading to a spar location under the front seats for many airplanes. Other airplanes have the spar located under the front edge of the rear seats with stability requirements met by locating the spar at 40 to 50% of chord, forward sweep to the spars, far forward or aft CG diagrams, or some combination of the above. Small airplanes have less than or non-existent under-floor space compared with larger aircraft. Space limitations also restrict the seat stroking space available in these designs. Some of the two-place homebuilt designs locate the seats between the spars with the bottom of the seat on the lower skin. Increasing the under floor depth increases weight, degrades appearance, and reduces performance with consequent loss of customer appeal.

The accidents studied in [2] were mostly off-airport and into soil rather than on hard surfaces. The US Army Crashworthiness Design Guide [5] reports that nearly 75% of all aircraft accidents occur off the runway. A limited number of whole airplane, pendulum-type drop tests have been conducted of both high wing and low wing single engine designs by NASA and the FAA [6-7] and show very different airplane responses to soil than to hard surfaces. The results of these tests show that traditional single engine designs tend to dig into the soil upon impact, producing approximately twice the deceleration of similar crashes on concrete. This results in the catastrophic failure of the fuselage structure with a complete loss of cabin integrity and survivable volume. The airplanes tested, typical of many general aviation airplanes, had very little energy absorbing material outside of the cabin. A more survivable scenario can be envisioned where energy absorbing structure ahead of the cabin absorbs the initial crash impact and forms a sliding

[1] Numbers in brackets indicate reference number.

surface for soil impacts to minimize soil scooping. Recent developments in automobiles, both street and racing, have shown that fatalities and injuries can be reduced substantially by designing the structure outside the cabin to absorb energy while keeping the cabin relatively undeformed. Similar development of helicopters for the US Army has shown the same results. The purpose of this project is to apply these concepts to a small general aviation airplane to extend the survival envelope and reduce the severity of injuries in survivable accidents. Two crash scenarios were selected for this project to match two of the prior tests [7]. The two conditions were the -30° on concrete and the -30° on soil with zero roll, yaw, and angle of attack and an impact velocity of about 82 ft/sec.

The introduction of composite materials into the aerospace industry represents one of the more significant recent technological developments. These materials offer a number of advantages over traditional monolithic materials as they provide smoother finish (lower drag), ease of fabrication of compound curved surfaces, and lower tooling costs. Several of the current composite kit airplanes show drag coefficients based on wetted area significantly below metal production airplanes. Therefore composite construction offers potential energy savings over the life of the product and the assembly of kits by relatively unskilled workers.

It was shown in Phase I [8] to be feasible to improve crashworthiness of small airplanes for low cost, weight, and performance penalties. The purpose of the Phase II project was to validate the goals with subscale and full scale testing allowing NASA to extend their full scale crash data base into small composite airplanes and to further explore impacts into soft soil. Specific tasks for Phase II of this project were as follows:

Task 1) Refine the seat development started in Phase I by analysis and further testing.

Task 2) Develop an dynamic analysis method for the engine mount. Verify the method with quasi-static ½ scale model tests, both onto a hard surface and into soft soil.

Task 3) Develop a dynamic analysis method for the impact event which includes the engine mount, airframe structure, and under floor energy absorbers

Task 4) Design and fabricate two airplanes and test at the NASA Impact Dynamics Research Facility, one onto a hard surface and the second onto soft soil. These tests should match the test conditions of prior NASA tests as closely as practical to allow direct comparison with prior data.

Task 5) Refine the design of the airplanes based on the results of the first two tests, fabricate two additional airplanes, and repeat the first two tests at the NASA Impact Dynamics Research Facility.

The project followed the general sequence shown above except that there was considerable overlap between tasks and some change in emphasis as lessons were learned. The analysis proceeded more slowly than anticipated due to the general difficulty of this type analysis, my lack of experience in this type analysis, and a combination of bugs and inadequate documentation for the program used. The analysis was a learning process, particularly in the following areas:

- How to locate springs (energy absorbers) and retain the springs in the proper position
- Spring unloading curves
- Value of windows, windshield, and doors
- Design allowables

Things that did not work usually locked up the computer with no error feedback. They might work in one model but not in another. Not every step will be described, rather the most successful techniques will be described with some references to failures and problems noted but not

necessarily fully explained. Discussion of failures and problems may ease the task of follow on work.

Analysis, testing of ½ scale models, and fabrication of full scale articles were all in process at the same time so the report will be organized by topics rather than by the sequence of the work. This results in some items being discussed out of sequence or referenced before there is a full discussion of the topic, but is thought to lead to a smoother information flow in the report.

2. Lessons From Prior Test and Design Philosophy

The observations below are based on my interpretation of the NASA/FAA tests [6-7] and are not necessarily reflected in the test reports.

The NASA/FAA tests [6-7] showed very different impact responses to hard surface and soft soil impacts. Hard surface impacts for both the high and low wing airplanes were survivable but had significant deformation of the floor space. Initial impact was on the nose gear followed by the cowling and engine and then the firewall and bottom of the cabin section. There was deformation of the foot space pushing the feet up toward the dummies. Impact forward of the center of gravity produces a moment tending to cause the airplane to rotate tail down. The high wing airplane had a fixed leaf spring gear which deformed the aft cabin floor upward resisting this rotation tendency. This deformation reduced the livable volume of the rear seat area and raised the rear of the front seats moving the dummies toward the instrument panel although they did not strike the panel. The low wing airplane had air/oil struts attached to the wings which deformed the wings rather than the aft cabin floor. The firewall/forward cabin floor area deformed upward similar to that for the high wing. Accelerations were higher normal to the floor than in the longitudinal direction.

Soft soil impacts gave very different results and were somewhat different for the high and low wing airplanes. The impact attitude for the high wing airplane was about seven degrees higher than for the low wing airplane and coupled with the higher center of gravity, this led to a different airplane response. Differences in the structural design of the high and low wing airplanes are also thought to have played a role in the different response. The high wing airplane had an under floor structure with both longitudinal and cross members between the floor and the outer skin. There was also a nose landing gear fitting extending up the firewall and under the fuselage. Firewall and fuselage skins were fastened together in a forward facing flange. The cowling was thin sheet metal with a cooling air exit opening around the nose gear. This structural arrangement allowed the lower edge of the firewall and under floor structure to scoop soil collapsing the structure behind the firewall so that a livable volume was not maintained. High axial loading low on the firewall and the high center of gravity caused the airplane to pitch tail up and exit the crater upside down tail first. The high angular acceleration failed the aft fuselage in down bending during the pitch over.

The low wing airplane was a retractable gear airplane with the gear down. An aft dynafocal engine mount was used with an extension under the engine to hold the nose gear. The nose gear contacted the soil first and rapidly retracted apparently through failure of an attachment to the drag leg. The cowl was thin sheet metal and appears not to have been a factor in the sequence. Either the front of the engine or the nose landing gear mount scooped soil and failed the engine mount in down bending with the engine remaining attached in a nose down attitude. The floor is also the outside skin on this airplane with four longitudinal hat section stiffeners on the bottom side of the floor. Firewall and skin are fastened together in a forward facing flange. Soil pressure forced the lower firewall edge back and up approximately 20 inches into the foot space. The pilot dummy's head struck the instrument panel and longitudinal deceleration was 60g in the pelvis.

One observation applicable to the four tests discussed is that the impact energy was absorbed primarily in the cabin structure. Engine mounts, cowlings, and nose gears provided little

protection for the occupant space. A study of the literature shows this to be typical for this class of airplane. It also shows that failures of seat attachments and restraint systems or their attachments are major factors in injuries or fatalities.

The design philosophy applied to this program was to apply energy absorbing structure outside the cabin area and strengthen the cabin structure so that the cabin area could survive the test impacts without significant deformation, design the engine mount and cowling combination to slide on the soil to reduce longitudinal loading in soft soil impacts, avoid design features that would catch the soil forming a scoop, and to provide energy absorbing seats and restraint systems that would protect the occupants to the test levels. Consideration was given to higher energy impacts but these could not be tested within the project constraints. Since the scope of the project would not allow comparison with both the high and low wing NASA tests and the current test airplane was low wing, the low wing test conditions were chosen for comparison.

3. Seat Evaluation

A method for analyzing the combination of seat cushions and under cushion energy absorbers was developed at the National Institute for Aviation Research of Wichita State University (WSU) for another proprietary program. This method was used to predict the performance of several thickness' of rate sensitive foam cushioning material over a range of under cushion rigid foam energy absorbers with the results shown in Figure 1(a). A series of seat tests were run on the horizontal deceleration sled located in the Impact Dynamics Laboratory at WSU to verify the analysis results. Tests included variations in thickness of the rate sensitive foam seat cushions and of the rigid foam (2 lb. density Last_A_Foam) energy absorbers. The energy absorbers had a hole pattern designed to reduce effective density to the level indicated by the analysis. Figures 1(b-d) show a representative picture of the pretest cushion and energy absorber and two post test pictures of the energy absorber. Lumbar load results are listed below.

Cushion	Energy Absorber	19 g lumbar load, lb.
None	None	1554
3 inch pink	None	1479
3 inch pink	1 inch	1353
3 inch pink	2 inch	1297
3 inch pink	3 inch	1274
1 inch green	1 inch	1590
1 inch green	2 inch	1412

The hole pattern was the same for all the energy absorbers and an aluminum plate covered the hole pattern (Figures 1(b-c)). The post test pictures show that the back part of the foam block failed under the loading for the tests with the three inch cushion and the aluminum plate was extended to the back edge of the block for the tests with the one inch cushion. That may have contributed to the higher loads. Seats for the full scale test airplane were based on these test results except where alternate seats are noted.

4. Test Facilities

4.1 Half Scale Test Setup

4.1.1 Test Rig

The half scale test rig was constructed in the WSU Structures Laboratory. A framework was constructed with side pieces at 30 degrees to the floor as shown in Figure 2(a). A model carriage rode on hardened steel rails fastened to the framework and was pushed along the rails by a

hydraulic actuator. Cam follower bearings were used to minimize friction. The complete rig with a model installed is shown in Figure 2(b).

The first two test attempts on a hard surface showed that the model would chip the concrete floor or gouge a steel plate if the model tried to slide on the surface. The method devised to eliminate this problem was to have the model contact a steel plate riding on another steel plate with axle grease between the plates to minimize friction. Since there was no relative motion between the mount and the top plate, there was no damage to the contact surface using this procedure.

Nearly one quarter of the mass of the airplane is in the installed propulsion system with most of that mass mounted on the engine mount. This has the effect of putting a concentrated load on the engine mount until the propulsion system is brought to rest and it was thought this should be simulated in the test. An extension to the carriage was made which allowed an auxiliary actuator to be placed between this extension and the model. A load could be placed on this actuator during the early portion of the stroke until it was judged that the propulsion system kinetic energy would be dissipated. During the first hard surface test, it was realized that this load was simply pushing through the stiffest portion of the mount to the floor which meant that the engine would also do the same thing and be brought to rest very quickly. Later discussion of the full scale hard surface tests will show that this did in fact happen. Use of the auxiliary actuator was discontinued for the hard surface tests but it was used for the soft soil tests where it was thought to still be appropriate.

4.1.2 Instrumentation

Instrumentation consisted of load cells on the primary and auxiliary actuators, a string potentiometer to measure carriage position, and strain gages on some of the engine mount tubes starting with mount 5. Signals from these transducers were fed through appropriate signal conditioning equipment to an analog to digital converter and then to a data translation program on a personal computer where the data were stored in a spreadsheet. Calibrations were conducted through the complete system to insure accuracy.

4.1.3 Difference between Static and Dynamic Loading

Fuselage bending moments are different in a dynamic event than in a static test. Bending moment in a quasi-static test, such as the half scale tests, increases linearly as distance behind the contact point increases whereas the angular accelerations of a crash event are relieving. Original planning was to test with a fuselage section back to the spar location but this leads to unrealistic bending moments and would make the test non-representative for the aft part of the cabin structure. For purposes of the half scale test, the cabin section was shortened and simplified to test only the area near the firewall and to use the cabin section only on the soft soil tests where it was needed for clearance. Hard surface tests were with the mount fastened directly to the test rig.

4.2 Full Scale Test Facilities

4.2.1 NASA Impact Dynamics Research Facility

The full scale crash tests were performed at the Langley Impact Dynamics Research Facility shown in Figure 3. The gantry is composed of truss elements arranged with three sets of inclined legs to give vertical and lateral support and another set of inclined legs to provide longitudinal support. The gantry is 240 feet high and 400 feet long. The supporting legs are spread 266 feet apart at the ground and 66 feet apart at the 216 foot level. An enclosed elevator and a stairway provide access to the overhead work platforms and catwalks permit safe traverse of the upper levels of the gantry. A movable bridge spans the gantry at the 216 foot level and traverses the length of the gantry. Shown in Figure 3 is an illustration of one of the test airplanes suspended from the gantry in the release position. The reinforced concrete impact surface permits tests to be repeated and allows comparison between tests. A soil bed approximately 2.5 to 3.0 feet deep

was placed on the concrete surface for tests 2 and 3. The soil bed was intended to replicate the prior NASA soil beds [9] but was somewhat softer. Details of the soil bed will be given in section 6. Detailed information about the facilities used and test procedures to carry out the full scale crash tests are reported in [10].

4.2.2 Instrumentation

4.2.2.1 Photographic

Three cameras were installed in the cabin. A wide angle lens camera was installed on the subpanel looking aft at the dummies. The 2 X 4 wood subpanel allowed this camera to rotate during test 1 so the subpanel was anchored more firmly for test 2 and changed to a more substantial structure for tests 3 and 4.

Two cameras (one for test 4) were mounted on the hat shelf behind the baggage compartment looking forward. The shelf was not strong enough in test 1 allowing excess camera motion so was reinforced for later tests.

Test 4 had one camera focused on the legs of the stroking rear seat.

A camera was mounted on a tripod fastened to the outside of the fuselage looking into the cabin for test 1. This camera failed and was not installed for the rest of the tests.

Two cameras were installed on the ground at each of the following locations:

forward of the impact point along the flight path

side of the impact point normal to the flight path

behind the impact point along the flight path

on the gantry above the impact point

At each location, one camera had a long focal length lens and one had a wider angle lens. All cameras were 16mm with a nominal framing rate of 400 frames per second.

4.2.3 Anthropomorphic Dummies

Two 50th percentile anthropomorphic dummies were used in tests 1, 2, and 3 and three were used in test 4. Each was instrumented with three axis accelerometers in the head, one accelerometer in the pelvis, and a lumbar load cell.

4.2.3.1 Accelerometers

Airframe accelerometers were installed as shown in Figure 4.

4.2.3.2 Strain Gages

Strain gages were installed on a number of the engine mount tubes as shown in Figure 5. Test 4 included gages only on the tubes connecting to the firewall.

4.2.3.3 Data Recording

The on board instrumentation was connected to a junction box in the aft fuselage and the signals were carried through an umbilical cable to a computer in the control room. They were recorded on a digital system as text files in engineering units. Data for test 1 were recorded at 10,000 samples per second for each channel while data for the last three tests were recorded at 5,000 samples per second for each channel.

Data were filtered according to SAE 211/1 Technical Standard [11]. Dummy accelerations and lumbar loads were filtered with Channel Frequency Class (CFC) 1000 and airframe accelerations and restraint system loads were filtered with CFC 60. Engine mount strain gage data were not filtered.

5. Hard Surface Impact

5.1 Analysis of Engine Mount

Terry Engineering acquired a two part finite element analysis program capable of running on a PC. The first part was a static linear elastic analysis program and the second part was for dynamic non-linear large deflection problems. A variety of different material properties are supported in the dynamic program.

A number of mount configurations were analyzed by the following process. A wire frame drawing of the engine mount was transferred to the preprocessor using an IGES transfer. Nodes and elements were defined in the preprocessor. The tubes were treated as beams for the analysis with material properties of 4130 steel. Beam elements consist of a center line, cross sectional area, and the moments of inertia in two axes. Two 25,000 lb. loads (representing 20g deceleration for a 2,500 pound airplane) were applied to the initial contact points on the mount at a 30 degree impact angle (Figure 6) and the linear elastic solution obtained. The process was repeated with tube sizes adjusted to keep stresses for tubes not intended to fail first under 70,000 psi (based on as welded condition [12]) using linear analysis. The tubes intended to fail first were sized to have stresses over 70,000 psi.

A dynamic analysis was then made using the same beam element and node layout as the elastic solution. Material properties were changed to resultant plasticity (elastic, plastic) with yield stress set at 70,000 psi. The firewall mount points of the mount were given a fixed boundary condition with the mount in the expected impact position of 30 degrees nose down. Impact was simulated by a "stonewall" weighing 2500 lb. having an upward vertical velocity of 40 ft/sec. The stonewall was initially in contact with the mount at the same nodes where the loads were applied for the elastic solution. The installed propulsion system mass (rigid body mass) was attached to appropriate nodes representing the engine mounts. This analysis doesn't allow the motions that an airplane has in an impact but the ½ scale tests don't either so the analysis represents these tests.

Sample data for the mount configuration selected for the first 1/2 scale test are shown in Figures 7(a-d). These data show the stonewall brought to rest in about 36 milliseconds with nearly constant force in the primary mount support tubes.

The desire was for the 1/2 scale model to be a true scale but tube sizes available did not allow that. Tube sizes were selected as near to 1/2 scale as possible, in general with larger wall thickness than desired. For example, the minimum wall thickness available is .028 which doubles to .056. Several of the wall thickness' in the analysis represented in Figures 7 were .035 or .049. We considered whether to maintain diameter and accept larger wall thickness or to try to match cross sectional area. It was decided to maintain diameter since I/σ would be more closely matched in this way. The dynamic analysis was rerun with tube sizes twice that of the model tubes and the results are shown in Figures 8(a-c). Failure modes are similar but with somewhat larger and less even forces in the primary support tubes.

The mount was laid out with the selected tube sizes after the above process and it was noted that the effective length of a number of the tubes is much less than used in the analysis. It was felt that the best course of action was to obtain test data to compare to the analysis so fabrication of

the first 1/2 scale mount proceeded and the mount is shown in Figure 9(a-b). A half scale "engine", also shown in Figure 9, was built to simulate the stiffness of the engine in the mount and to simulate the size of the oil pan. The tube across the top of the simulated engine represents the front cylinders since it was expected that the cowling would deform back against the front cylinders during soft soil impacts.

5.2 Half Scale Hard Surface Tests

5.2.1 Mount 1

This first mount was dramatically over strength. The lower attach bolts failed in tension at well beyond the expected loads with little permanent deformation in the rest of the mount. There was localized crushing of some tubes at joints and some weld cracking at the same joints.

5.2.2 Mount 2

A number of tube sizes were reduced for mount 2 and the lower attach points changed to load the attach bolts in double shear. This had the effect of allowing rotation of the lower joint and the wall condition was changed to reflect this additional degree of freedom in the calculations. This mount was still greatly over strength and only sustained flattening of the lower tubes and localized tube crushing at joints in several tests at well above predicted loads. One of the forward elements was removed for the later tests with no significant change in results. None of the tubes buckled as the analysis indicated should happen.

5.2.3 Mount 3

Tube sizes were further reduced for mount 3 and it showed a progressive failure pattern but with less load than desired (Figure 10).

5.2.4 Mount 4

Several tube sizes were increased for mount 4 and a similar failure pattern at somewhat higher load was obtained (Figure 11). Both mounts 3 and 4 had failures of the lower rail which was thought to be a potential problem in soft soil. The fracture left a forward facing tube which could penetrate the cowling and on into the soil.

5.2.5 Mount 5

Detail design changes were made for mount 5 to try to delay this fracture while tube sizes were maintained the same as 4 (Figure 12(a-d)). These changes had little effect because the failure mechanism was not correctly analyzed. The failure was in bending at a weld joint and not a tensile failure of the tube itself as had been assumed. Figure 12(a) shows mount 5 installed on the test rig prior to test and Figures 12(b-d) show representative pictures during the test. All quasi-static tests were run continuously at about two inches per minute stroke rate. Data for mounts 3-5 are compared in Figure 13. Details of the failures were changed from the earlier mounts but the overall results were similar for mounts 4 and 5. Instrumentation for mounts 1 through 4 included actuator stroke and force. Five strain gages were installed on mount 5 to give additional details of the failure patterns. Gages were installed at the locations shown in Figure 14 with the data shown in Figure 15

Yield strength of the material was calculated from the data of gage 5 to be about 98,600 psi and the stress at buckling was about 145,000 psi. Early calculations had used yield strength of 70,000 psi [12]. Calculations after this test used 95,000 psi based on this test data.

5.2.6 Comparison of ½ Scale tests to Analysis

Engine mount analysis continued throughout the ½ scale test period with refinements trying to improve the correlation with test data. The simulated engine used in the tests stabilizes the engine mount rail whereas the early calculations without any engine simulation showed buckling in the rail. A real engine in a real crash would also be expected to provide some stability to the rail and it was thought important to match the failure sequence of the mount tubes as well as possible

in the analysis. The first attempt to replicate the engine using rigid links supported on springs simulating the engine mount isolators was unsuccessful. It was found that a rigid mass, simulating the powerplant installation mass and moment of inertia, could be added to the calculations. This stabilized the rail but the overall failure pattern changed from that observed in the tests, basically the mass held the front of the mount down more than observed in the half scale tests. Mass was reduced to 1/100 times installed powerplant mass which retained the rigid mass characteristic but brought the calculated failure pattern closer to test (inertial loads are negligible for the stroke rates used in these tests).

Calculated loads in the three support tubes were resolved into the load normal to the firewall (test rig actuator load) and compared to the load from test mount 5 (Figure 16). There is an unexplained drop in the load near 1.5 inch displacement but otherwise there is some agreement in the shape of the curve but the load is too low. Reasoning that the measured buckling stress from test 5 was about twice the plastic yield stress used in the calculations (70,000 psi), doubling the calculated load produced much better agreement. This case is also plotted in Figure 16. The load displacement curves were integrated to obtain energy absorbed for the test data and two times the calculated load with the following results.

Test 5	41411 in lb.
2 * calculated	36642 in lb.

Test energy absorbed is 13% higher than twice calculated. Measured wall thickness' were the order of 5% high for several tube samples representing the test mounts leading to a closer agreement between calculated and measured energy absorption.

Test loads for mount 5 were of the desired magnitude with reasonable correlation with analysis using the adjusted yield strength, so mounts were fabricated for the first two full scale test airplanes based on mount 5. Fabrication of the lower rails was changed to eliminate the welds which failed on mounts 3 through 5. Additional design details for these mounts are given in section 5.4 below.

5.2.7 Mount 6

Mount 6 was fabricated after completion of the first two full scale mounts and was the same as mount 5 except that the rails were bent at key locations rather than welded. It was intended to be as close to a half scale model of the first two full size mounts as available tube sizes would allow. Mount 6 was used on both the first two soft soil tests (see below for discussion of the soft soil tests) with only minor bending of the front of the mount where it goes around the front of the engine. The primary actuator load was much higher than it had taken to deform mount 5 on a hard surface indicating either that mount 6 was much stronger than mount 5 or the soft soil loading was different than expected. We decided to test mount 6 on a hard surface to compare the results to the two soil tests and to the results of mount 5 on a hard surface. Test results (Figure 17) showed that the intended similarity in strength to mount 5 had been achieved and that the lower rail fracture had been eliminated. Mount 6 is shown prior to test in Figure 18(a) and after test in Figure 18(b). This test also confirmed that loading in soft soil is of a different nature than hard surface loading and this will be discussed in more detail in section 6 below.

Scaling from half scale to full scale, the cross sectional area of the tubes increases by a factor of four. With no friction, vertical force on the engine mount is twice the actuator force for the 30° angle of the tests leading to the expected full scale vertical load being eight times the half scale actuator force. The expected vertical force for the full scale test would result in about 20 g vertical deceleration of the full scale airplane based on the results of tests of mounts 5 & 6. Based on the analysis and test results of the half scale mount, we expected the full scale mount to deform similar to mount 6 as shown in Figure 18(b) and for the airplane deceleration to be the order of 20g. Neither of these results was achieved in test 1 because the full scale mount was much too strong as will be shown in the discussion of full scale test 1 below.

5.3 Airplane Dynamic Analysis

The engine mount analysis models were 3 dimensional and had run times up to 8 hours. It was decided to simplify the full airplane model in an attempt to get reasonable model development time, reasonable run times, and to develop internal loads so that the first two airplanes could be built on schedule. The first attempts simplified the engine mount by taking the 2 dimensional view of the mount and treating all the elements as having twice the area and moment of inertia of the tubes for the design mount. Engine mount materials were elastic-plastic. Various simplification methods were considered for the fuselage and the first method used was to have upper and lower longerons, vertical members at the frame locations, and a diagonal behind the firewall to give shear strength. Elements in this model were arbitrary simple constant cross section steel elements and material was linear elastic. This model is illustrated in Figure 19.

Rigid masses (which do not show in the preprocessor drawing) simulated the powerplant installation, two front seat passengers, one rear seat passenger, and the empennage. Rigid masses have both mass and moment of inertia and are attached to nodes. The rest of the airplane mass was simulated by nodal masses (which also do not show) placed according to a Cirrus Design weight estimate taking into account the structural mass of the model. Both horizontal and vertical mass locations were considered in the spread. Total mass represents three passengers and mid mission fuel (2500 pound gross weight).

The design concept called for the floor to be the primary structural element in the lower fuselage with foam blocks under the floor in three locations for energy absorbers. Both foam blocks and edge loaded composite sandwich panels had been looked at in Phase I of the contract. Data from a number of sources indicate that edge loaded panels work well only for unidirectional loads while foam blocks tend to work well for omnidirectional loads. Further, foam blocks are much cheaper to fabricate and install than panels. Springs representing these blocks used a general non-linear spring formulation which allowed user specified load versus deflection data both for loading and unloading. The foam blocks used for under floor energy absorption were thought to have little or no rebound under dynamic conditions so the unloading curve was quickly brought to zero and kept at zero to simulate the out of contact condition. This spring model was used for many of the dynamic analysis runs but there were many failures along the way until finally getting to a model that wouldn't run at all as we tried to make the model more realistic. A great deal of confusion was caused by the fact that changing an element or material property in the engine mount would cause the run to fail in the first few steps, long before any of the springs touched the ground. Yet by process of elimination, the problem was found to be in the spring unloading curve. The zero slope portion of the curve appears to have caused problems in the program and when the tail of the unloading curve was changed to a small finite slope the problem went away.

The spring loading curve was based on the cross sectional area of the blocks and the spring rate given for rigid, closed-cell, polyurethane foam increased by 30% for dynamic loading as given by the manufacturer [13].

The line of action of the springs is not restrained in the analysis program. A large number of methods of restraining the ends were tried without success. The final method chosen, only because it worked, was to make a 4 element lever with the element nearest the structure having a high modulus (steel) but with a low yield strength (9,500 psi). The other three elements were treated as linear elastic steel. Initially the springs were attached between the end of the lever and a node on the fuselage floor so they collapsed to zero length when fully compressed. Later in the project, it was realized that the line of action of the spring was indeterminate when the spring approached zero length and a post was attached to the floor with the spring attached to the top of the post. This had the further value that the only loads on the post were the spring loads and these loads could then be read out to verify the spring action. More time was spent trying to get the springs to work correctly than in any other aspect of this analysis.

For the engine mount analysis, the mount had been stationary and the stone wall moving. The airplane model reversed this with the stone wall considered fixed in space and the model was given an initial velocity of 40 ft/sec downward. Model angle was set at 30 degrees to the stone wall.

Engine mount tube sizes were varied to bring the forward part of the airplane to rest while keeping seat decelerations under 20 g for the initial impact. Spring loading curves were varied to keep seat decelerations under 20 g for the secondary impact. The design goal was to absorb the energy outside the cabin structure to maintain the people space undamaged. This means that the initial ground reaction will be farther from the center of gravity than if the energy is absorbed in cabin deformation. The result is higher angular acceleration of the airplane and a more severe secondary impact or aft fuselage slap down.

Springs were initially located under the firewall, under the main spar, and under the rear spar. The rear spar location was found to cause a "jolt" at the crew seat location. Various positions of the rear spring were tried and moving the spring aft to a position just aft of the rear seat was found to eliminate the "jolt".

While this model was used to develop internal loads for design of the first two full scale test airframes, no results are shown since the model is not representative of the real structure and several problems were later found in the analysis.

5.4 Design Concept, Tests 1& 2

The basic fuselage structure was a fiberglass sandwich shell consisting of a rigid polyurethane foam core with two ply face sheets aft of the cabin door and four ply face sheets forward. Frames were located at the firewall, aft of the baggage compartment, and forward stabilizer attachment. There was a spar box across the floor over the main wing spar. Wing skins were similar to the aft fuselage skins and there was a tip to tip continuous "I" beam main spar attached to the spar box using two bolts. Fuel was carried in integral tanks located outboard of a planned landing gear well aft of the main spar. There was an aft close out spar attached to the fuselage with a single bolt on each side. Ballast was attached to this aft spar to simulate the mass of flaps and ailerons. Each wing contained four ribs, one at the root, one at the inboard end of the fuel tank, one mid tank, and one at the end of the fuel tank. Design of elements specific to the first two test airplanes are described below.

The design of the first full scale engine mount was completed based on the results of half scale test five and the analysis described above. Two locations in the ½ scale mounts failed in tension while the rest of the failures were compression buckling. It was thought that energy absorption of the mount would be improved if a higher elongation material was used for the two elements failing in tension. Stainless steel and mild steel both have higher elongation to failure but with about half the strength of the 4130 steel used for the rest of the mount. Tube sizes for the two tension tubes were increased to account for the lower strength and one tube was made of mild steel and one of stainless steel and the first mount is shown in Figure 20. It should be noted that the primary energy absorbers in the mount were the compression tubes and tube size of the tension tubes has little to do with impact response of the mount.

This first analysis carried all loads in the lower fuselage below the door sill because the desire was not to have structural elements in the windshield. The fuselage sidewall is shallow to get under the cabin doors resulting in a very substantial beam being required for the compression loads leading to a higher than desired weight penalty. The first two airplanes were built based on this analysis and had large beams under the door and heavy steel tube structure tying the central portions of the engine mount to these beams (pictures referenced in section 5.5). They were heavier than needed.

The floor had added stiffeners to carry the lower engine mount loads and struts continued through the spar at four locations to carry these loads into the rear floor. The rear floor was made of wood so that test instrumentation could be installed easily. Stiffeners were installed above the under floor foam blocks to transfer the loads into the spar box or sidewalls.

Certain simplifications were made to keep the project within the cost limits. Teledyne Continental Motors supplied run out engines which were installed without propellers, exhaust systems, or plumbing. Ballast was fastened to the propeller flange to simulate propeller mass. No landing gear was installed, partly for cost reasons and also because the gear up impact was thought to be the worst case. Basically all systems were left out because it was thought that they would have little effect on the crash dynamics. Water was used in the fuel tanks to simulate the impact dynamics of fuel but no lines were installed.

A simple plywood instrument panel mounted on a wood subpanel was installed at the correct position to check for dummy impact on the panel. One of the interior cameras was mounted on the subpanel.

Two 50th percentile anthropomorphic dummies were used on each of the first two tests. Dummies were restrained with a lap belt and a dual shoulder harness. The copilot's shoulder harness was fastened to the upper cabin structure through an inertia reel while the pilot's shoulder harness was fastened to the seat structure through an inertia reel. A roll bar at the aft edge of the door supported the copilot's harness loads. Seats for the first two airplanes, except for the pilot seat for test 1, were simple composite seats designed to hold seat cushions and under cushion foam energy absorbers as described in section 3 above. The pilot seat for test 1 had a fiberglass diaphragm suspended above the seat bottom designed to deform as a shear panel under the dummy loads. This did not work well and the diaphragm was removed for test 2 and replaced by the foam energy absorbers as described above. The copilot's seat (Figure 21(a)) was fiberglass while the pilot's seat (Figure 21(b)) was carbon fiber to provide the required stiffness for the shoulder harness loads. Seats were bolted to steel brackets mounted to the spar box.

The cowling for test 1 was a simple shell not designed to carry any crash loads. Test 2 had a cowling which was a scaled up version of the ½ scale soft soil cowl described below. It will be further described in section 6 on soft soil tests.

Doors were simulated by simply cutting out a portion of the sidewall structure and retaining it in place with four screws through tabs bonded to the structure. Door frames were not simulated for either the airframe or the door. The right rear window was left out so that the umbilical cord could pass through the opening.

Swing fittings were installed in each wing at the quarter chord point, a forward fitting at the firewall fastened to the upper mount points, and a tail fitting where the forward edge of the horizontal stabilizer would be. No tail surfaces were installed but ballast simulated the mass of the empennage.

5.5 Full Scale Test 1, Hard Surface

5.5.1 Test Conditions

The first full scale test was run at the NASA Impact Dynamics Research Facility on May 1, 1996. This test was designed to be a 30 degree impact angle, zero degree angle of attack impact on hard surface. The measured angle of attack was 6 degrees leading to an angle of impact relative to the ground of 24 degrees. Roll and yaw were small. Impact velocity was about 85 ft/sec, slightly higher than planned (Table 1).

5.5.2 Test Data

The airplane is shown rigged ready for pull back in Figure 22(a) and in the pullback position in Figure 22 (b). An impact sequence in shown in Figure 23. Representative post test pictures are given in Figures 24(a-e) and data are given in Figures 25-44.

Primary data were recorded digitally with a limited time for data recording and the timing of the data collection was such that data for the secondary impact were not recorded. Backup data were recorded in analog format with a longer timing cycle which included the secondary impact. Timing counts were not coordinated between data groups so there is no way to accurately determine impact times for the different analog traces. A number of the analog traces were saturated and there are anomalies in the data which do not appear to be coming from the instruments reducing the ability to fully analyze the data. While there are problems in the analog data, the data shown in Figure 33 show the characteristic indicated by the analysis that there are two impacts and that the second impact increases in strength going aft in the airplane. It also shows that there were two peaks in the copilot pelvis acceleration which appear to be of approximately equal magnitude. However, the data are misleading because the second peak saturated the data system so the real magnitude is not known. These data were filtered using the SAE 211/1 standard with filter class 1000 for the pelvis acceleration. There is little difference between filtered and unfiltered with class 1000. The rest of the data in this figure were filtered with class 60 which does introduce some questions in the data. For example, the lower right engine mount trace shows a section with nearly a square wave with a small peak on each end. That is a saturated portion of the original signal so the peaks were added by the filter algorithm.

The filter algorithm causes the ends of the traces to be inaccurate. The beginning of the traces is not shown but the end where the data were cut off early is not accurate because the filter algorithm causes the last value to be zero even if the last point has a finite value. This is a problem only with the digital data from test 1 since the later tests and the analog data had long enough data recording times that neither end is shown.

The engine mount (Figure 24(a-b)) was expected to deform similar to the hard surface test of mount 6 as shown in Figure 18(b). There is much less deformation in the full scale mount than mount 6 and further, the deformation is of a different type. Whereas the tubes between the rails buckled on the half scale tests, they punched into the rails with very little buckling on the full scale mount. It appears that material strength and/or resistance to column buckling is higher under dynamic loading than static loading by a greater margin than expected. For example, Figure 42 shows strains about twice the level at which buckling occurred in the half scale tests and this tube was nearly straight after the test. Airframe accelerations were consequently higher than expected. The half scale test of mounts 5 and 6 indicated an acceleration of about 20 g while Figure 25 shows several times that much at the firewall. The higher than expected loads forward leads to higher than expected angular acceleration. Combining the linear and angular accelerations leads to the measured acceleration in the Z direction decreasing moving aft and in fact changing direction between the baggage compartment and the tail. This characteristic is predicted by the analysis and can be seen in the data by comparing Figures 25, 26, and 28. One indication of the high angular acceleration is the fracture in up bending of the aft fuselage (Figure 24(c)) with the tail Z accelerometer measuring the order of 100 g (Figure 26).

There was no loss of livable volume in the cabin with the film showing only small cabin deformation during the impact and neither dummy hit the instrument panel. It should be noted that there is more distance between the people and the instrument panel than in some current airplanes. There were fractures at the intersections of all structural members crossing the cabin at their attachment to the side walls which showed evidence of cabin deformation but the amount was too small to affect the occupants.

The left hand seat gave a lumbar load approaching 3800 pounds (Figure 27) with no visible evidence of permanent deformation of the diaphragm. Performance of the right hand seat as seen in the copilot lumbar load (Figure 30) was better with a maximum lumbar load of about 2400 pounds. Figure 24(e) shows the right seat under cushion energy absorber after the test. This energy absorber was originally two inches thick but had been reduced to one inch due to a head clearance problem. Both lumbar loads were well above the 1500 pound limit but the right seat results were encouraging in that they were well below the pilot's rigid seat data. Lumbar loads were not recorded for the second impact on either seat by either data system.

There was no fuel spray from the fuel tanks. Fuel leaks were small and slow, well away from the engine compartment, and appear to have been from manufacturing flaws.

5.5.3 Comparison of Analysis to Test Results

By the time of this test, the dynamics analysis model had been modified to a much more realistic structural model. No comparison was made with the analytical model used for design of the first two airplanes but the test data were compared to the later model and this comparison will be described below.

5.5.4 Key Observations

The engine mount strength and deformation pattern did not match the ½ scale test data or the analysis.

Dynamic strain to failure of the engine mount elements was higher than for static testing.

5.6 Airplane Dynamic Analysis Revisions

After the first two airplanes were under construction a more realistic model was developed as shown in Figure 45. This is also a two dimensional model for simplicity. A windshield post was added in an attempt to reduce the size of the side beams required and thereby the weight of the airplane. Steel tubing material properties were used for the windshield post (linear elastic) and engine mount (elastic plastic or resultant plasticity) elements. Linear elastic properties for fiberglass laminate (+/- 45°) were used for the rest of the airframe elements except for the door frames. The vertical member supporting the aft end of the windshield post is actually the front door frame which more resembles a hoop than a post. Effective stiffness of that frame was calculated using a static analysis of the frame as shown in Figure 46. The rear door frame was arbitrarily set at half the stiffness of the front door frame initially but later they were the same. Top and bottom beams areas were based on the fuselage perimeter measured between the 45 degree tangency's on either side of the section loft and material thickness' (.085 for two sides of the aft fuselage sandwich) for typical structure for this type of airplane. Frames (other than the door frames) were estimated based on typical frames. Sidewall shear was simulated by plate elements with material thickness of .080 aft of the rear door frame (based on two plies inside and outside and two sides of the airplane) and .170 forward where additional plies were used. Core materials were neglected. Four node quad plates were used for all shear elements, some elements look like triangles but the program uses one node twice to make them a four node quad plate. Areas containing doors, windows, and windshield were left open. It was thought that the low modulus of elasticity of the window and windshield material would make them ineffective and that the doors could open easily.

Parametric studies were run of variations in the windshield post, door frame, and cabin top including both straight and curved sections. Seat decelerations were sensitive to buckling of any of these members. If the element was stabilized by shear panels, modulus of elasticity and cross sectional area were found to be the important parameters with moment of inertia of little importance. Moment of inertia of the element was very important for unstabilized elements.

This model showed that the side beams carried very little load in contrast to the results of earlier analyses and the floor loads decreased as well. But it was not representative of the airplanes built and there was still a desire not to have the windshield post so it was removed from the model. The model had been based on design information for the baseline airplane but study of the fuselage as built showed that the side walls under the door were much heavier than the design information indicated and the model was revised to reflect the actual construction in that area. The longeron was changed to area and moment of inertia of the test aircraft resulting in the model of Figure 47. Beam elements are shown in the model by rectangles where the width of the rectangle is representative of the beam moment of inertia so the relative size of the beams can be seen in the model. Rear seat velocities at the secondary impact were lower than with the prior model but the seat deceleration was very high.

It was observed that seat velocity was essentially constant during the time of the spring compression and the high seat deceleration occurred after the spring bottomed. This phenomena was studied using an animation which showed that the fuselage was deformed in a downward arc at the time of the spring impact and the arc was reducing throughout the spring stroke allowing the seat to continue downward unattenuated. Pictures from test 1 had been transferred from video to the computer showing that the impact attitude (flight path angle was 30 degrees as planned) for the first test was 24 degrees instead of the planned 30 degrees and that there was substantial flexibility in the fuselage indicating that the above phenomena might be correct. A later reading of the film showed the impact attitude was indeed 24 degrees but the fuselage deflection was small meaning the model was not correctly predicting the fuselage flexibility and that the resolution of the video to computer transfer was not good enough to determine these kinds of details.

This meant my calculations were not matching the airplane characteristics very well. In developing the model, I had assumed that the windshield, doors, and windows were not effective in fuselage bending because of low modulus of elasticity and the following events. The windshield had popped out in test 1, the doors had come loose, and the pilot side window fractured. There was no window installed in the right side rear location to allow exit of instrumentation cables. The video of test 1 was reviewed carefully to determine when these events occurred and it appeared they occurred on the second impact, aft fuselage slap down. This could not be determined with 100% certainty due to camera motion but I believe it to be correct.

The analytical model was modified to contain shear panels representing the doors and windows and a beam representing the windshield (Figure 48). Area and moment of inertia for the windshield beam was estimated as 90 degrees of arc of a 22 inch radius circle. Modulus of elasticity was set at 400,000 psi as shown on a data sheet for cast acrylic. The door in the model of Figure 48 was not separated from the rest of the structure while the doors of the test airplanes were attached at 4 points. Production doors would be expected to have 2 hinges and 2 latches also. Figure 49 shows the model modified by making the door separate and attaching it to the structure at 4 nodes. There was no significant difference in airplane dynamics and internal loads were essentially the same except for cabin top loads which increased somewhat. This model took nearly twice as long to run so most of the structural loads development used the faster running model. Figure 49 shows a different engine mount than the other figures but this comparison for the different door models was made on the same engine mount.

It was discovered that the gravitational acceleration was not active with the rigid body masses but was with the nodal masses. It should be noted that gravitational acceleration has only a second order effect on the results because it is small compared to the inertial accelerations. Gravitational acceleration had been verified early in the model development and it is not known why the system had changed. The model was changed to eliminate the rigid body masses and replace them with nodal masses. Inputs for nodal masses do not allow specifying moment of inertia so each rigid body mass was divided into two nodal masses placed twice the radius of gyration apart and centered on the center of gravity of the mass in order to keep the correct moment of inertia. This

required adding beams for the engine and the flight crew to position the masses correctly. The aft fuselage was modified to allow the proper placement of the empennage but nodes already in the model were close enough for the rear seat passenger. The modifications can be seen in Figures 47-49.

Early runs with the engine represented by a rigid body mass had the rigid body tied directly to nodes in the engine mount which had the effect of making the engine mount rail rigid between the tie points. Half scale tests showed that the rail deformed by bending upward between mount points as shown in Figures 18(b) and 95(b). Small triangular brackets (Figures 47-49) were added to the rail with the engine mass tied to the tips of the triangles to allow some flexibility in the rail and make the model more representative of the test results. This modification brought the model into closer agreement with test results.

Sliding friction cannot be used with two dimensional elements so the analysis neglected the horizontal component of velocity. A run was made with that component included to verify this method of analysis. There was no difference other than the horizontal position of the airplane verifying that considering only the vertical velocity component was valid for this model. It would not be valid with friction. Friction can be included with three dimensional elements but time did not allow development of a three dimensional model.

Prior to learning that the impact attitude was 24 degrees instead of the planned 30 degrees, considerable effort was expended trying to change the analysis parameters to obtain a closer match between the analysis and test data. Dynamic analysis had used a resultant plasticity material model with yield strength set at 95,000 psi based on test results of samples of the engine mount material versus the published value of yield strength of 70,000 psi. Strain gage data on the engine mount in test 1 show strain rates of 1 to 1.5 in/in/sec. Data for mild steel [14], data not available for 4130 steel, show that yield strength is increased by about 50 to 75% at these strain rates. The increase appeared to be somewhat higher for compression than for tension. Further, our static tests, see section 5.2, showed strength of the material used in these tests to be substantially higher than the reference values [12]. Wall thickness was also on the high side of the tolerance for the samples tested. The model was run with yield strengths of 125,000, 150,000, 175,000, and 200,000 psi in an attempt to get closer to the full scale test results. Values of firewall acceleration and time to the aft fuselage slap down are shown below for the 30 degree impact attitude calculation.

yield strength	firewall acceleration, g	slap down time, sec
95,000	32.7	.135
125,000	38.8	.135
150,000	46.9	.140
175,000	52.9	.140
200,000	59.2	.140

Firewall acceleration was about 50 g based on a 39 point moving average of the analog data (digital data shown in Figure 25 shows higher acceleration and the differences are unexplained) so compares best at yield strength between 150,000 and 175,000 psi while time to slap down shouldn't be expected to agree with test data due to the actual angle and calculation angle. Note that Z axis is normal to the airplane reference line in the test data and the Y axis is normal to the impact surface in the analysis (Y axis was used instead of Z axis in analysis because sample constant acceleration calculations showed more uniform accelerations). Deformation of the engine mount also showed about the correct deformation although the mechanism is different. The analytical model (beam) doesn't allow for the deformations in cross section of the test mount.

The analysis above was made with one of the preliminary models containing a windshield post and without windows and doors. When the model with structural parameters representing the first test airplane including doors, windows, and windshield was run with the impact angle at 24 degrees and yield strength set at 150,000 psi (Arcrft11, run 2, Figures 50-51), the results closely matched the flexibility of the fuselage and the firewall deceleration calculated to be 40 to 50 g (Figure 51(a)). Seat decelerations determined from Figures 51(b-c) are in reasonable agreement with test 1 data. There are oscillations in the calculation making it difficult to determine an average acceleration. The program will plot acceleration but oscillations are so strong in those data as to make them useless.

Touch down time for the aft under floor foam was at 70 milliseconds based on the film of the test. Aft spring touch down was calculated to be about 85 milliseconds after impact. The aft fuselage failed under acceleration loads early in the event changing both the moment of inertia of the airplane and the kinetic energy and this may have changed the time to slap down. Initial acceleration at the tail post calculated to be about 104 g (Figure 51(d)) which agrees closely with the test data.

Calculated load in the engine mount post is shown in Figure 52(a) and the sum of the loads in the two posts from test 1 is shown in Figure 52(b). The test load was obtained by averaging the strain gage readings and multiplying by the modulus of elasticity and the nominal cross sectional area. Wall thickness of sample tube elements tended to be about 5% greater than nominal and there appears to be a bias in the data prior to impact. With these corrections, the data for the engine mount post were thought to be in reasonable agreement with the analysis.

This analysis (two dimensional model) can only simulate a symmetrical hard surface impact. The engine mass has been included but the engine size and shape has not been included. Tests 1 and 4 both had the oil pan hit the surface early fracturing the pan. All four engine mount brackets broke in test 1, but remained in the mount, and this cannot be simulated at this time. The analysis program is supposed to allow stopping the analysis, make changes in parameters, and restart. Attempts to do this were unsuccessful and more development would be needed to make this process work. Engine isolators were not modeled. One attempt was made to do this without success.

At this point the analysis matched the test data well enough to proceed with design of the next two test airplanes and that was deemed to be higher priority than trying to improve the analysis.

5.7 Design Concepts, Tests 3 & 4

The project plan was to conduct two tests, one on hard surface and one on soft soil, and refine the design based on the test results and the analysis and then repeat the first two tests. The engine mount and cowling had worked well on the soft soil test and accident data indicated that there are more soil impacts than hard surface. Therefore it was decided to design the last two airplanes to have engine mounts and cowlings equivalent to those on test 2, test 2 results are described in section 6 below, and to simplify and reduce the weight of the airframe structure compared to the first two airplanes. Those two airplanes had been both heavier than necessary and difficult to build. The seats and restraint systems should also be improved to solve the problems shown in the first two tests.

The analysis model which had best represented the results of test 1 (Arcrft11, run2) was modified to the engine mount tube sizes of the test 2 mount. As explained above, the analysis had indicated that windshield, windows, and doors contribute to strength so these were included in analysis. A number of structural variations were studied including changes in the aft portion of the engine mount and fuselage concept changes. Results of the analysis for the final design concept are shown in Figures 53-54 with the impact attitude changed from the 30 degree design condition to the 26 degree attitude obtained in test 4. The final design concept will be discussed below and

is illustrated in Figure 55 with some details shown in Figure 56. The basic structure remained the same as discussed in section 5.4 except for a change in the wing for test 4. A preproduction wing was used for test 4 which had a "C" section spar instead of "I" section of the first two wings and only three ribs instead of four, otherwise the structure was similar to the first two wings. The wing from test 1 was reworked and used again for test 3.

The engine mounts for airplanes 3 and 4 were the same as for test 2 except for changes made to improve clearance against engine accessories. Connection point for the posts to the upper rail was moved aft one inch and the attachments points of the posts to the firewall were moved down two inches and outboard two inches. The pad in the cowling for test 2 was four layers of ¼ inch Nomex honeycomb with a single layer of fiberglass cloth between layers. Foam was substituted for the honeycomb to allow wet lay-up with the construction remaining the same otherwise. Details of this construction will be discussed more in section 6.3 below.

The structure behind the firewall and the engine mount would be simplified if the engine mount did not have the two central posts to the firewall. A new model of the mount was made eliminating these tubes and the analysis showed that the mount collapses inward at low load without those two posts. A cross piece between the two sides of the mount solves the problem but can't be used at the proper location because of the engine accessory case. Several types of cross beams designed to pass under the accessory case were evaluated analytically with poor results. Lateral support beams from the mount to the lower corners of the firewall were found to work well analytically. However, under high enough impact conditions the engine will tend to rotate up and back through the firewall. It was thought that the central tubes and the supporting structure behind the firewall would tend to keep the engine out of the cabin. An aluminum cross tube (Figure 56(a)) was located behind the firewall to take the engine mount loads and provide a ductile material to provide further resistance to engine penetration into the cabin. This square extrusion is not as light as a beam designed for the moment distribution but it was economical to acquire and install for this test series.

Airplanes 1 and 2 had the lower engine mount brackets in line with the floor to transfer loads directly into the floor. Dynamics analysis showed a significant difference in airplane response if the lower mount points were moved up to the break in the firewall. Basically, it gave about two inches more stroke before hitting a hard resistance point. The lower mount points were redesigned as shown in Figure 56 (a-c). Loads were transferred into the floor through a firewall brace simulating a nose wheel well as shown in Figure 56(a). This brace also resisted the vertical loads in the firewall. Solid sections were incorporated in the floor and firewall under the braces for shear strength.

The upper engine mount loads were taken into the fuselage by a straight beam (Figure 56(a)) behind the aluminum cross tube which transferred the loads into a beam under door by shear. These beams were small in comparison to those in the first two airplanes and can be seen in Figures 56(a) and (d). Figure 56(d) also shows the simulated instrument subpanel and the air bag installation for test 3. A wide angle lens camera was mounted on the subpanel and it was found in test 1 that substantial torsional rigidity was needed to keep this camera in position. Two 2 by 10 boards were used as an inexpensive way to provide secure camera and air bag mounting and to simulate the size and position of the subpanel.

The cabin top had failed in test 1 and analysis showed that a stiffener was needed to prevent buckling if the windshield carried any load. A stiffener was added.

Both test 1 and the analysis indicated that the rear seat area had higher decelerations than the front seats in the hard surface impact. Two changes were made to try to improve survivability in this area. The rear energy absorber was extended outside the loft for more stroke with a fairing as illustrated in Figure 55. And a stroking rear seat was installed as shown in Figure 56(e). This

seat will be described more below. A partial frame was added as shown in Figure 56(f) to resist shoulder harness loads for the rear seat passenger. Loads from the rear energy absorber were taken by a "Z" section cross beam (Figure 56(e)) behind rear seat which formed the front edge of the baggage compartment.

One of the wing rear spar attachment bolts had failed in test 2. While having parts separate from the airplane removes kinetic energy, it also increases the probability of breaking fuel lines and changes the loading on the energy absorbers. It is not known if this is favorable or not at this time since attempts to stop and restart the analysis with changes had not been successful. Rear spar attach fitting strength and the bolt size were increased for airplanes 3 and 4.

Two steps were taken to reduce the angular velocity of the hard surface impact with the first and primary step being the reduced engine mount strength. A very simplified analysis indicated that a stabilizer might provide significant aerodynamic resistance to rotation so a simple wooden stabilizer was installed for test 4. An aft fuselage stiffener was added, the core material for the upper aft fuselage was changed to provide better adhesion of fiberglass to the core, and an aft fuselage frame was added about midway between the aft of the baggage compartment and the empennage. These changes were all to delay the core to skin bond line failure seen in test 1.

Test 2 was survivable except that both dummies were thrown forward into the instrument panel, the pilot because of a seat failure and the copilot because of a shoulder harness failure. An air bag was added for the pilot and airframe mounted load limiting shoulder harnesses were installed for both occupants for test 3. These will be described more fully below.

5.8 Full Scale Test 4, Hard Surface

5.8.1 Seats

The analysis described above and the test data from test 1 both show that the rear seat is subject to high acceleration during the second impact, "slap down", and that there is not enough stroke in the under floor energy absorber to attenuate the impact to the level required for a non stroking seat to limit the lumbar loads. Figure 54(c) shows the velocity of the rear seat at the second impact to be about 380 inches/sec. The stroke required to decelerate at a constant 20 g to zero velocity is 9.34 inches while the extended energy absorber only has a five inch stroke. Only about 3.5 inches stroke is available within the loft lines. It was thought that a combination of the extended energy absorber and a stroking rear seat could limit the lumbar loads to less than the allowed 1500 pounds. A JAARS "S" leg middle seat was acquired and mounted in the rear seat position (Figure 56(e)) for test 4. This seat limited lumbar loads to less than 1500 pounds in sled tests to loading higher than the FAR 23.562, Test 1 requirements. While this seat is in use by two non-profit organizations, it is not commercially available.

The pilot's seat was a developmental seat from Impact Dynamics, Inc. (IDI) currently under development for a new airplane program. This seat, shown in Figure 57, is designed to meet the FAR 23.562 requirements when mounted over the main spar. The energy absorbing material is contained within the seat and the mounting is assumed to be rigid with respect to the airframe. It is planned to be adjustable fore and aft but was mounted to a steel framework fastened to the spar box for this test. The back angle is also adjustable but was fixed for this test. The restraint system was airframe mounted.

The same copilot seat as used in the first two tests was used for tests 3 and 4. New energy absorbers were fabricated for each test using the design of the tests described in section 3.

5.8.2 Test Conditions

Test 4 was planned as a repeat of test 1 with the addition of the rear seat and was conducted June 19, 1997. Impact attitude was at 26 degrees instead of the planned 30 degrees and impact velocity was 83.2 ft/sec. (Table 1). Roll and yaw were small.

5.8.3 Test Data

The airplane is shown rigged ready for pull back in Figure 58(a) and in the pullback position in Figure 58 (b). An impact sequence in shown in Figure 59. Representative post test pictures are given in Figures 60(a-h) and data are given in Figures 61-76.

The windshield shattered at about 30 milliseconds after impact followed shortly by failure of the forward roll bar and side beams under the doors just aft of the forward edge of the door as shown in Figure 60(a-b). Both doors also came loose early. This allowed the forward fuselage to rotate upward approximately 12 degrees (Figure 59) and the engine mount did not deform as much as predicted (Figures 60(c-d)). Analysis had indicated the engine mount would collapse completely as shown in Figure 53 but the analysis did not allow for the forward fuselage failure, loss of the doors, or for the physical size of the engine and it's oil pan. This engine has a cast aluminum oil pan and the front portion was shattered by the impact as shown in Figure 60(e). Forward mount brackets (portion attached to the engine) were broken but the aft brackets were intact. The mount did deform more than in test 1 and the deformation was more like that from the quasi-static tests.

There was no loss of cabin space and the deformation of the forward cabin was not enough to cause major damage to the legs of the front seat occupants. There was some fracturing of the slanted firewall segment on both sides as shown in Figures 60(f-g) but no penetration. There was no loss of structural integrity of the firewall at the braces near the floor but there was damage to the firewall beside the braces both above and below the cross tube as shown in Figure 60(h). Bond line failures along the upper engine mount support beam and some failure of the side shear panel can be seen in Figure 60(i). Bond lines also failed on both sides of the "Z" beam above the rear energy absorber as shown in Figure 60(j). There were a number of other areas of failures of bond lines and fracturing of fibers in transition locations.

The aft fuselage failed in down bending and the stabilizer attachment failed on the second impact. These failures were neither unexpected or undesirable. Failures at this time reduce the energy available for rebound. The main wing spar lower cap failed by delamination presumably on the second impact.

The under floor energy absorbers did not show permanent deformation but the pictures indicate near full compression of them. The airplane did rebound into the air about one foot and out of contact with the ground for about 40 feet. It then stayed on the ground for the rest of the slide out. The airplane in test 1 had two rebounds but of less height.

Accelerations at all locations were much lower than for test 1 including the tail post (Figure 62) which was less than half that for test 1. The pilot's lumbar load was well under the 1500 pound limit at about 1100 pounds (Figure 64). Copilot's lumbar load was over the limit at near 1700 pounds (Figure 66) yet the under cushion energy absorber showed no permanent deformation. This is not understood since the same design had performed well in the tests described in section 3. The foam material was from a different batch and it may be that there is enough variability from batch to batch to make the difference. There is a lot of high frequency hash on the pilot's pelvis trace but changing the filter to delete this confirms that the pilot's pelvis had lower accelerations than the copilot's pelvis showing that the lumbar loads have the correct relationship.

Lumbar loads for the rear seat passenger (Figure 69) were lower than expected, in fact, lower than tests for the same type seat in sled tests. NASA checked all the calibration factors after the test and could find no error. It has been suggested that lumbar loads should be approximately 60

or 70 times the pelvis acceleration in g based on the weight of the portion of the body above the lumbar location. The first peak in lumbar load is approximately 60 times the acceleration but the second peak doesn't follow that relationship. The dummy leaned forward under the first impact and continued to move during the second impact. Some of the upper body weight was supported by the shoulder harness and the angle of the body and the motion of the body were relieving to lumbar loads. This is in contrast to sled tests where the body has little forward motion for the FAR 23.562, Test 1. Harness loads were below the limit for all occupants and none of the occupants struck other structure.

Strain gages were installed only on the engine mount elements that attach to the firewall due to time and budget constraints. They would not be expected to compare well to the analysis due to the different airframe failure modes.

5.8.4 Comparison of Analysis to Test Results

The analysis shown in Figures 53-54 is for the impact attitude of test 4. Loss of the windshield early produced a different failure pattern with side beam fracture and less deformation of engine mount than predicted. Some of the impact features were correctly predicted. Firewall acceleration is approximately correct if the short duration spike is neglected. The pilot's seat had two accelerations of nearly equal magnitude while the rear seat has lower initial acceleration followed by a much higher acceleration. Aft fuselage slap down time was approximately correct.

Design of the side beam had been based on the internal loads without the windshield in place but with the doors in place. The 2D analytical model did not allow the doors to flex out of plane or simulate the reduced stiffness due to door curvature. Doors actually have considerable curvature similar to the door frames and pictures show the door flexing well out of contour before failure of the attachments. Door stiffness could be simulated in the same manner as the door frame but this was not done and the model is therefore not representative. Earlier calculations with the door panels deleted showed much higher side beam loads and this is thought to be the reason for the side beam failure. There was a combination of bond line and fiber failures in the beam. The sequence of failures is not known. The beam was basically a closed hat section and the strength is greatly reduced if the bond line fails.

5.8.5 Key Observations

This was a survivable test with IDI seats in the forward locations and JAARS seats in the rear location. There was no loss of cabin volume and minimal injuries would be expected for occupants of the IDI and JAARS seats.

Engine mount deformation was more like the quasi-static tests than test 1 but deformed less than expected due to failure of the cabin side beams.

Failure of the side beams leads to questions about higher energy impacts, is there enough remaining structure to absorb additional energy. A more progressive failure with higher residual strength is desired.

Better simulation of the doors and their attachments is needed in the analysis.

Windshield material is not capable of carrying these loads without shattering. Either a windshield post is needed or strength of the side beams must be increased. Analysis indicated excessive airframe flexibility for heavy side beams but without either windshield or doors and test 4 tends to verify this result.

Many of the structural failures were bond line failures.

5.9 Impact Attitude Variations

The dynamics analysis for the design model for tests 3 and 4 was run at impact attitudes of 30, 26, 20, 10,and 0 degrees while holding the vertical velocity constant at 40 ft/sec. Plots showing the variation in seat accelerations for the various angle are shown for the front seats in Figure 77 and the rear seats in Figure 78. The accelerations increase with decreasing impact attitude for both seats with a larger velocity change in the first impact until there is only one impact for the zero degree condition. It does not appear practical in this size airplane to absorb all the energy in the airframe for low angle impacts for this impact velocity. Unless significant energy can be absorbed by a fixed landing gear in addition to the under floor energy absorbers, all seats should be of the stroking type as exemplified by the JAARS seats.

6. Soft Soil Impact

6.1 Half Scale Soft Soil Tests

6.1.1 Soil Characterization

As stated earlier, the test plan was for the soft soil tests, both full scale and ½ scale, to be conducted onto soil beds of the same characteristics as prior NASA tests [6-7]. Soil characteristics for these tests [9] are replotted in Figures 79-80.

6.1.2 California Bearing Ratio

CBR measures surface strength of the soil. The test device [15] consists of a two inch diameter cylinder and a plate with a slightly over two inch hole in the center (Figure 81). This plate is to have a minimum weight of 10 pounds and is placed on the soil with the test cylinder penetrating the soil through the center hole. CBR is the pressure required to penetrate .1 inches into the soil divided by the reference pressure of 1000 psi, then multiplied by 100 to convert to percent. A CBR of 100 is intended to represent the soil strength of a well-graded crushed gravel surface. Corrections are available for greater than .1 penetration.

For the ½ scale tests in the WSU Structural Test Laboratory, the engine mount test rig hydraulic and data systems were used to push the CBR tester (Figure 81) into the ground and record the data.

6.1.3 Airfield Index

Airfield Index (AI) is measured with a cone penetrometer [9] which is a 30 degree included angle cone of .5 inch base diameter (Figure 82). The cone is pushed into the ground at a slow steady rate. AI calibration is linear with a force of 10 pounds corresponding to an AI of 1.0. AI is a measure of the relative shear strength of soils and will vary somewhat with the type of soil. It is therefore necessary to correlate the measurements with other types of strength measurements. However, the cone penetrometer provides an efficient and rapid method for measuring the relative soil strength and, more importantly, the variation of soil strength with depth.

For the ½ scale tests in the WSU Structural Test Laboratory, the engine mount test rig hydraulic and data systems were used to push the cone penetrometer into the soil and record the data.

6.1.4 Soil Box for ½ Scale Tests

A plywood box was built 4 ft by 8 ft by 2 ft deep. Later modifications to the box to clear the test rig and increase lateral strength of the box resulted in a depth of about 22.5 inches (Figure 83). The box was filled with soil available on the WSU campus. When dry, this was basically dust with very little organic matter.

6.1.5 Soil Preparation

Initial soil tests showed the soil to be very low on both CBR and AI. NASA had compacted their soil bed by driving tractors and graders over it as layers of soil were added to the soil bed. This was clearly not practical in our test box. The first method tried was to hit the soil using a controlled number of blows to a wood 4x4 with a five pound hammer. The dry soil did not develop the proper characteristics so water was added. This was done by trial and error until reasonable results were obtained. The correct water content was enough to cause the soil to make a cohesive lump when a handful was squeezed but not so much as to be able to squeeze water out of the soil.

The prospect of trying to tamp the complete soil bed by the method above was daunting so a gasoline powered tamper was rented and the soil was tamped in layers similar to the NASA process. The soil was found to be much too hard so it was dug out and tamped again just on the surface. This yielded acceptable characteristics and was used for the first ½ scale test. CBR results are given below and AI data are given in Figure 84. Seven measurements are shown on this figure and show that the AI values generally fall within the range of the NASA data. One curve shows an obvious clod and these were occasionally found. Our preparation made sure they were small. The results shown below and in Figure 84 are typical of the soil bed measurements made throughout the ½ scale tests.

Location No.	CBR, .1 depth	CBR, .2 depth
2	2.6	3.4
3	2.9	3.9
4	4.2	6.1
5	3.3	4.3
6	6.6	6.9

The tamper was rented again for the next test and the soil dug out and retamped but we could not complete the test that day due to unavailability of the forklift required to move the box into test position. The next day, the soil was like a brick.

Renting the gasoline powered tamper required a substantial investment of time and money and further it was difficult to control the amount of tamping. A manual tamper was acquired which was an approximately 10 inch square steel plate having a 4 foot handle and following procedure developed for subsequent tests.

Soil was removed from the box until about 8 inches was remaining in the box. The soil was tamped with the manual tamper 5 times moving to a fresh spot until all the soil was tamped. Approximately 6 inches of soil was added to the box and the tamping repeated. Water was added at each level and mixed into the soil to obtain uniform dampness as described above. This process was repeated until all the soil was back in the box and tamped. CBR and AI measurements were made and if they were in the correct range, testing could proceed. If not, soil was removed and the process repeated. In general, soil preparation was made just before testing because it was found that the surface could harden if left overnight. It was also found that the surface dried rapidly in the low humidity environment of Kansas. After some experience with this drying, a plastic vapor barrier was used to cover the box when not in use. The vapor barrier maintained the humidity in the box requiring only surface treatment when it was kept in place. It was also found that it was unnecessary to dig out the complete box after a test if the vapor barrier had been used. Only the part near the test crater had to be reworked.

6.1.6 Mount 6 Test 1

The primary purpose of the cowling is to transfer soft soil loads to the energy absorbing structure of the engine mount. Two concepts were considered. First, the lower cowl surface would be made strong enough to act like a ski. It was initially thought that this would require a substantial thickness of the lower cowl which would reduce the stroking distance available for the engine mount and would complicate the installation of cowl flaps and exits for exhaust pipes. Second, side beams in the cowl would be strong enough to allow the lower cowl surface to carry the soil loads as a membrane. The second concept was selected for the first tests. The forward portion of the cowl was expected to push up against the engine cylinders to help support the forward end of the beams and the aft portion of the beams will be fastened to the firewall. This attachment must carry both lateral and torsional loads. Figure 85 shows the first 1/2 scale cowling with the beams clearly shown.

It had been realized that this concept was flawed prior to the first test in that the side beams and their attachment to the firewall would not allow the cowl to rotate upward as desired. However, the test was carried out to gain whatever knowledge could be gained.

Half scale mount 6 was built to the same configuration as the last mount (mount 5) tested on a hard surface with one exception. The lower mount rail was continuous instead of having a butt joint at the initial ground contact point since this joint had failed early in the last three tests. It was basically a one half scale version of the first two full scale mounts delivered to NASA. There was no noticeable deformation of either the cowl or the engine mount in the first soft soil test even though the actuator force reaches about double the maximum load reached for mount 5 on a hard surface. Strain gages showed very low loads in the engine mount elements and it was realized that the cowling was carrying most of the load. The cowling cracked under the lower mount rails and there was some surface cracking where there was a local change in stiffness.

Soil behavior was different than expected. Soil toward the front of the cowl appeared to be shoved forward and to the side. There was a "bow wave" of loose soil well ahead of the cowl. Soil in the crater under the forward part of the cowl was soft while we had expected it to be compacted, and was compacted under the aft part of the cowl. A relatively sharp line was evident between the portion that was pushed ahead and aside and where the cowl had slid over the soil and pushed down compacting the soil.

6.1.7 Wood Cowl Tests

After the first test of a cowl and engine mount in the soil, it was realized that the data didn't adequately define the vertical reaction force of the soil, all instrumentation was on the engine mount and substantial load was being carried by the cowl. For tests on a hard surface, we had assumed the normal force to be twice the axial force based on no friction at the surface but it was apparent that this was not the case in the soft soil. A wooden block was fabricated to the side view cowl contours in a two dimensional shape. It was thought that the 2 dimensional shape would allow easier analysis of the results. This was mounted on a pivot with a strut containing a load cell resisting vertical motion as shown in Figure 86(a). It was pushed into the soil bed in the same manner as the cowl and mount (Figure 86(b)) with forces shown in Figures 87.

Action of the soil was similar to that for the cowl. An unsuccessful attempt was made to develop a pressure distribution that would give the forces measured. Some experiments with a adding a friction term indicated a possible explanation for the measured forces.

6.1.8 Soil Friction Tests

A test sled was built with four runners of 5 sq. in. each (1.25 wide by 4 long) having a platform to support test weights of 50 lb. each (Fig. 88(a-b)). Tests were run with 200, 400, and 500 lb. added. The sled is estimated to weigh about 5 lb. The sled was pulled by a hydraulic cylinder through a load cell and the data were recorded onto a spreadsheet. The soil was smoothed and

retamped locally after each test. Two problems were observed. First, the weight of the actuator was adding weight to the front of the sled causing it to dig into the soil more on the front runners than the aft runners. The cylinder front was blocked up for the fourth and fifth tests to take this weight off. Second, it was observed after the fourth test that the smoothing and tamping was leaving a groove in the soil. Prior to the fifth test the soil was loosened over a larger area with the digging fork and then the area was tamped leaving a smooth surface. It is therefore thought that the first and fifth tests were the most accurate. We estimated that the cylinder was adding about 20 lb. to the system and the data adjusted to reflect the sled and cylinder weights as appropriate. Small errors in estimating weights of the sled and cylinder were not thought to be significant due to the small variation in friction with contact pressure and the fact that the sled and cylinder were a small fraction of the loaded sled weight.

Each test showed starting friction to be higher than moving friction with friction reducing with increasing contact pressure.

Test Number	Contact Pressure	μ (start)	μ (moving)
1	11.25	.60	.53
2	21.25	.50	.45
3	26.25	.50	.42
4	25.25	.49	.36
5	25.25	.50	.40

Speed of motion was approximately the same as used in tests of the cowls and the wood cowl at about two inches per minute.

6.1.9 Wood Block Tests

We had observed in the cowl tests that part of the soil appears to be pushed out of the way so a test was devised to measure the force of this motion. A block (Figure 89(a-b)) was fabricated 18 inches wide and an average of 7.1 inches high. The active surface was normal to the line of force in the test rig and the surfaces behind the front face were cut back to minimize any frictional effects. It was pushed into the soil at an angle of 30 degrees using the same test rig as for cowls and the wood cowl. Force was from a hydraulic cylinder measured by a load cell. A supporting strut, with load cell, normal to the line of actuation held the block in position and measured moment around the support pins. Data were recorded into a spreadsheet. Recorded forces and an equivalent pressure (uniform over the face of the block) are shown in Figure 90(a-b).

There was considerably more normal force than expected. Inspection of the soil after the test showed that the soil under the block was soft. It did not show any of the pressure compacting evident in the cowl and wood cowl tests. Soil had been pushed forward and upward in front of the block. Near where the top of the block had stopped, the soil was easily indented with a thumb. Near the bottom face of the block, the soil was very hard. An attempt was made to push the Al probe into this area with little success. I would estimate in excess of 100 lb. was applied with very little penetration. The Al probe was easily pushed into the soil under the block and near the top of the front face. Soil was dug from low on the front face and it was compacted to 2 to 3 inch depth. These chunks could be easily broken up by hand. The surface ahead of the block also fragmented into chunks 1 to 2 inches deep and were also easily broken up.

When the block is fully in the soil, the soil spills freely over the top of the face. Coupling this with the change in hardness of soil over the face of the block, it was assumed that a triangular pressure distribution could approximate the loads. The pressure under the block could also be assumed to be a triangular distribution. Initially, it was not assumed that there was any pressure under the block if the block sheared the soil cleanly but the data indicate that the pressure field

wraps around the lower lip of the block providing an upward force or lift. This pressure field is most likely a function of the type of soil and the moisture content so these results may not be general to all types of soil. We considered the question of whether the results could be influenced by friction. The data given are for the block at rest so sliding friction can't explain these results. The following results were obtained for the maximum stroke position.

Force	4665.53 lb.
Normal force	2381.36 lb.
Front face maximum pressure	73.01 psi
Bottom face maximum pressure	63.65 psi

The results above, both soil friction and the pressure load, were used to refine the block loading for the simulated cowl and a pressure and friction distribution found that matches the applied loads well. This distribution was found by iteration and can't be claimed to be the correct answer. An additional force measurement would be needed to give higher confidence in these data but the results match the forces measured on the wood cowl and seem reasonable based on observation of the crater and results of the "wood block" and friction tests. The results were used in developing the cowl and engine mount concepts and are given in Table 2.

6.1.10 Mount 6 Test 2

The same cowl and mount used in test 1 were used in test 2 with the cowl modified by removing the side beams, reinforcing the cracked areas, and adding a honeycomb pad under the cowling bottom as shown in Figure 91. There was not enough room between the cowl and engine mount to place the pad inside the cowl. They were reinstalled and retested as soil test 2 with several photos of the test in progress shown in Figure 92. Forces are shown in Figure 93. The auxiliary actuator (with load cell) shown pushing on the top of the dummy engine is intended to represent the inertial forces of the engine during the early part of the stroke. This force is removed later in the stroke as shown in Figure 93. Again there was no noticeable permanent deformation of the engine mount except a small bend in the upper front part where it pressed against the cowl. There were cracks in the fiberglass under this part of the mount and some permanent deformation of the honeycomb under the contact points in the lower cowl. Several of the holes where the cowl attaches to the firewall showed evidence of partial failure. Strain gage data show higher engine mount strains than in test 1 but lower than needed to deform the mount. It should be noted that total forces applied to this system were more than three times the load needed to start deformation of mounts 3 and 5 in hard surface tests showing that the loading is much different and/or load carried by the cowl reduces the engine mount loading. When the side beams were removed, part of the beam structure originally built into the side walls was left, an .040 thick band of unidirectional fiberglass, and indications are that substantial load is being carried in this material. These remnants of the side beam bowed out under the loads acting as a support for the cowling skin allowing it to take some soil loads as a membrane.

Soil behavior was similar to the first test. The data obtained from test 1 and 2 did not allow a full definition of the engine mount loading but a new half scale mount was fabricated with tube sizes adjusted based on the strain gage data.

6.1.11 Mount 6 Hard Surface Test

After these first two soft soil tests using mount 6, it was tested on a hard surface to make sure that the mount had not been strengthened compared to mount 5. It had been intended to be an improved version of mount 5 with changes to eliminate the failure in the lower rail that left a forward facing tube which might penetrate the cowl. Figure 94, which compares test 2 in soft soil with the hard surface test, shows that mount 6 did achieve the desired result. See section 5.2.7 for a description of the hard surface test of mount 6.

6.1.12 Mount 8 - ½ Scale Soft Soil Test 3

Half scale mount 8 was built based on the strain gage readings from soil test 2. The soil bed was prepared in a manner similar to previous tests. The engine mount was installed on the same fuselage section as soil test 2 and the same cowling installed. It was not practical to remove the unidirectional fibers from the cowl sidewall so the screws were left out of the sidewalls to simulate weaker cowl sidewalls. Fiberglass reinforcement was added to the lower cowl where the screw holes had elongated in the previous test. The model is shown through the test sequence in Figure 95(a-d).

The model was pushed into the soil (soil test 3) nearly 22 inches (actuator stroke) with data given in Figure 96. Simulated engine inertia load was maintained on the dummy engine for approximately the first 10 inches of stroke. The mount started permanent deformation shortly after removal of the simulated engine load with the first failure in the rear posts. The engine mount deformed upward in a manner very similar to the hard surface tests with the cowling maintaining a smooth surface for the soil forces to be transferred to the mount. First failure on hard surfaces is the forward diagonal at the surface contact point. It appears that the stiff cowl structure (honeycomb pad) prevented high loading at this forward area. The forward upright did not fail throughout the test but pushed up on the upper mount rail causing it to deform in up bending. The upper rails failed later at the weld under the main post (Fig. 95(d)).

Soil characteristics in the crater and near the cowl were similar to those described above for earlier tests and are shown in a sketch in Figure 97. AI measurements made in the compacted portion were approximately double pretest measurements decaying to the pretest values about eight inches below the surface. Also shown in the sketch is that the portion of the cowl behind the honeycomb pad deformed upward into a fold which could catch some soil. The pad stopped forward of the vertical portion of the firewall.

6.1.13 Mount 9 - ½ Scale Soft Soil Test 4

Half scale mount 9 was the same as mount 8 except for adjustments in 3 tube sizes. A new cowl was modified with a segmented pad to reduce stiffness in the longitudinal direction in an attempt to reduce bridging of the mount by the cowl. In this case, the honeycomb pad was inside and the aft end of the cowl was extended aft under the front of the airplane. The fuselage section was modified for this cowl. The soil bed was prepared as before and soil test 4 conducted. The forward diagonal did buckle earlier than in the prior test but otherwise there appeared to be little, if any, benefit to the modified cowl structure. Actuator load had more variation than the prior test with lower minimum load. It was judged that test 3 had the better characteristics so the full scale engine mount and cowl for the first full scale soil test was based on mount 8 and the cowl tested with it.

As in the prior test, the portion of the cowl behind the honeycomb pad deformed upward into a fold which could catch some soil. The pad had been extended to approximately in line with the vertical portion of the firewall.

6.1.14 Shot-put, Dynamic versus Static

All of our laboratory test were static (approximately 2 in/min stroke rate) which does not show the effect of acceleration of the dirt ejected from the crater. To get some idea of the dynamic effects, a 12 pound shot-put was purchased and dropped into the same soil bed as test 4. Drop heights were varied from 2 to approximately 17 feet and the crater depth measured. The same shot-put was then pushed into the soil using the test rig actuator, load cell, and data gathering system. Energy versus crater depth (stroke) was calculated for the static tests and compared to the dynamic results (Figure 98(a)) and showed more energy absorbed dynamically than statically at the same crater depth. The ratio of dynamic to static energy increases with increasing drop height and is shown in Figure 98(b). Due to ceiling height limitations, the highest velocity of the shot-put

was limited to slightly over ¾ of the full scale test vertical velocity component. No soil was ejected from the crater by the shot-put, in fact the edge of the crater sloped down into the crater for approximately ½ inch from the edge. An airplane impact is expected to eject soil from the crater increasing the dynamic energy absorption. These tests indicate that impact dynamic forces could exceed twice the quasi-static forces.

6.2 Full Scale Test 2, Soft Soil

6.2.1 Test Conditions

The second full scale test (first soft soil test) was conducted at the NASA Impact Dynamics Research Facility September 20, 1996. Design test parameters were test velocity of 81 feet/sec at 30 degree impact angle with zero angle of attack. Actual test conditions were 84 feet/sec with an angle of attack of approximately 2.7 degrees (Table 1). Impact was on soft soil intended to replicate the soil characteristics of prior NASA tests [6-7] and of the ½ scale tests conducted for this project.

A California Bearing Ratio tester was not available but it was thought that the airfield index was more important since it measures through the depth of the soil bed whereas the CBR represents only the surface characteristics. Airfield index data are given in Figure 99 and are lower than the earlier tests or the ½ scale tests. Rebuilding the soil bed to match more closely with prior tests was considered but it was decided that soil dynamics were probably more important than the index reading and therefore to continue the test without change to the soil bed.

6.2.2 Test Data

An impact sequence in shown in Figure 100 and shows the airplane coming out of the crater at low speed coming to rest a short distance from the crater. Representative post test pictures are given in Figures 101(a-f). The cowling and engine mount performed nearly as designed and very similar to the ½ scale tests, that is, the cowling maintained a sliding surface (Figure 101(b-c)) and the engine mount deformed upward (Figure 101(e)) to prevent the front of the airplane from simply sticking in the ground. Several engine components, such as oil cooler, magnetos, and starter, were closer to the mount posts than planned due to a somewhat idealized CAD model used in the design. These parts rotated up into the mount posts bending the posts as shown in Figure 101(e) so that energy was absorbed both in the lower part of the mount and in the posts.

Design of the cowling was similar to that for ½ scale test 3. Figures 102(a) shown the honeycomb pad under construction and Figure 102(b) show the completed lay-up just before curing. The pad was four layers of ¼ inch Nomex honeycomb with a single ply of fiberglass between layers. The cowling shell had been made before design of the cowl was complete and a skirt had to be added to extend the cowl to the slanted firewall surface. This made for a change in stiffness just forward of the firewall and the cowl broke on both sides at this location (Figures 101(b-c)). This left a forward facing scoop but there was very little soil inside the cowling indicating this failure was late in the sequence.

Test data are given in Figures 103-123. There was no loss of cabin volume. Both dummies hit the instrument panel because the pilot seat came loose at the rear attachments due to an installation error and the copilot shoulder harness inertia reel bracket failed at about 3240 pounds (Figure 108). Shoulder harness force is limited to 2000 pounds in FAR 23 so it appeared a that a significant reduction in load for the harness was required. It can be determined from the pictures that the dummies were forward of the seat backs and there was some slack in the harnesses at impact. The airplane is suspended in an approximately 65 degree nose down position for several minutes in the pretest period. There were load cells on the harnesses and the weight of these cells tends to extend the harnesses and a slow motion of the belt won't lock the inertia reels. The dummies had been taped to the seats with tape fastened over the shoulder to the seat back. The tape is partially cut to initiate tearing at impact and it appears it may have released early. While

the forward position of the dummies and slack in the harnesses may have contributed to the high harness loads, it was thought that a further reduction in harness loads was advisable for the next soft soil test. The measures taken will be described in section 6.3. Airframe decelerations (Figures 103-104, 107) were in the survivable range so it was thought that the test was survivable assuming the seats and harnesses worked properly.

Soil was pushed forward by the forward part of the cowl but heavily compacted under the aft part of the cowling in our ½ scale tests. It did not appear to be this way after the full scale test. Airfield index tests were run after the test both in the fuselage portion where soil appeared to have been pushed out of the crater and where the wing appeared to have compressed the soil. Readings were in the same range as before the test. We could find no evidence of soil compaction in the crater similar to that of the ½ scale tests. The crater depth was measured in a grid pattern and the volume of the crater integrated. Approximately 7 cubic feet of soil was ejected from the crater. Soil density measurements showed this soil to weigh about 80 pounds per cubic foot leading to the weight of soil ejected of 560 pounds or .224 times the weight of the test airplane. Figure 43, Volume III of Reference 5 gives the impulsive aircraft acceleration for these test conditions to be a little under 15g which is close to the data for the X axis shown in Figure 103. This tends to confirm that momentum exchange in ejecting soil from the crater is the primary factor in the X axis deceleration while the Z axis deceleration is probably the result of some combination of momentum exchange and energy absorption of the engine mount or airframe.

There was no visible deformation of the under floor energy absorbers in this test although test 4 shows that this may not mean there was no deformation. The airplane did not develop the angular velocity of the prior hard surface test.

The right rear wing attach bolt failed allowing the right wing to swing well forward during the event. The left bolt was bent but did not release the wing. Fuel tanks did not rupture.

6.2.3 Key Observations

The cowling and engine mount worked as designed forming a sliding surface with no scoops on the lower surface. Fractures of the cowling sides made forward facing scoops although very little soil was found inside the cowling. These fractures were caused at least in part, by the fabrication sequence.

Airframe decelerations were survivable and the importance of retaining dummies and harnesses in correct place prior to impact was illustrated. Failure of one seat and one shoulder harness indicated the desirability of improved restraint systems such as air bags and/or load limiting shoulder harnesses.

6.3 Full Scale Test 3, Soft Soil

6.3.1 Restraint Systems

Both dummies hit the instrument panel in the first soft soil test, one because of a seat attachment failure and one because of failure of the shoulder harness inertia reel attachment bracket. Two approaches were taken to improve restraint for the second soft soil test. An air bag was installed on the pilot's side and both shoulder harnesses had load limiters installed. In this way, there could be a direct comparison between the combination of air bag and load limiting and use of the load limiter alone. Both sides would see essentially the same loading since it was a symmetrical impact.

6.3.1.1 Air Bag

Simula Technologies, Inc., provided a developmental air bag system for the third airplane drop test. The air bag system used in the test is a derivative of the Simula Passenger Air Bag System

(PABS) currently being certified for bulkhead rows in the Jetstream 41. The air bag system used in the test consisted of two components: an air bag module mounted on the pilot's side instrument sub-panel, and a crash sensor mounted on the floor near the firewall. The installed air bag is shown in Figure 56(d) and the sensor was mounted on the floor just below the bottom of the picture. It was between the two braces shown near the center of the firewall behind the lower engine mount fittings. The copilot's position was tested without an air bag in order to provide comparative occupant data.

The air bag module consisted of a molded plastic cover and metal housing from the PABS, a modified automotive driver-side air bag inflator, and an air bag designed specifically for this test. The assembled module measured approximately 2 inches deep by 6 inches wide by 7 inches tall and was mounted to the instrument sub-panel (represented by the wood 2x10's) by means of an adapter. The module weighed approximately 4 lb. Modules for a production air bag system could be integrated into an aircraft instrument panel or glare shield in the same manner as automotive passenger-side air bags are integrated into a car dashboard. Also, the packed size and shape of a production air bag module can be varied from the dimensions of the module used in this test in order to improve integration into the aircraft.

The air bag itself was relatively small, approximately 52 liters, which is similar in size to an automotive driver-side air bag. The shape, however, was a derivative of the air bag used in the PABS. Inflation of the air bag was provided by a conventional sodium azide automotive driver-side inflator specifically tailored for this test to insure proper air bag performance. The air bag inflation is initiated by an electrical signal coming from the crash sensor and the air bag fully deploys in about 50 ms. Because it is a derivative of the PABS, the air bag used in the test was vented. Vented air bags offer the advantage of rapid deflation, which is considered important for egress in transport and commuter aircraft. Non-vented air bags may be more appropriate in light aircraft, however, because non-vented bags remain inflated for several seconds to provide protection from secondary impacts.

The crash sensor used in the drop test was borrowed from Simula's Inflatable Body and Head Restraint System (IBAHRS)–an inflatable shoulder harness developed for military helicopters. The IBAHRS sensor was used mainly because it was already at the NASA Langley facility for a previous AGATE drop test. A crash sensor similar to the one developed for PABS could be developed for a production light aircraft air bag system that would be lighter and less expensive than the IBAHRS sensor. The crash sensor detects the accelerations associated with a crash, processes the acceleration information to discriminate between an actual crash and accelerations due to gust loads and landings, and sends an electrical signal to the inflator to deploy the air bag in a crash. The crash sensor is powered by aircraft power. A capacitor discharge system is integrated into the sensor to deploy the air bag when needed even in the event of aircraft power loss. A press-to-test diagnostic circuit on the IBAHRS sensor checked the air bag system readiness prior to the test. The IBAHRS sensor weighs about 3 lb. A production crash sensor for a light aircraft air bag system would weigh less.

The total air bag system weight for the test (air bag module, IBAHRS crash sensor, and wiring) was less than 8 lb. A two air bag production system integrated into the aircraft would likely weigh between 10 and 12 lb.

There was no flight control system installed in the test airplane so the air bag could be installed without consideration of possible interference with controls. The production version of the test airplane is planned to have a side stick controller simplifying the task of preventing air bag and controls interference. Air bags are currently under development for military helicopters with control sticks and an inadvertent deployment without causing loss of flight control has been demonstrated successfully in simulators. More work is needed to determine the best way to install air bags with control wheels.

6.3.1.2 Shoulder Harness Load Limiter

The developmental restraint system included inertia reels and wire bending load limiters which were designed to stroke at about 1600 to 1700 pounds. The load limiters were installed in the single strap between the inertia reel and the junction with the double shoulder straps. A bypass strap limited the extension to less than the wire bender stroke of about five inches.

6.3.2 Test Conditions

The third full scale test (second soft soil test) was conducted at the NASA Impact Dynamics Research Facility May 15, 1997. Design test parameters were test velocity of 81 feet/sec at 30 degree impact angle with zero angle of attack. Actual test conditions were 82.3 feet/sec with an angle of attack of approximately 6.5 degrees (Table 1). Impact was on soft soil intended to replicate the soil characteristics of prior NASA tests [6-7] and in the ½ scale tests conducted for this project. Airfield Index measurements are given in Figure 124 and show the soil to be similar to the ½ scale tests near the surface but somewhat softer underneath.

6.3.3 Test Data

6.3.3.1 Airframe

An impact sequence in shown in Figure 125 and shows the airplane making a crater and then coming out of the crater at low speed. It then slid off the soil bed and came to rest on the concrete surface just out of the frame for these pictures. Representative post test pictures are given in Figures 126(a-l) and data are given in Figures 127-146.

The crater depth was measured in a grid pattern and the volume of the crater integrated. Approximately 4.8 cubic feet of soil was ejected from the crater. Soil density measurements showed this soil to weigh about 80 pounds per cubic foot leading to the weight of soil ejected of 390 pounds or .155 times the weight of the test airplane. Figure 43, Volume III of Reference 5 gives the impulsive aircraft acceleration for these test conditions to be approximately 11g. Figure 127 shows two acceleration peaks approximating 20g with a central portion lower but above 11g. The correlation between data and Figure 43 of Reference 5 is not as good as for test 2. As in test 2, airfield index readings were in the same range as before the test showing no evidence of soil compaction in the crater as was found in the ½ scale tests.

Performance of the cowling and engine mount was similar to that of test 2 except that the forward portion of the engine mount broke free and remained attached to the engine as the engine was thrown forward away from the airframe (Figure 126(b-e)). Strain gage data shown in Figures 135-140 show that the engine mount absorbed energy for 140 to 160 milliseconds before breaking away and this time interval covered the primary event. Strain gage data from the posts (Figures 135-136) indicate that the mount failure occurred as the airplane rotated up out of the crater which reverses loading on the engine mount. Several differences can be noted between test 3 and test 2 where the mount did not fail in this manner. Impact attitude was 3.9 degrees lower which was shown in the hard surface analysis to be a more severe impact. Engine mount post attachments to the upper rails had been moved aft one inch to increase engine accessories clearance and this nearly doubled the distance from the aft engine mount brackets to the post. The engine and accessories rotated upward bending the posts in test 2 which probably relieved loads in the rails. There was more clearance between the accessories and the mount in this test so the posts were not bent.

The cowl worked well, similar to the cowl in test 2 except that it fractured where the forward portion of the pad met the central portion of the pad (Figure 126(e)). The cowling pad for test 2 was made from honeycomb as described above and had a less abrupt intersection of the two portions of the pad. Foam was used for the pad on test 3 to allow use of wet lay-up fiberglass. Observation of the half scale tests showed the skirt of the cowl to be in compression and fastening

the skirt to the belly skin is difficult with the energy absorbing foam in place so the skirt was not fastened to the belly for airplanes 3 and 4.

Both wings broke forward because the fittings built into the rear spar pulled through the end of the spar. These fittings were aluminum inserts, shown in Figure 126(f), designed to increase bearing strength. The wing for test 3 was the same wing used in test 1. This wing was refurbished to fix the visible damage prior to test 3 but it cannot be determined if there was prior damage to these fittings. It should be noted that test 1 on hard surface produced higher loads normal to the floor than parallel to the floor while test 3 on soft soil produced the opposite results. Upper main spar caps failed at the side of the fuselage while the lower spar caps separated from the web in what appeared to be a bond line failure, possibly with an incomplete bond.

The slanted floor of the firewall was fractured toward the outside edges as shown in Figures 126 (g-h) but was not penetrated so the foot space was not compromised.

The air bag, shown deployed in Figure 126(k), appeared to work as designed. Film from the internal cameras show that the bag was fully inflated before the dummy contacted the bag. There was no head impact on any hard surface but the head data was lost because the instrument wires pulled out of the connector. One particularly impressive result was that there was little pilot motion after initial impact compared to the copilot where there was considerable flailing during the slide out.

The load limiter on the pilot's shoulder belt stroked about 1 inch while the copilot's (Figure 126(l)) stroked about 1.75 inches with the difference thought to be a result of the air bag for the pilot. The copilot flailed during the slide out apparently because the inertia reel released after the initial impact. His head hit the subpanel when the airplane hit the concrete surface. HIC was calculated to be less than 900 where 1000 is considered to be the threshold of injury.

6.3.4 Key Observations

The lighter, less labor intensive airframe designed for the third and fourth airframes worked well for this test, as well as the heavier airframe worked for test 2.

Both the air bag and load limiters appeared to have positive benefits for this crash scenario. The load limiter kept the occupant loads below limits but allowed more head and upper body motion than the combination of air bag and load limiter. The combination of air bag and load limiter would be expected to reduce neck injury potential due to head motion.

The restraint systems should resist occupant motion during secondary aircraft motions after the initial impact.

This was a survivable test with minimal injuries expected.

7. Weight Penalty

It is difficult to estimate the weight penalty for the design features utilized for these tests because there was not a complete baseline airplane meeting certification requirements for comparison. Some increments can be estimated and are listed below.

The cowling weighed approximately 22 pounds more than the estimated cowling for this airplane. Since part of the cowling appeared to be overly strong, this could probably be reduced with the right type of testing.

The engine mount weighed about 20 pounds which is little different than a normal bed mount. There is probably some penalty compared to an aft dynafocal mount designed only for flight and landing loads.

The square aluminum tube behind the firewall calculated to weigh 8 pounds for the design wall thickness, a higher wall thickness was used due to availability. This tube was not optimum design and the part could be reduced by a least half with good design. Some solid core was required in both the firewall and the floor behind the lower engine fittings to transfer loads between face sheets. The solid core and extra plies used on the test airplanes added about 8.7 pounds. Most firewalls have both vertical and lateral stiffeners and consideration of these weights could reduce the total weight penalty to about 8 to 10 pounds.

The braces behind the firewall were in the location for a nose wheel well and would probably add only a small weight increment if properly designed.

Longitudinal support for the tube and engine mount required a beam under the door and the supports for the cross tube of the above paragraph. These items weighed about 10.7 pounds on the test airplanes. There would normally be a door frame and there normally would be some extra structure to support the upper engine mount points. However, the beam needs to be stronger than the normal door frame and an estimate of the added weight for these items is approximately 8 pounds.

One frame was added to the aft fuselage and some additional plies were added to the upper aft fuselage. The additional stiffness was added for the loads of test 1 and test 4 had only about half the loads. Changing to honeycomb core in this area and addition of a dorsal fin would be expected to eliminate the need for the stiffener applied to the top of the fuselage and the added plies. The extra frame added about .4 pounds.

The under floor energy absorbers weighed approximately 7.6 pounds and the baggage compartment frame which supported the aft energy absorber weighed about 4 pounds. Some frame is required there for normal structure so assume a penalty of about 2 pounds.

The floor is structural in this concept and the belly skin is a minimum thickness fairing. This is thought to have more manufacturing than weight implications but there may be a small weight penalty.

Summing the penalties listed above leads to an airframe weight penalty of about 50 pounds. Some of these items are thought to be stronger than necessary and the side beams may be under strength. Additional knowledge of the dynamic properties of materials and the ability to test components dynamically would allow improved design and possibly reduce the weight penalty. It is assumed that roll bars will be necessary and that some structure will have to be added to the simple shell to meet other requirements so not every small reinforcement added to the test airplanes has been counted. This increment is thought to be representative. The overall weight penalty will be smaller if crashworthiness is designed in from the beginning rather than trying to add the features later. The analysis also indicates that the weight penalty may be less if a windshield post is used to carry the bending load into the upper cabin structure rather than taking all the bending load below the doors.

Air bags for the front seats would be expected to add 12 pounds. Weight increment for the load limiters is estimated to be about 1 pound. Properly designed seats are not expected to increase the weight.

8. Summary of Results

These tests indicate that improved survivability is possible, compared to prior NASA tests of conventional airplanes, for symmetrical impacts at approximately stall speed for this class of airplanes for a relatively severe impact angle onto both hard and soft soil surfaces. The airframe weight penalty is approximately 50 pounds with air bags adding another 12 pounds and load limiting shoulder harnesses an additional 1 pound.

No single feature was responsible for the improved survivability, rather the combined effects of all the features discussed were required for the full benefits.

The same airframe design is suitable for both hard surface and soft soil impacts.

Dynamic conditions can't be simulated in quasi-static testing.

Subscale static testing can help understand failure and energy absorbing patterns.

Subscale soil testing was particularly valuable in understanding soil impact behavior.

Absorbing energy in the engine mount, rather than in the cabin structure, increases accelerations at the rear seat for hard surface impacts by moving the ground reactions farther from the center of gravity. This leads to a second impact as the airplane rotates tail down with the strength of the second impact increasing aft. Rear seat loading is higher than front seat loading for this class of airplane during this second impact.

Soft soil impacts have longitudinal loads higher than normal loads with the reverse being true for hard surface impacts. Both air bags and shoulder harness load limiters proved beneficial for the soft soil impacts.

Loads applied at the seat tracks were higher than FAR 23.562 certification loads.

Analysis indicates seat accelerations increase as impact attitude decreases for the same flight path angle and velocity.

Off axis impacts were not tested or analyzed.

9. Recommendations

1. An inexpensive method for the dynamic testing of materials and components needs to be developed and made available to the industry.

2. An inexpensive method for the dynamic testing of configurations, full or subscale, needs to be developed and made available to the industry.

3. The analysis should be extended to include seats, occupants, and restraint systems, three dimensional structures, soil impact, and off axis impacts.

4. These results have shown that survivability can be improved but it is clear that impact energy can exceed the design limits of any reasonable energy absorbing system. Further, the number of impact scenarios is infinite. Crashworthiness standards need to be developed that are achievable, reasonable, and that can be applied without full scale airplane impact testing.

5. While not a technical topic, some change in the product liability climate needs to be made that does not penalize companies or individuals for conducting crashworthiness research and development and for making product improvements.

10. References

1. "National Transportation Safety Board, General Aviation Crashworthiness Project: Phase Two -- Impact Severity and Potential Injury Prevention in General Aviation Accidents", NTSB/SR-85/01, March, 1985

2. "National Transportation Safety Board, General Aviation Crashworthiness Project: Phase III -- Acceleration Loads and Velocity Changes of Survivable General Aviation Accidents", NTSB/SR-85/02, September, 1985

3. "AOPA'S 1993 Aviation Fact Card", Aircraft Owners and Pilots Association, 1993-1995

4. "National Transportation Safety Board, Annual Review of Aircraft Accident Data, U.S. General Aviation Calendar Year 1982", NTSB/ARG-86/01, February, 1986

5. "Aircraft Crash Survival Design Guide", Simula, Inc., USARTC-TR-79-22, January 1980

6. Vaughan, Victor L. Jr. and Hayduk, Robert J., "Crash Tests of Four Identical High-Wing Single-Wing Airplanes", NASA Technical Paper 1699, 1980

7. Castle, Claude B. and Alfaro-Bou, Emilio, "Crash Tests of Three Identical Low-Wing Single-Engine Airplanes", NASA Technical Paper 2190, 1983

8. Terry, James E., Hooper, Dr. Steven J. and Nicholson, Mark, "Design and Test of an Improved Crashworthiness Small Composite Airframe", Phase I Report, NASA SBIR Contract NAS1-20178, 1994

9. Cheng, Robert Y. K., "Soil Analyses and Evaluations at the Impact Dynamics Research Facility for Two Full-Scale Aircraft Crash Tests", NASA Contractor Report 159199, December 1977

10. Vaughan, Victor L. Jr. and Alfaro-Bou, Emilio, "Impact Dynamics Research Facility for Full-Scale Aircraft Crash Testing", NASA TN D-8179, 1976

11. SAE, "Surface Vehicle Recommended Practice", SAE J211/1, Rev. Mar95

12. "Strength of Metal Aircraft Elements", ANC-5 Bulletin, 1955

13. *General Plastics Last-A-Foam ® FR-3700 for Crash & Fire Protection of Nuclear Material Shipping Containers*, General Plastics Manufacturing Company, 1993

14. Jones, N., *Structural Impact*, Cambridge University Press, 1989

15. "Standard Test Method for Bearing Ratio of Soils in Place", ASTM D 4429 - 84, 1984

	NASA, Low Wing		Terry Engineering			
	Soft Soil	Hard Surface	1 Hard Surface	2 Soft Soil	3 Soft Soil	4 Hard Surface
Flight Path Angle, degrees	-31	-29	-30	-30	-30	-30
Pitch Angle, degrees	-27.3	-26	-24	-27.2	-23.5	-26
Velocity, ft/sec	82	80.7	85	84	82.3	83.2

Roll and Yaw were small for all tests

Table 1, Full Scale Test Conditions

wood cowl test #1

13.3 inch stroke - max normal load cell

segment	length	theta	area	X arm	Z arm	local pressure	element force	normal force	axial force	moment	friction	normal friction	axial friction	moment friction	net normal	net axial	net moment	friction coefficient
1	0.8683	72.7032	14.32695	38.3613	3.36996	20	286.539	85.21979	273.573	4191.072	128.9426	-123.108	38.3489	-4593.34	-37.8881	311.9219	-402.2709	0.45
2	1.5357	70.6298	25.33905	37.9775	2.23108	20	506.781	168.1277	478.0795	7451.704	222.9836	-210.355	73.9762	-7823.71	-42.2273	552.0557	-372.0059	0.44
3	1.6386	67.6088	27.0369	37.4108	0.749152	20	540.738	206.0259	499.9509	8082.133	232.5173	-214.979	88.59114	-7976.16	-8.95299	588.542	105.96884	0.43
4	1.798	63.7917	29.667	36.7016	-0.81496	20	593.34	262.0839	532.3198	9185.077	249.2028	-223.574	110.0752	-8295.24	38.50953	642.3951	889.83492	0.42
5	2.1071	58.3325	34.76715	35.7515	-2.51822	20	695.343	365.0918	591.7853	11562.33	285.0906	-242.632	149.6876	-9051.4	122.4598	741.473	2510.9291	0.41
6	3.8614	45.0438	63.7131	33.8412	-4.77415	22	1401.688	990.4427	991.8433	28782.56	560.6753	-396.737	396.1771	-15317.5	593.7054	1388.02	13465.085	0.4
7	1.6648	29.5941	27.4692	31.7603	-6.54447	26	714.1992	621.0423	352.6853	17416.35	285.6797	-141.074	248.4169	-6106.31	479.9682	601.1022	11310.038	0.4
8	5.4462	19.5768	89.8623	28.4708	-7.86798	28	2516.144	2370.715	843.0251	60863.26	1006.458	-337.21	948.2861	-17061.7	2033.505	1791.311	43801.523	0.4
9	3.302	12.3715	54.483	24.2924	-9.13414	30	1634.49	1596.541	350.1633	35585.37	653.796	-140.065	638.6164	-9235.73	1456.476	988.7797	26349.639	0.4
10	2.8386	9.3727	46.8369	21.2794	-9.71901	30	1405.107	1386.351	228.8132	27276.89	547.9917	-89.2372	540.677	-7153.76	1297.114	769.4903	20123.129	0.39
11	2.607	7.4445	43.0155	18.5865	-10.119	32	1376.496	1364.895	178.3337	23564.06	523.0685	-67.7668	518.6601	-6507.87	1297.128	696.9938	17056.193	0.38
12	2.4633	6.0491	40.64445	16.0692	-10.4177	36	1463.2	1455.054	154.1817	21775.34	541.3841	-57.0472	538.3701	-6525.28	1398.007	692.5518	15250.057	0.37
13	2.3642	4.9771	39.0093	13.6667	-10.6501	38	1482.353	1476.765	128.5959	18812.94	533.6472	-46.2945	531.6354	-6294.66	1430.47	660.2313	12518.28	0.36
14	1.4962	4.2515	24.6873	11.743	-10.8081	39	962.8047	960.1557	71.37189	10503.71	336.9816	-24.9802	336.0545	-3925.45	935.1755	407.4264	6578.2611	0.35
			560.8581					13308.51	5674.722	285052.8		-2315.06	5157.573		10993.45	10832.29	169184.66	

load cell data	
axial force	10877
normal force	9997
moment	169949

Fv/Fa = 1.367805

actuator normal =		9952.04
Resultant	=	15433.55
Arm	=	10.96
θ	=	45.43

vertical component	horizontal component	effective μ
14877.61	4105.0343	0.27592

6 inch stroke

segment	length	theta	area	X arm	Z arm	local pressure	element force	normal force	axial force	moment	friction	normal friction	axial friction	moment friction	net normal	net axial	net moment	friction coefficient
4	1.798	63.7917	29.667	36.7016	-0.81496	10	296.67	131.0419	266.1599	4592.539	157.2351	-141.065	69.45222	-5233.9	-10.0228	335.6121	-641.3643	0.53
5	2.1071	58.3325	34.76715	35.7515	-2.51822	12	417.2058	219.0551	355.0712	6937.4	221.1191	-188.188	116.0992	-7020.36	30.86733	471.1704	-82.95737	0.53
6	3.8614	45.0438	63.7131	33.8412	-4.77415	12	764.5572	540.2415	541.0054	15699.58	405.2153	-286.733	286.328	-11070.4	253.5086	827.3334	4629.2213	0.53
7	1.6648	29.5941	27.4692	31.7603	-6.54447	16	439.5072	382.1799	217.0371	10717.76	219.7536	-108.519	191.0899	-4697.16	273.6613	408.1271	6020.5908	0.5
8	5.4462	19.5768	89.8623	28.4708	-7.86798	20	1797.246	1693.368	602.1608	43473.76	808.7607	-270.972	762.0157	-13710.3	1422.396	1364.176	29763.433	0.45
9	3.302	12.3715	54.483	24.2924	-9.13414	24	1307.592	1277.233	280.1306	28468.3	523.0368	-112.052	510.8931	-7388.59	1165.181	791.0237	21079.711	0.4
10	2.8386	9.3727	46.8369	21.2794	-9.71901	26	1217.759	1201.505	198.3048	23639.97	487.1038	-79.3219	480.6018	-6358.9	1122.183	678.9066	17281.073	0.4
								5444.624	2459.87	133529.3		-1186.85	2416.48		4257.773	4876.35	78049.708	

load cell data	
axial force	4848
normal force	4616
moment	78472

Fv/Fa = 1.310207

actuator normal =		4591.159
Resultant	=	6473.59
Arm	=	12.06
θ	=	41.13

vertical component	horizontal component	effective μ
6351.8813	1249.4101	0.196699

8 inch stroke

segment	length	theta	area	X arm	Z arm	local pressure	element force	normal force	axial force	moment	friction	normal friction	axial friction	moment friction	net normal	net axial	net moment	friction coefficient
3	1.6386	67.6088	27.0369	37.4108	0.749152	10	270.369	103.0129	249.9755	4041.066	143.2956	-132.487	54.59686	-4915.54	-29.474	304.5723	-874.4765	0.53
4	1.798	63.7917	29.667	36.7016	-0.81496	13	385.671	170.3545	346.0079	5970.3	204.4056	-183.384	90.28789	-6804.07	-13.0297	436.2958	-833.7736	0.53
5	2.1071	58.3325	34.76715	35.7515	-2.51822	15	521.5073	273.8188	443.839	8671.75	260.7536	-221.92	136.9094	-8278.72	51.89933	580.7484	393.02667	0.5
6	3.8614	45.0438	63.7131	33.8412	-4.77415	17	1083.123	765.3421	766.4243	22241.07	487.4052	-344.891	344.4039	-13315.8	420.4511	1110.828	8925.3097	0.45
7	1.6648	29.5941	27.4692	31.7603	-6.54447	20	549.384	477.7249	271.2964	13397.19	247.2228	-122.083	214.9762	-5284.31	355.6415	486.2726	8112.884	0.45
8	5.4462	19.5768	89.8623	28.4708	-7.86798	23	2066.833	1947.373	692.4849	49994.82	930.0748	-311.618	876.318	-15766.9	1635.755	1568.803	34227.948	0.45
9	3.302	12.3715	54.483	24.2924	-9.13414	25	1362.075	1330.451	291.8027	29654.48	544.83	-116.721	532.1803	-7696.45	1213.73	823.9831	21958.033	0.4
10	2.8386	9.3727	46.8369	21.2794	-9.71901	27	1264.596	1247.716	205.9319	24549.2	505.8385	-82.3728	499.0865	-6603.47	1165.343	705.0184	17945.73	0.4
11	2.607	7.4445	43.0155	18.5865	-10.119	29	1247.45	1236.936	161.6149	21354.93	498.9798	-64.646	494.7744	-6208.16	1172.29	656.3893	15146.767	0.4
								7552.73	3429.377	179874.8		-1580.12	3243.534		5972.607	6672.911	105001.45	

load cell data	
axial force	6693
normal force	6182
moment	105094

Fv/Fa = 1.309599

actuator normal =		6176.556
Resultant	=	8955.43
Arm	=	11.72
θ	=	41.83

vertical component	horizontal component	effective μ
8765.1431	1836.3117	0.209502

Table 2, Estimated Wood Cowl Loads

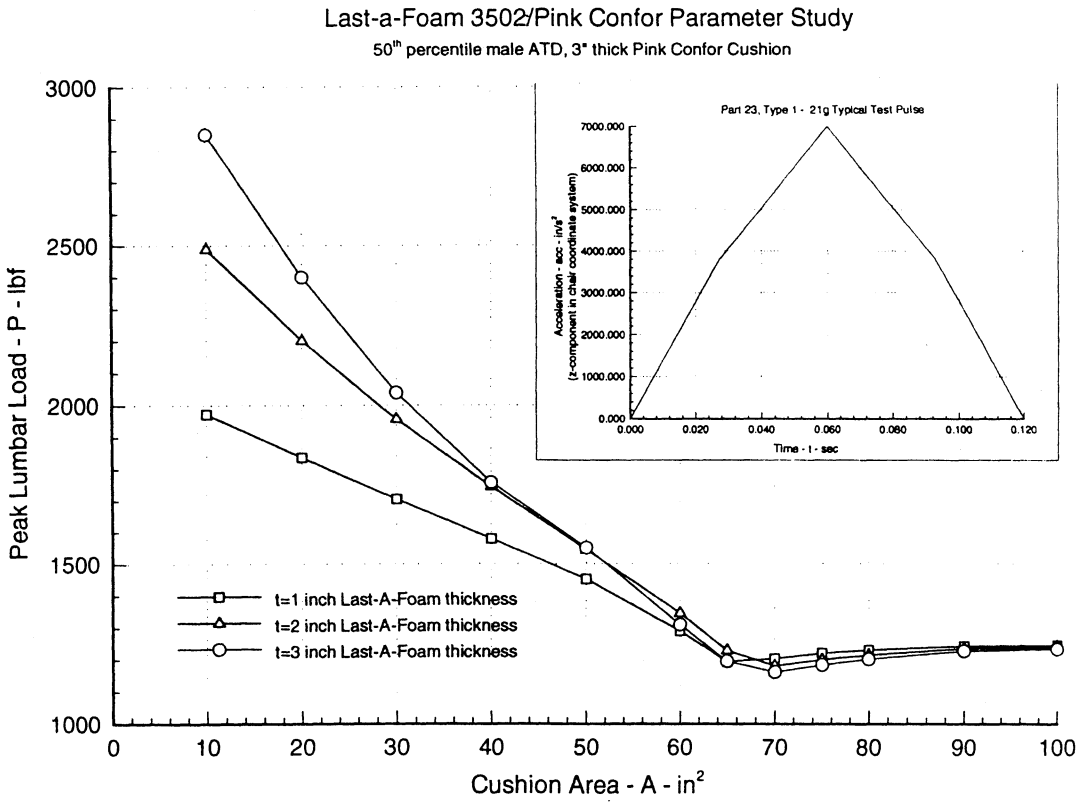

(a), Analysis

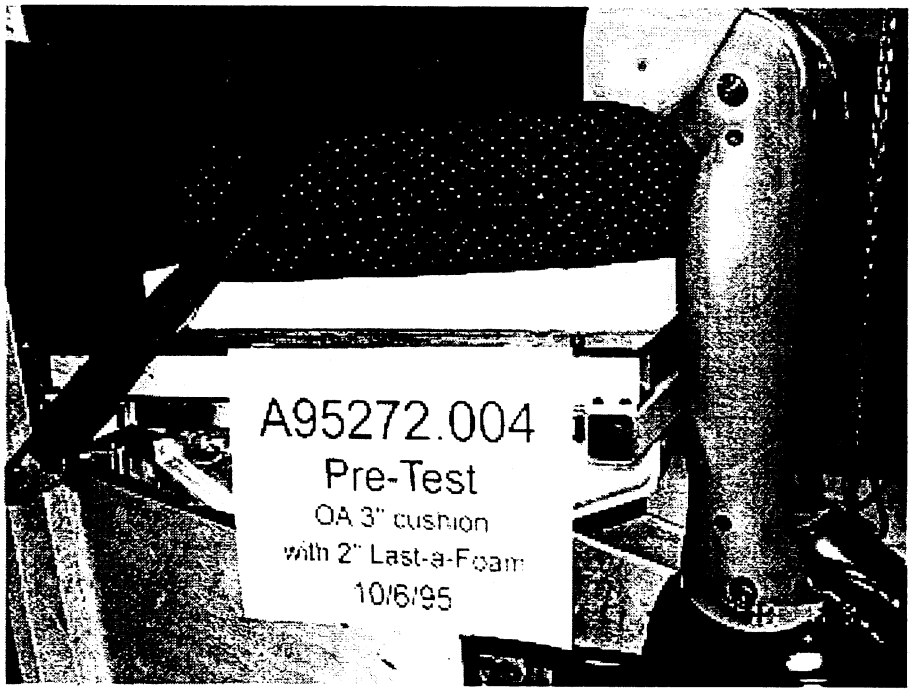

(b), Representative Cushion and Energy Absorber

Figure 1, Seat Cushion and Energy Absorber

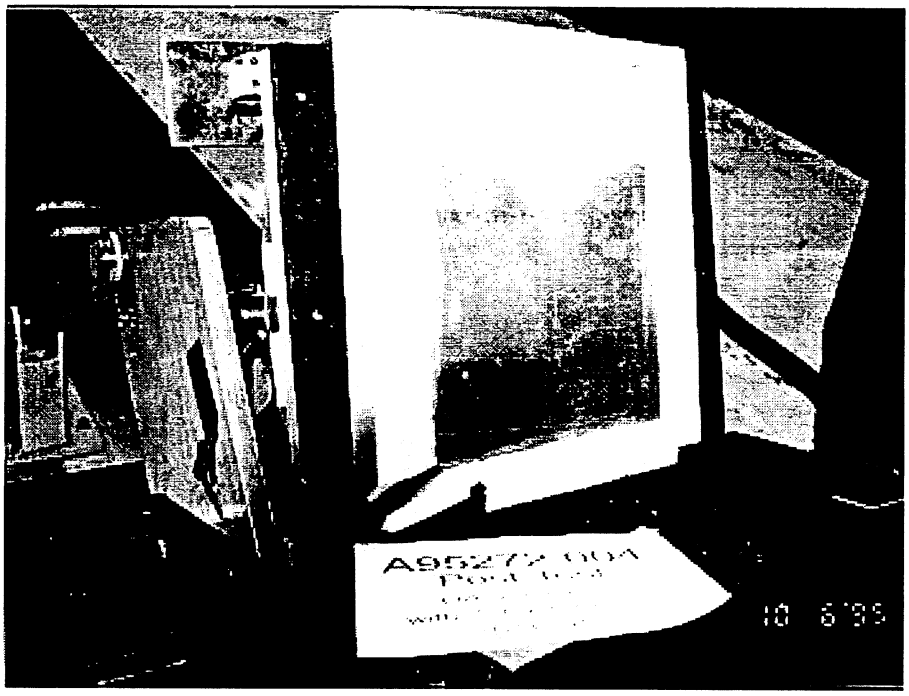

(c), Post Test Showing Aluminum Plate

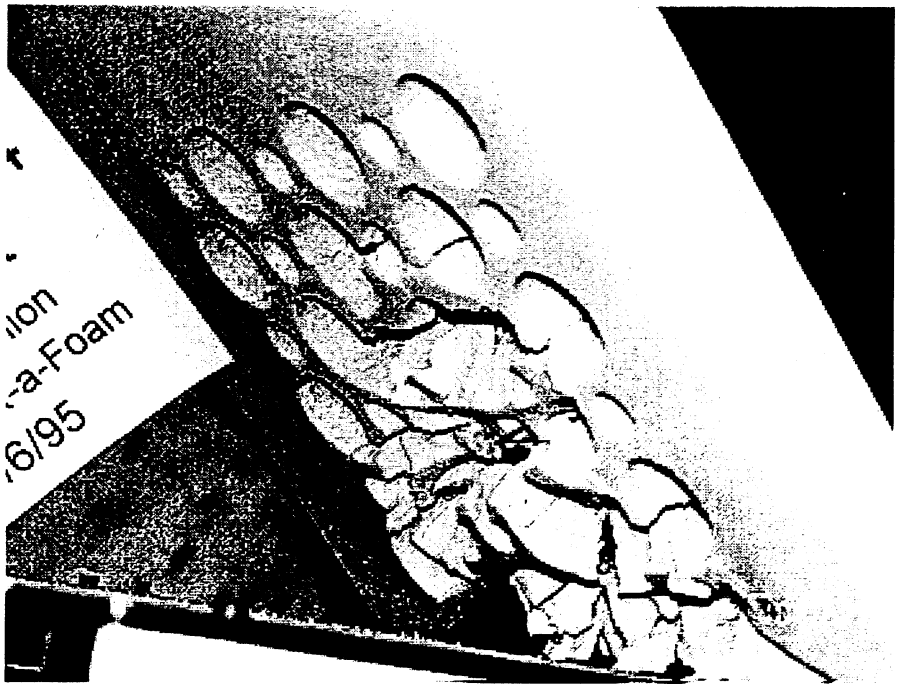

(d), Post Test Energy Absorber

Figure 1, (continued)

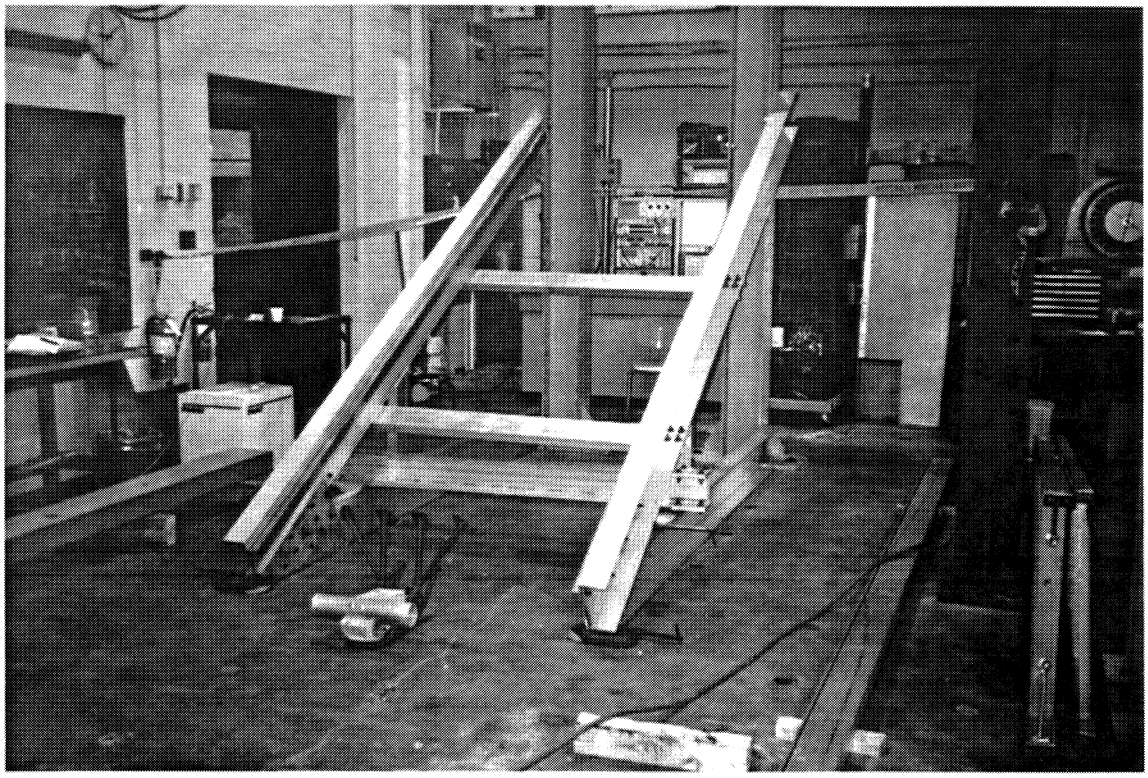

(a), Framework

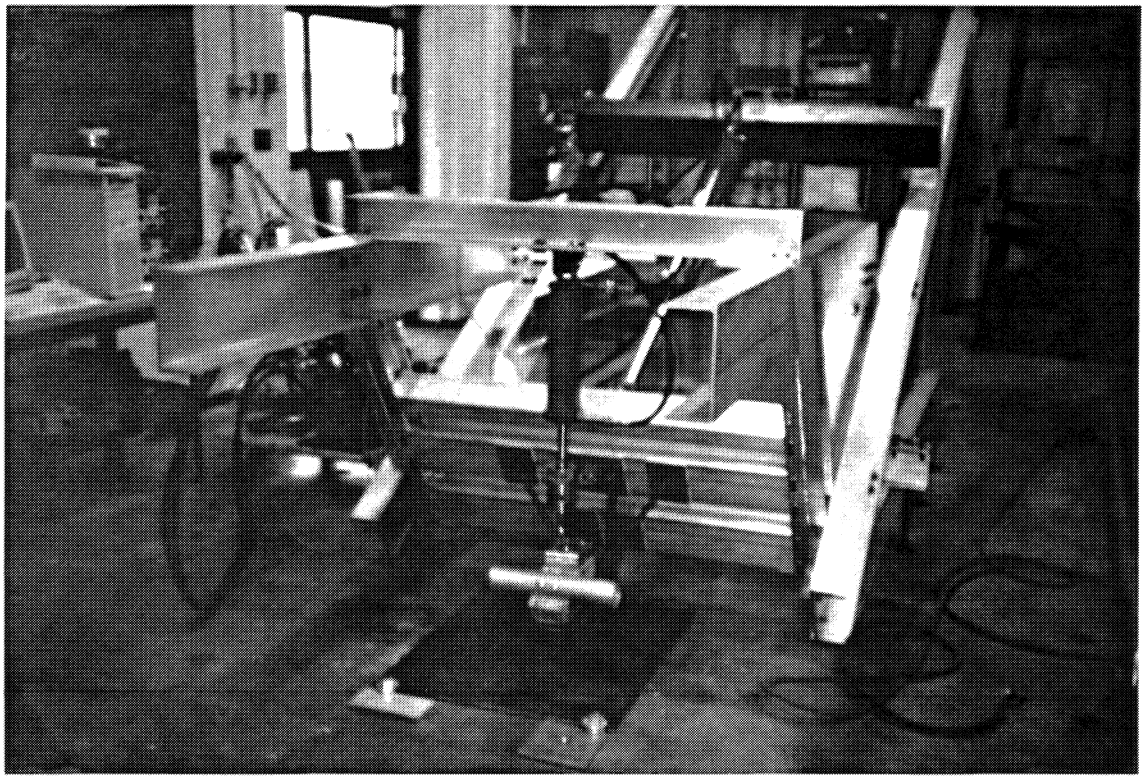

(b), Completed Test Rig with Model Engine Mount

Figure 2, Half Scale Test Rig

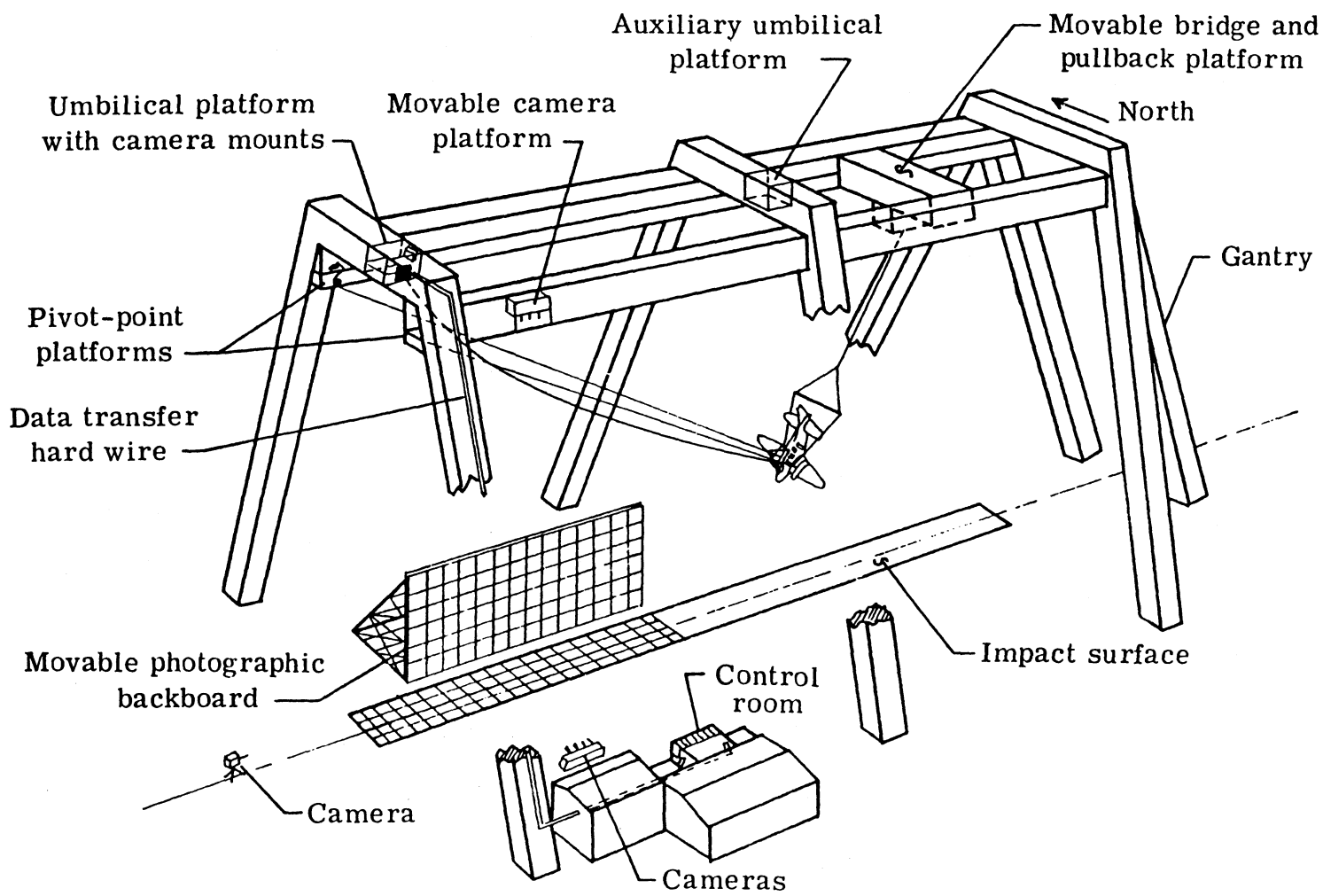

Figure 3, Diagram of Impact Dynamics Research Facility

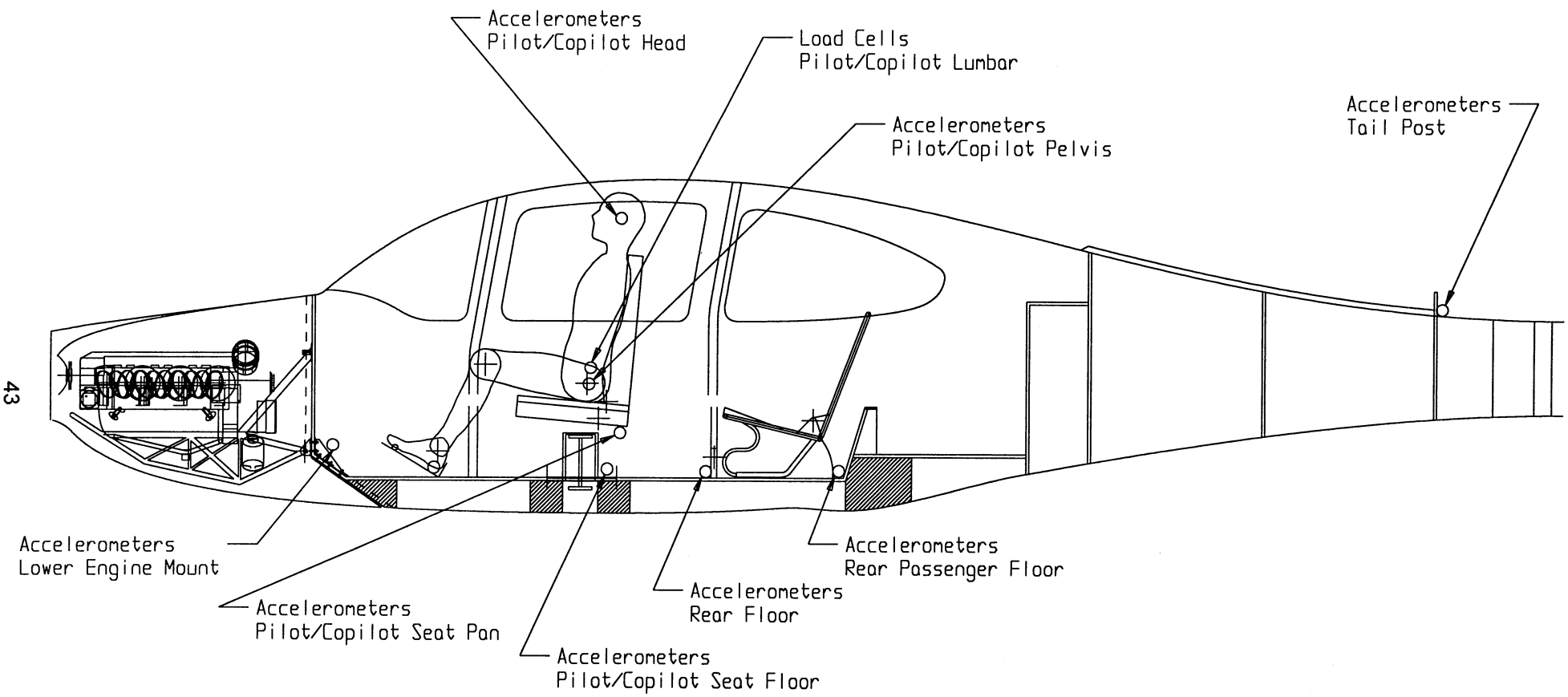

Figure 4, Instrumentation Layout

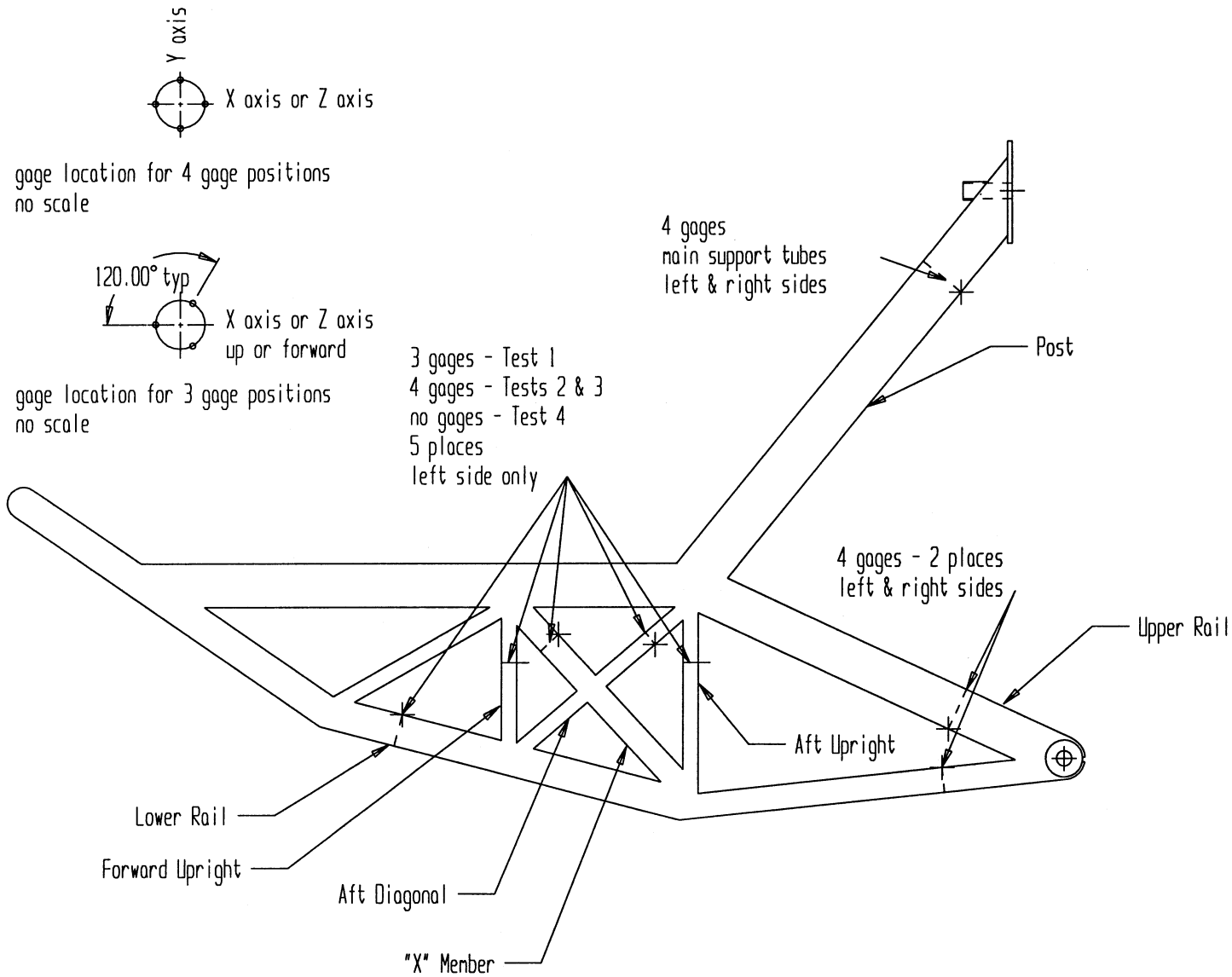

Figure 5, Engine Mount Strain Gage Locations

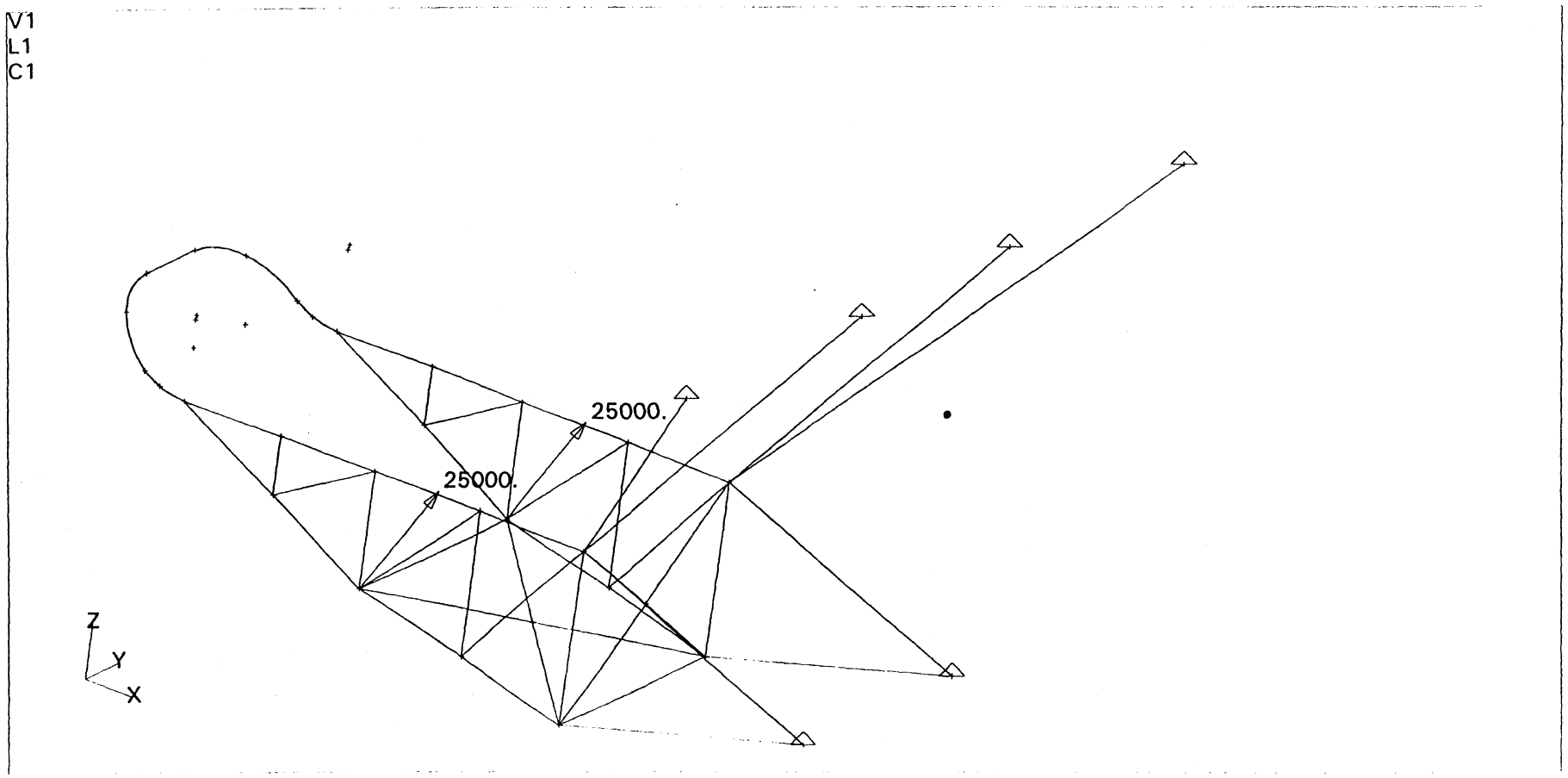

Figure 6, Engine Mount Static Analysis

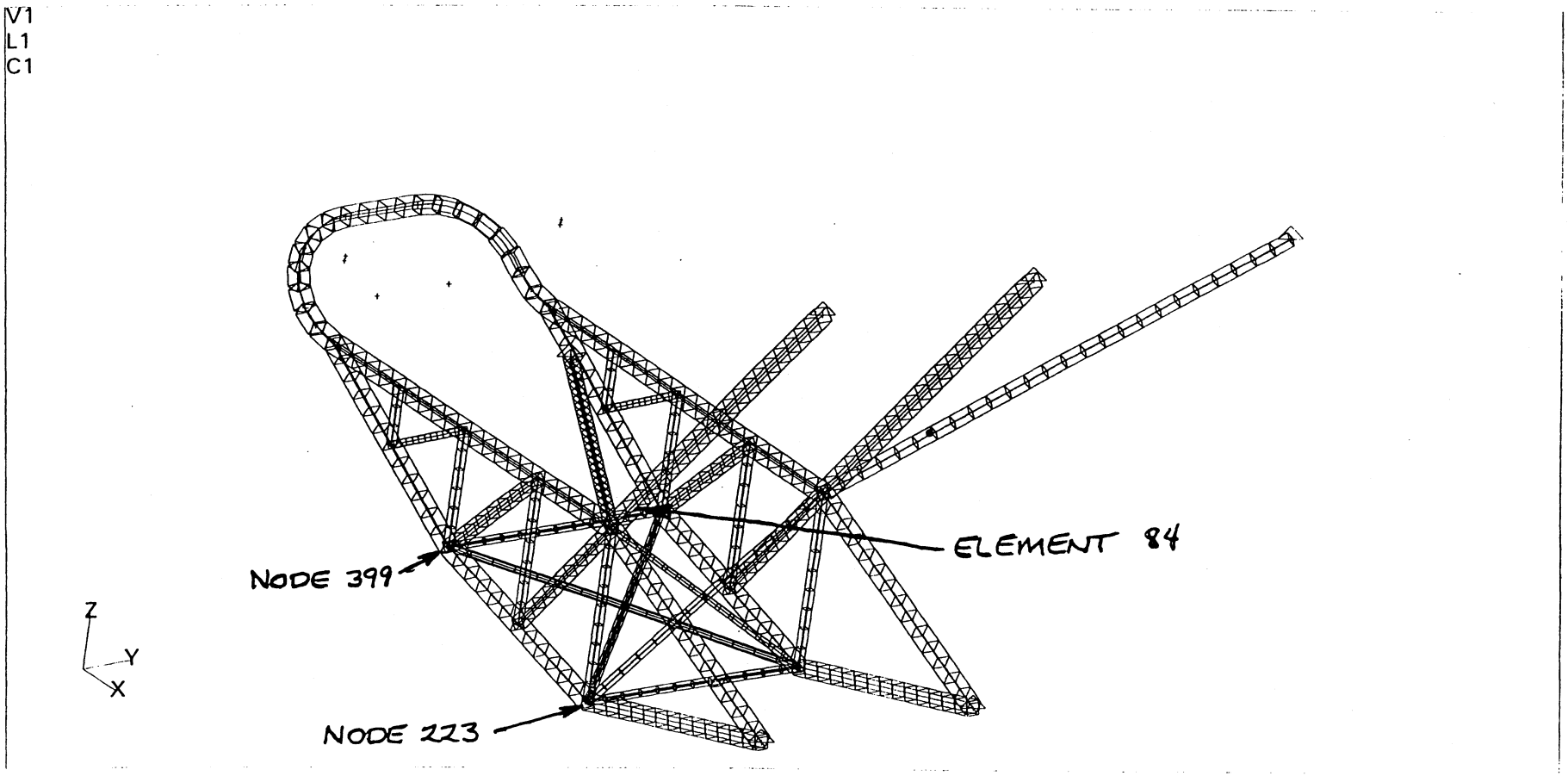

(a) Model

Figure 7, Engine Mount Dynamic Analysis

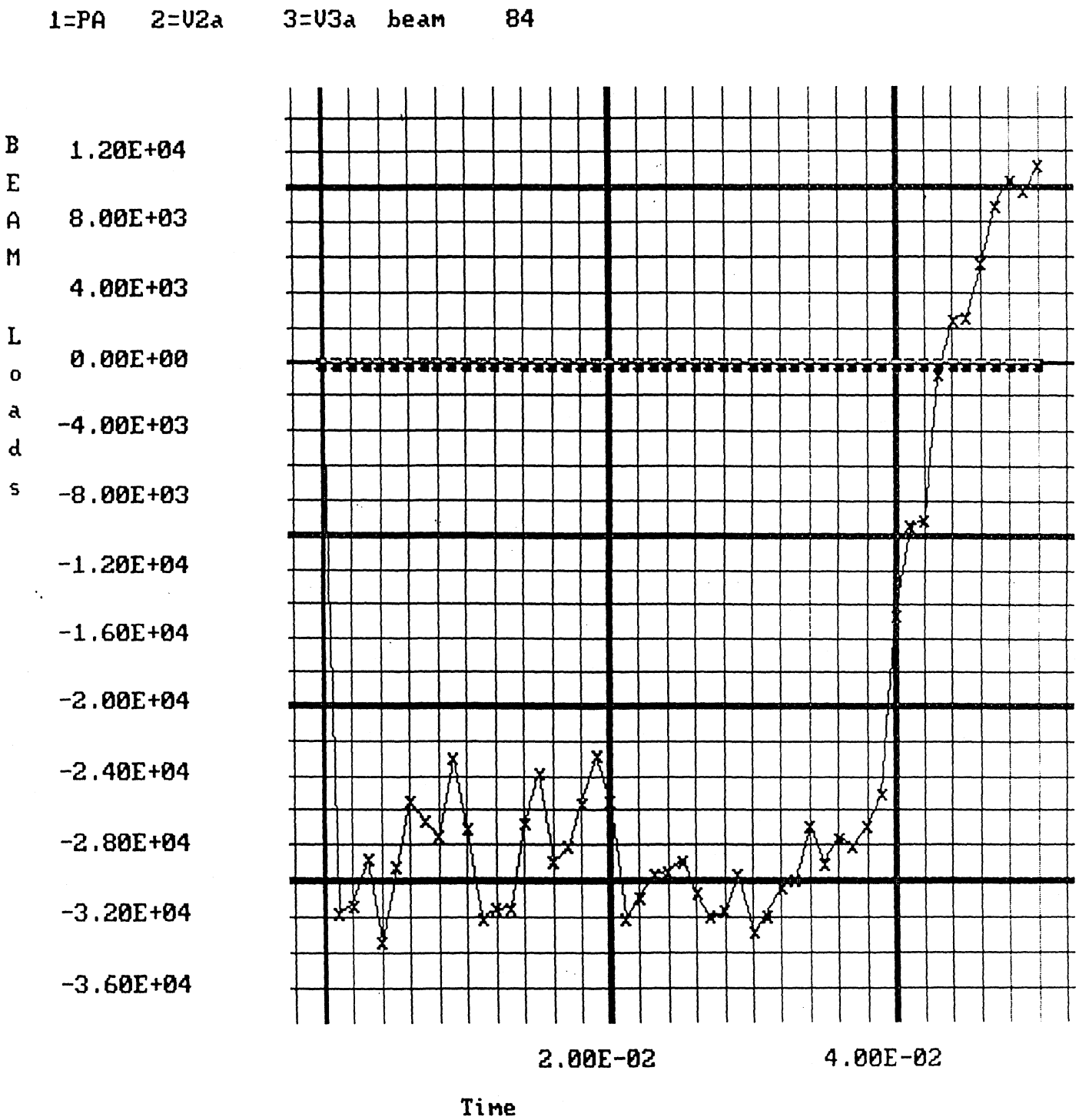

(b), Load Element 84

Figure 7, (continued)

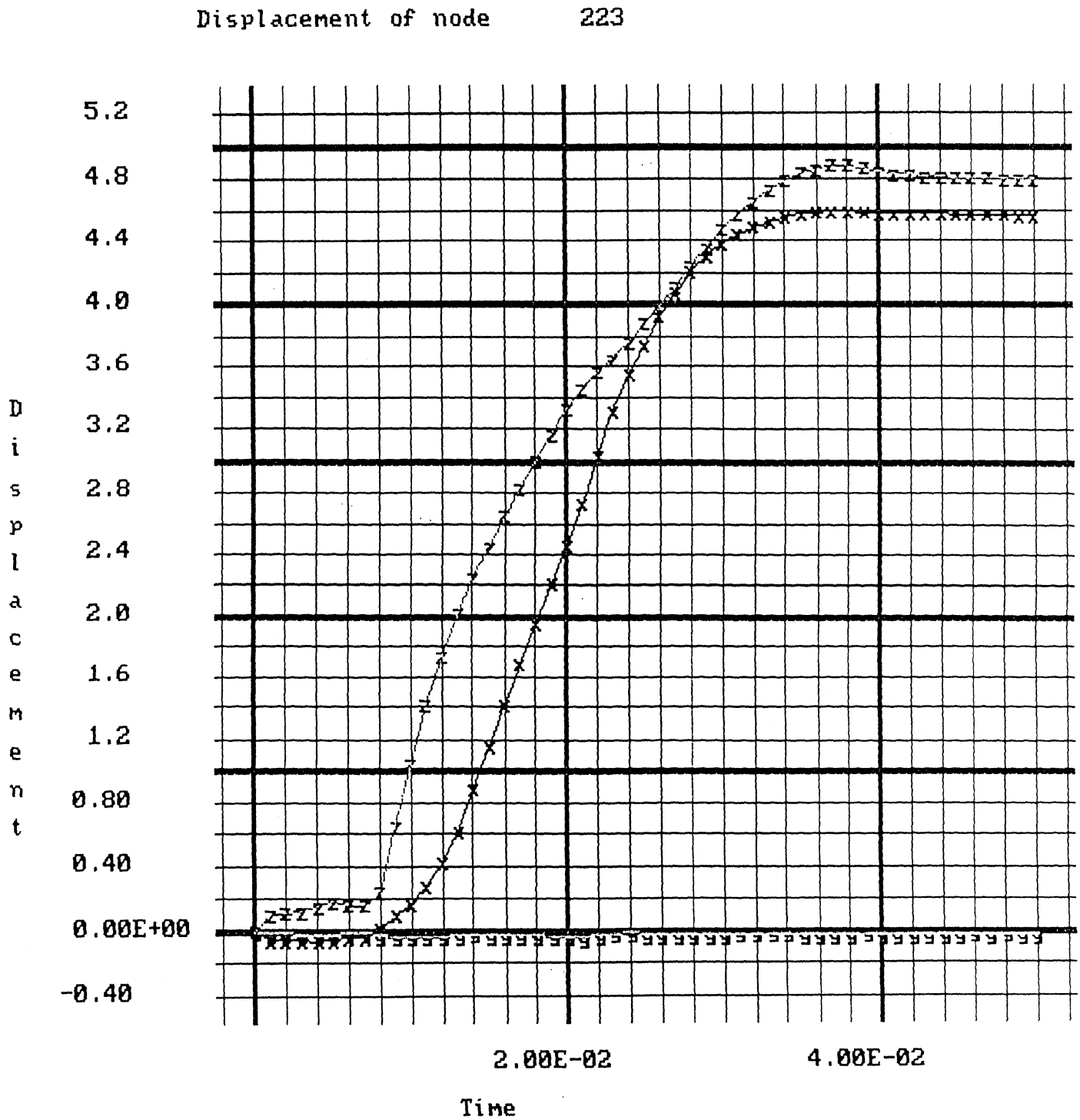

(c), Displacement Node 223

Figure 7, (continued)

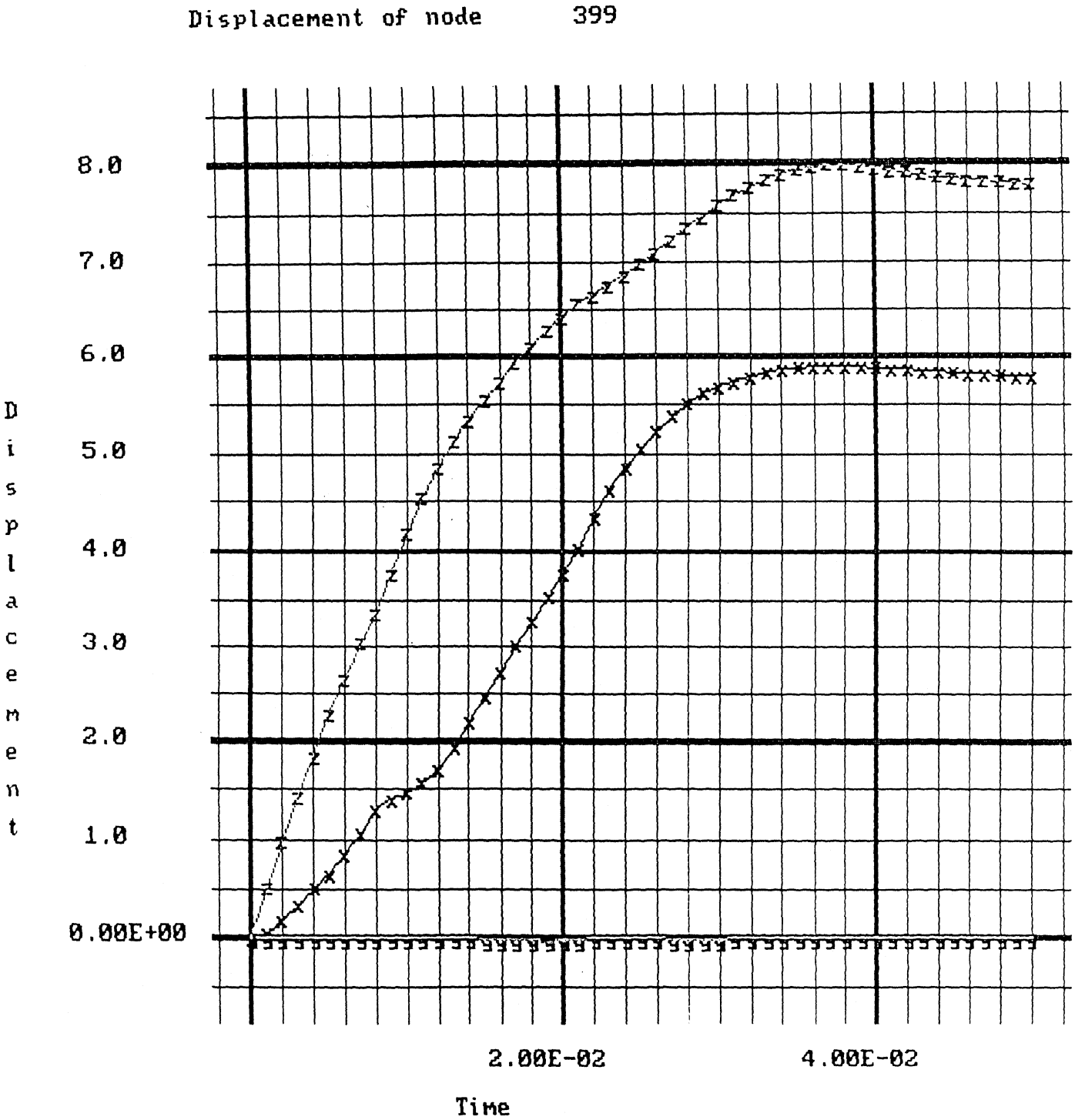

(d), Displacement Node 399

Figure 7, (concluded)

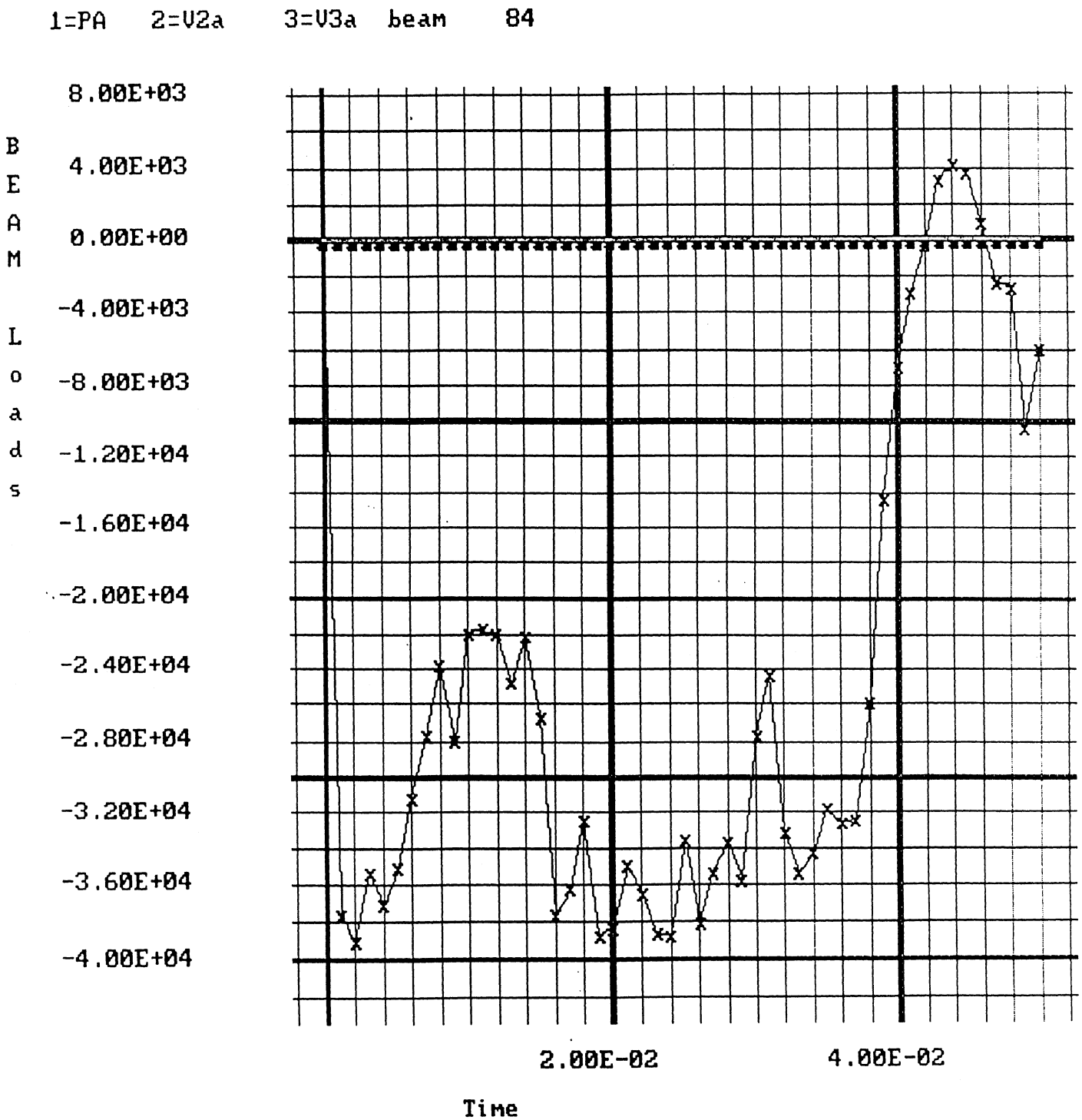

(a), Load Element 84

Figure 8, Engine Mount Dynamic Analysis, Adjusted Tube Sizes

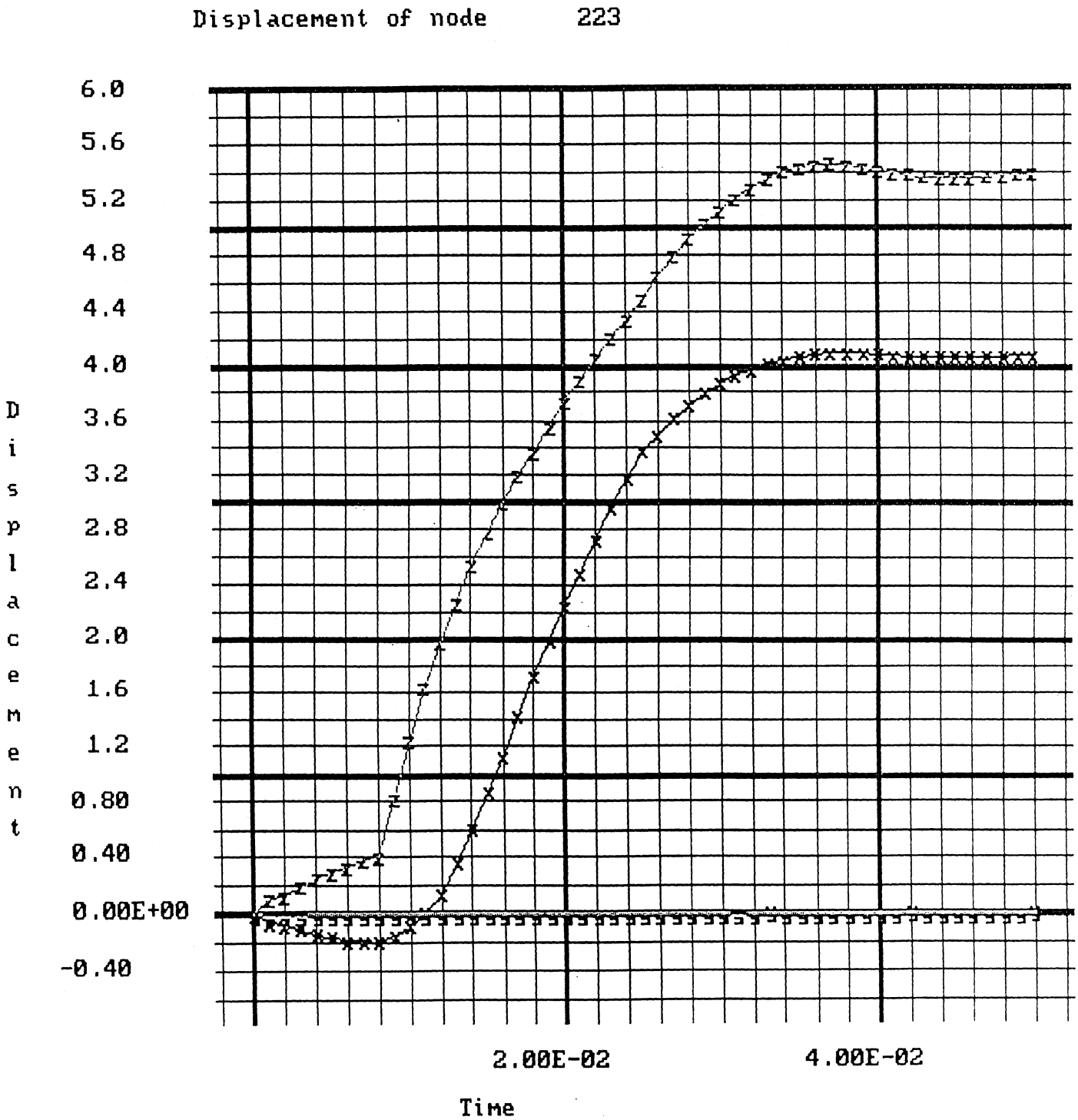

(b), Displacement Node 223

Figure 8, (continued)

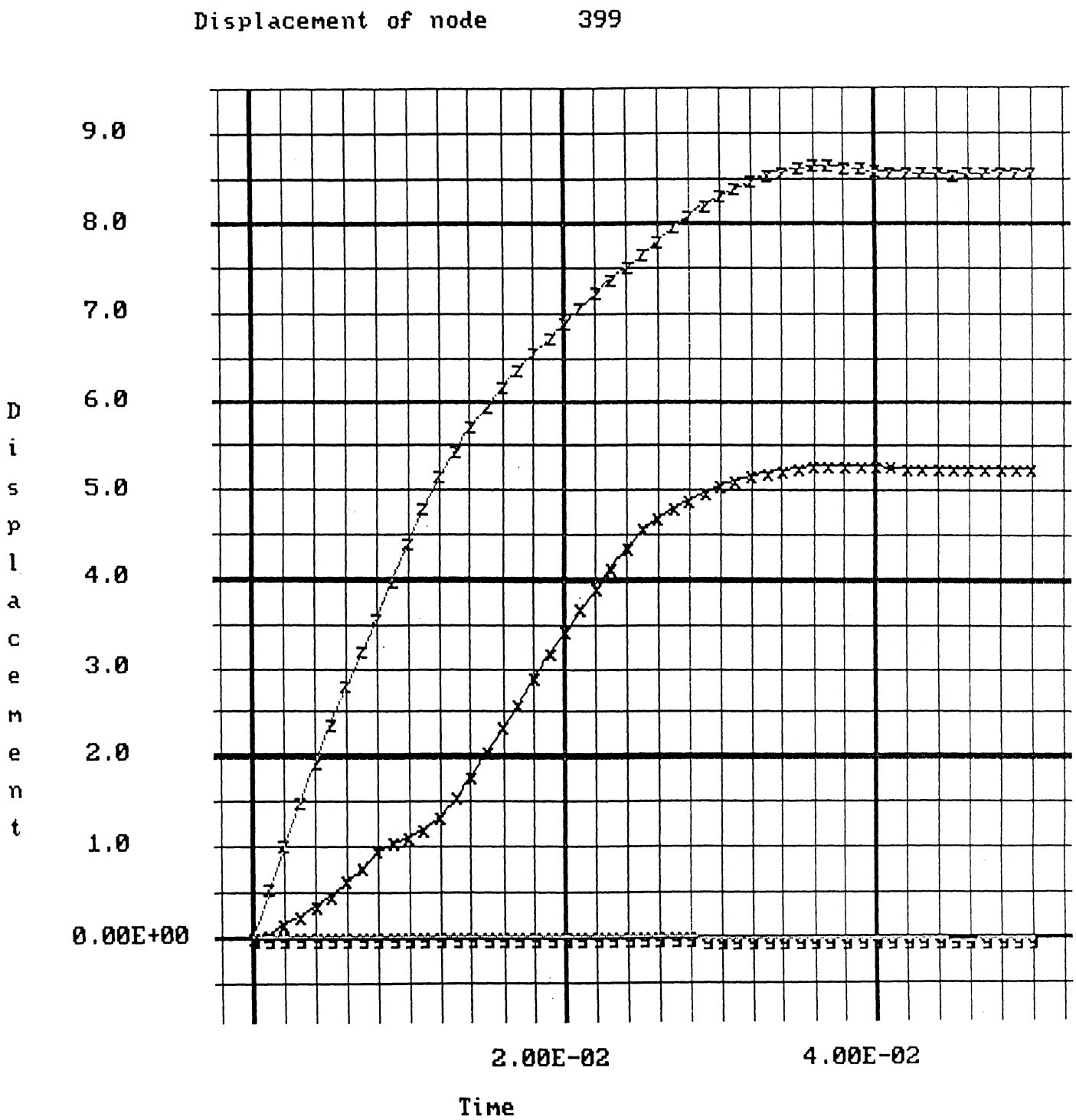

(c), Displacement Node 399

Figure 8, (concluded)

(a), Parts

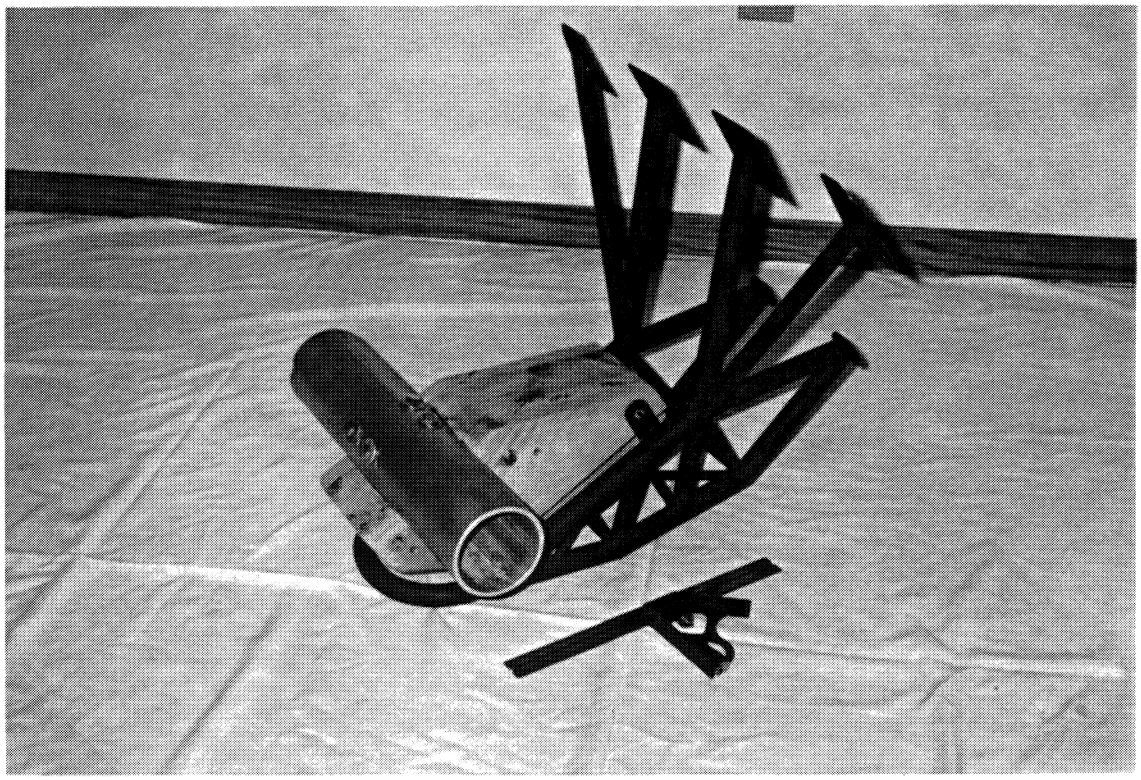

(b), Assembled

Figure 9, First Half Scale Engine Mount

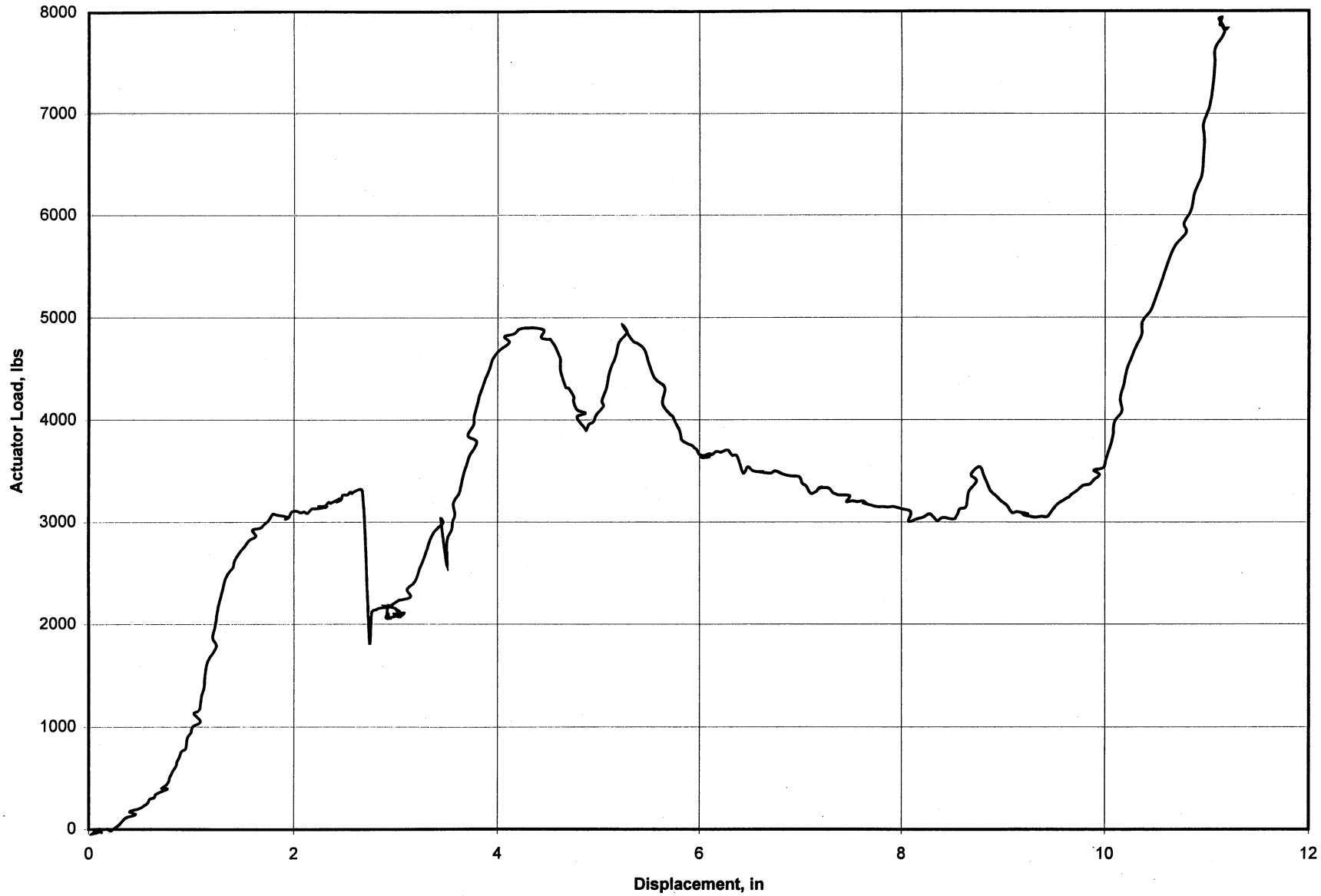

Figure 10, Half Scale Mount 3 Test Data

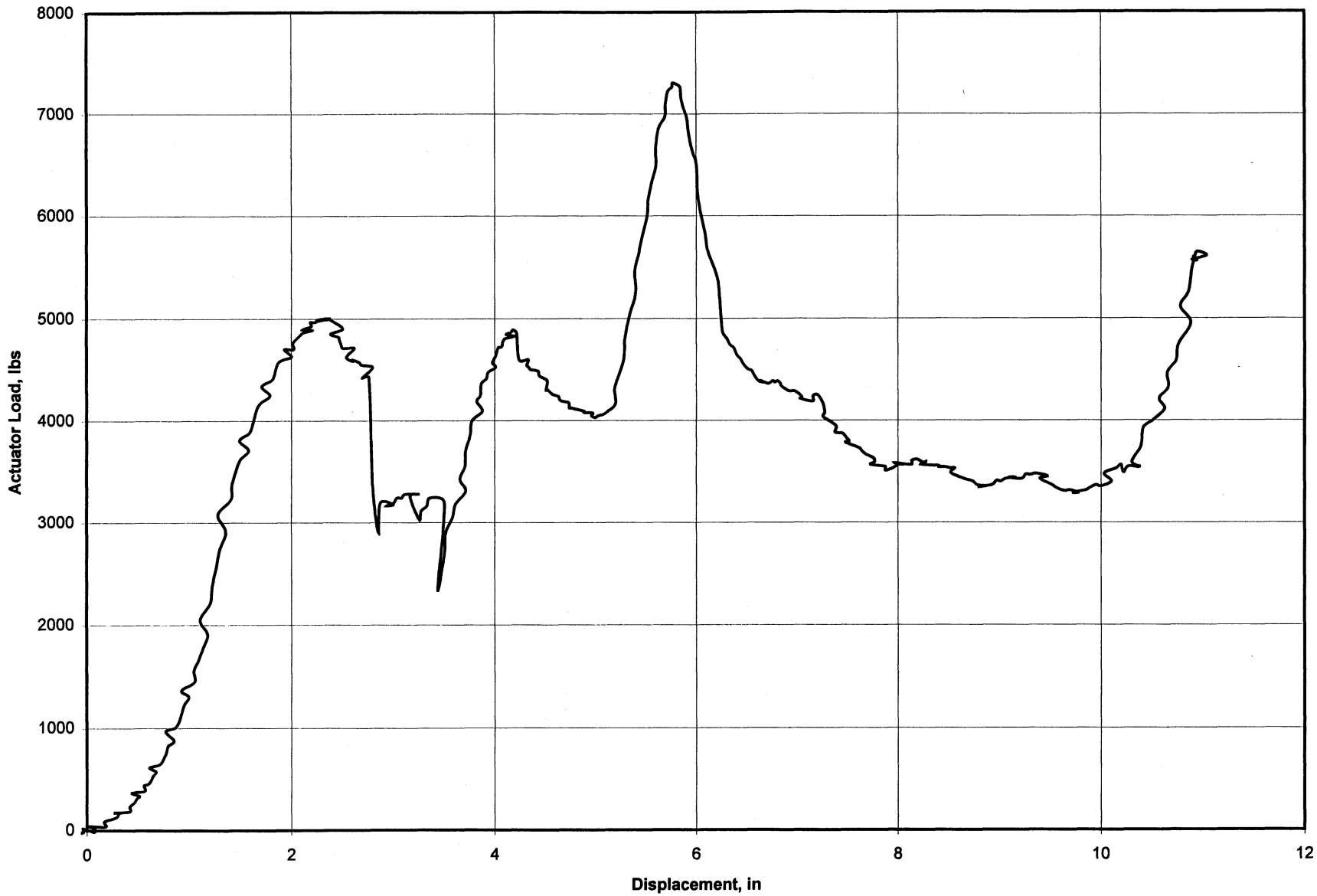

Figure 11, Half Scale Mount 4 Test Data

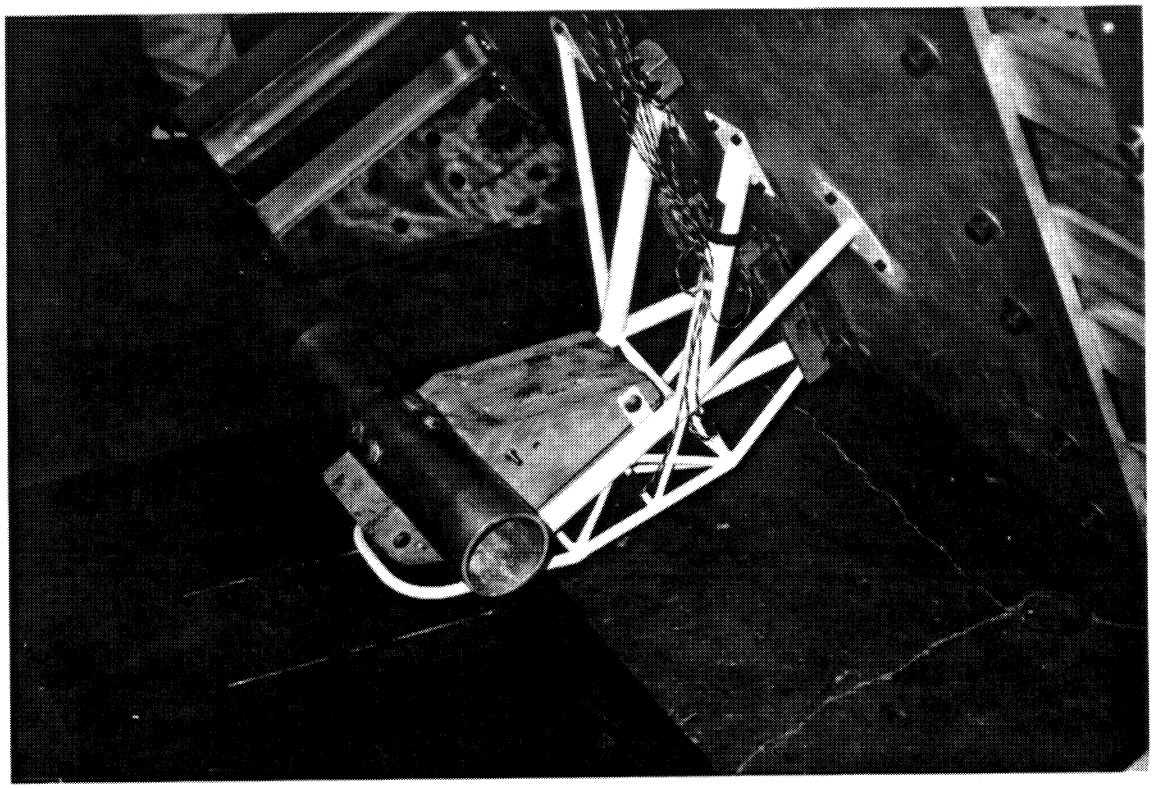

(a), Pretest

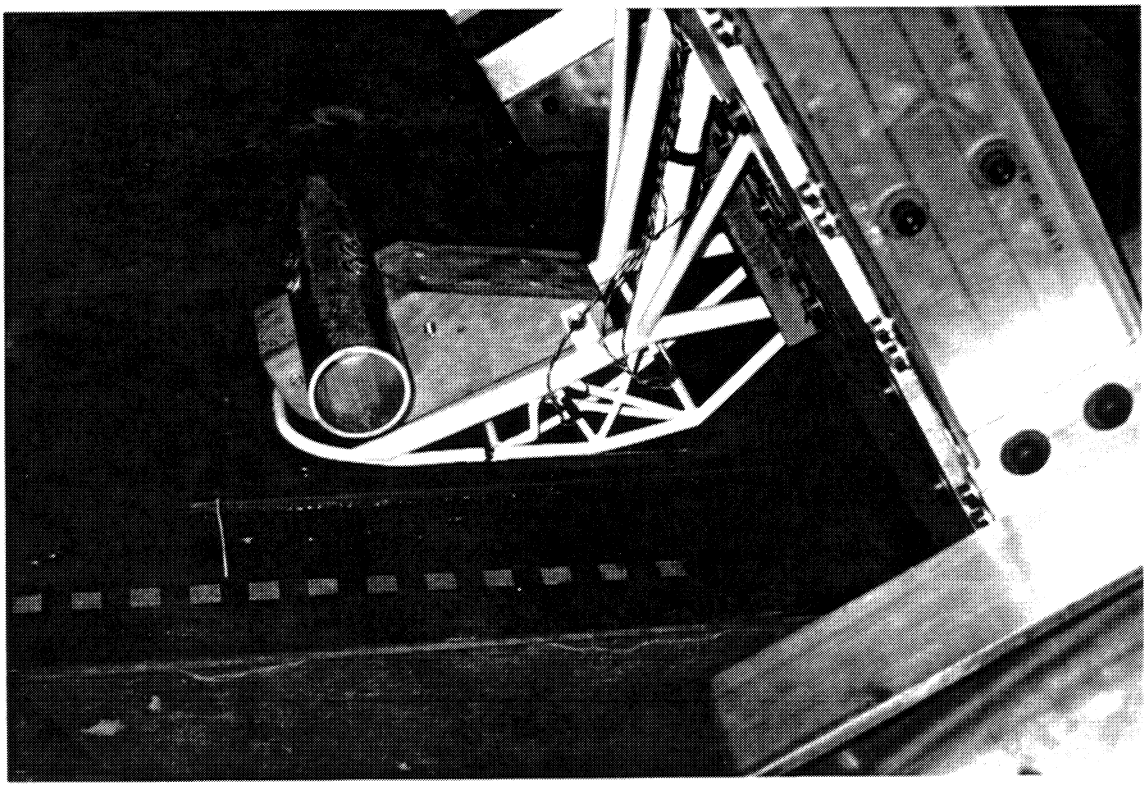

(b), During Test

Figure 12, Half Scale Engine Mount 5

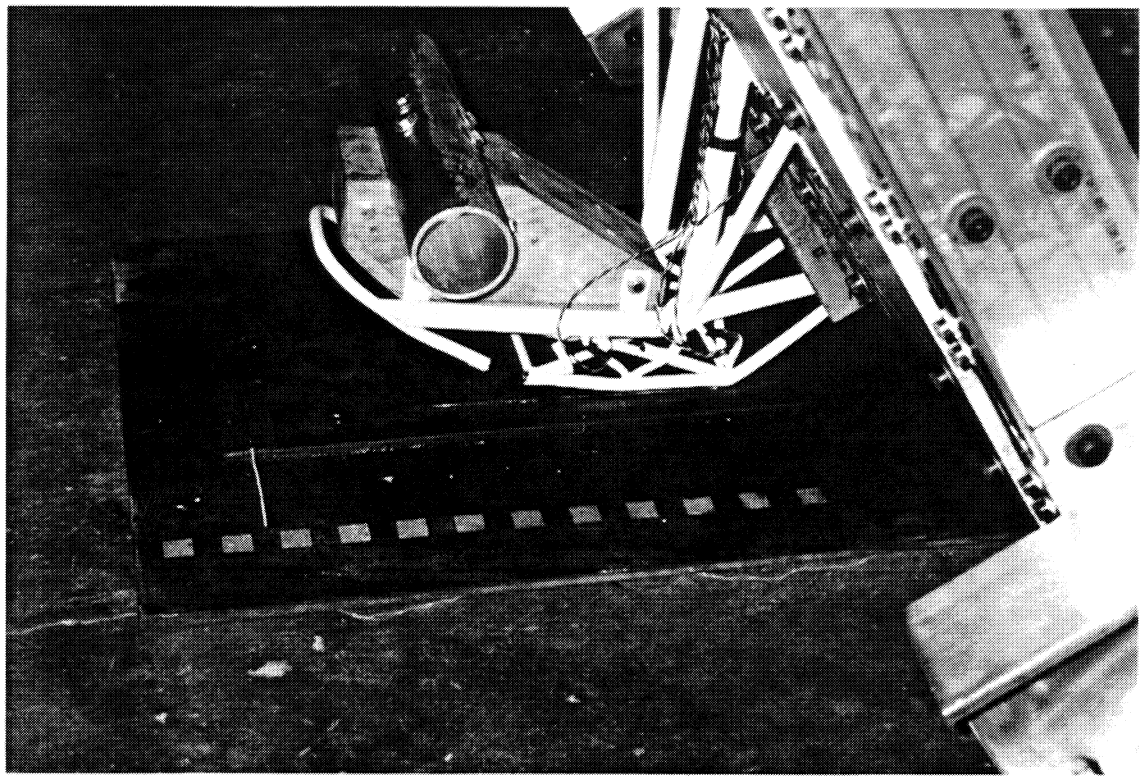

(c), During Test

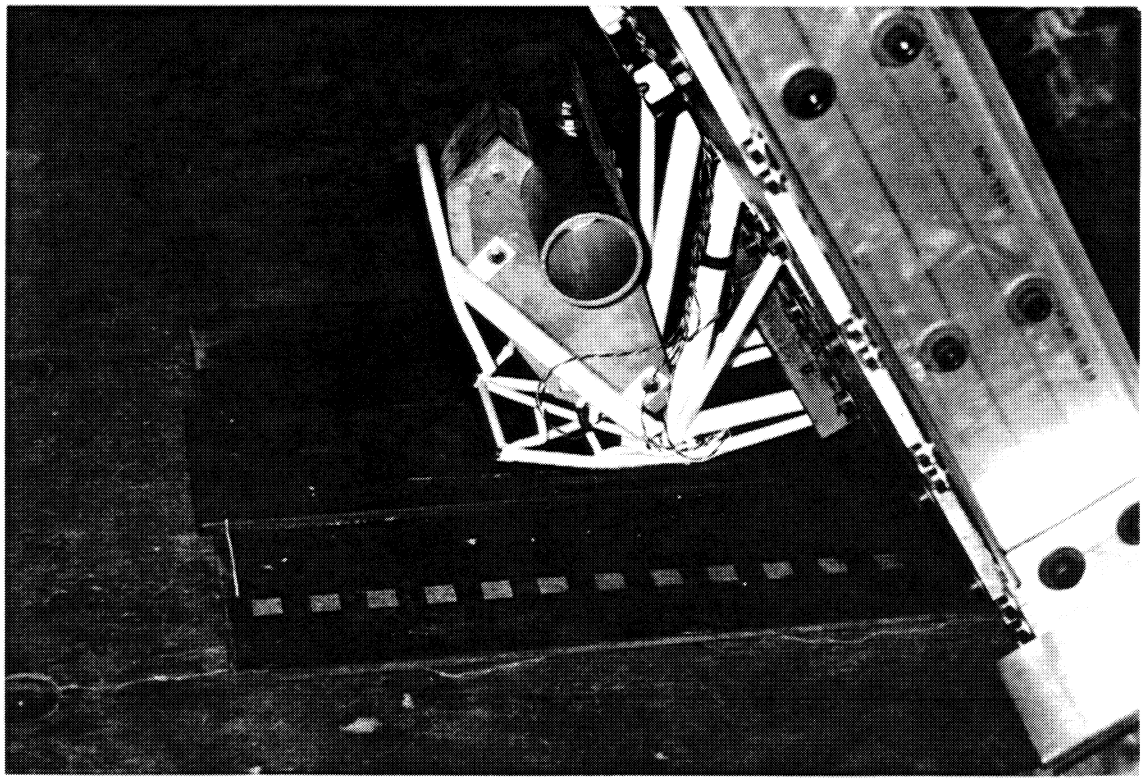

(d), End of Test

Figure 12, (concluded)

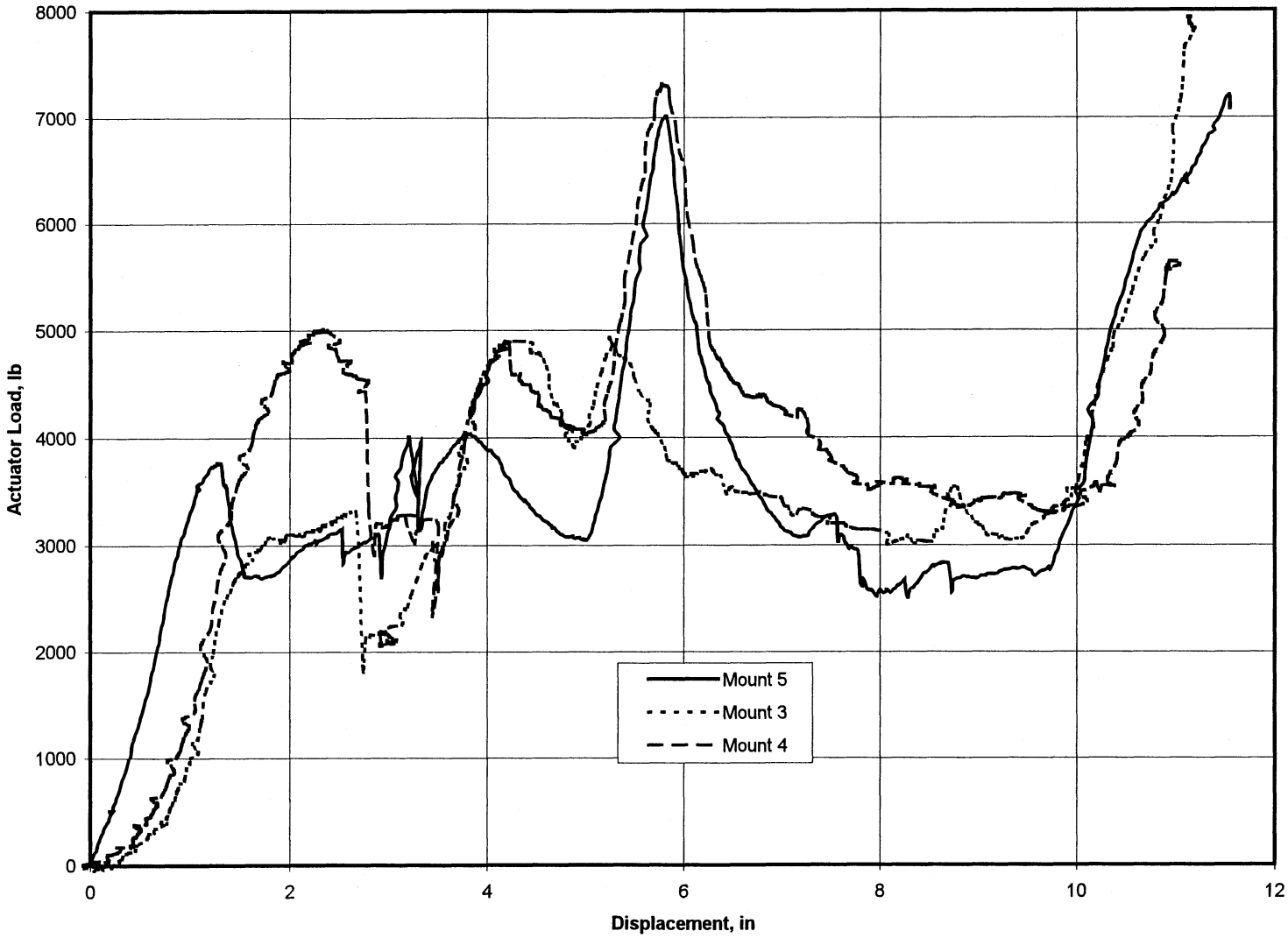

Figure 13, Comparison of Test Data for Three Half Scale Mounts

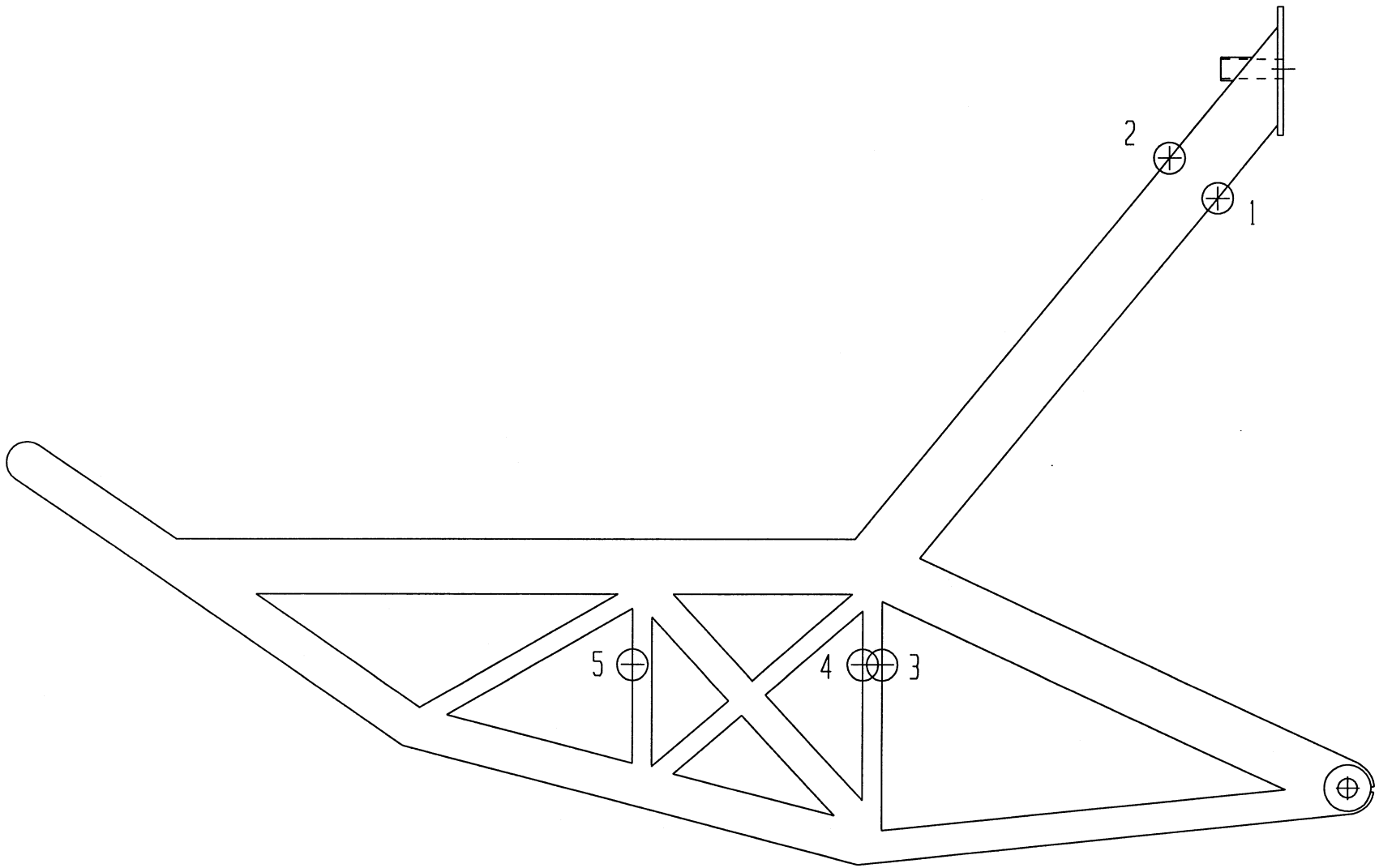

Figure 14, Half Scale Engine Mount Strain Gage Locations

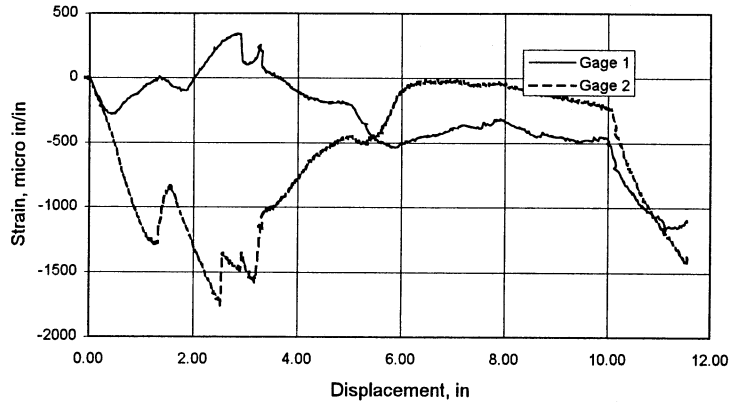

(a), Post

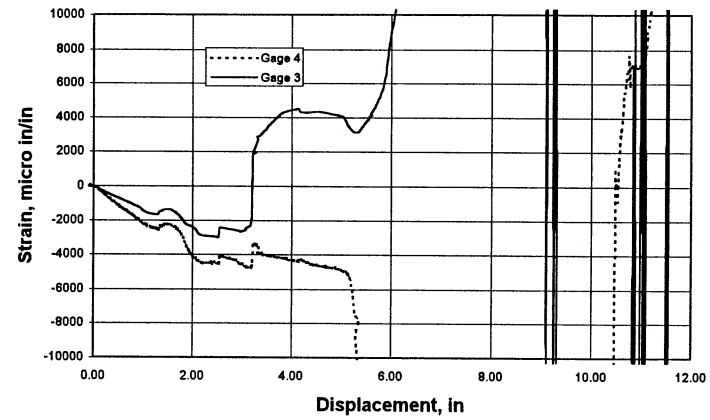

(b), Aft Upright

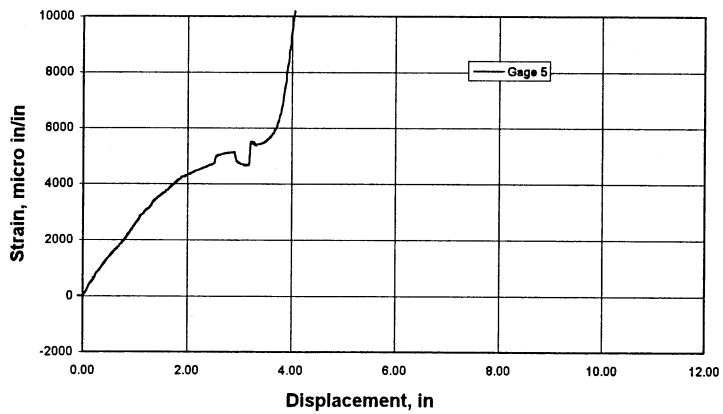

(c), Forward Upright

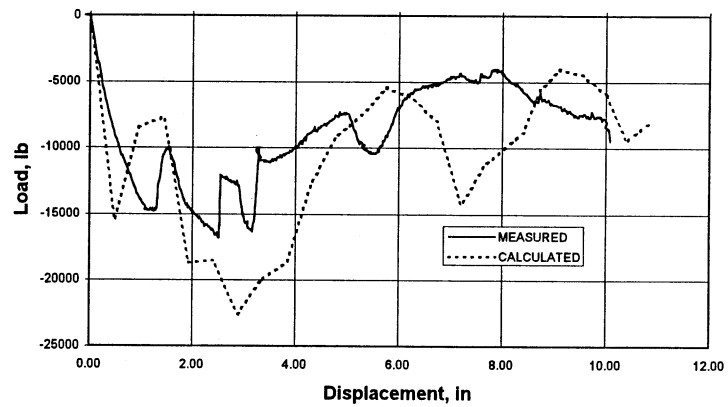

(d), Post Load - Calculated vs. Measured, Full Scale Values

Figure 15, Strain Gage Data for Half Scale Mount 5

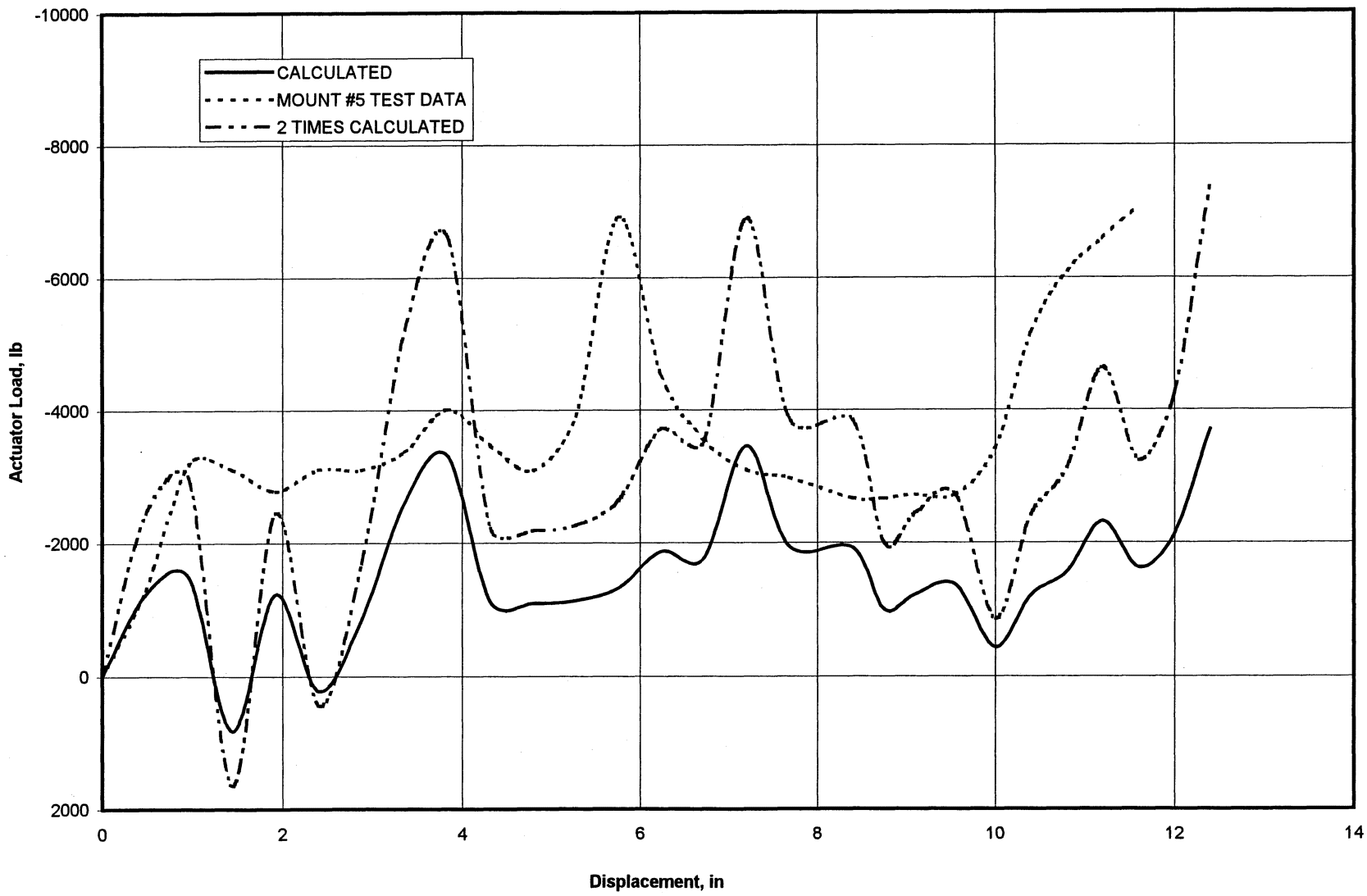

Figure 16, Comparison of Engine Mount Analysis to Test

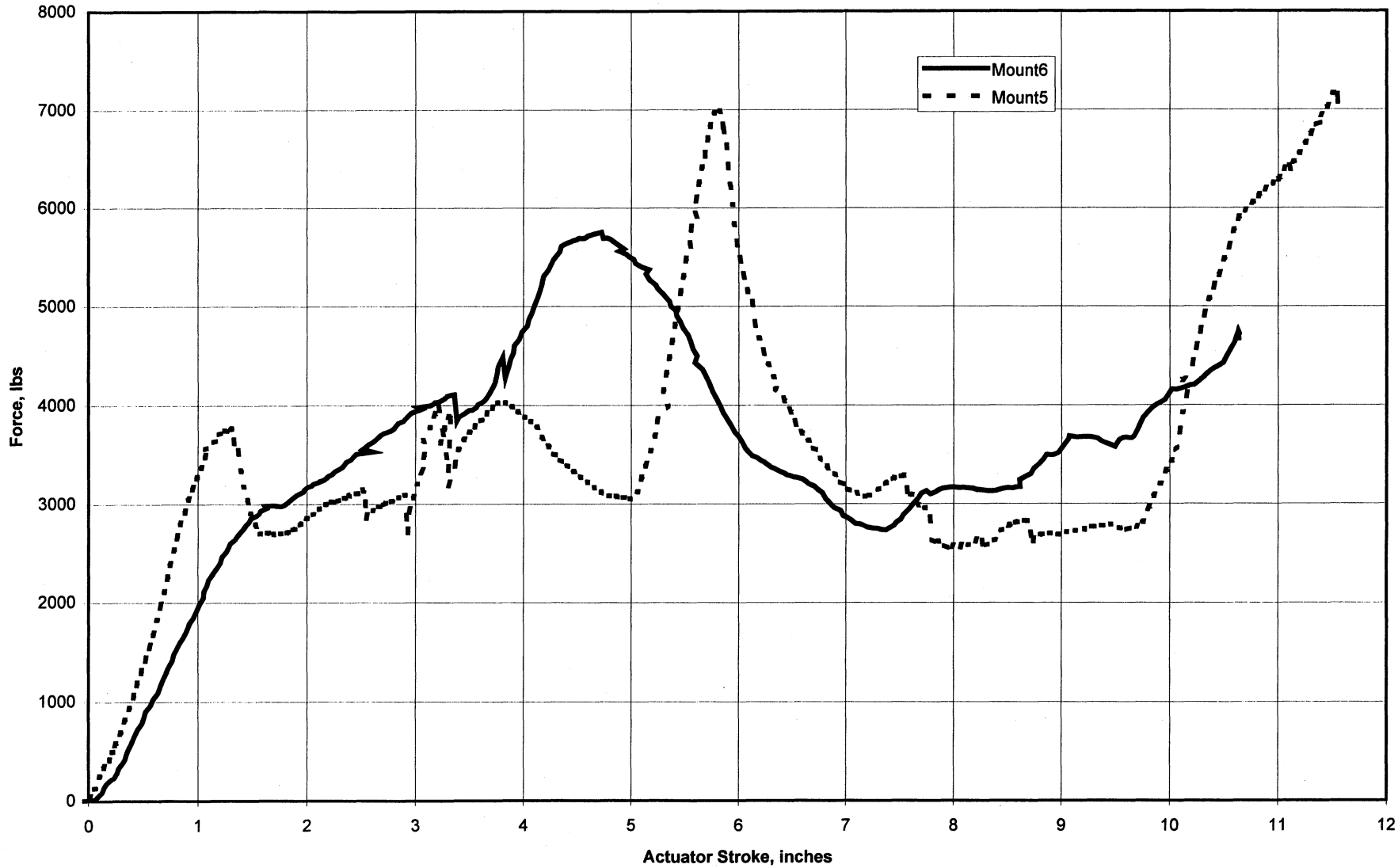

Figure 17, Data Comparison for Half Scale Mounts 5 and 6

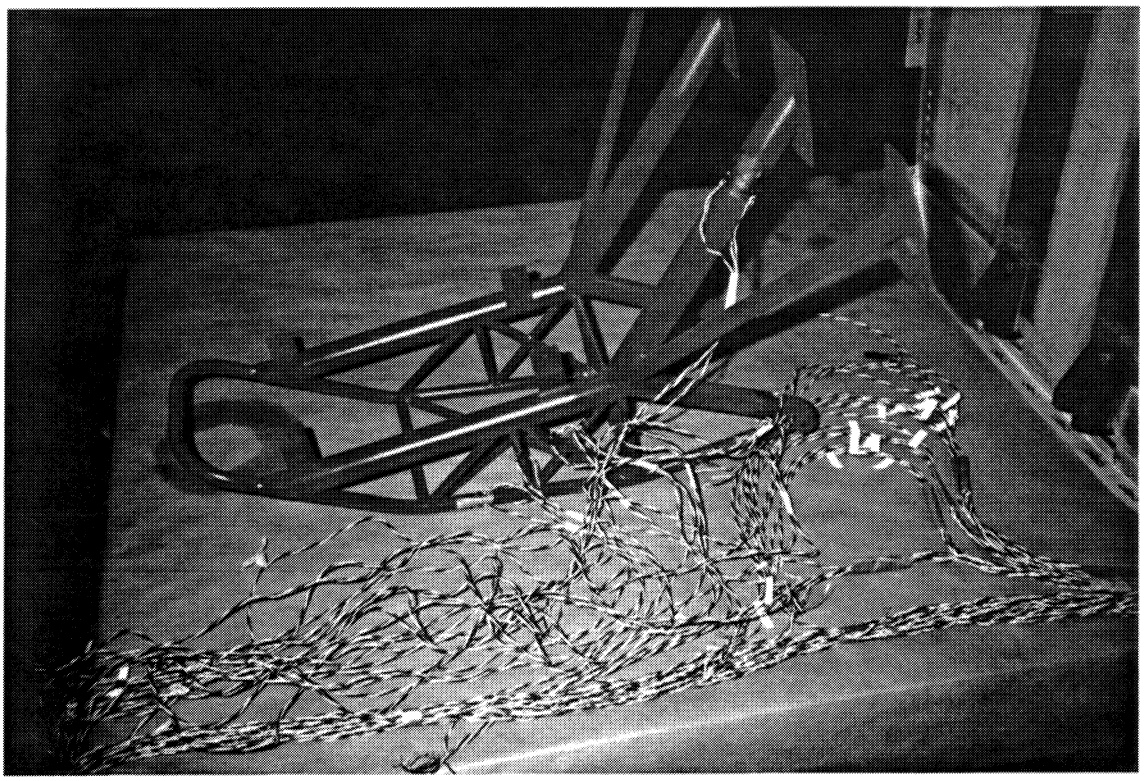

(a), Pretest Showing Strain Gage Installation

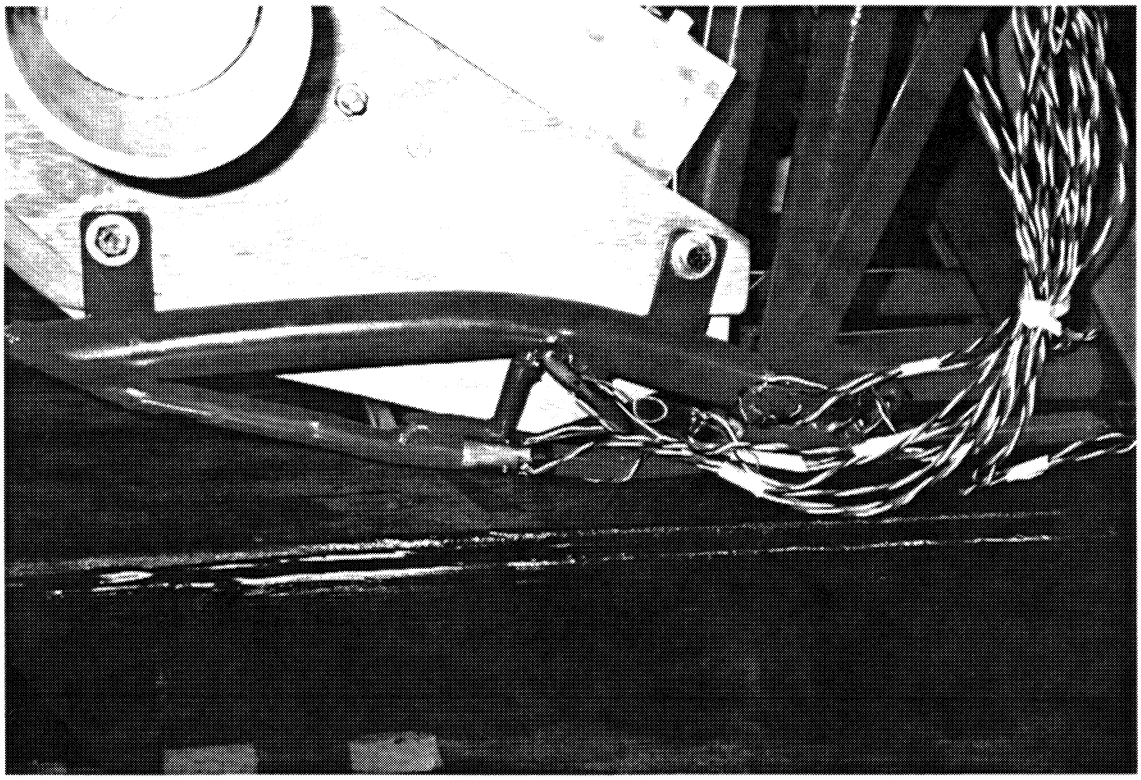

(b), Post Test

Figure 18, Half Scale Mount 6

aircrft1 model

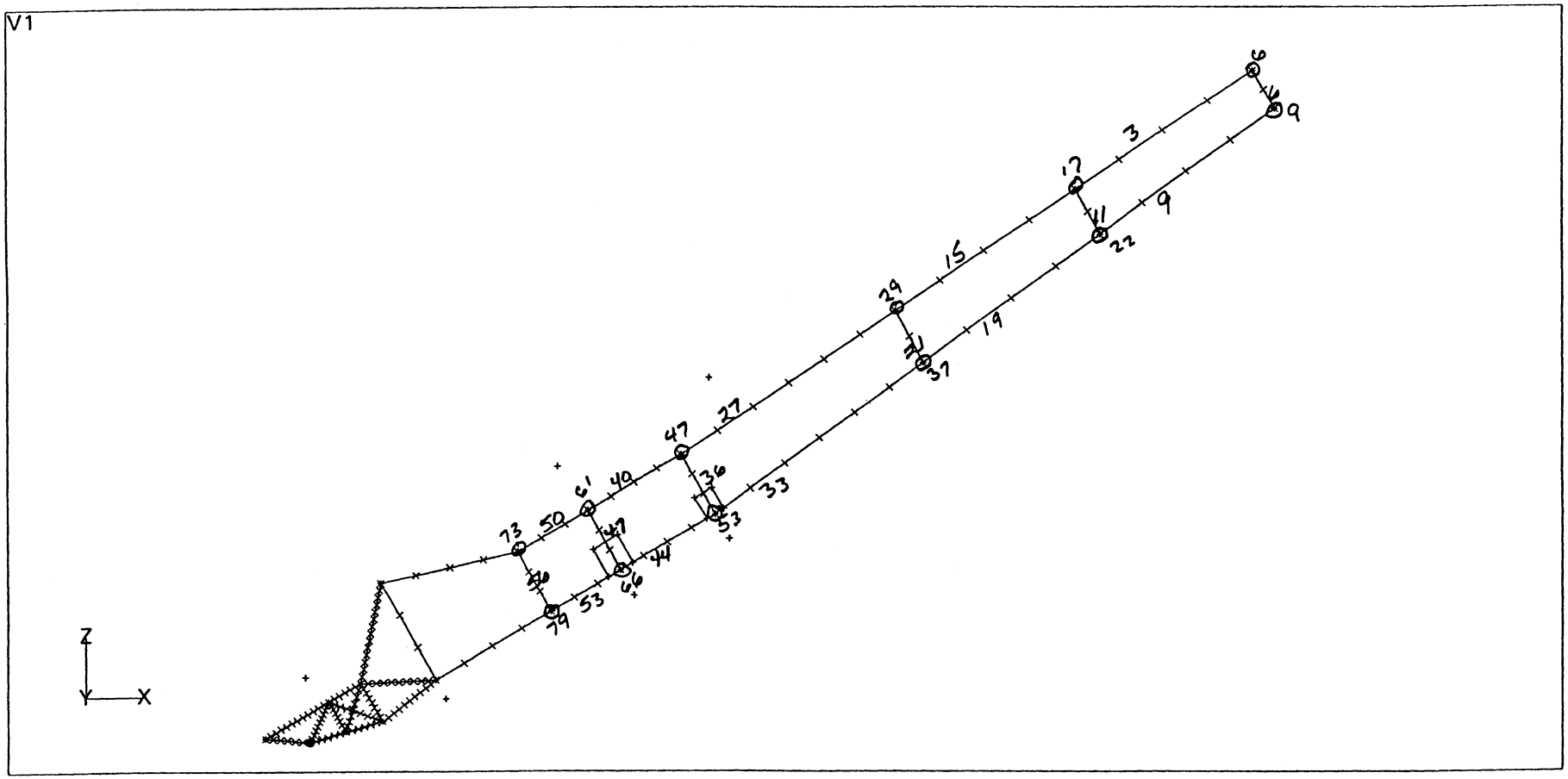

Figure 19, First Aircraft Dynamics Analysis Model

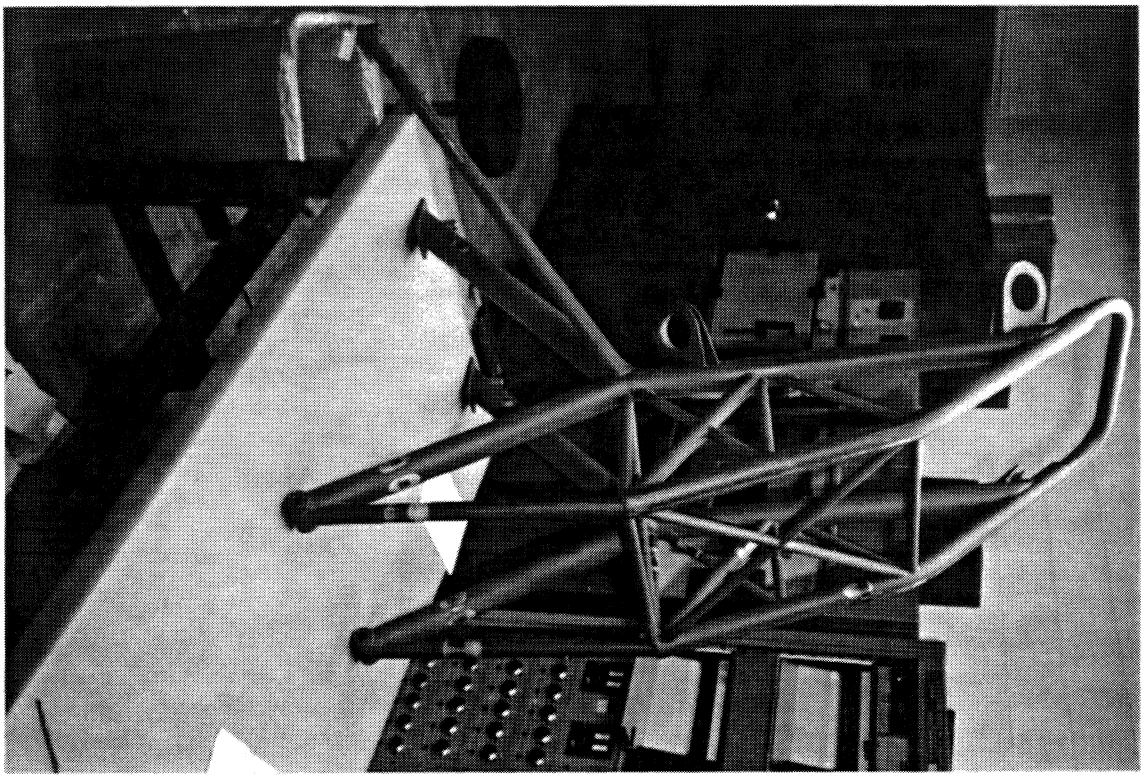

Figure 20, First Full Size Engine Mount with Strain Gages Installed

(a), Copilot

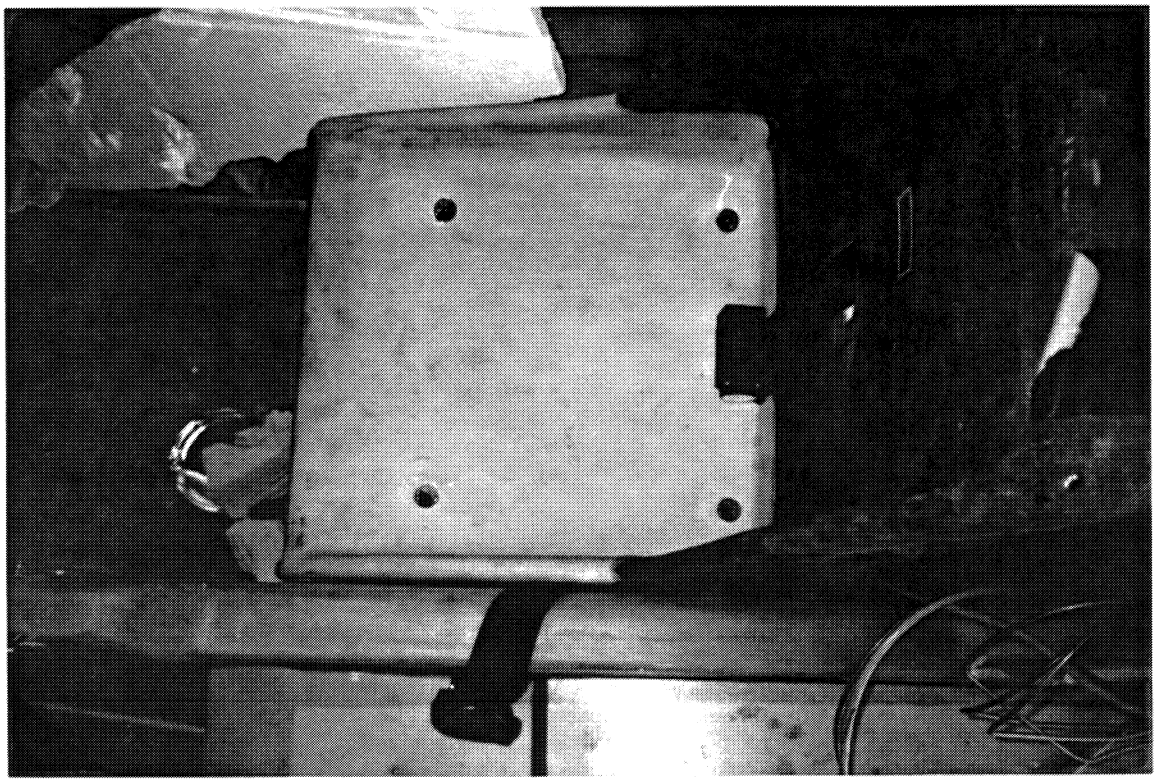

(b), Pilot

Figure 21, Full Scale Test Seats

(a), Impact Position

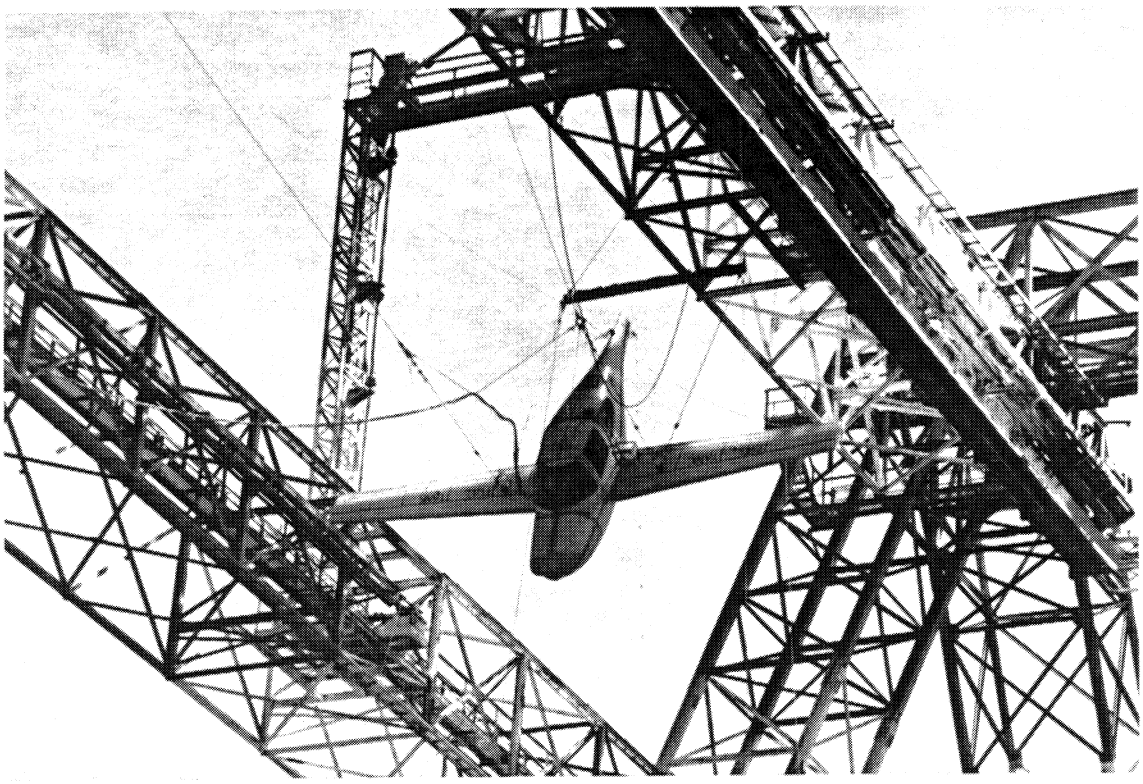

(b), Pullback Position

Figure 22, First Full Scale Test Airplane

Impact

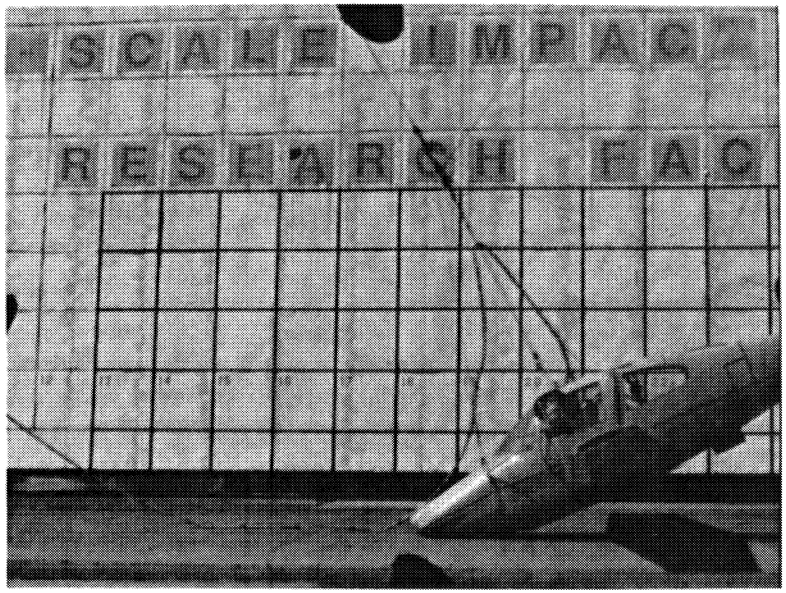

t = .010 seconds

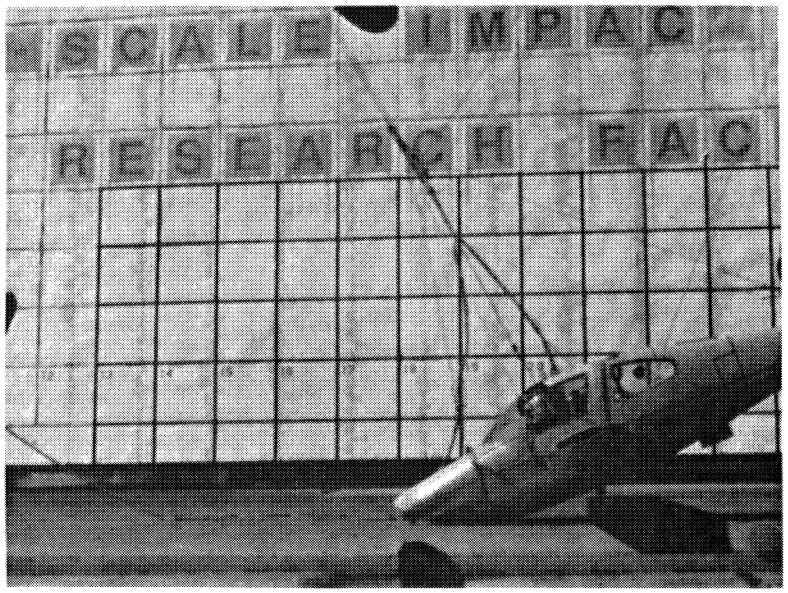

t = .020 seconds

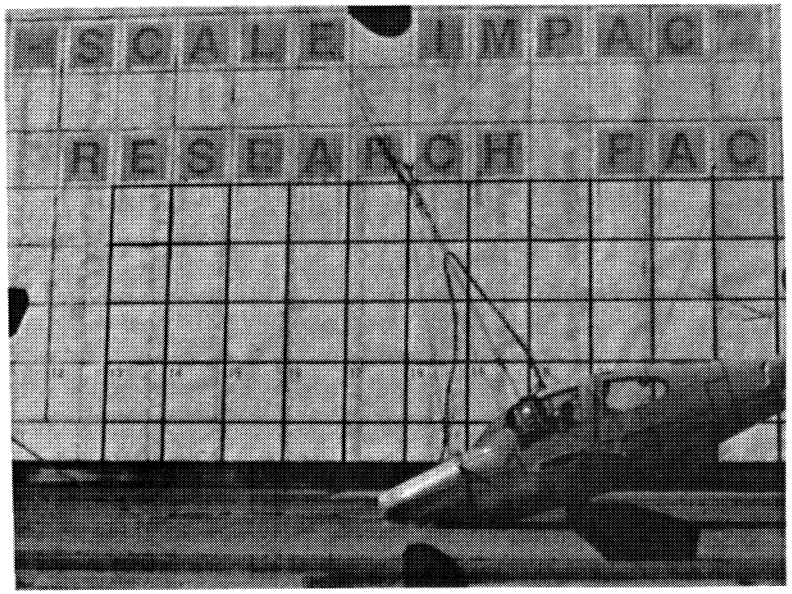

t = .030 seconds

Figure 23, Crash Sequence Photographs for Test 1

t = .040 seconds

t = .050 seconds

t = .060 seconds

t = .070 seconds

Figure 23, (continued)

t = .080 seconds

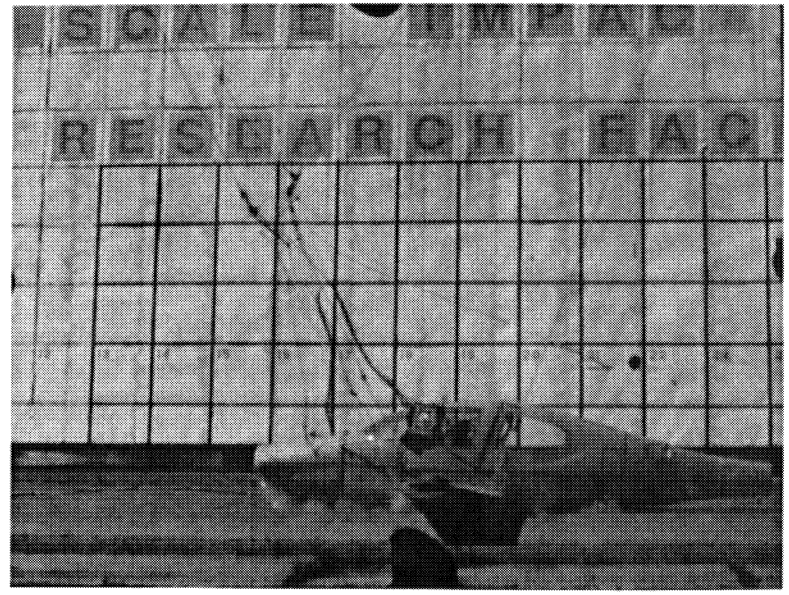

t = .090 seconds

t = .100 seconds

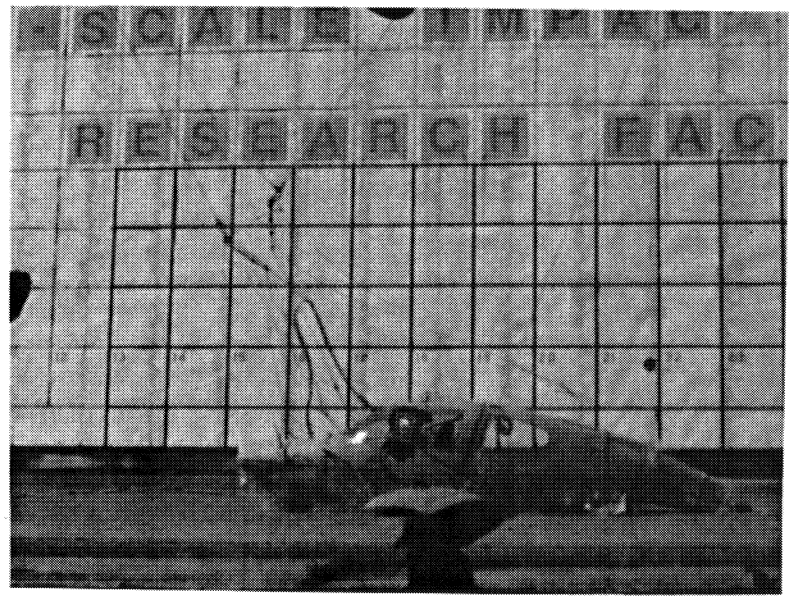

t = .110 seconds

Figure 23, (concluded)

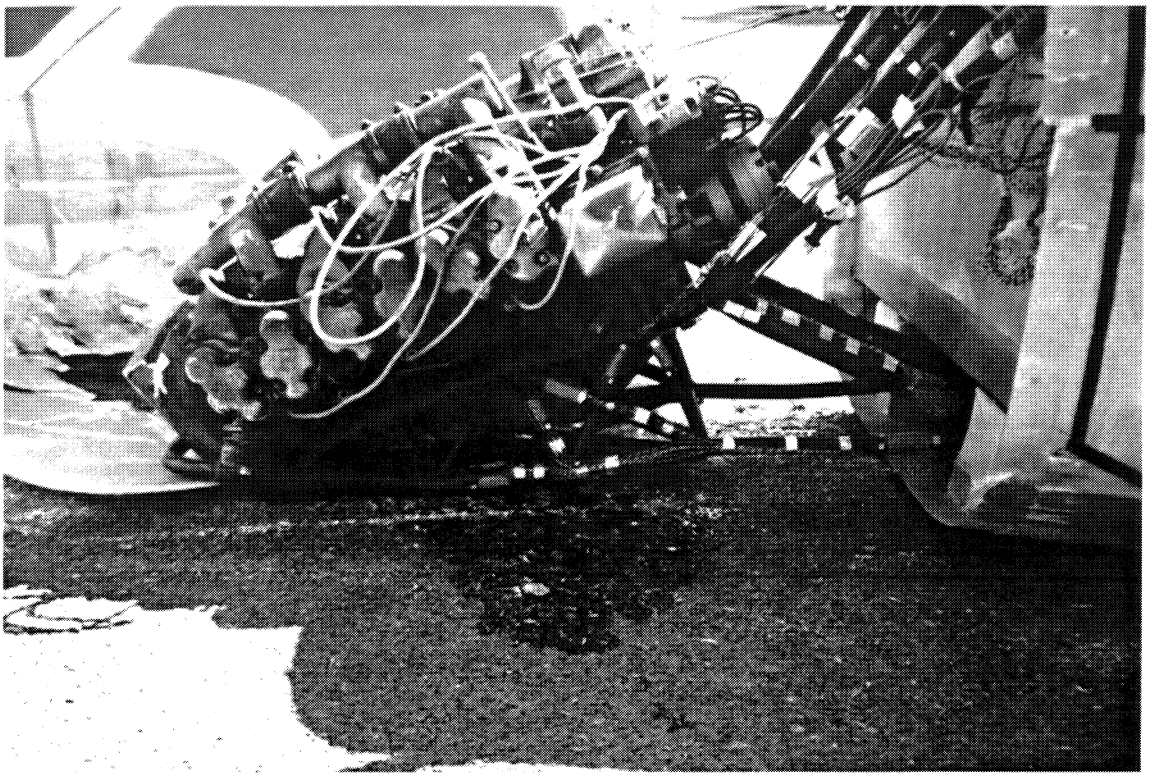

(a), Engine and Engine Mount

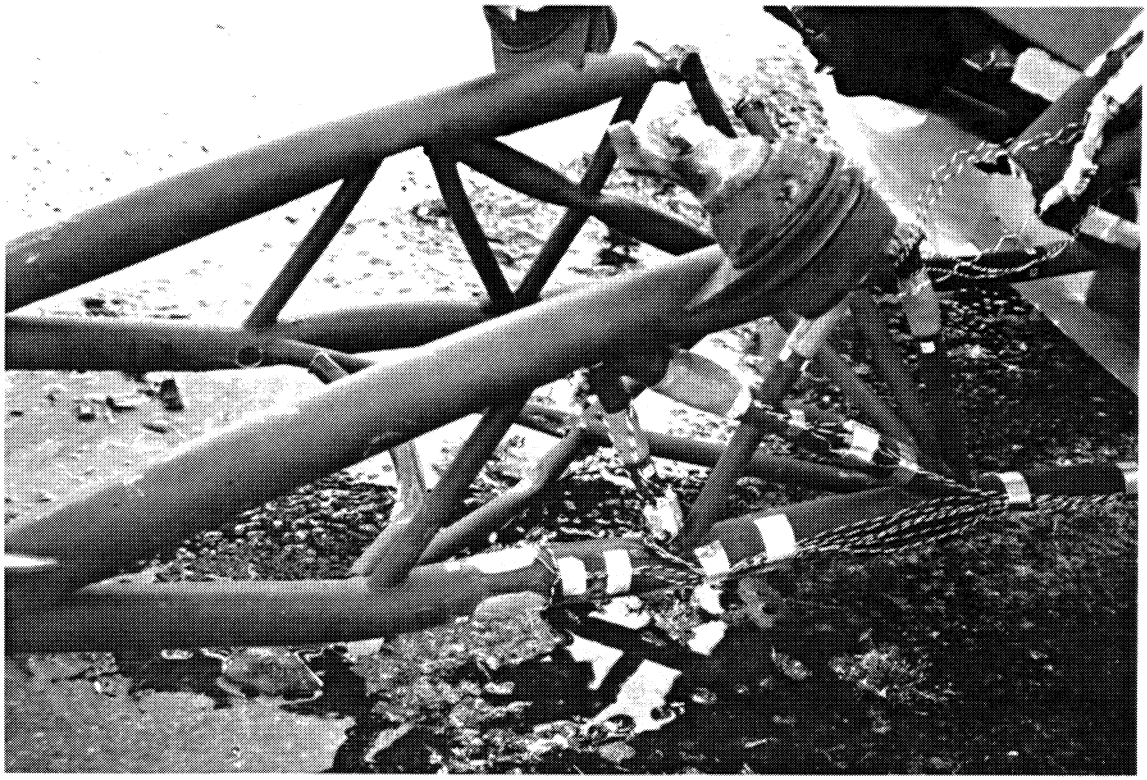

(b), Engine Mount Close Up

Figure 24, Post Crash Damage for Test 1

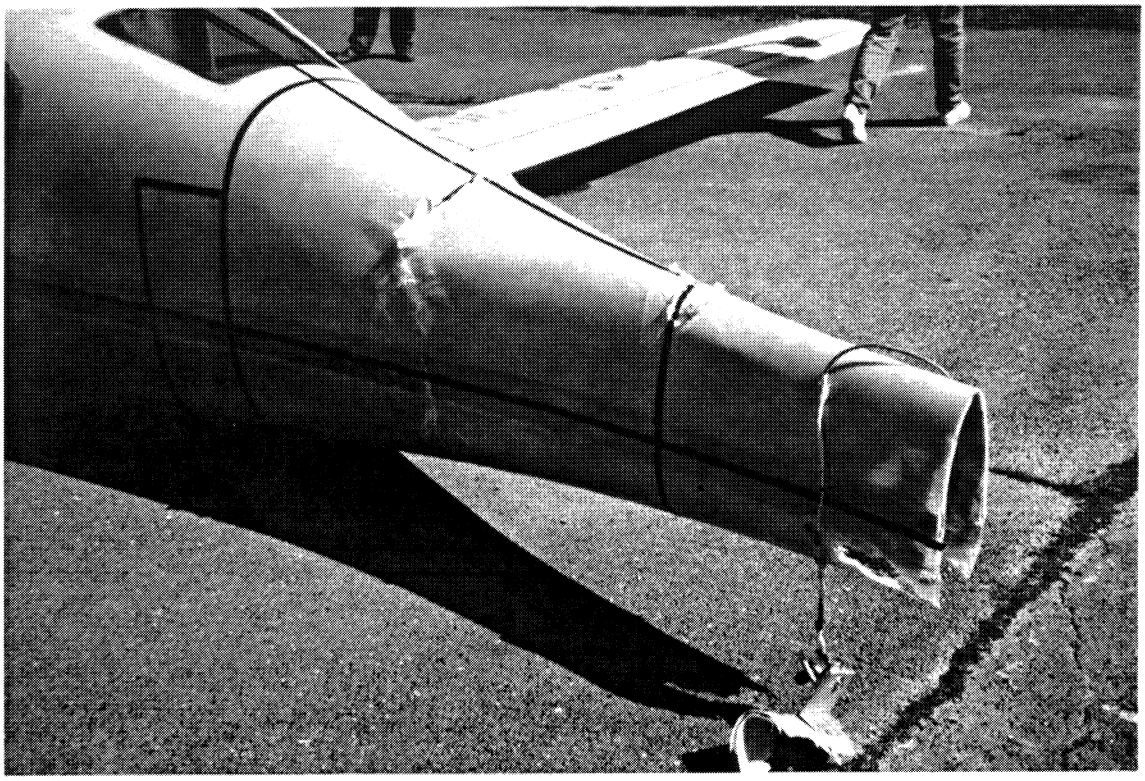

(c), Aft Fuselage

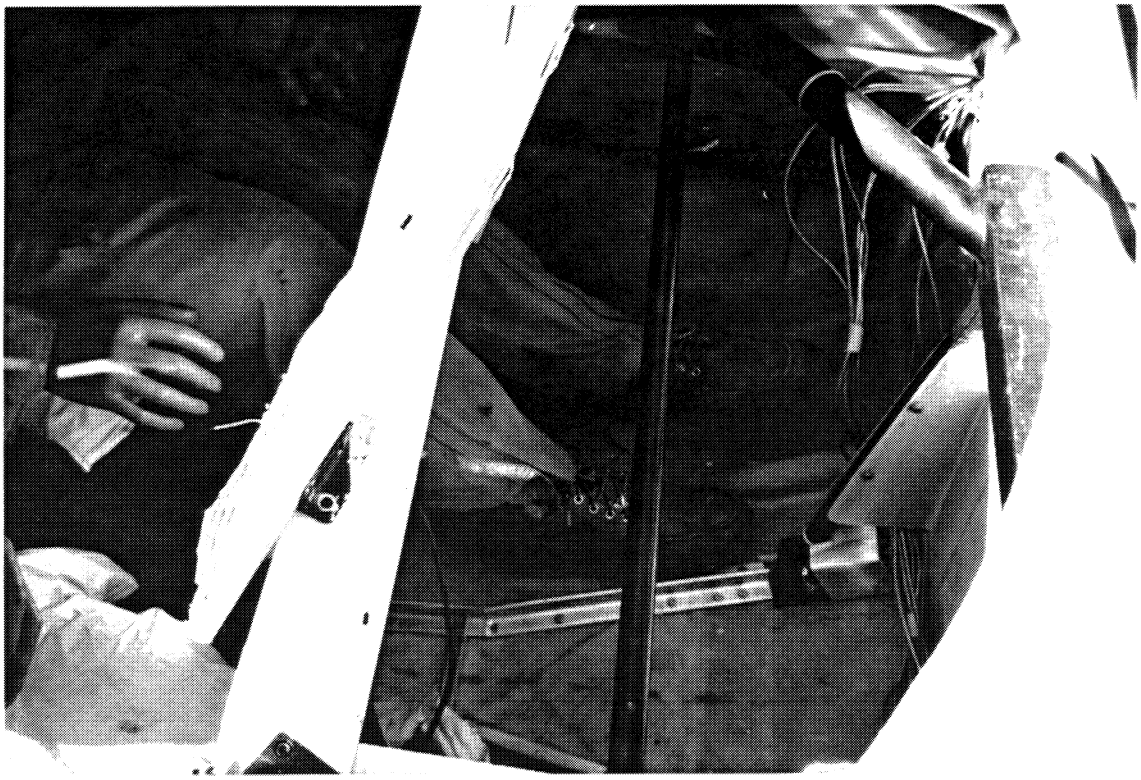

(d), Pilot's Foot Space

Figure 24, (continued)

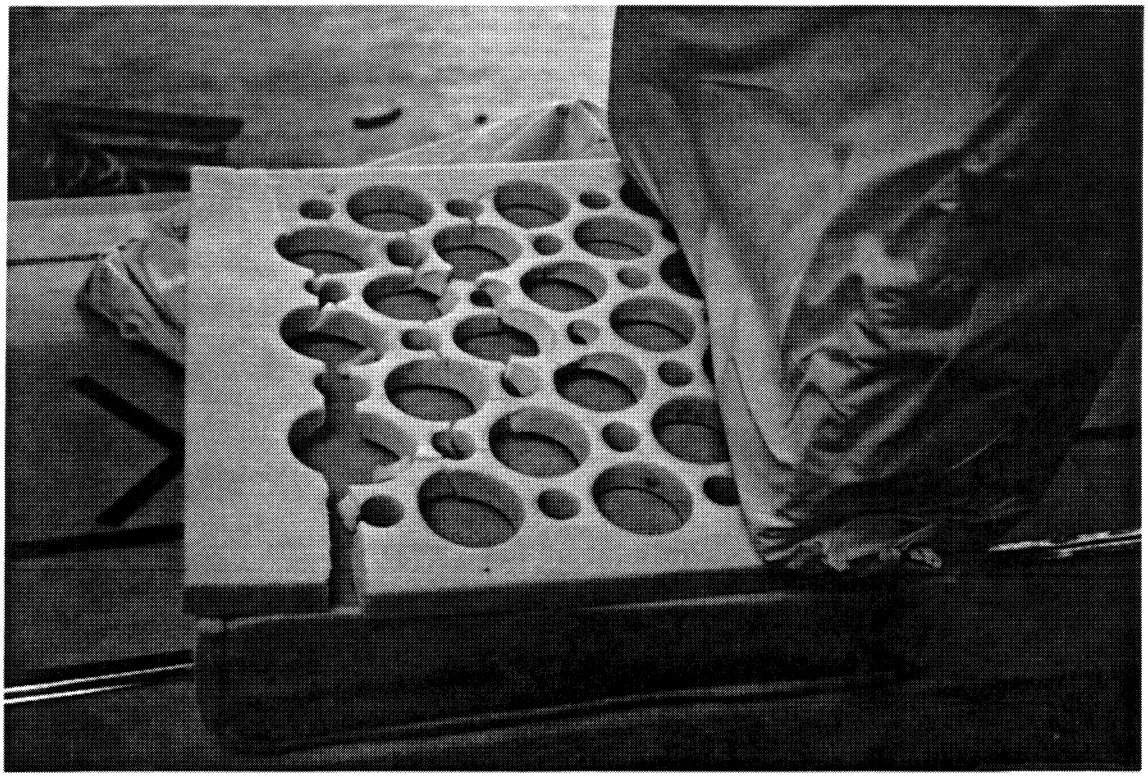

(e), Copilot Under Cushion Energy Absorber

Figure 24, (concluded)

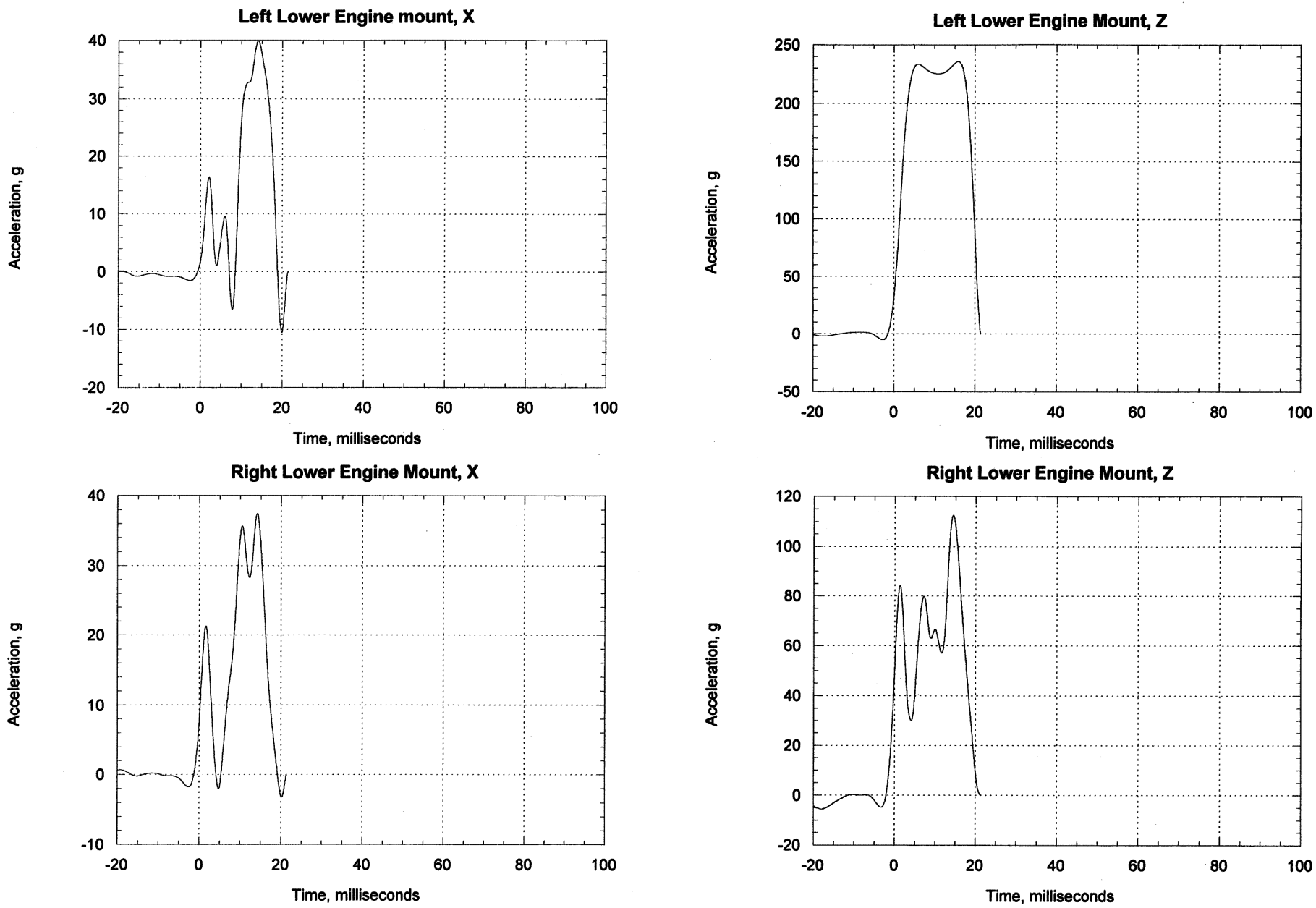

Figure 25, Test 1, Lower Firewall Accelerations

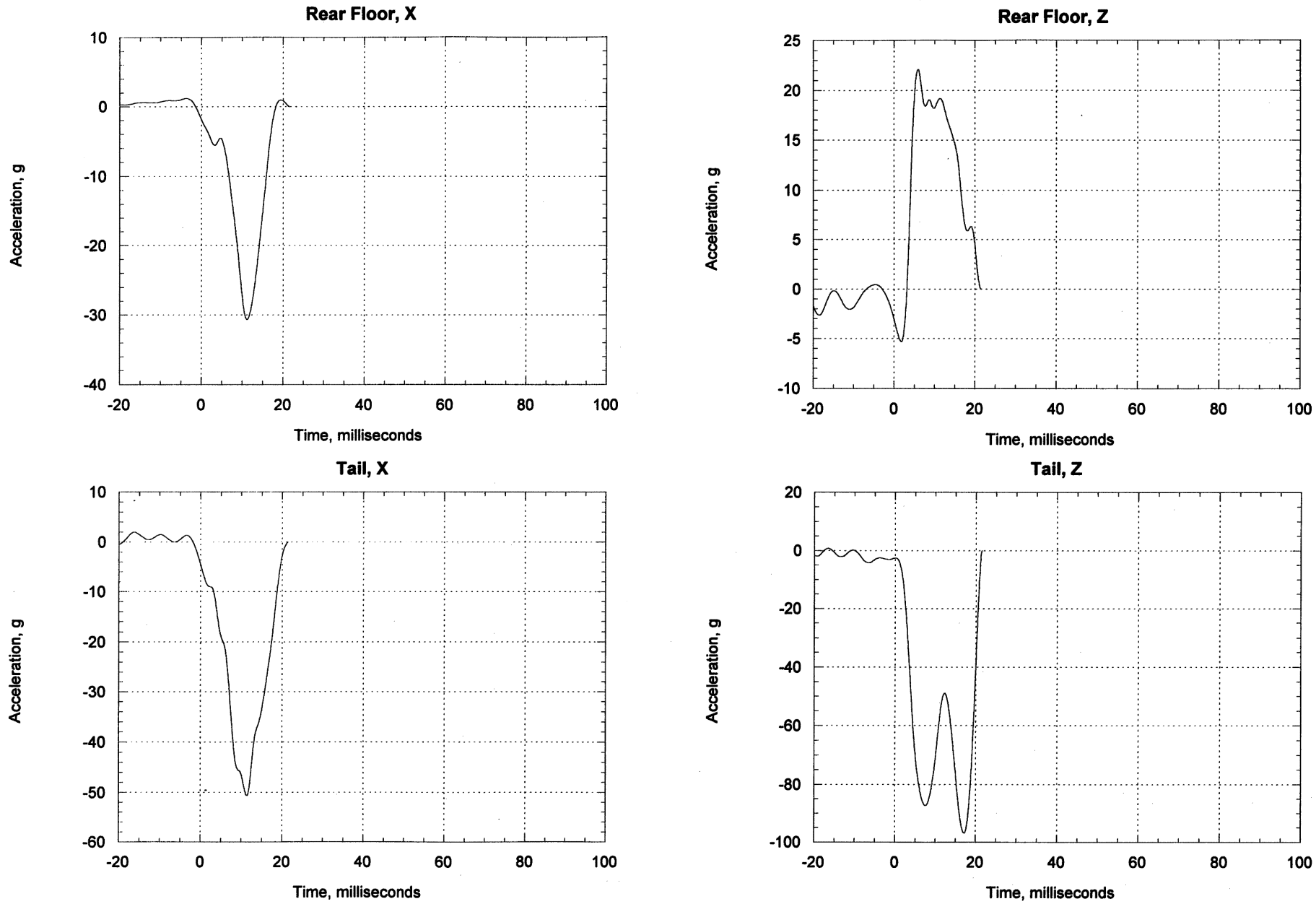

Figure 26, Test 1, Aft Airframe Accelerations

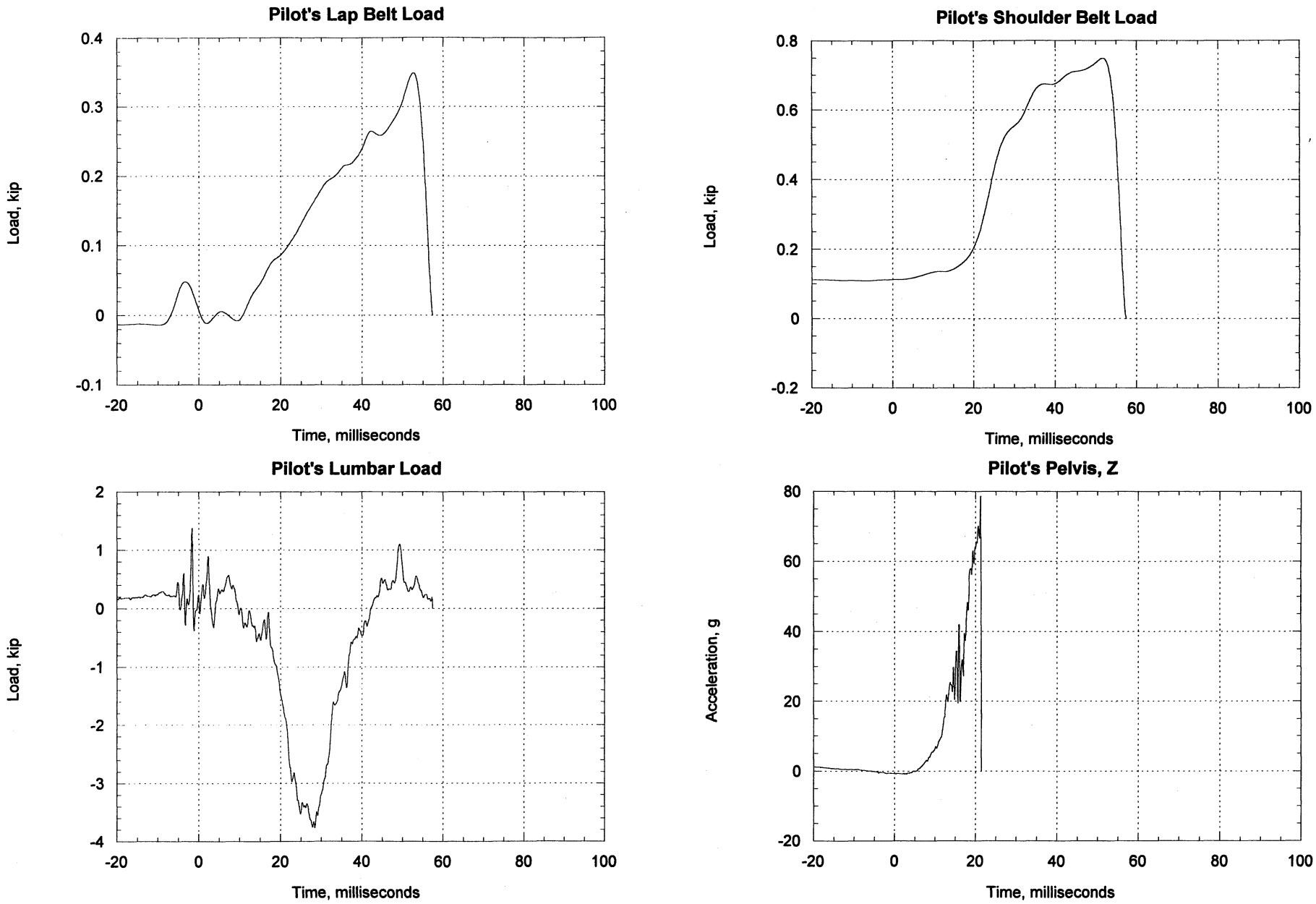

Figure 27, Test 1, Pilot

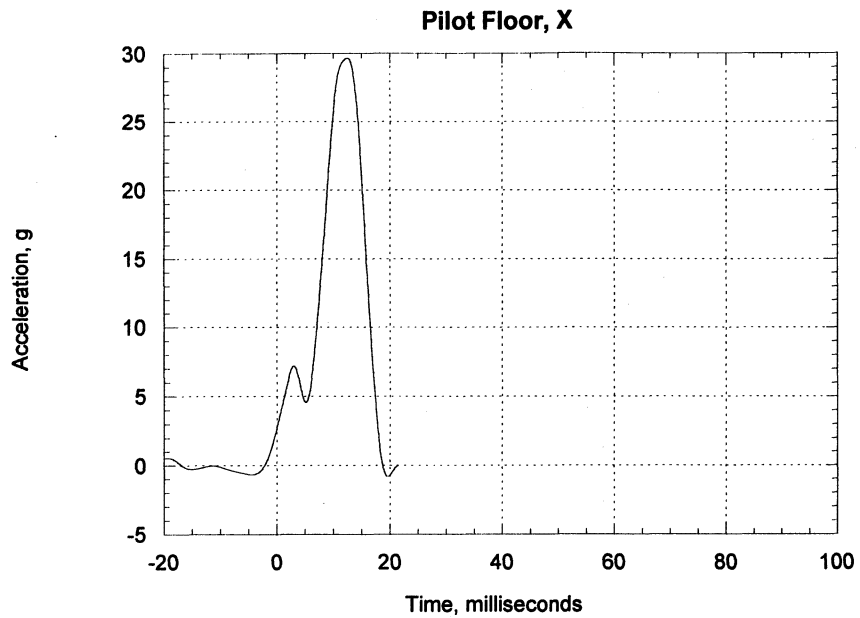

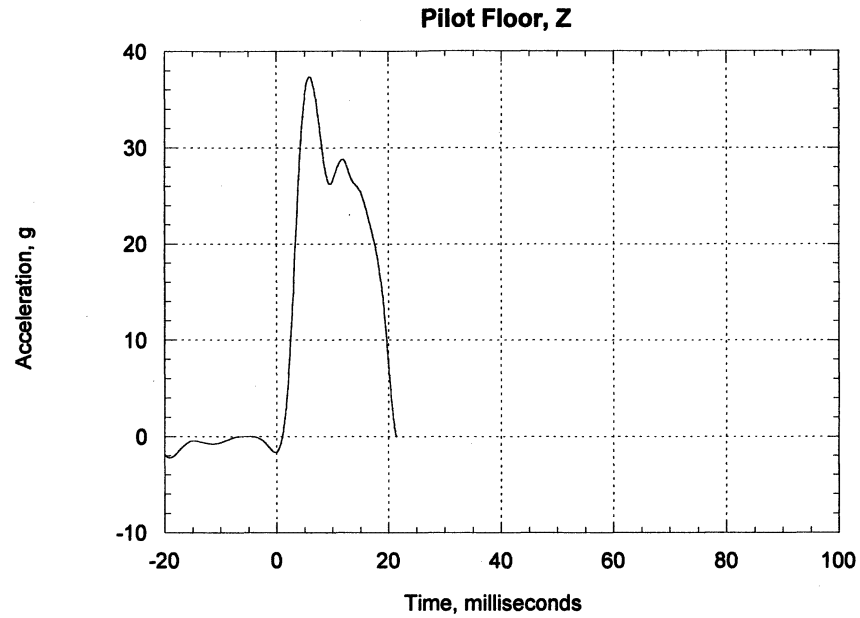

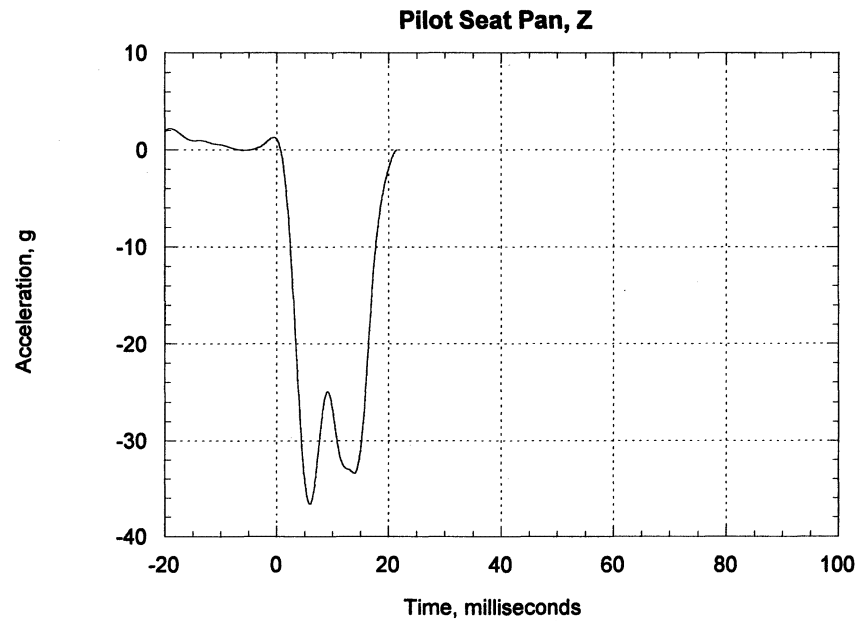

Figure 28, Test 1, Pilot's Seat & Floor

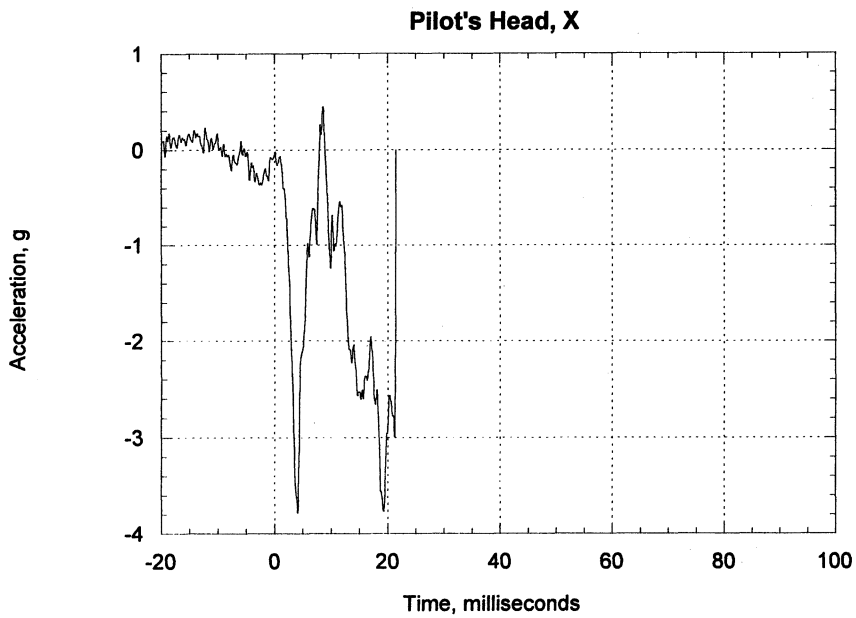

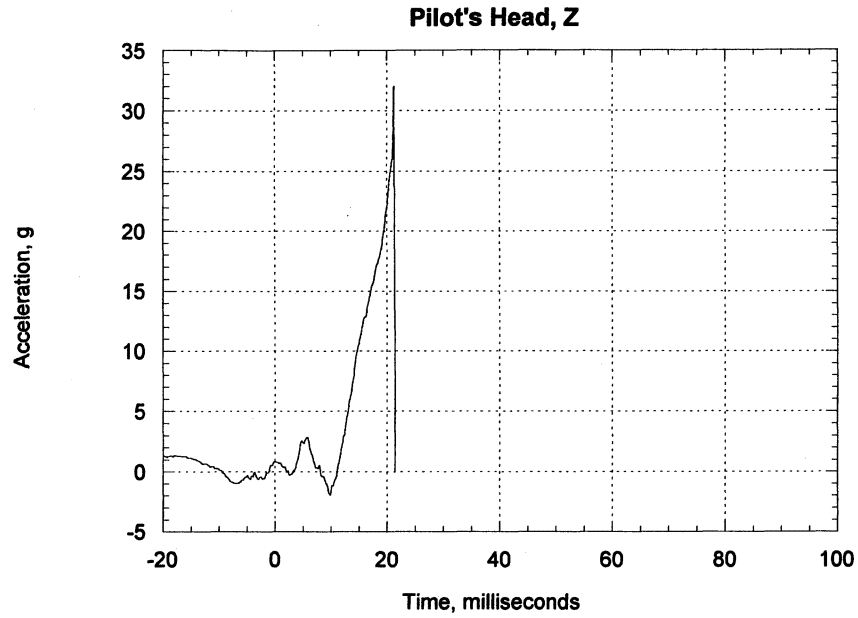

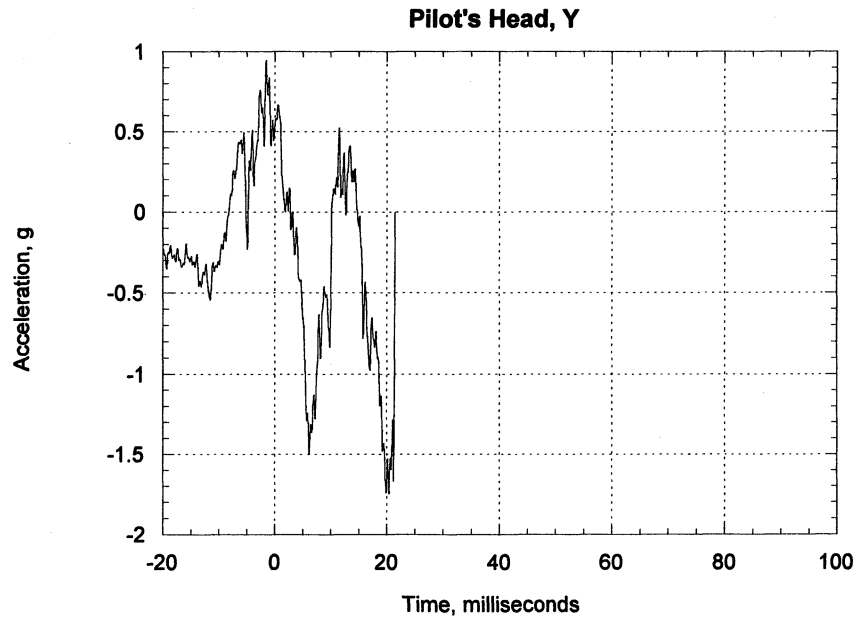

Figure 29, Test 1, Pilot's Head

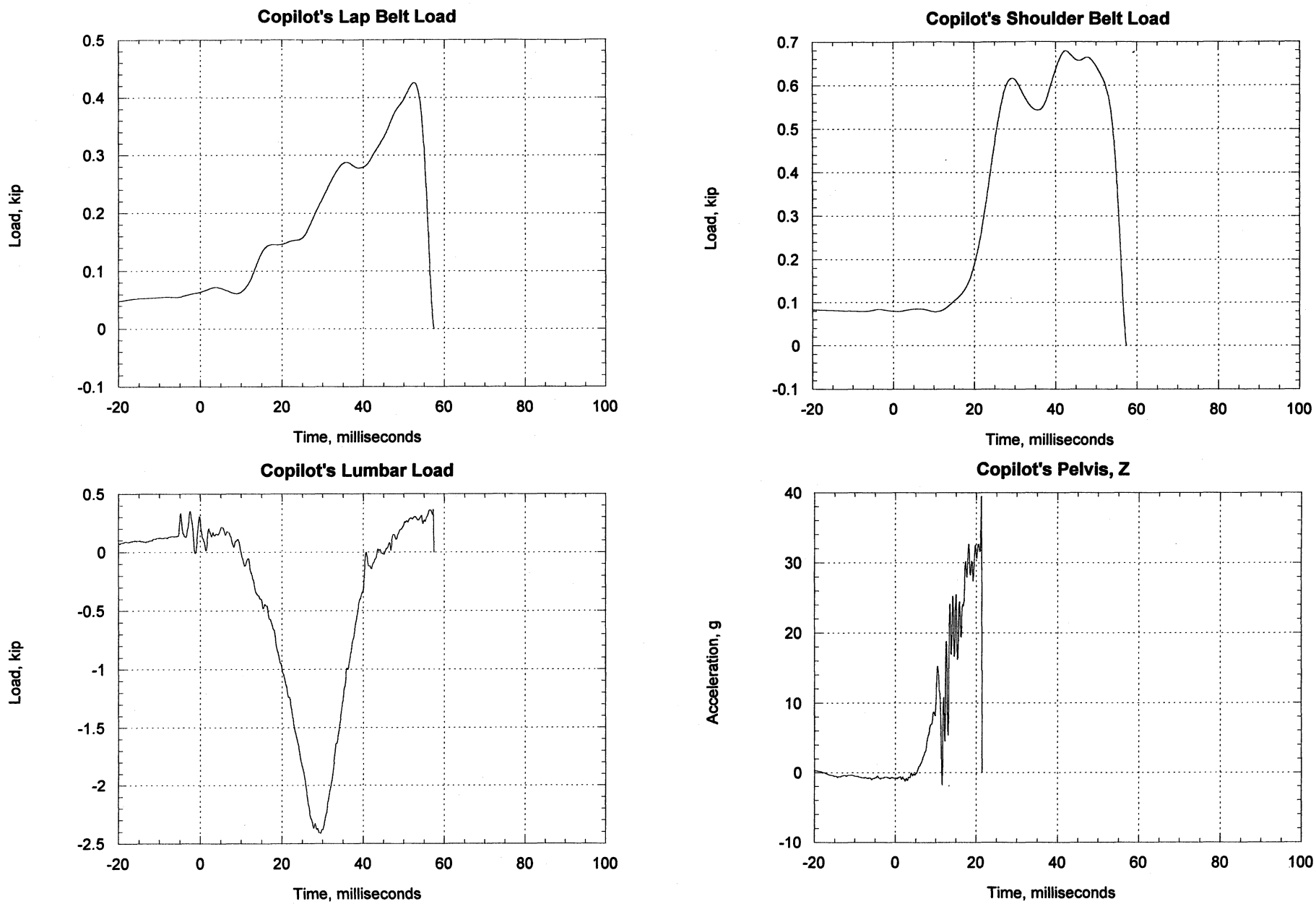

Figure 30, Test 1, Copilot

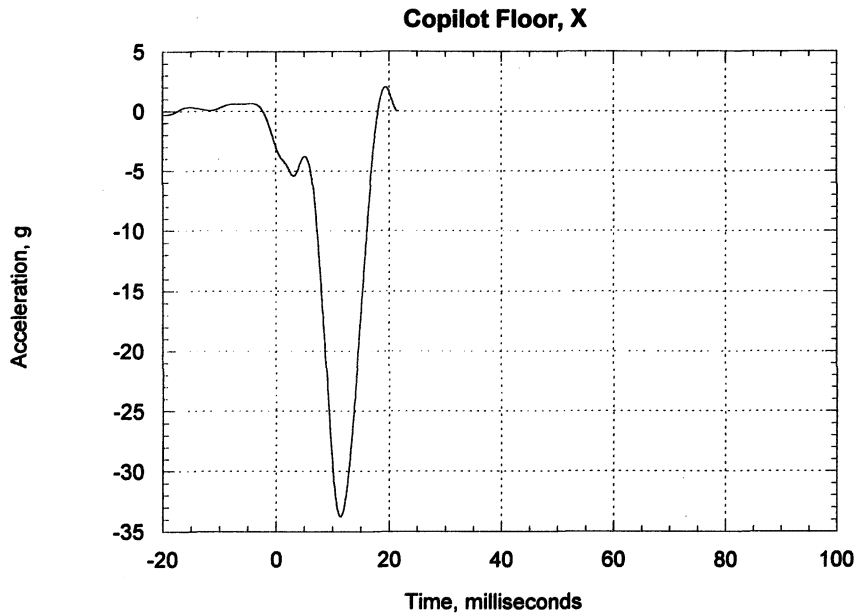

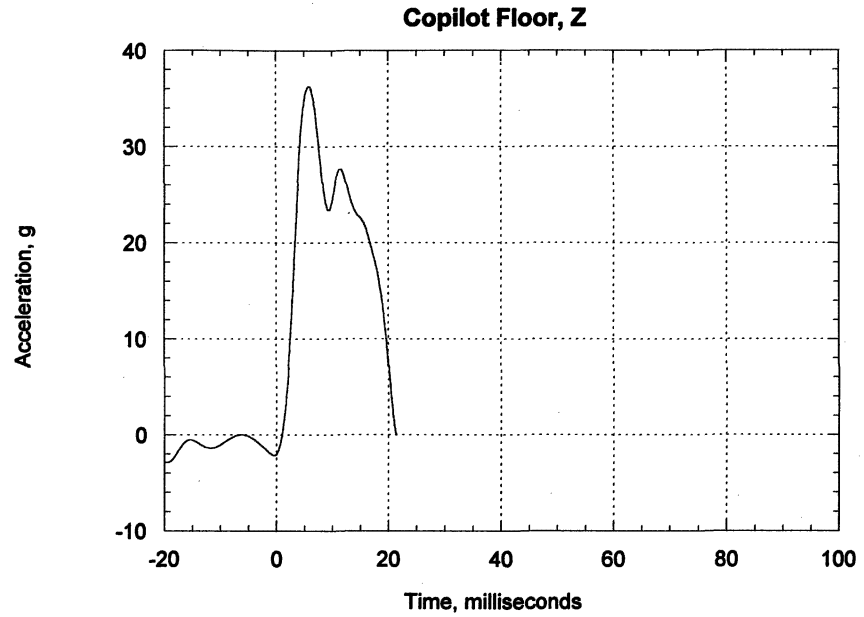

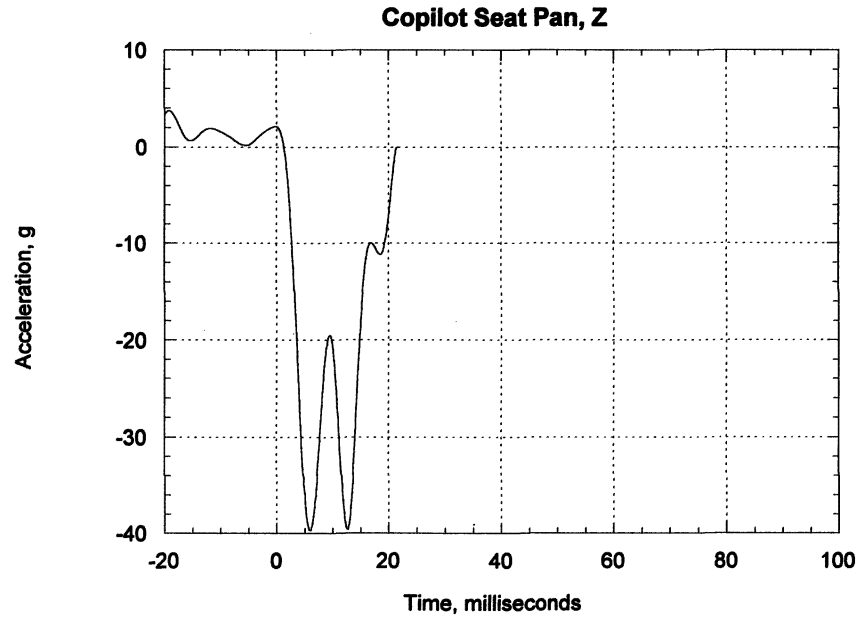

Figure 31, Test 1, Copilot's Seat & Floor

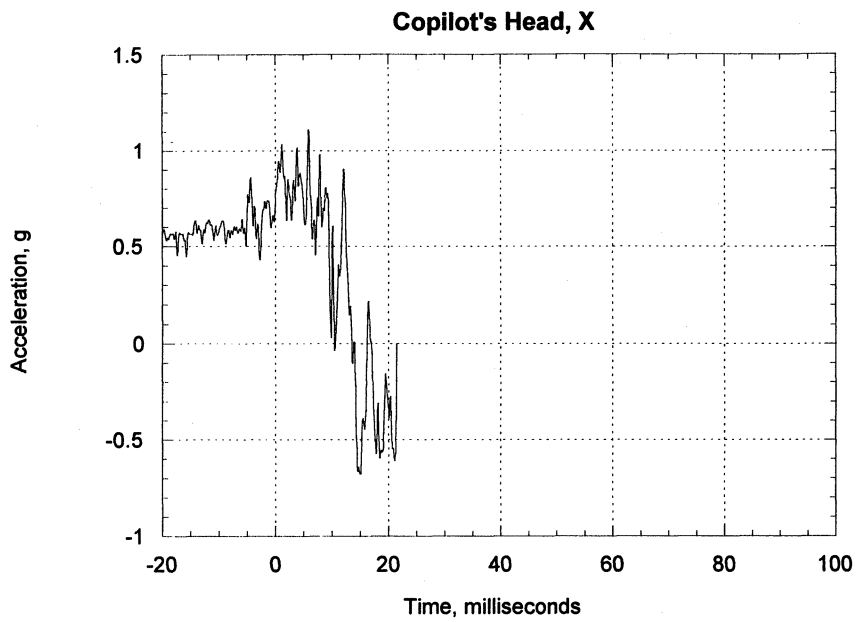

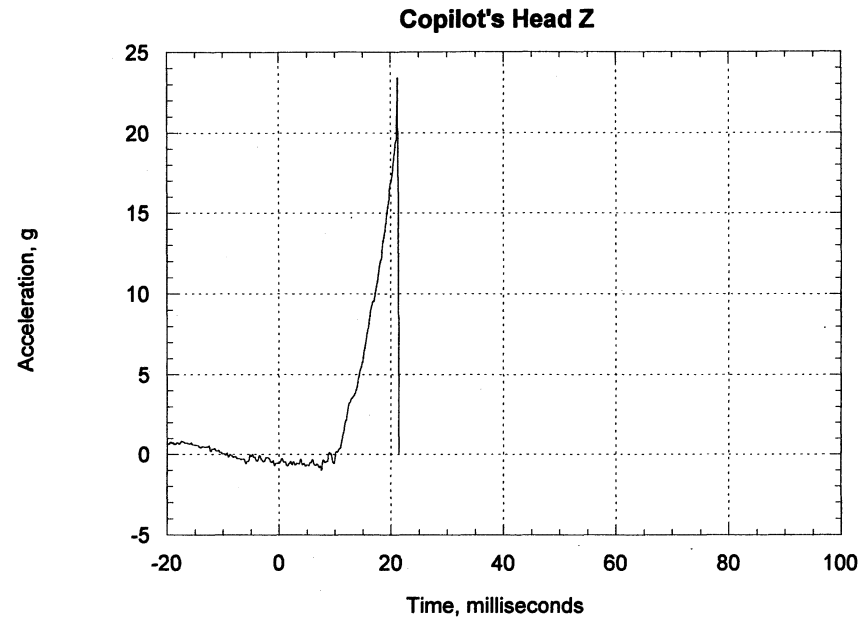

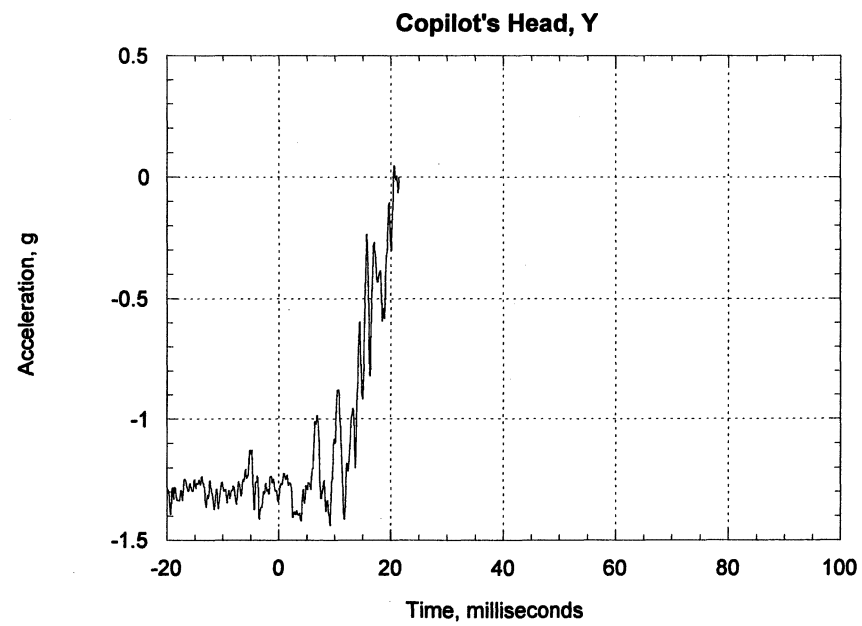

Figure 32, Test 1, Copilot's Head

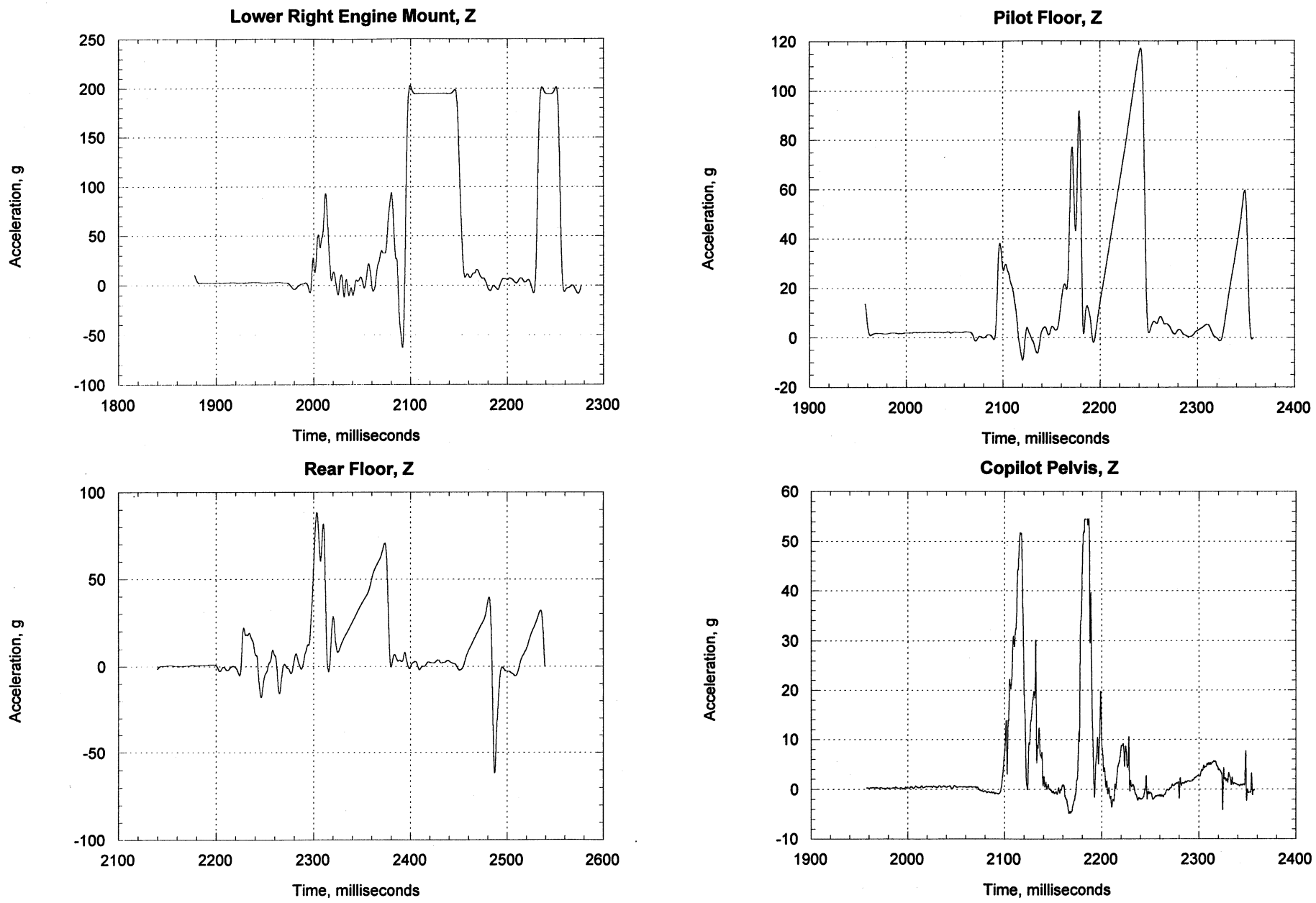

Figure 33, Test 1, Analog Data

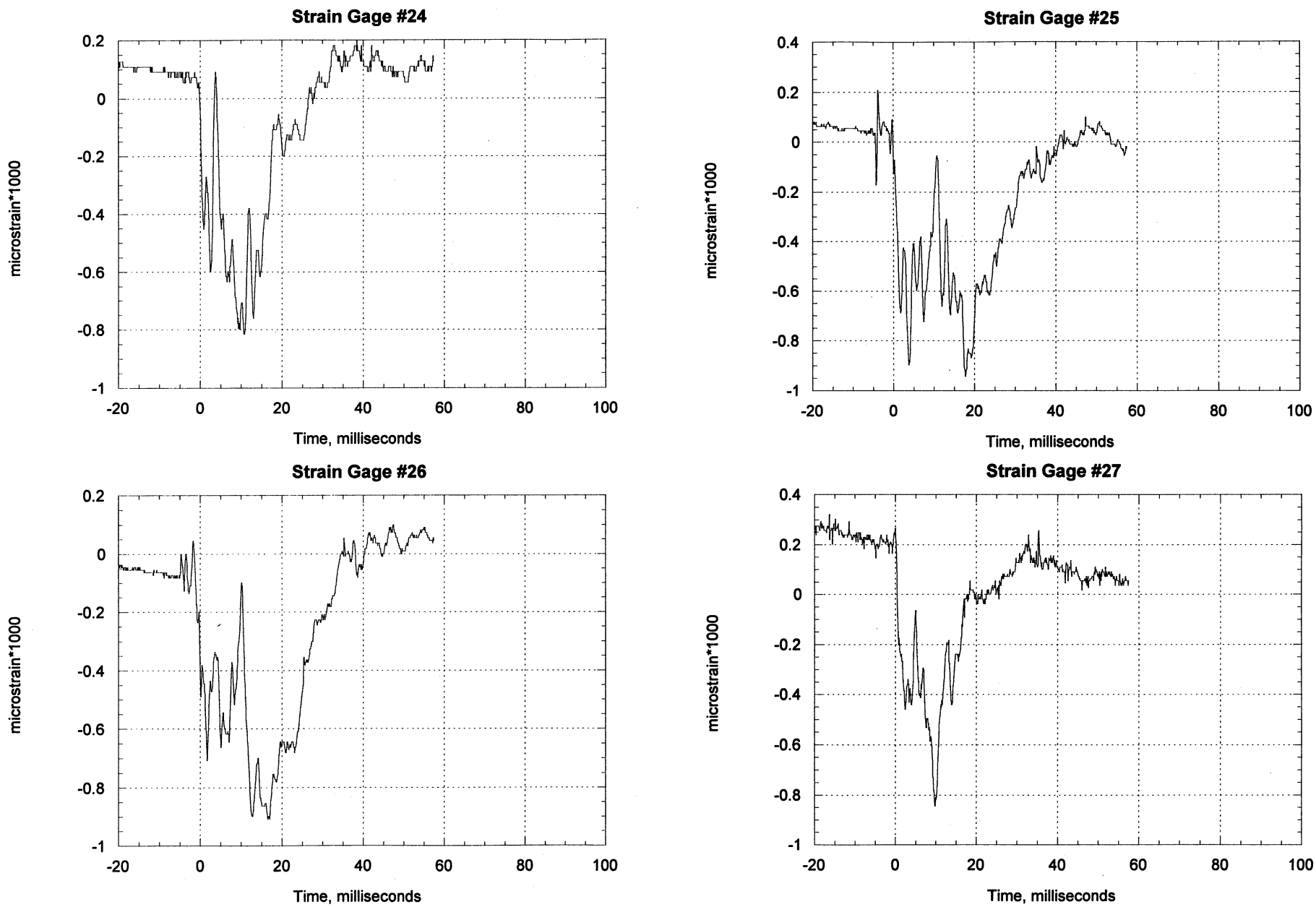

Figure 34, Test 1, Engine Mount, Left Post

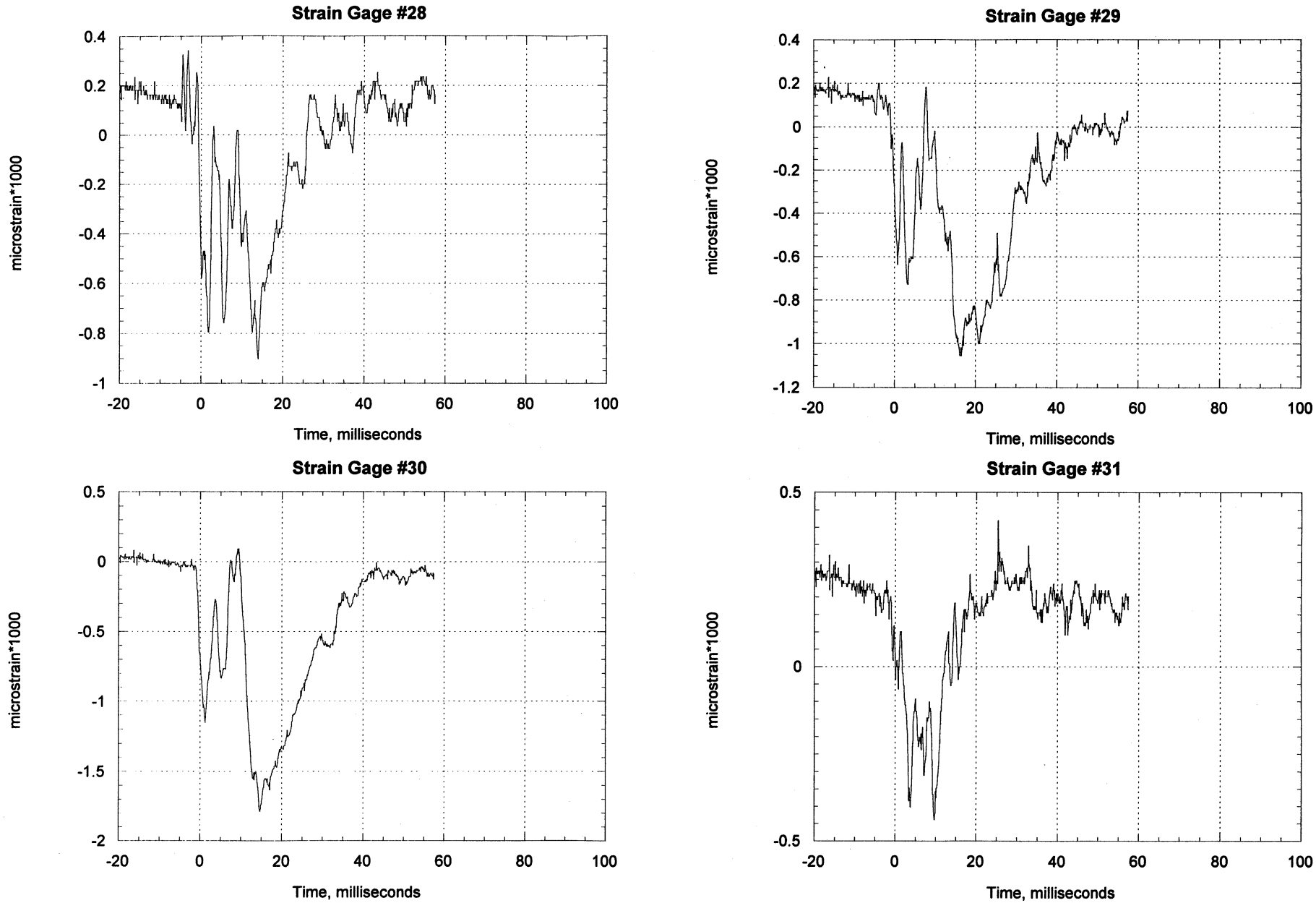

Figure 35, Test 1, Engine Mount, Right Post

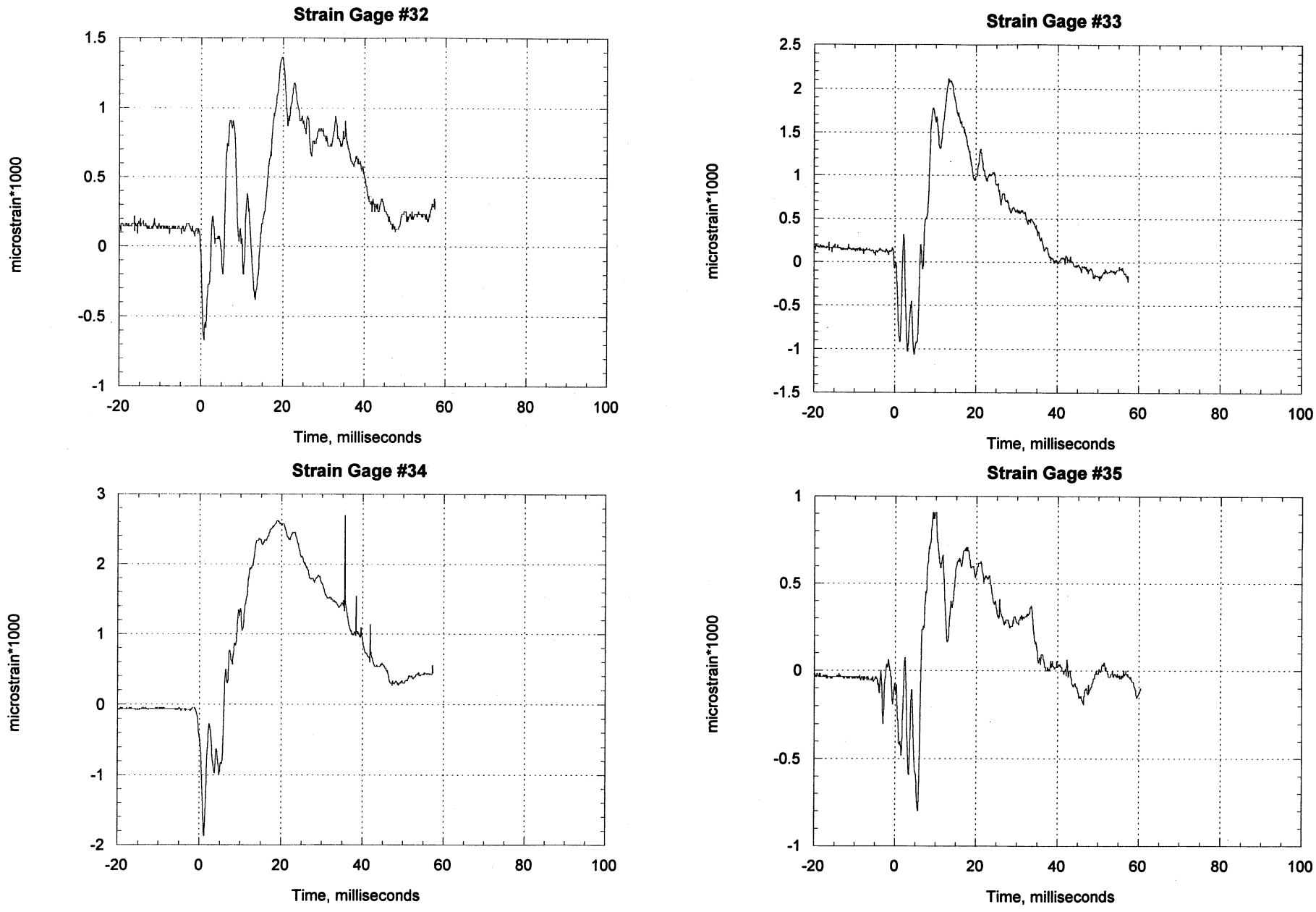

Figure 36, Test 1, Engine Mount, Left Aft Upper Rail

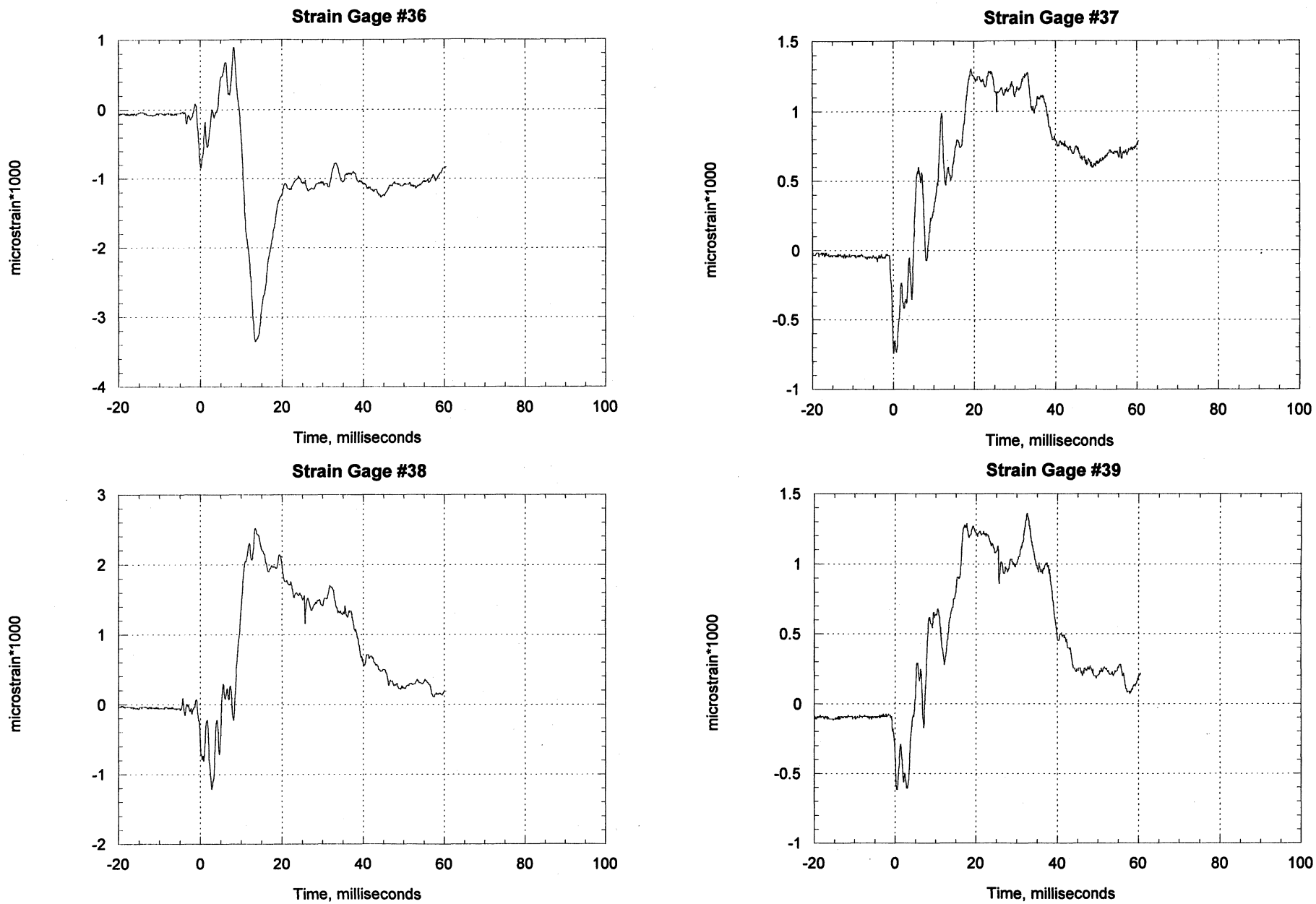

Figure 37, Test 1, Engine Mount, Right Aft Upper Rail

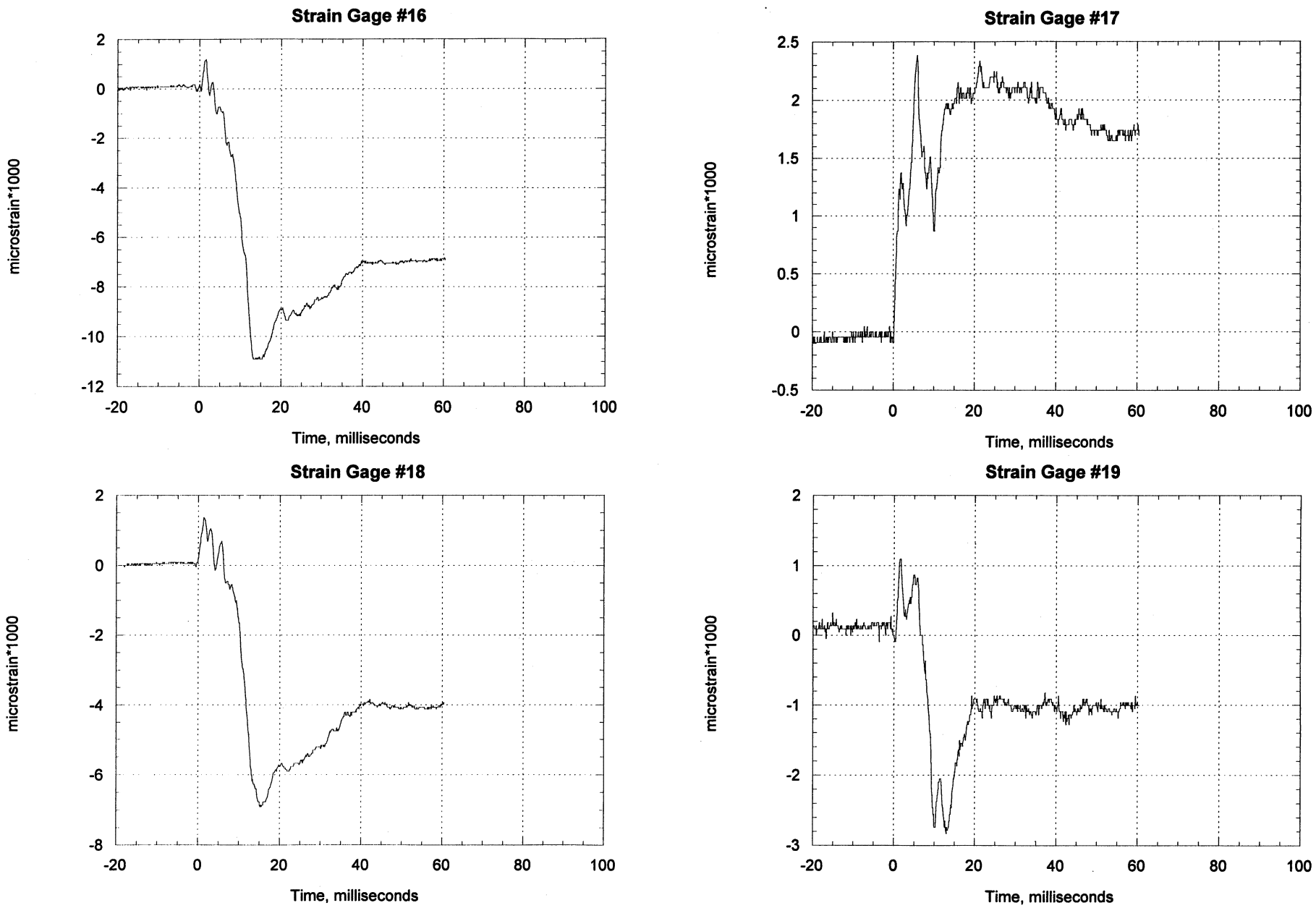

Figure 38, Test 1, Engine Mount, Left Aft Lower Rail

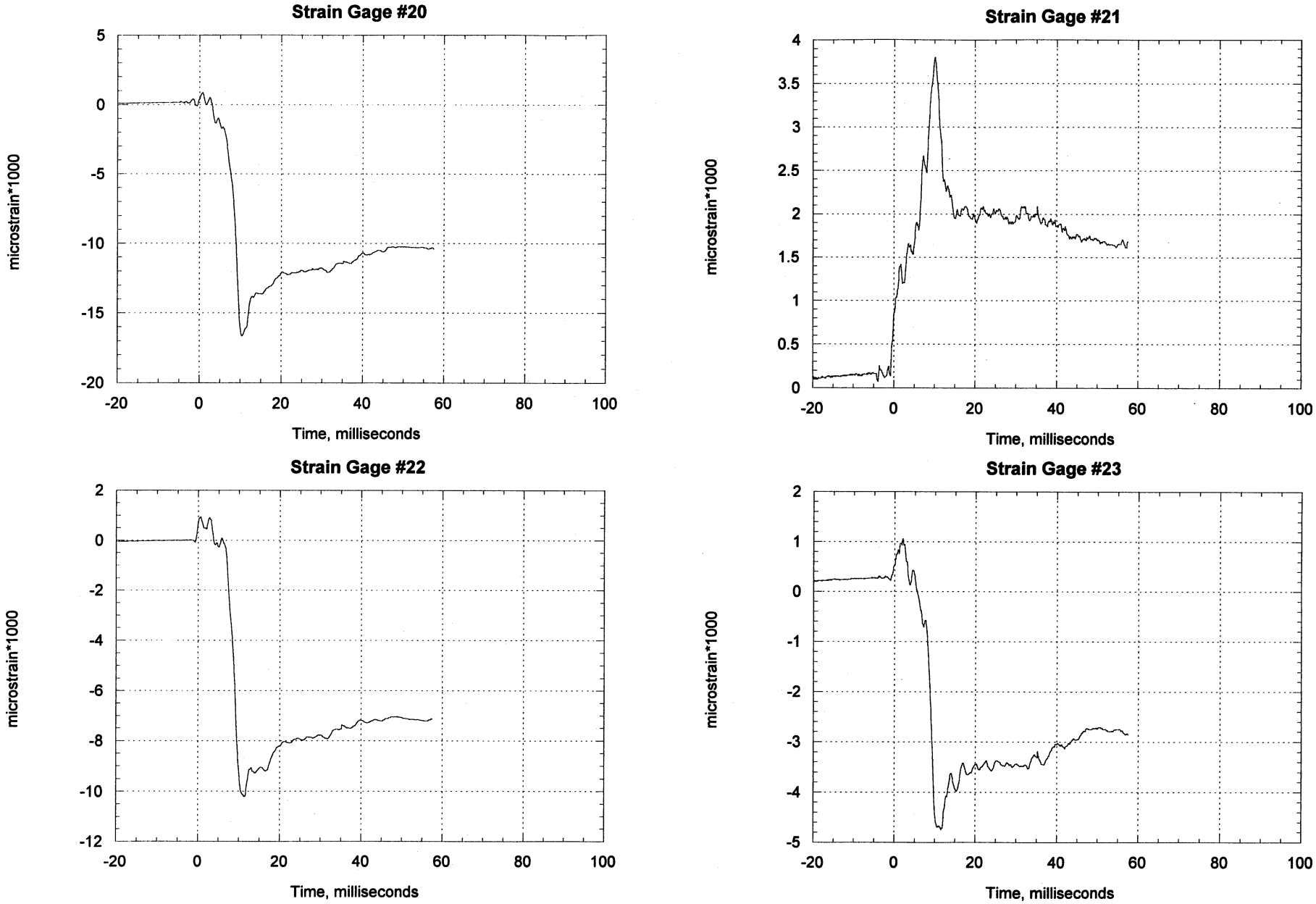

Figure 39, Test 1, Engine Mount, Right Aft Lower Rail

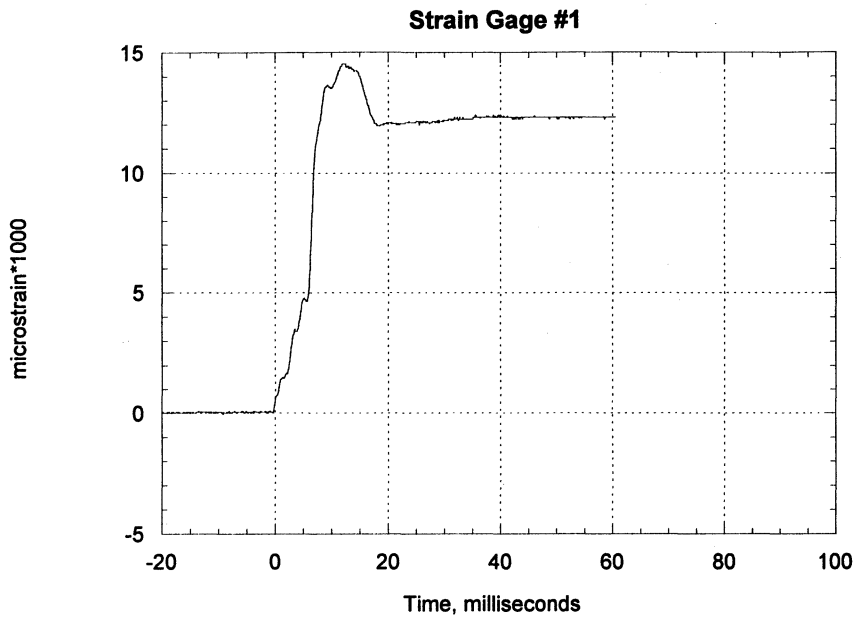

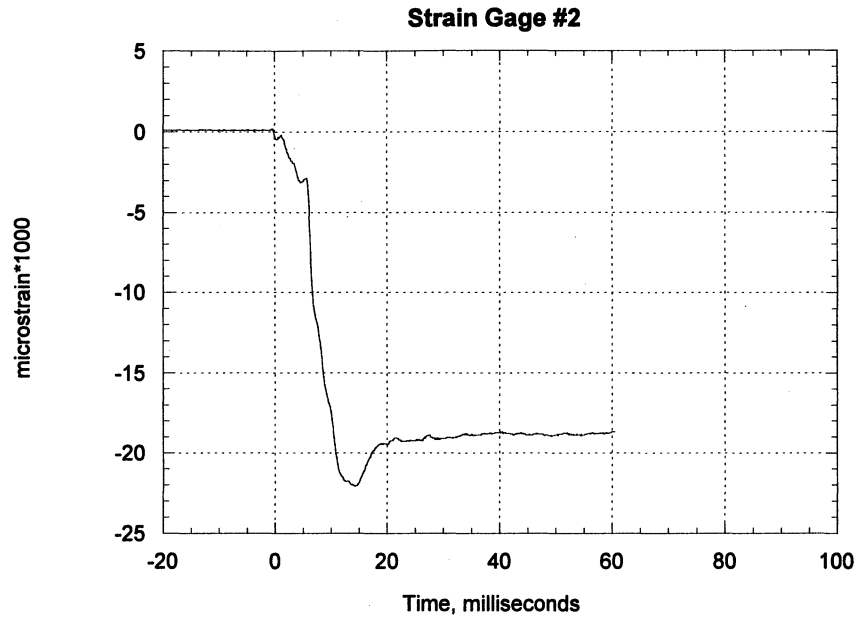

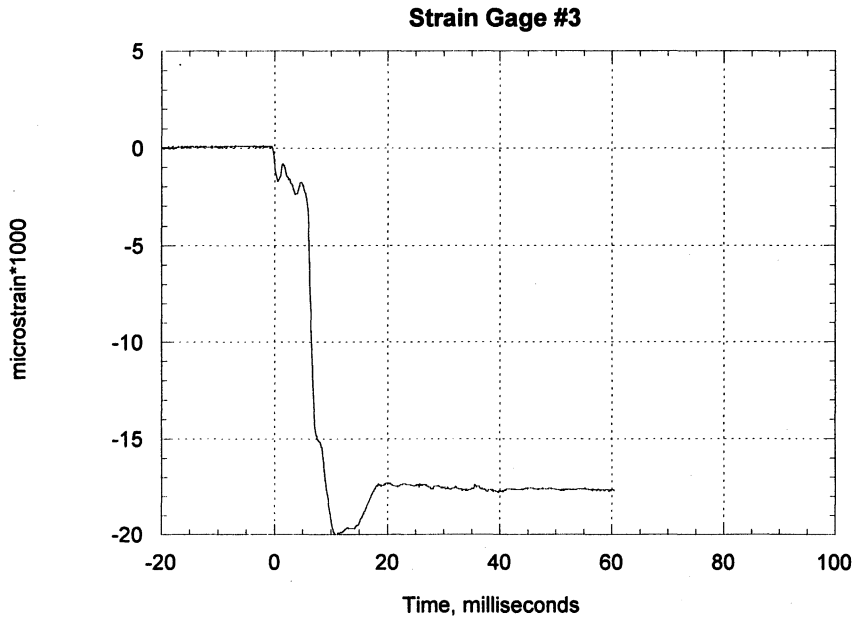

Figure 40, Test 1, Engine Mount, Forward Lower Rail

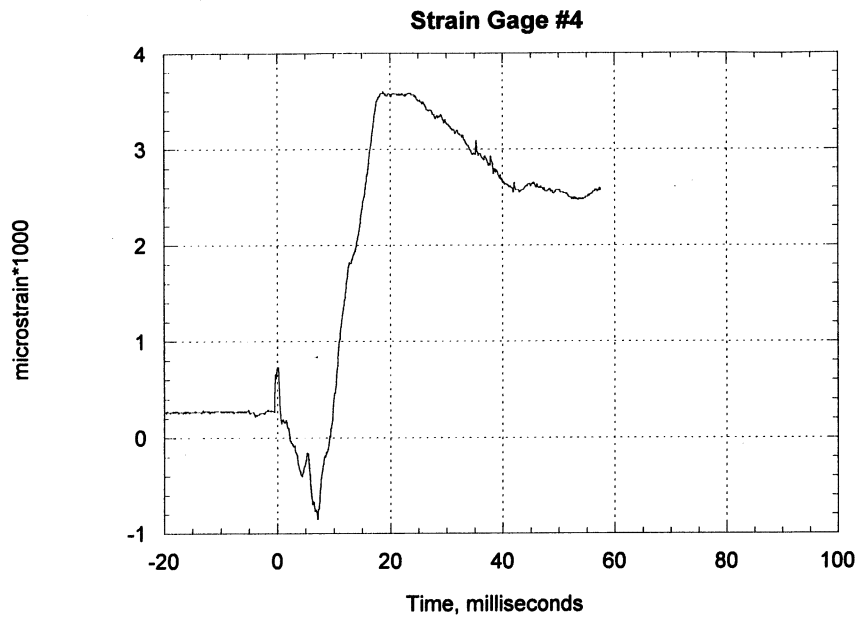

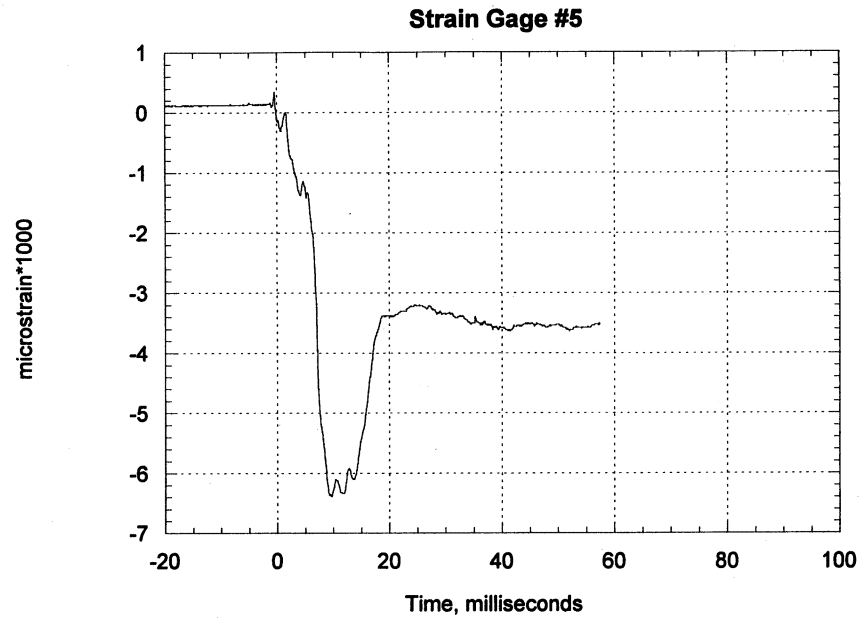

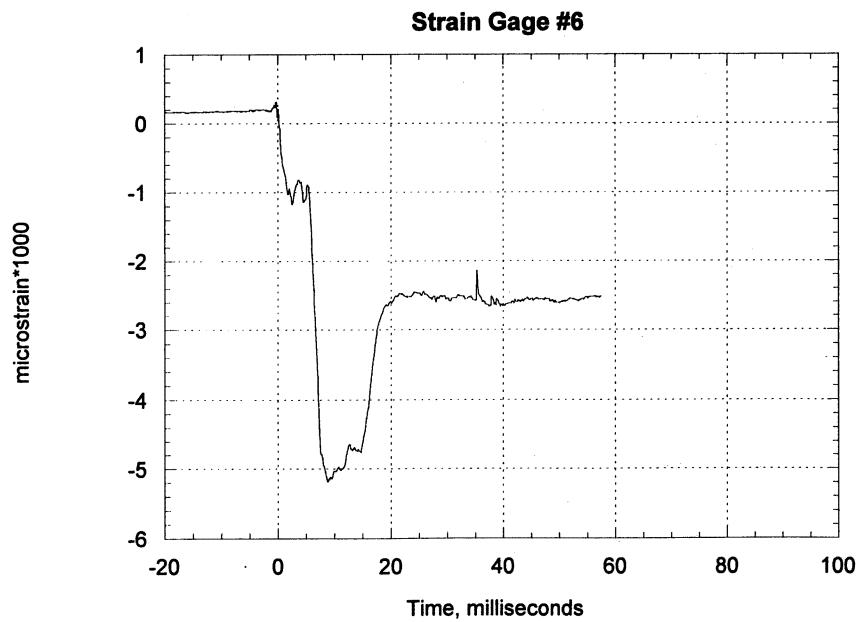

Figure 41, Test 1, Engine Mount, Forward Upright

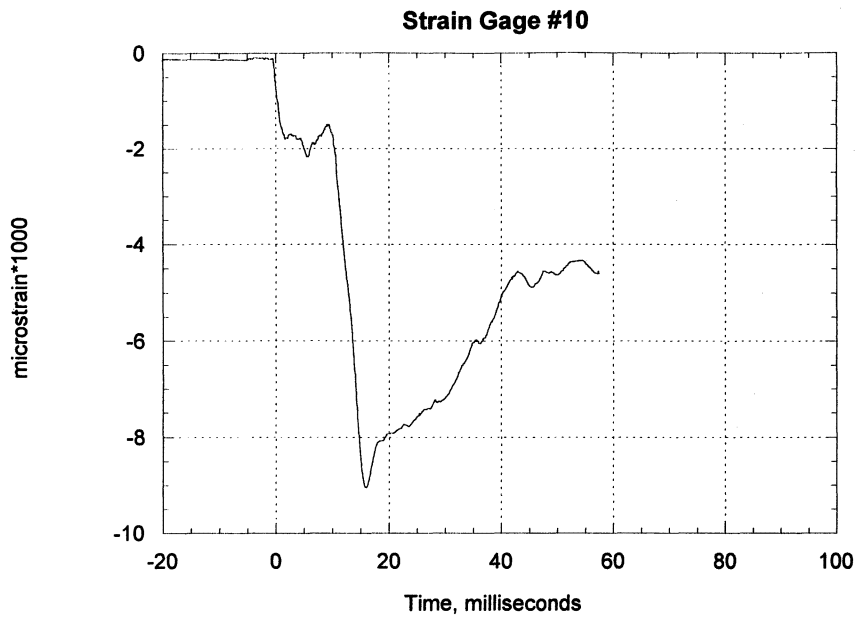

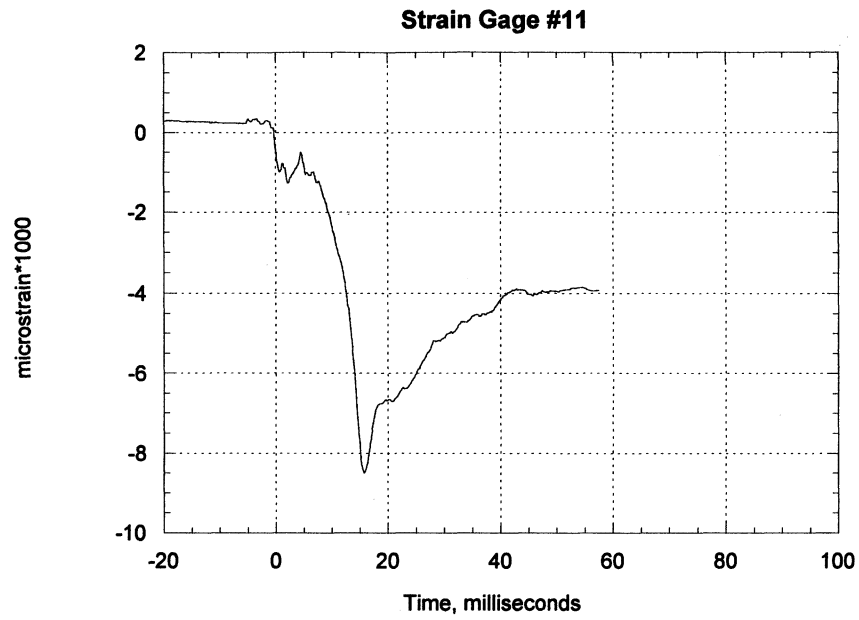

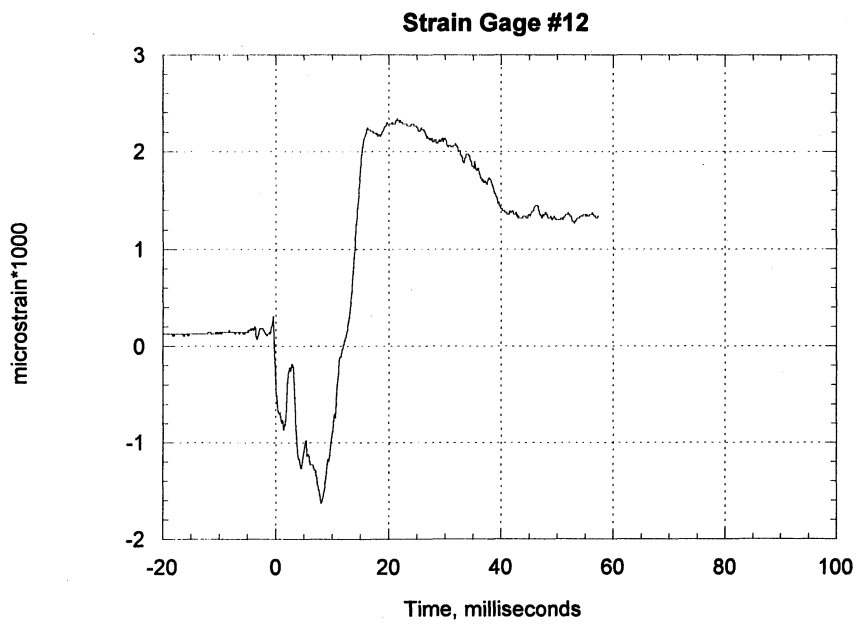

Figure 42, Test 1, Engine Mount, Aft Diagonal

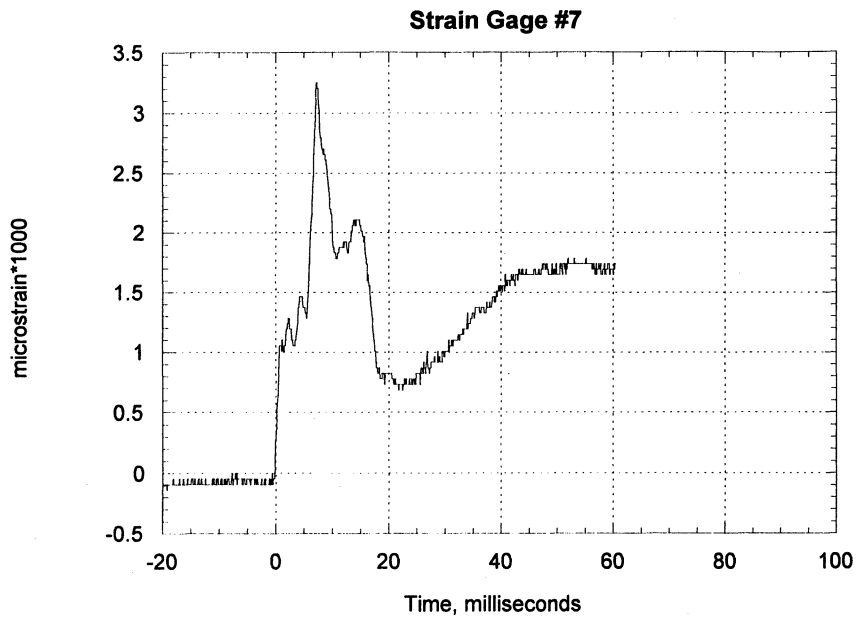

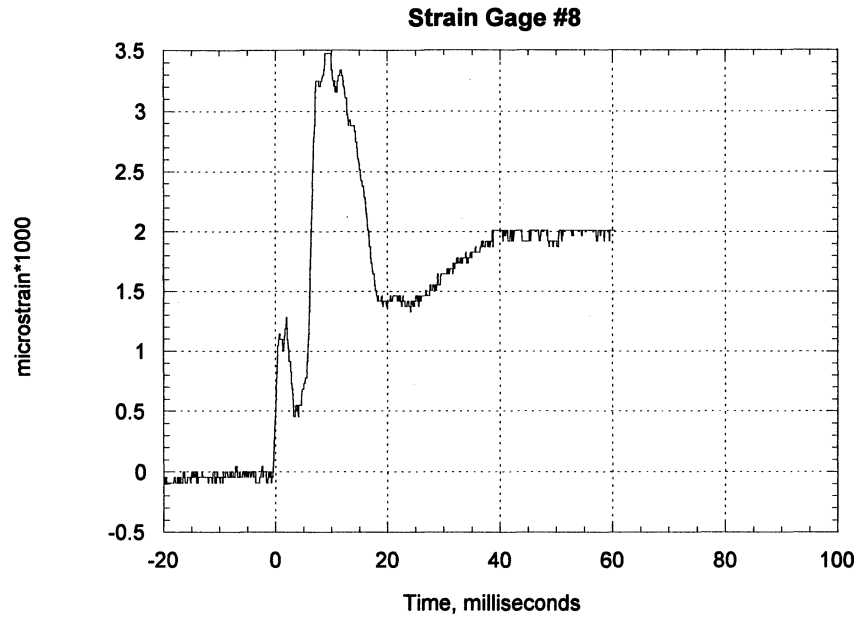

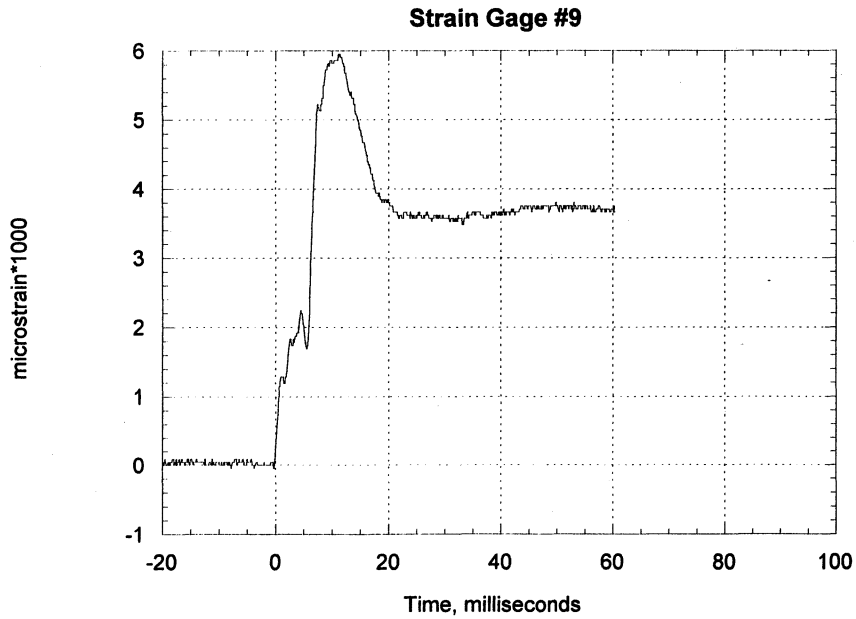

Figure 43, Test 1, Engine Mount, "X" Member

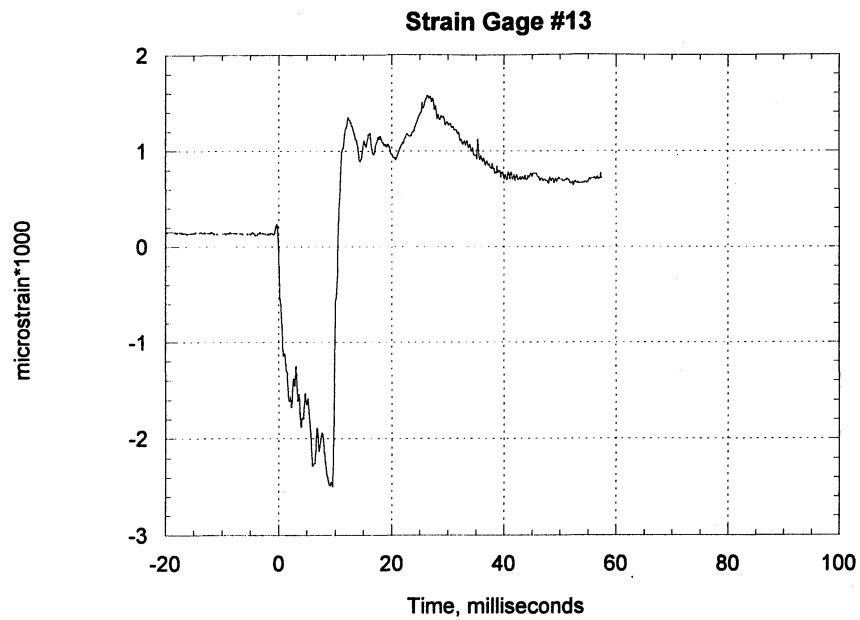

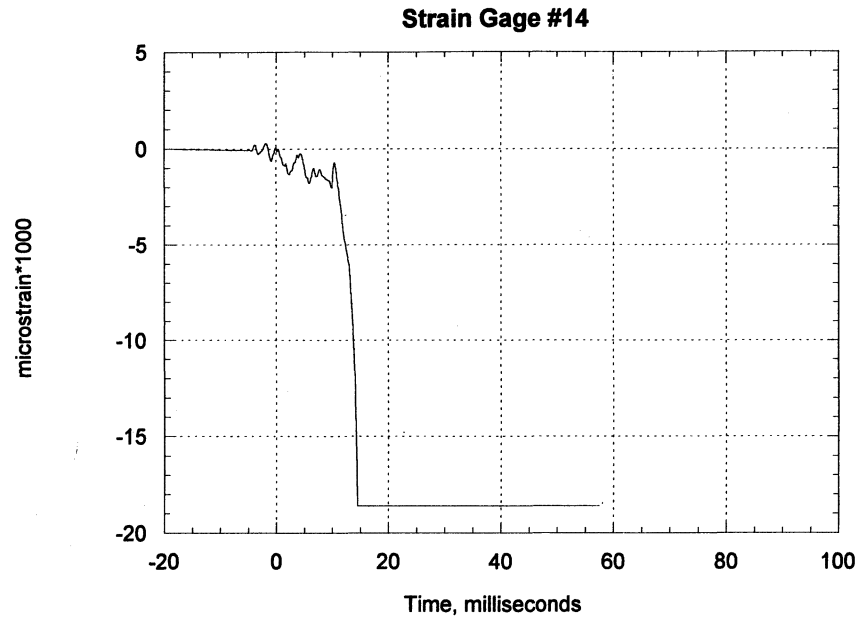

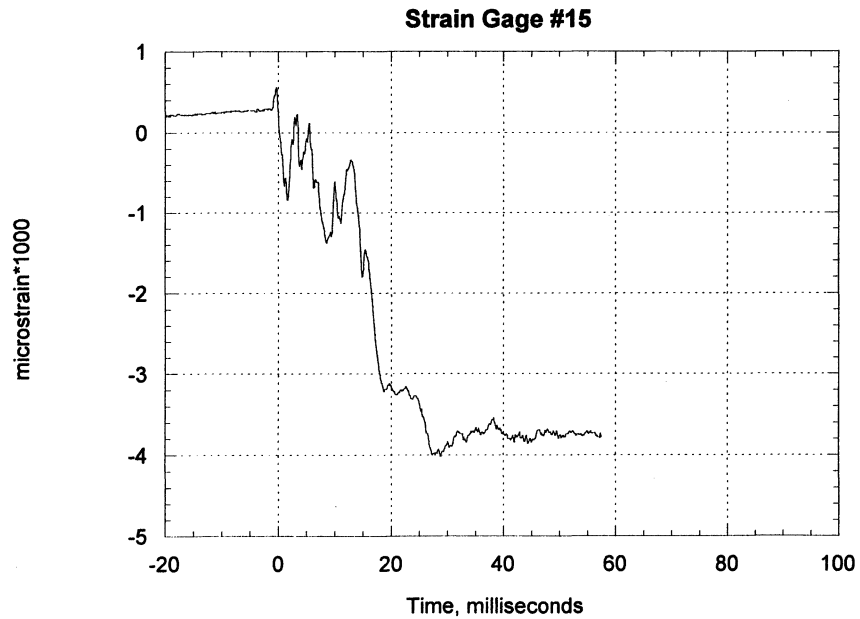

Figure 44, Test 1, Engine Mount, Aft Upright

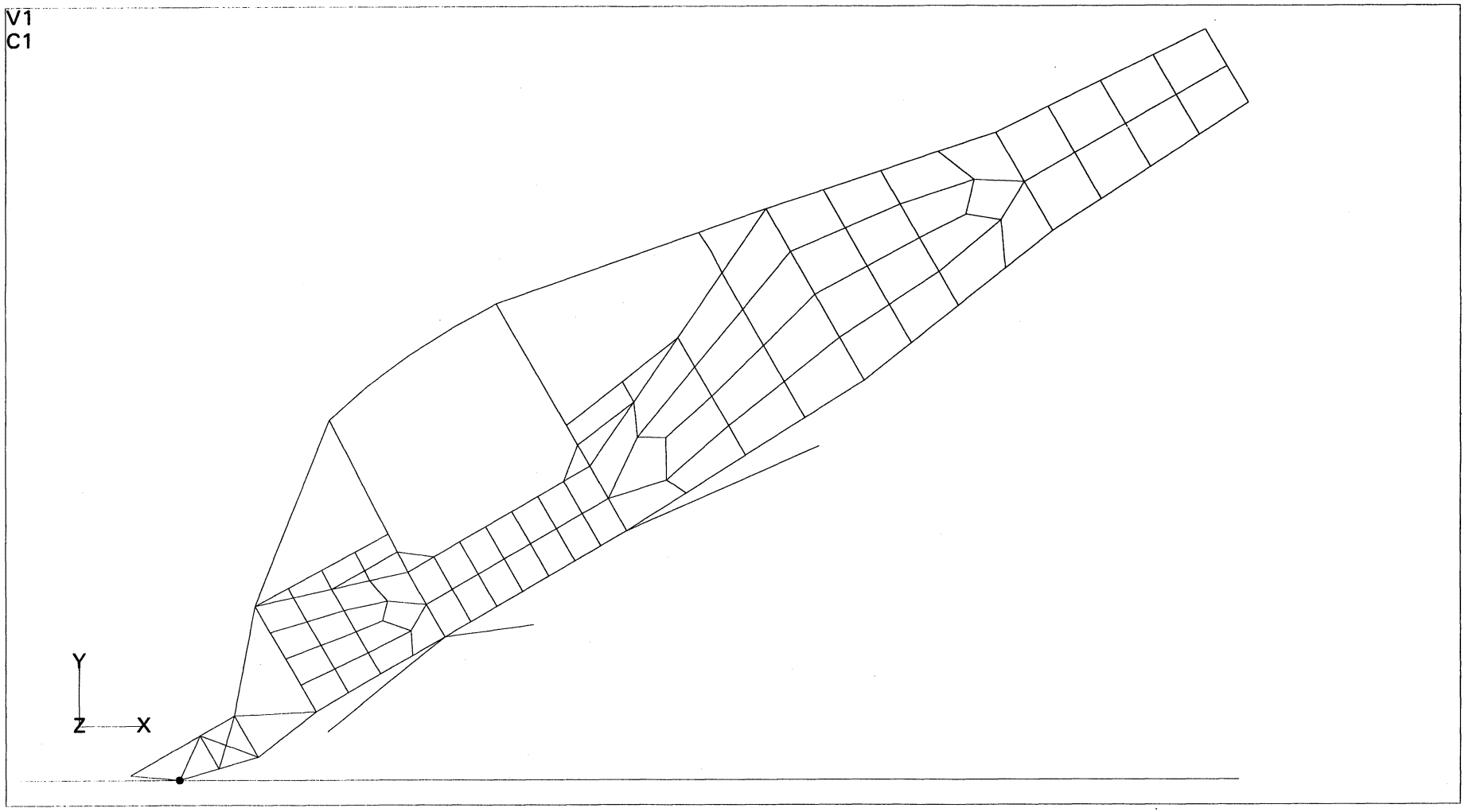

Figure 45, Dynamic Analysis Model, Windshield Post and Shear Panels

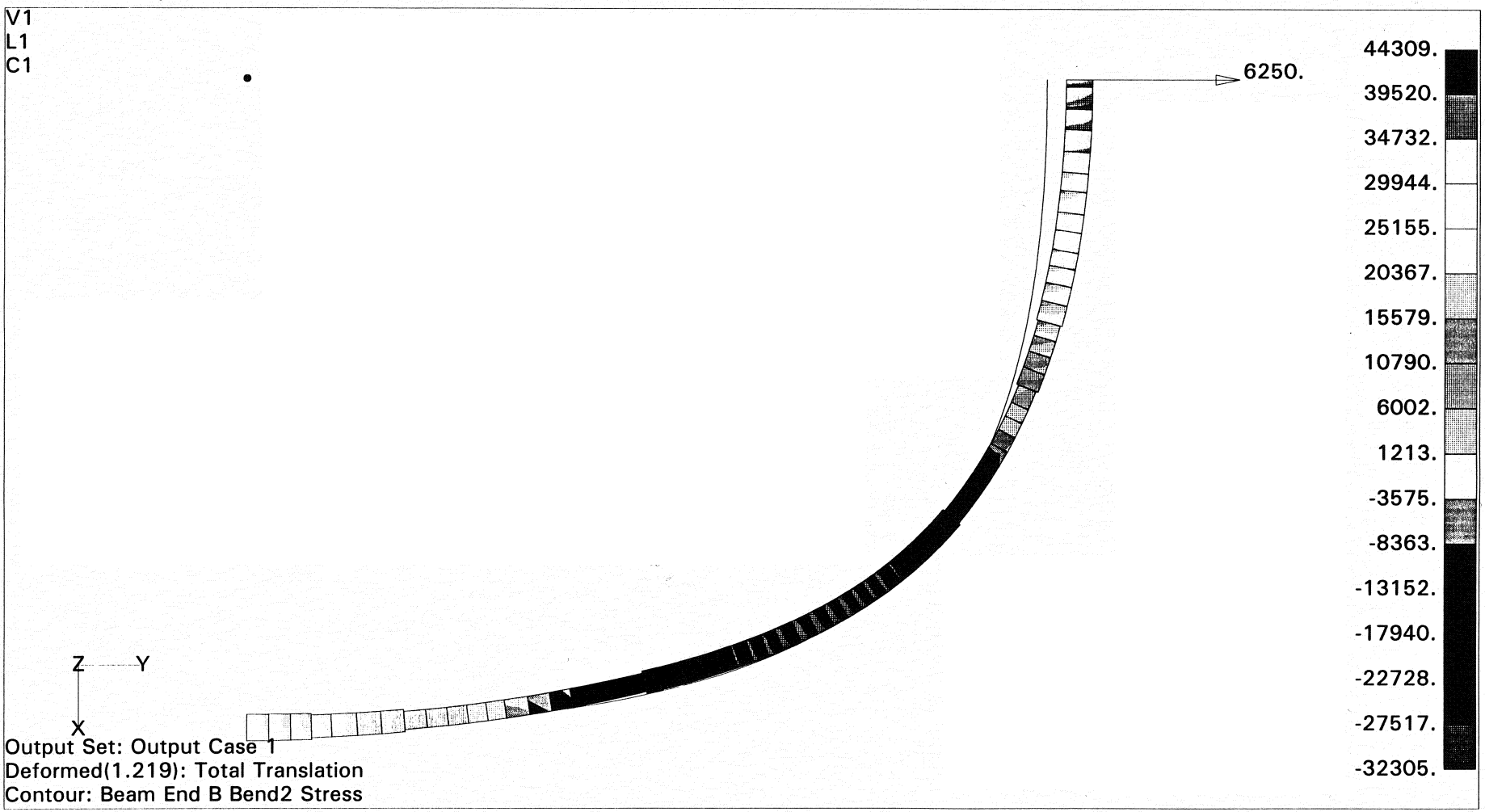

Figure 46, Static Analysis, Front Door Frame

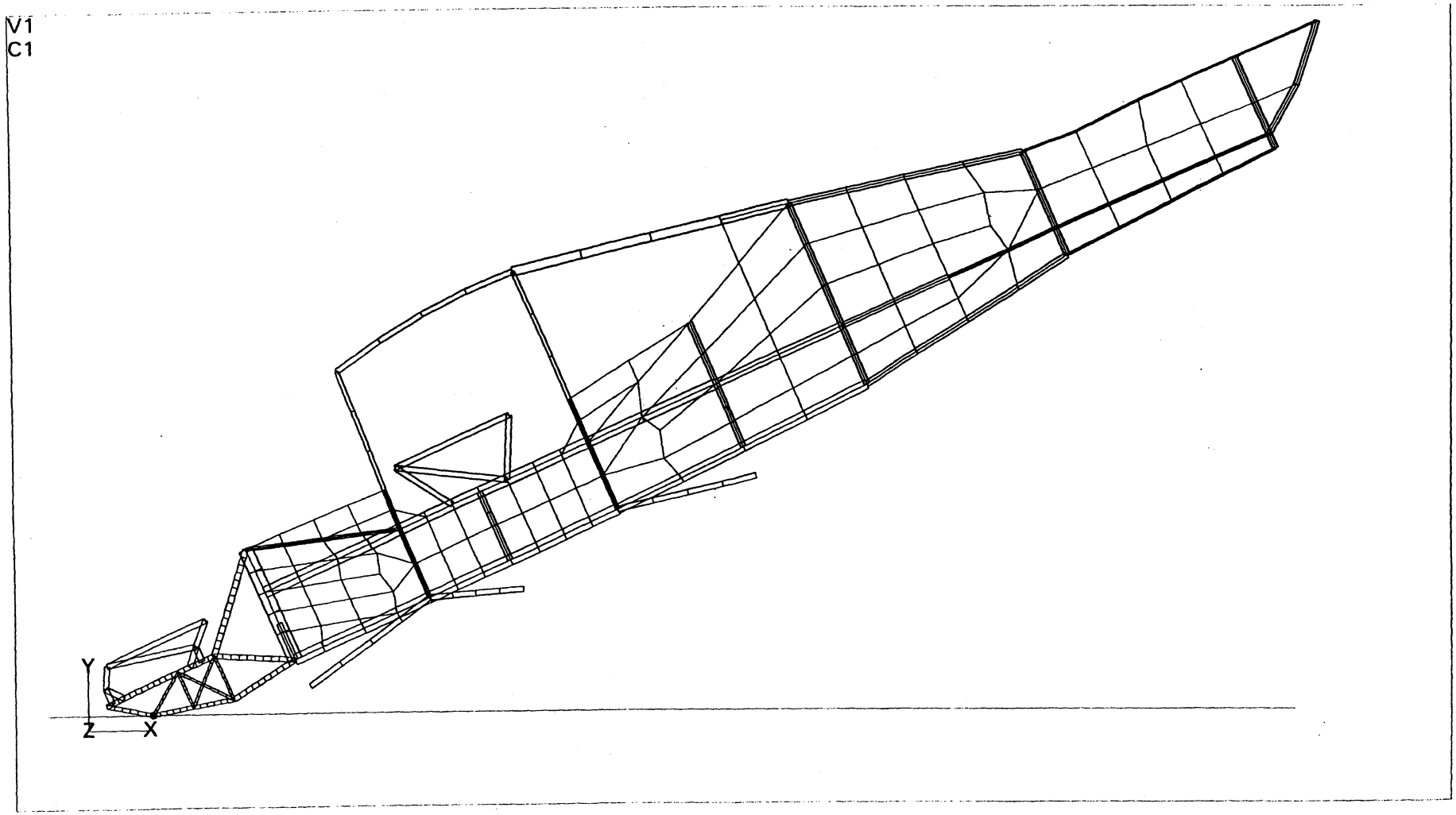

Figure 47, Dynamic Analysis Model, Structural Elements to Match First Two Test Airplanes

Arcrft11 Model

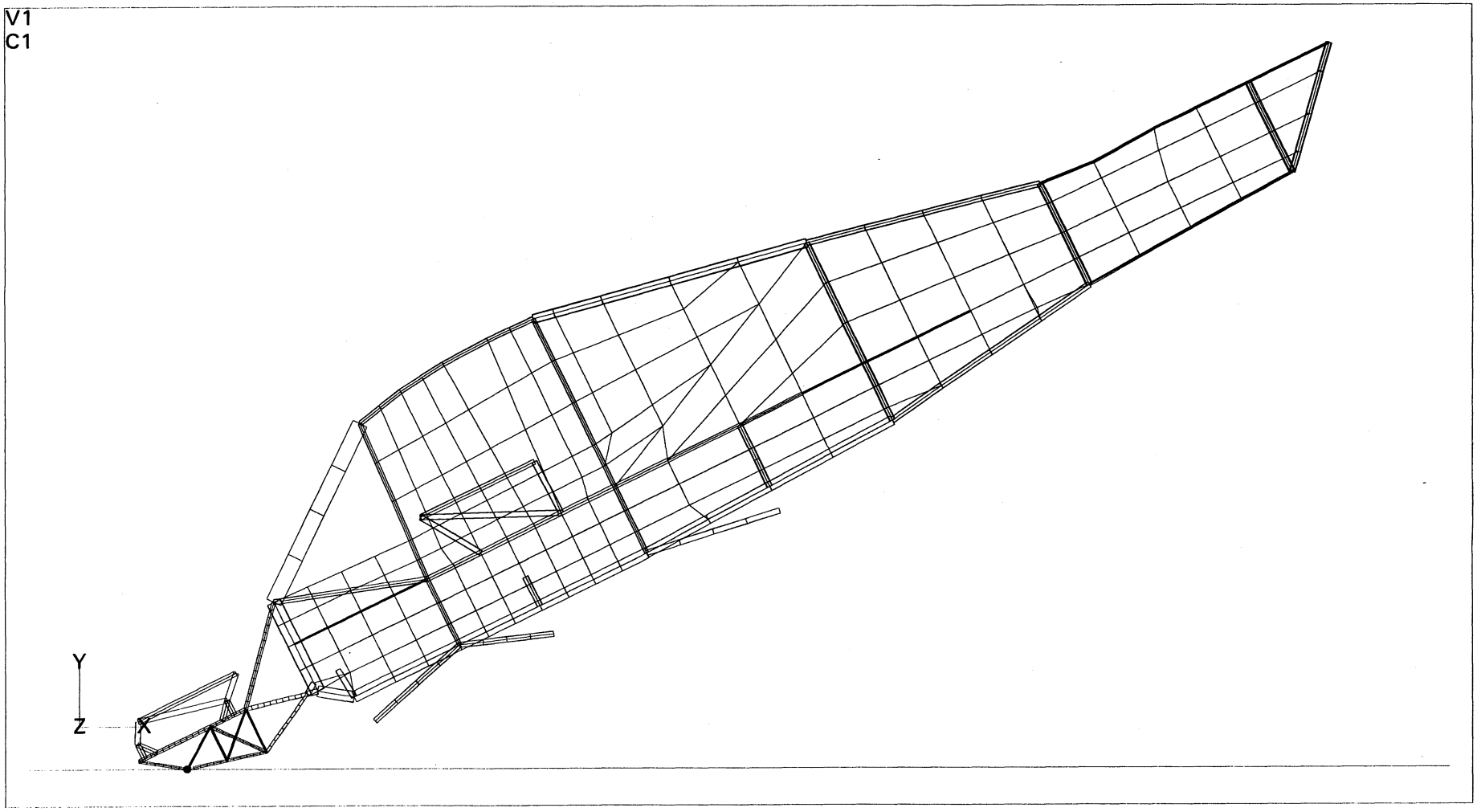

Figure 48, Dynamic Analysis Model, Doors, Windows, and Windshield Added

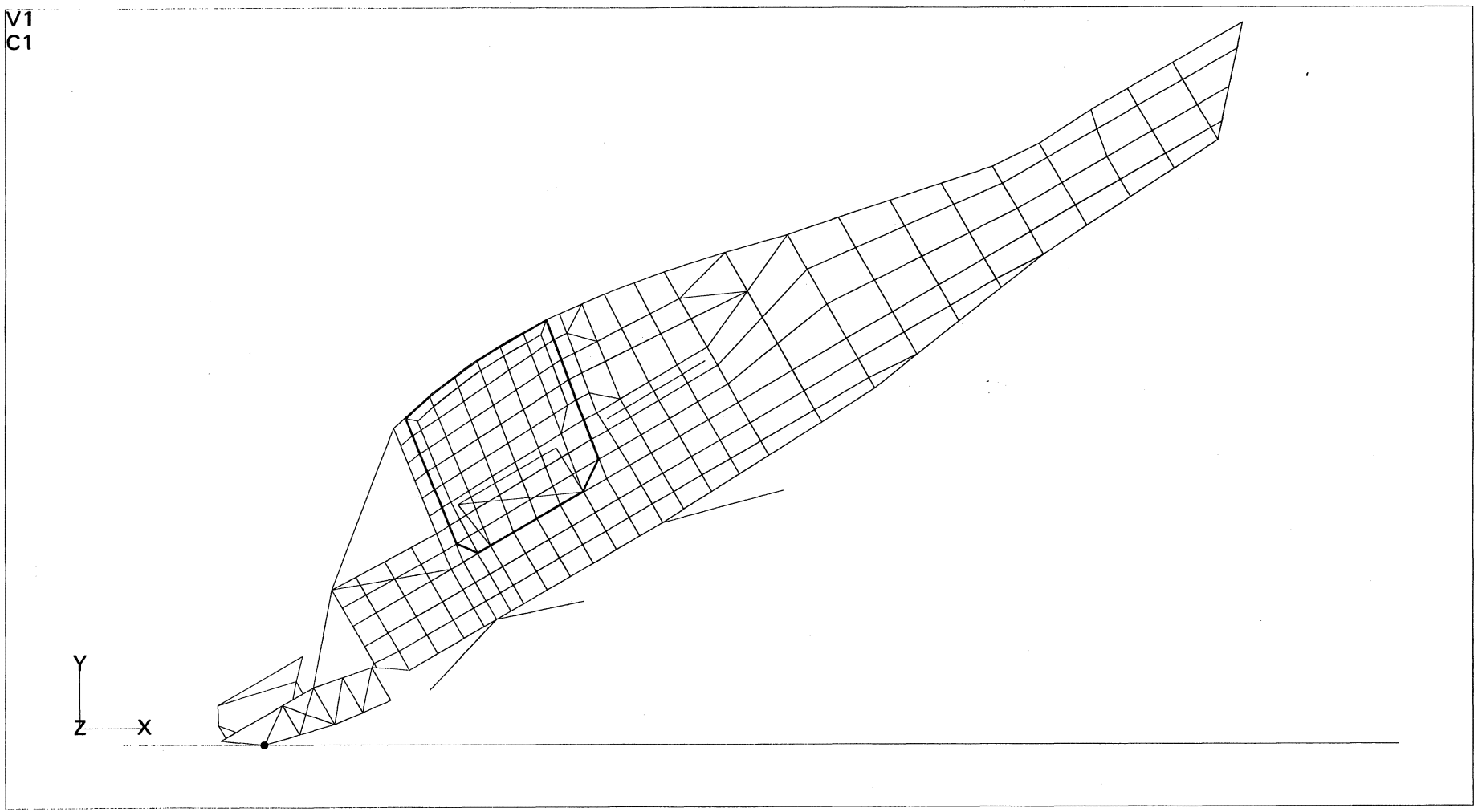

Figure 49, Dynamic Analysis Model, Separate Door Attached at Four Nodes

Arcrft11, Run 2

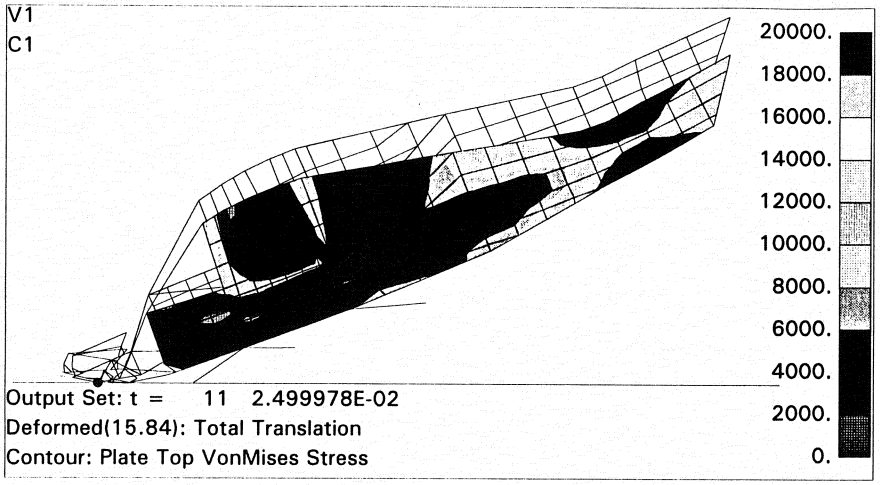

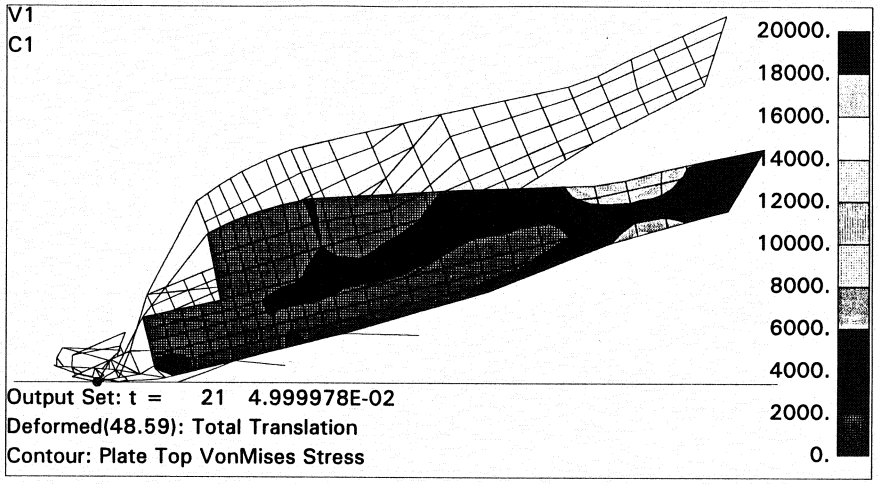

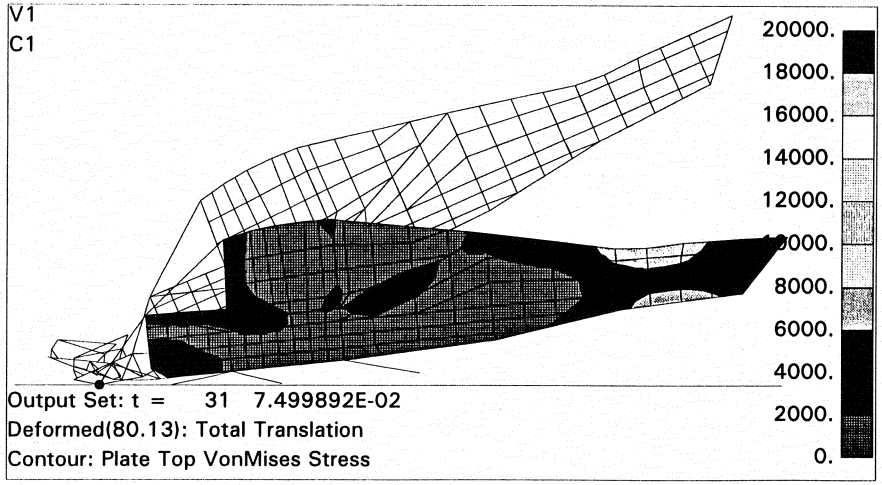

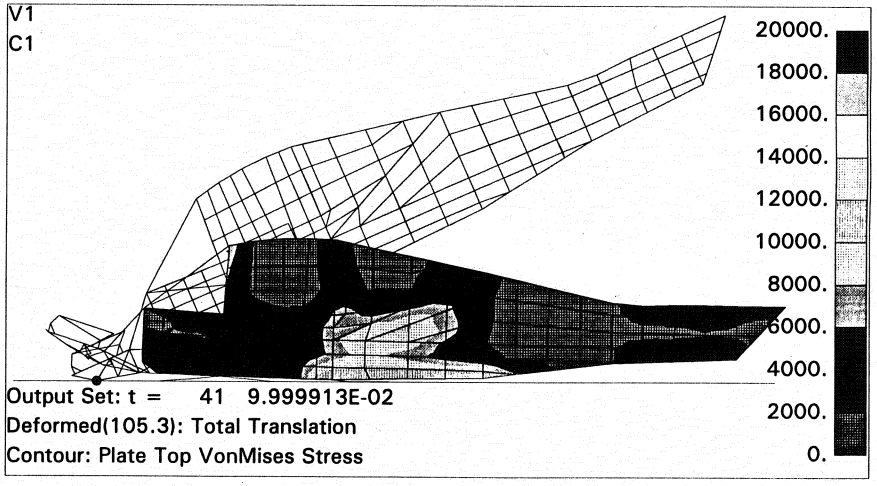

Figure 50, Dynamic Analysis, Model to Match Test 1

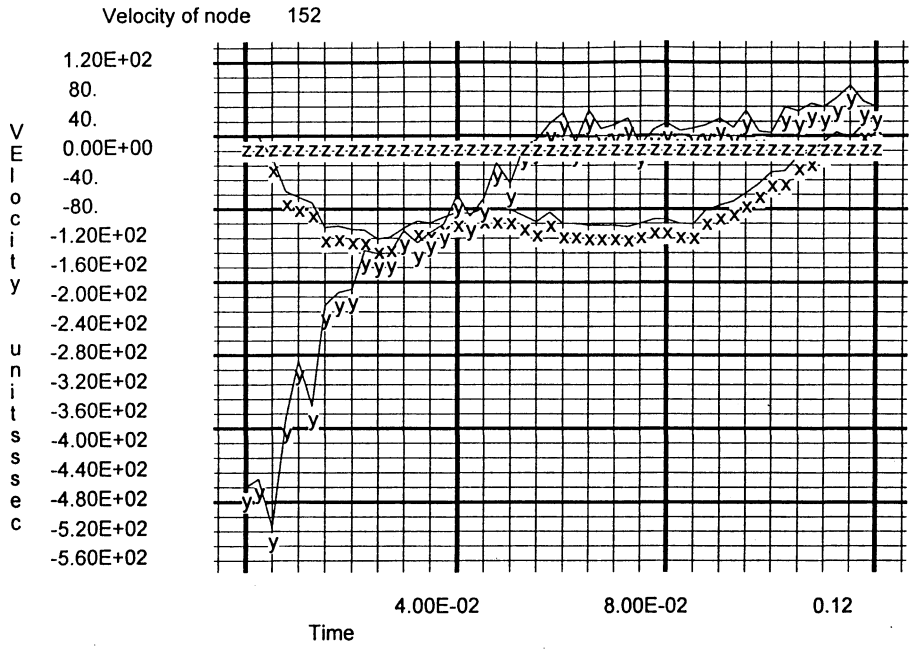

(a), Firewall

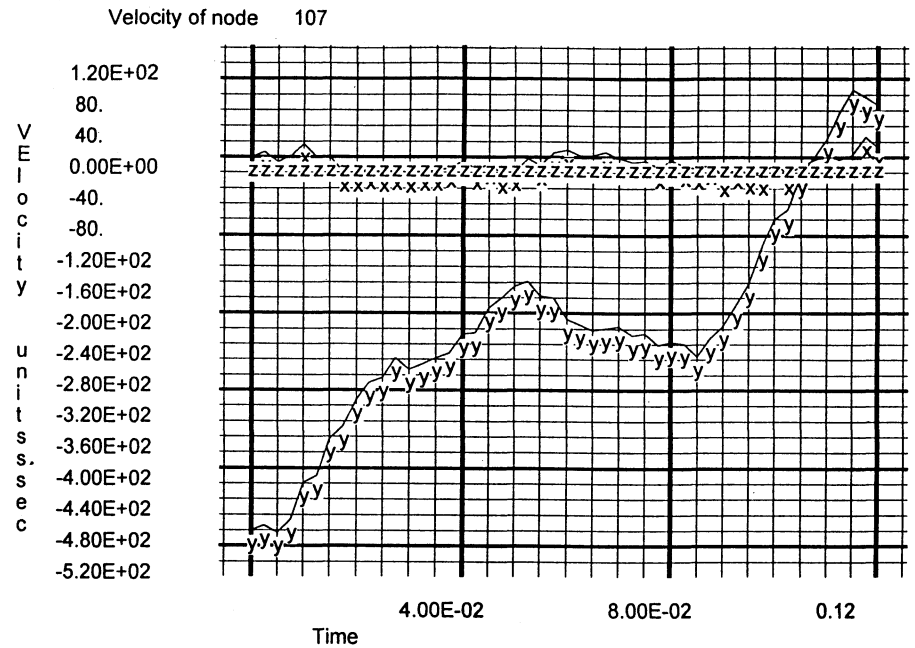

(b), Front Seat

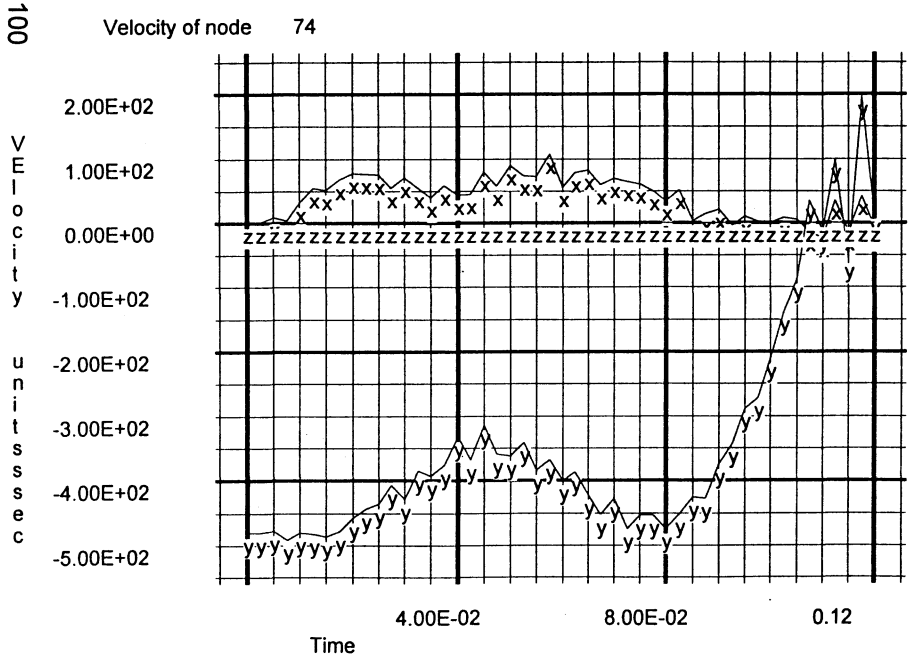

(c), Rear Seat

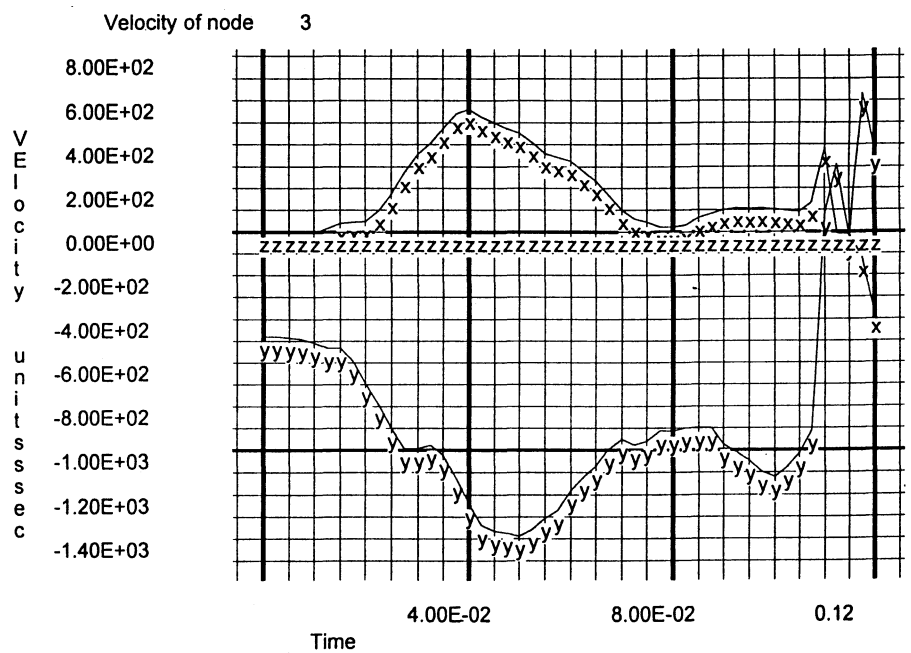

(d), Tail Post

Figure 51, Dynamic Analysis, Model to Match Test 1

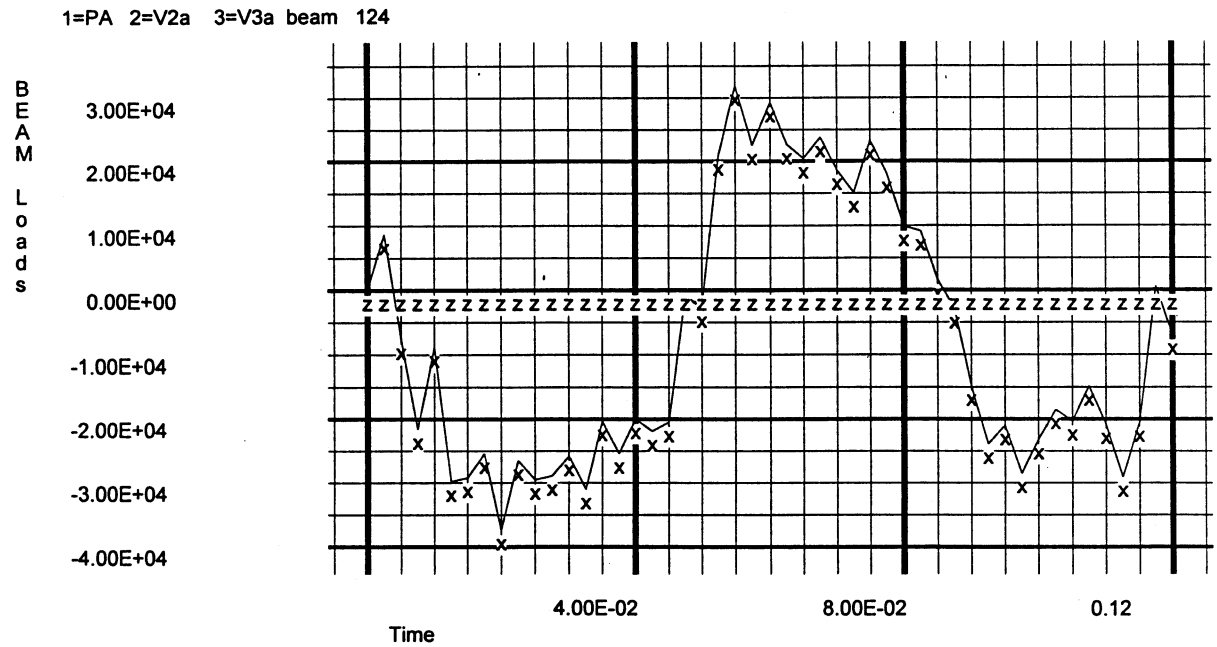

(a), Calculated

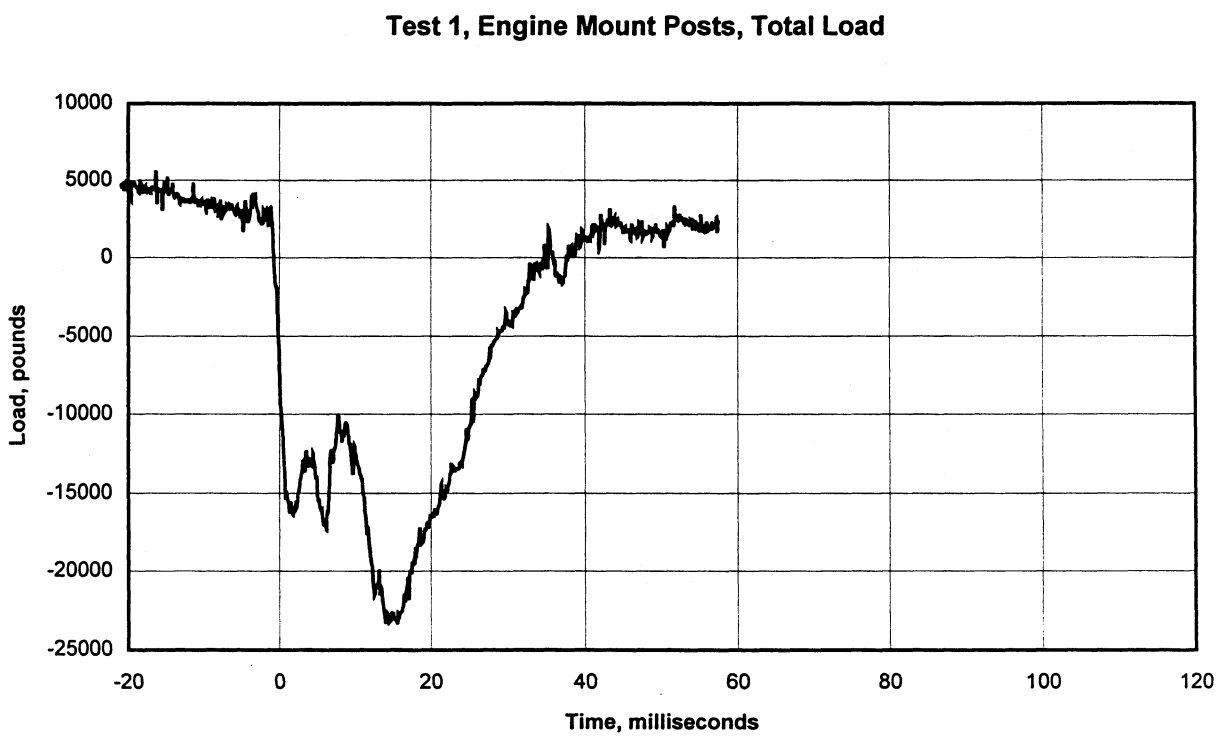

(b), Test Data

Figure 52, Engine Mount Loads, Test 1

Arcrft11, Run 10

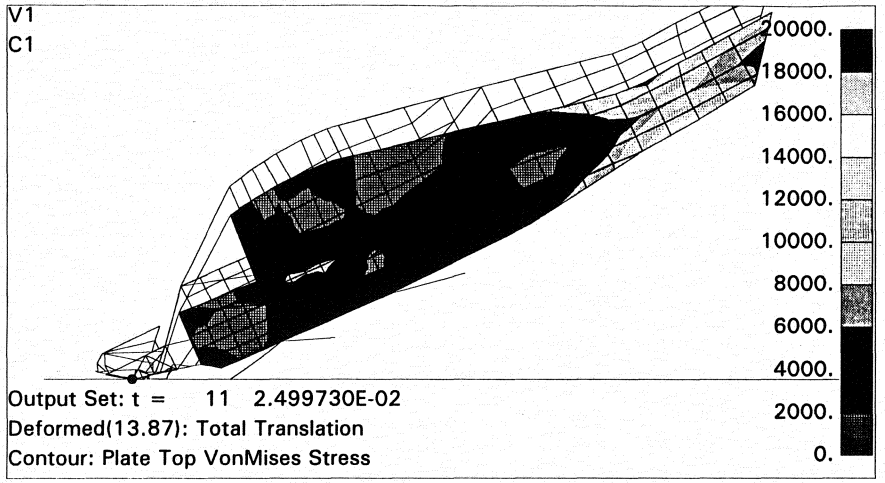

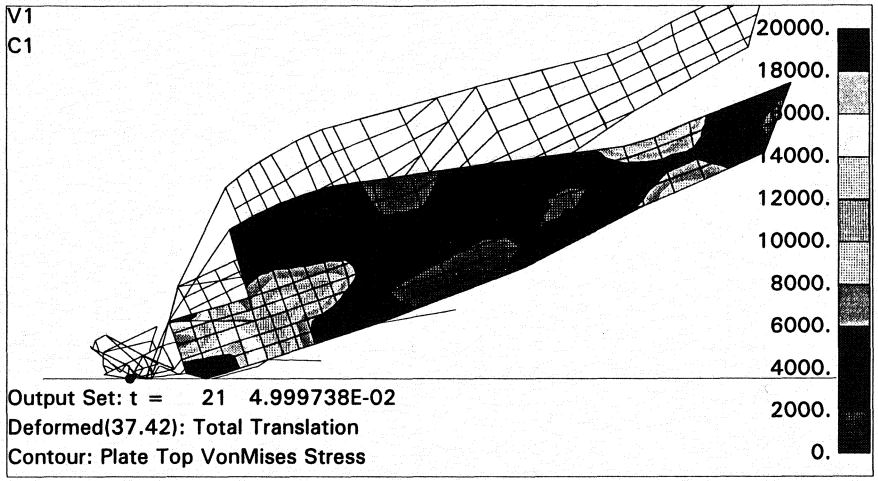

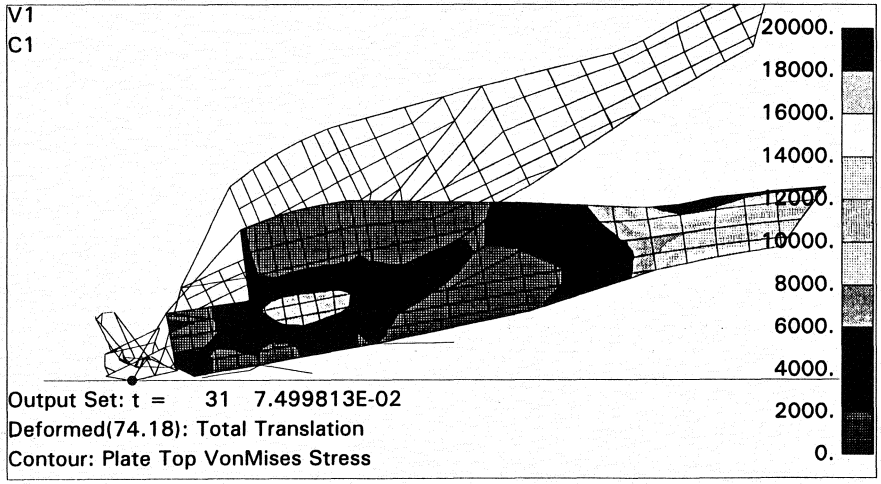

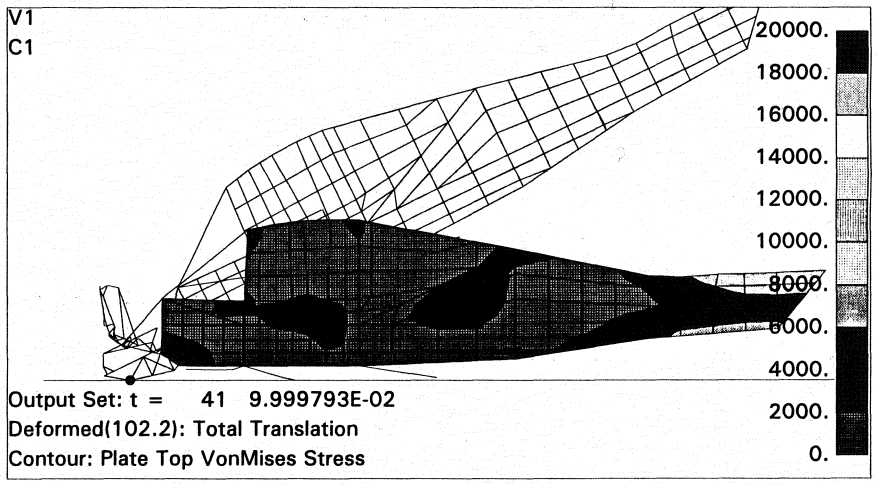

Figure 53, Dynamic Analysis, Design Condition for Airframes 3 and 4

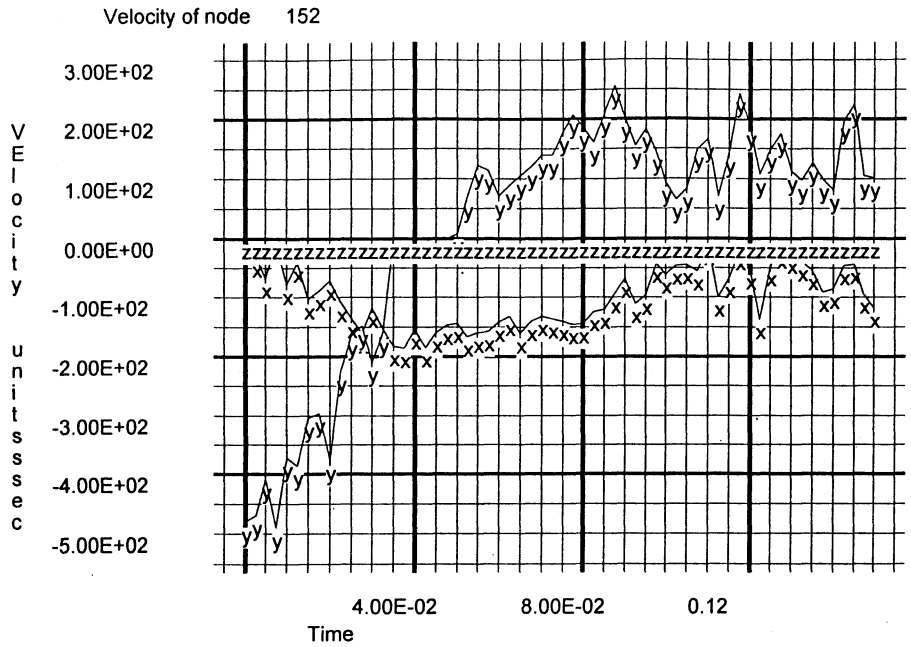

(a), Firewall

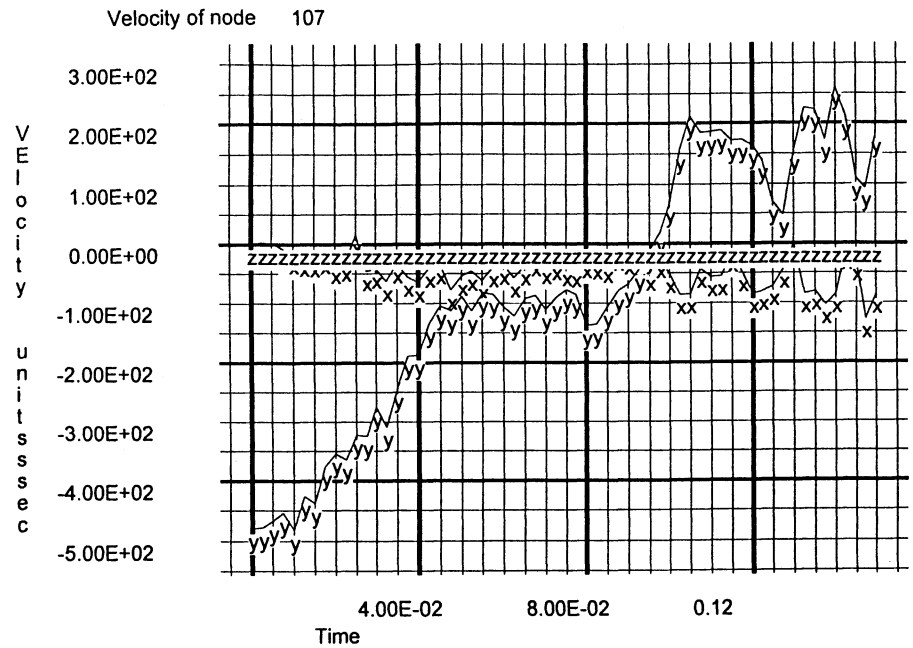

(b), Front Seat

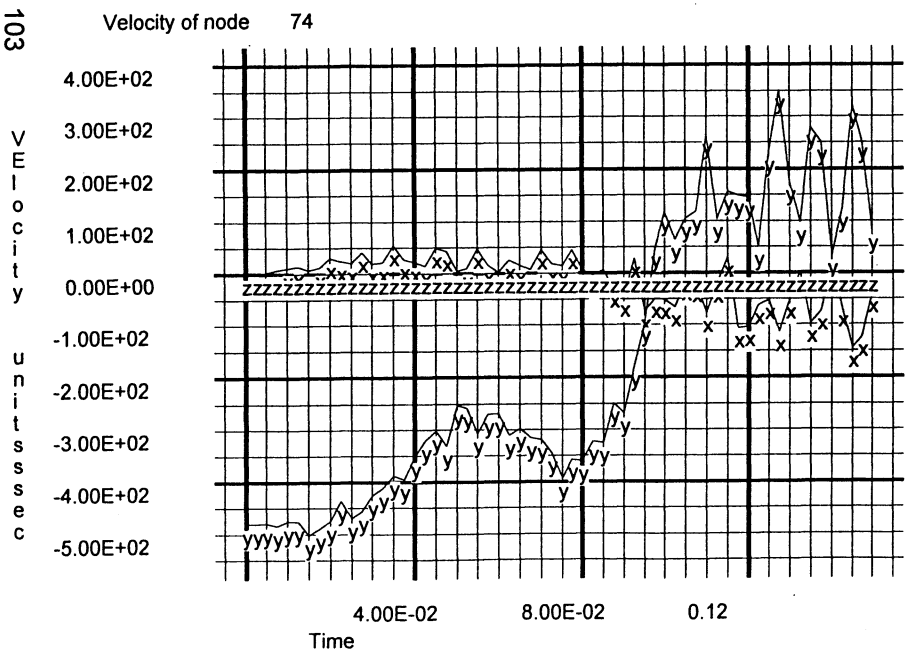

(c), Rear Seat

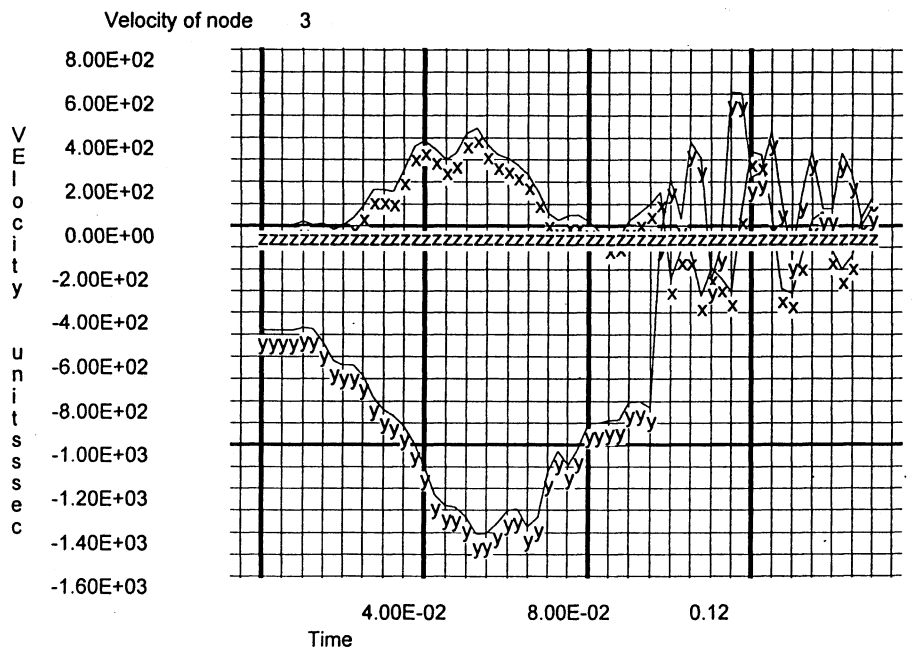

(d), Tail Post

Figure 54, Dynamic Analysis, Design Condition for Airframes 3 and 4

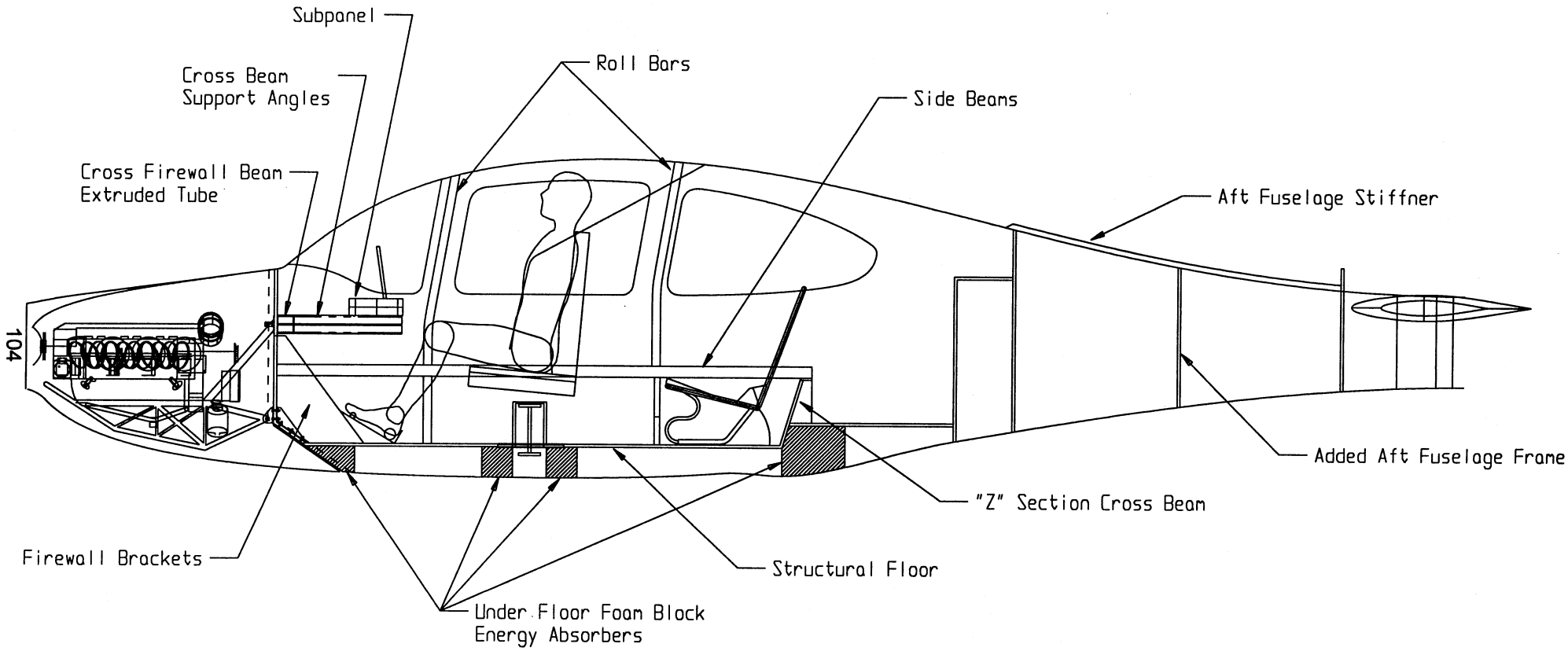

Figure 55, Structural Concept, Airplanes 3 and 4

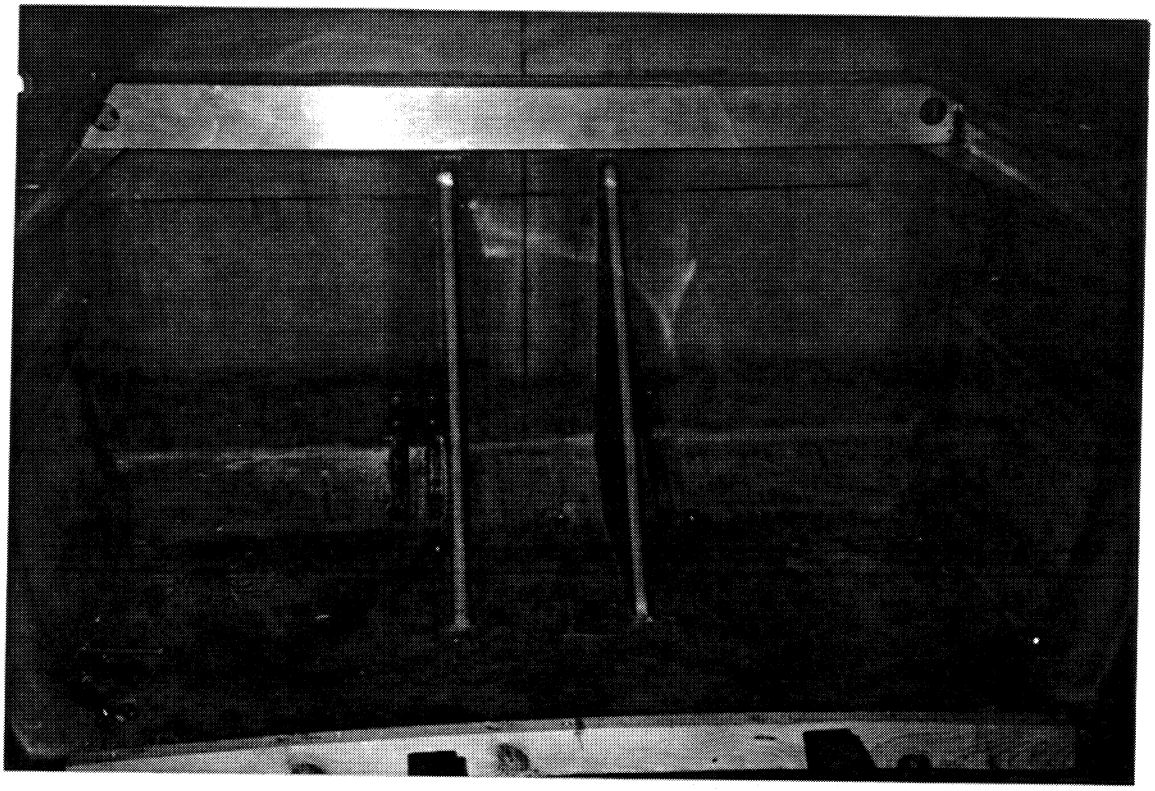

(a), Back Side of Firewall

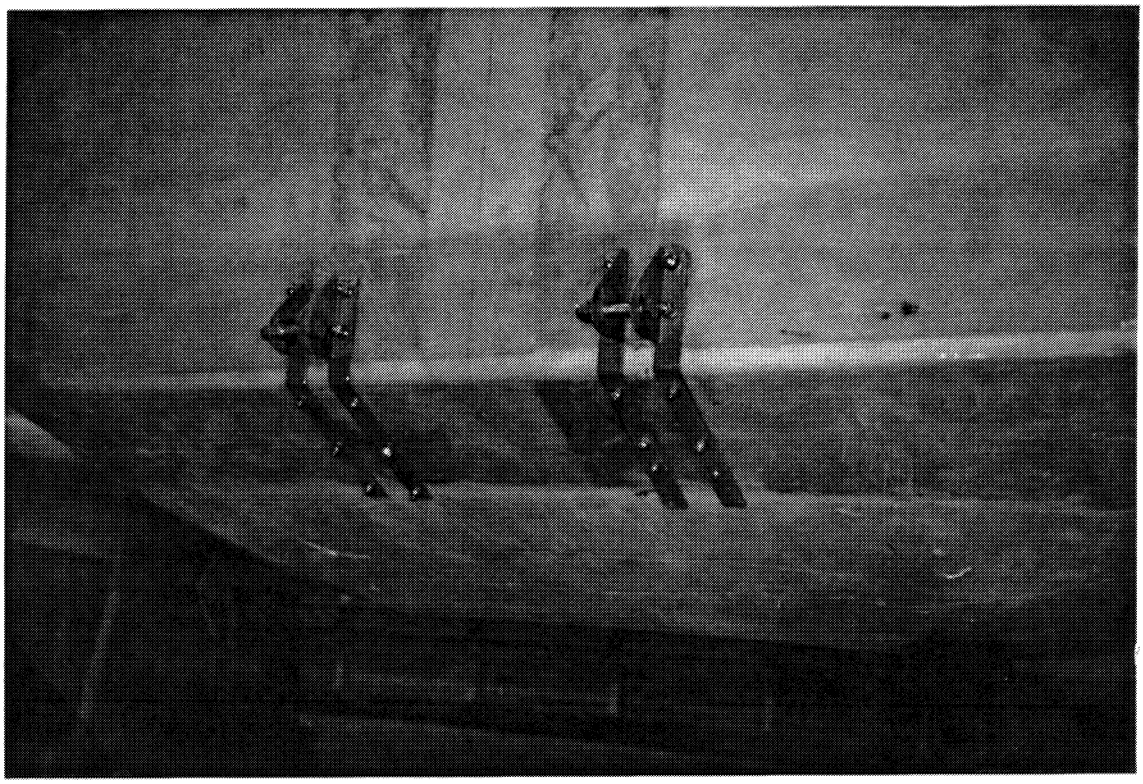

(b), Lower Engine Mount Fittings

Figure 56, Structural Concept Pictures, Airframes 3 and 4

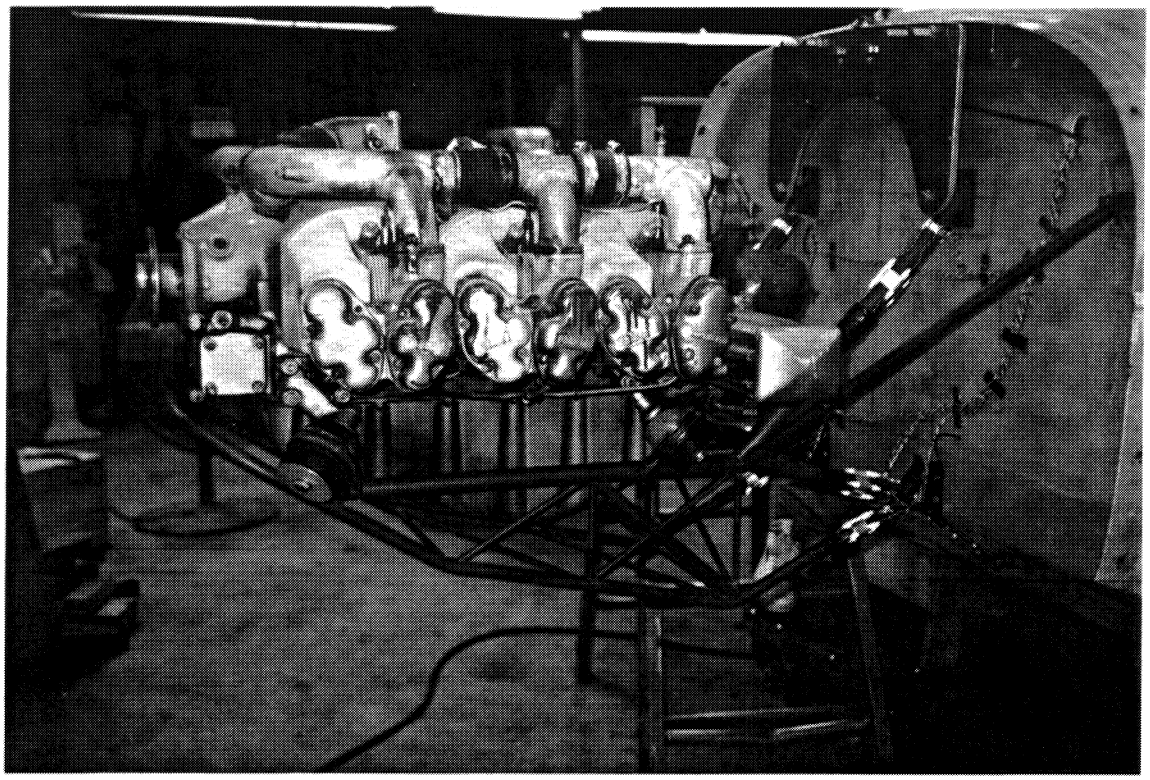

(c), Engine Mount

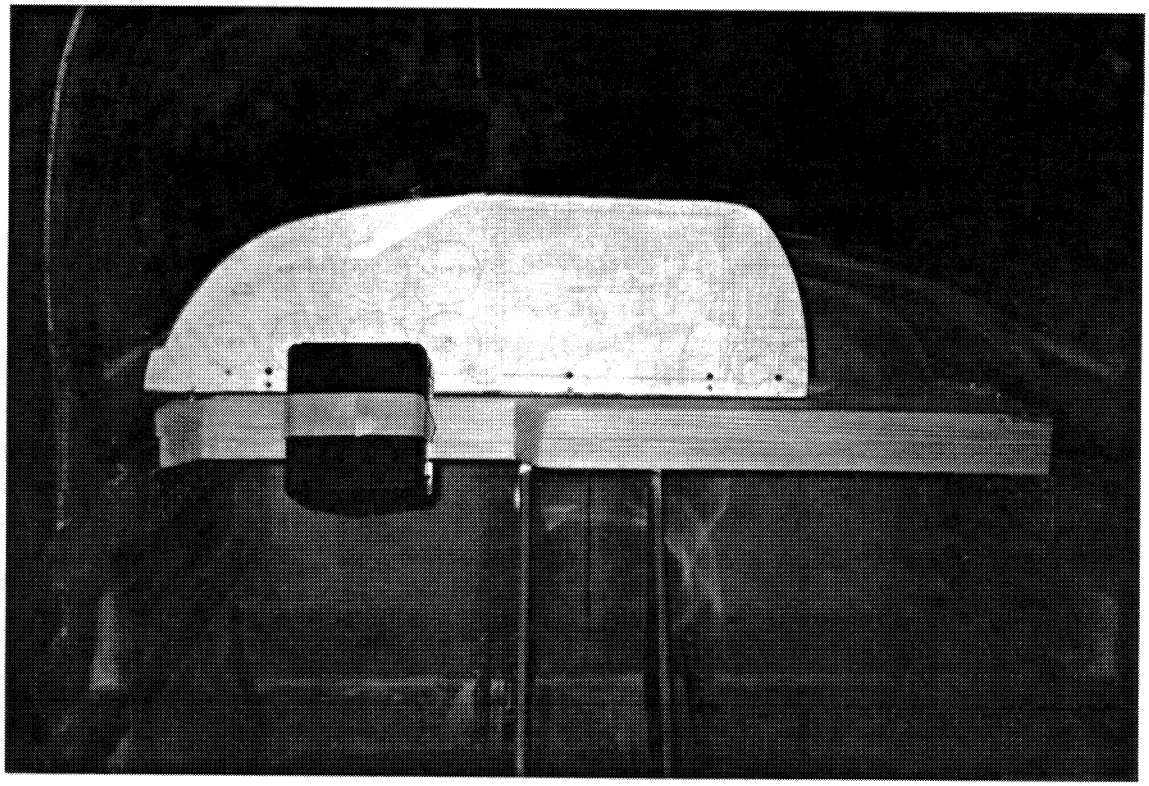

(d), Simulated Instrument Panel, Subpanel, and Installed Air Bag

Figure 56, (continued)

(e), JAARS Seat in Rear Location

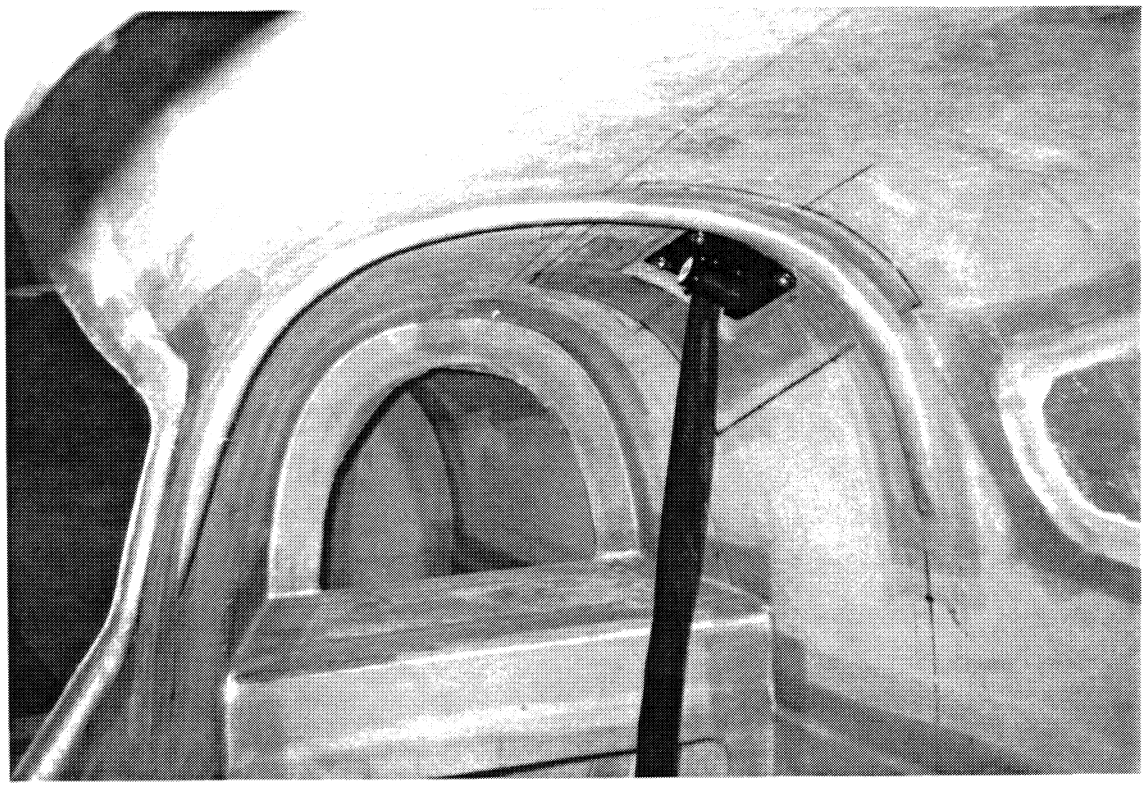

(f), Camera Shelf and Shoulder Harness

Figure 56, (concluded)

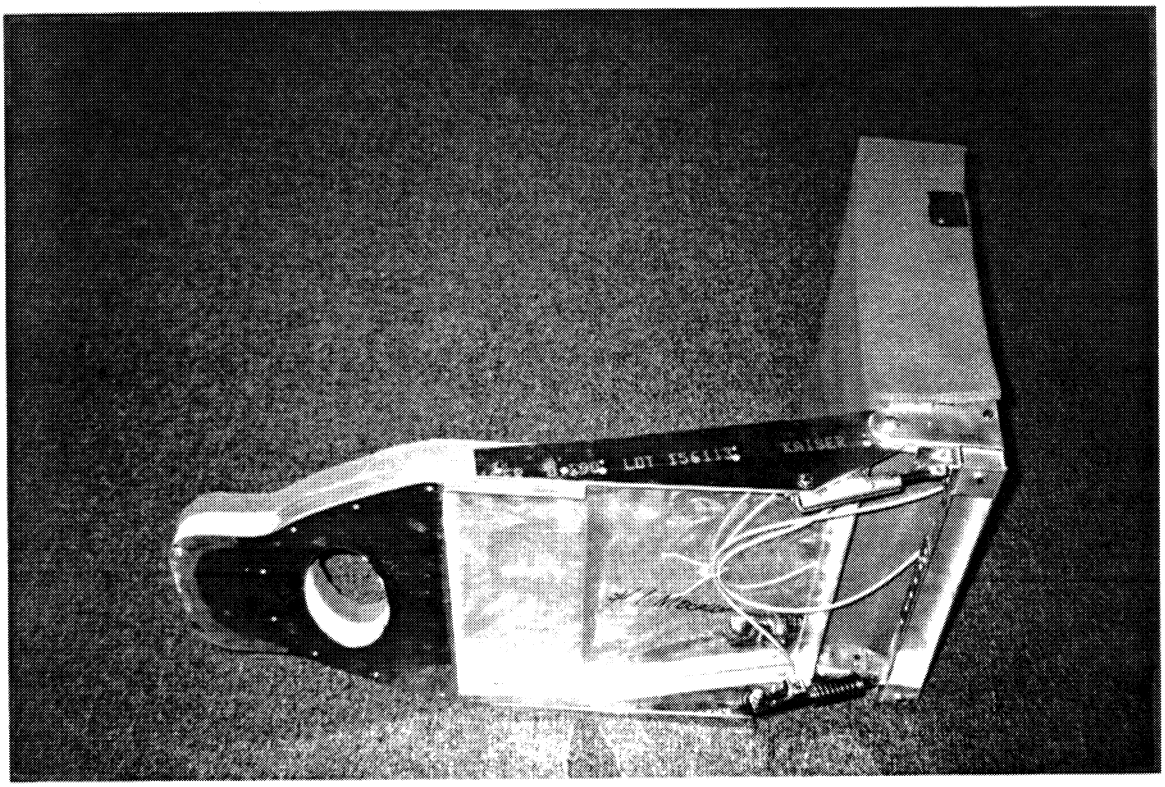

(a), Back View

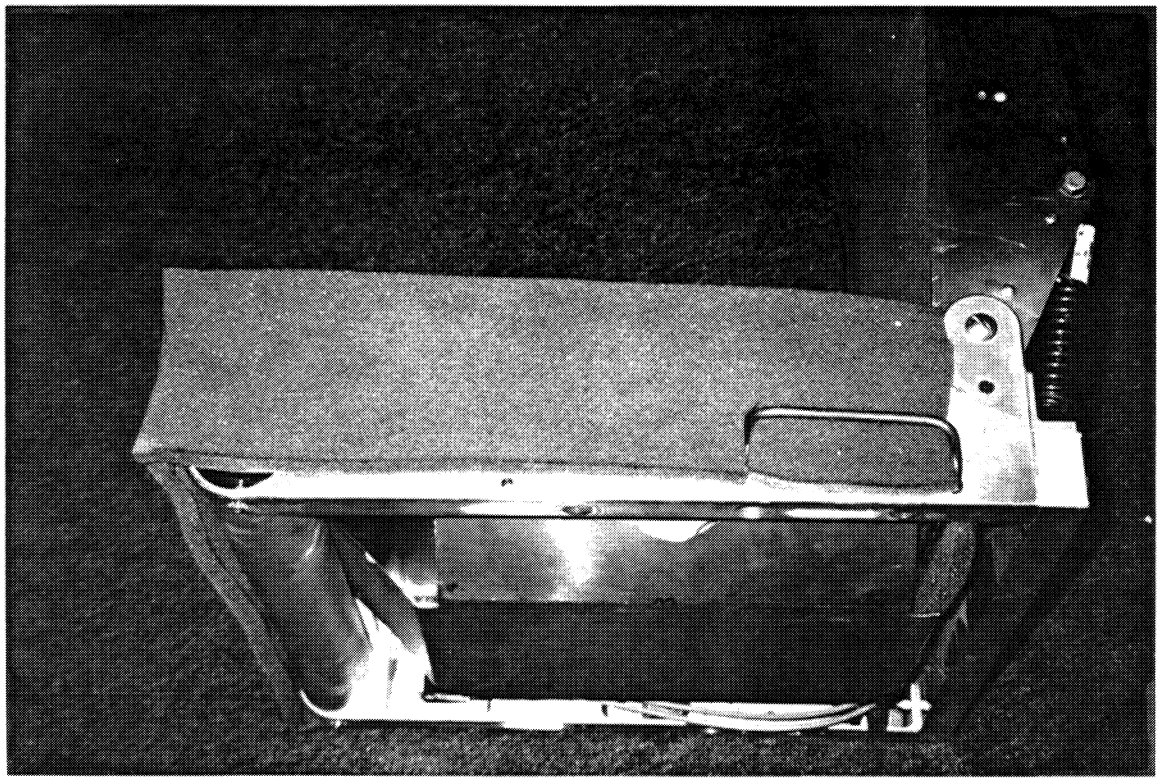

(b), Bottom View

Figure 57, IDI Seat for Pilot Location, Test 4

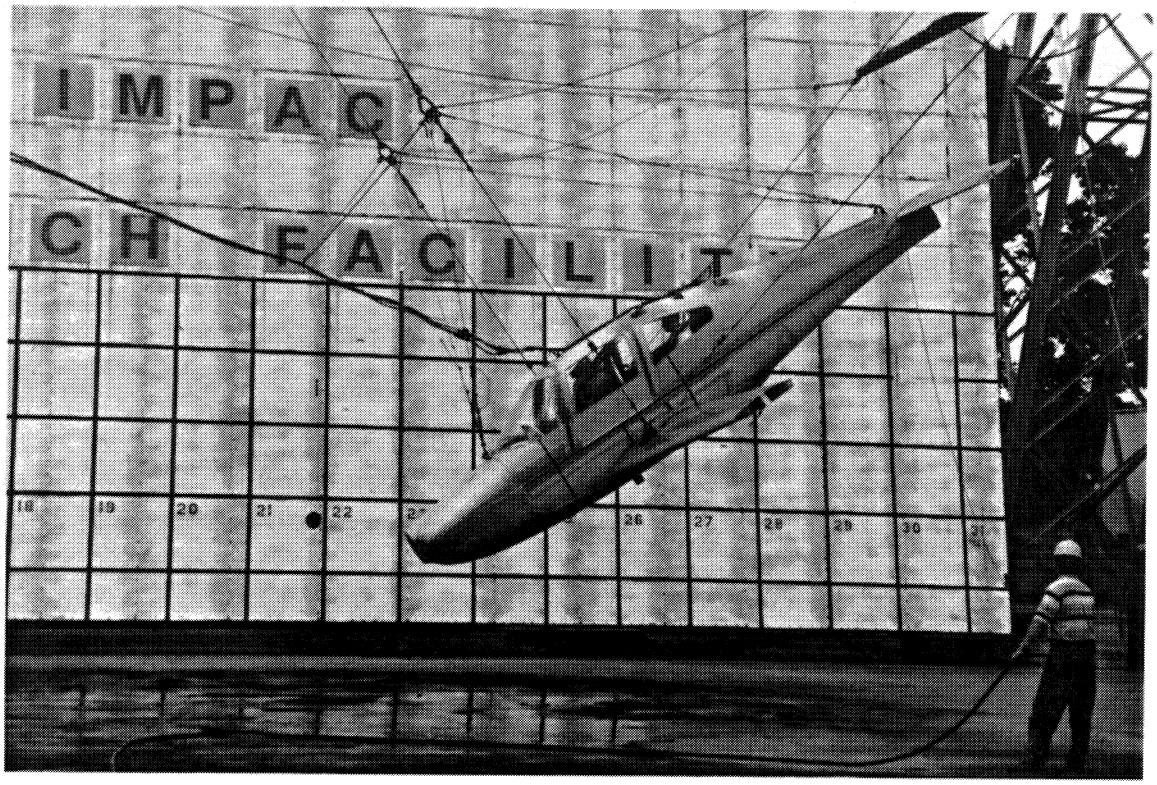

(a), Start of Pullback

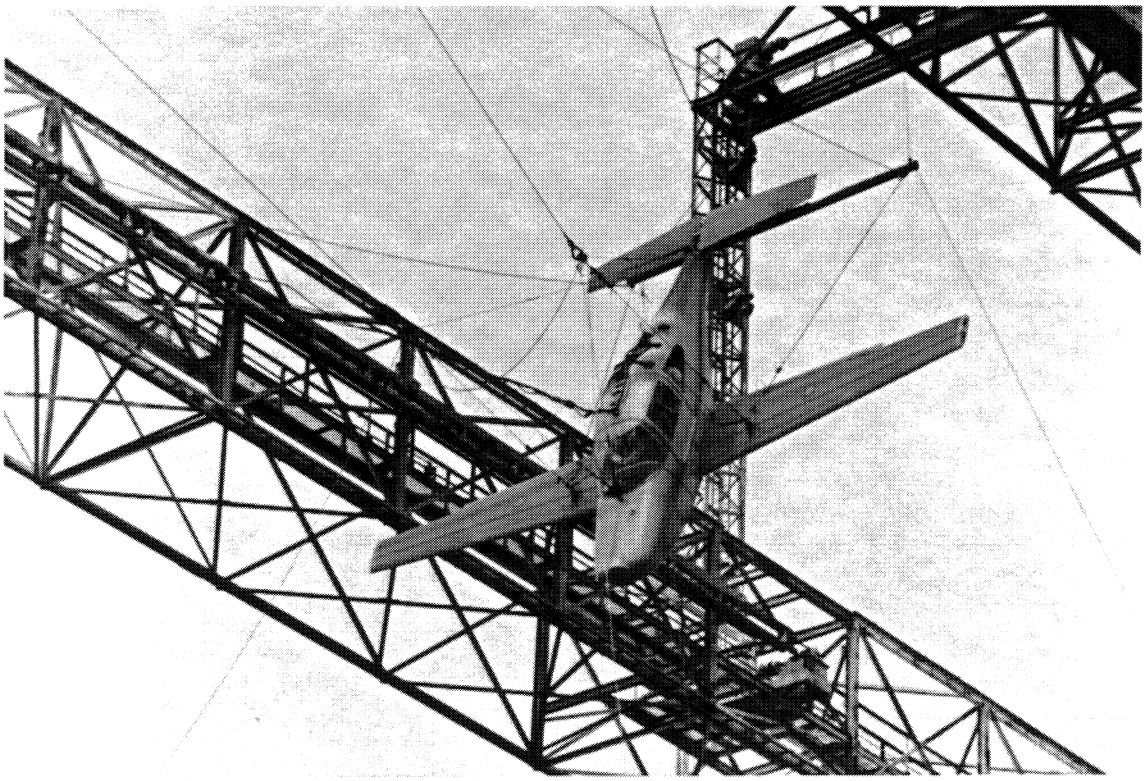

(b), Pullback Position

Figure 58, Test 4 Airplane

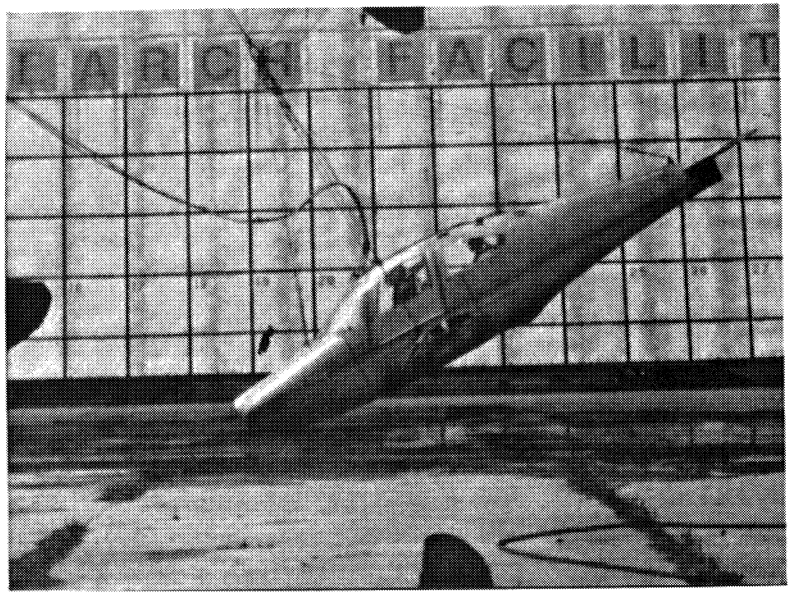

Impact

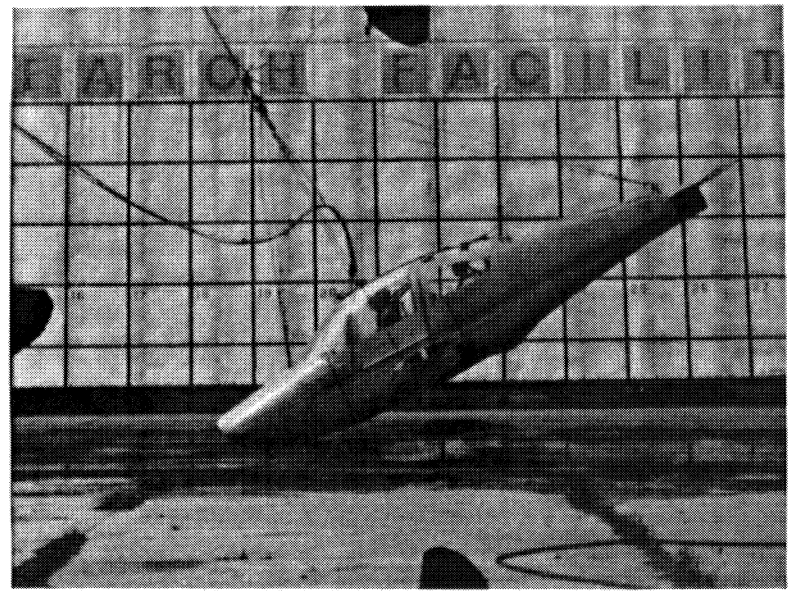

t = .010 seconds

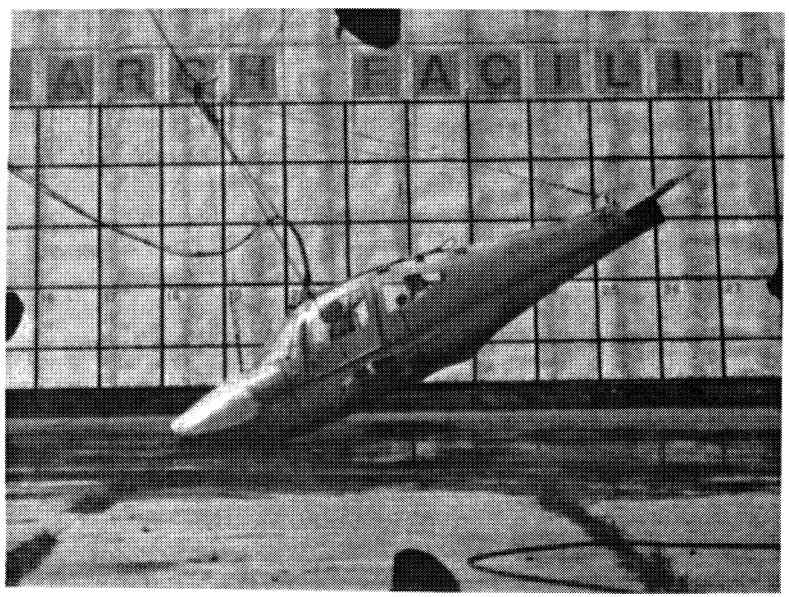

t = .020 seconds

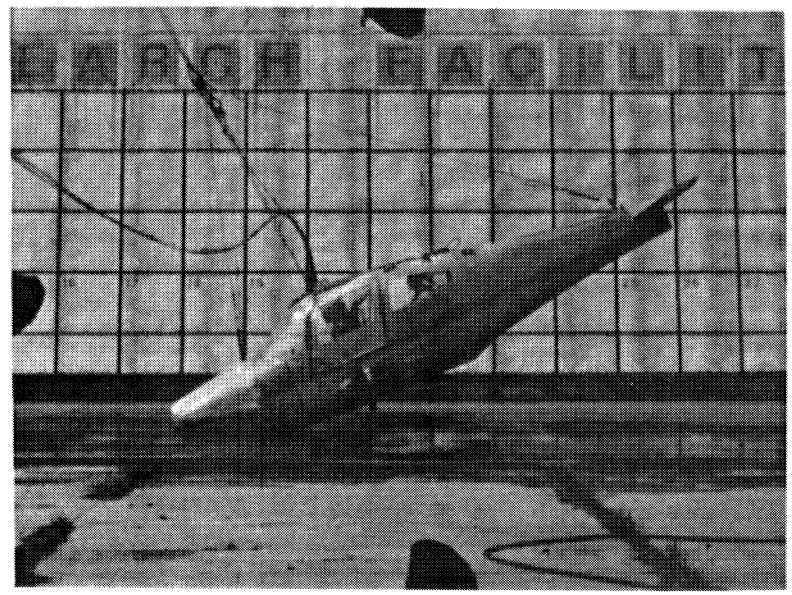

t = .030 seconds

Figure 59, Crash Sequence Photographs for Test 4

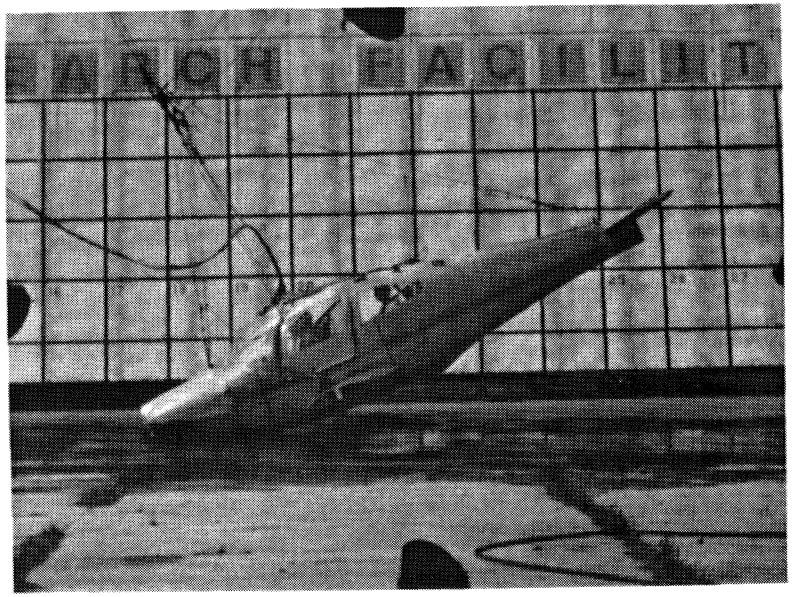

t = .040 seconds

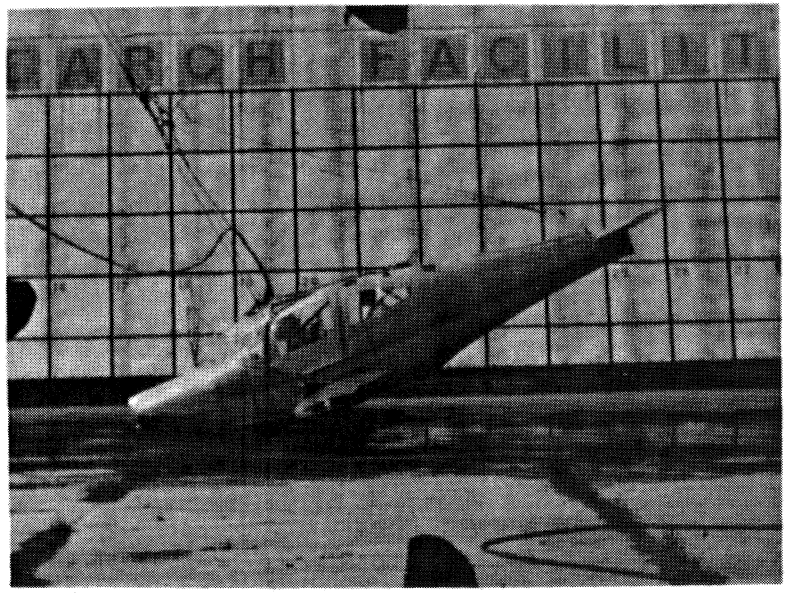

t = .050 seconds

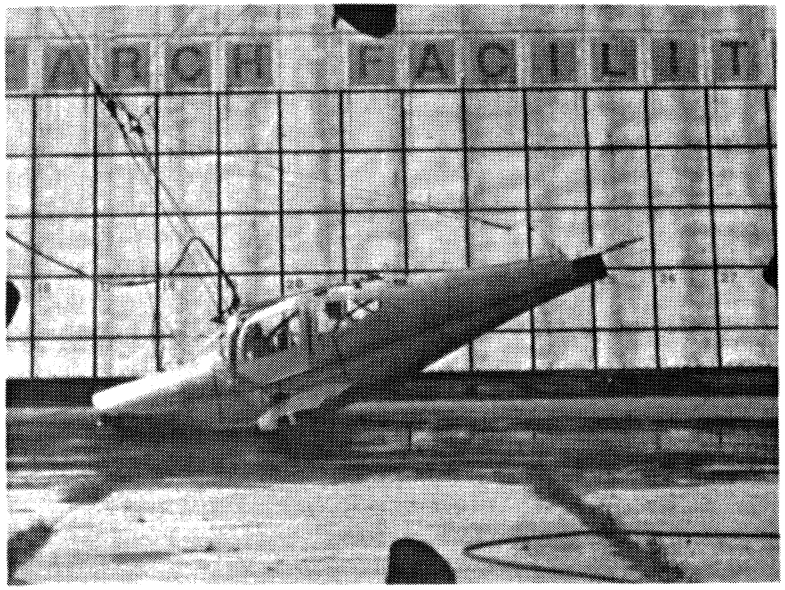

t = .060 seconds

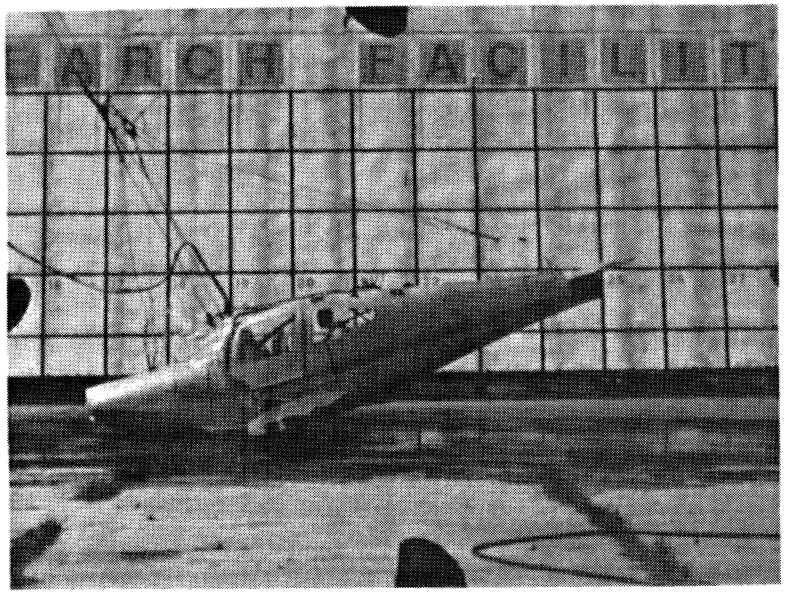

t = .070 seconds

Figure 59, (continued)

t = .080 seconds

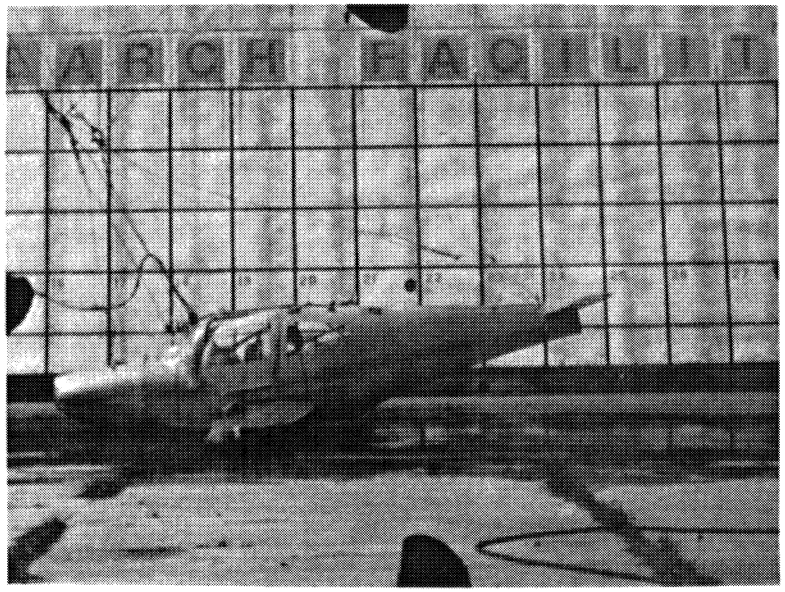

t = .090 seconds

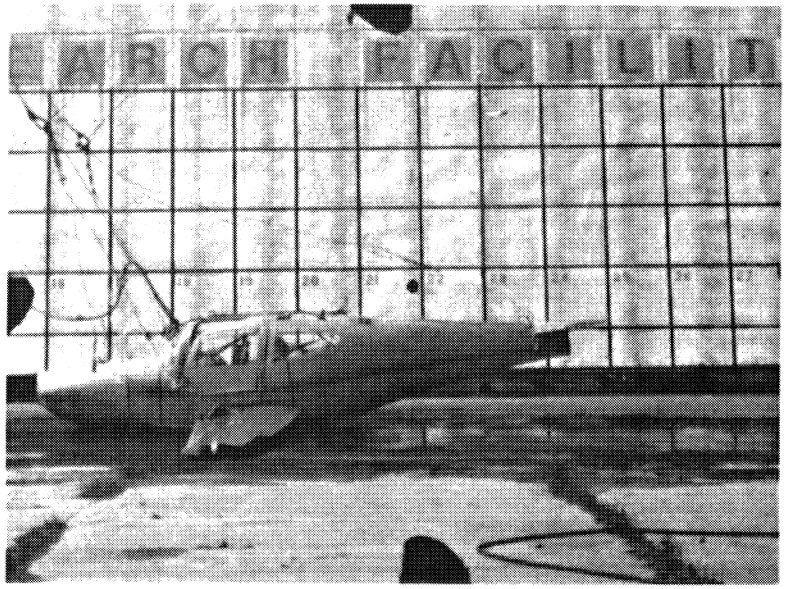

t = .100 seconds

t = .110 seconds

Figure 59, (continued)

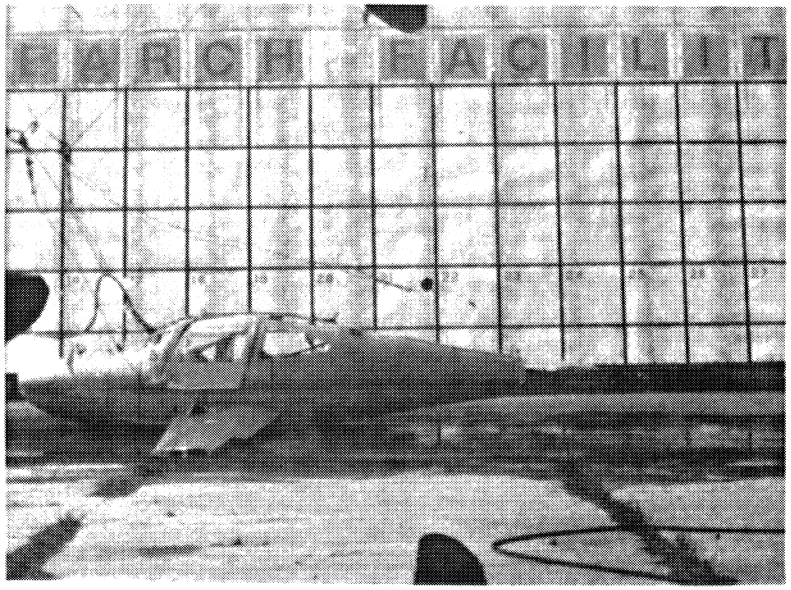

t = .120 seconds

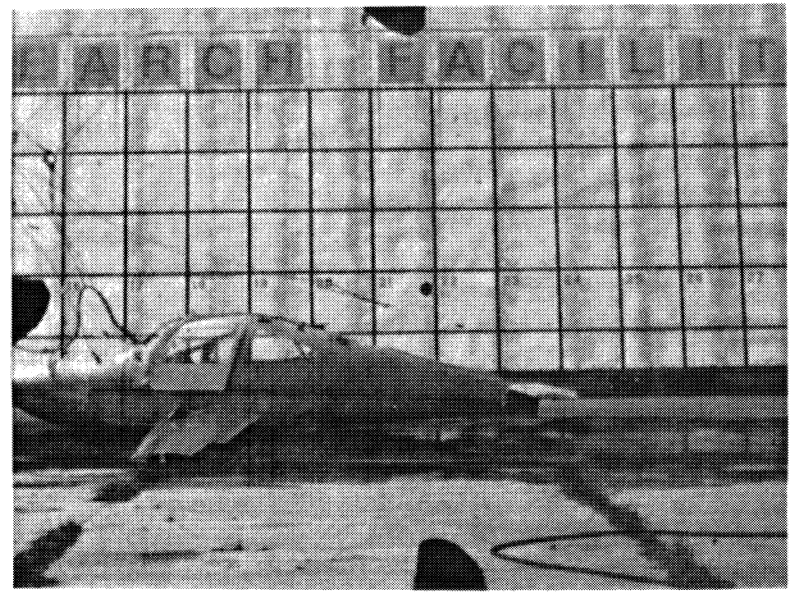

t = .130 seconds

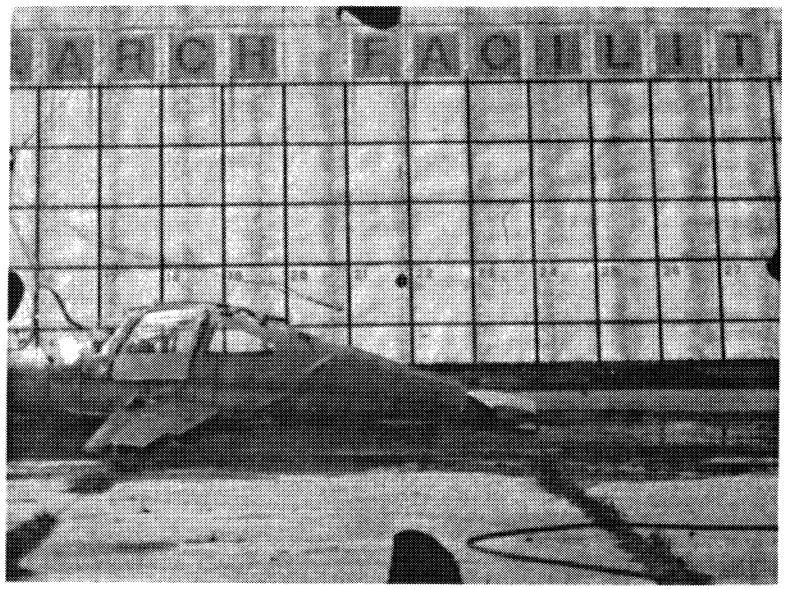

t = .140 seconds

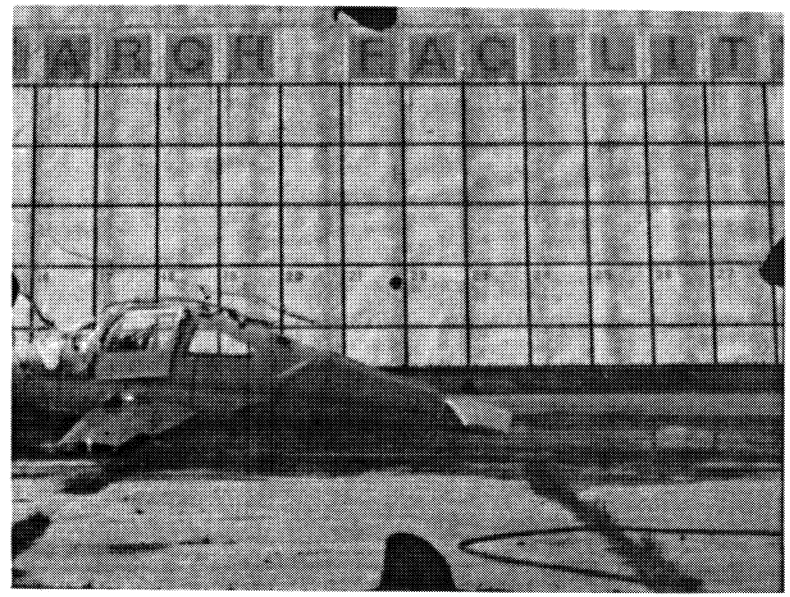

t = .150 seconds

Figure 59, (concluded)

(a), Cockpit View

(b), Right Side Beam

Figure 60, Post Crash Damage forTest 4

(c), Engine Mount with Engine

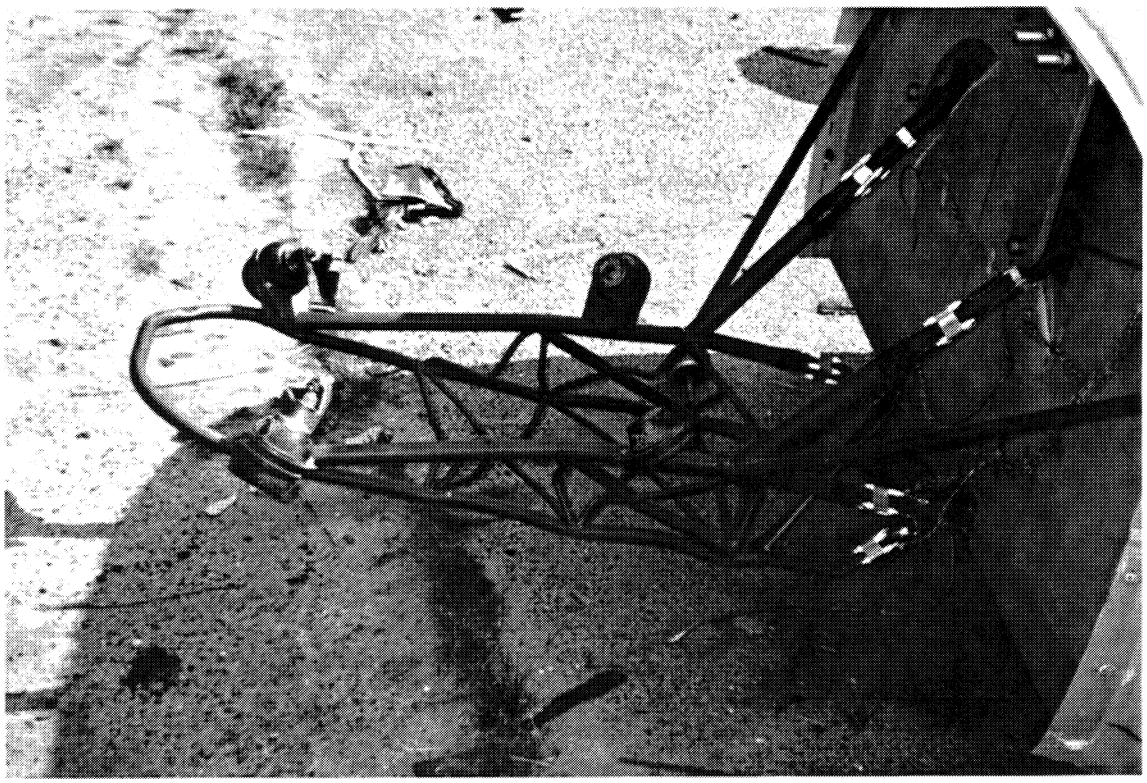

(d), Engine Mount

Figure 60, (continued)

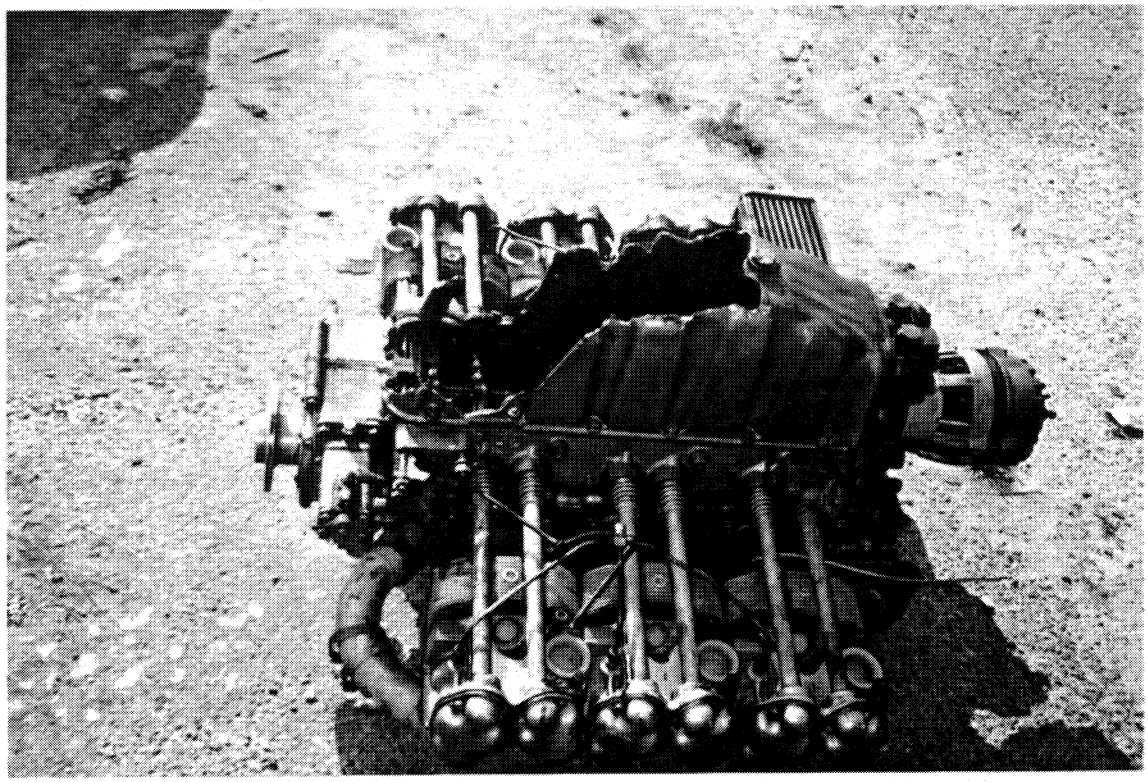

(e), Engine

(f), Pilot Foot Space

Figure 60, (continued)

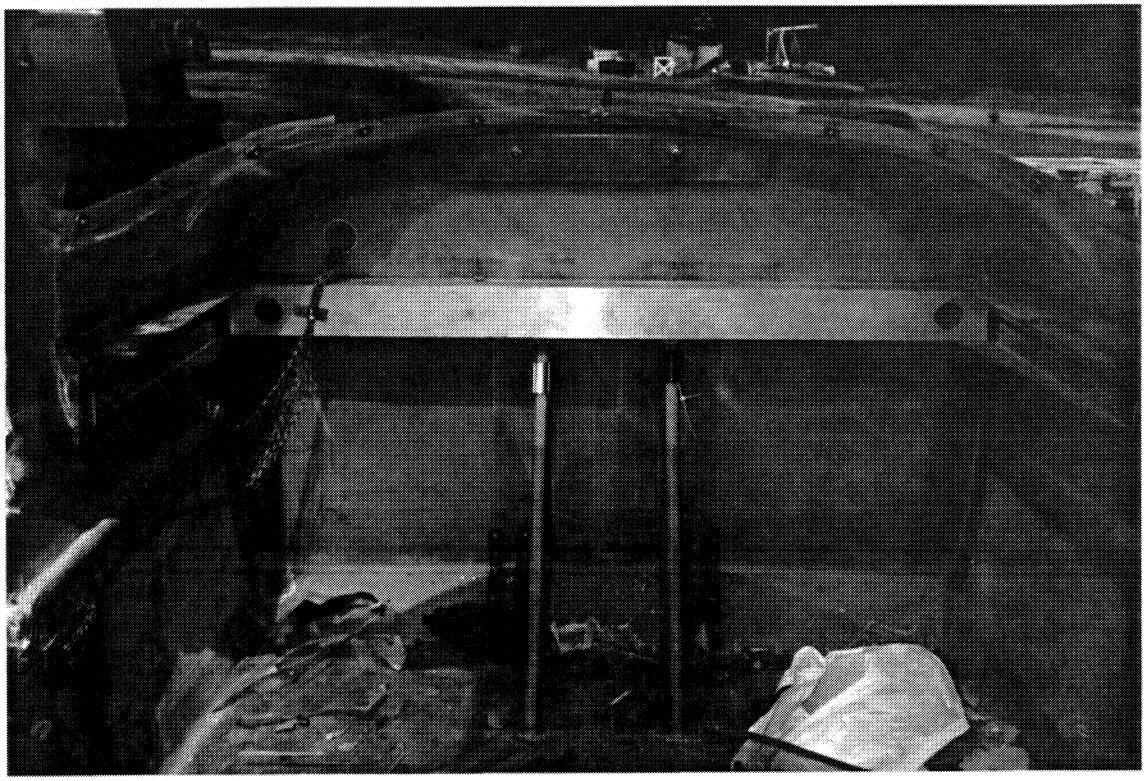

(g), Back Side of Firewall

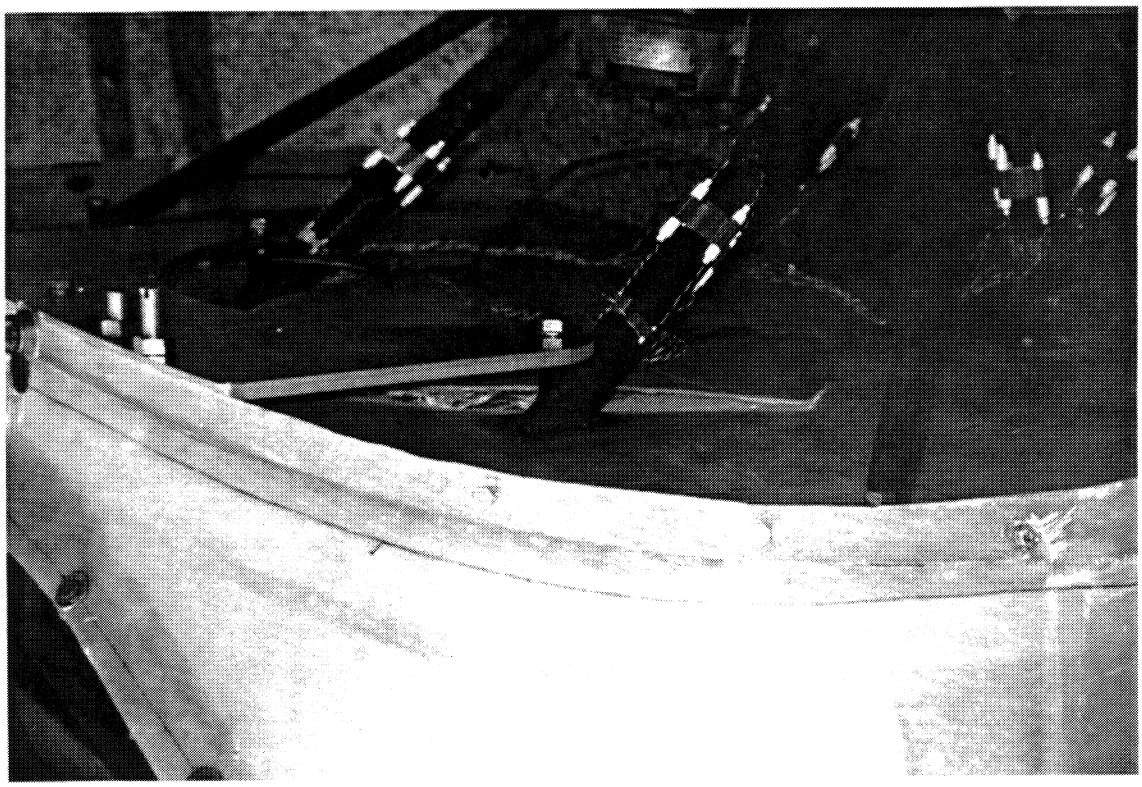

(h), Firewall

Figure 60, (continued)

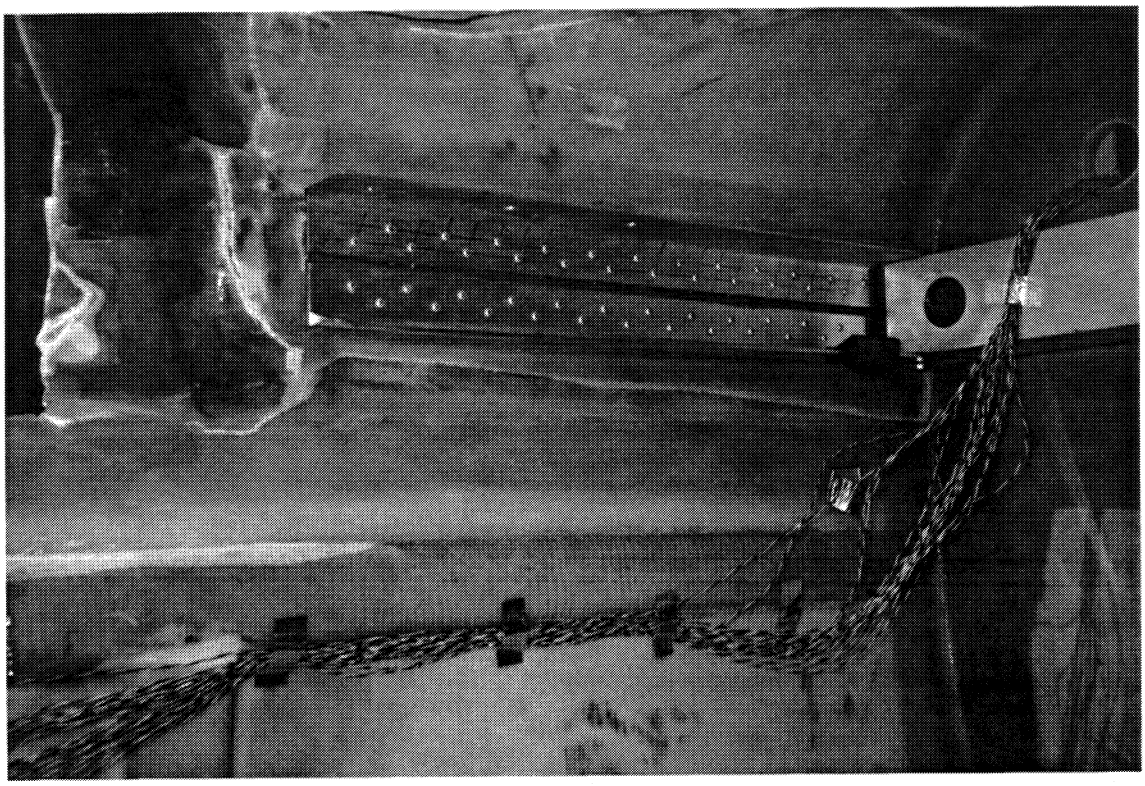

(i), Side Beams, Inside View

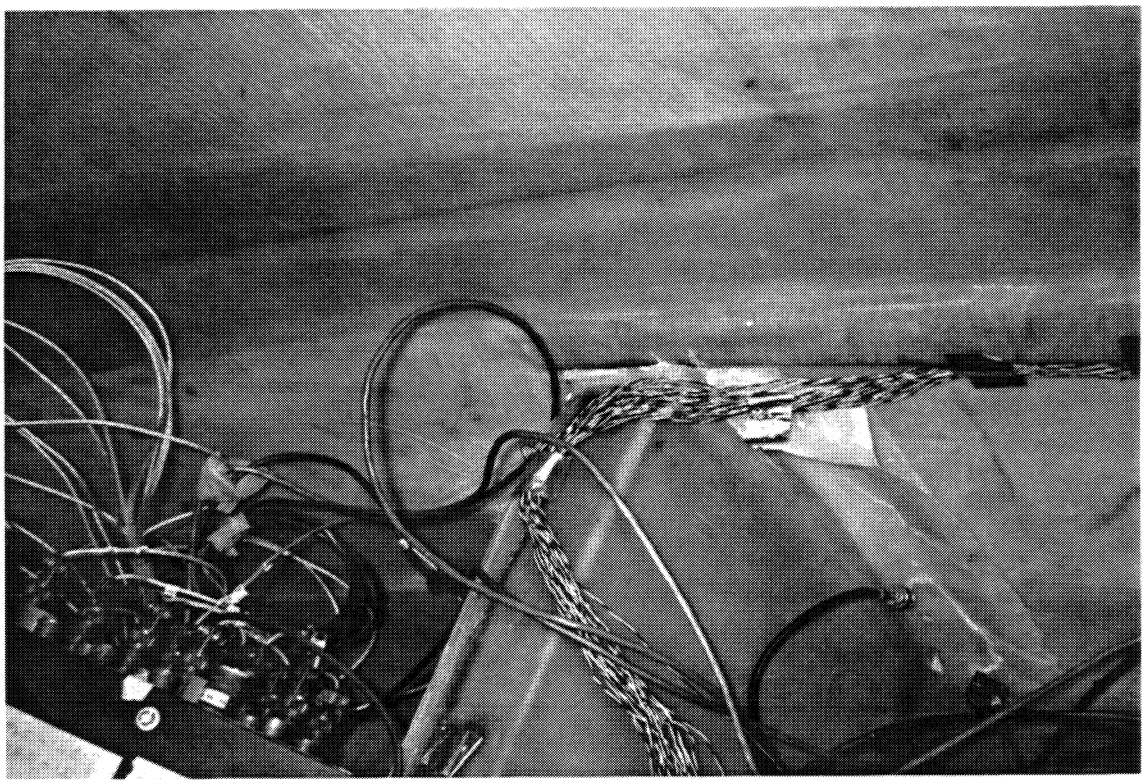

(j), Z Section Beam over Aft Energy Absorber

Figure 60, (concluded)

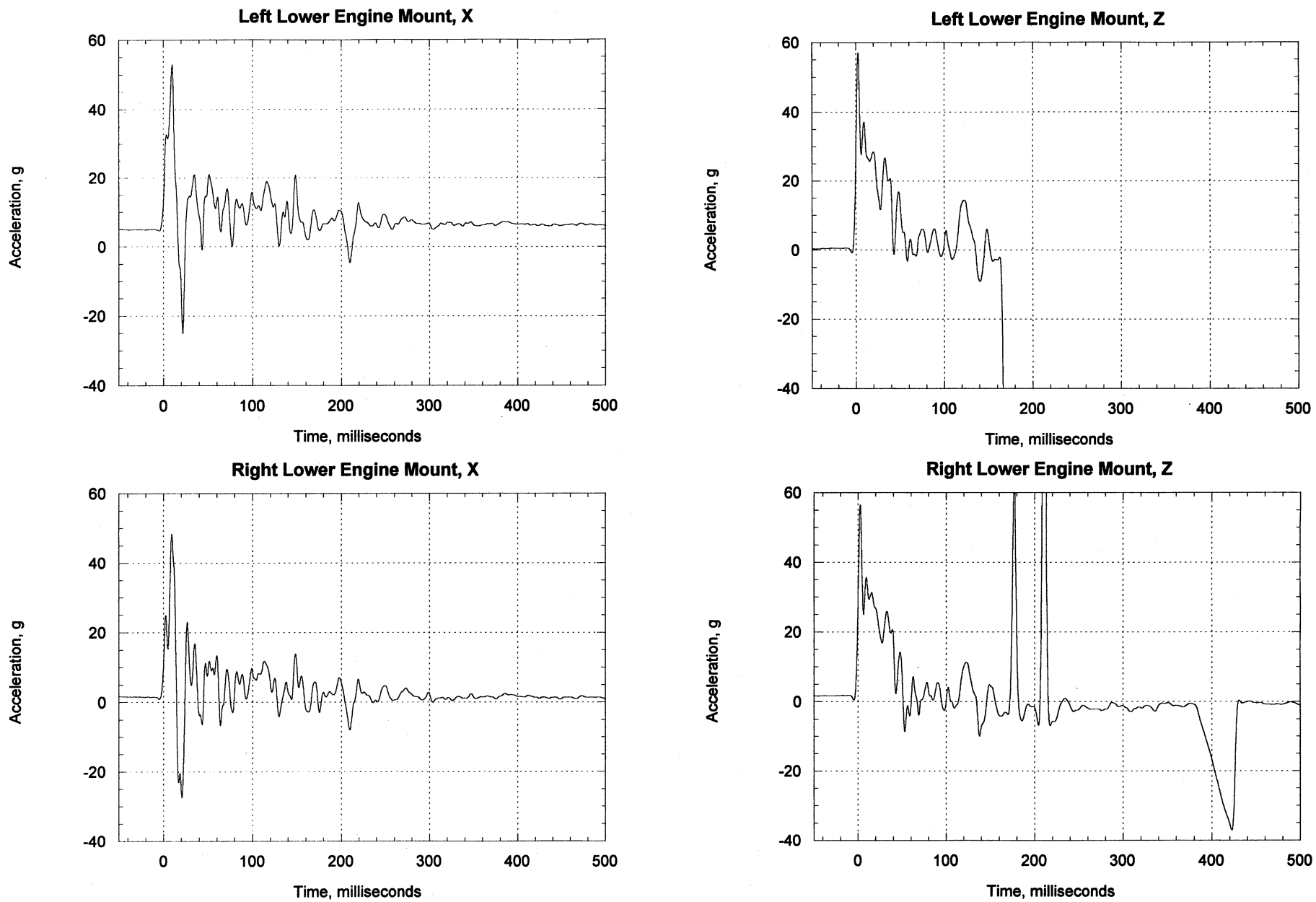

Figure 61, Test 4, Lower Firewall Accelerations

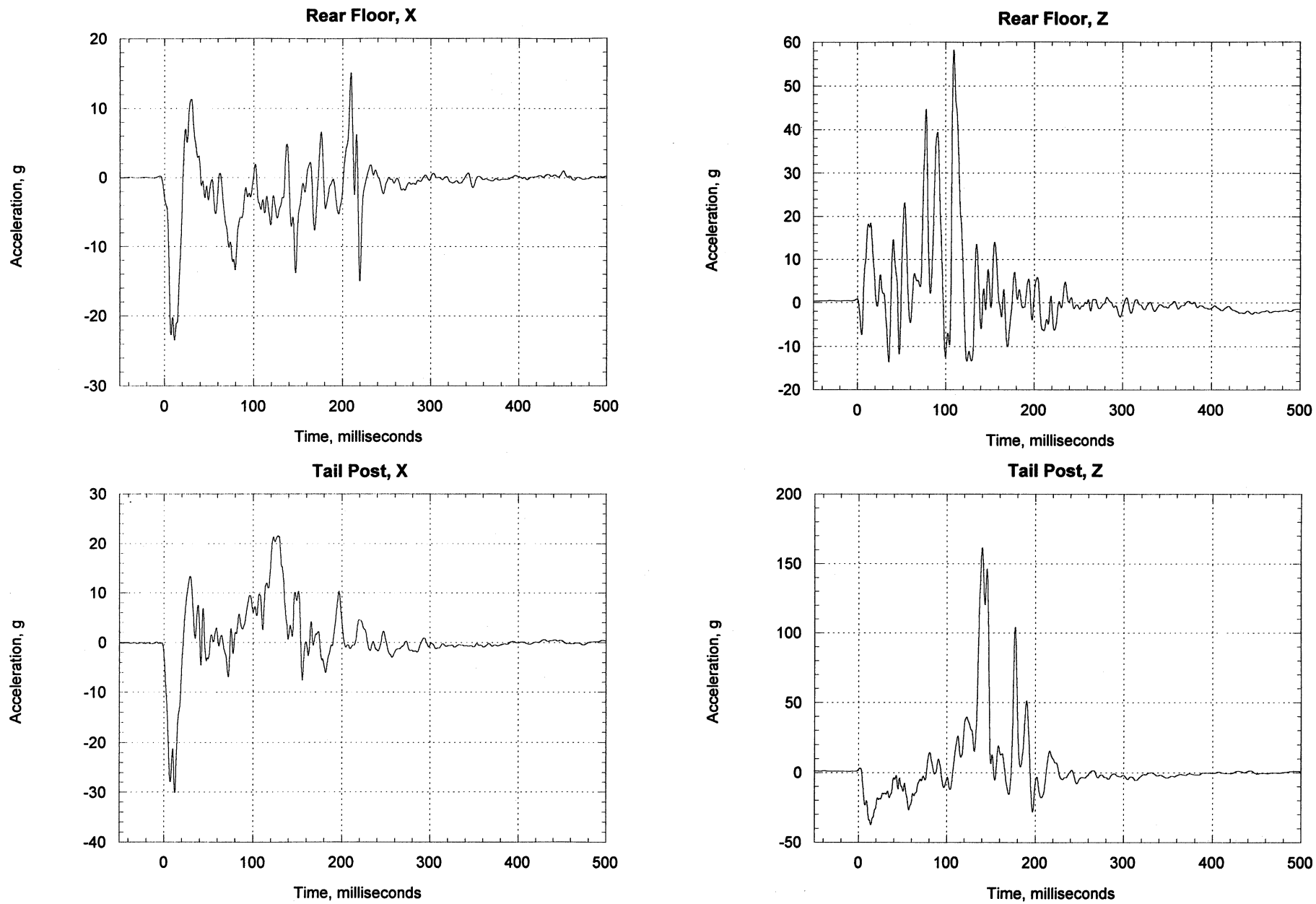

Figure 62, Test 4, Aft Airframe Accelerations

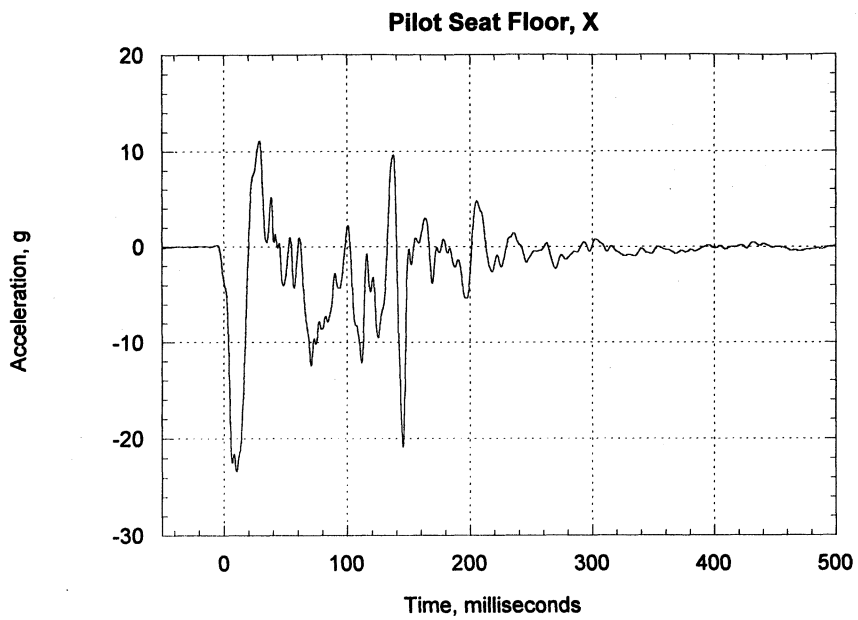

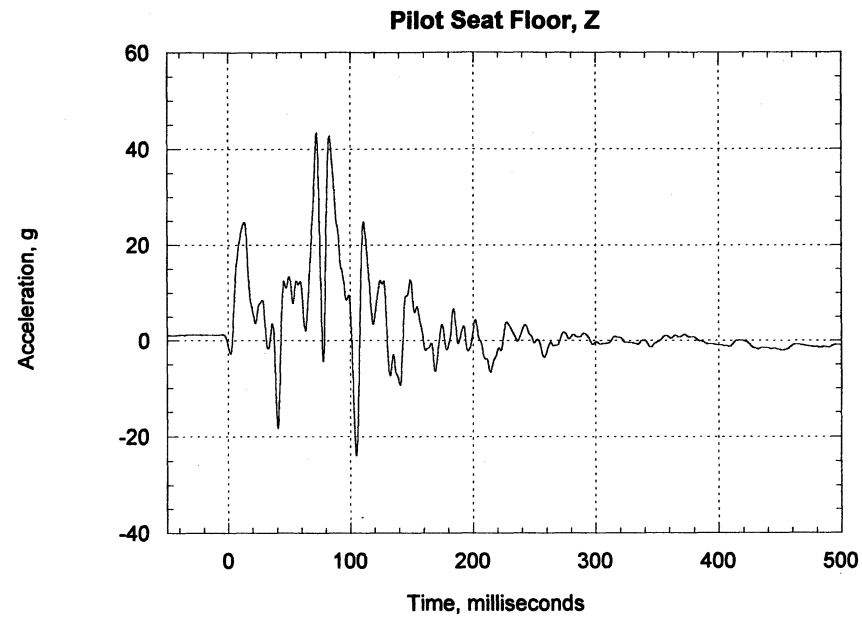

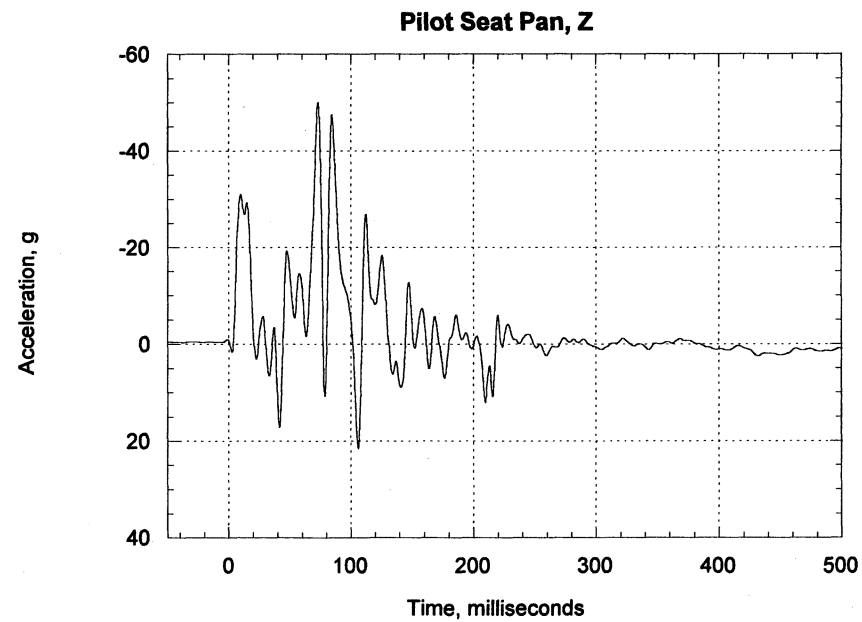

Figure 63, Test 4, Pilot's Seat & Floor

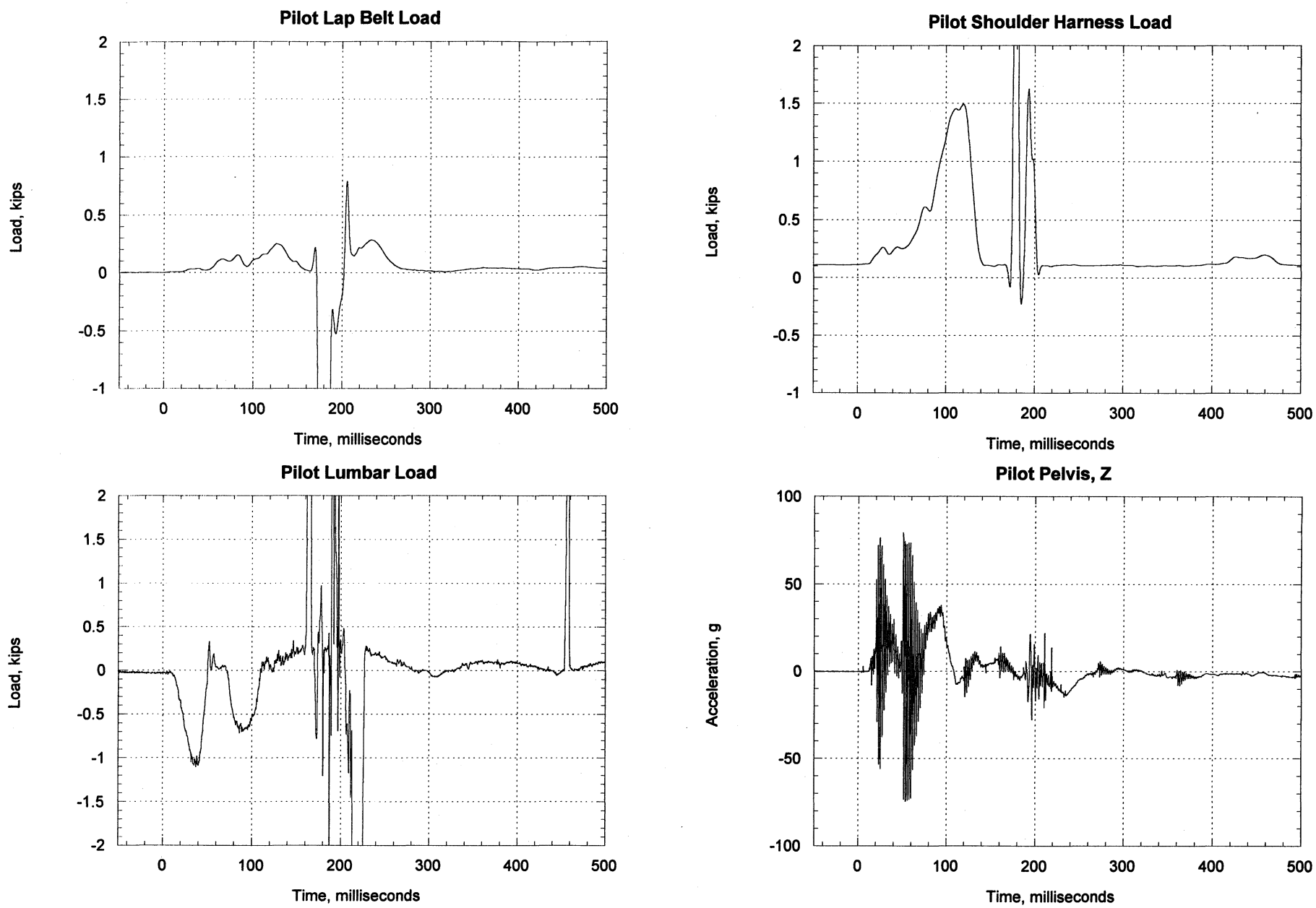

Figure 64, Test 4, Pilot

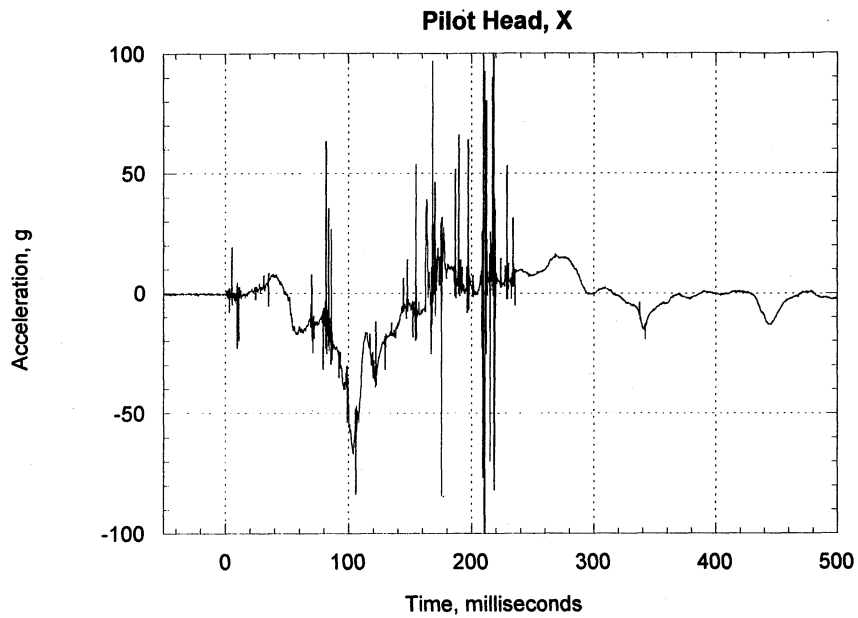

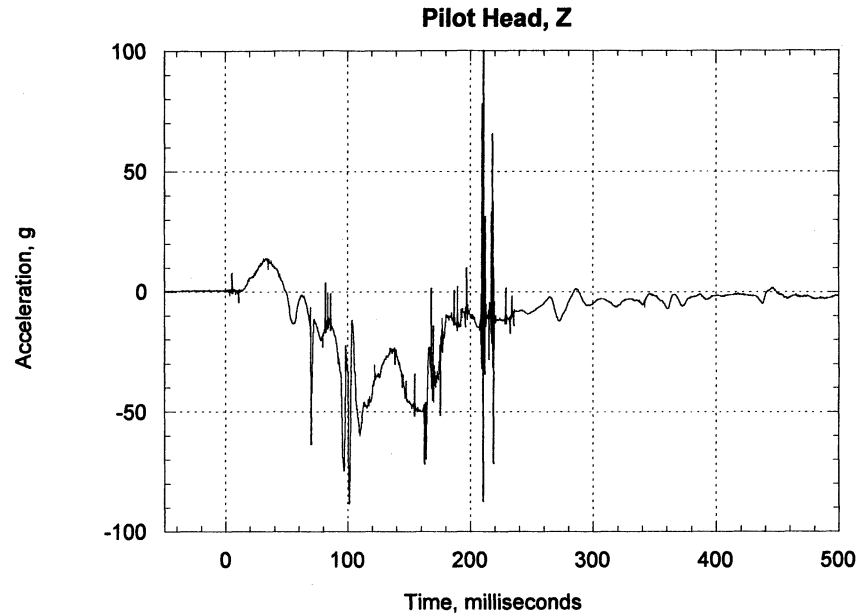

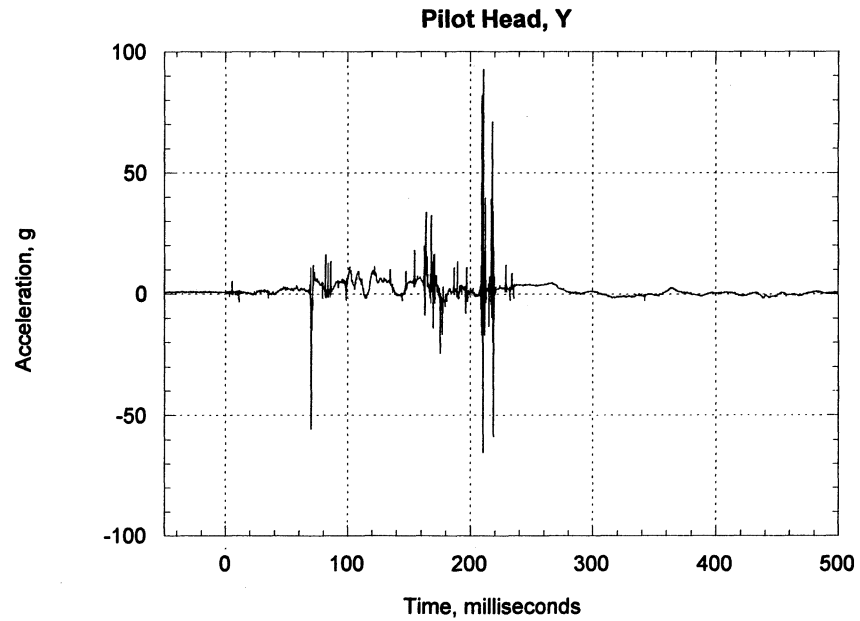

Figure 65, Test 4, Pilot Head

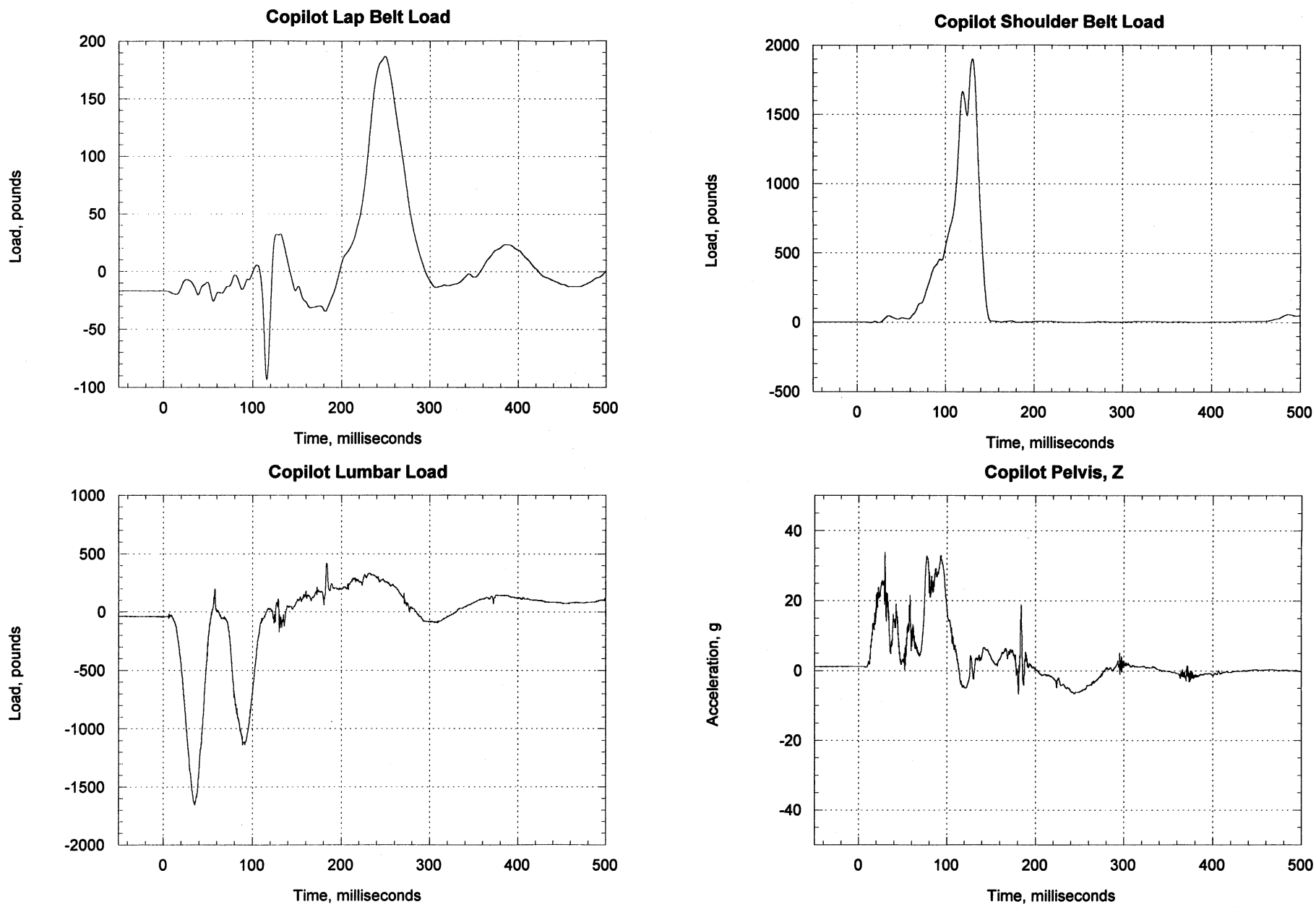

Figure 66, Test 4, Copilot

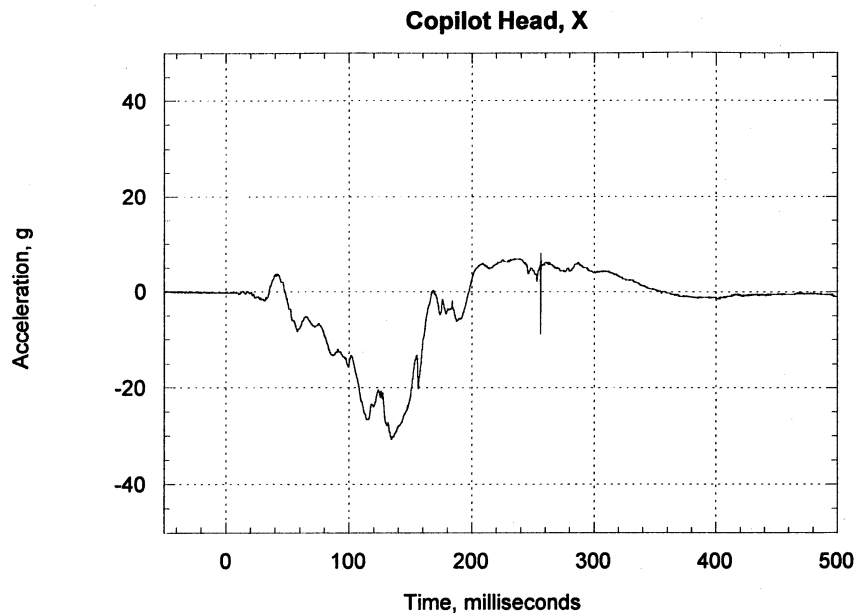

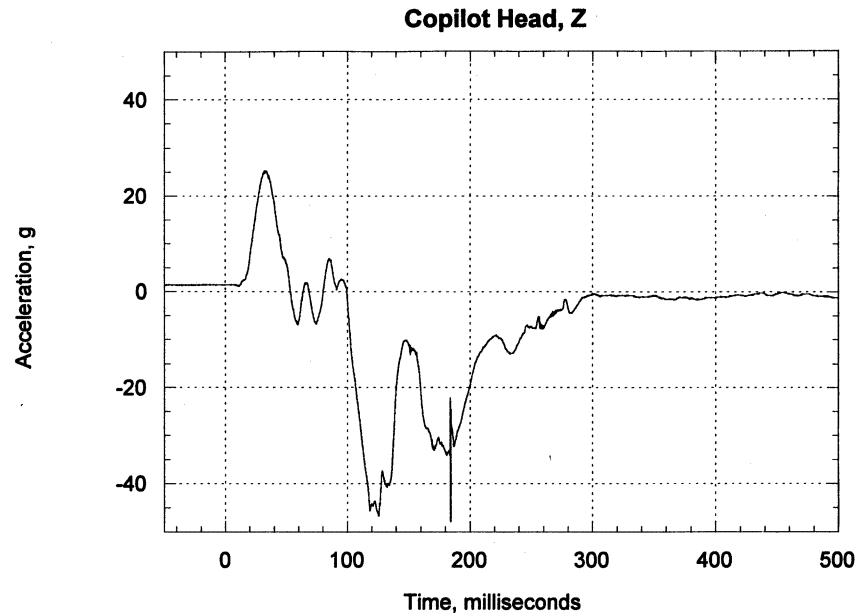

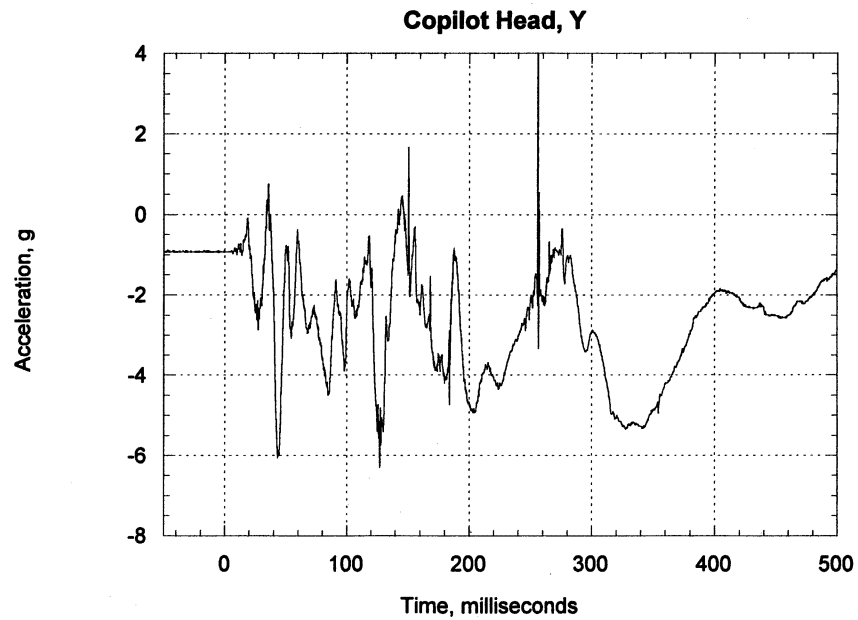

Figure 67, Test 4, Copilot Head

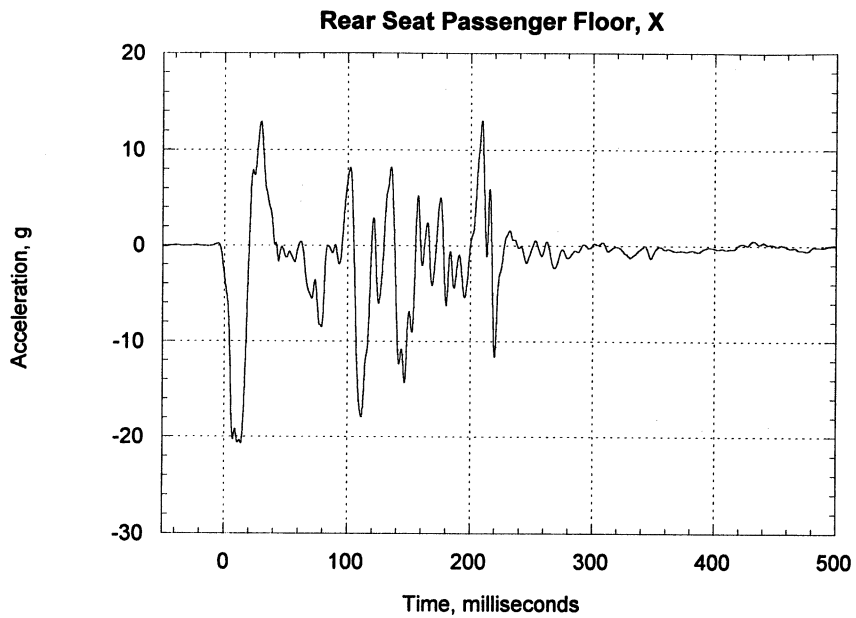

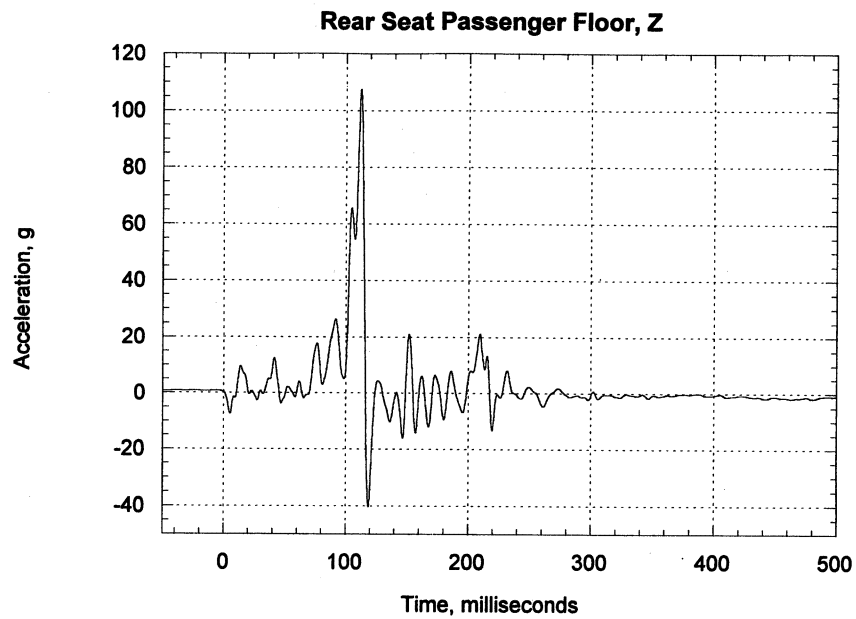

Figure 68, Test 4, Rear Seat Floor

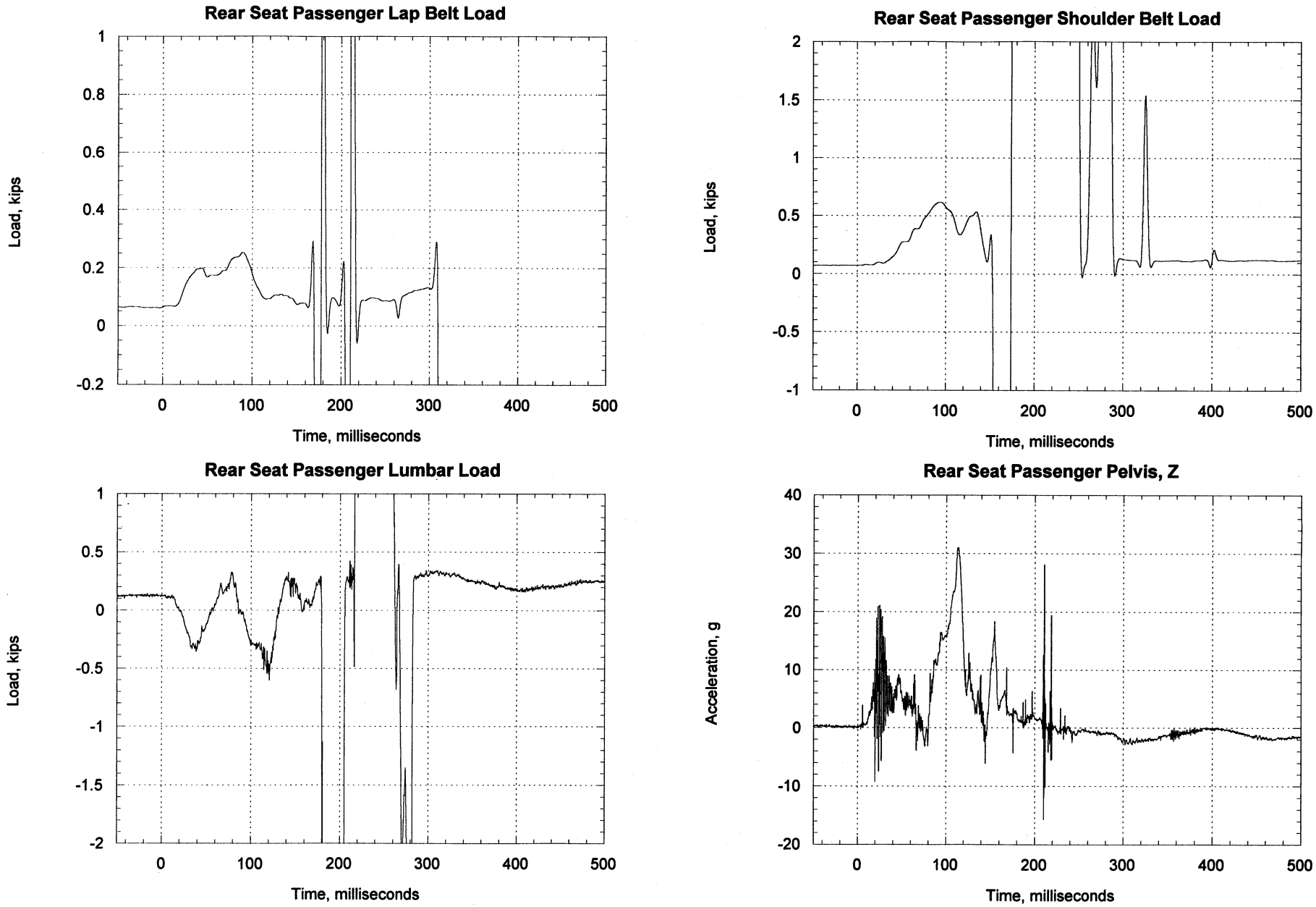

Figure 69, Test 4, Rear Seat Passenger

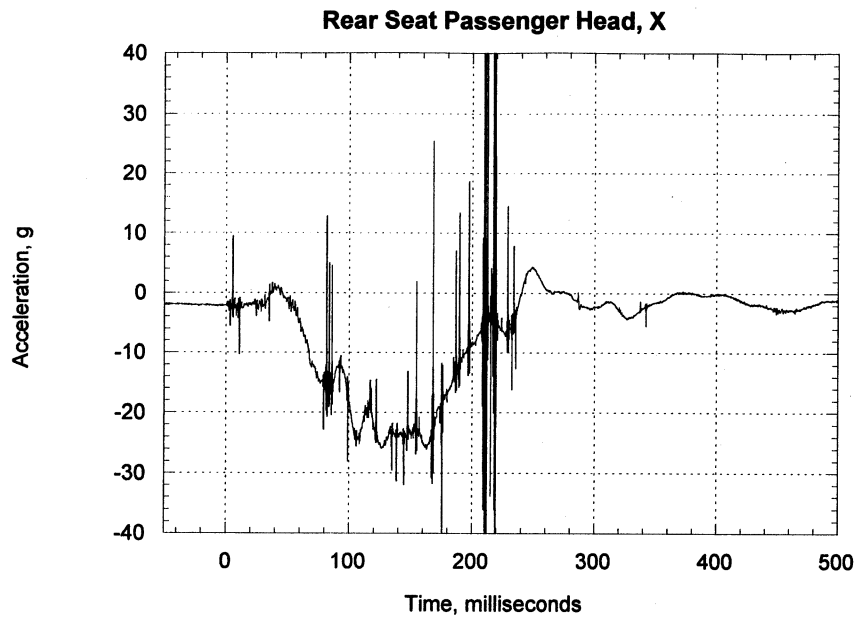

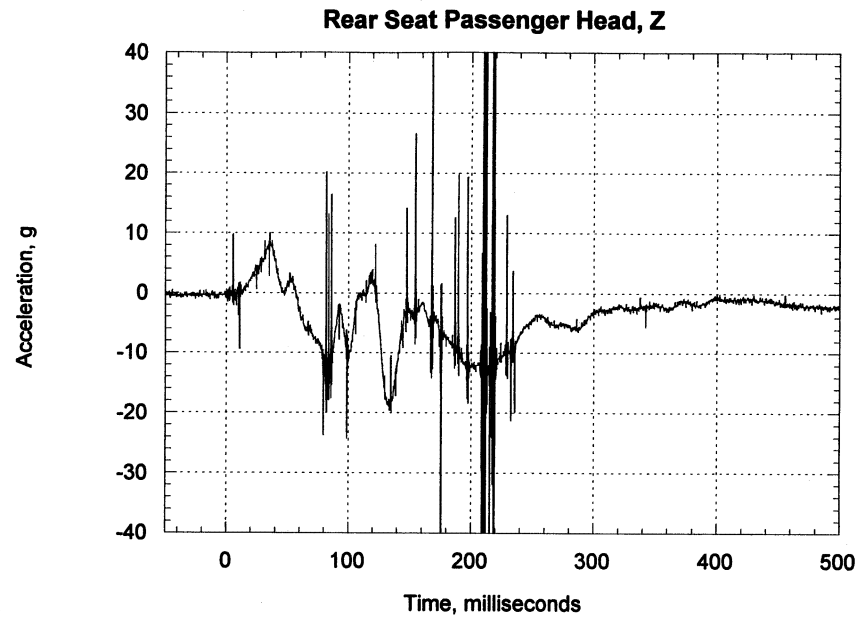

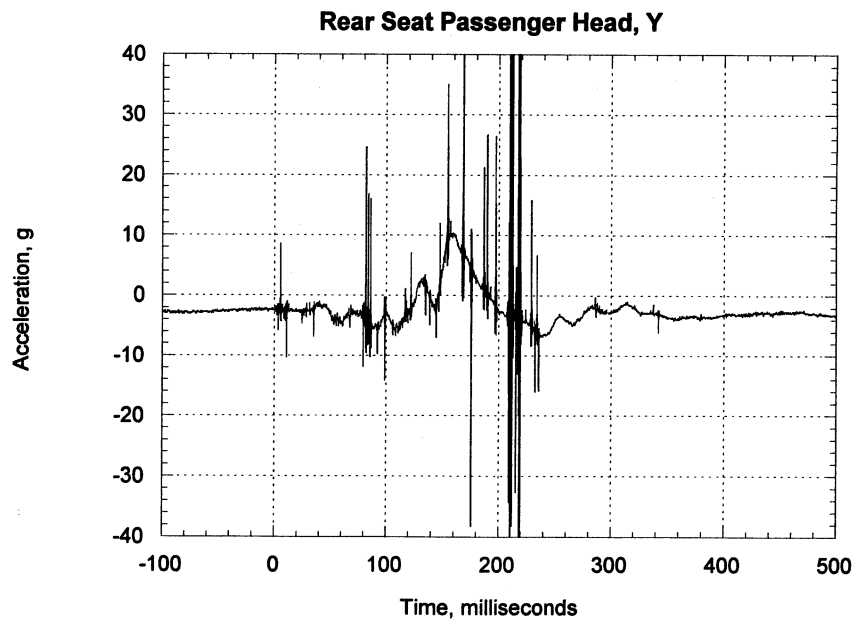

Figure 70, Test 4, Rear Seat Passenger Head

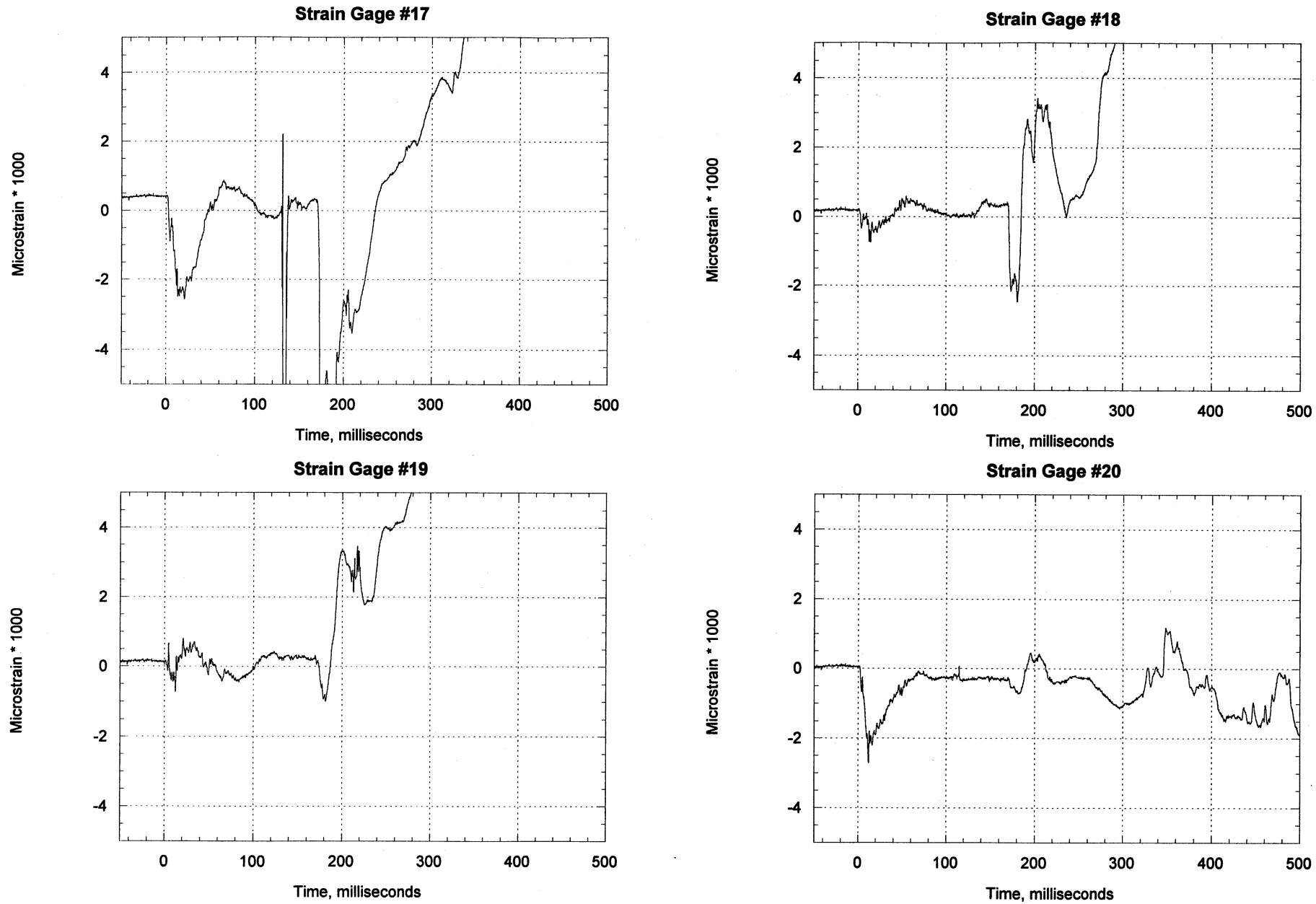

Figure 71, Test 4, Engine Mount, Left Post

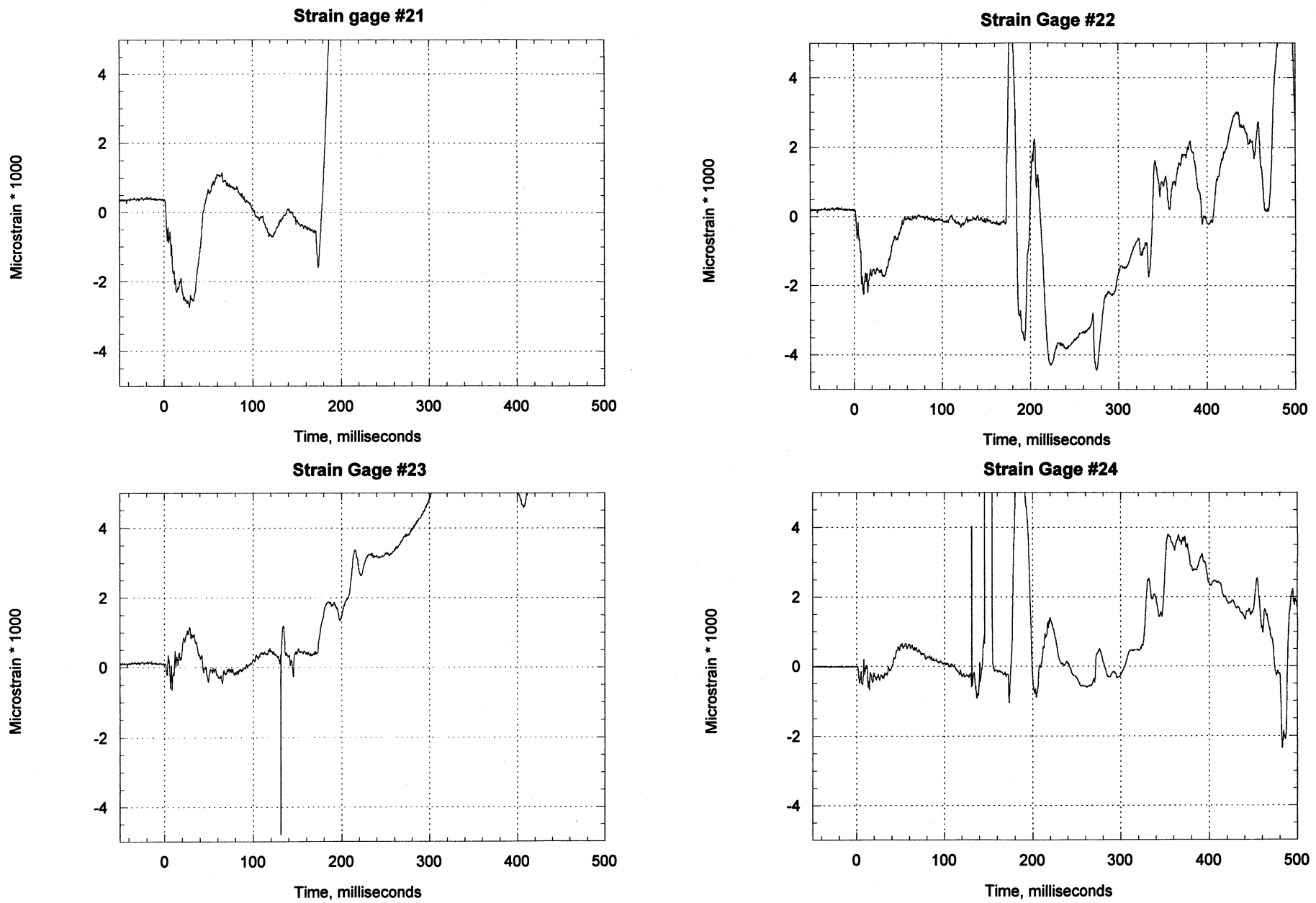

Figure 72, Test 4, Engine Mount, Right Post

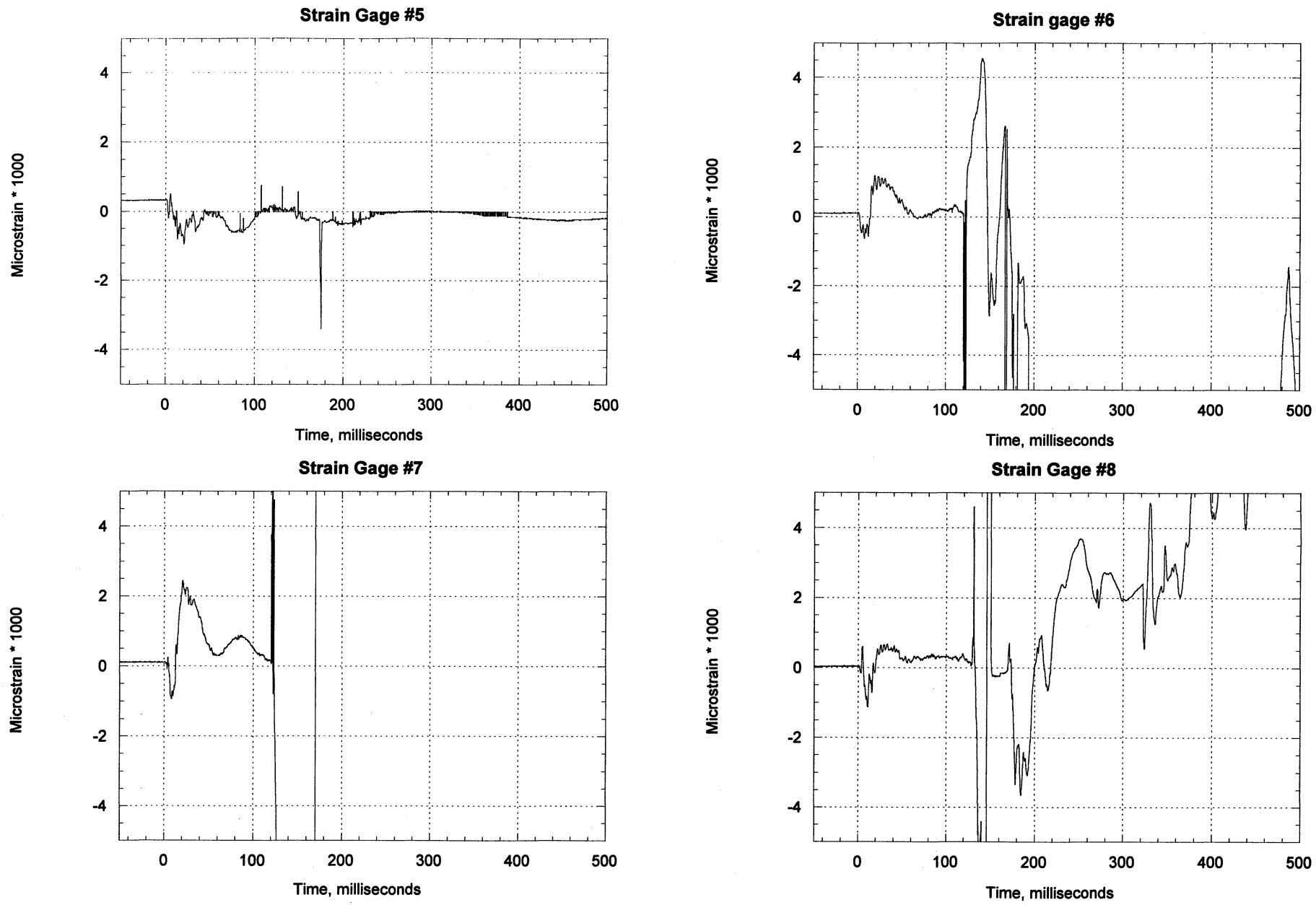

Figure 73, Test 4, Engine Mount, Left Aft Upper Rail

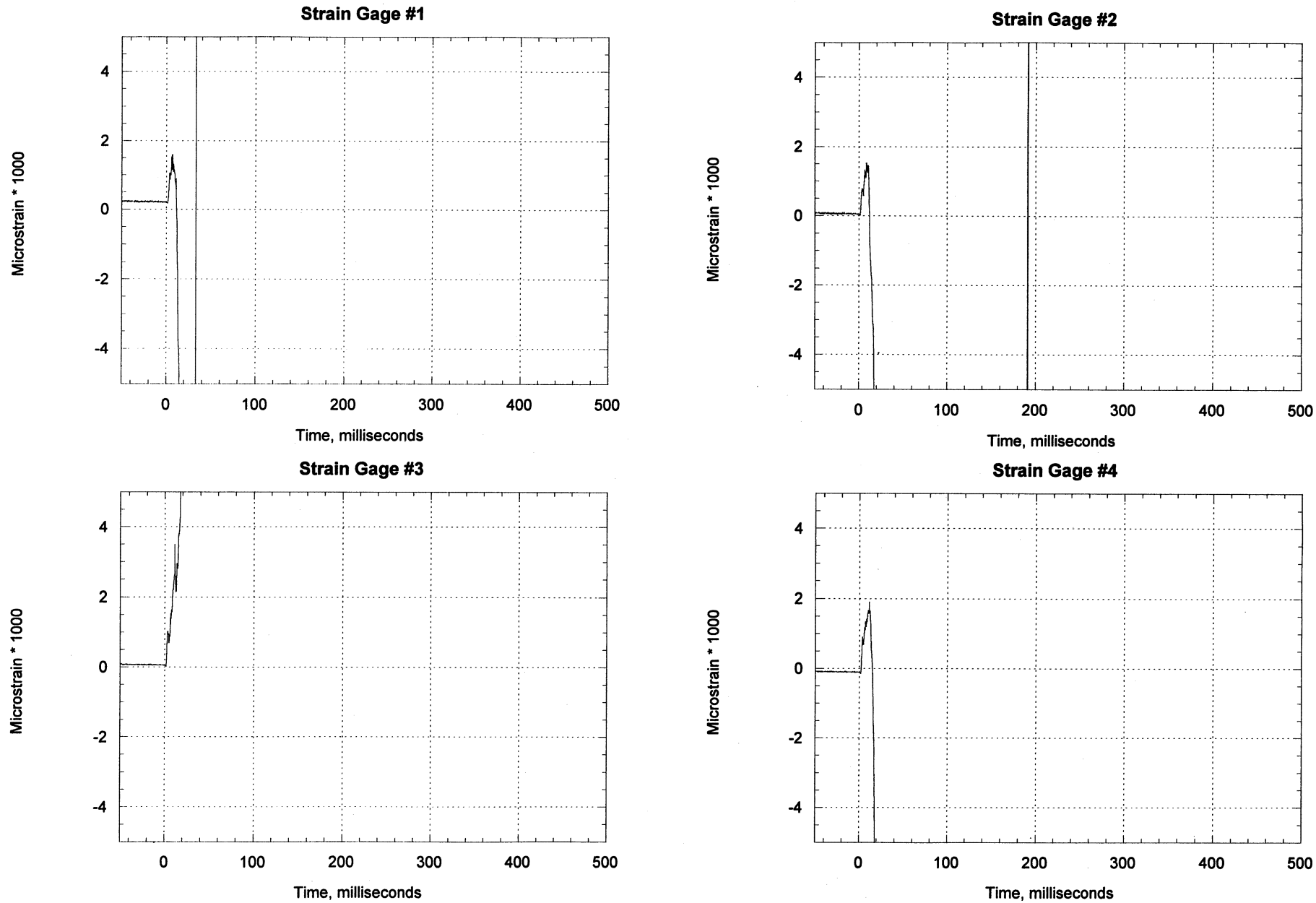

Figure 74, Test 4, Engine Mount, Left Aft Lower Rail

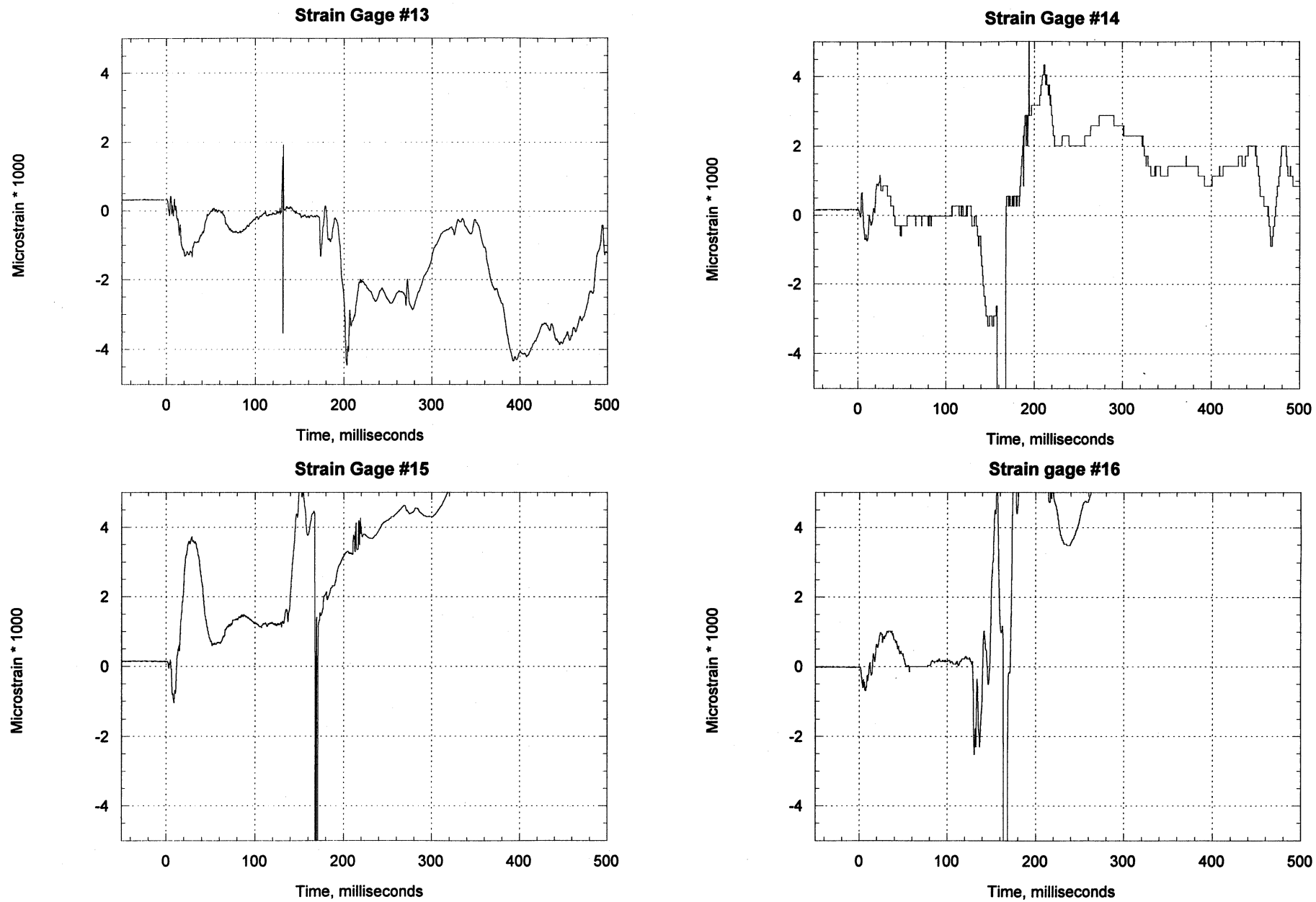

Figure 75, Test 4, Engine Mount, Right Aft Upper Rail

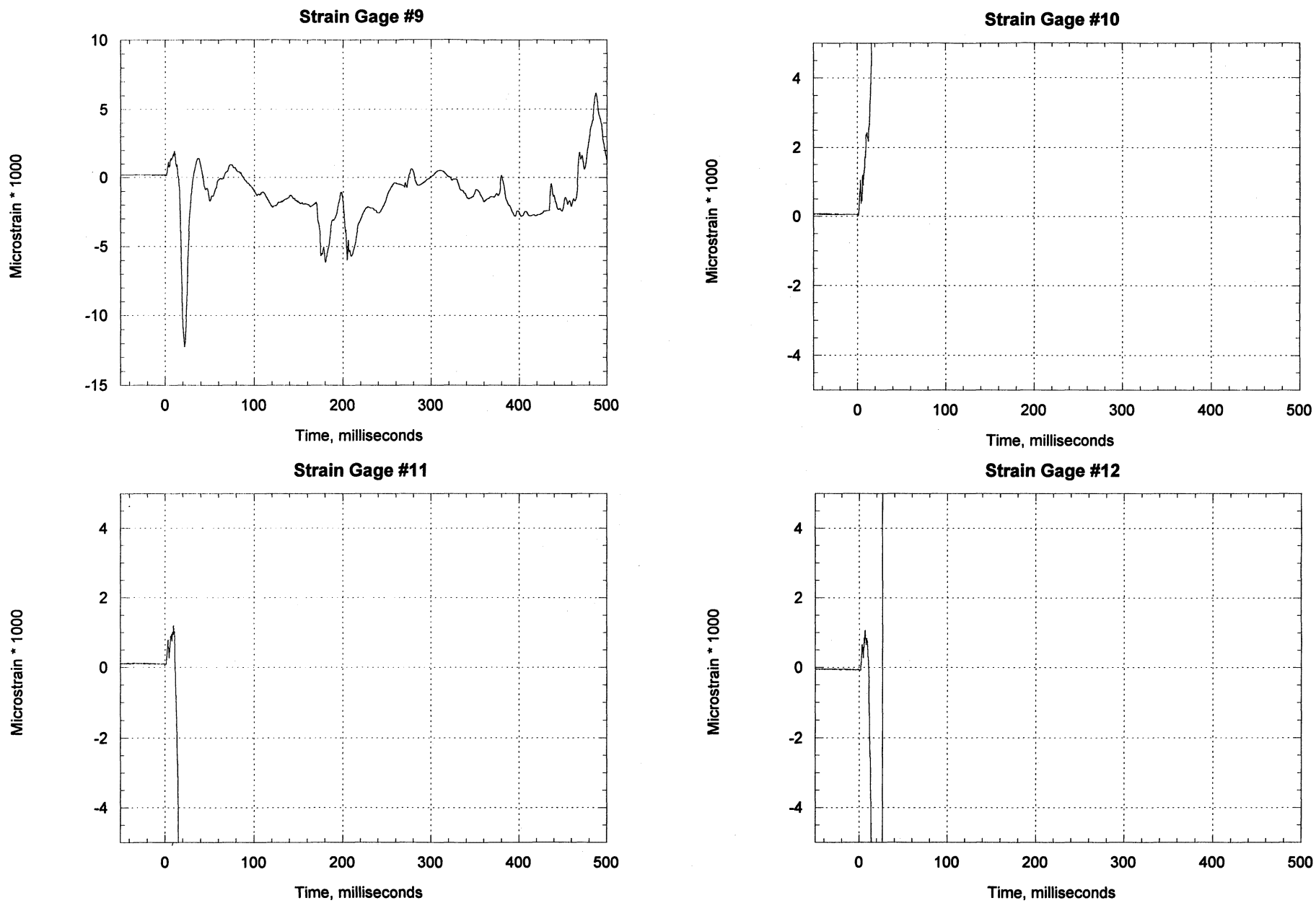

Figure 76, Test 4, Engine Mount, Right Aft Lower Rail

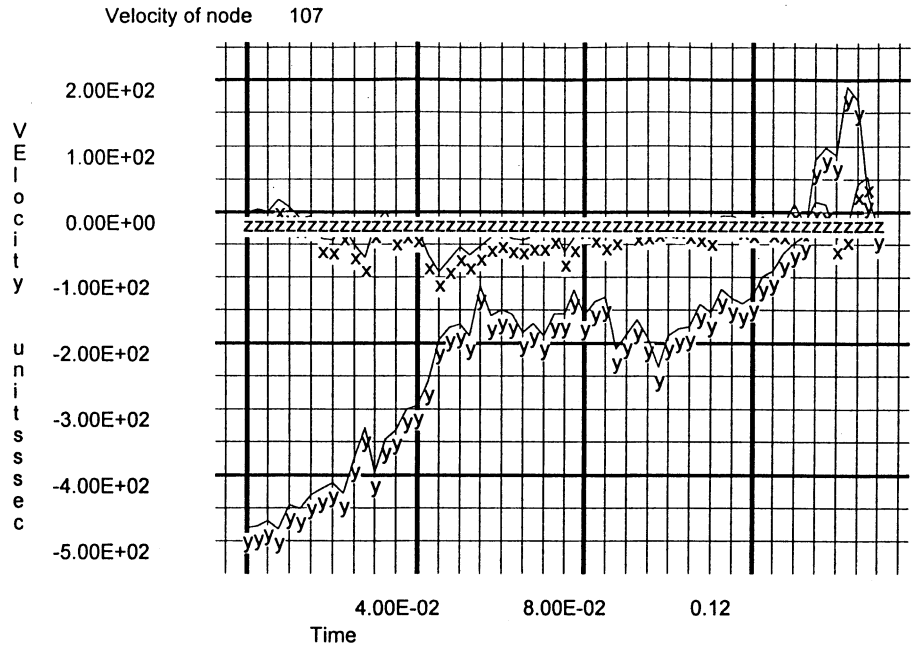

(a), 30 degrees

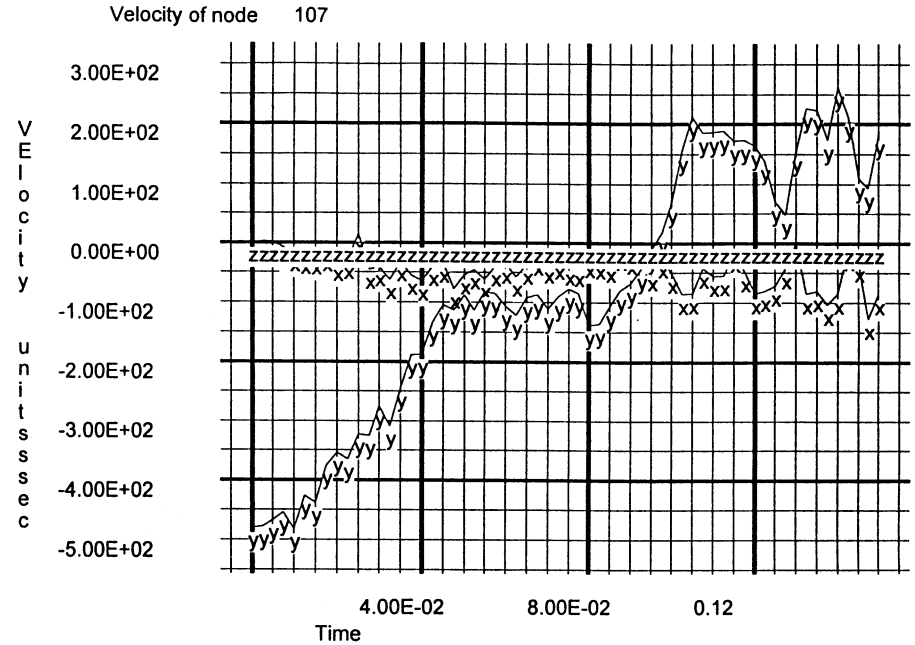

(b), 20 degrees

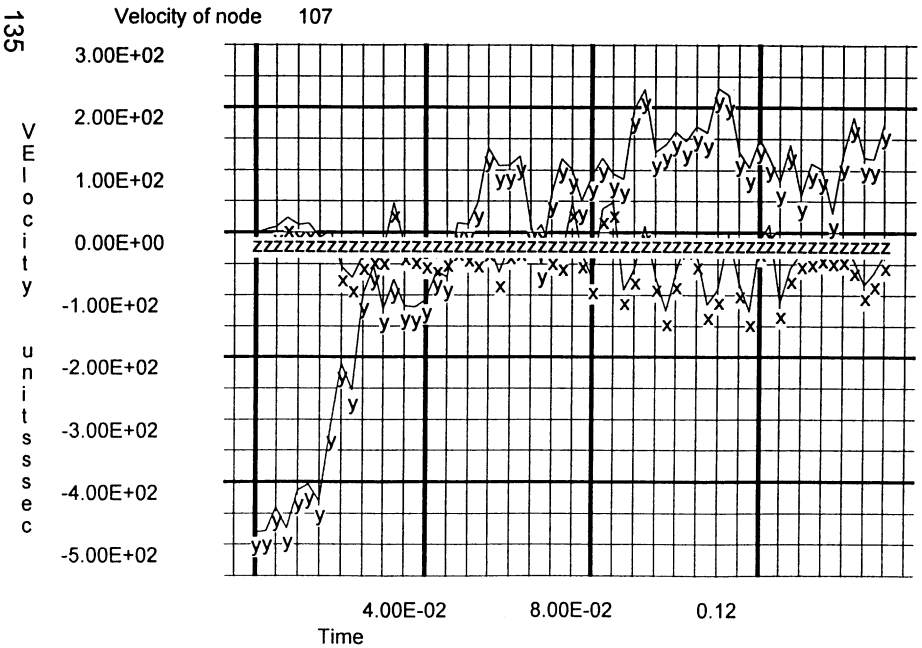

(c), 10 degrees

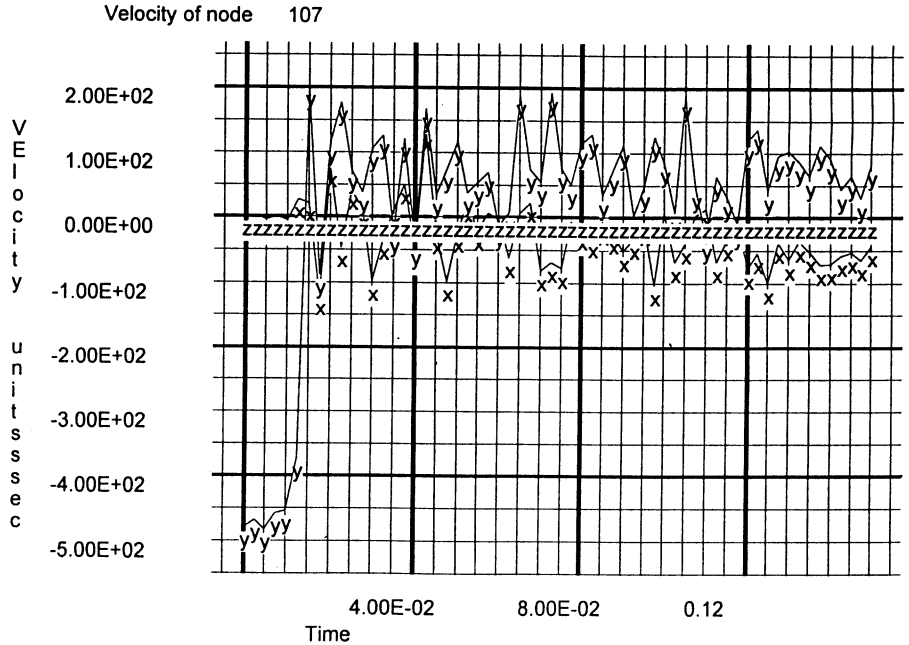

(d), 0 degrees

Figure 77, Dynamic Analysis, Impact Attitude Variation for Constant Impact Velocity, Front Seat

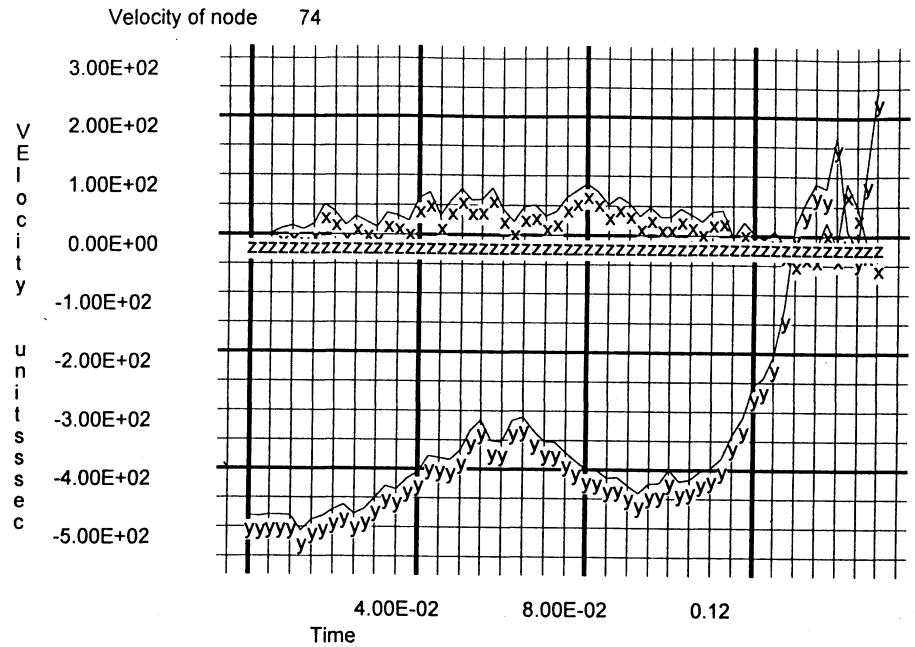

(a), 30 degrees

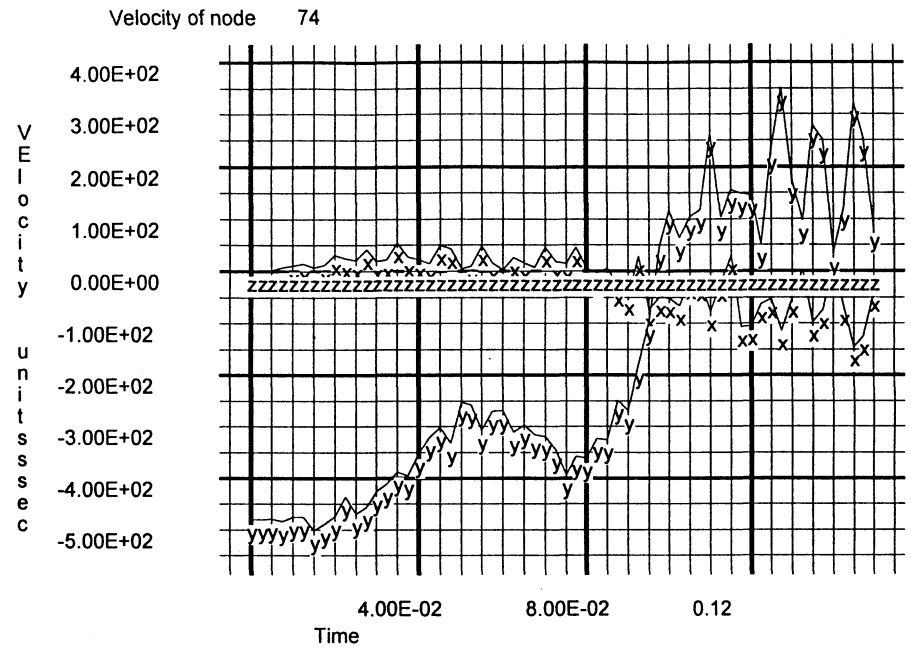

(b), 20 degrees

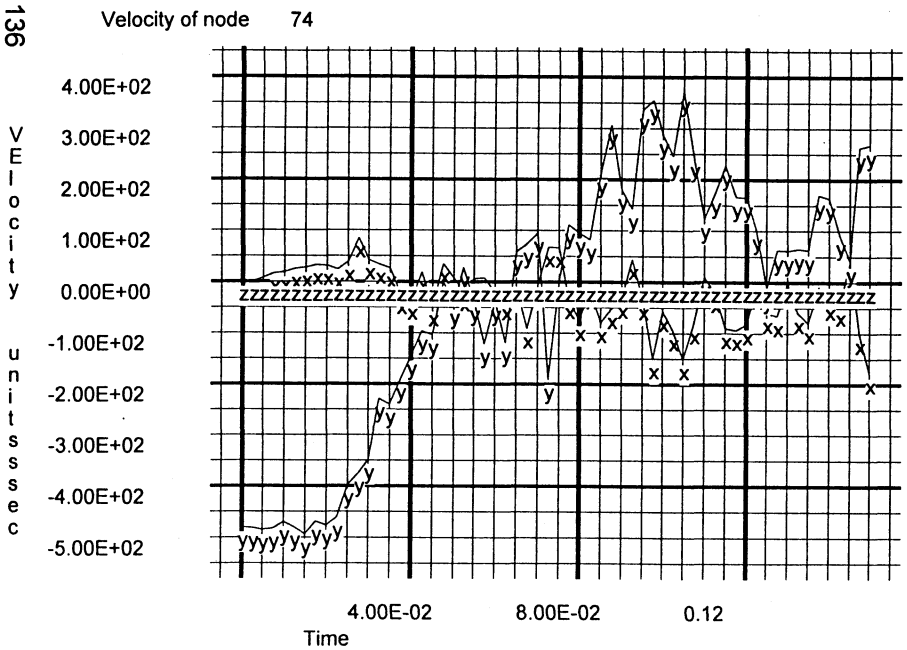

(c), 10 degrees

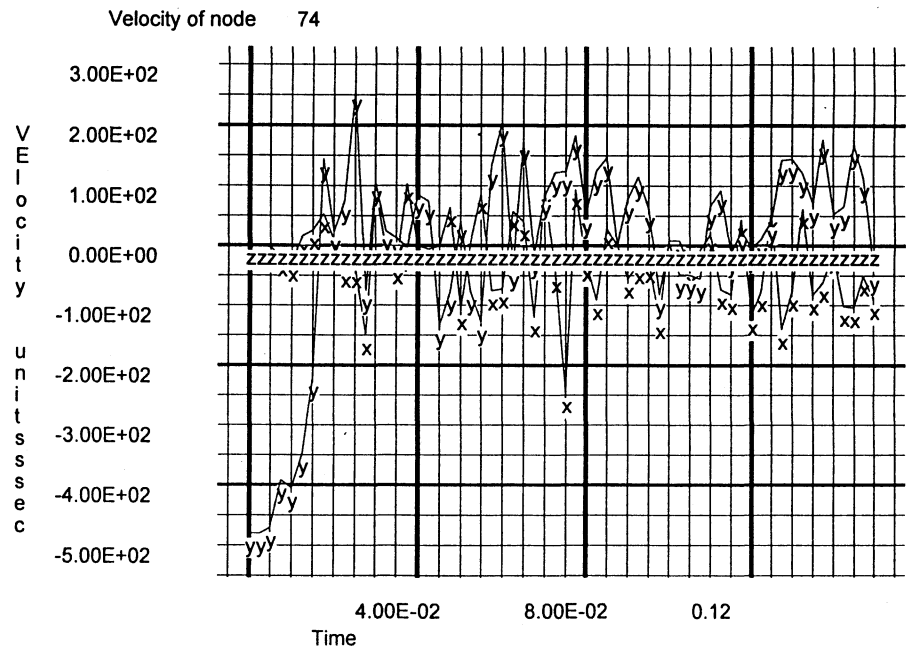

(d), 0 degrees

Figure 78, Dynamic Analysis, Impact Attitude Variation for Constant Impact Velocity, Rear Seat

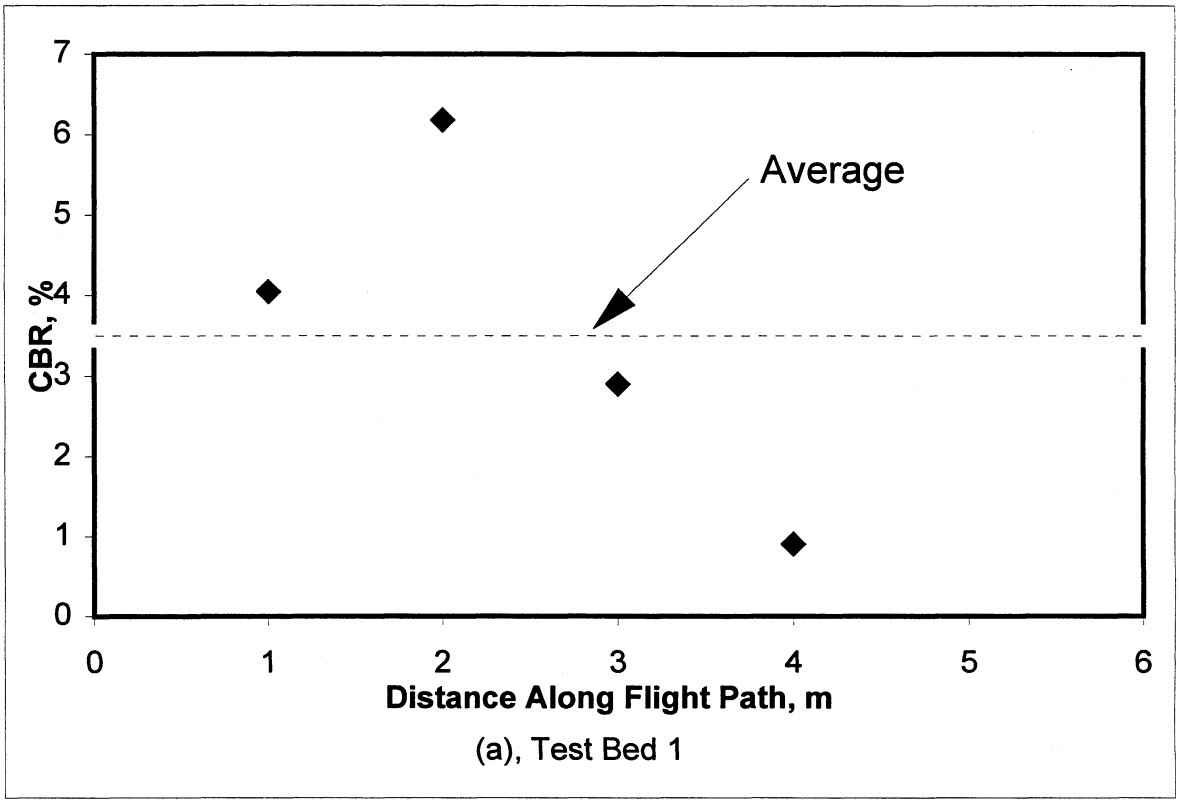

(a), Test Bed 1

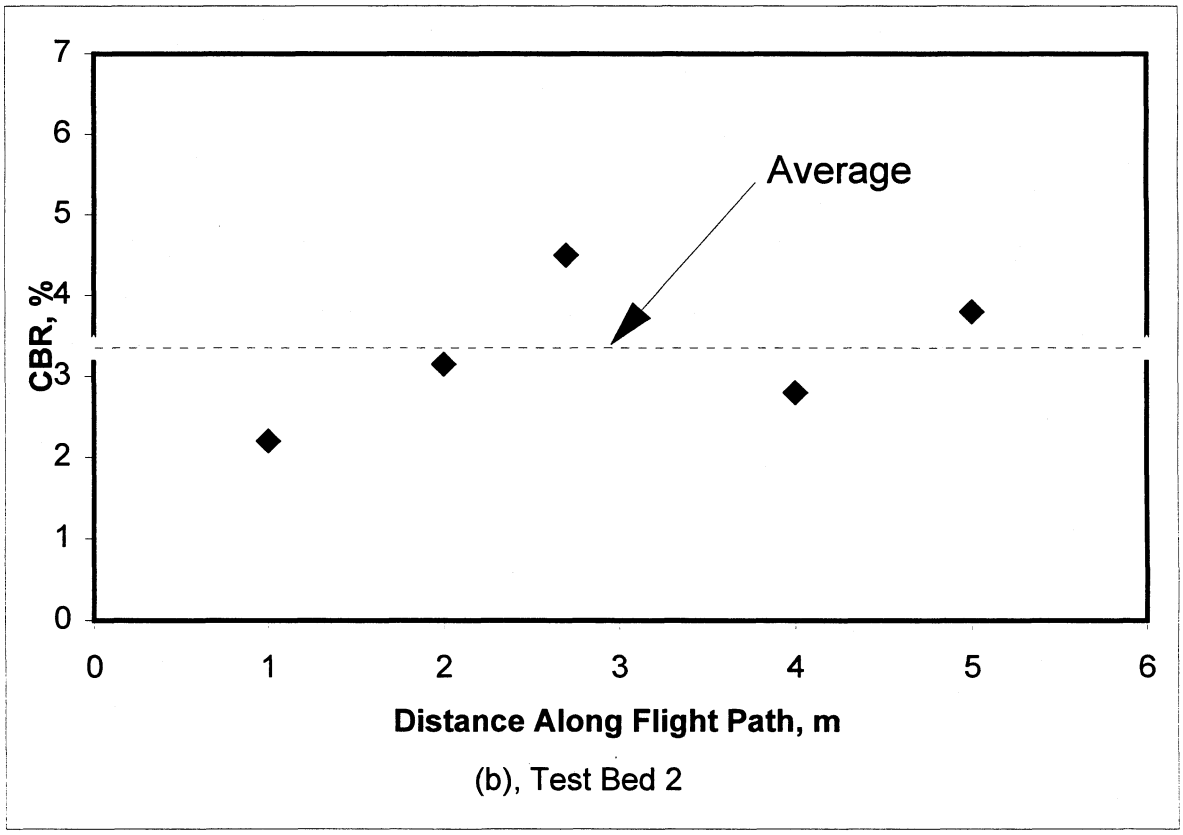

(b), Test Bed 2

Figure 79, California Bearing Data for Prior NASA Tests

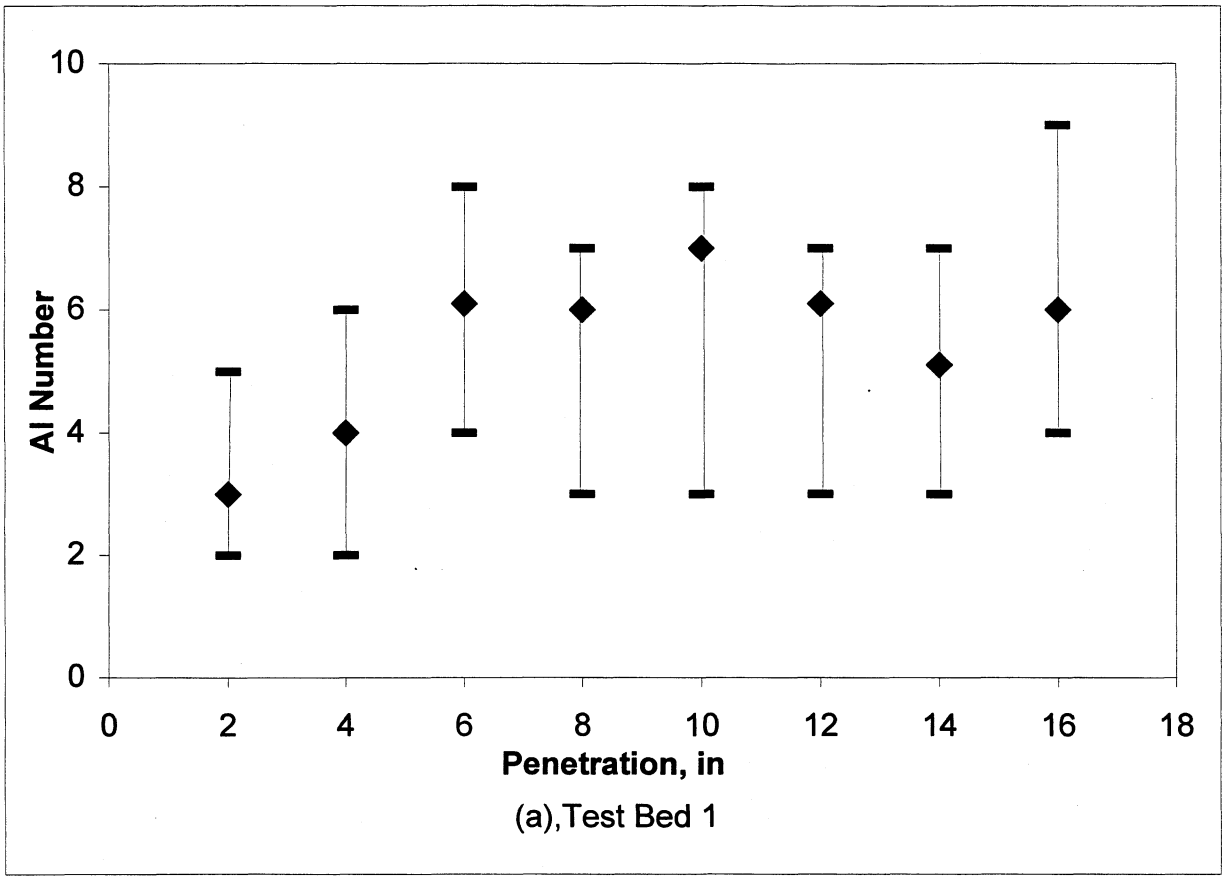

(a),Test Bed 1

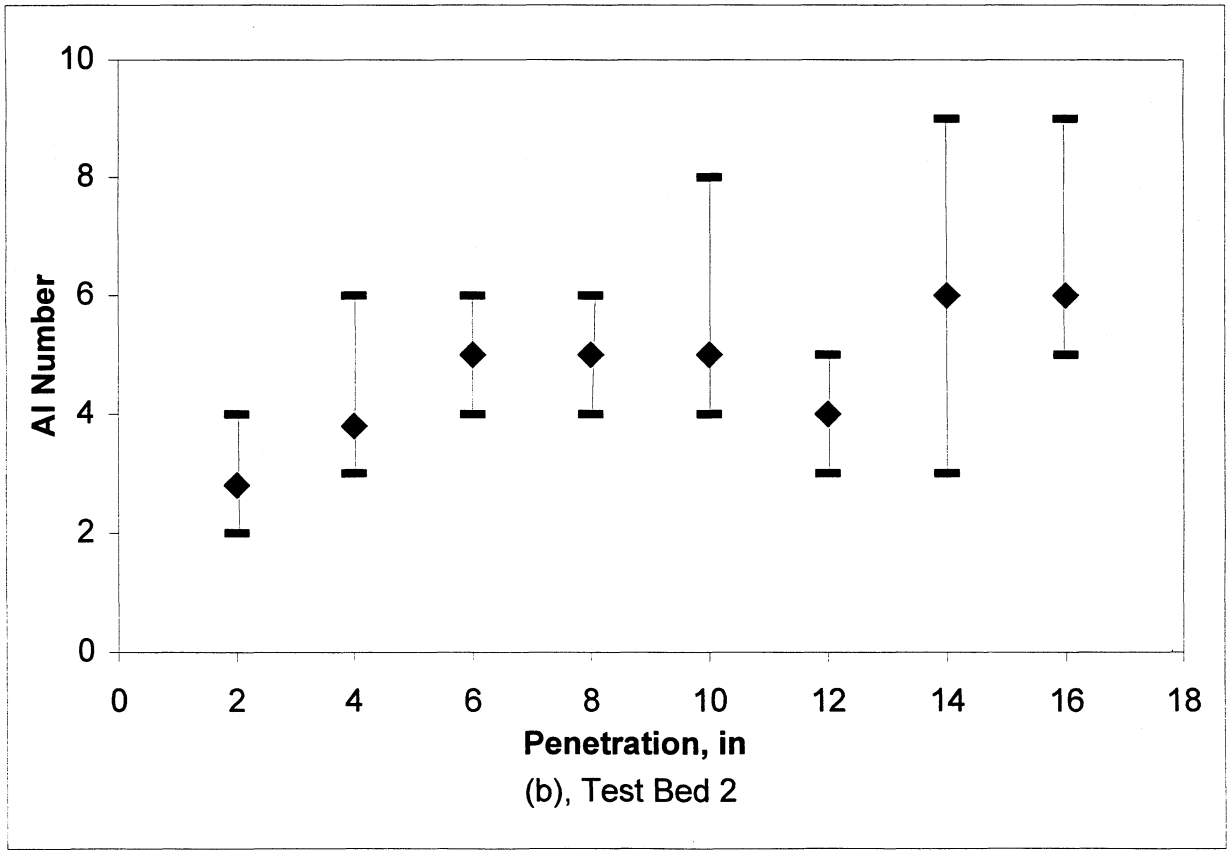

(b), Test Bed 2

Figure 80, Airfield Index for Prior NASA tests

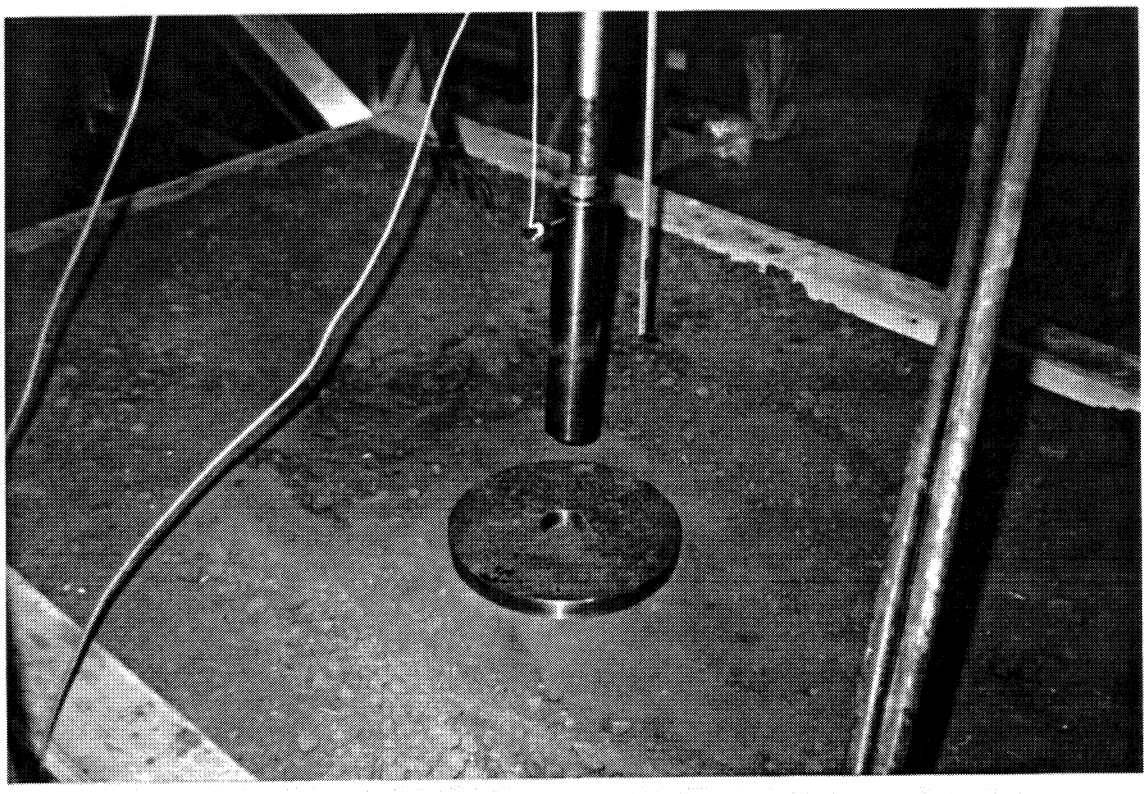

Figure 81, California Bearing Ratio (CBR) Test Device in Soil Box

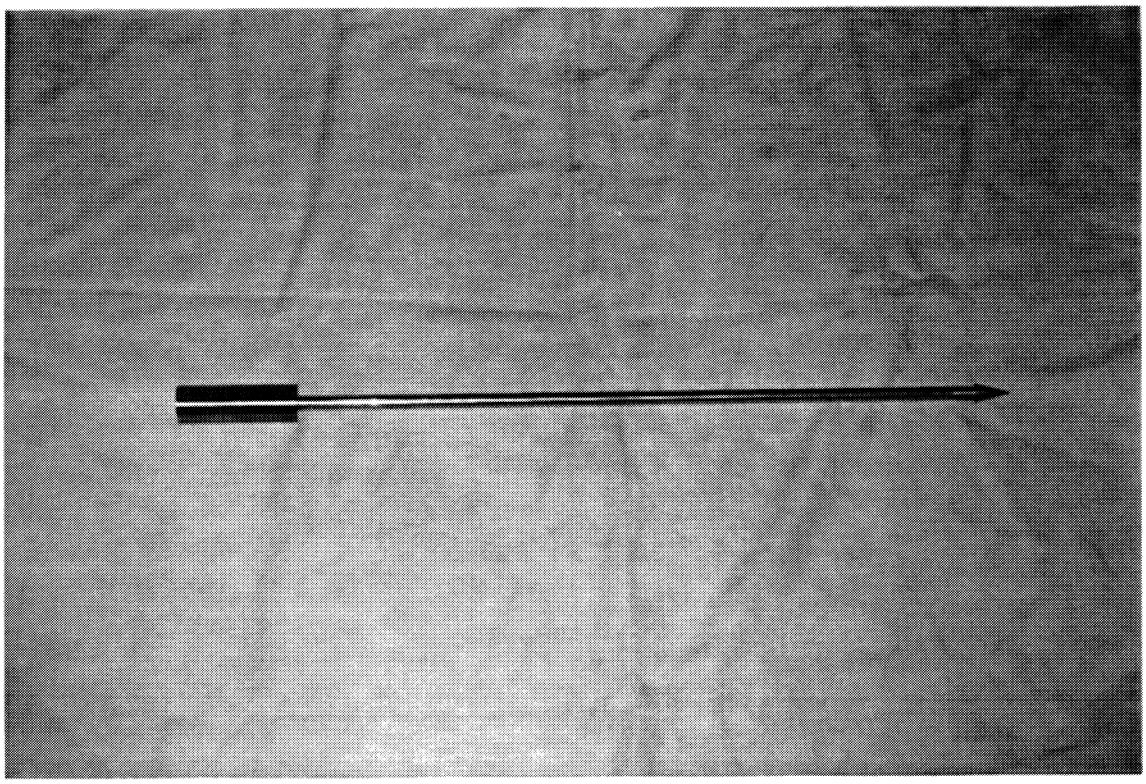

Figure 82, Cone Penetrometer (Airfield Index (AI)) Test Device

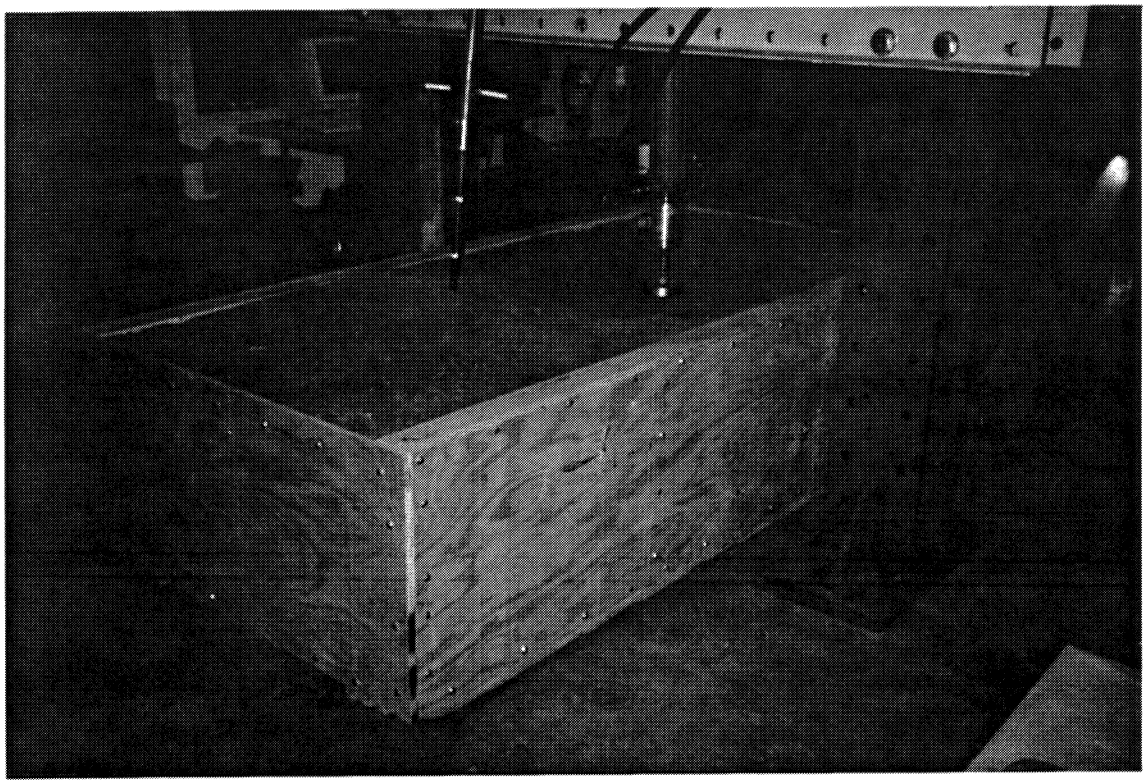

Figure 83, Soil Box in WSU Structural Test Laboratory

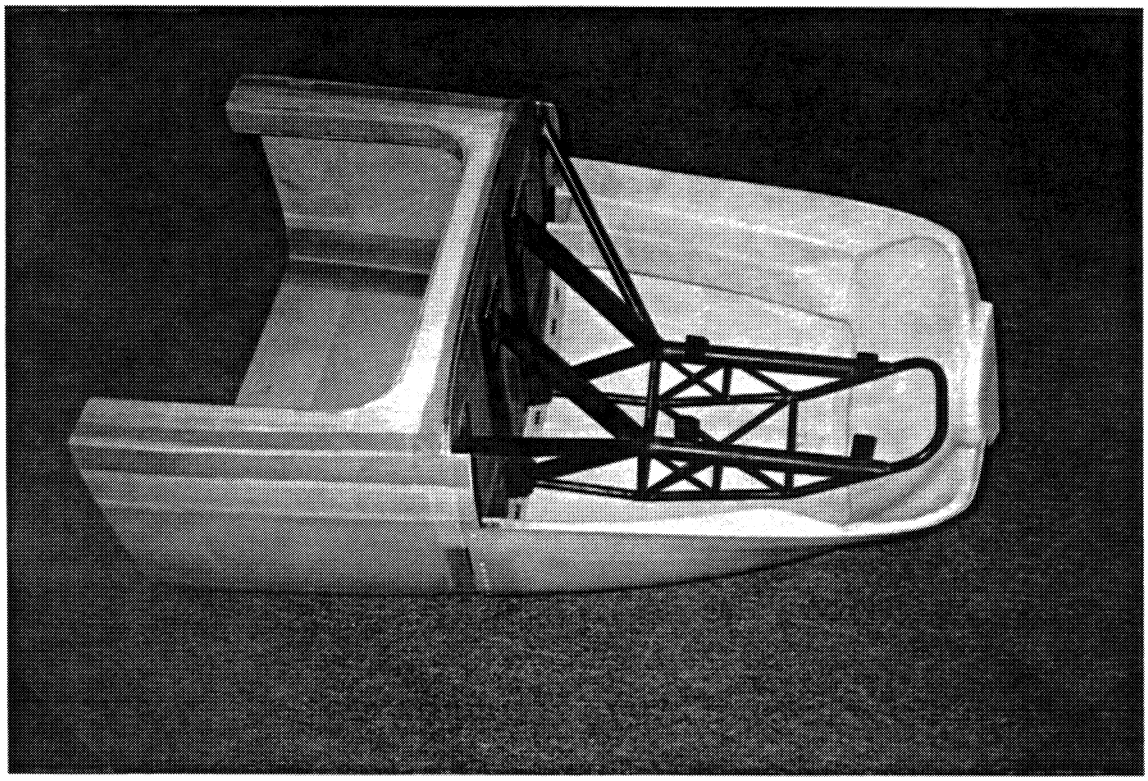

Figure 85, Half Scale Model for First Soil Test

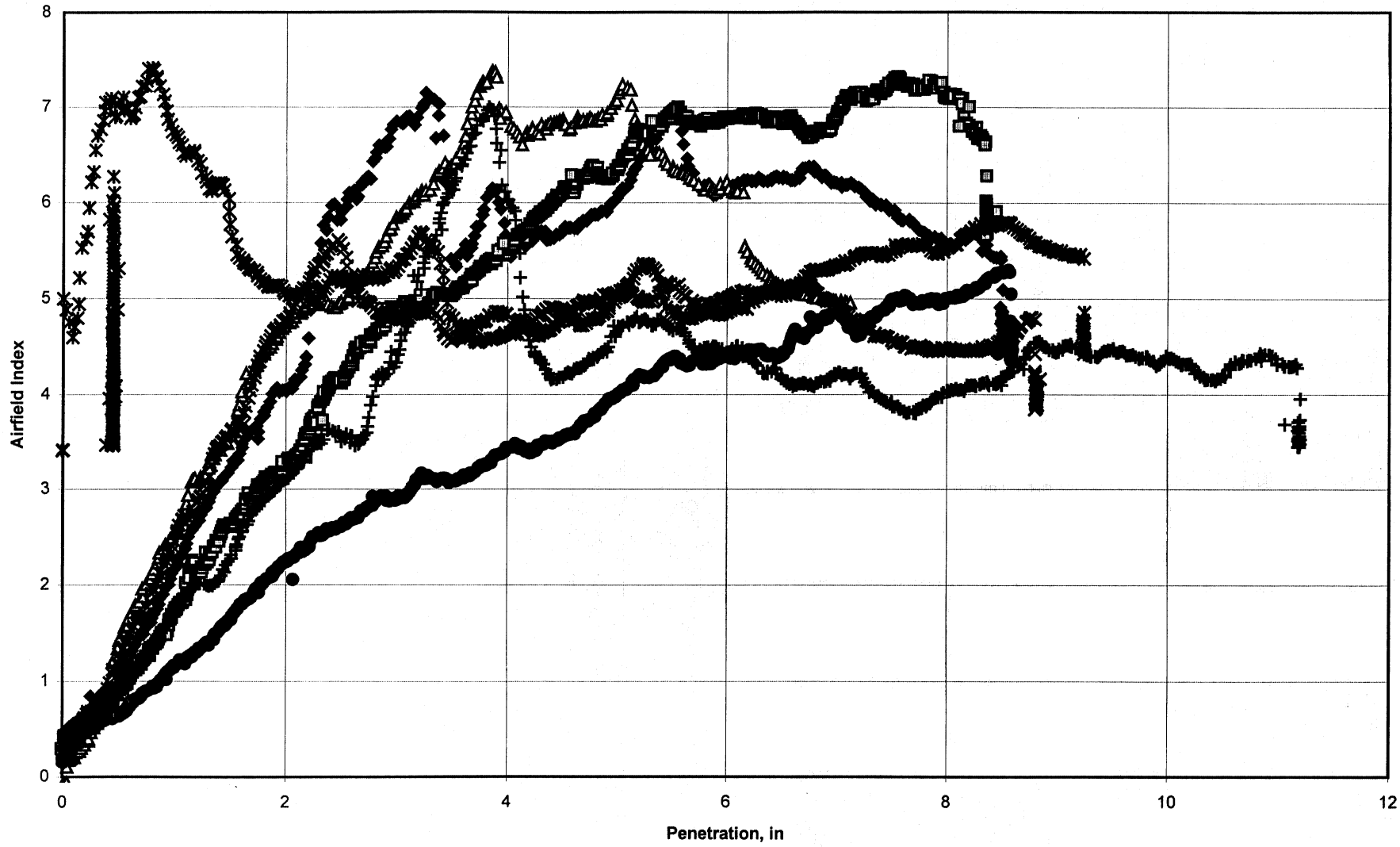

Figure 84, Airfield Index Measurements for Soil Bed 1, WSU Lab

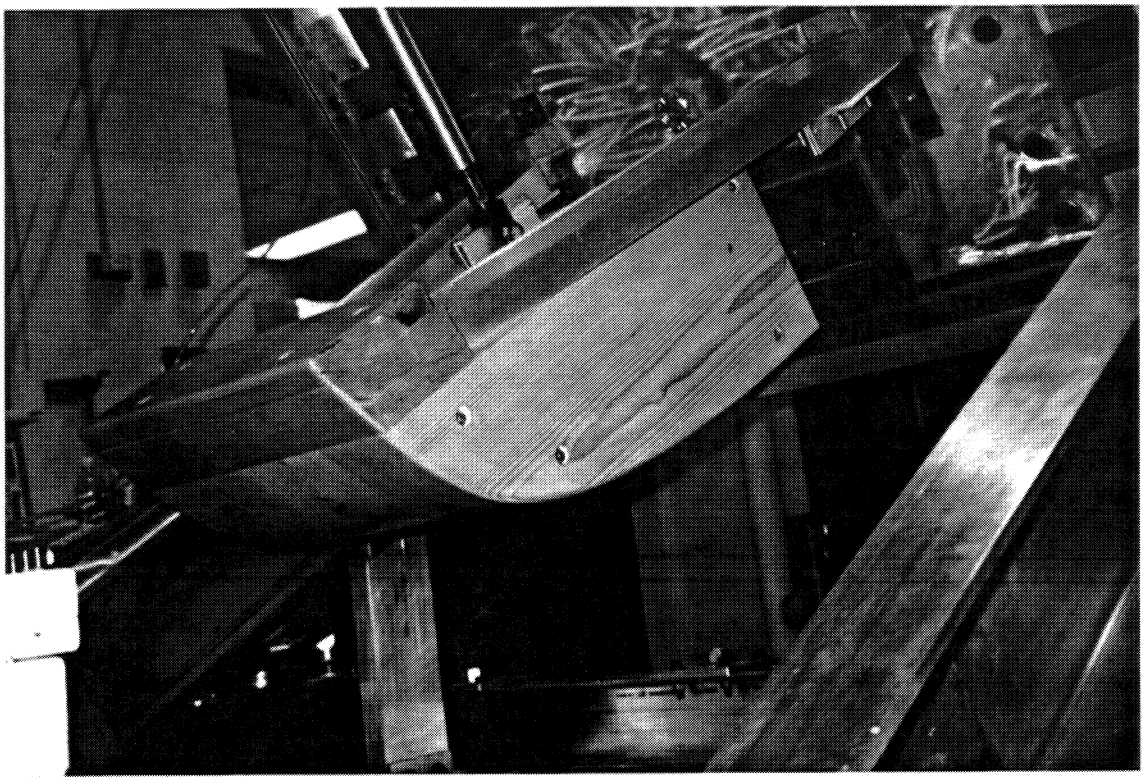

(a), Pretest

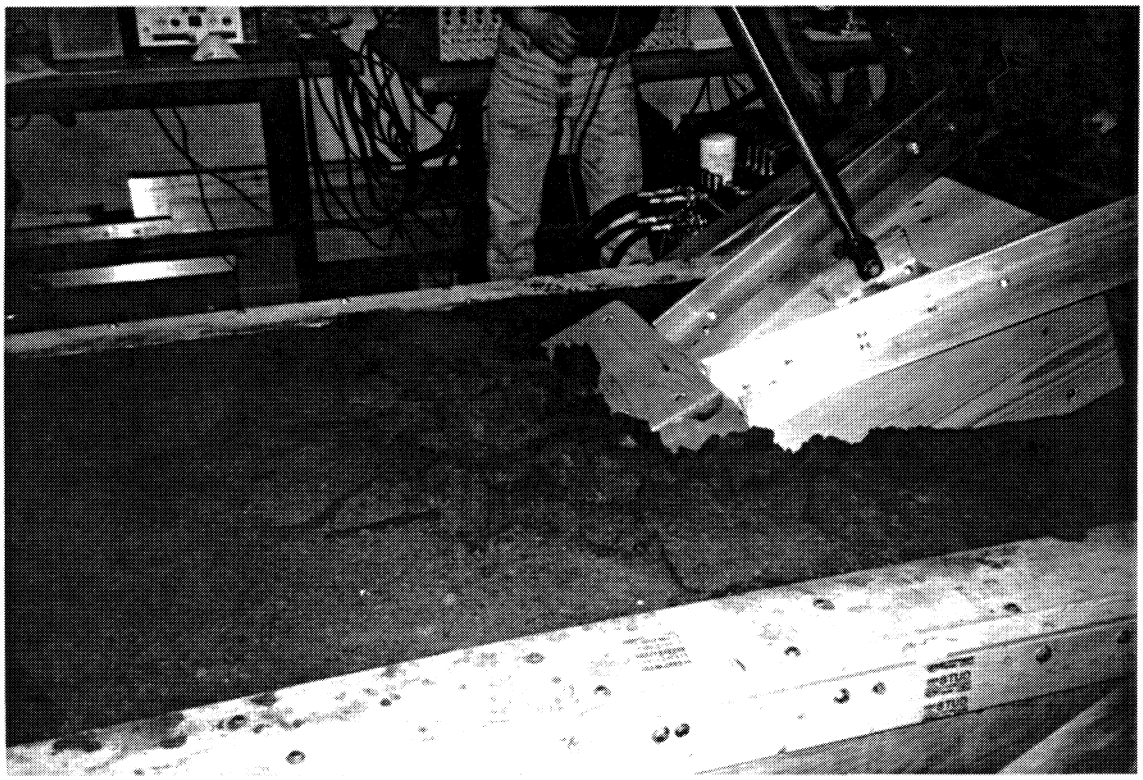

(b), During Test

Figure 86, Wood Cowl Test Device

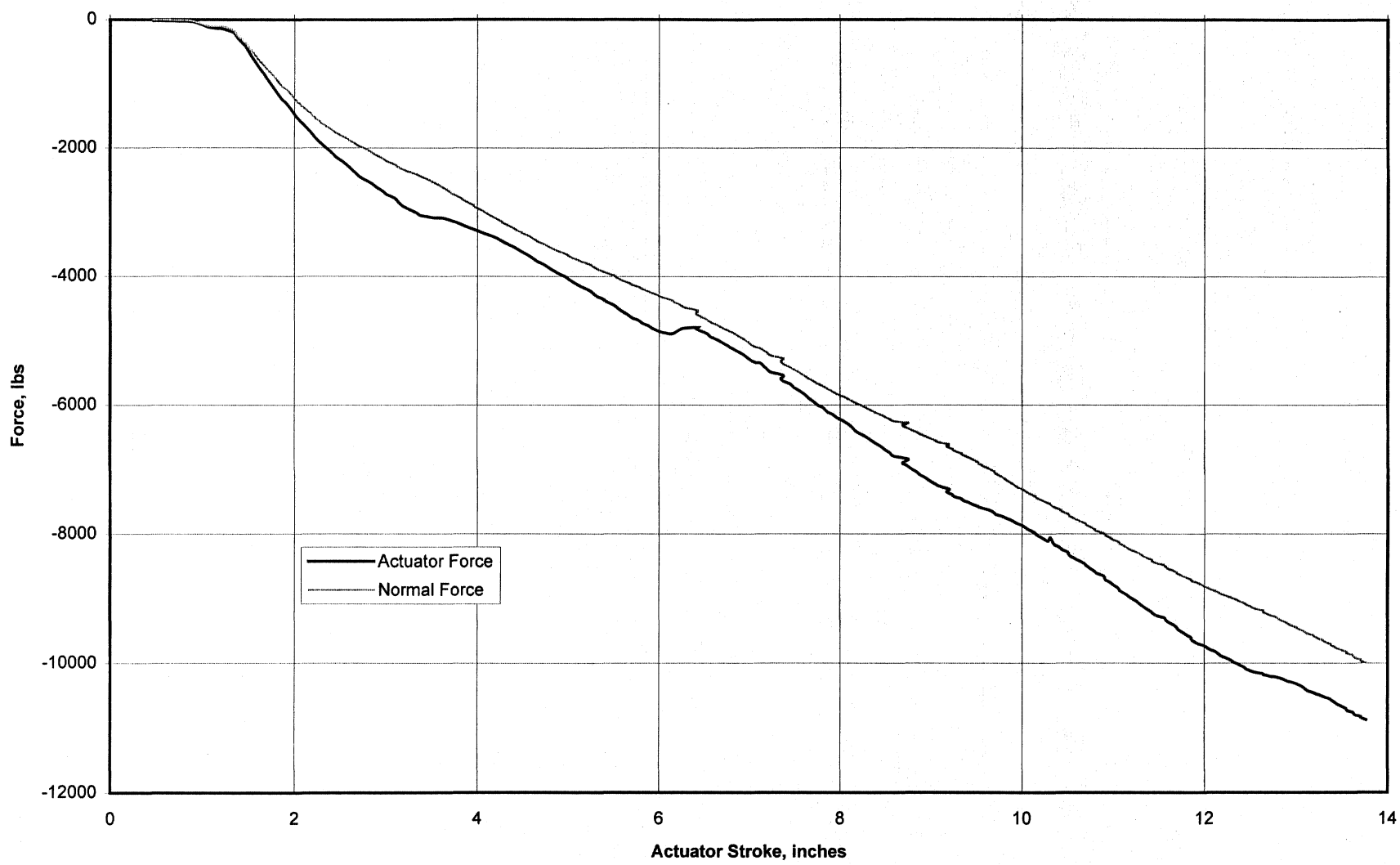

Figure 87, Wood Cowl Test Data, Soil Bed 2

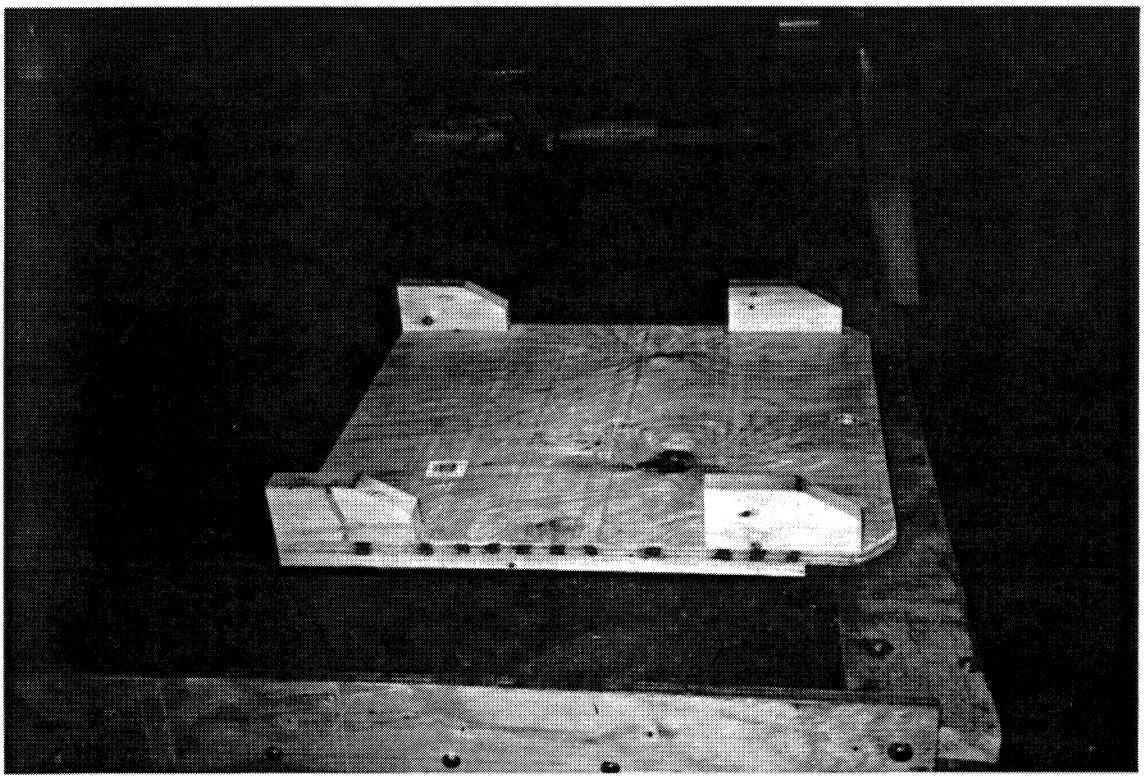

(a), Test Sled

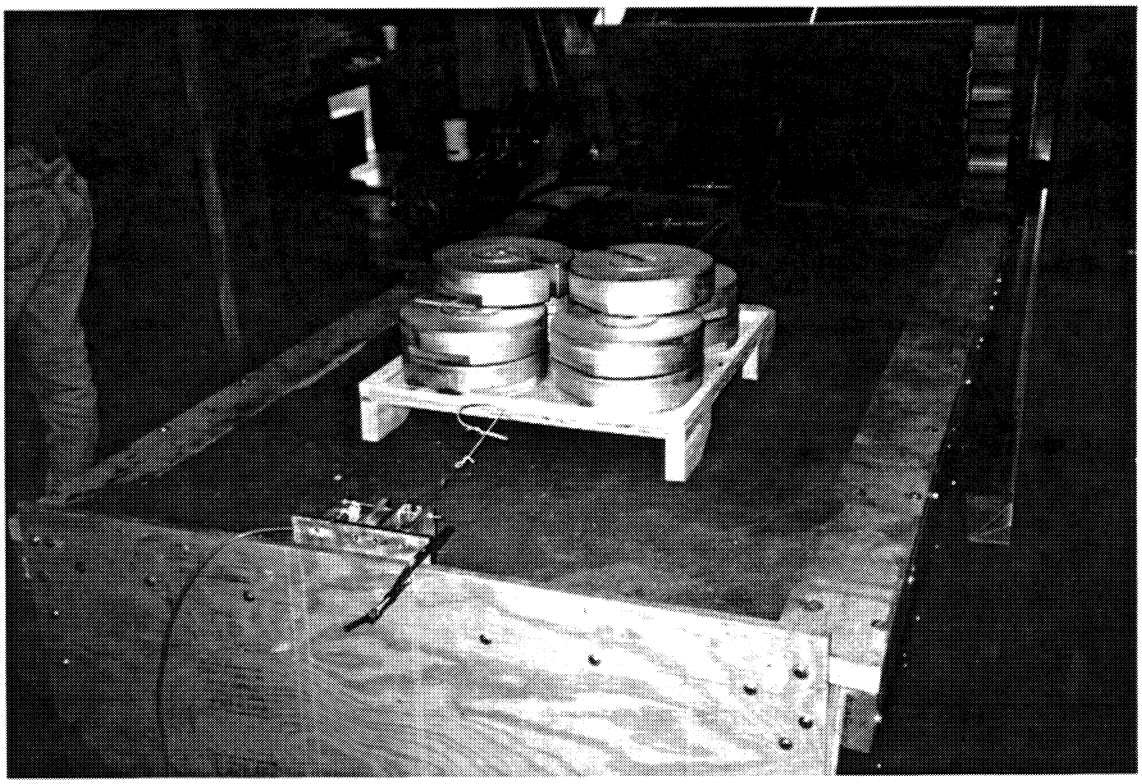

(b), Loaded for Test

Figure 88, Soil Friction Test

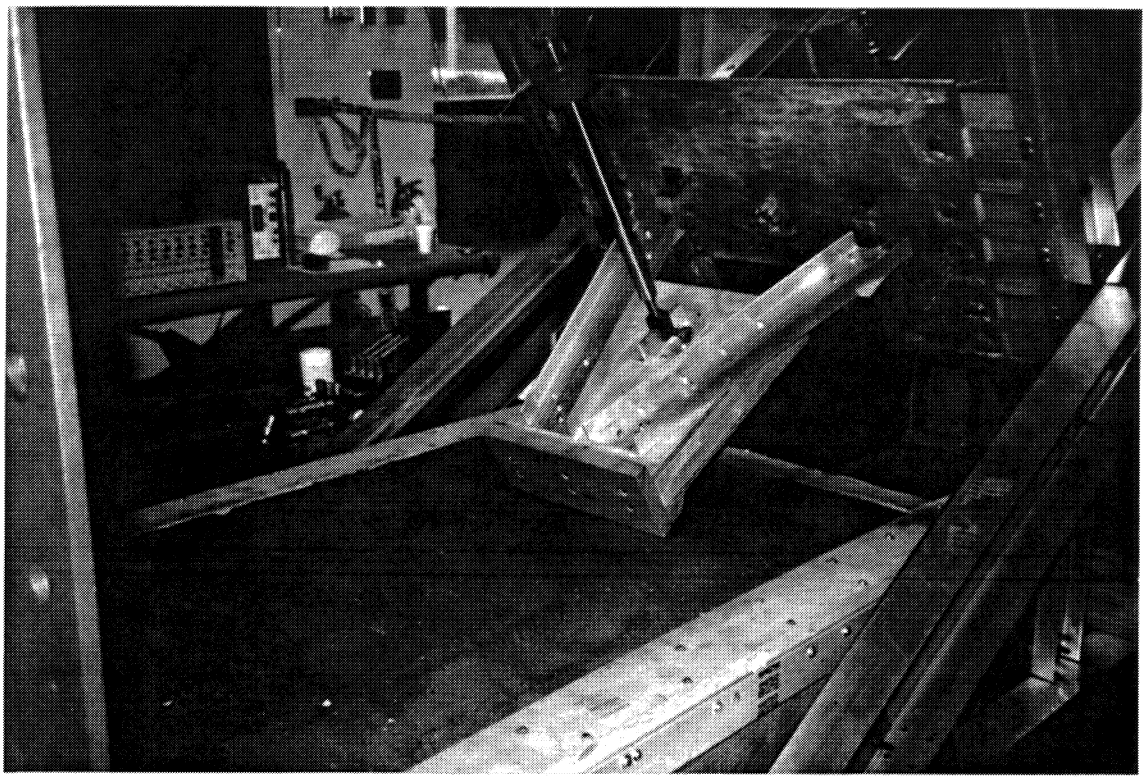

(a), Pretest

(b), During Test

Figure 89, Soil Block Test

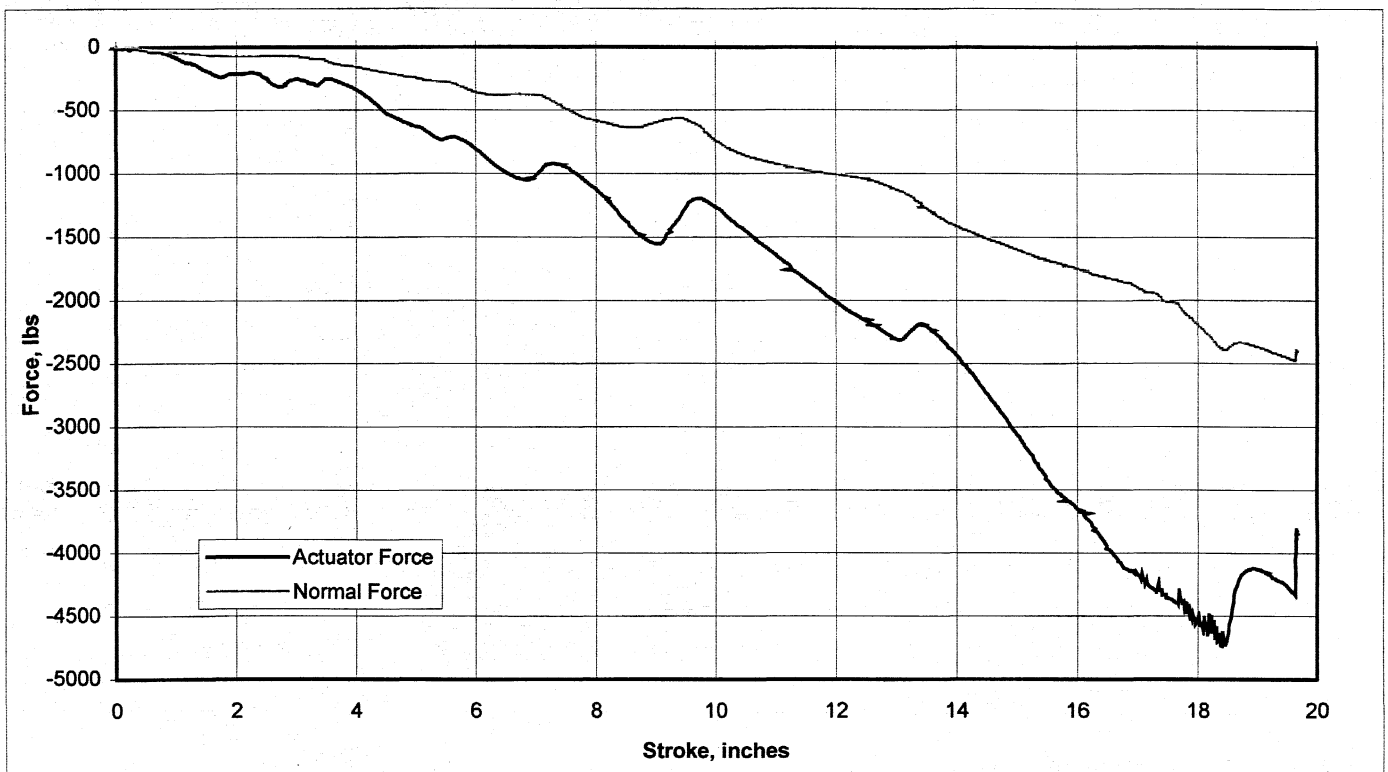

(a), Test Data, Soil Bed 3

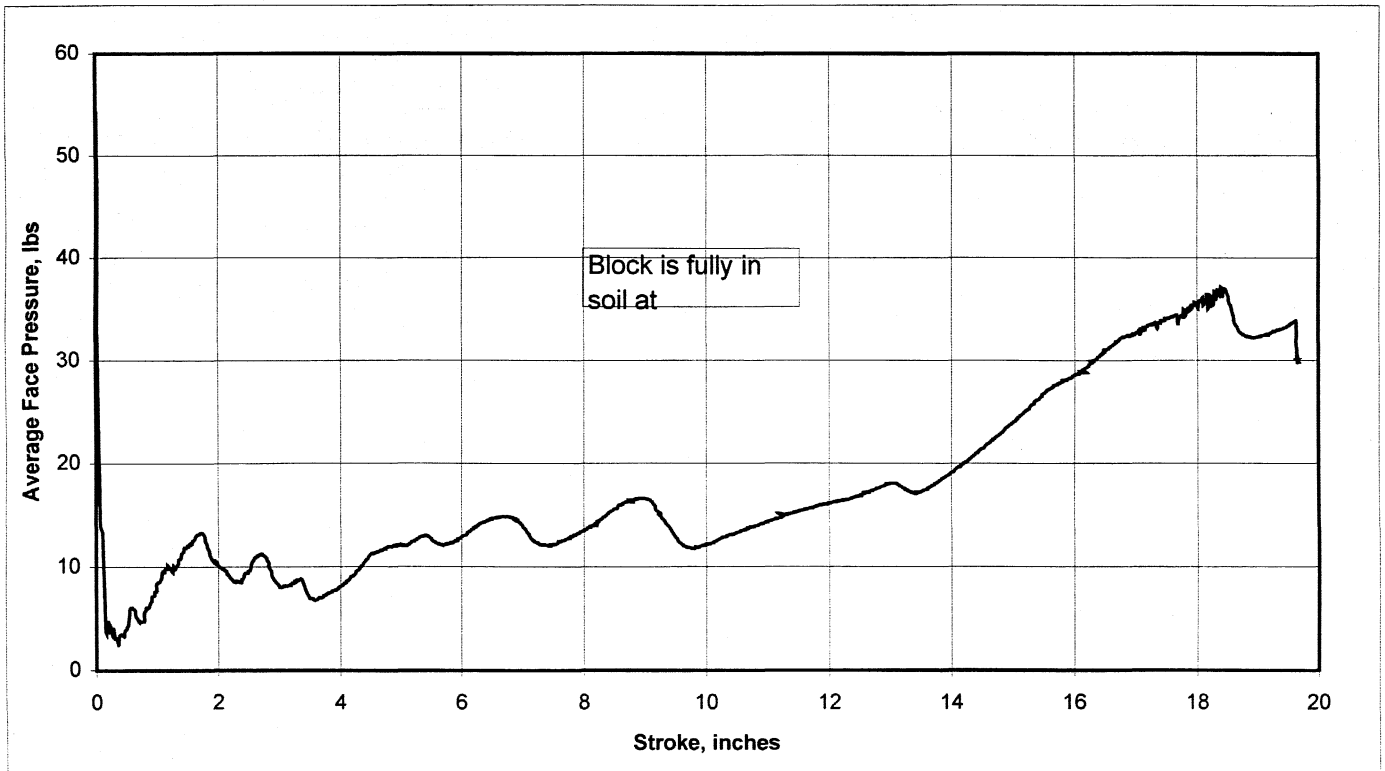

(b), Average Face Pressure

Figure 90, Soil Block Data

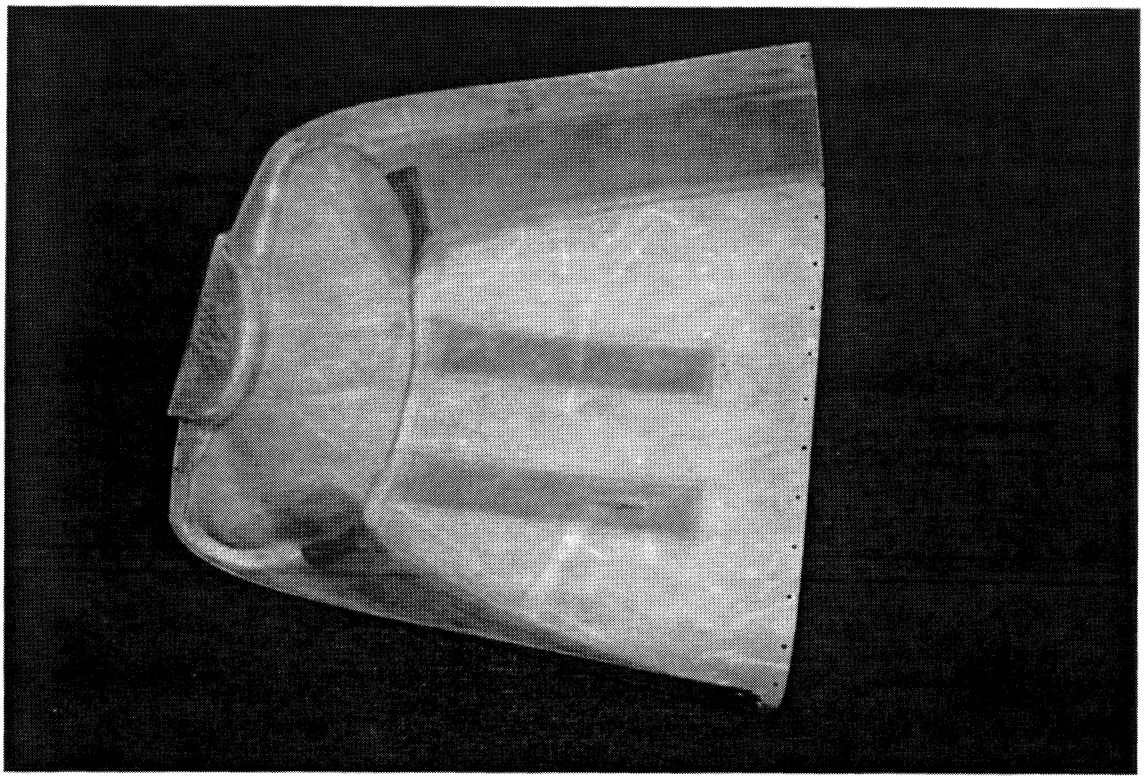

(a), Internal Repairs

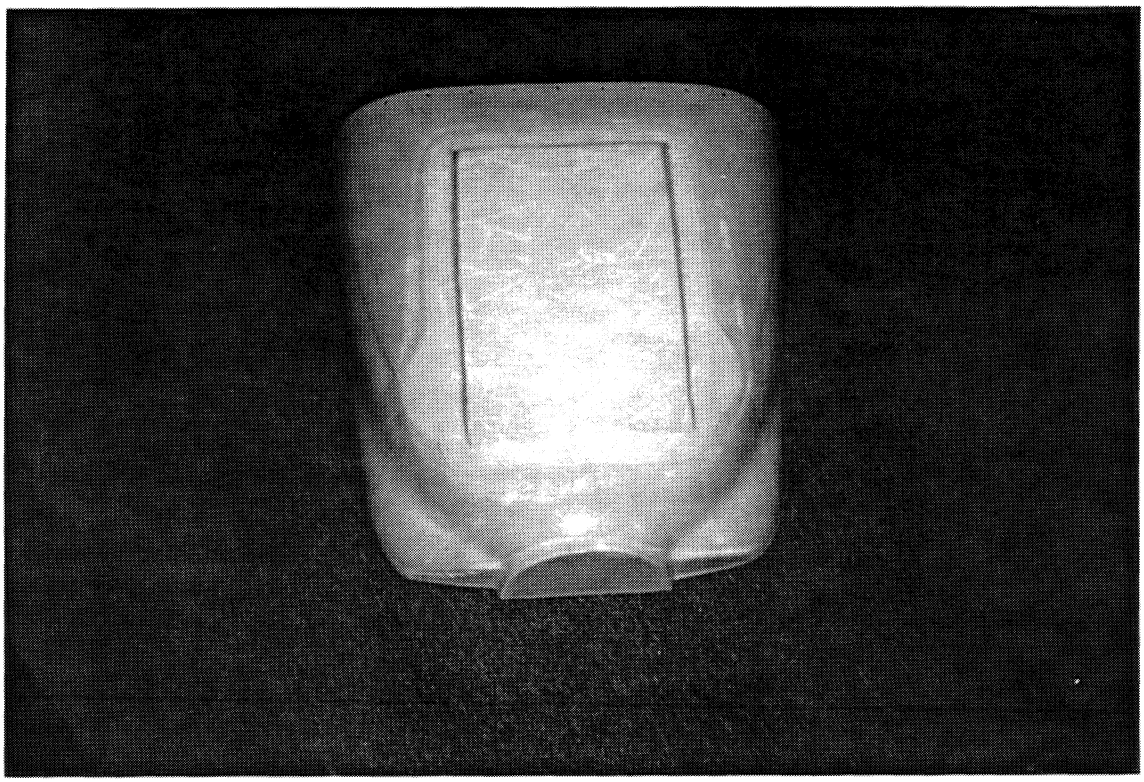

(b), Added External Reinforcement

Figure 91, Cowling for Soil Test 2

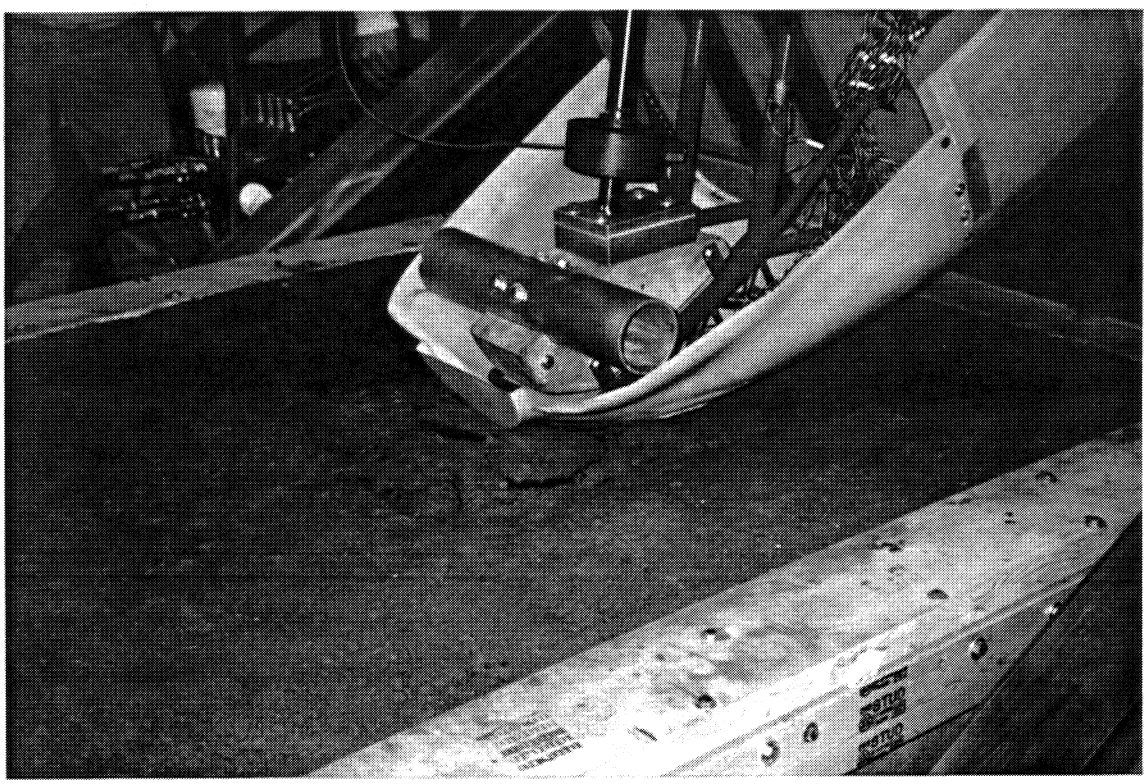

(a), During Test

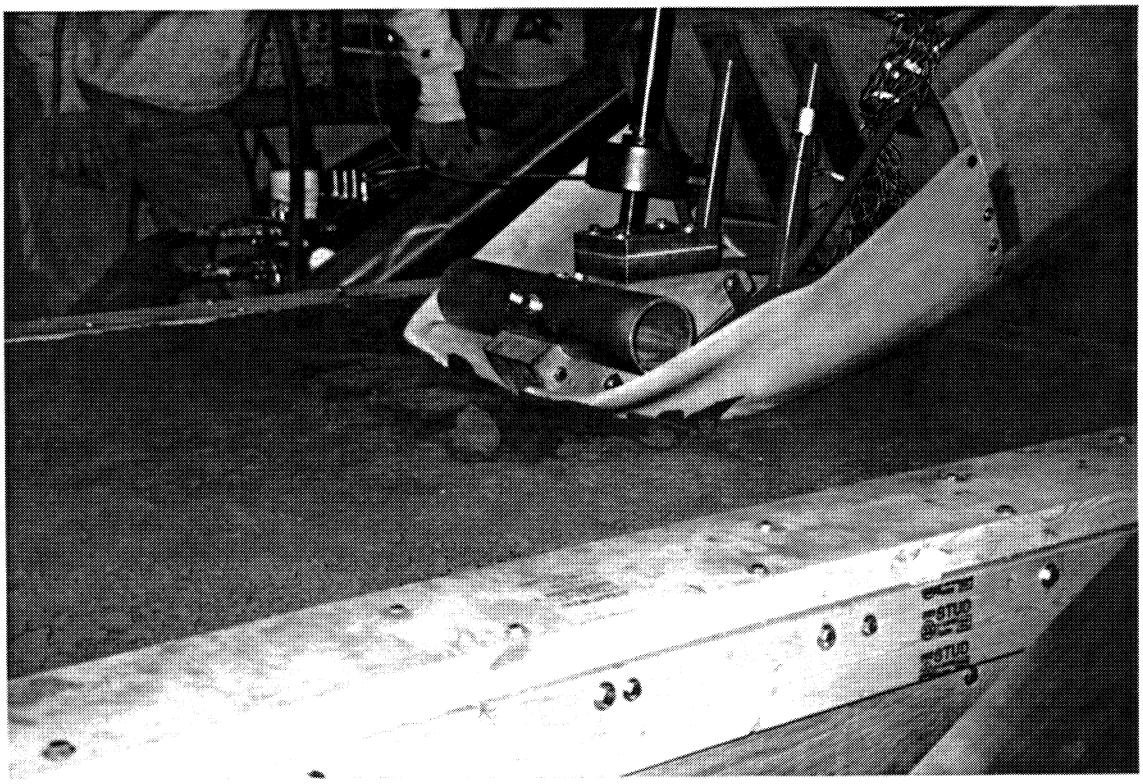

(b), During Test

Figure 92, Soft Soil Test 2

(c), During Test

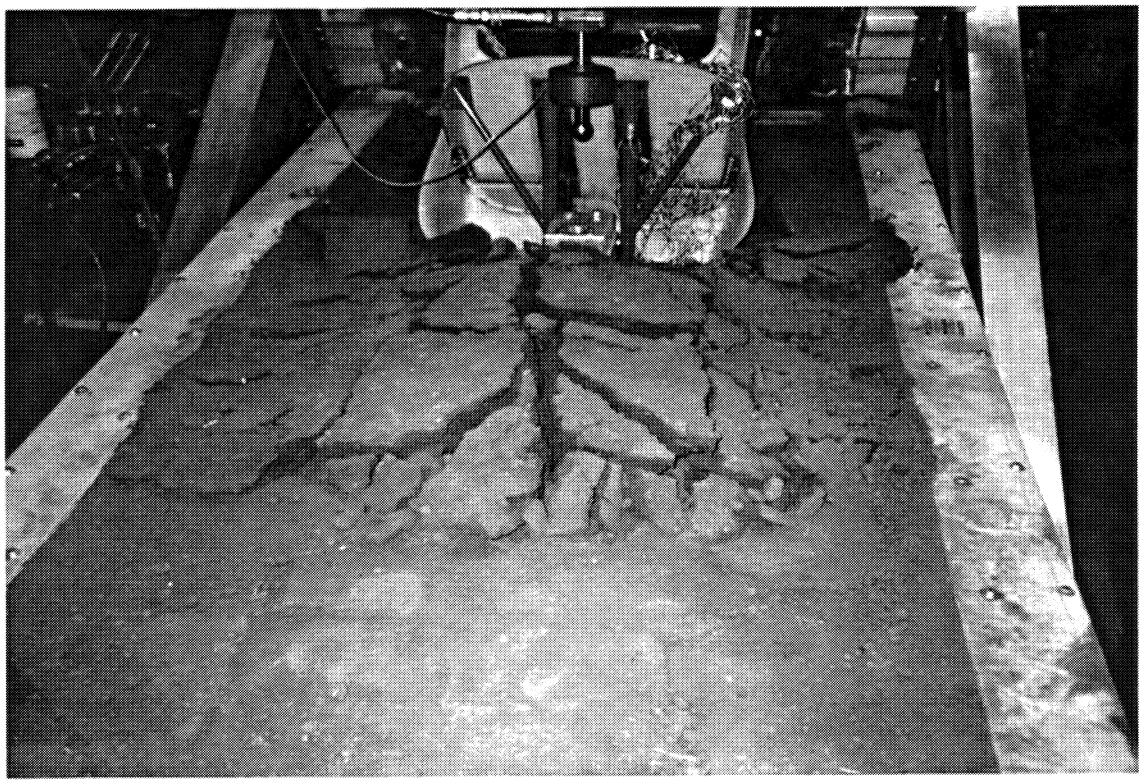

(d), During Test

Figure 92, (concluded)

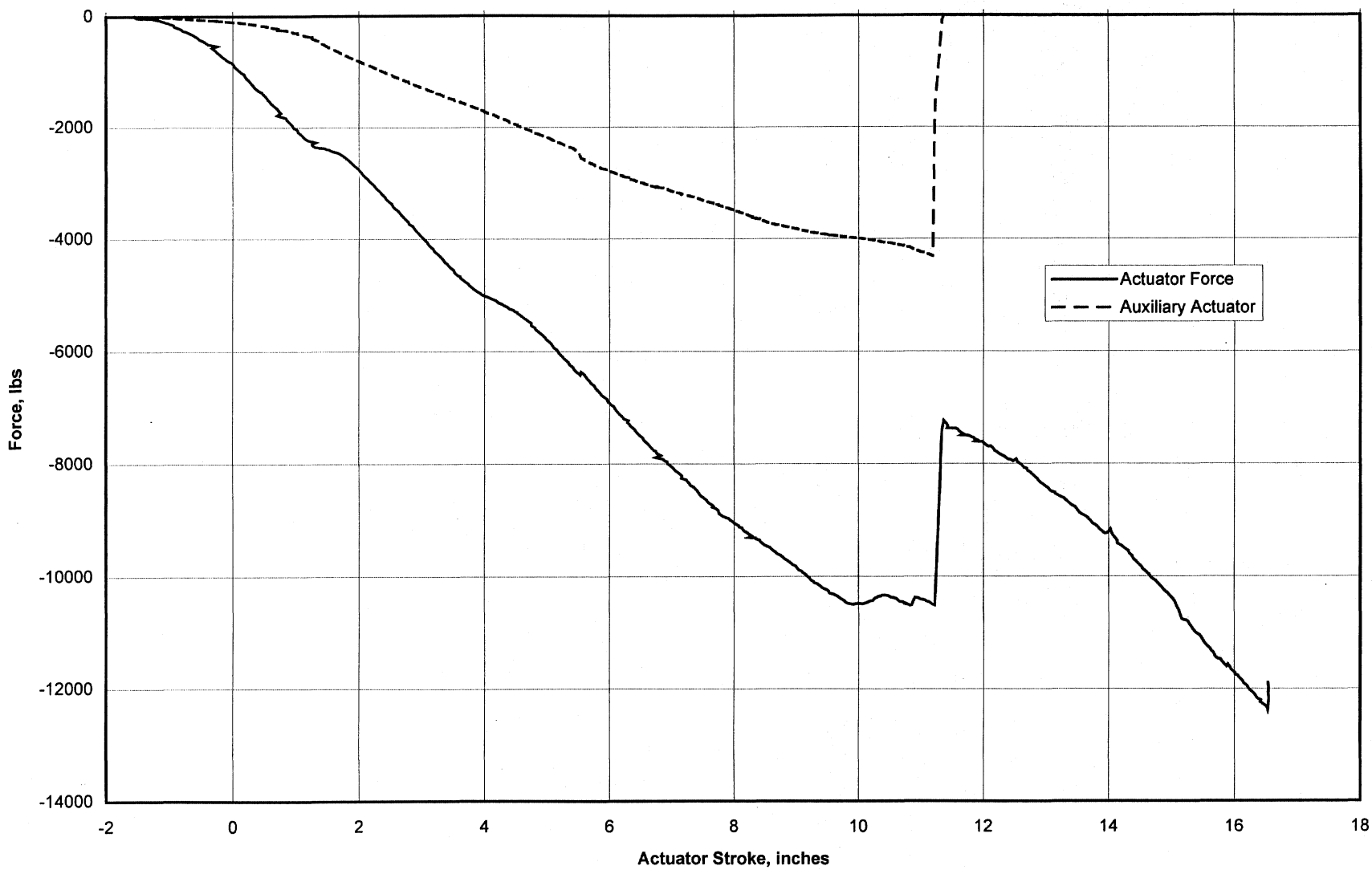

Figure 93, Soft Soil Half Scale Test 2 Data

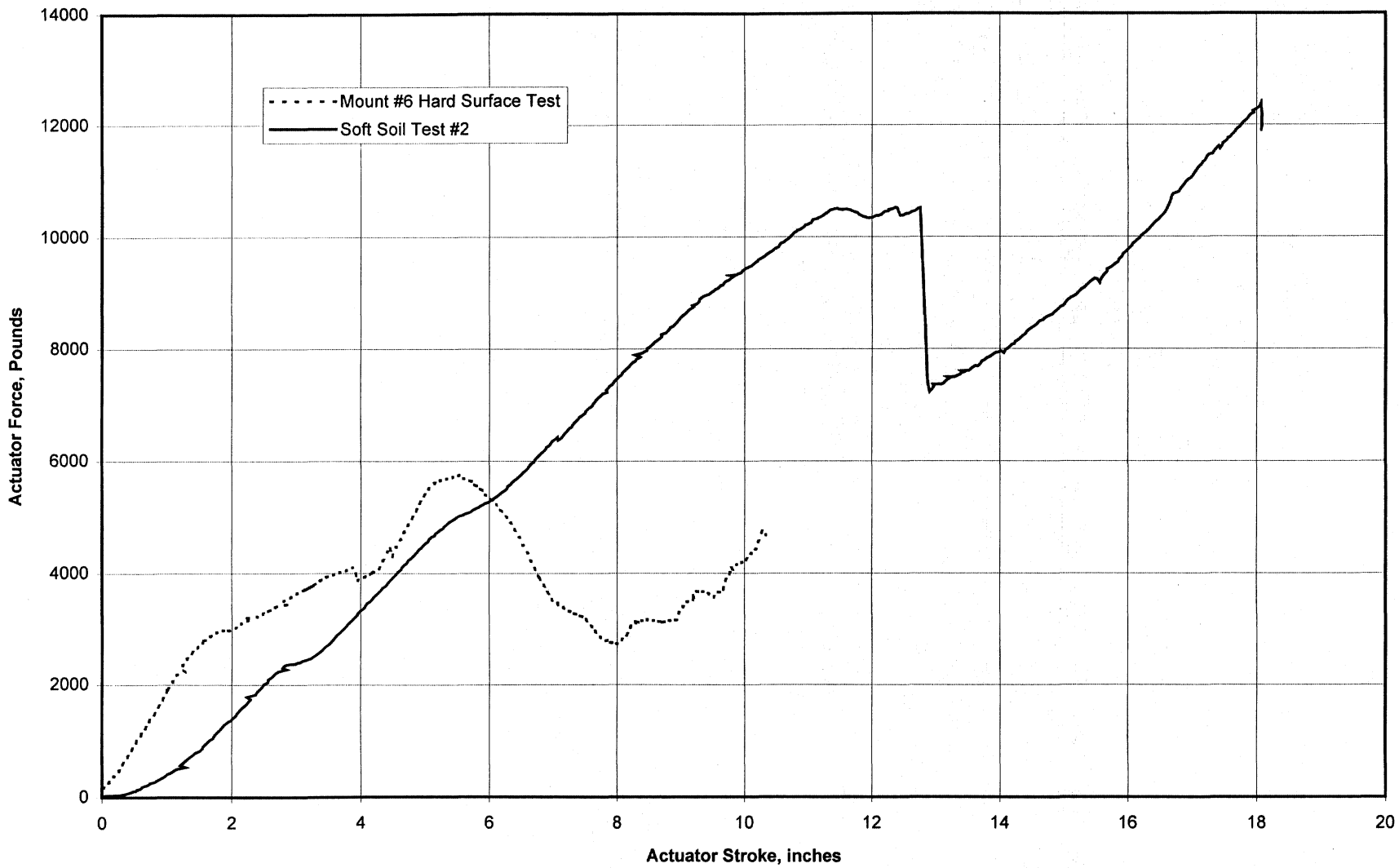

Figure 94, Comparison of Hard Surface Test to Soft Soil Test for Half Scale Mount 6

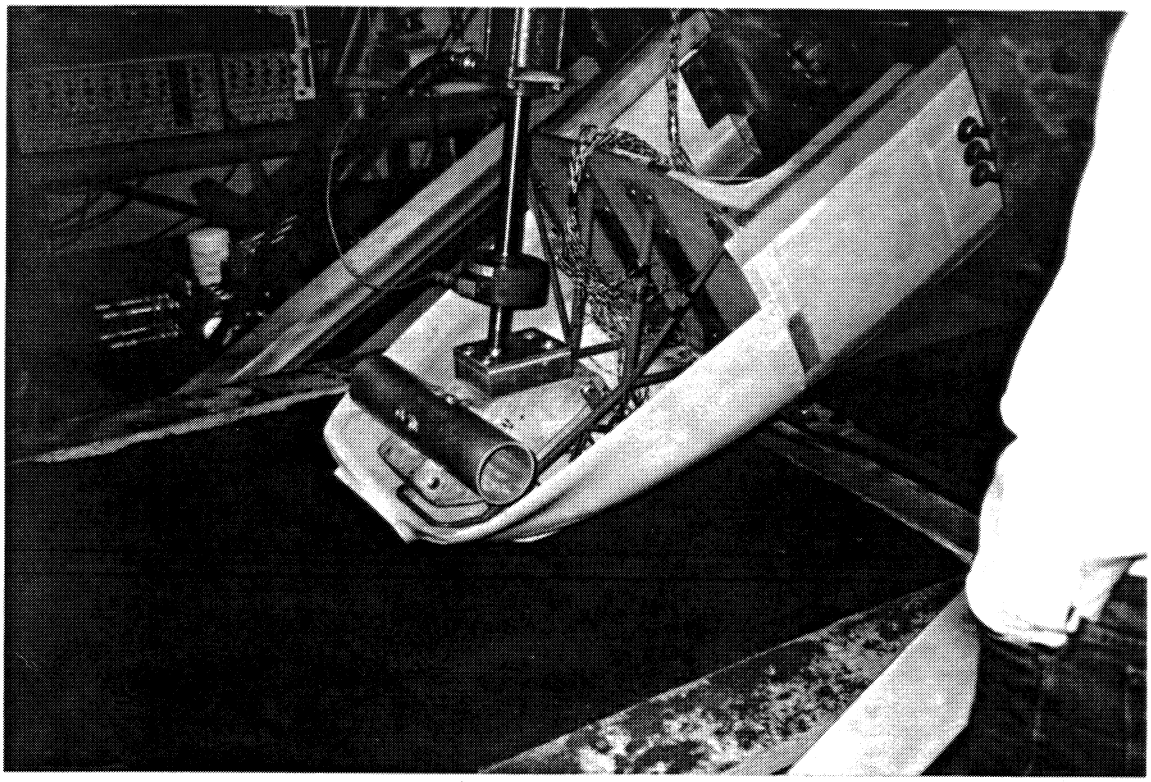

(a), Half Scale Mount 8 Ready for Test

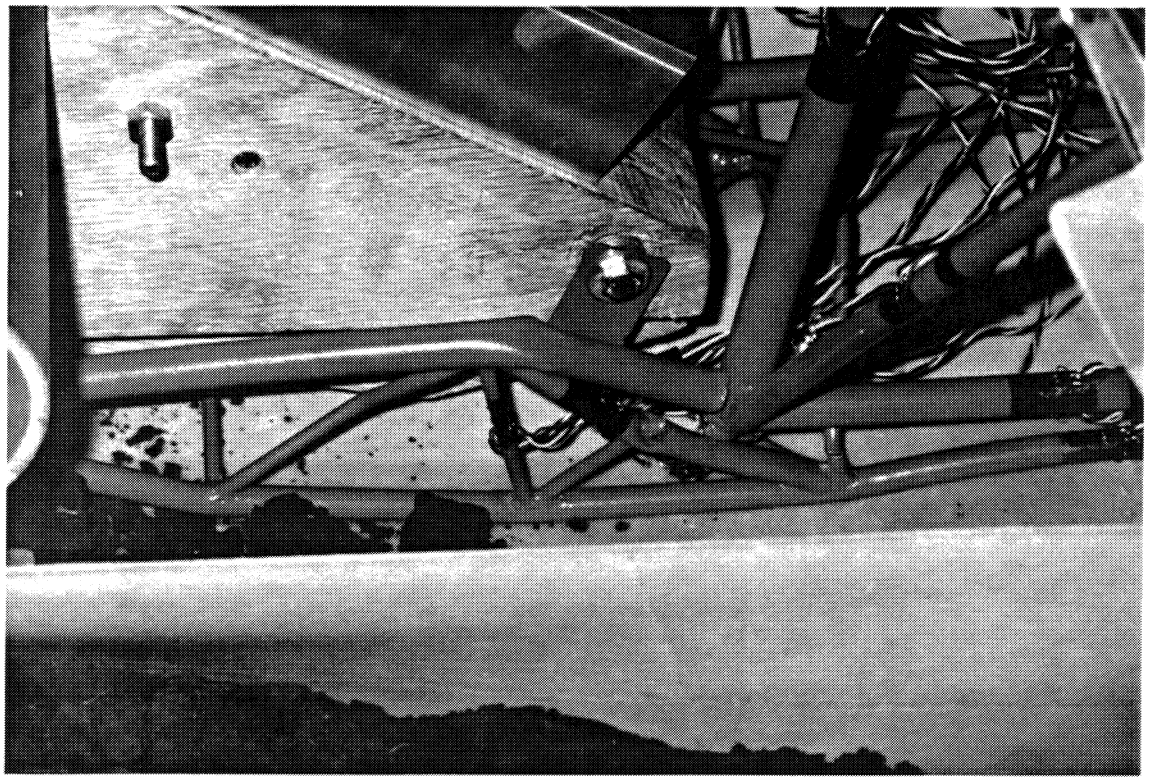

(b), During Test

Figure 95, Soft Soil Test 3

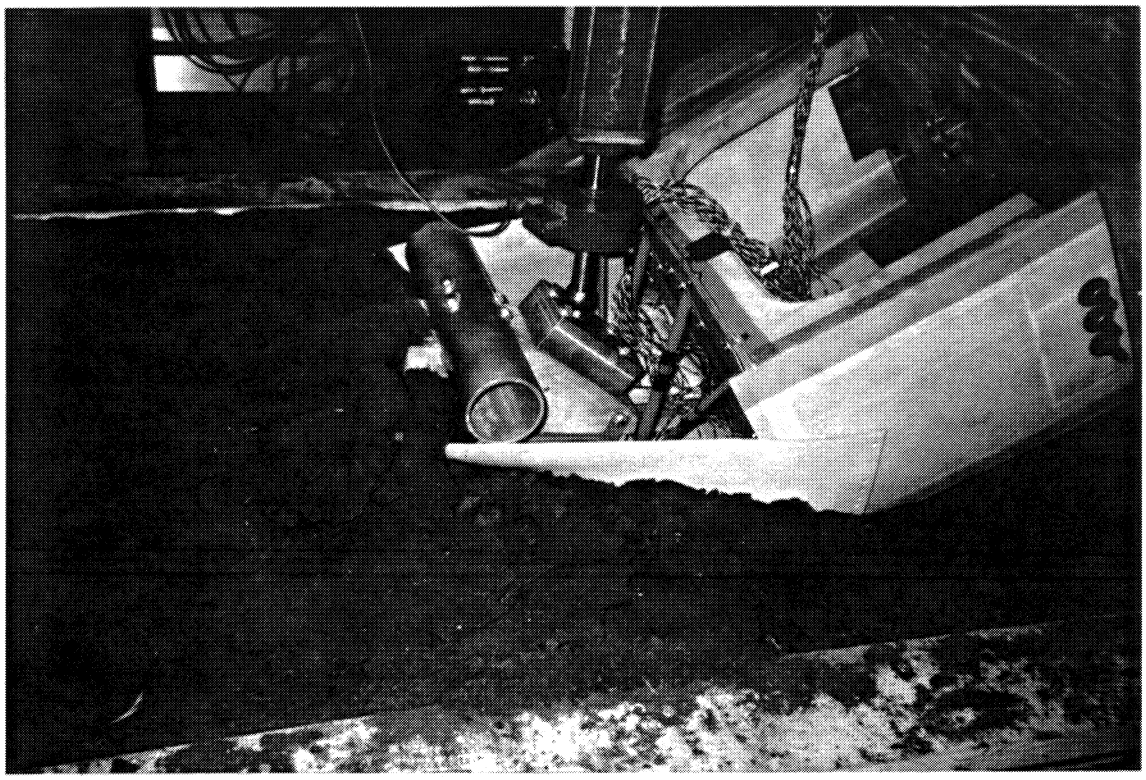

(c), During Test

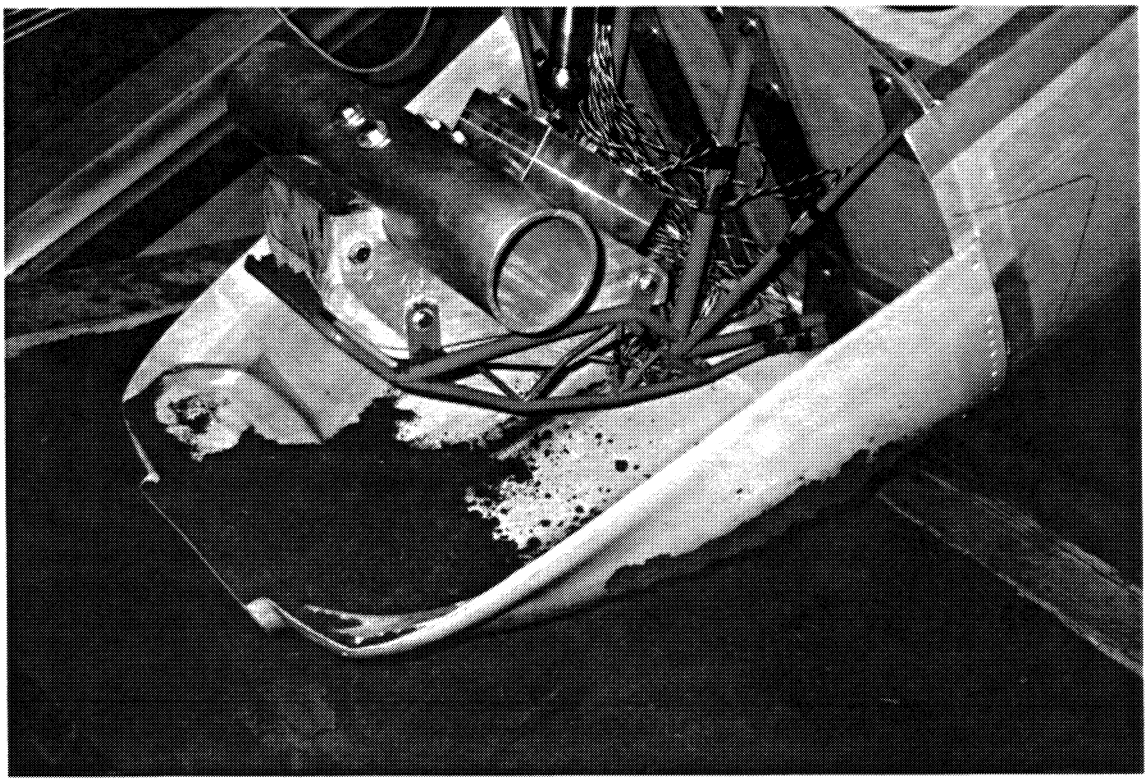

(d), Post Test

Figure 95, (concluded)

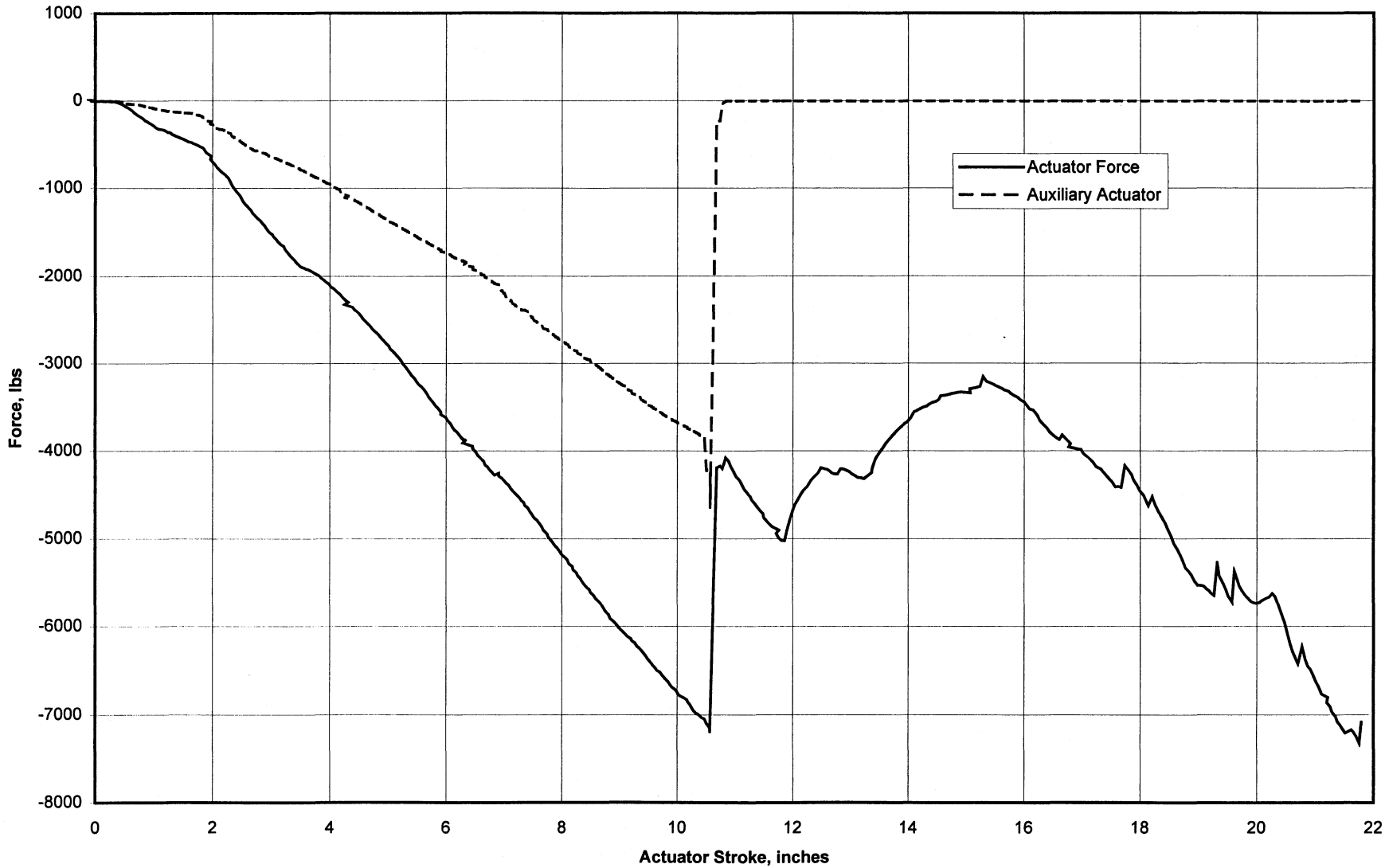

Figure 96, Soft Soil Half Scale Test 3 Data

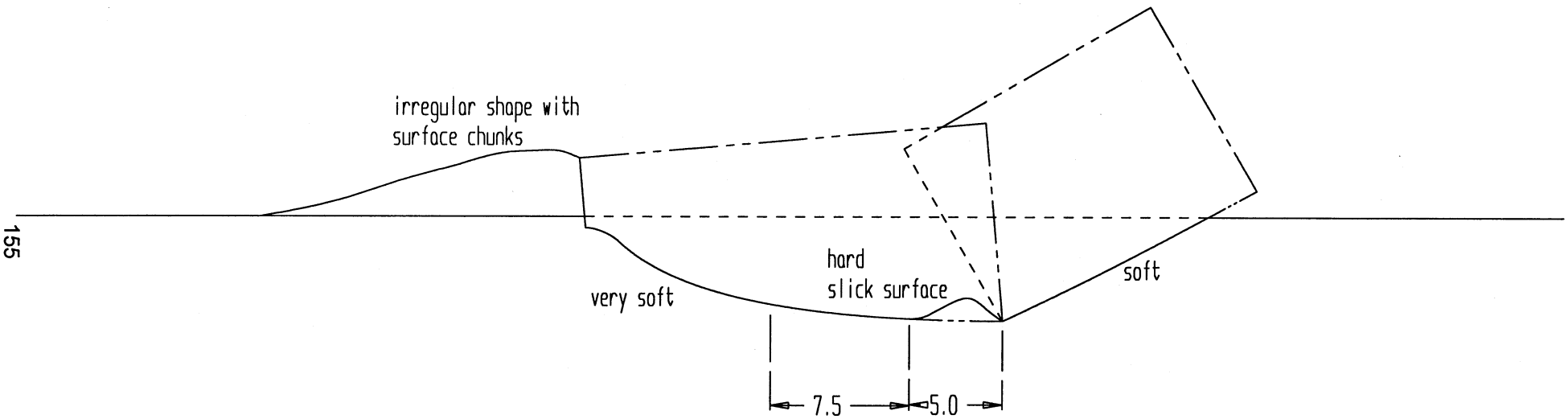

Figure 97, Crater Shape, Soil Test 3

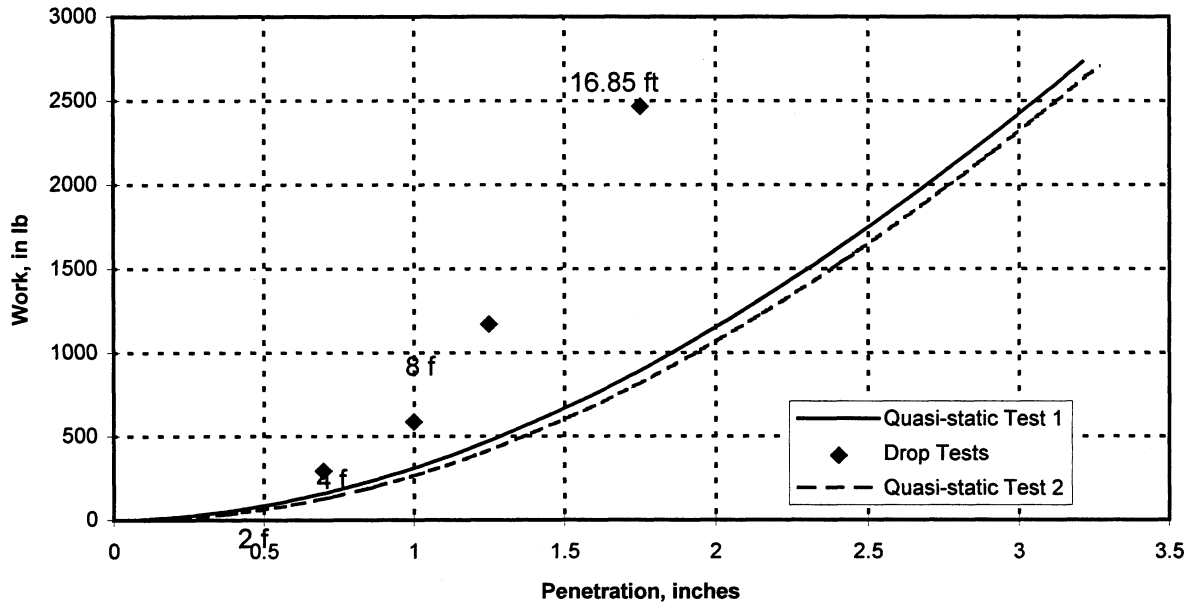

(a), Work versus Penetration

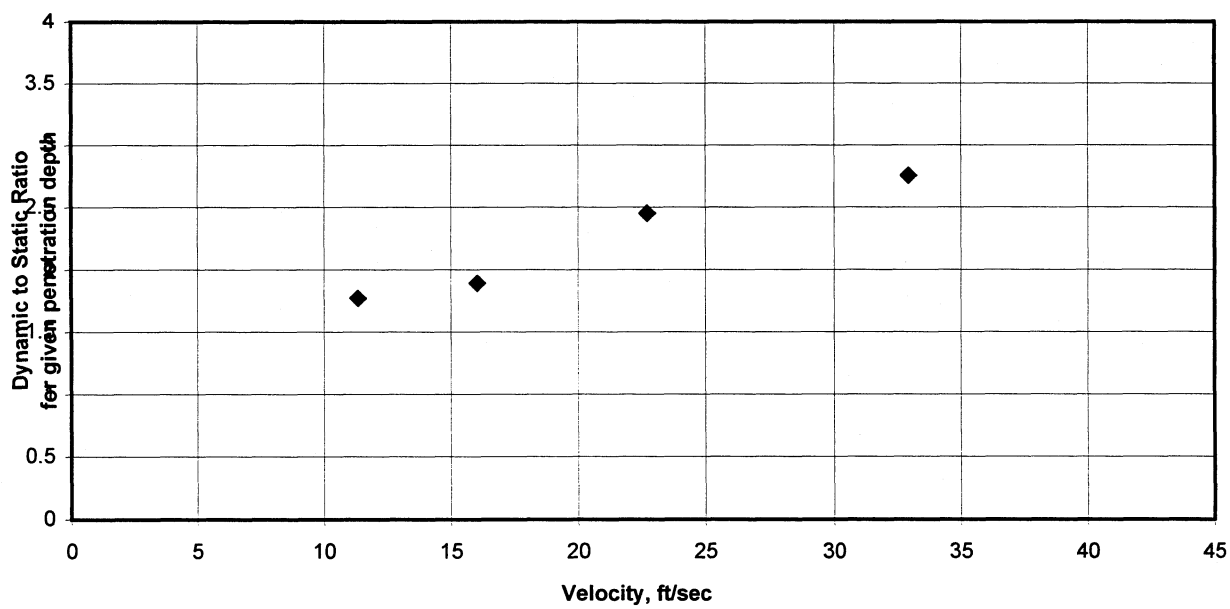

(b), Dynamic to Static Work Ratio

Figure 98, Shotput Tests in Soil Bed 5

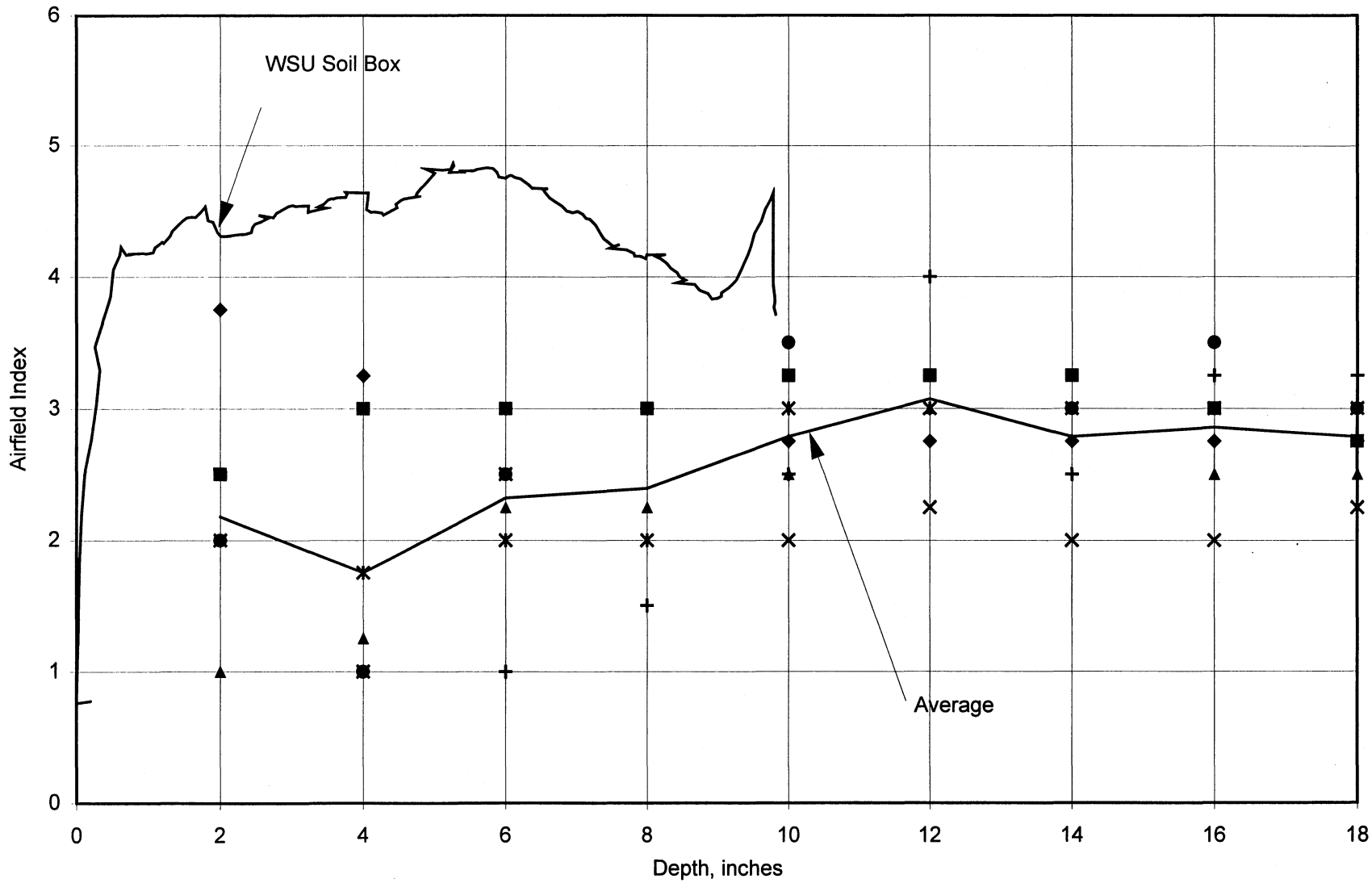

Figure 99, Soil Characteristics for Full Scale Test 2

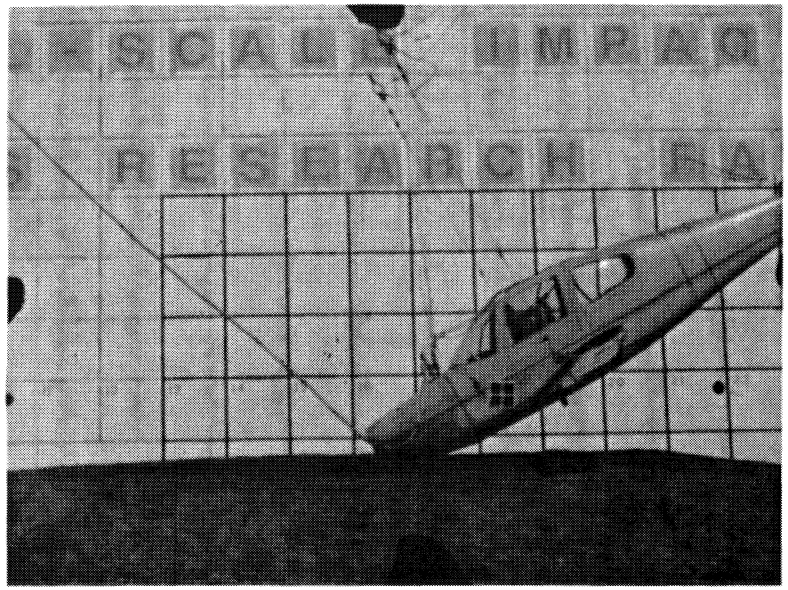

Impact

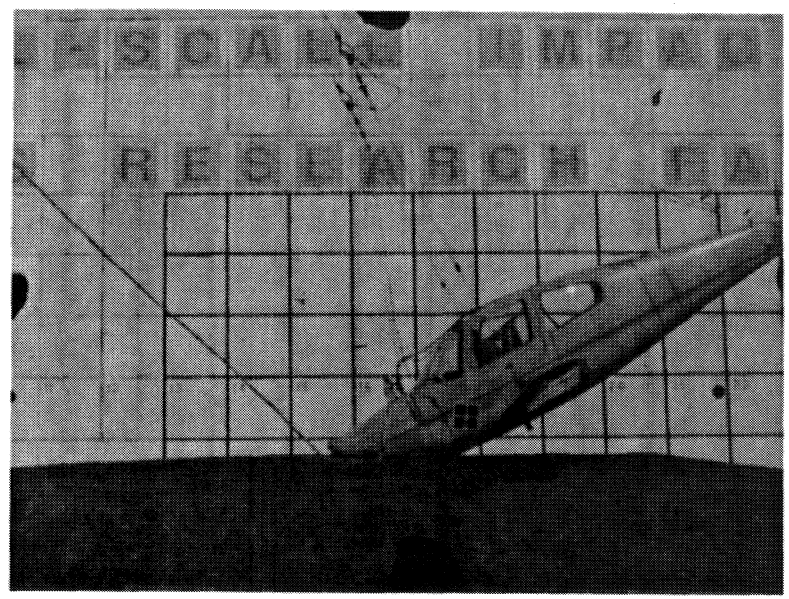

t = .020 seconds

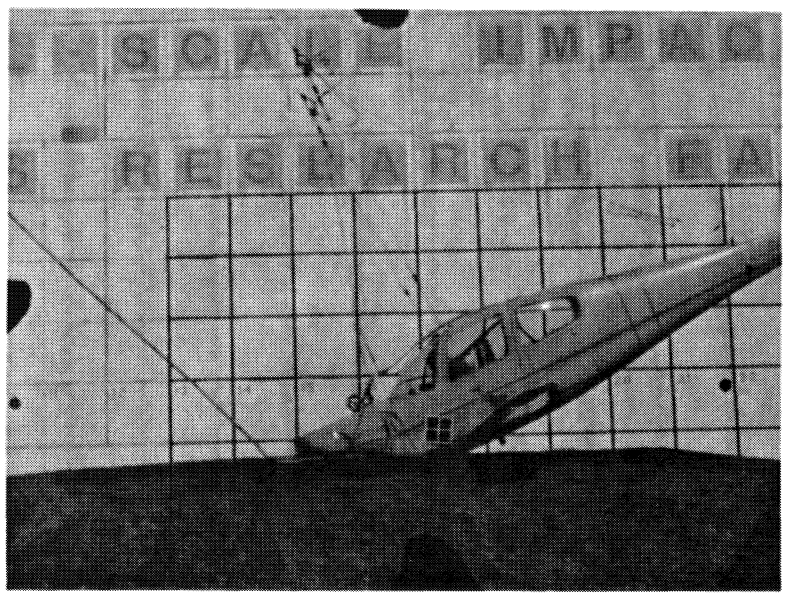

t = .040 seconds

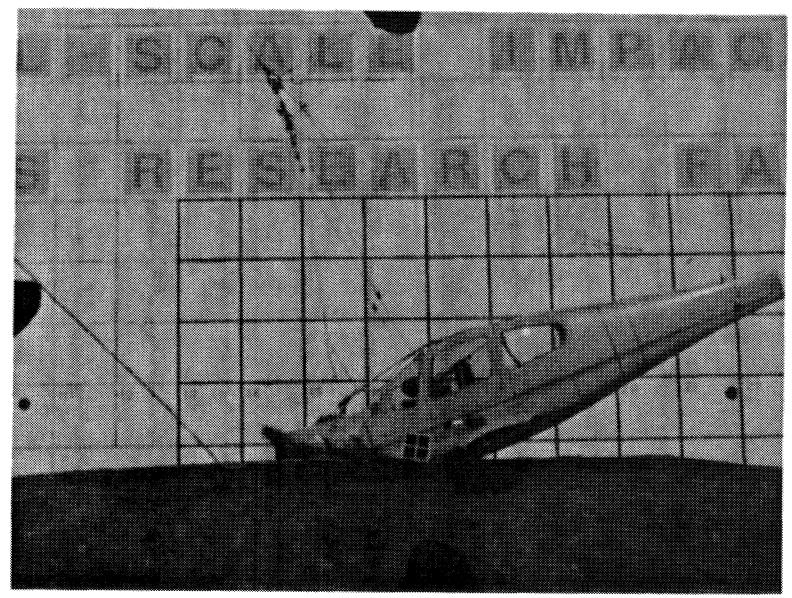

t = .060 seconds

Figure 100, Crash Sequence Photographs for Test 2

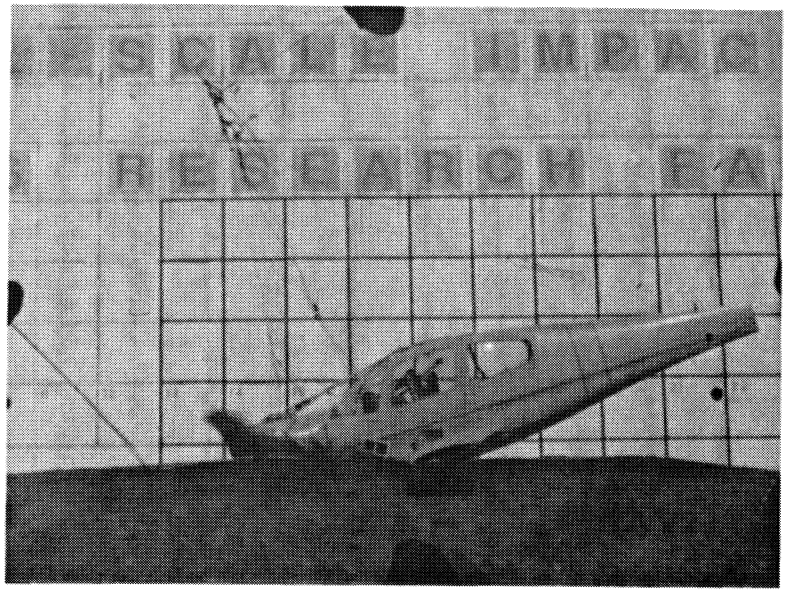

t = .080 seconds

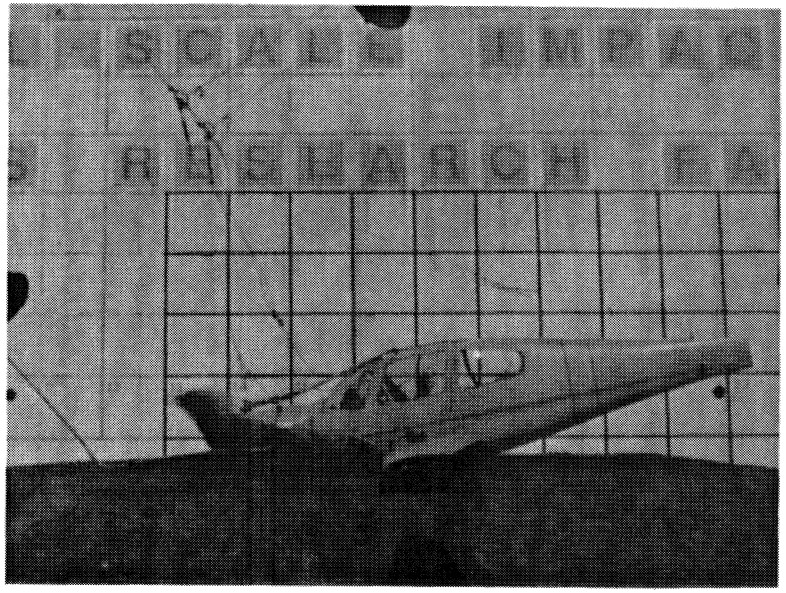

t = .100 seconds

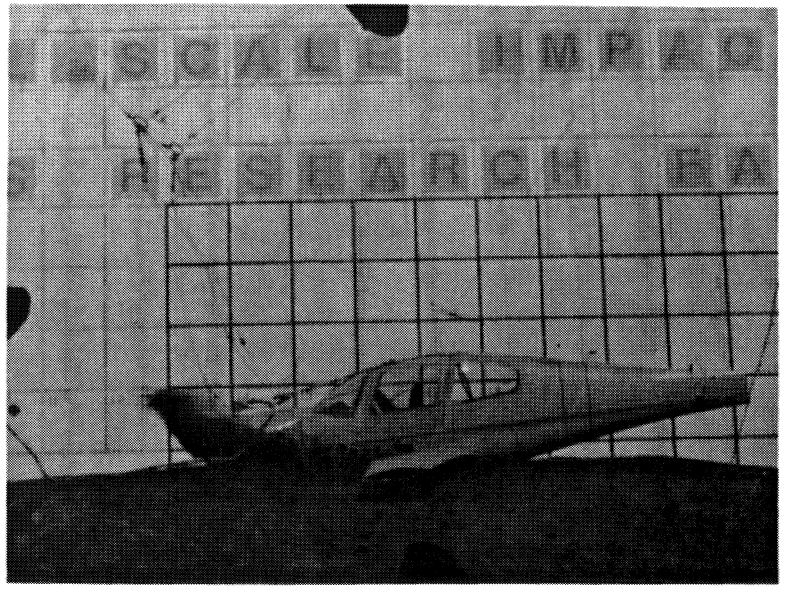

t = .120 seconds

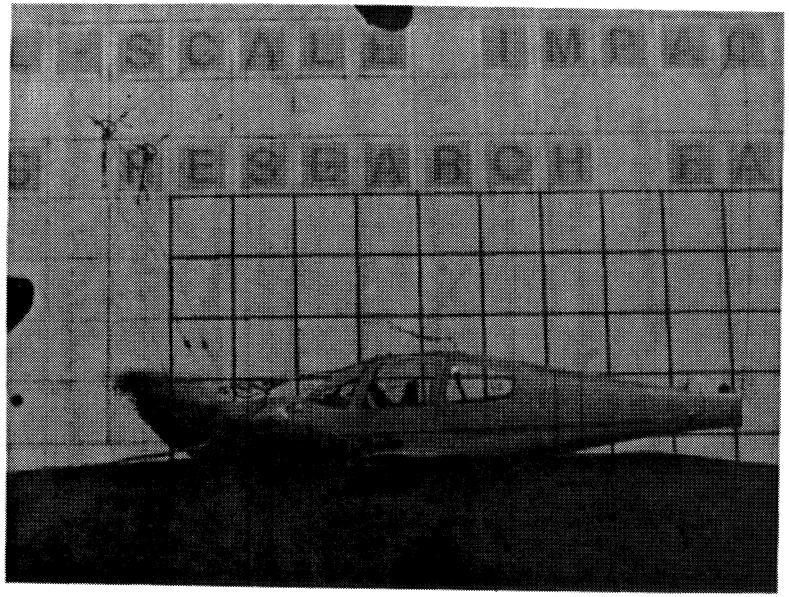

t = .140 seconds

Figure 100, (continued)

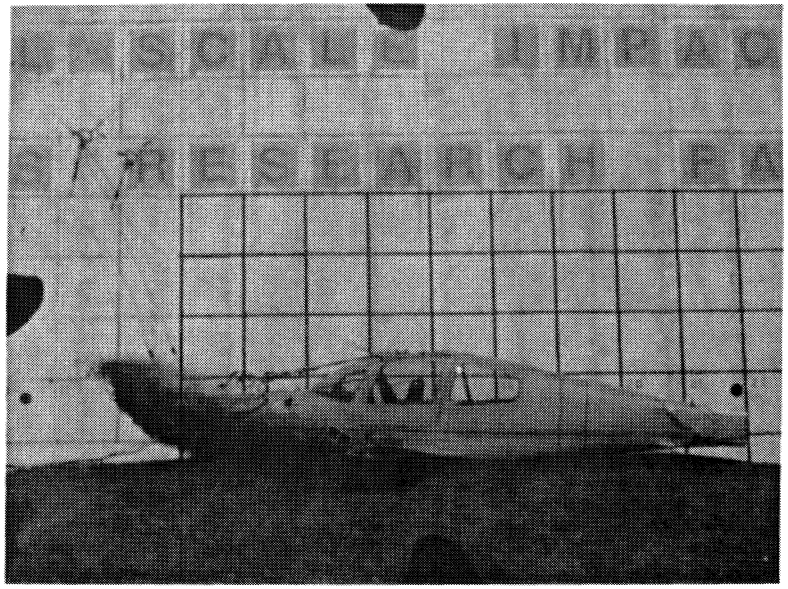

t = .160 seconds

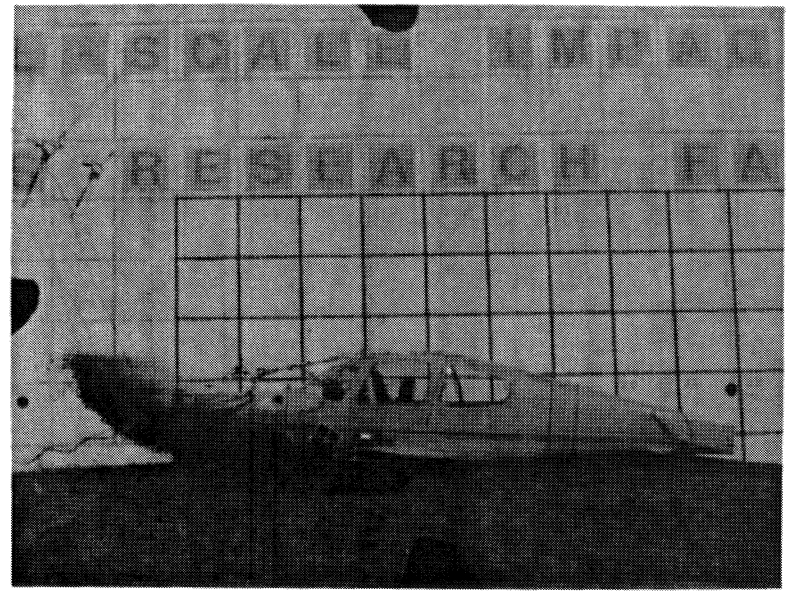

t = .180 seconds

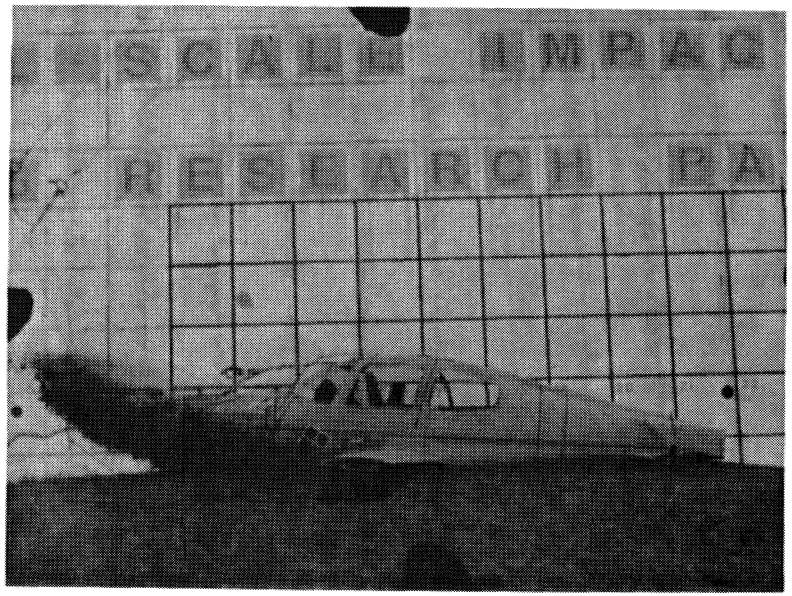

t = .200 seconds

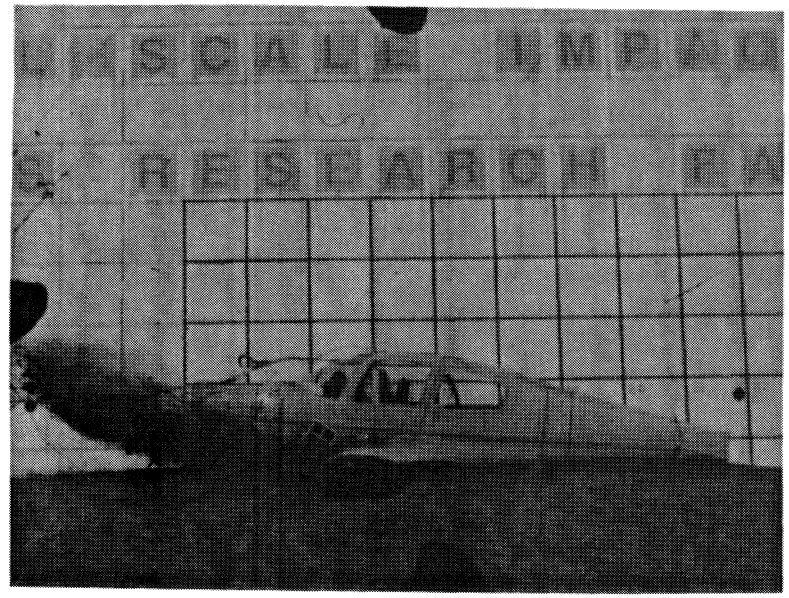

t = .220 seconds

Figure 100, (continued)

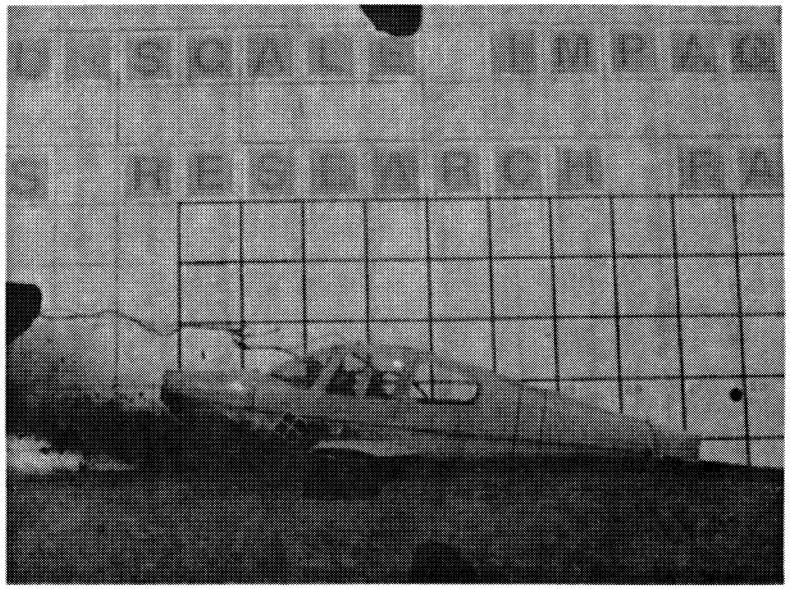

t = .300 seconds

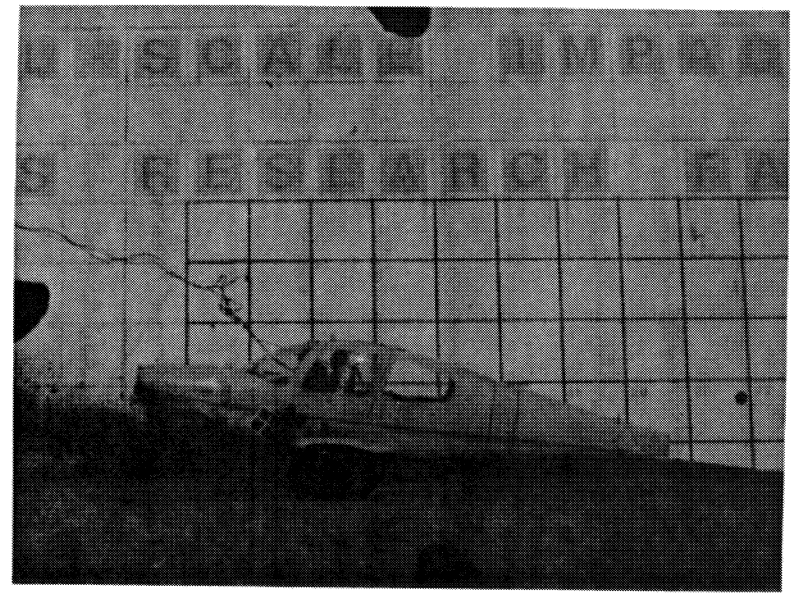

t = .400 seconds

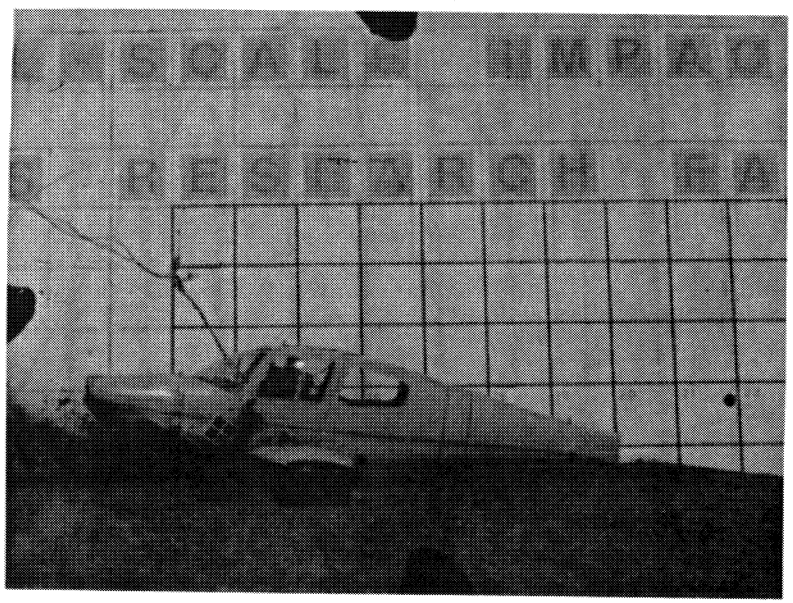

t = .500 seconds

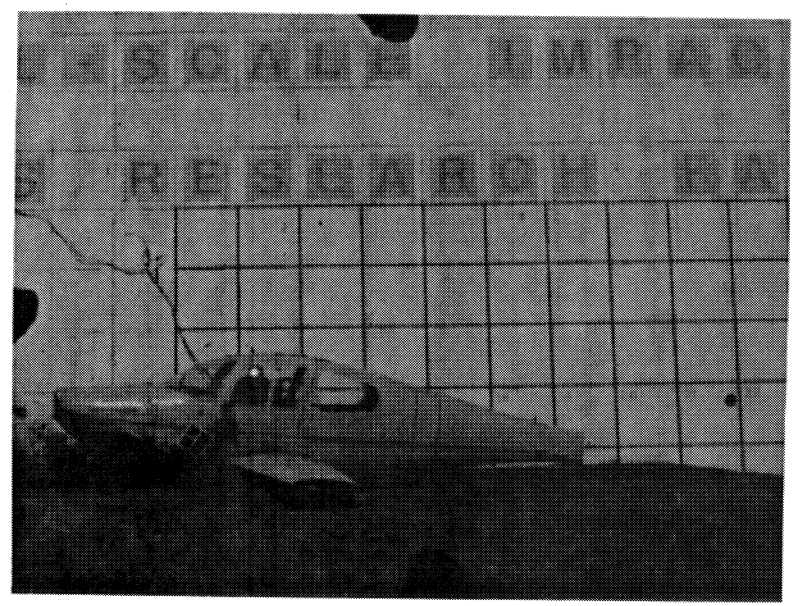

t = .600 seconds

Figure 100, (concluded)

(a), Rest Position

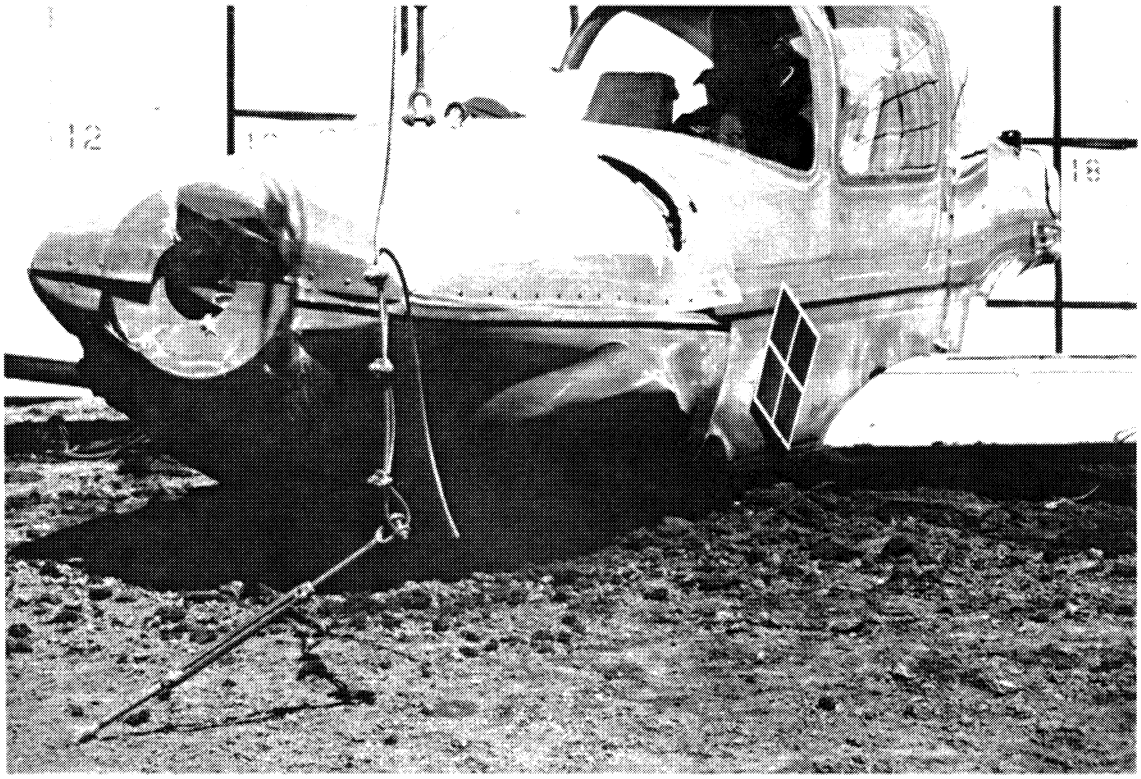

(b), Front View Showing Cowl

Figure 101, Post Crash Damage for Test 2

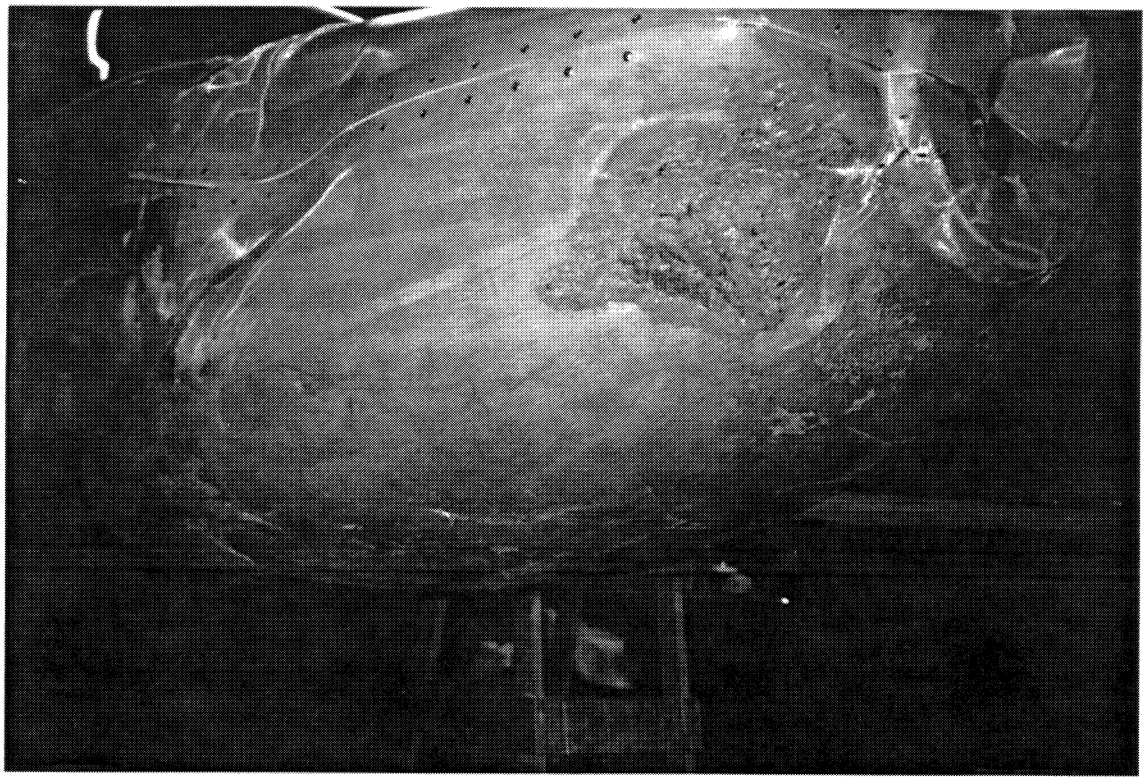

(c), Cowl

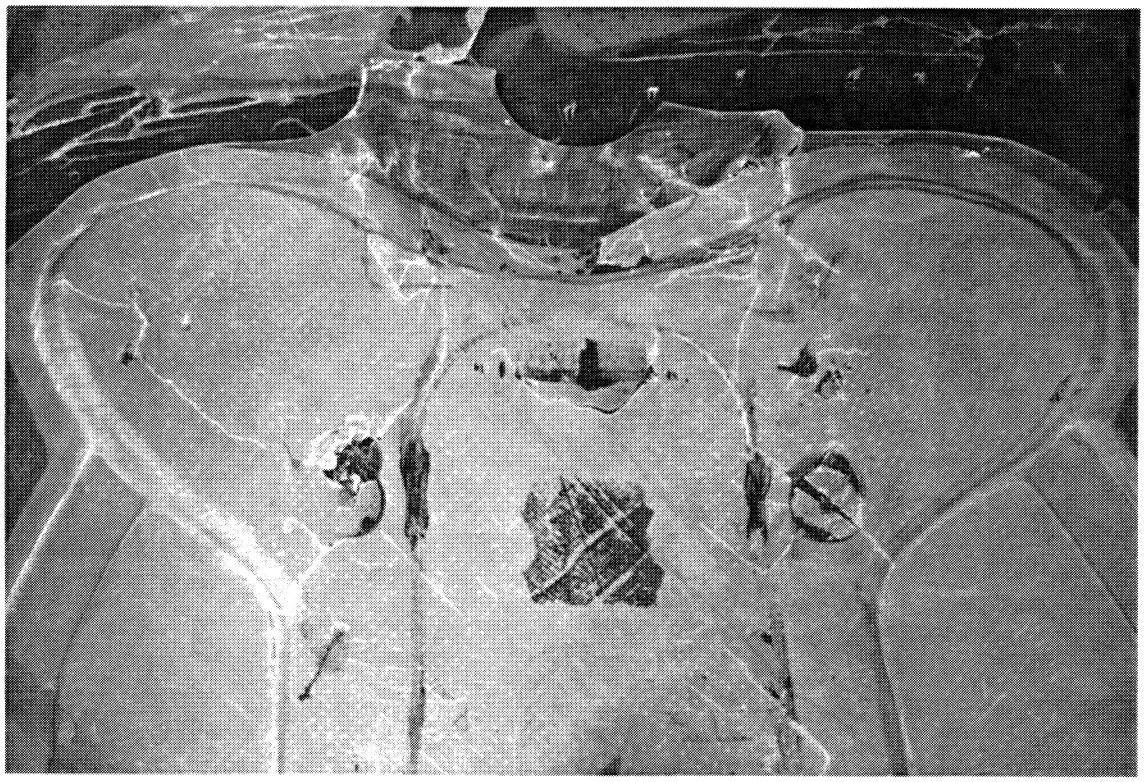

(d), Inside Cowl

Figure 101, (continued)

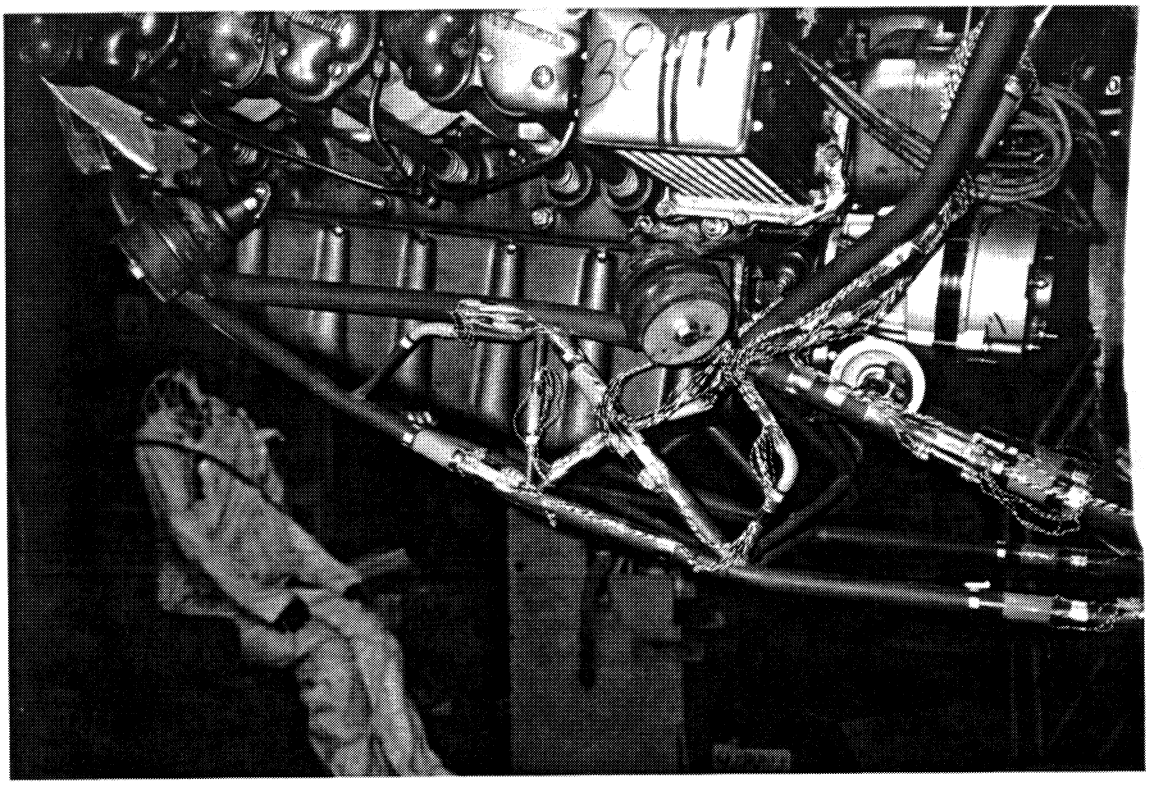

(e), Engine Mount

(f), Dummy Positions

Figure 101, (concluded)

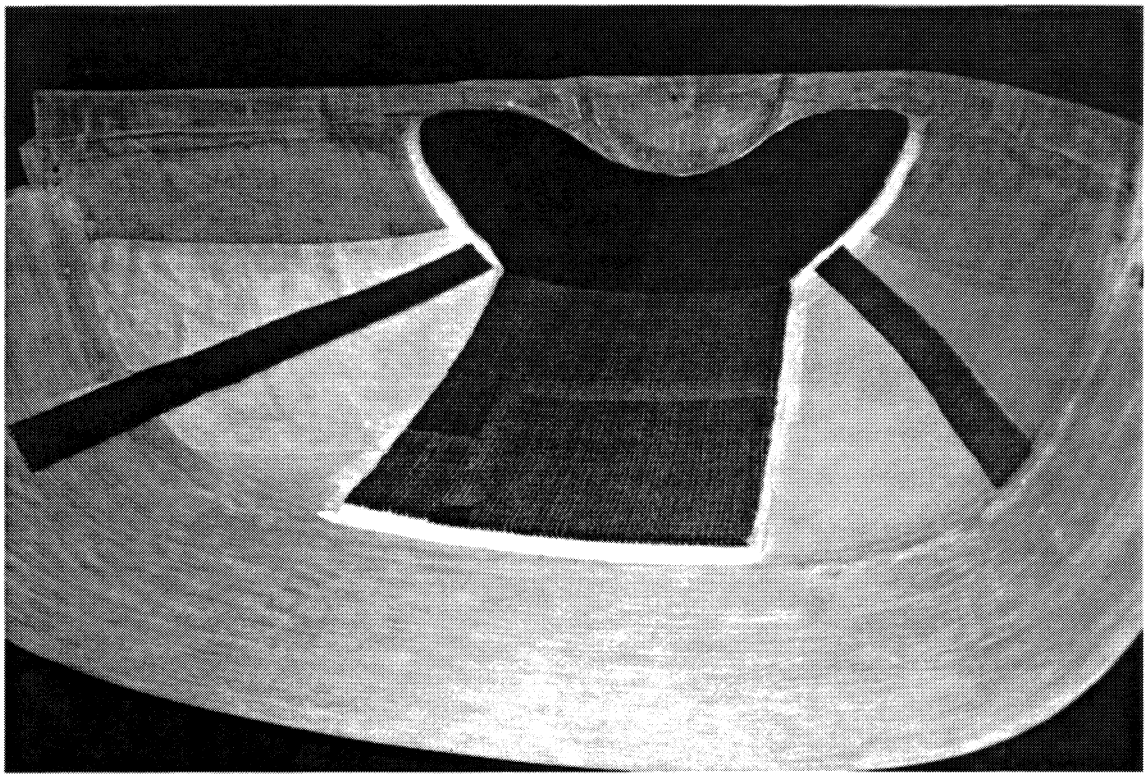

(a), Pad Lay-up in Progress

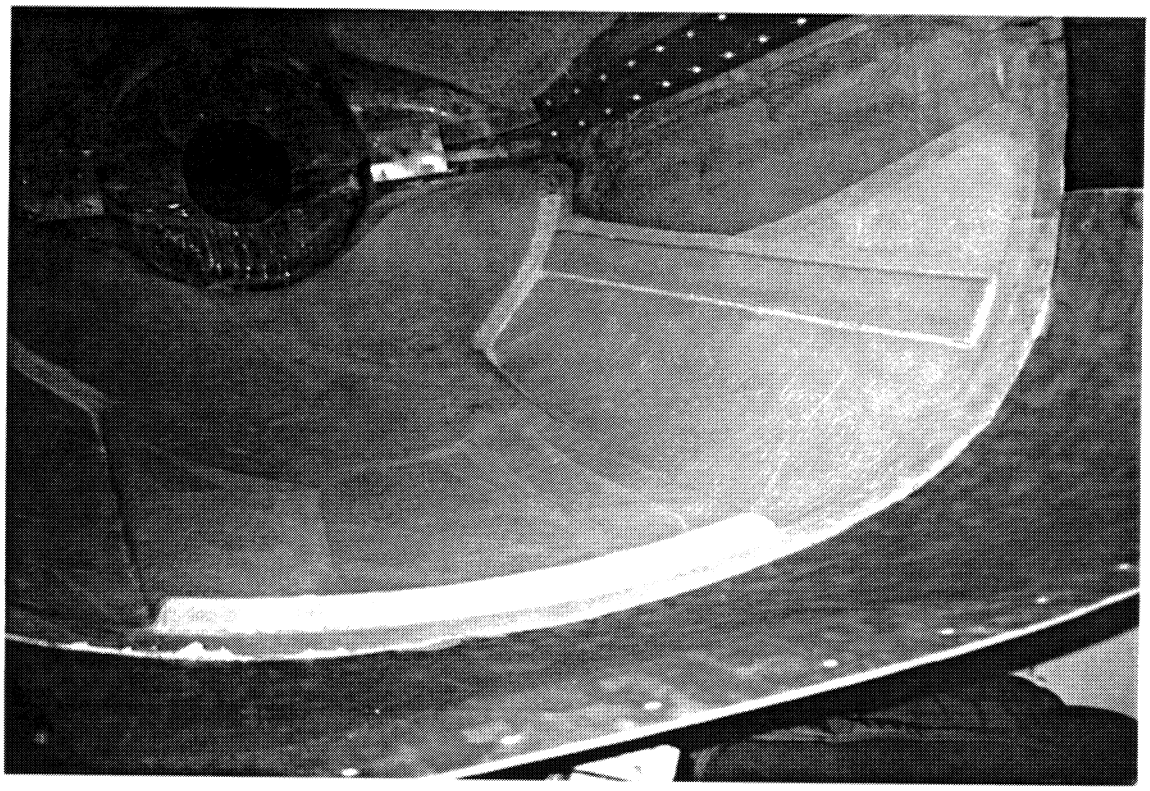

(b), Completed Pad

Figure 102, Test 2 Cowling

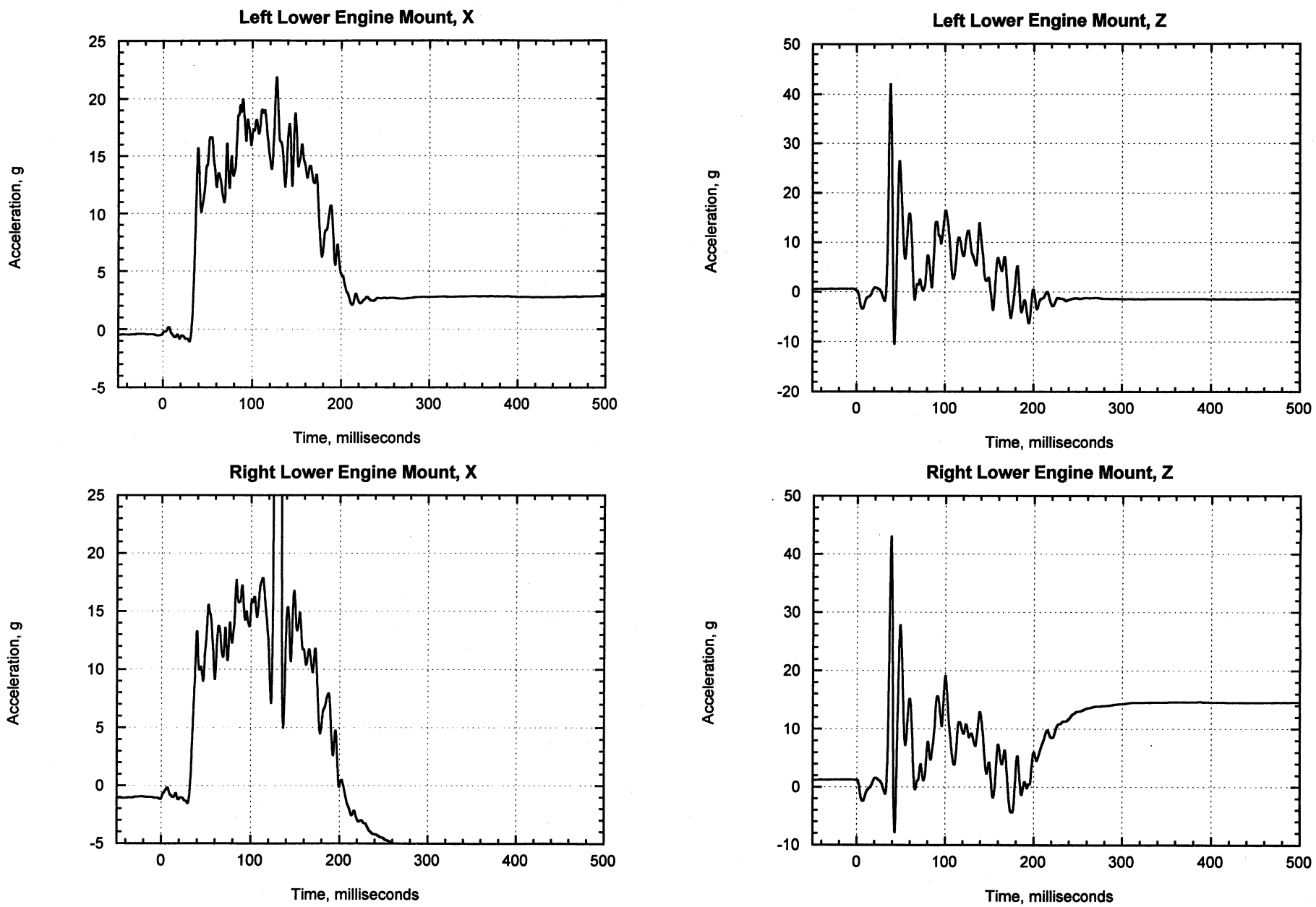

Figure 103, Test 2, Lower Firewall Accelerations

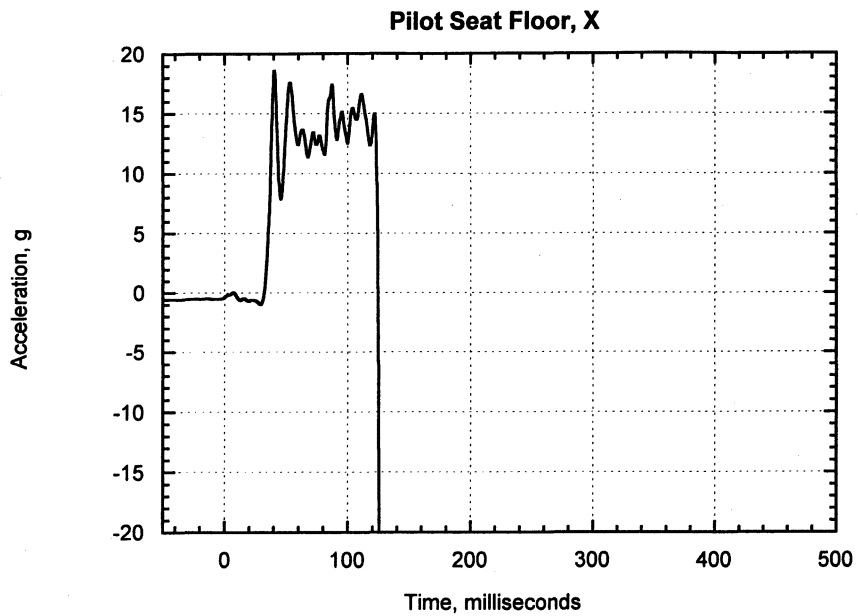

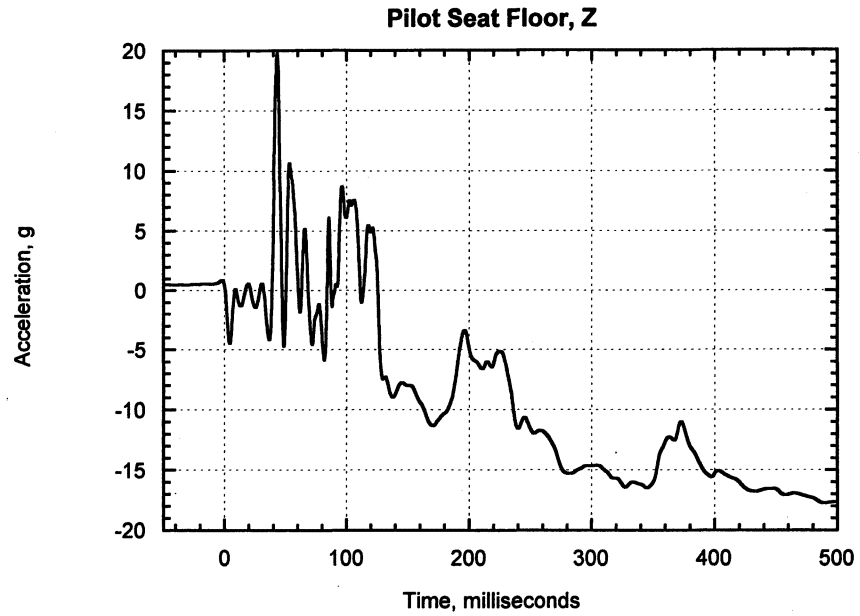

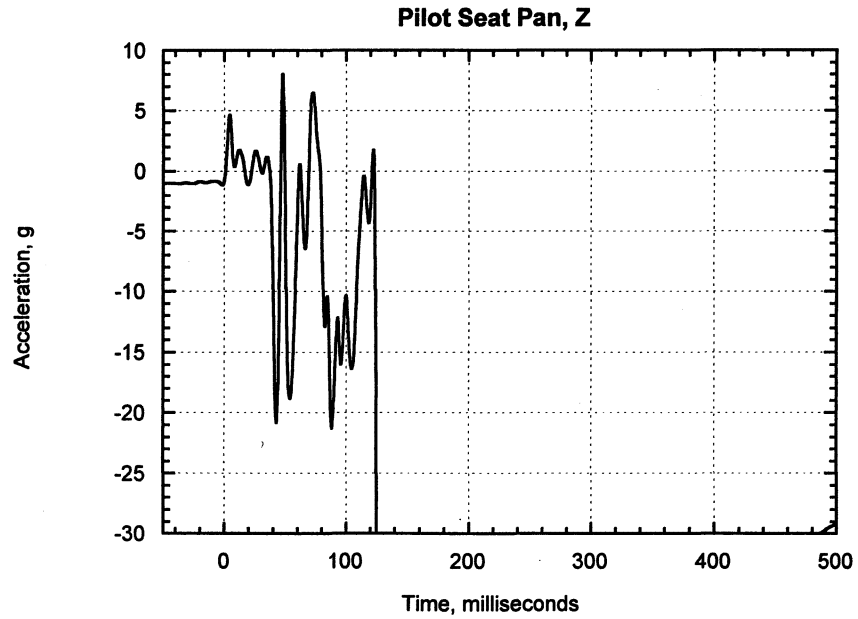

Figure 104, Test 2, Pilot's Seat & Floor

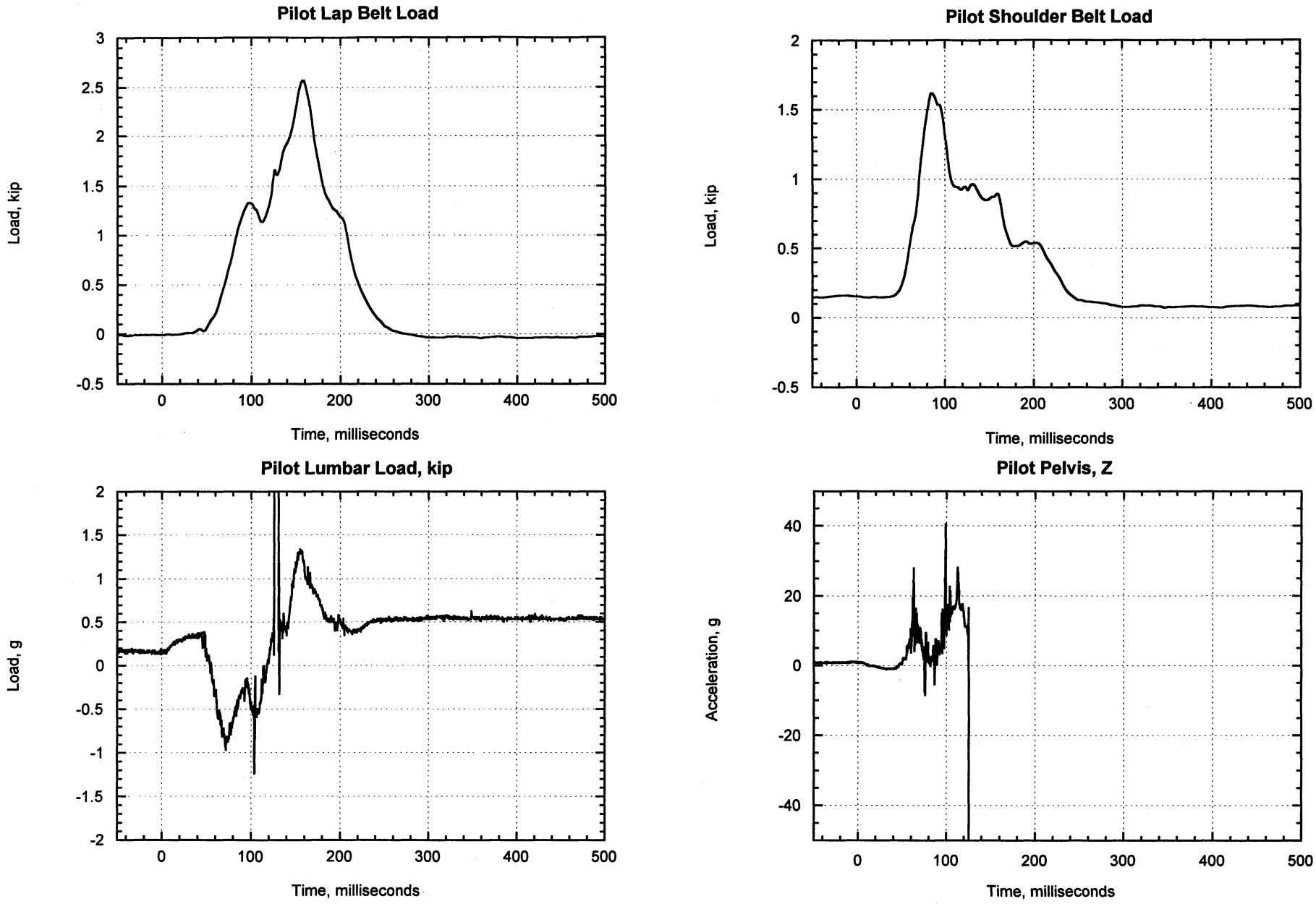

Figure 105, Test 2, Pilot

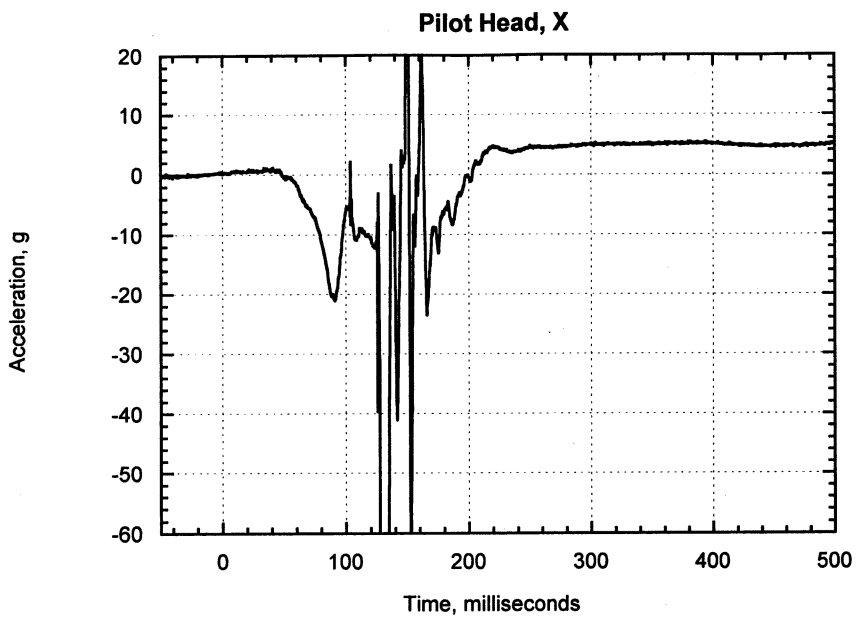

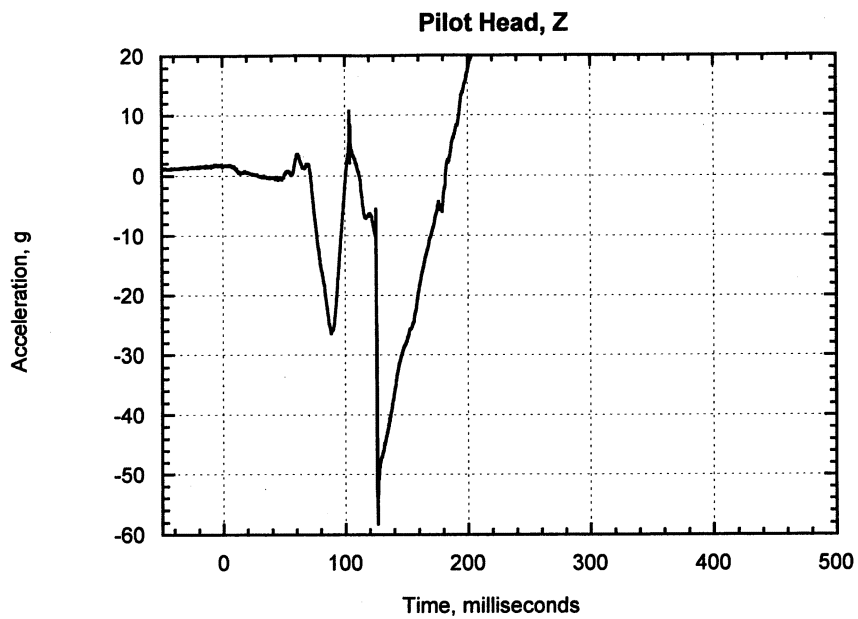

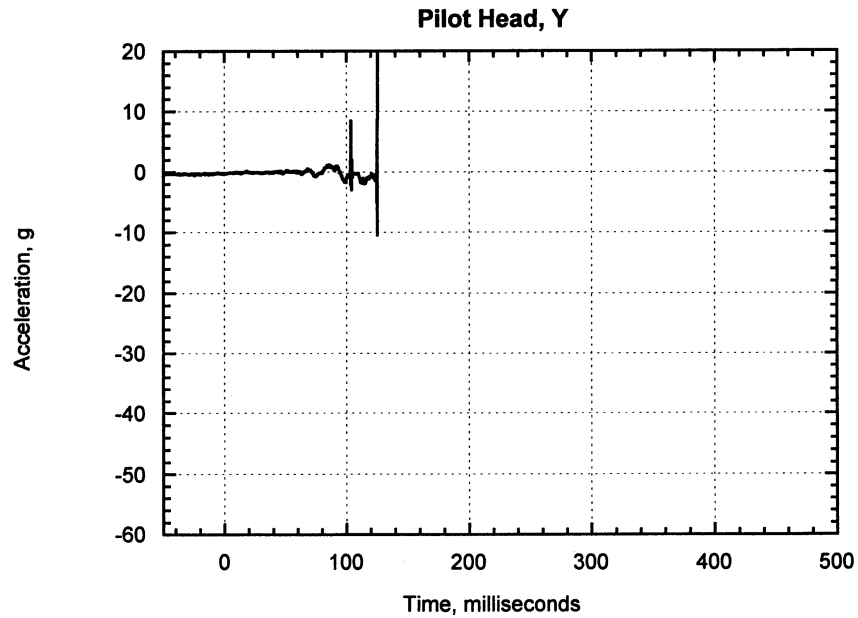

Figure 106, Test 2, Pilot Head

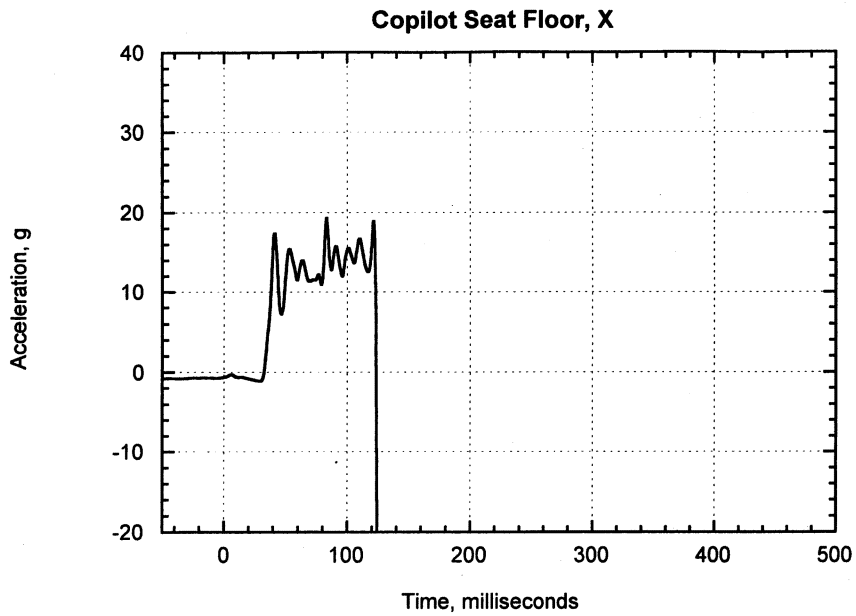

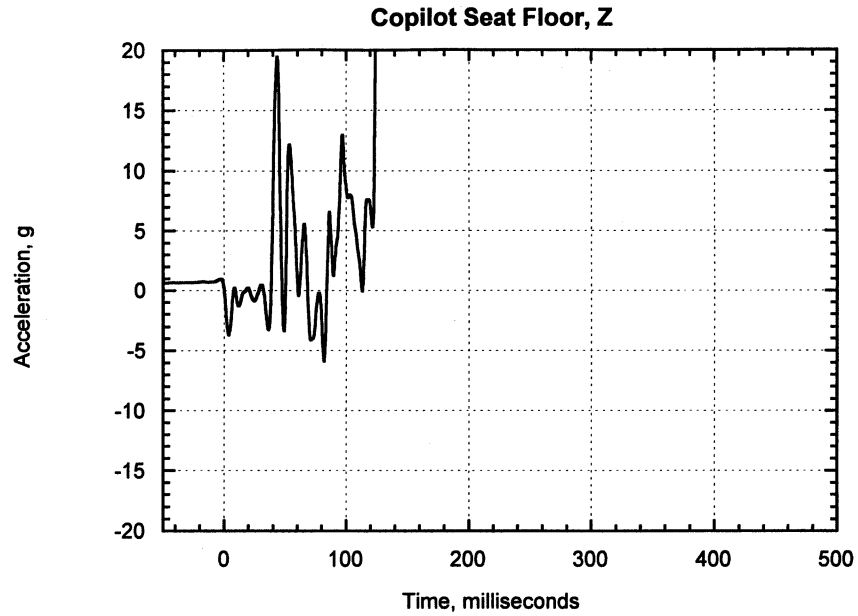

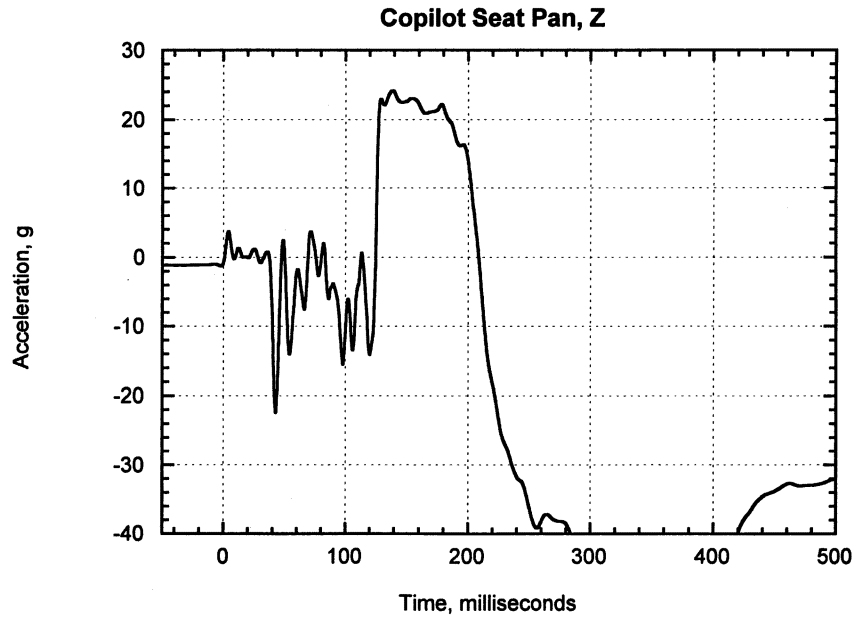

Figure 107, Test 2, Copilot's Seat & Floor

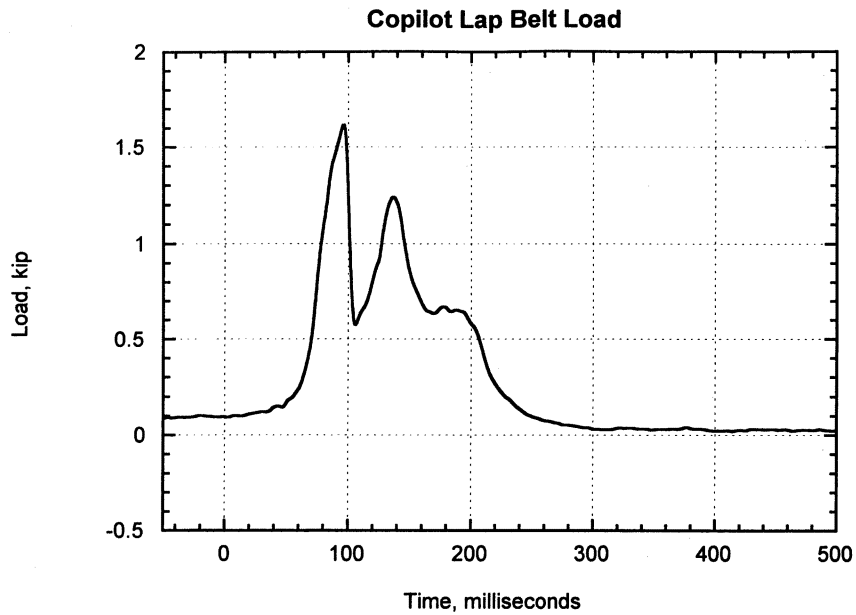

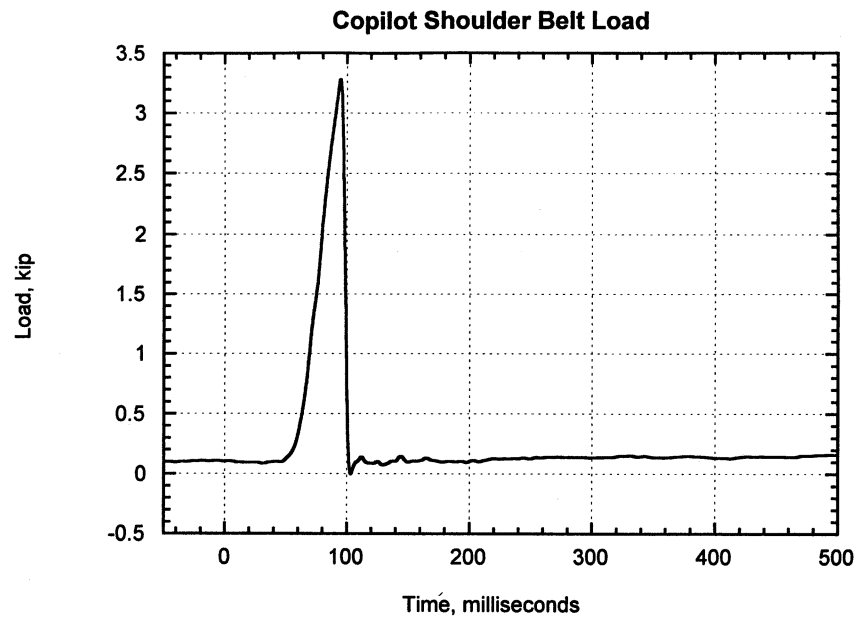

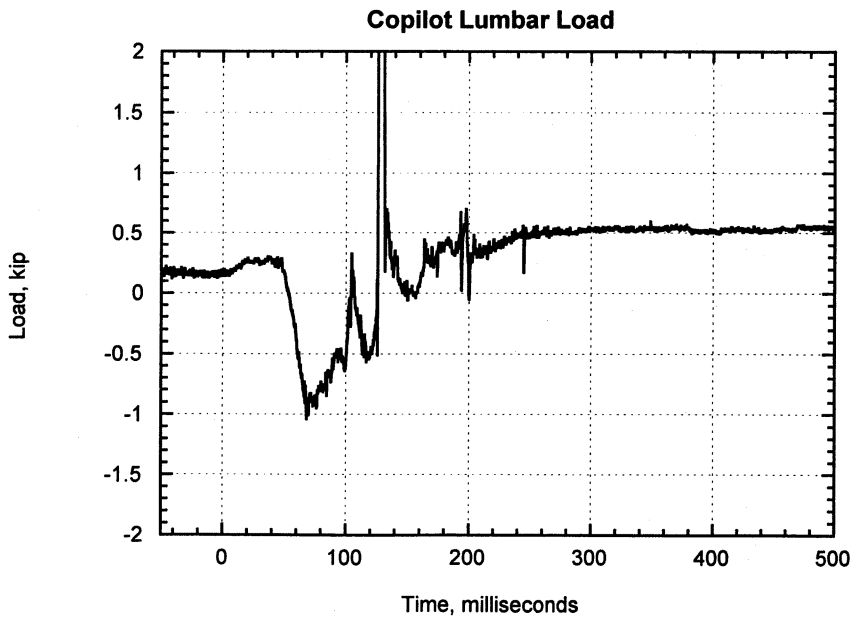

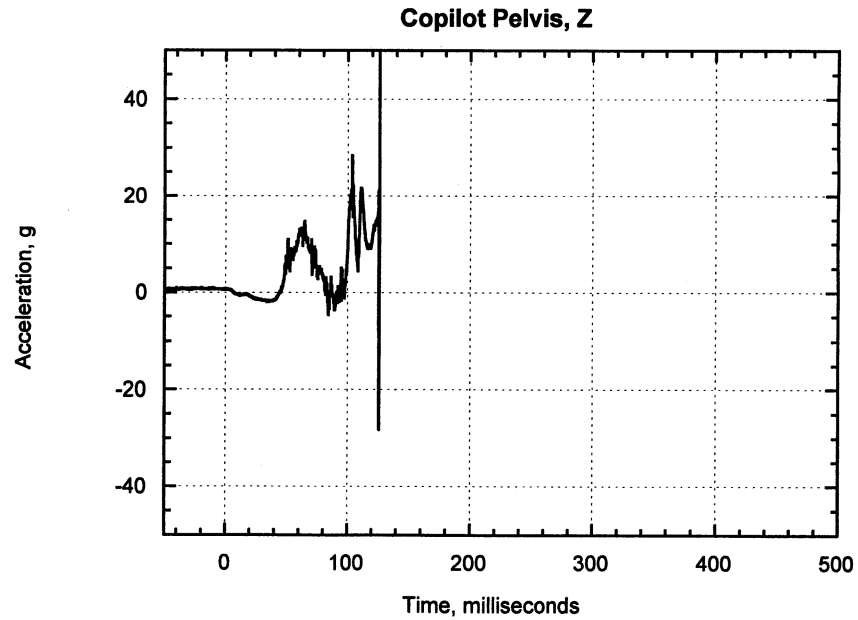

Figure 108, Test 2, Copilot

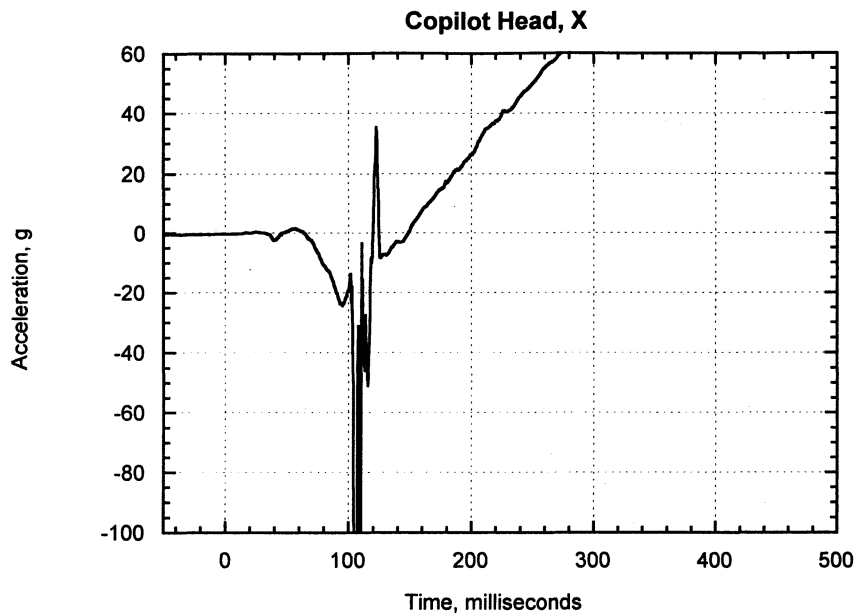

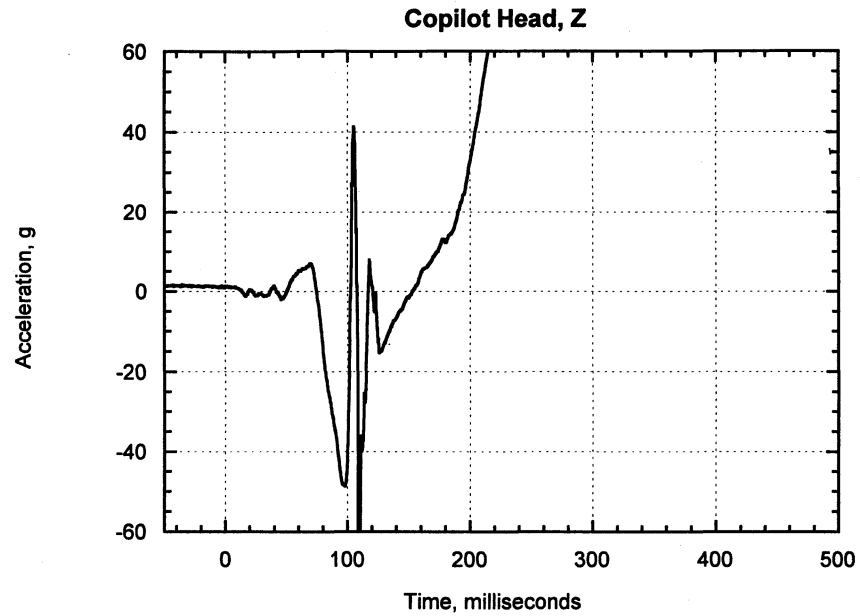

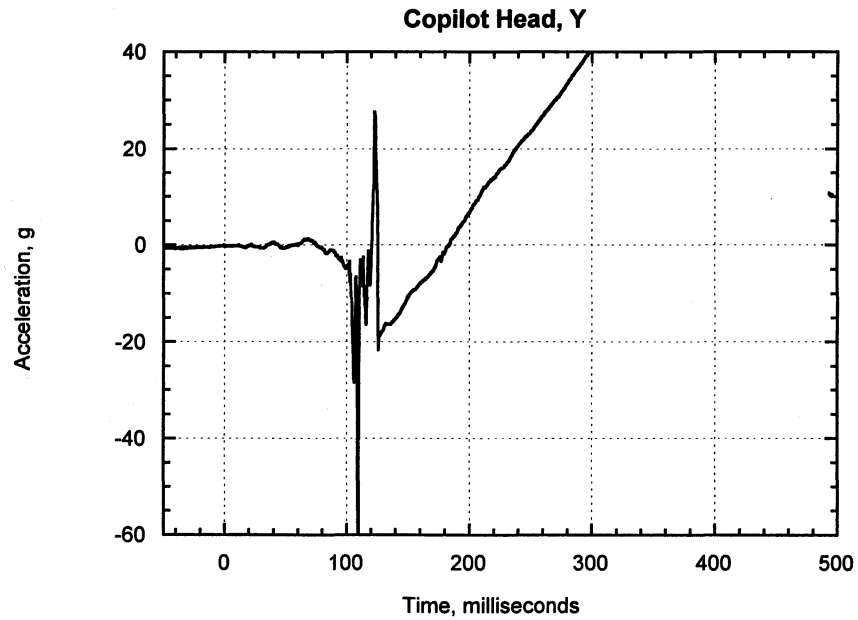

Figure 109, Test 2, Copilot Head

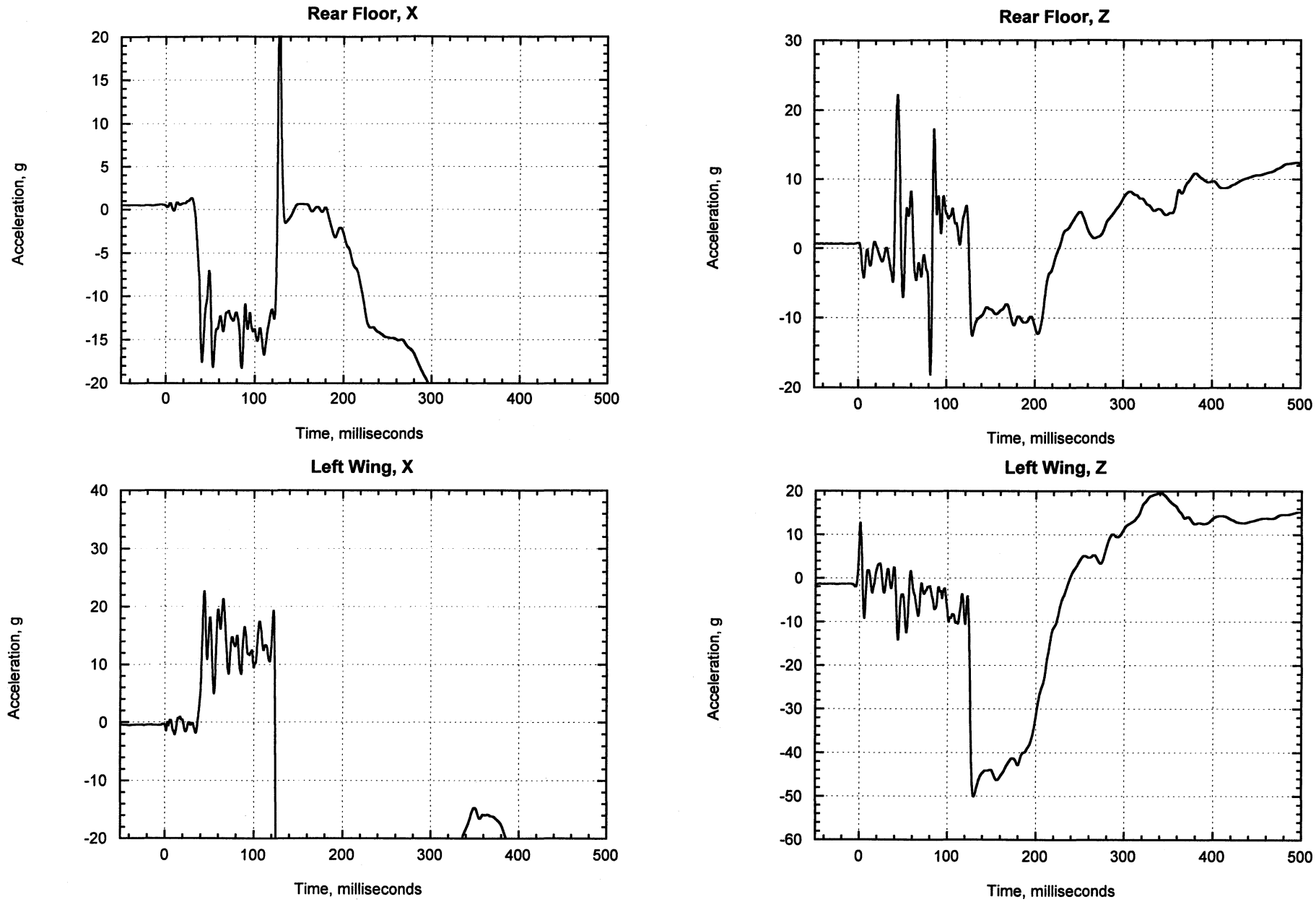

Figure 110, Test 2, Rear Floor and Left Wing

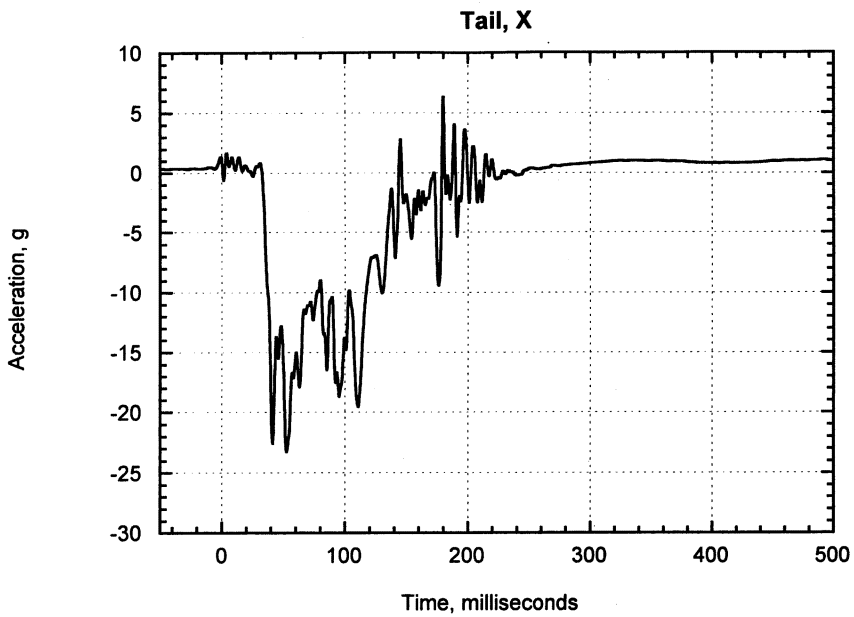

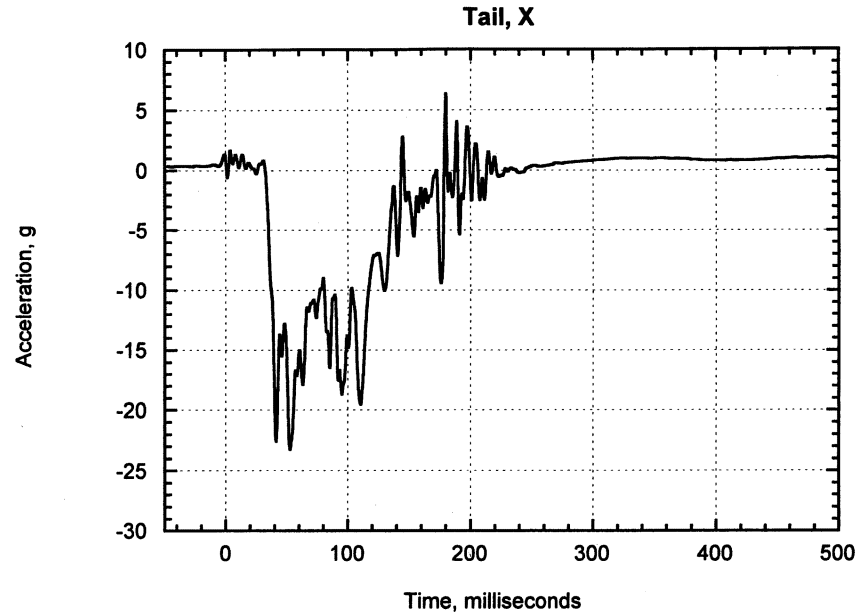

Figure 111, Test 2, Tail Accelerations

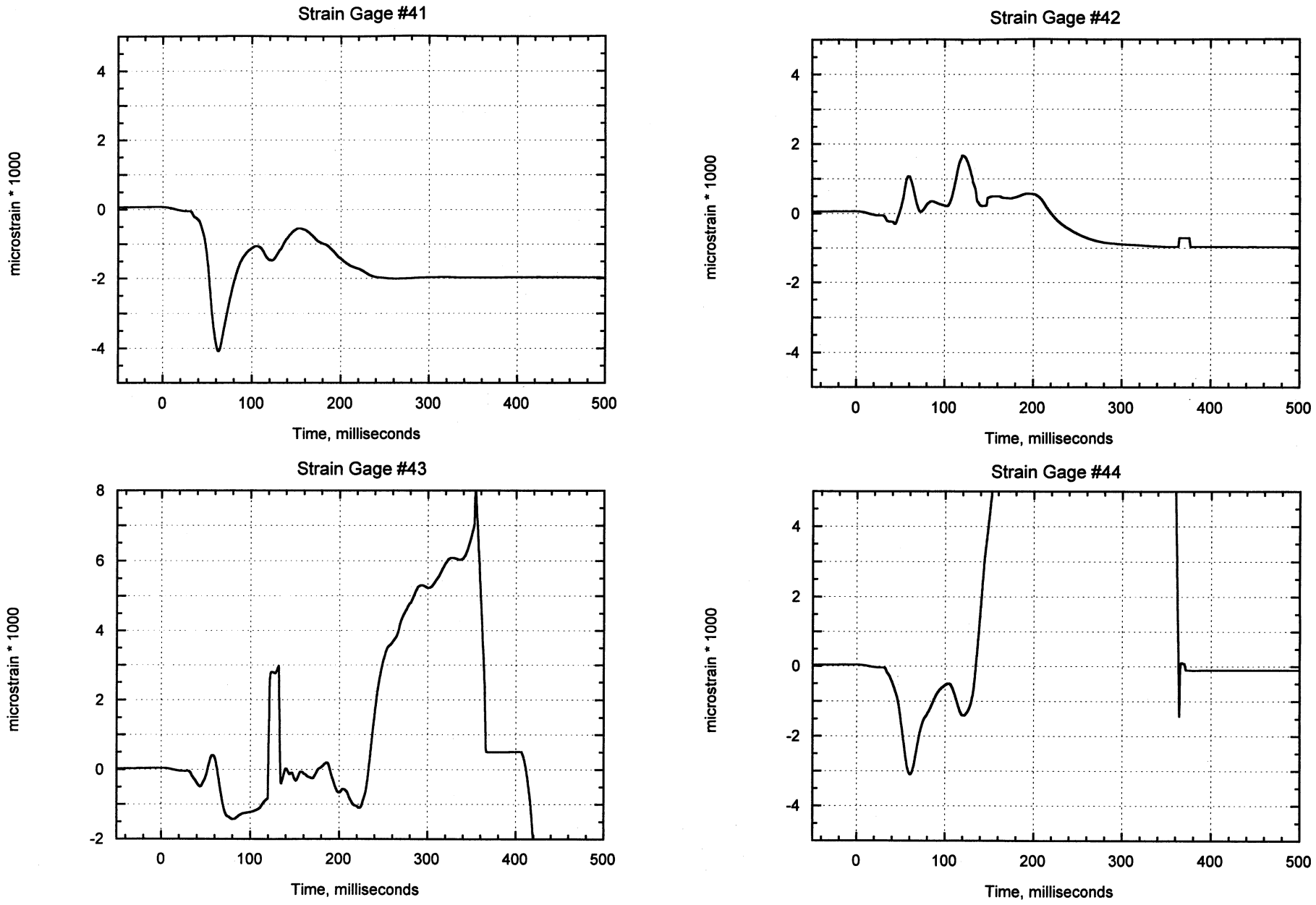

Figure 112, Test 2, Engine Mount, Left Post

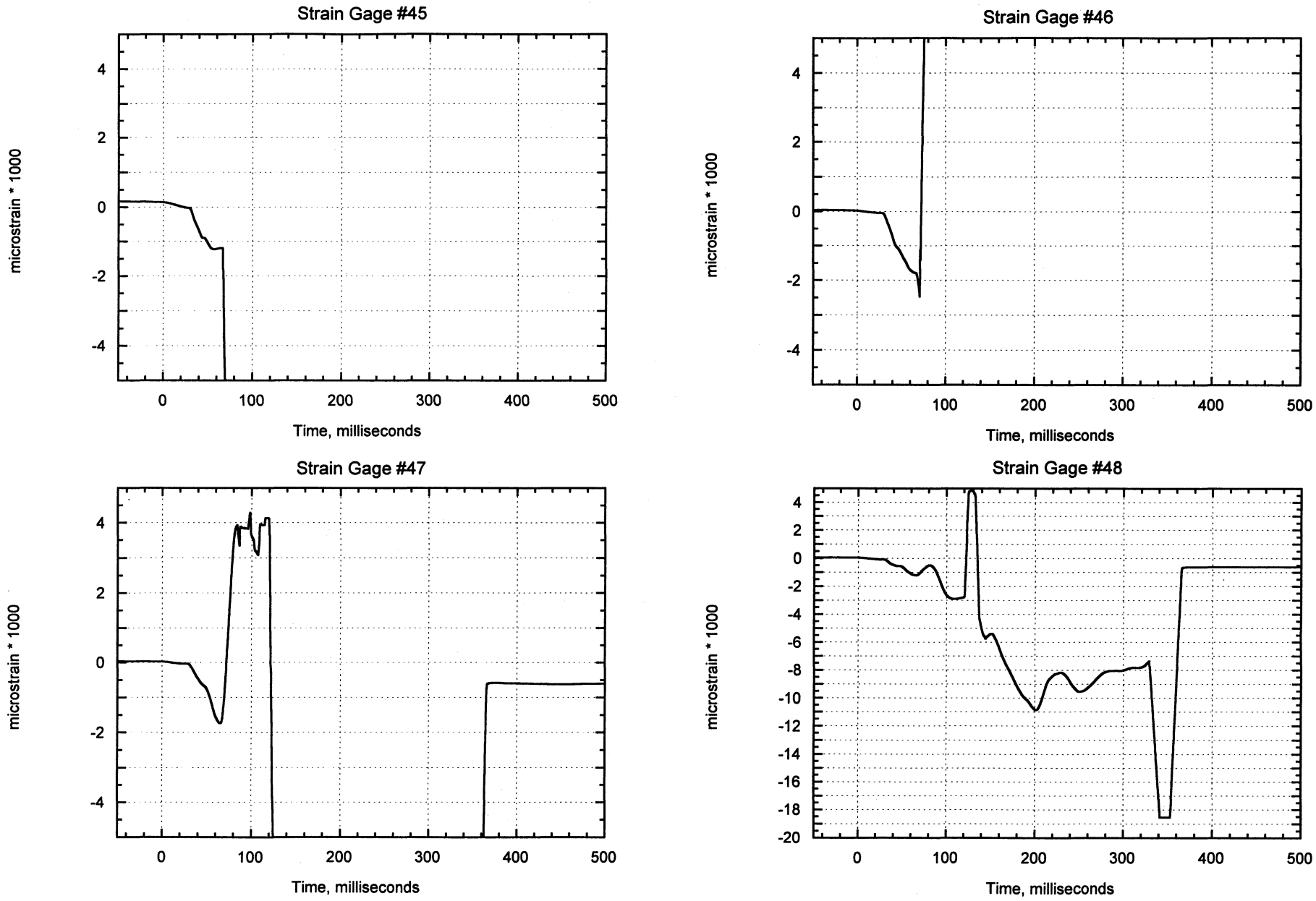

Figure 113, Test 2, Engine Mount, Right Post

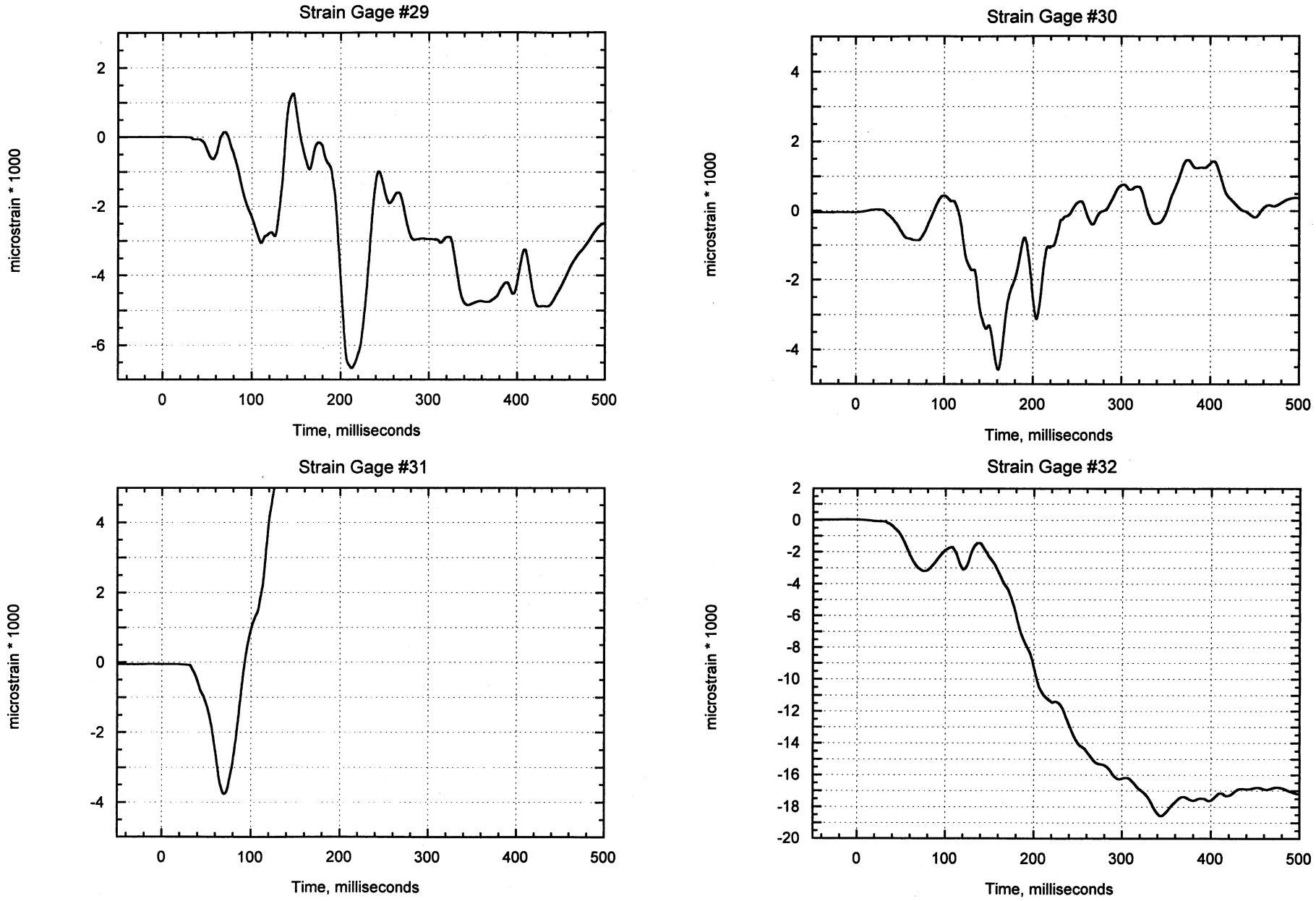

Figure 114, Test 2, Engine Mount, Left Aft Upper Rail

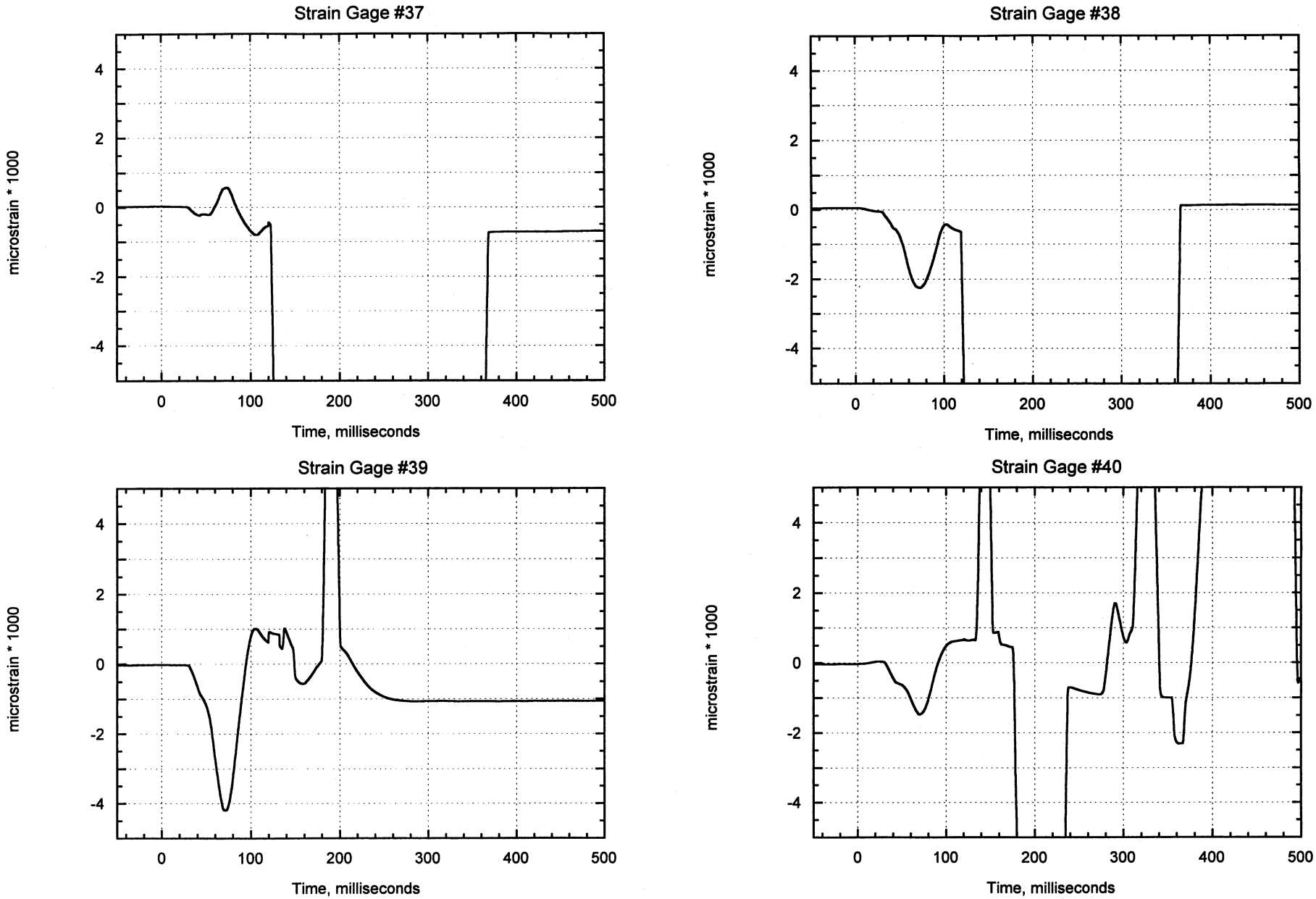

Figure 115, Test 2, Engine Mount, Right Aft Upper Rail

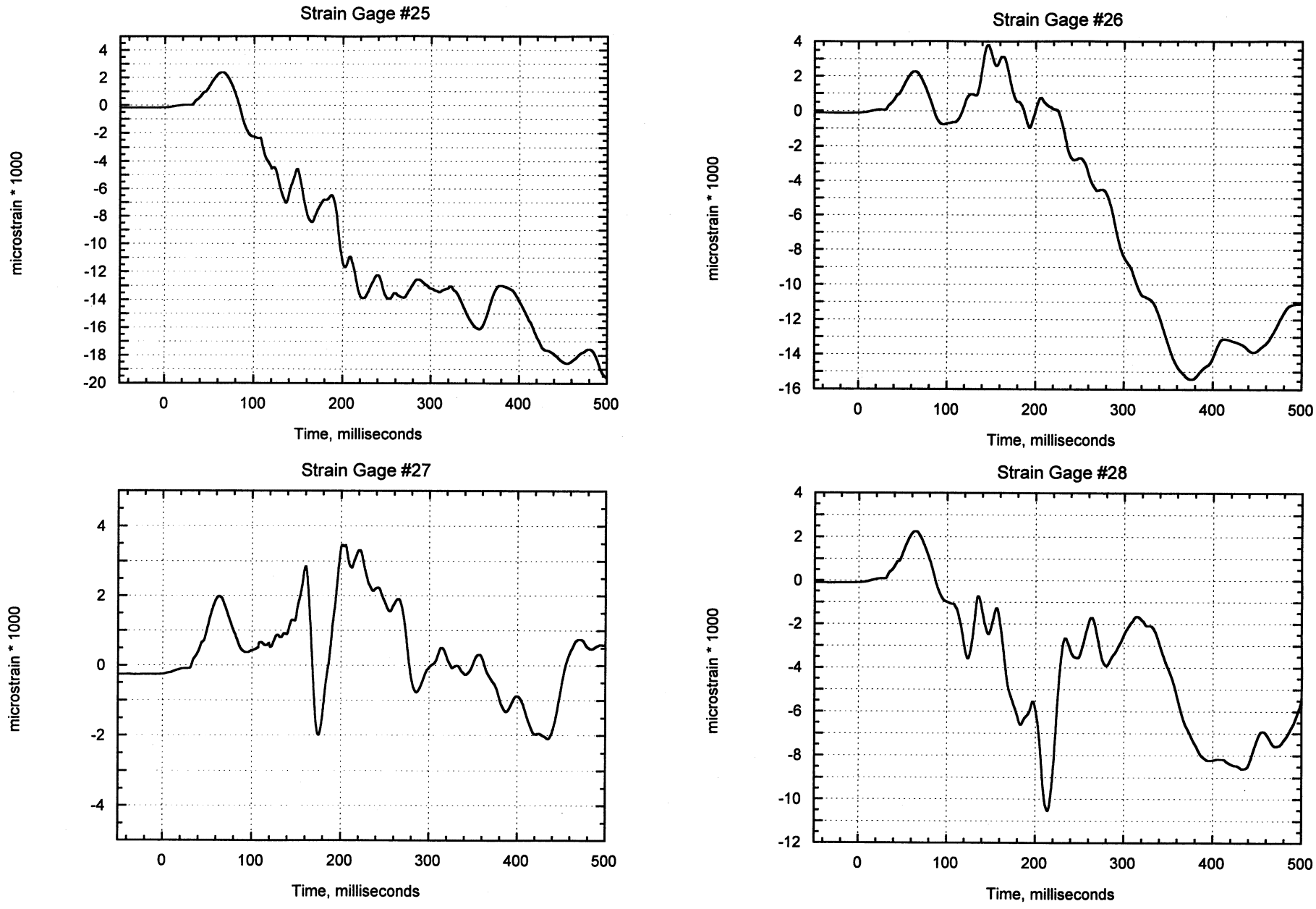

Figure 116, Test 2, Engine Mount, Left Aft Lower Rail

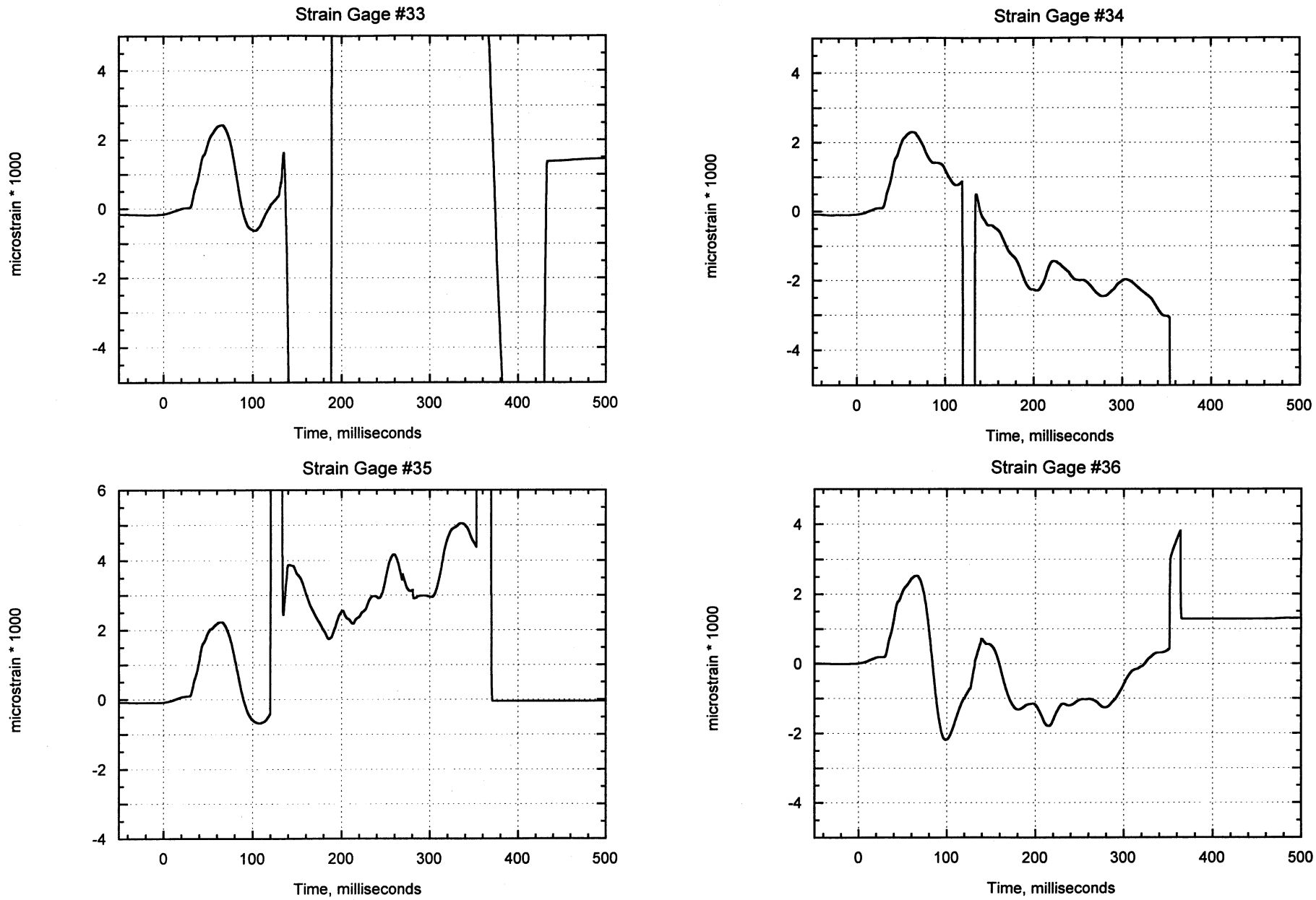

Figure 117, Test 2, Engine Mount, Right Aft Lower Rail

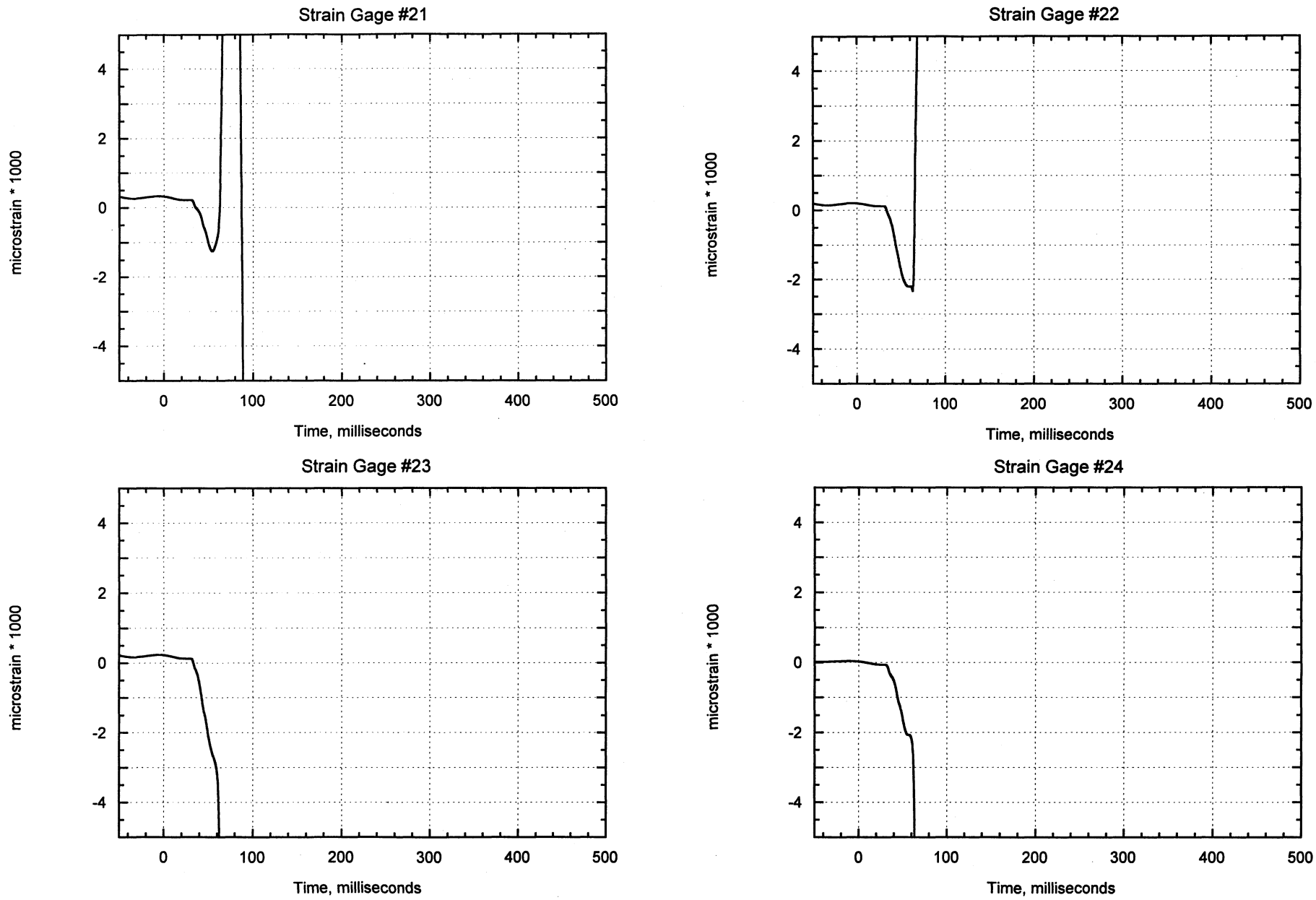

Figure 118, Test 2, Engine Mount, Left Aft Upright

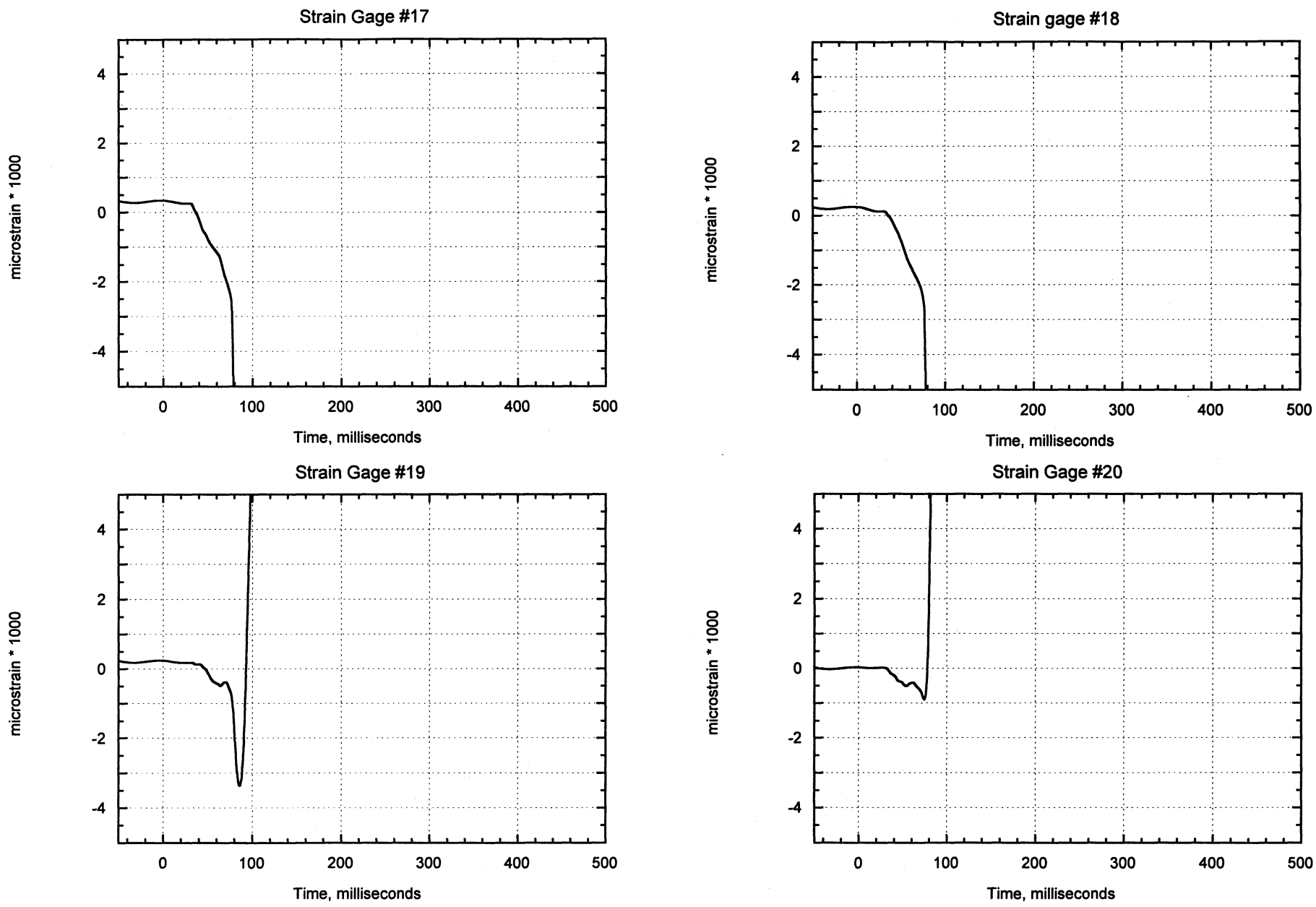

Figure 119, Test 2, Engine Mount, Left Aft Diagonal

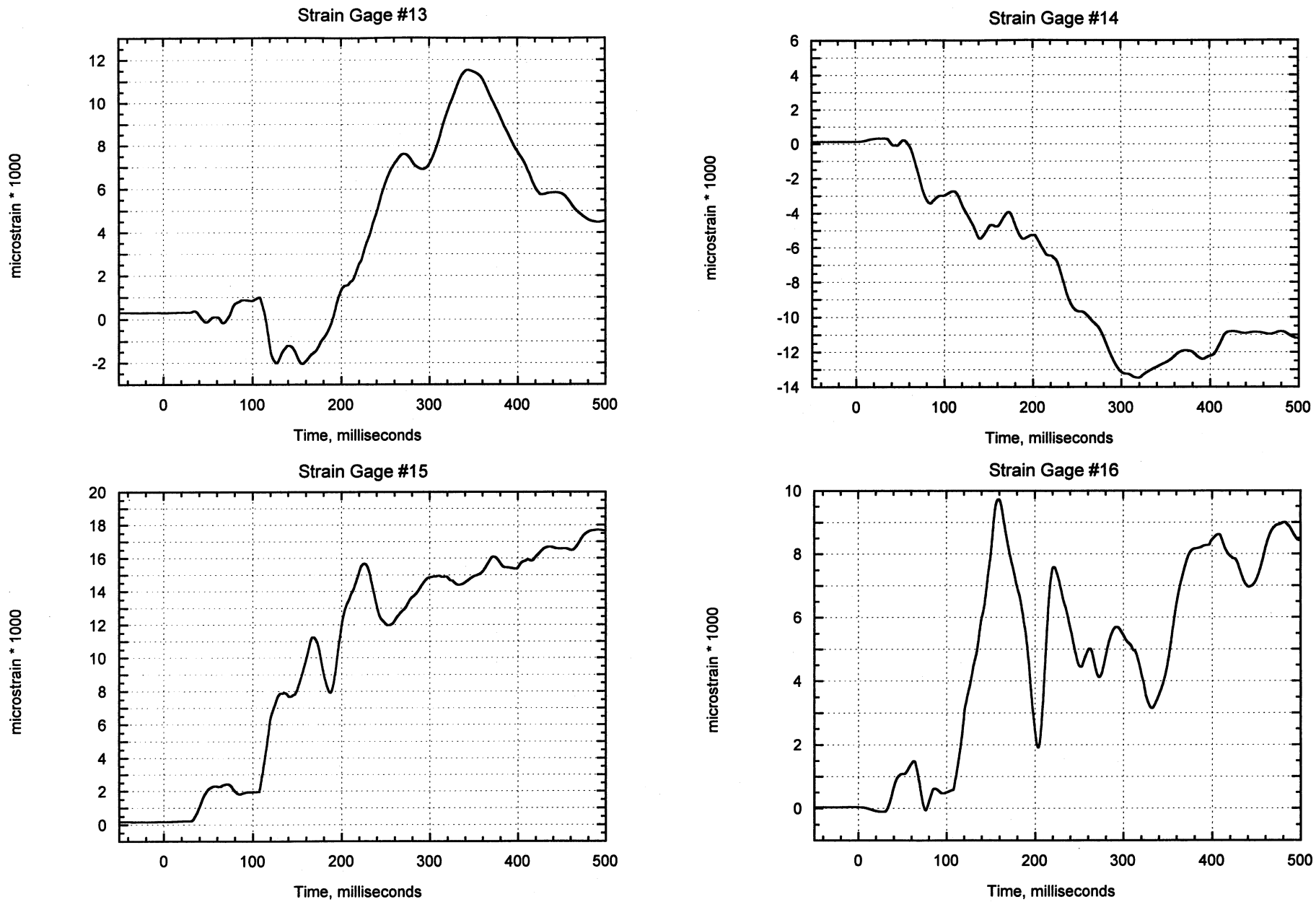

Figure 120, Test 2, Engine Mount, Left "X" Member

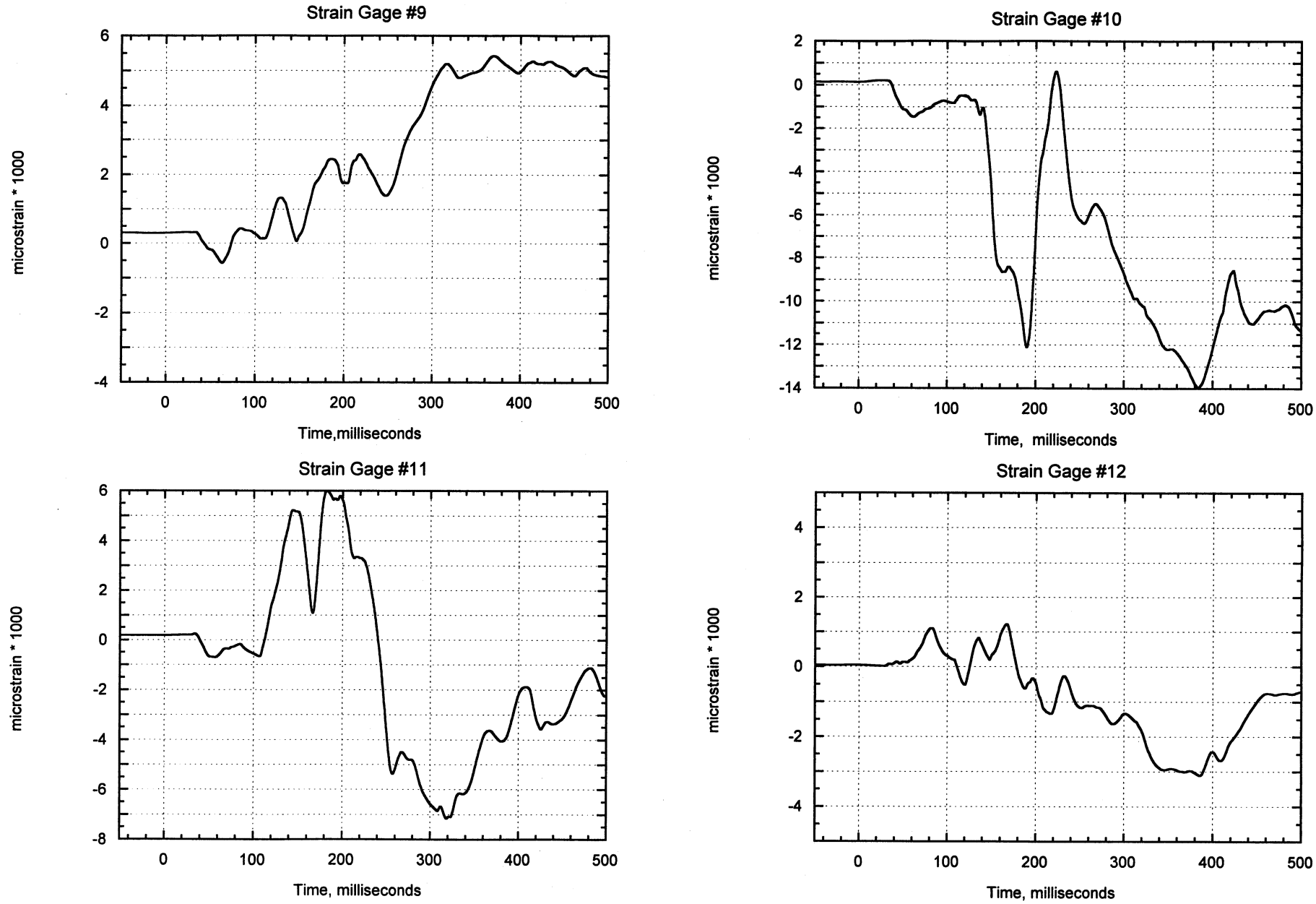

Figure 121, Test 2, Engine Mount, Left Forward Upright

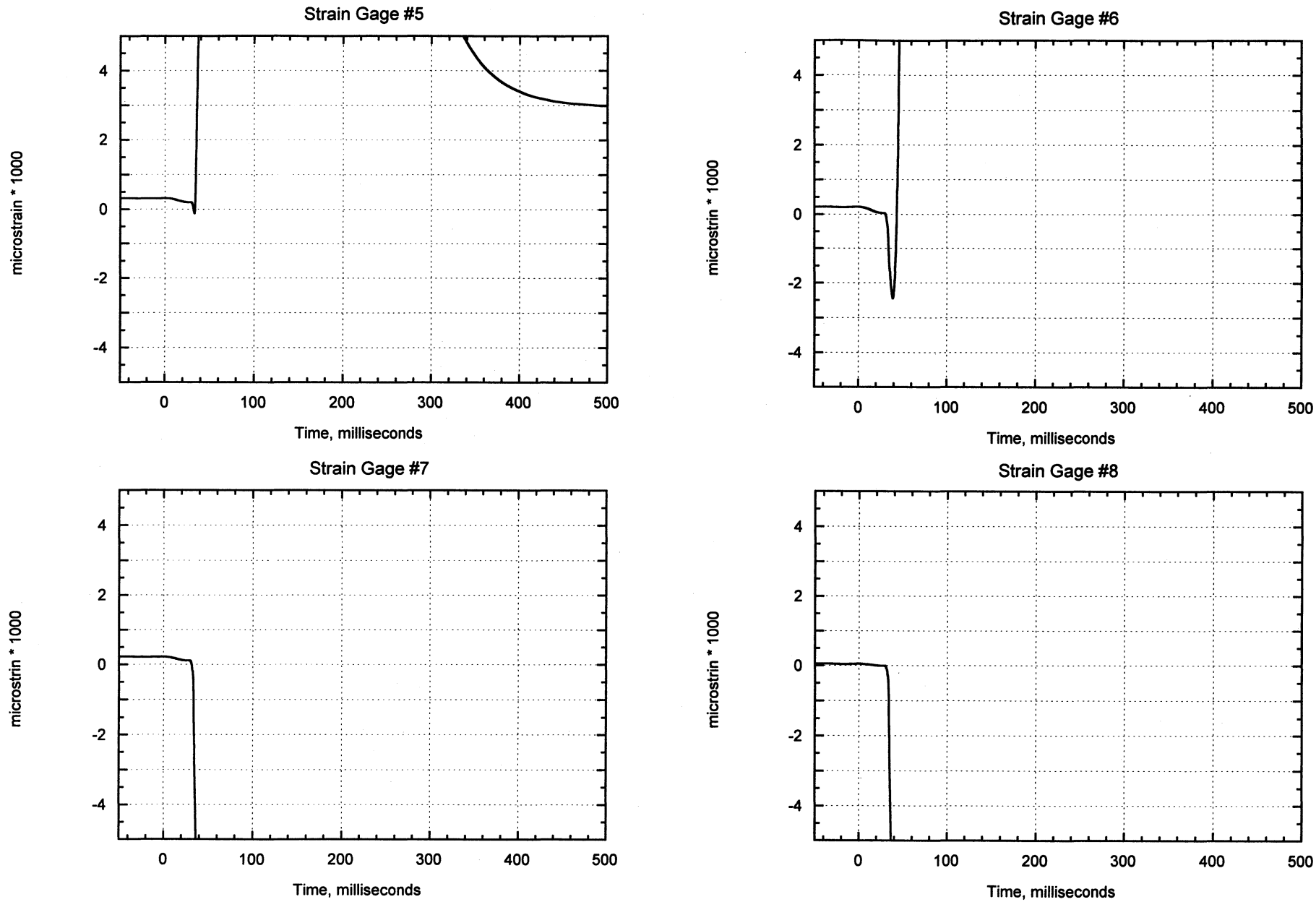

Figure 122, Test 2, Engine Mount, Left Forward Diagonal

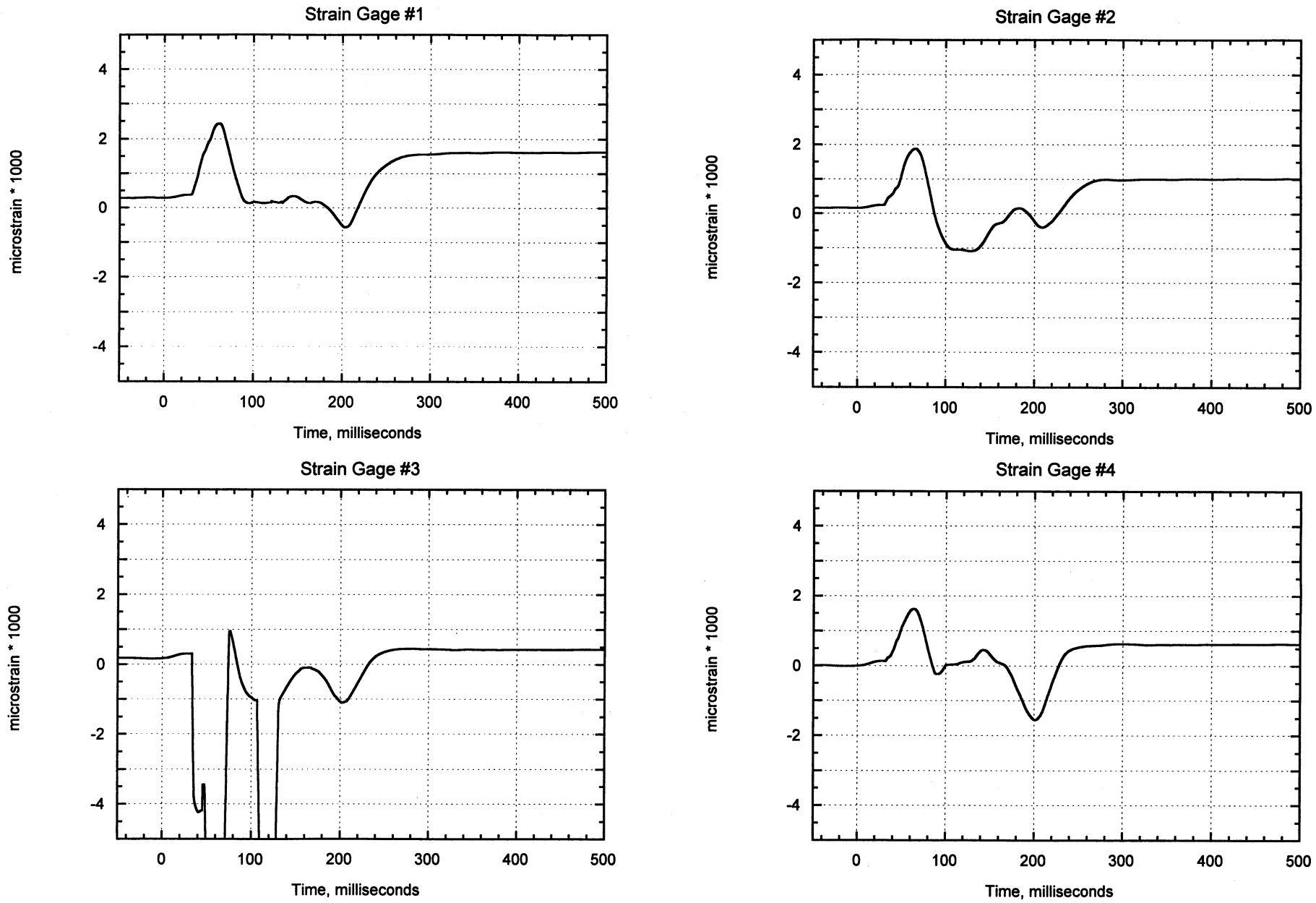

Figure 123, Test 2, Engine Mount, Left Forward Lower Rail

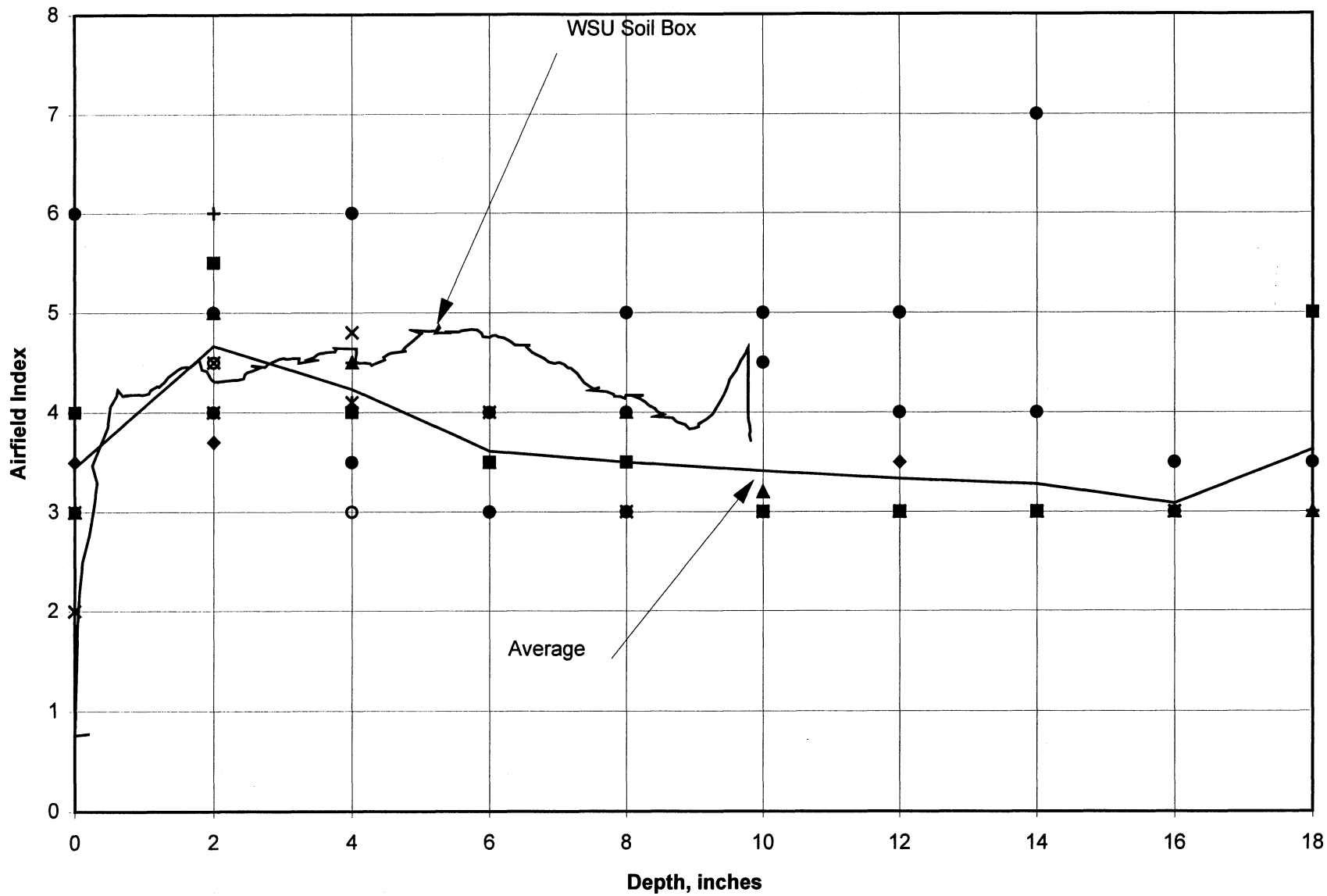

Figure 124, Soil Characteristics for Full Scale Test 3

Impact

t = .020 seconds

t = .040 seconds

t = .060 seconds

Figure 125, Crash Sequence Photographs for Test 3

t = .080 seconds

t = .100 seconds

t = .120 seconds

t = .140 seconds

Figure 125, (continued)

t = .160 seconds

t = .180 seconds

t = .200 seconds

t = .220 seconds

Figure 125, (continued)

t = .240 seconds

t = .260 seconds

t = .280 seconds

t = .300 seconds

Figure 125, (concluded)

(a), Post Test Airplane Position and Crater

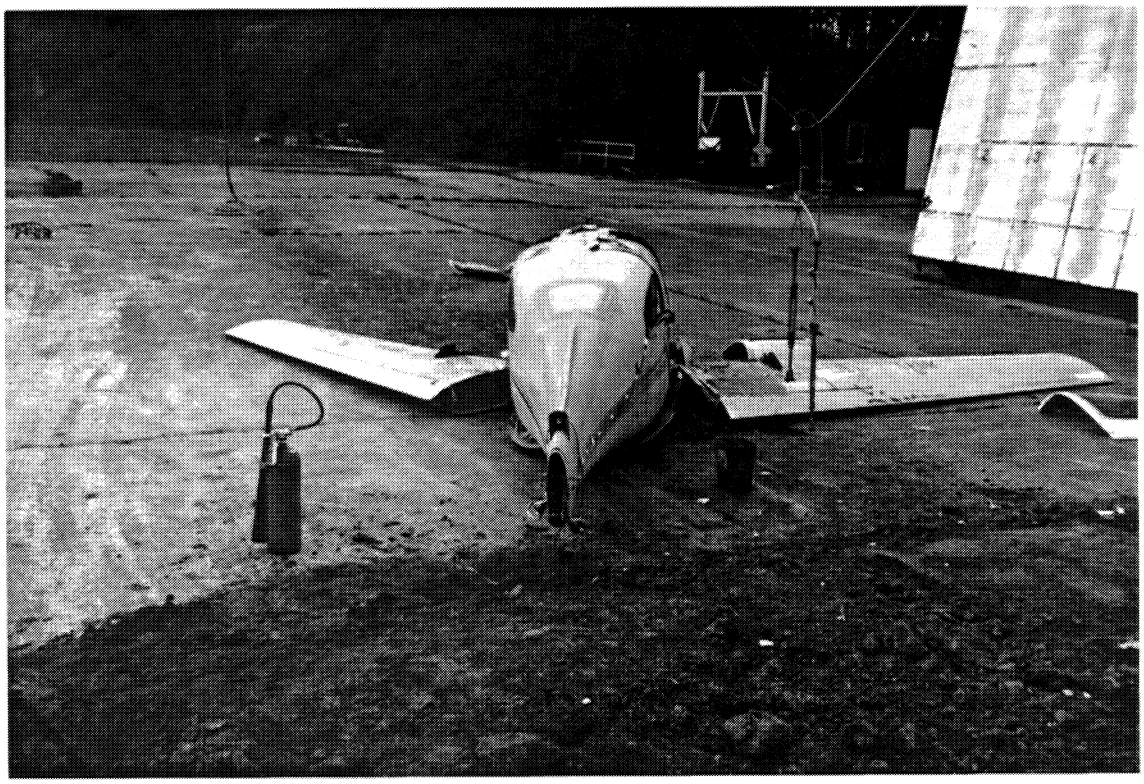

(b), Post Test Airplane

Figure 126, Post Crash Damage for Test 3

(c), Front View

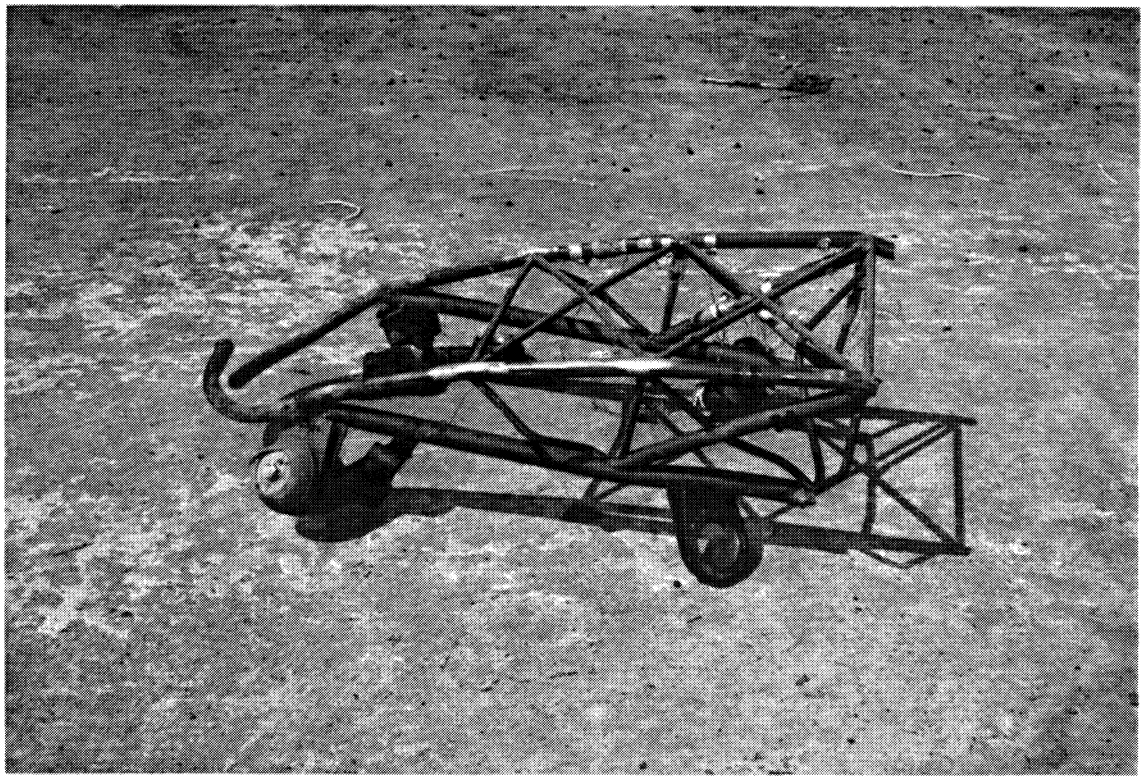

(d), Engine Mount

Figure 126, (continued)

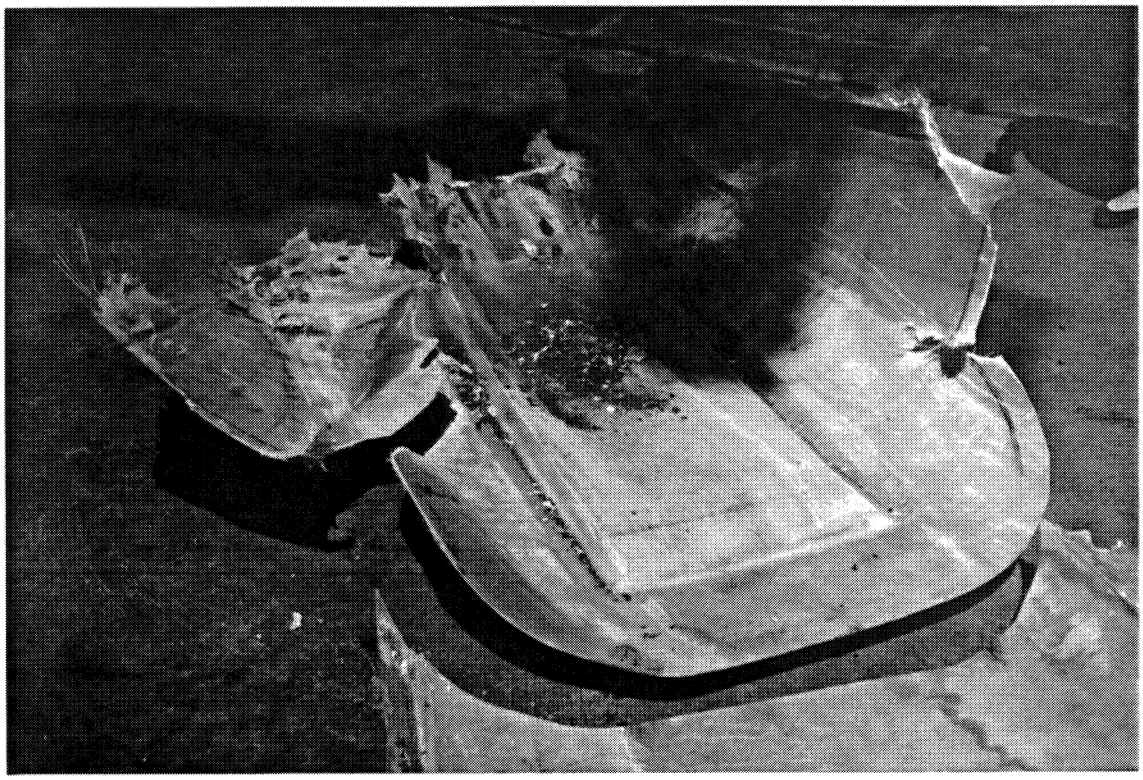

(e), Lower Cowling

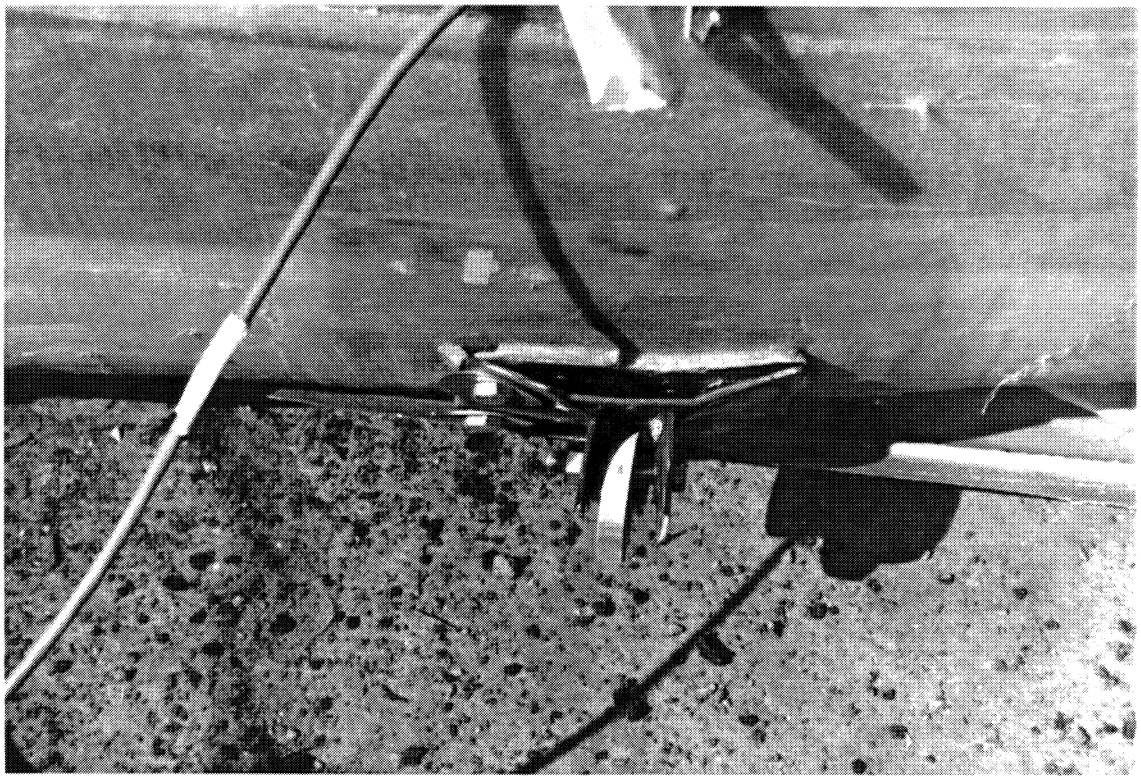

(f), Rear Wing Spar Fitting

Figure 126, (continued)

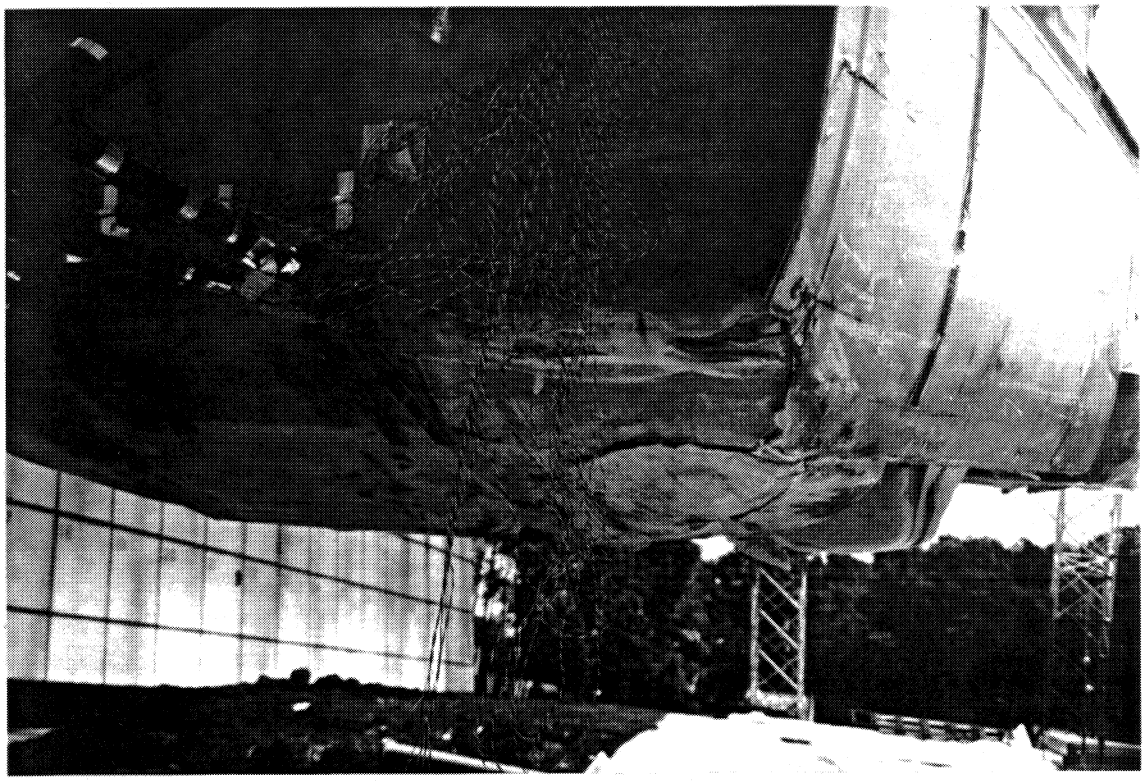

(g), Left Side Lower Firewall and Energy Absorber

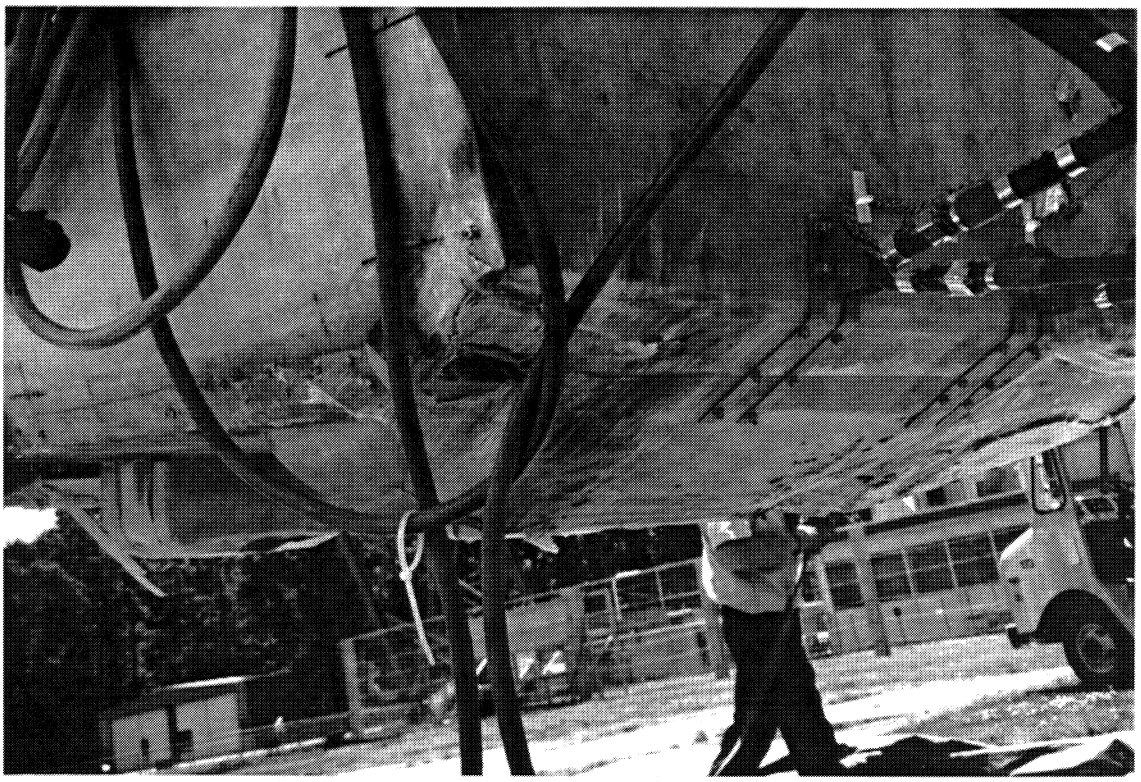

(h), Right Side Lower Firewall and Energy Absorber

Figure 126, (continued)

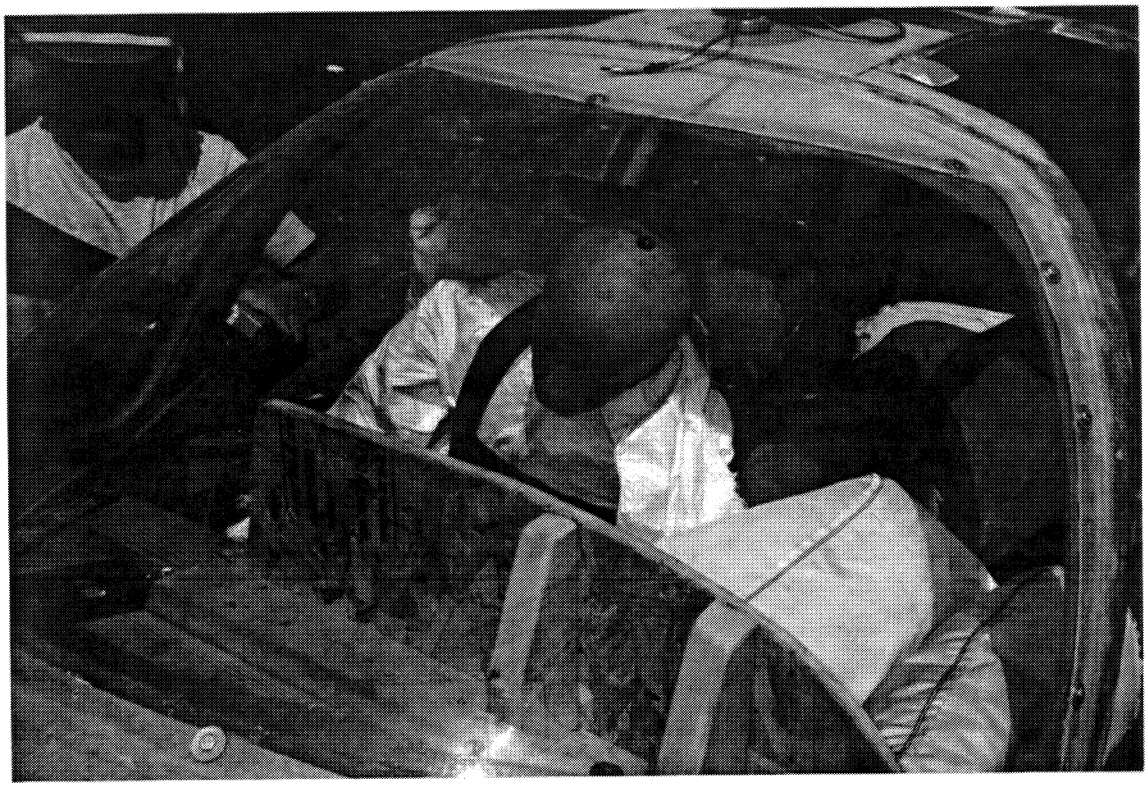

(i), Crew Position

(j), Crew Position

Figure 126, (continued)

(k), Deployed Air Bag

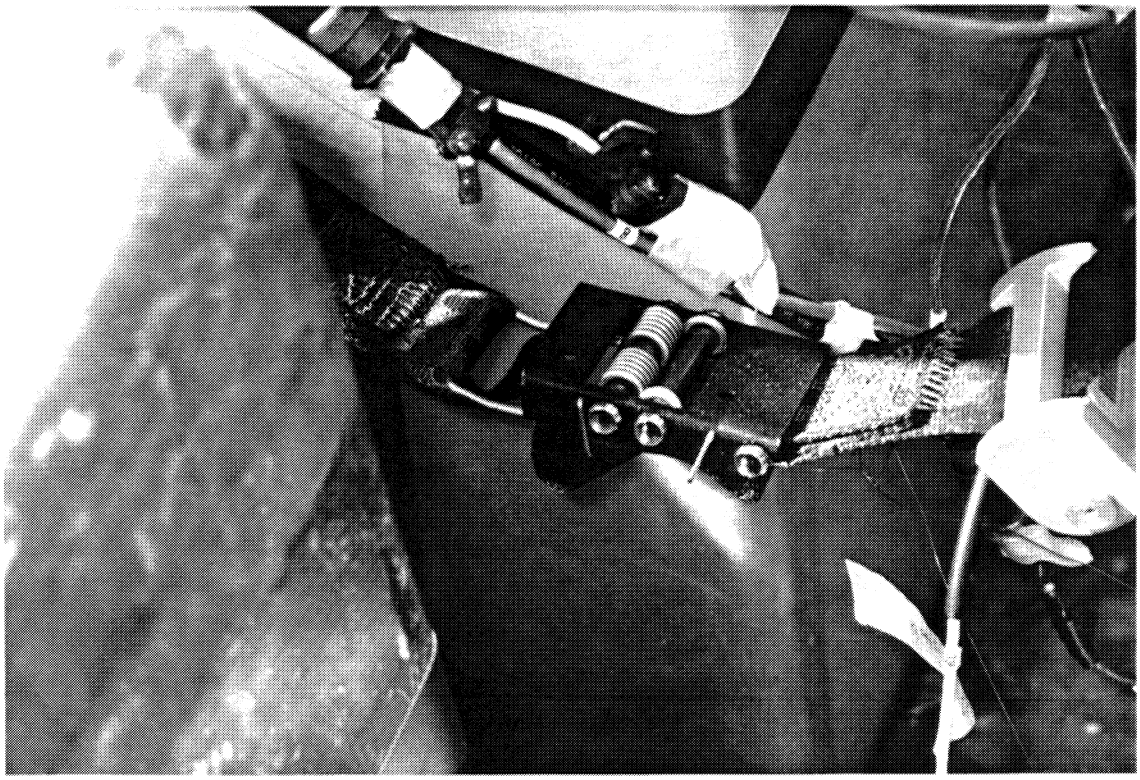

(l), Copilot's Load Limiter

Figure 126, (concluded)

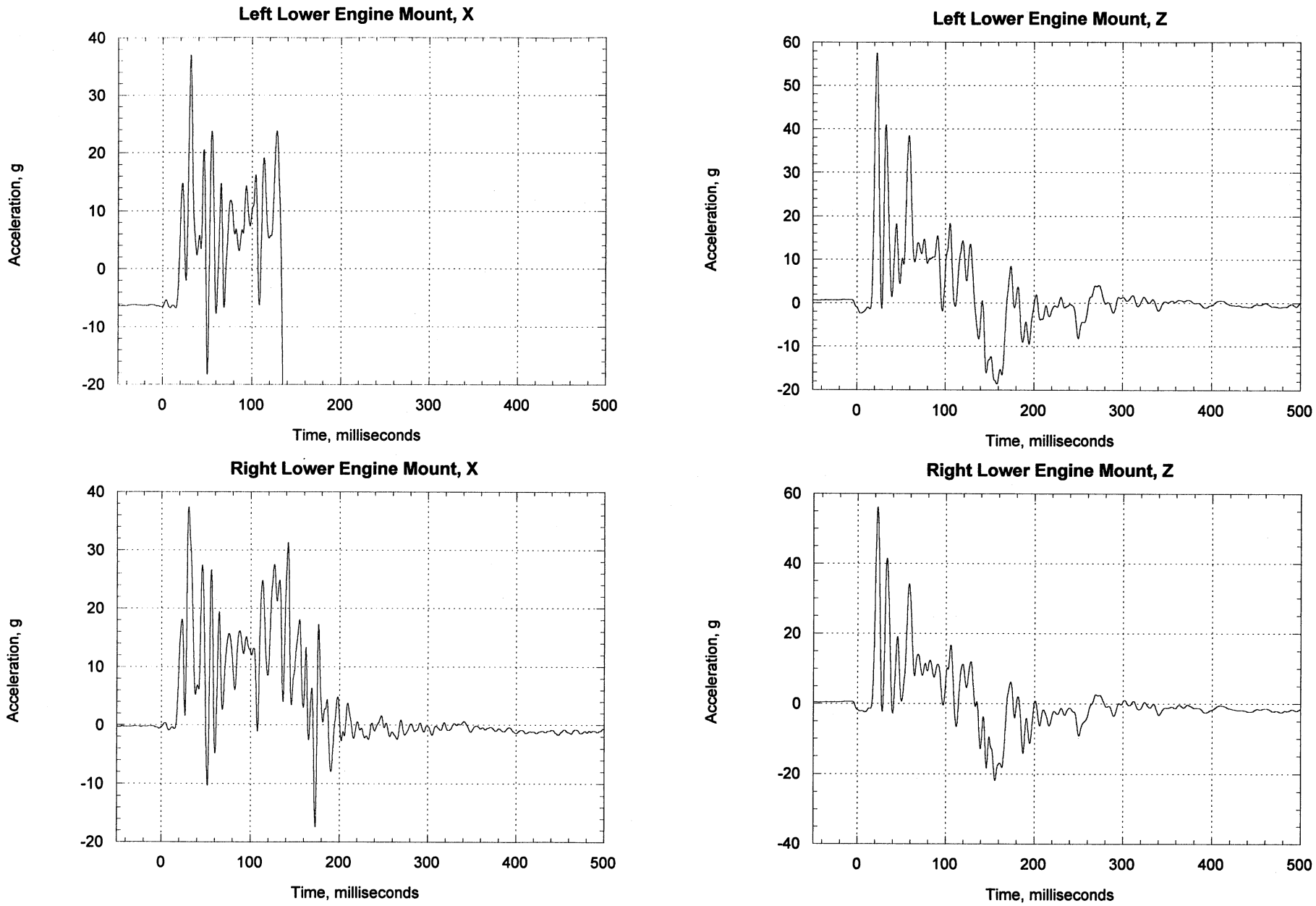

Figure 127, Test 3, Lower Firewall Accelerations

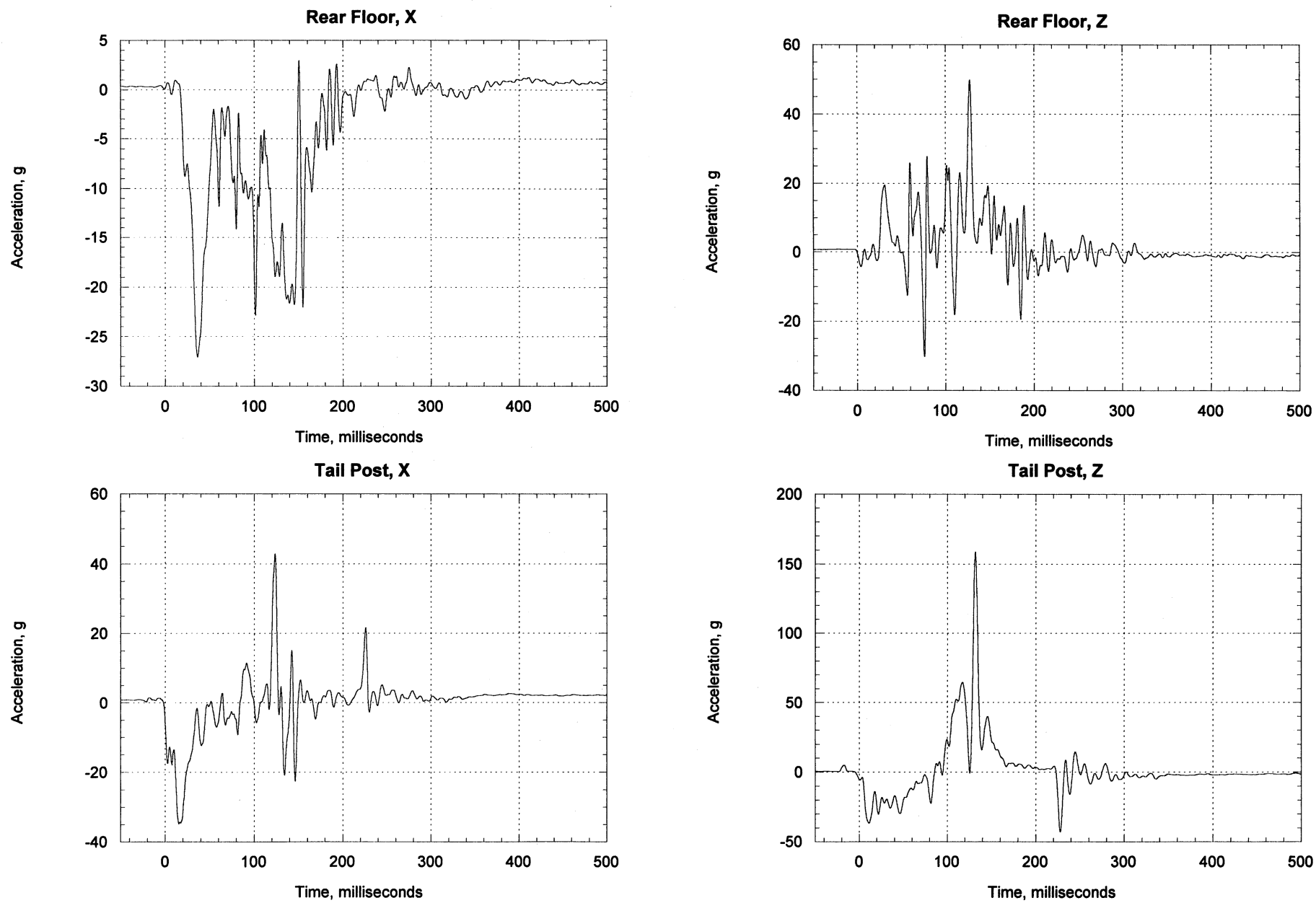

Figure 128, Test 3, Aft Airframe Accelerations

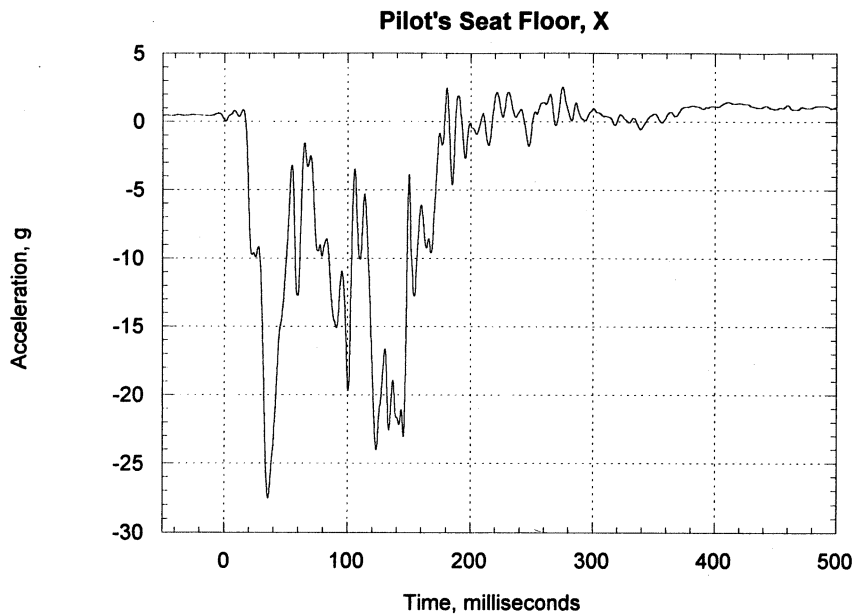

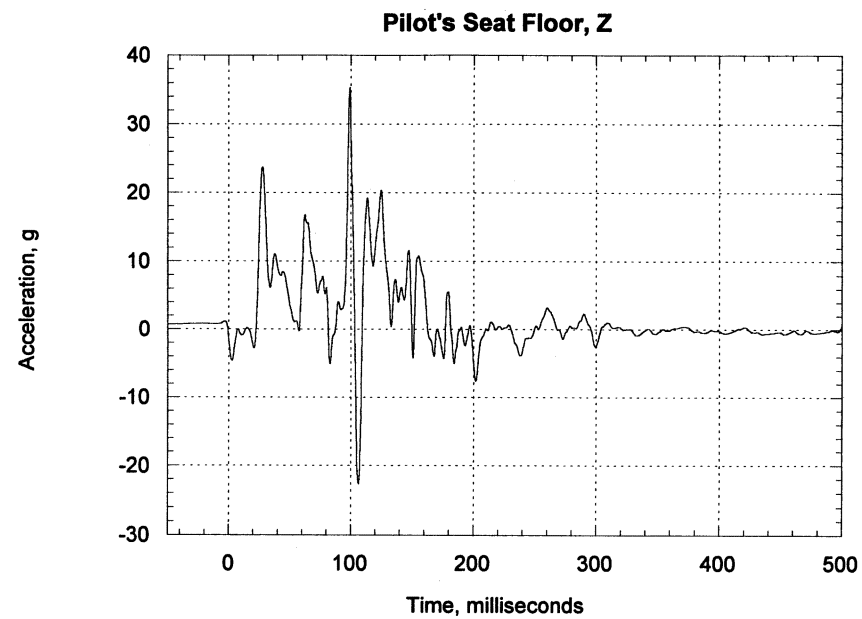

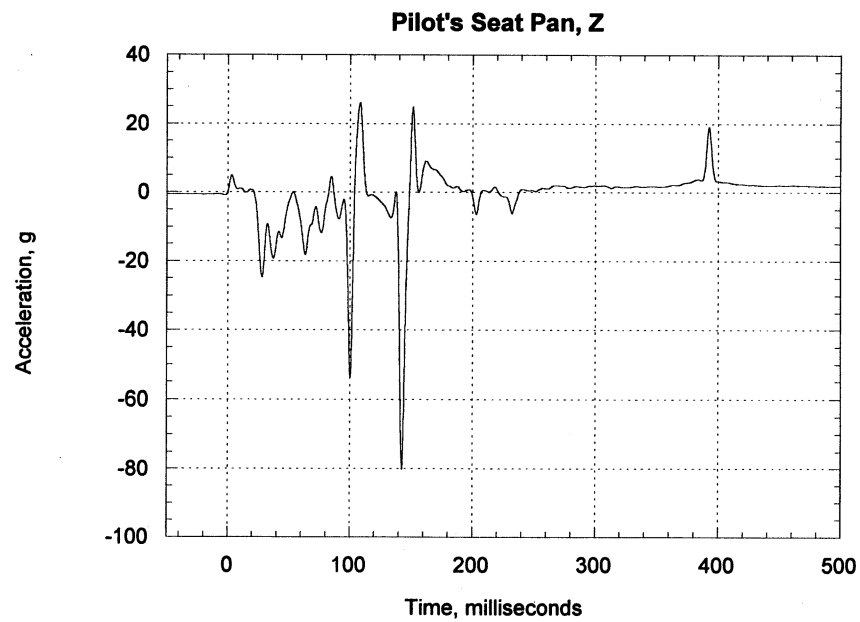

Figure 129, Test 3, Pilot's Seat & Floor

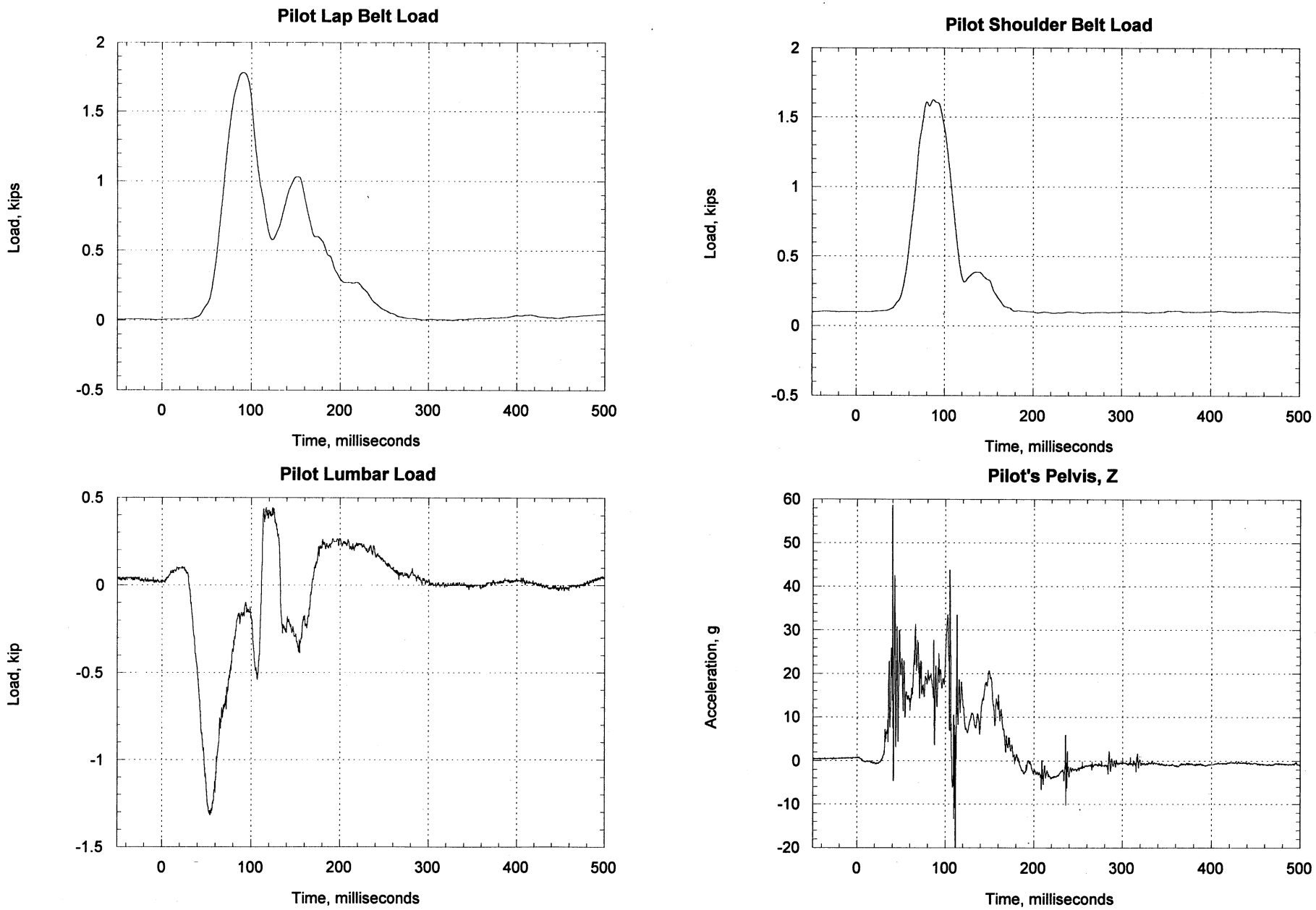

Figure 130, Test 3, Pilot

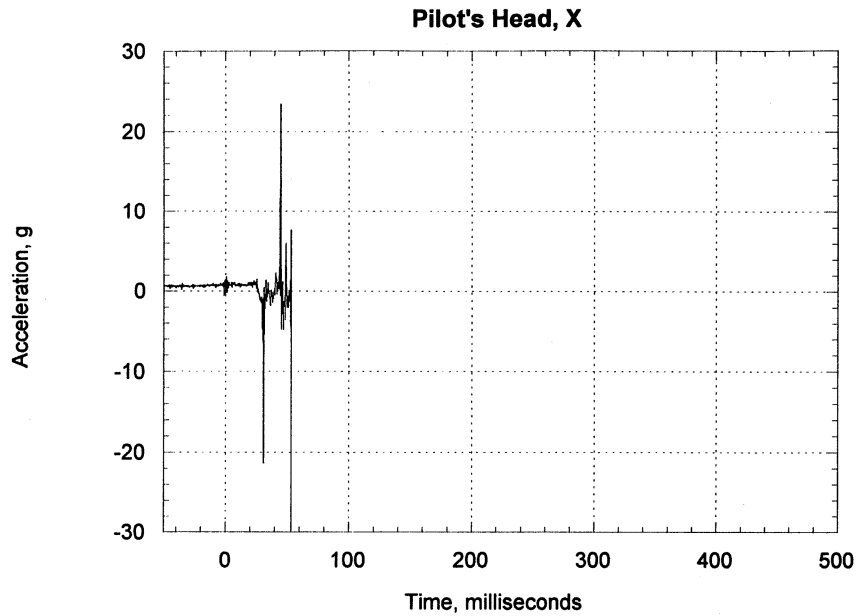

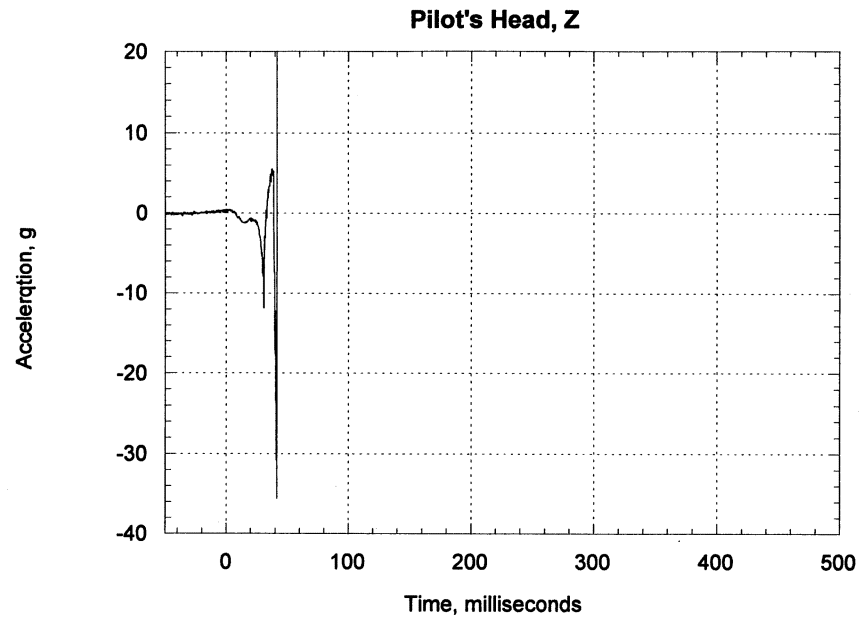

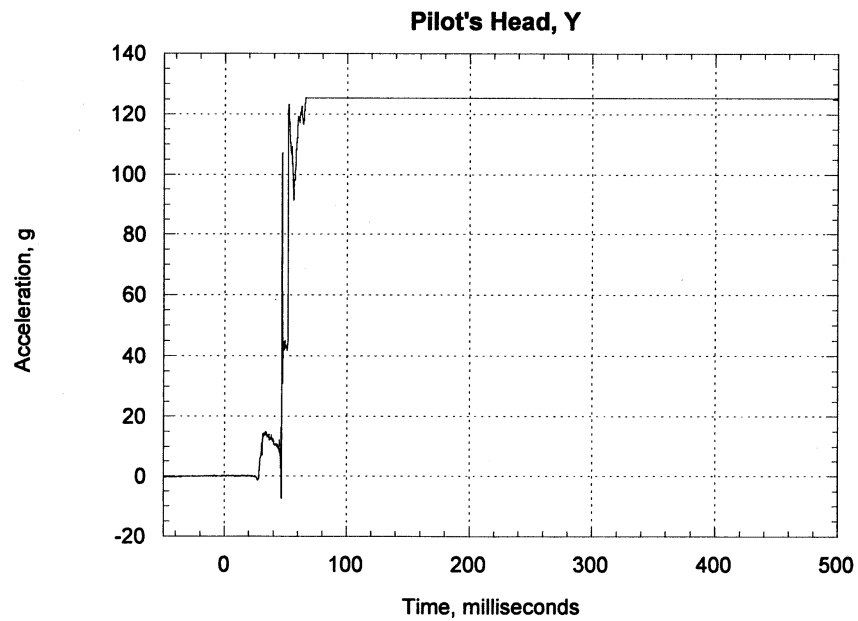

Figure 131, Test 3, Pilot's Head

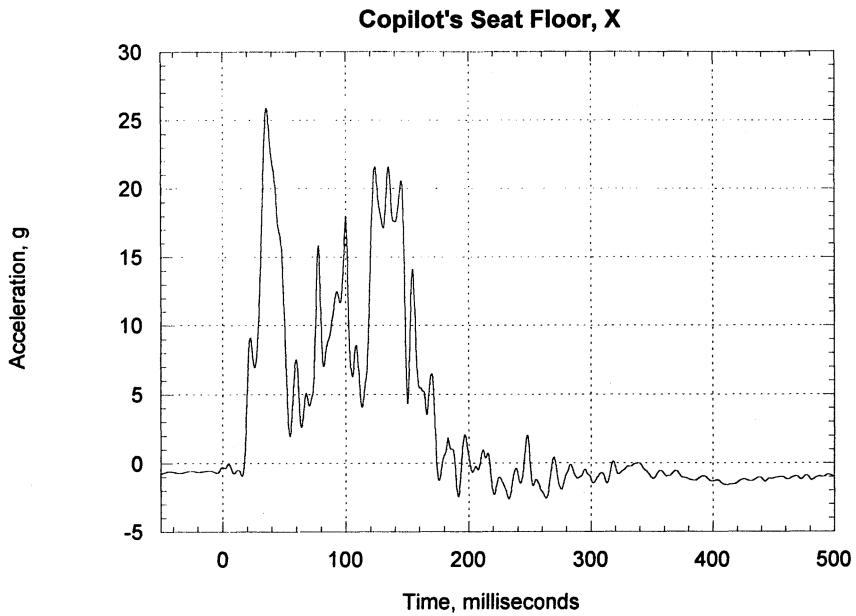

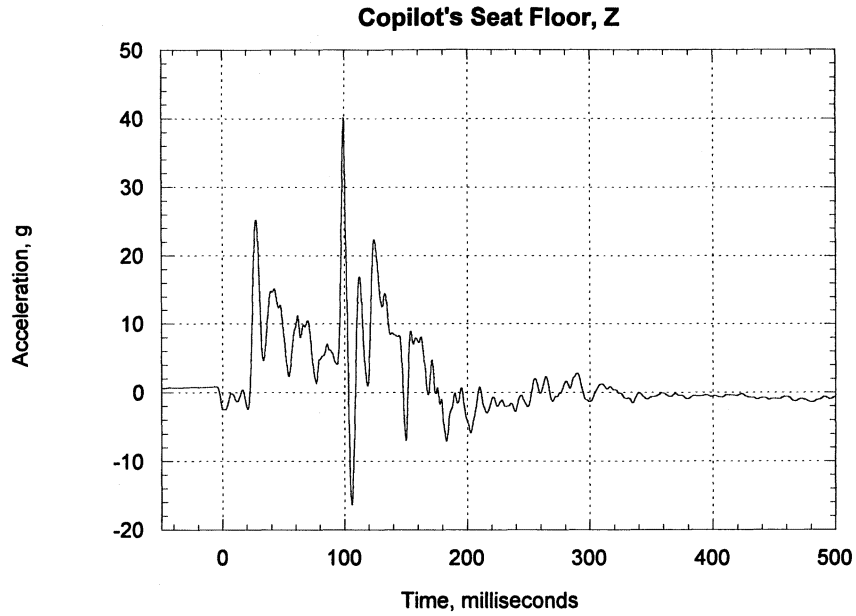

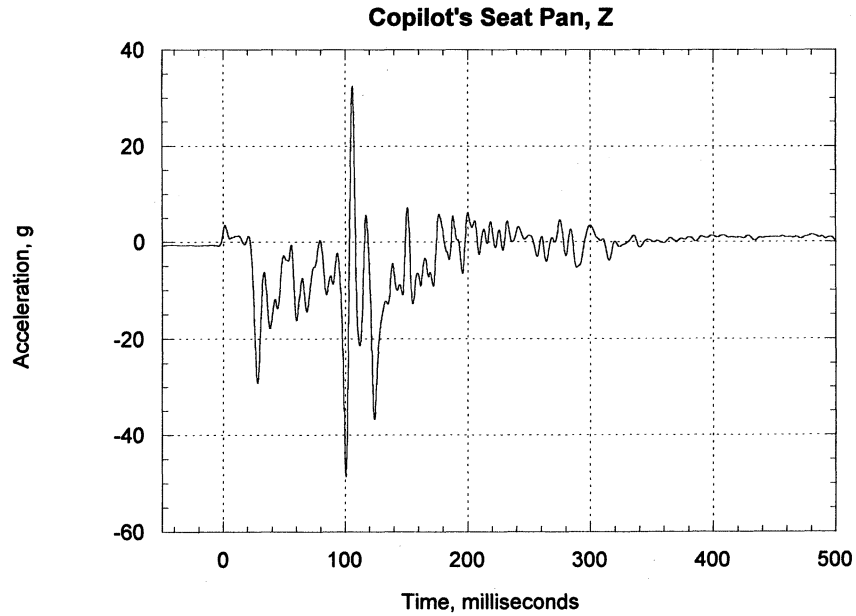

Figure 132, Test 3, Copilot's Seat & Floor

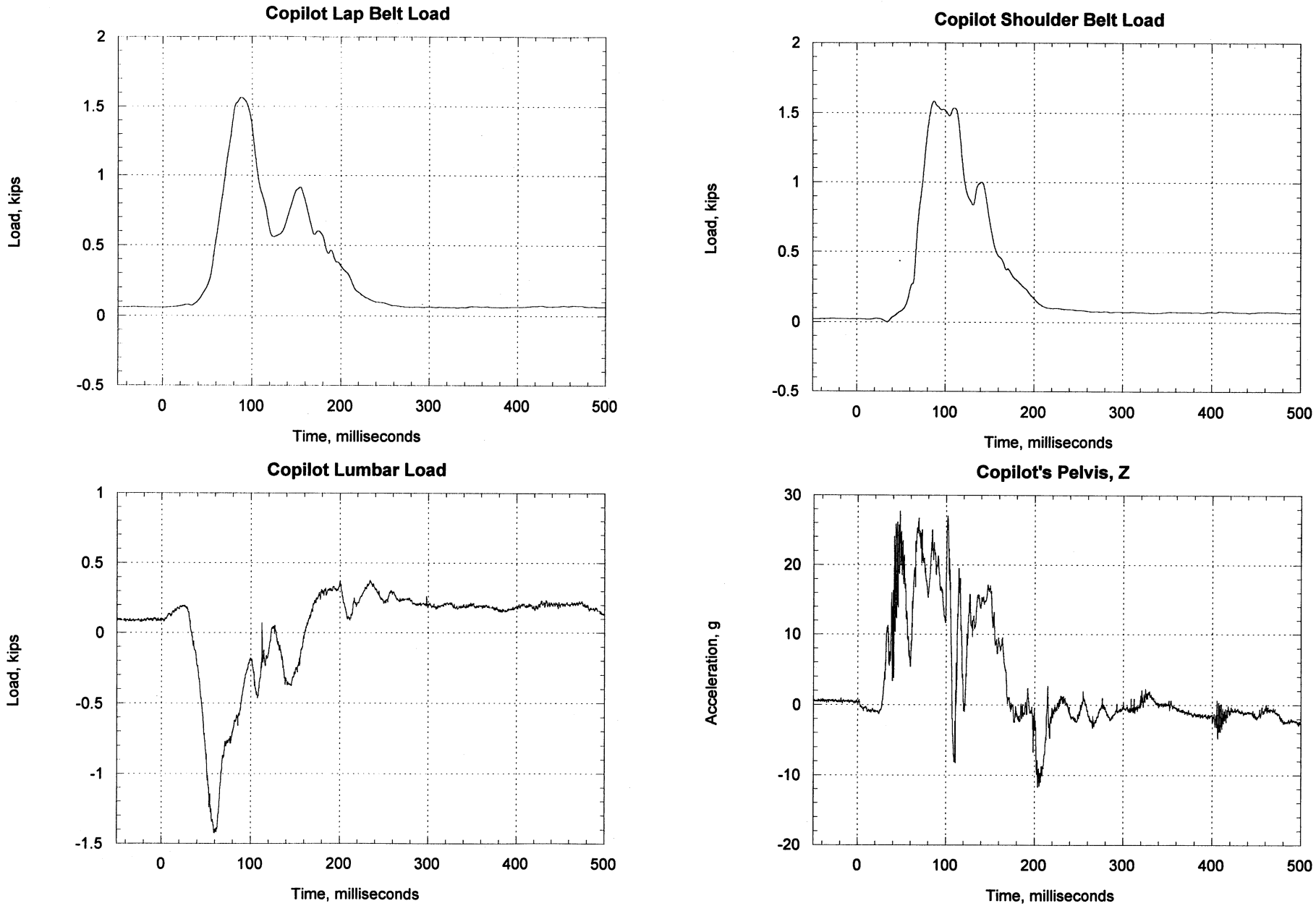

Figure 133, Test 3, Copilot

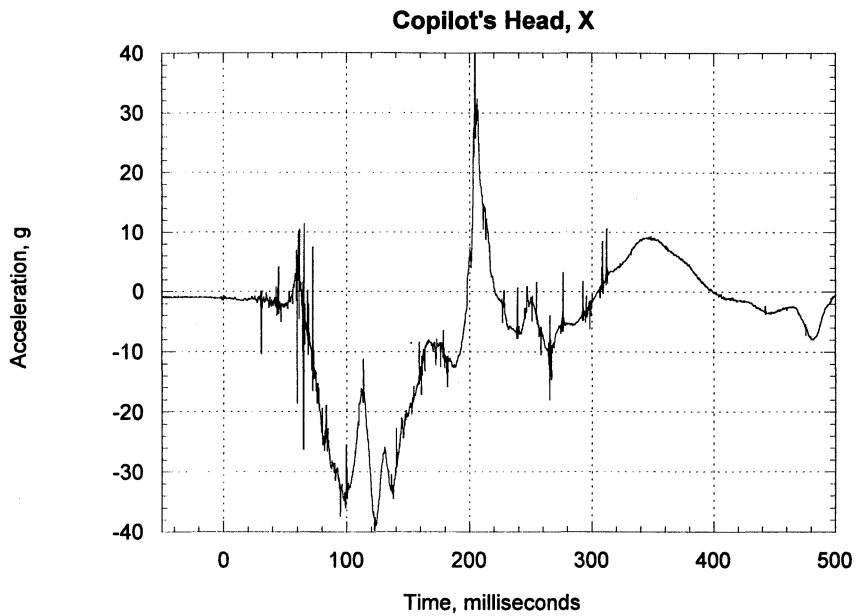

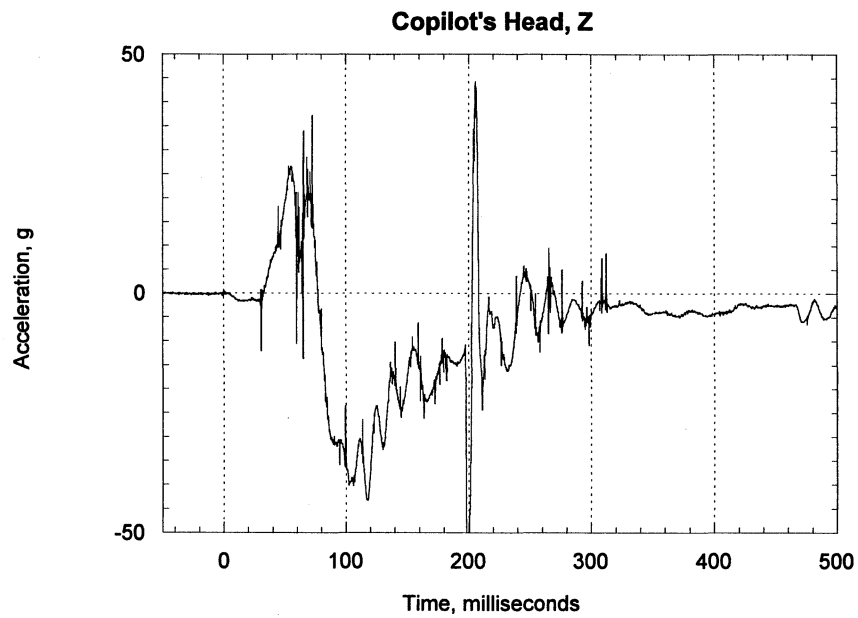

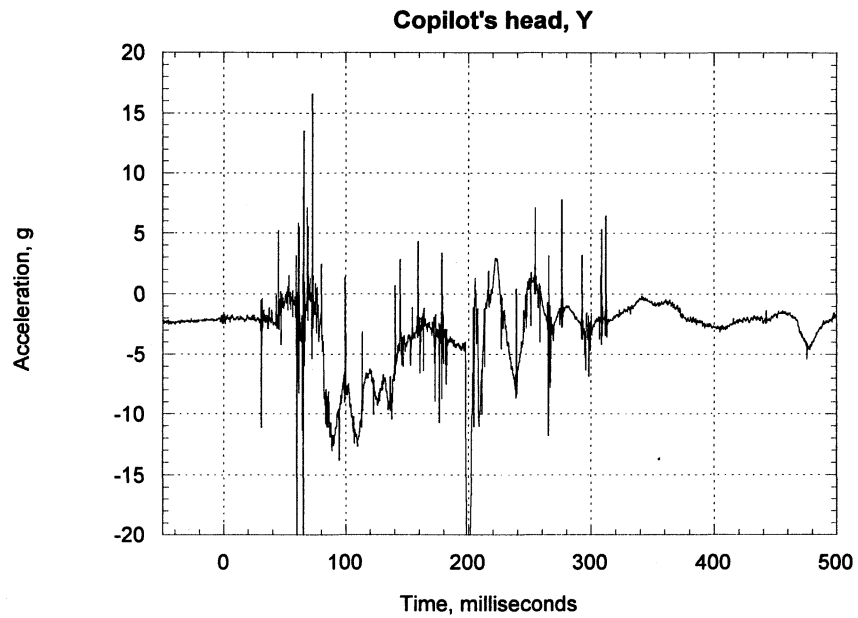

Figure 134, Test 3, Copilot's Head

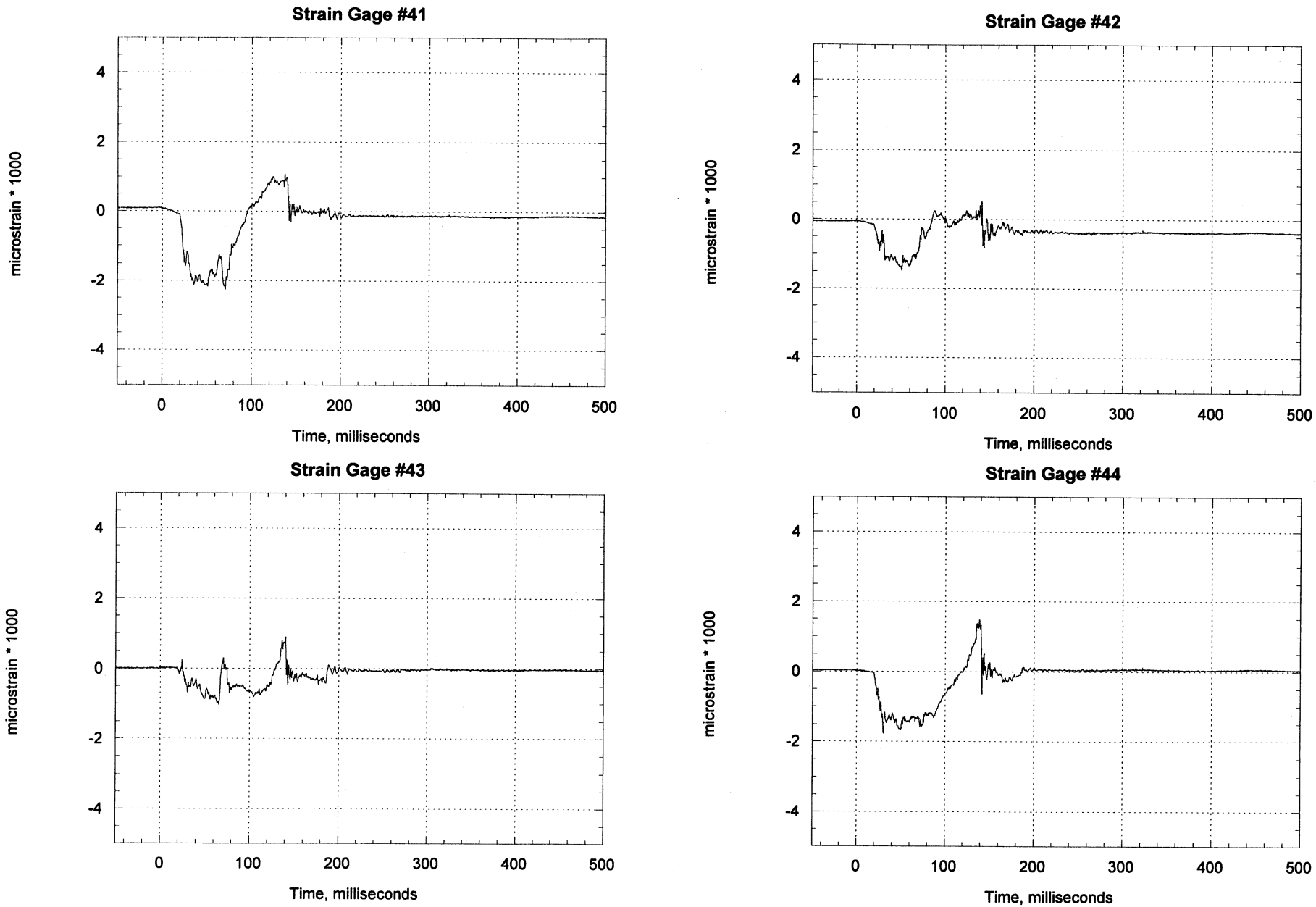

Figure 135, Test 3, Engine Mount, Left Post

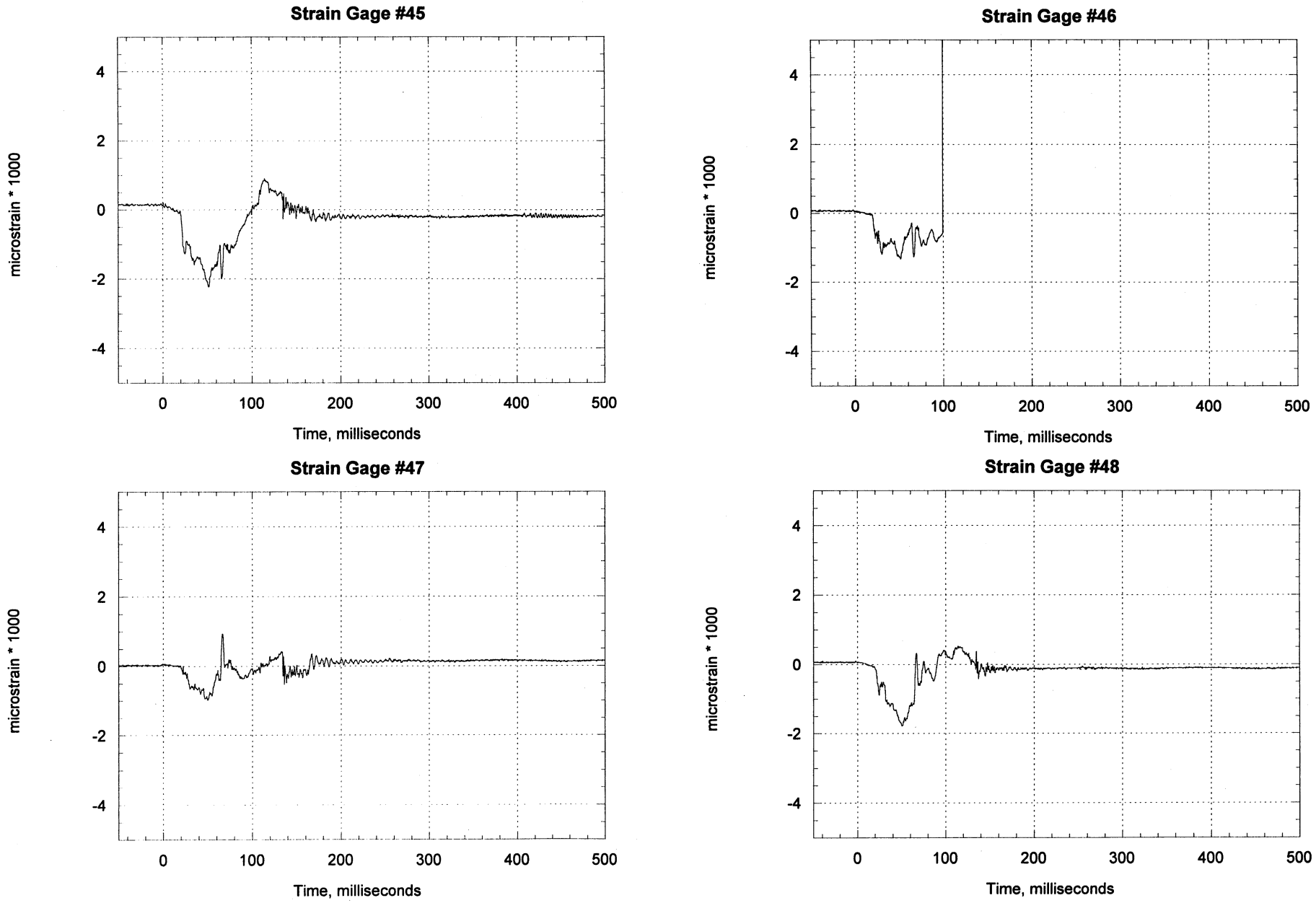

Figure 136, Test 3, Engine Mount, Right Post

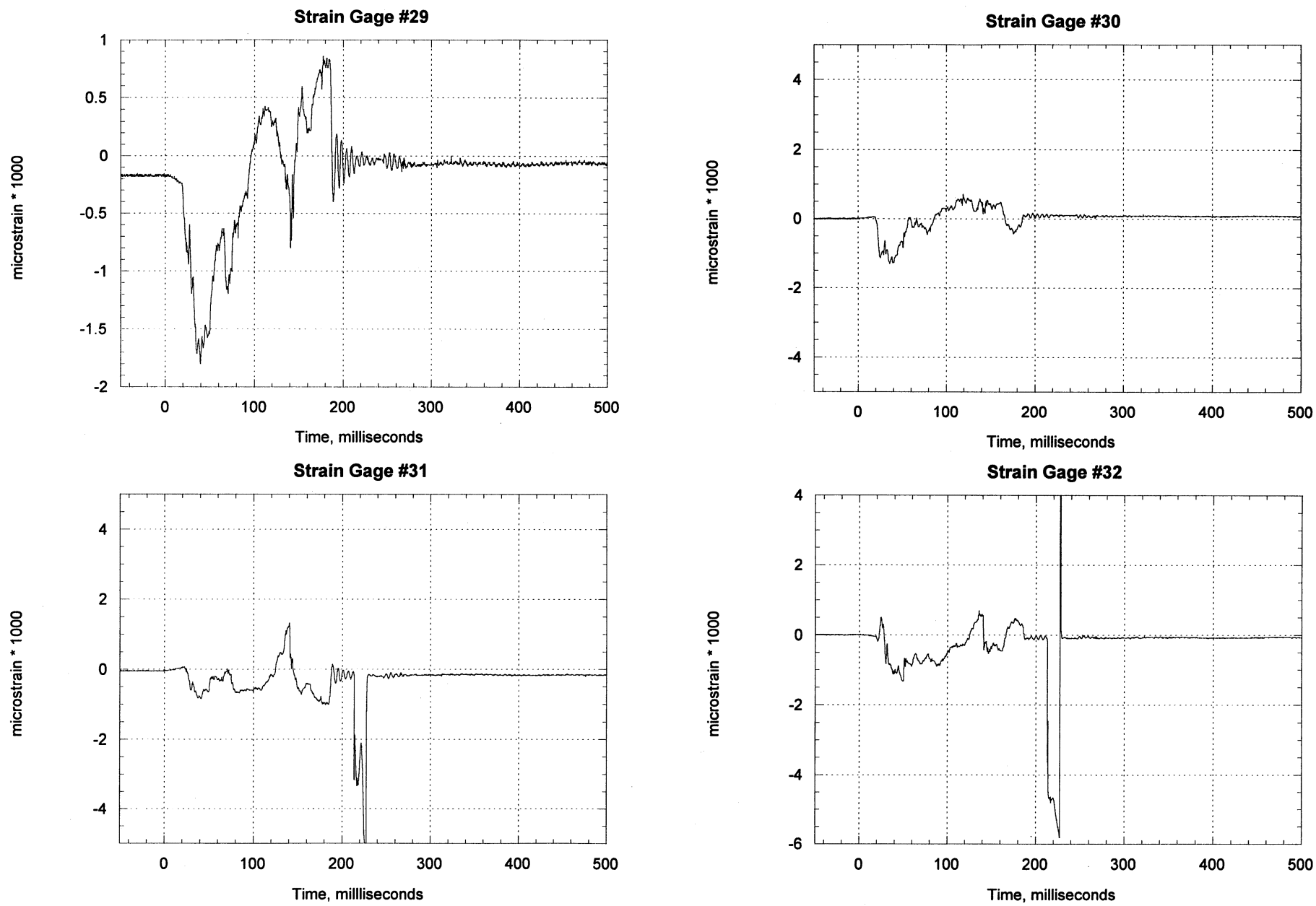

Figure 137, Test 3, Engine Mount, Left Aft Upper Rail

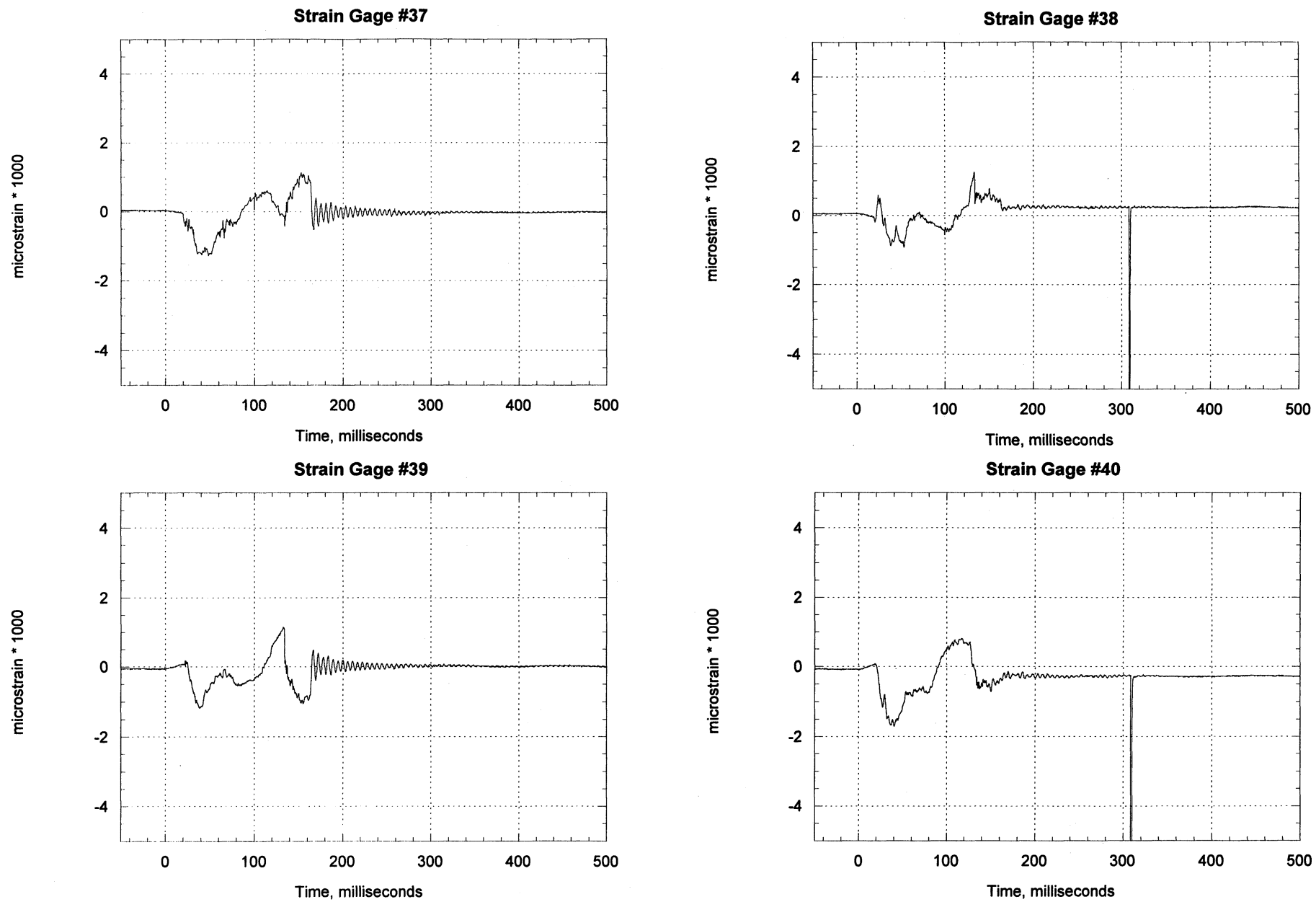

Figure 138, Test 3, Engine Mount, Right Aft Upper Rail

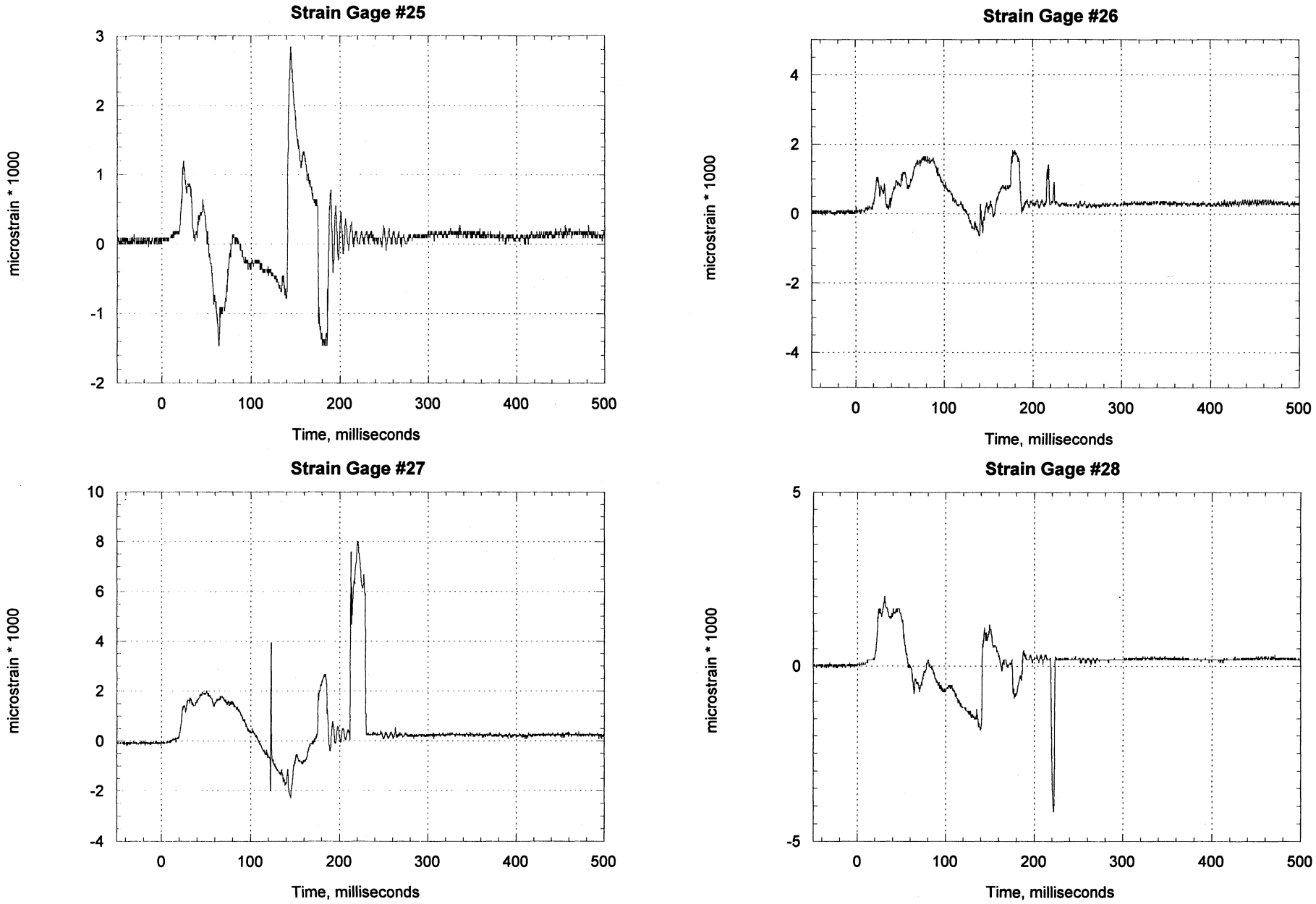

Figure 139, Test 3, Engine Mount, Left Aft Lower Rail

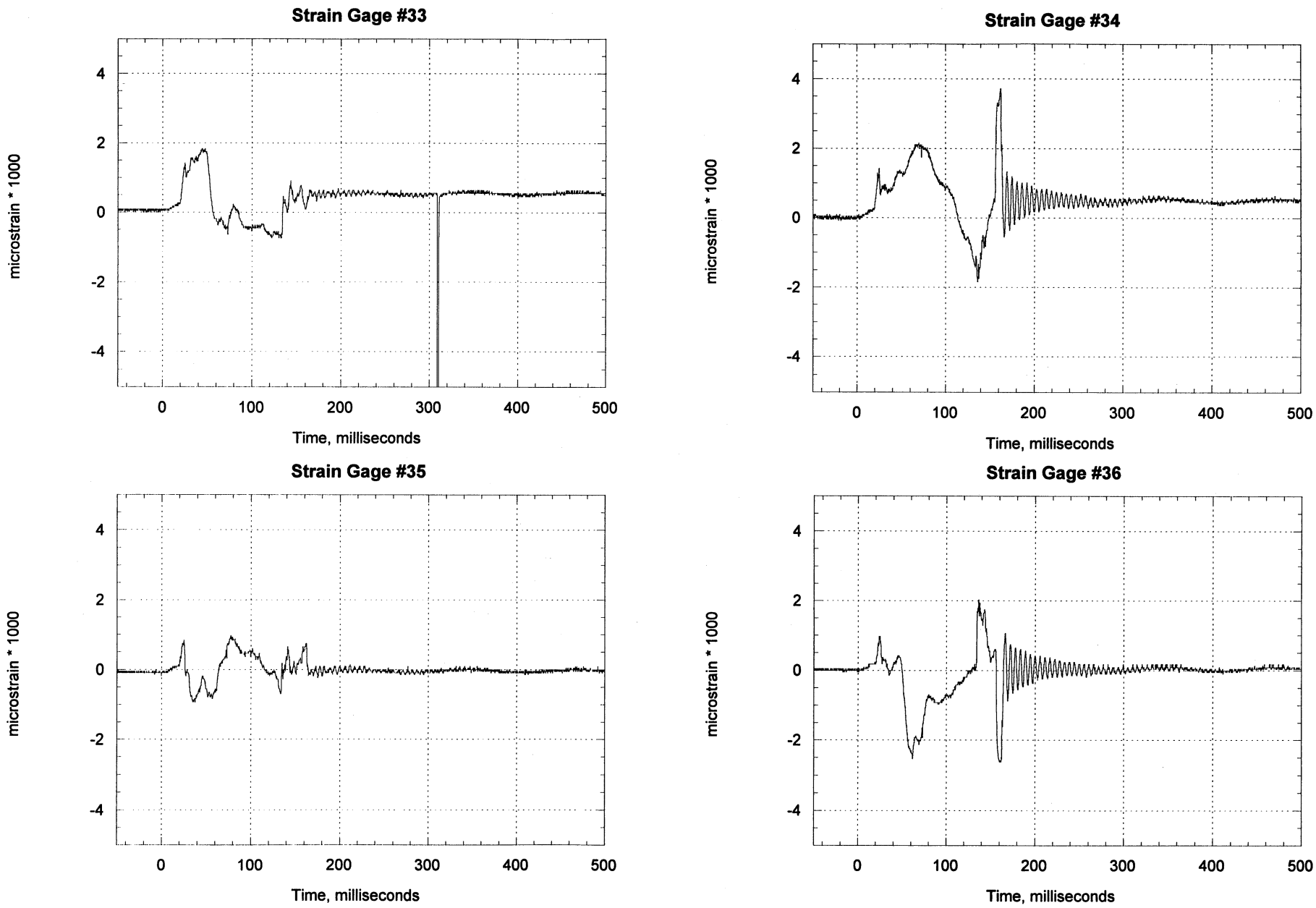

Figure 140, Test 3, Engine Mount, Right Aft Lower Rail

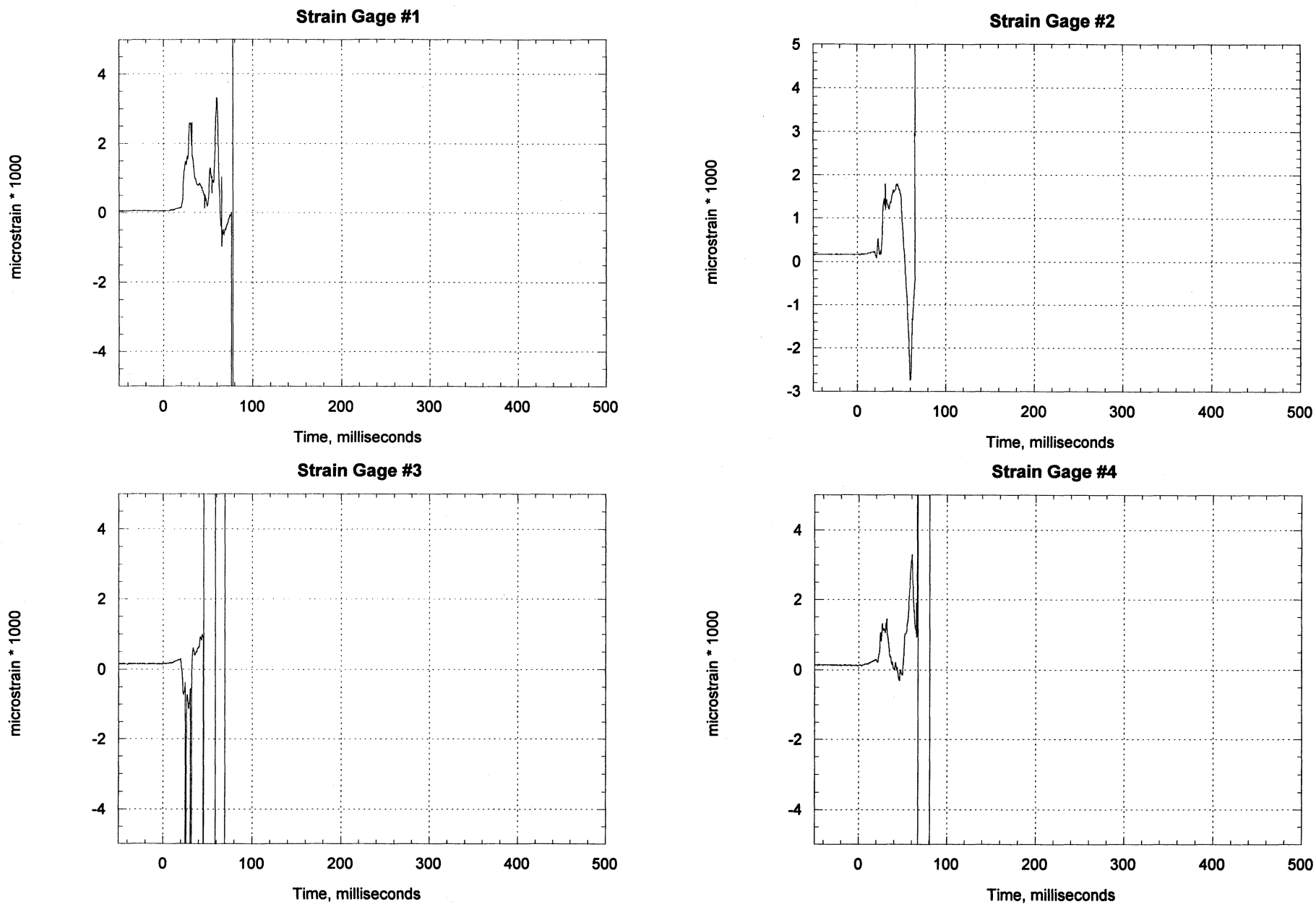

Figure 141, Test 3, Engine Mount, Forward Lower Rail

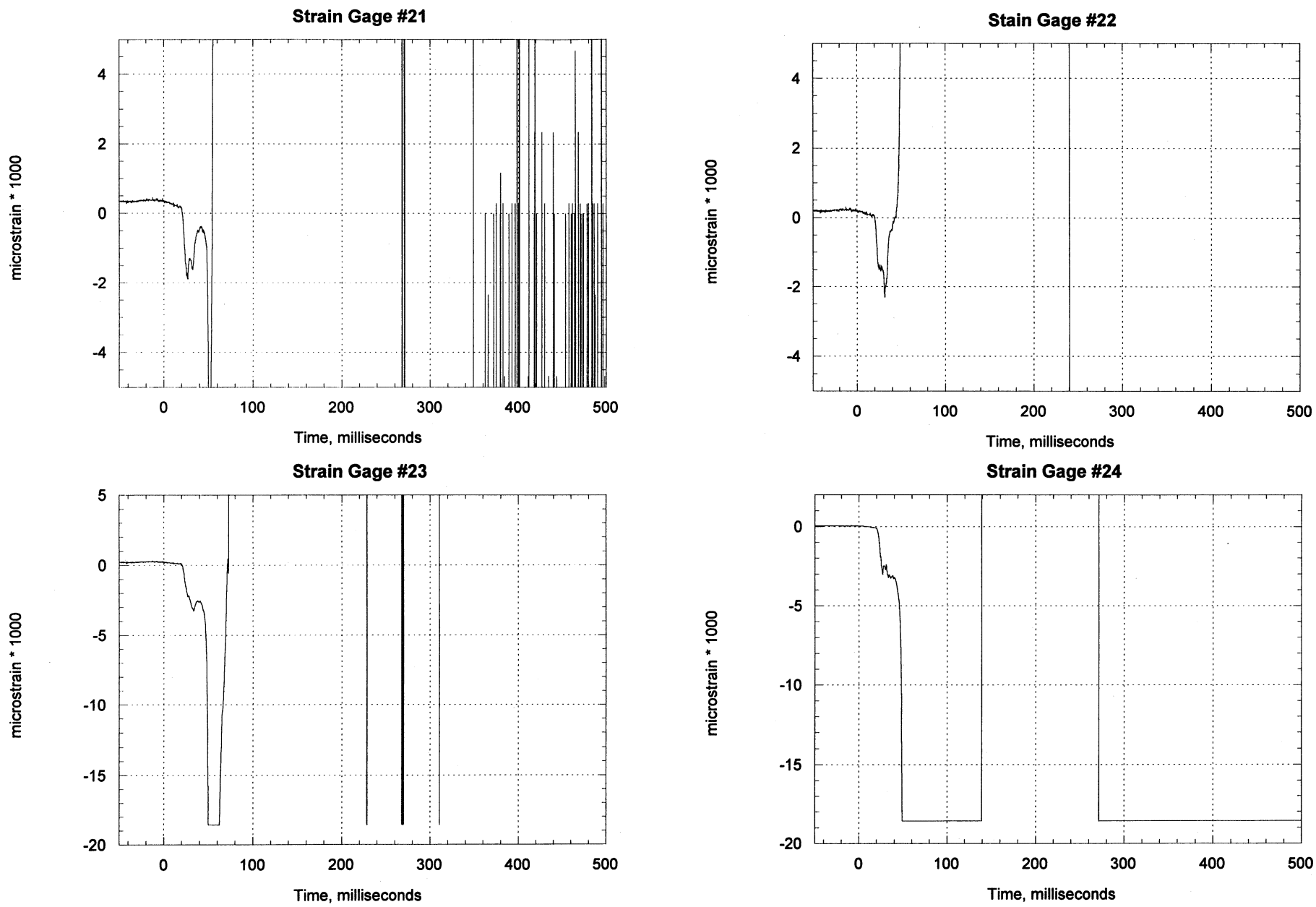

Figure 142, Test 3, Engine Mount, Aft Upright

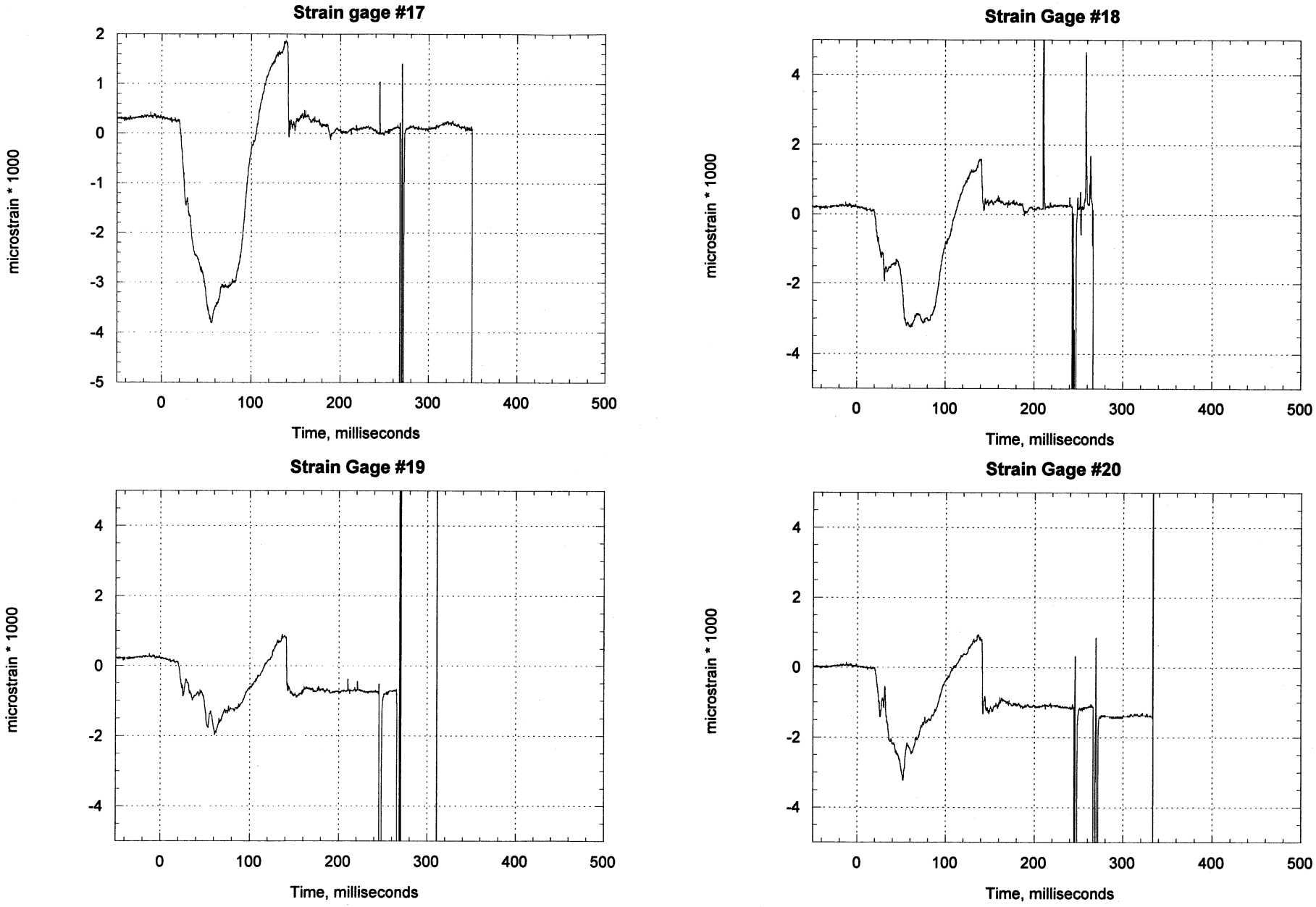

Figure 143, Test 3, Engine Mount, Aft Diagonal

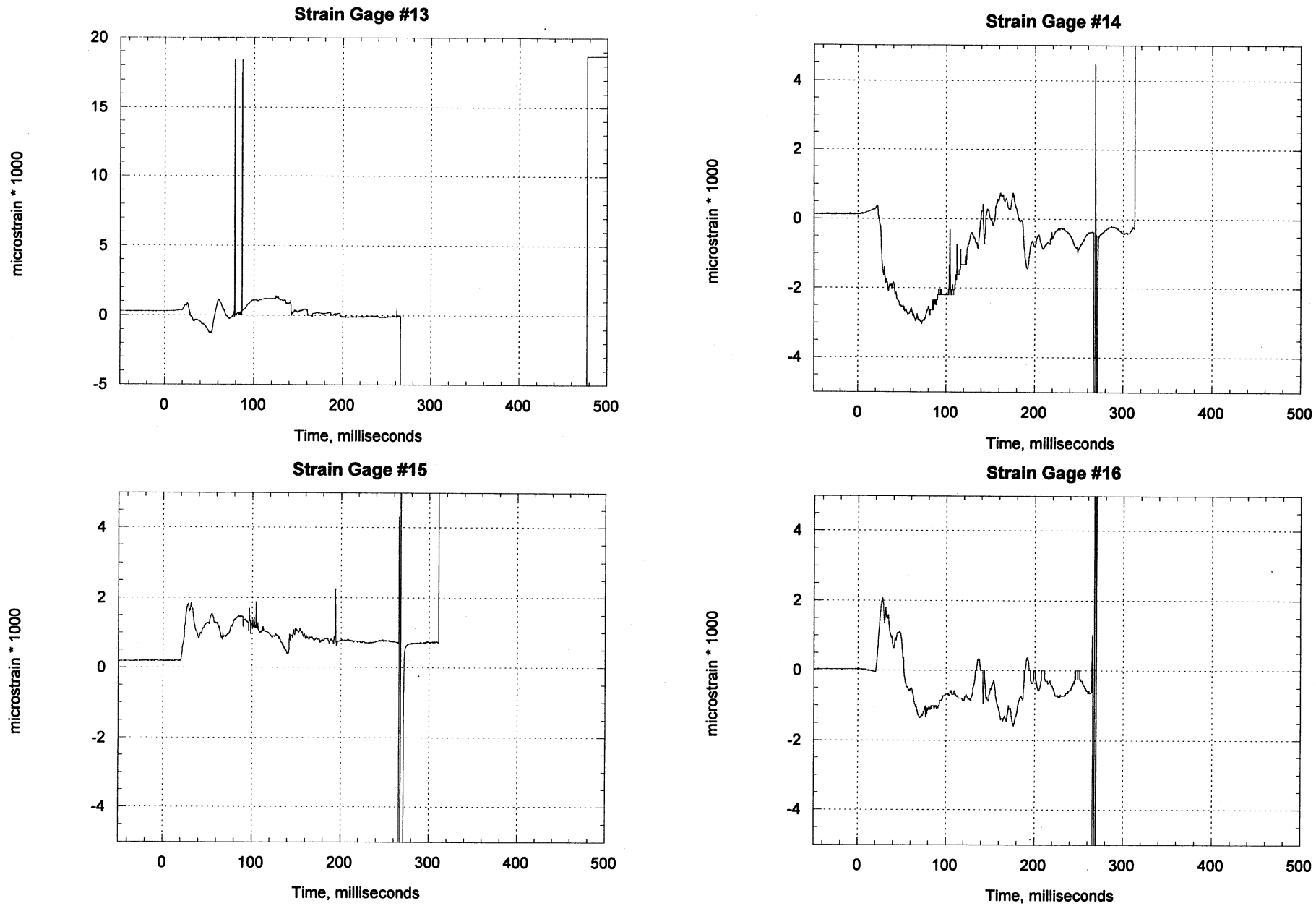

Figure 144, Test 3, Engine Mount, "X" Member

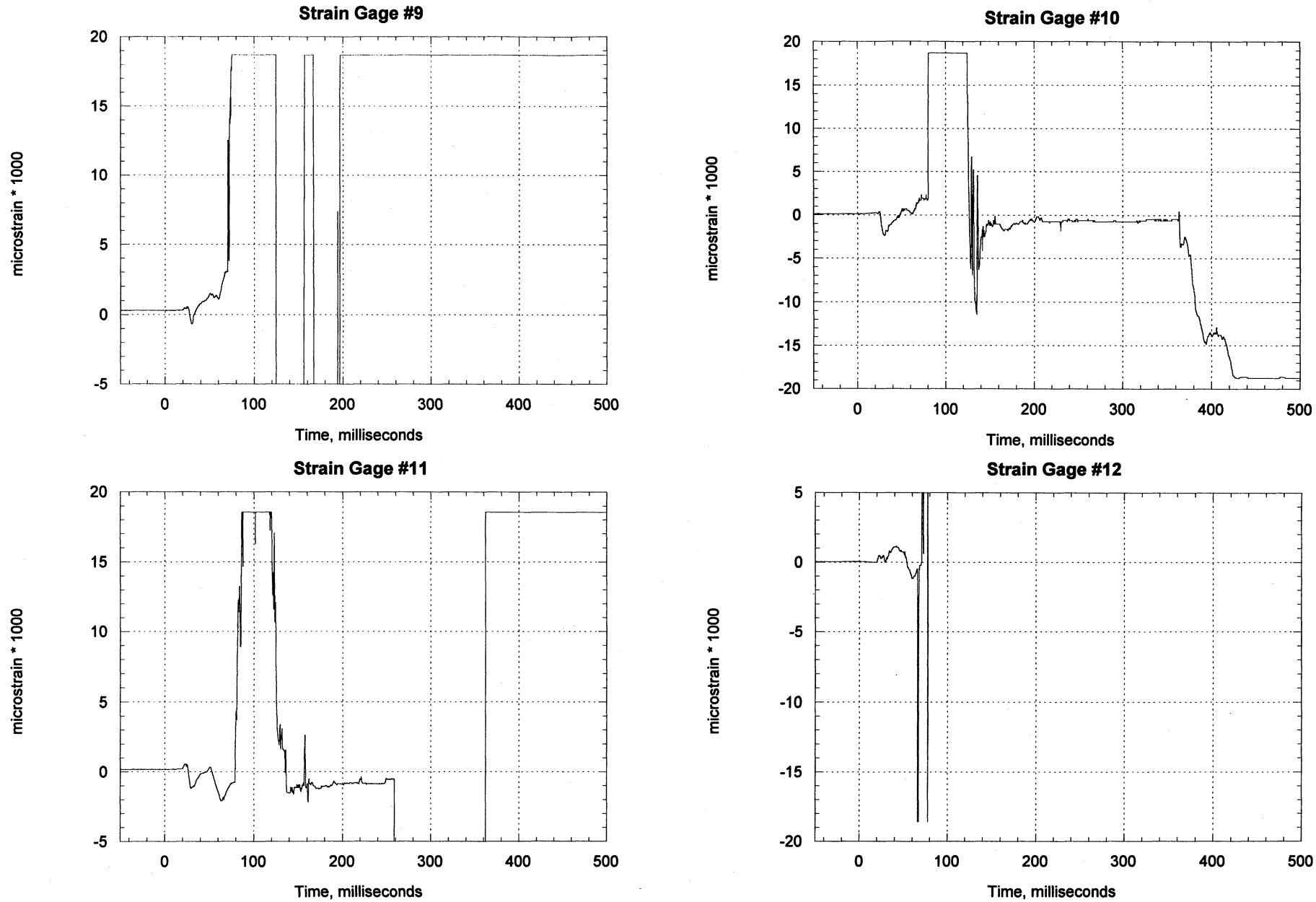

Figure 145, Test 3, Engine Mount, Forward Upright

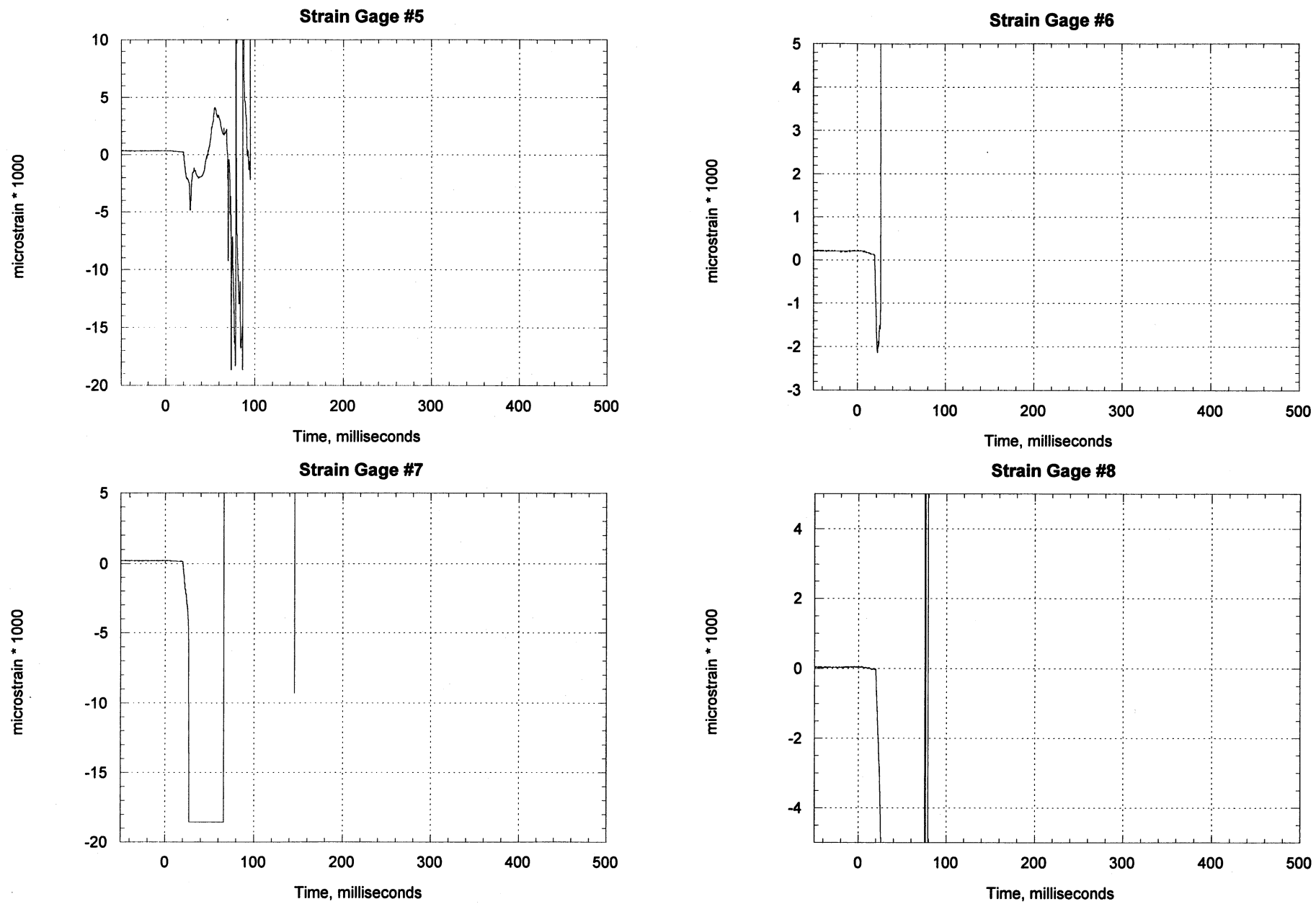

Figure 146, Test 3, Engine Mount, Forward Diagonal

REPORT DOCUMENTATION PAGE

Form Approved
OMB No. 0704-0188

The public reporting burden for this collection of information is estimated to average 1 hour per response, including the time for reviewing instructions, searching existing data sources, gathering and maintaining the data needed, and completing and reviewing the collection of information. Send comments regarding this burden estimate or any other aspect of this collection of information, including suggestions for reducing this burden, to Department of Defense, Washington Headquarters Services, Directorate for Information Operations and Reports (0704-0188), 1215 Jefferson Davis Highway, Suite 1204, Arlington, VA 22202-4302. Respondents should be aware that notwithstanding any other provision of law, no person shall be subject to any penalty for failing to comply with a collection of information if it does not display a currently valid OMB control number.
PLEASE DO NOT RETURN YOUR FORM TO THE ABOVE ADDRESS.

1. REPORT DATE *(DD-MM-YYYY)*
08-2002

2. REPORT TYPE
Contractor Report

3. DATES COVERED *(From - To)*

4. TITLE AND SUBTITLE
Design and Test of an Improved Crashworthiness Small Composite Airframe

5a. CONTRACT NUMBER
NAS1-20427

5b. GRANT NUMBER

5c. PROGRAM ELEMENT NUMBER

6. AUTHOR(S)
Terry, James E.; Hooper, Steven J.; and Nicholson, Mark

5d. PROJECT NUMBER

5e. TASK NUMBER

5f. WORK UNIT NUMBER
728-50-10-01

7. PERFORMING ORGANIZATION NAME(S) AND ADDRESS(ES)
Terry Engineering
147 Williamsburg
Andover, Kansas 67002-9770

8. PERFORMING ORGANIZATION REPORT NUMBER

9. SPONSORING/MONITORING AGENCY NAME(S) AND ADDRESS(ES)
National Aeronautics and Space Administration
Washington, DC 20546-0001

10. SPONSOR/MONITOR'S ACRONYM(S)
NASA

11. SPONSOR/MONITOR'S REPORT NUMBER(S)
NASA/CR-2002-211774

12. DISTRIBUTION/AVAILABILITY STATEMENT
Unclassified - Unlimited
Subject Category 05
Availability: NASA CASI (301) 621-0390 Distribution: Nonstandard

13. SUPPLEMENTARY NOTES
An electronic version can be found at http://techreports.larc.nasa.gov/ltrs/ or http://techreports.larc.nasa.gov/cgi-bin/NTRS
Langley Technical Monitor: Lisa E. Jones

14. ABSTRACT

The purpose of this small business innovative research (SBIR) program was to evaluate the feasibility of developing small composite airplanes with improved crashworthiness. A combination of analysis and half scale component tests were used to develop an energy absorbing airframe. Four full scale crash tests were conducted at the NASA Impact Dynamics Research Facility, two on a hard surface and two onto soft soil, replicating earlier NASA tests of production general aviation airplanes. Several seat designs and restraint systems including both an air bag and load limiting shoulder harnesses were tested. Tests showed that occupant loads were within survivable limits with the improved structural design and the proper combination of seats and restraint systems. There was no loss of cabin volume during the events. The analysis method developed provided design guidance but time did not allow extending the analysis to soft soil impact. This project demonstrated that survivability improvements are possible with modest weight penalties. The design methods can be readily applied by airplane designers using the examples in this report.

15. SUBJECT TERMS
Crashworthiness; Energy absorbing structure; Energy absorbing seats; Air bag; Restraint systems; Dynamic impact testing; Dynamic analysis

16. SECURITY CLASSIFICATION OF:			17. LIMITATION OF ABSTRACT	18. NUMBER OF PAGES	19a. NAME OF RESPONSIBLE PERSON
a. REPORT	b. ABSTRACT	c. THIS PAGE			STI Help Desk (email: help@sti.nasa.gov)
					19b. TELEPHONE NUMBER *(Include area code)*
U	U	U	UU	227	(301) 621-0390